

**UNIVERSIDADE DE LISBOA**  
**INSTITUTO SUPERIOR TÉCNICO**

**Durability of all-composite civil engineering structures in  
service conditions. Development of an inspection and diagnosis  
system**

**André Miguel Pereira Castelo**

**Supervisor:** Doctor João Pedro Ramôa Ribeiro Correia  
**Co-Supervisors:** Doctor Susana Bravo Cabral da Fonseca  
Doctor Jorge Manuel Calição Lopes de Brito

**Thesis approved in public session to obtain the PhD Degree in  
Civil Engineering**

**Jury final classification: Pass with Distinction**

**2023**



**UNIVERSIDADE DE LISBOA**  
**INSTITUTO SUPERIOR TÉCNICO**

**Durability of all-composite civil engineering structures in  
service conditions. Development of an inspection and diagnosis  
system**

**André Miguel Pereira Castelo**

**Supervisor:** Doctor João Pedro Ramôa Ribeiro Correia  
**Co-Supervisors:** Doctor Susana Bravo Cabral da Fonseca  
Doctor Jorge Manuel Caliço Lopes de Brito

**Thesis approved in public session to obtain the PhD Degree in Civil Engineering**

**Jury final classification: Pass with Distinction**

**Jury**

**Chairperson:** Doctor Eduardo Nuno Brito Santos Júlio,  
Instituto Superior Técnico, Universidade de Lisboa

**Members of the Committee:** Doctor João Pedro Ramôa Ribeiro Correia,  
Instituto Superior Técnico, Universidade de Lisboa  
Doctor José Manuel de Sena Cruz,  
Escola de Engenharia, Universidade do Minho  
Doctor José Dinis Silvestre,  
Instituto Superior Técnico, Universidade de Lisboa  
Doctor Maria Paula Marques da Costa Rodrigues,  
Laboratório Nacional de Engenharia Civil

**Funding Institution: Fundação para a Ciência e Tecnologia**

**2023**



## Abstract

The use of fibre reinforced polymer (FRP) composites in civil engineering has become increasingly popular due to their high strength-to-weight ratio, corrosion resistance and durability. However, despite the empirical evidence of their good performance, even in relatively harsh environmental conditions, there is a lack of information on their long-term durability, which is essential for their acceptance as a mainstream structural material. This thesis intends to comprehensively understand the behaviour of glass-FRP (GFRP) composite materials throughout their service life. The thesis consists of two parts: (i) development of an inspection, diagnosis, and rehabilitation system, and (ii) evaluation of the durability of pultruded GFRP profiles for civil engineering purposes.

The inspection, diagnosis, and rehabilitation system developed in the first part of the thesis comprises four groups of entities: anomalies, probable causes, diagnosis methods, and rehabilitation techniques. A data analysis based on a field study of 31 infrastructures containing 410 GFRP substructures allowed identifying the most common anomalies that can be detected during the in-service stage of GFRP constructions. The type, age, and location of the substructures proved to be relevant to the type of anomalies detected.

The second part of the thesis evaluated the durability of GFRP composites made of polyester (UP) and vinylester (VE) resins under different environmental conditions, including chemicals (water, acidic and alkaline) and weathering (natural and accelerated). The results obtained show that, among the various chemicals, immersion in an alkaline environment caused the highest reduction in mechanical properties, while exposure to water vapour resulted in a higher reduction in comparison to the other vapour environments. For weathering, the results confirmed that VE specimens exhibited better performance than UP specimens. The use of a surface veil and surface protective coatings did not have a clear influence on strength retention. The incorporation of UV stabilizer additives improved the mechanical properties of UP specimens.

**Keywords:** GFRP, inspection system, durability, chemical environments, weathering.



## Resumo

A utilização de polímeros reforçados com fibras (PRF) na Engenharia Civil aumentou consideravelmente nos últimos anos, devido à sua elevada relação resistência-peso, resistência à corrosão e durabilidade em condições ambientais adversas. No entanto, apesar das evidências do seu bom desempenho, continua a existir falta de informação relativamente ao seu comportamento a longo prazo, fator que é essencial para a sua aceitação como material estrutural corrente. Esta tese tem como objetivo compreender o comportamento dos materiais compósitos GFRP (do inglês, *glass fibre reinforced polymer*) ao longo da sua vida útil. A tese é composta por duas partes: (i) desenvolvimento de um sistema de inspeção, diagnóstico e reabilitação; e (ii) avaliação da durabilidade de perfis pultrudidos de GFRP para aplicações da Engenharia Civil.

Na primeira parte da tese, foi desenvolvido um sistema de inspeção, diagnóstico e reabilitação para estruturas em compósitos, composto por quatro grupos de elementos: anomalias, causas prováveis, técnicas de diagnóstico e técnicas de reabilitação. Através da análise de dados, recolhida durante a inspeção de 31 infraestruturas contendo 410 subestruturas em GFRP, foi possível identificar as anomalias mais comuns durante a fase de serviço das construções. A tipologia, idade e localização das subestruturas mostraram-se relevantes para o tipo de anomalias detetadas.

Na segunda parte da tese, foi avaliada a durabilidade de elementos GFRP, constituídos por resinas de poliéster e viniléster, sob diferentes condições ambientais, nomeadamente (i) ambientes químicos (neutros, ácidos e alcalinos) e (ii) envelhecimento ambiental (natural e acelerado). No estudo sobre os efeitos de ambientes químicos, a imersão em ambientes alcalinos provocou a maior redução de propriedades mecânicas, enquanto a exposição ao vapor de água provocou uma maior redução em comparação com os restantes ambientes de vapor. No estudo sobre os efeitos do envelhecimento ambiental, as amostras de viniléster exibiram melhor resistência ao envelhecimento do que as amostras de poliéster. A aplicação de um véu de superfície e de camadas de proteção superficial não teve uma influência clara na variação das propriedades mecânicas.

**Palavras-chave:** GFRP, sistema de inspeção, durabilidade, ambientes químicos, envelhecimento ambiental



## Acknowledgements

This thesis is the culmination of over six years of research. Although it is an individual work, it would not have been possible without the combined efforts, support, and goodwill of the many people with whom I have had the honour and pleasure of working and collaborating. I would like to express my appreciation to all those who have helped me on this long journey.

Firstly, I cannot express enough how grateful I am to my thesis supervisor, Professor João Ramôa Correia, and my co-supervisors, Doctor Susana Cabral-Fonseca and Professor Jorge de Brito. Their unwavering support, patience, and encouragement throughout the entirety of this project has been nothing short of remarkable and invaluable. Without their guidance, dedication, and expertise, I would not have been able to complete this work to the best of my abilities.

I am truly fortunate to have had the privilege of working with such outstanding scholars who have generously shared their knowledge and expertise with me. Their valuable insights, feedback, and constructive criticism have challenged me to grow both personally and academically. Their encouragement and friendship have meant the world to me, and I will be forever grateful for their mentorship. I could not have asked for better mentors, and I am honoured to have had the opportunity to work with them. In particular, I want to express my deepest gratitude to Prof. João Correia, for his unyielding support, dedication and guidance, without which this work would not have been possible. I owe a great deal to his support, for his invaluable advice, knowledge, guidance, dedication, scientific exigence and rigour.

This thesis was conducted in collaboration with Laboratório Nacional de Engenharia Civil (LNEC), where most of this thesis experimental work was conducted. I thus want to thank Doctor Maria Paula Rodrigues and Doctor Susana Fonseca for always making me feel welcome, and for providing me with a unique learning experience in a different work environment. All LNEC personnel made me feel at ease and they were always available and helpful, assisting me through the different experimental tests. In particular, I would like to thank Filomena Noble, Nuno Silvestre, Otilia Lourenço, and Rúben Rocha.

In my thesis, I also developed a substantial amount of lab work at IST, which would not have been possible without the help, guidance and companionship of the technicians that were there to support me, namely Fernando Alves, Fernando Costa, Pedro Costa and Jorge Pontes, and also to the Civil Engineering Research and Innovation for Sustainability (CERIS) research unit from IST, which provided me with the work conditions needed to develop this work.

I would like to express my gratitude to our industry partners, Sociedade Técnica de Estruturas Pultrudidas (STEP) and ALTO Perfis Pultrudidos, for their generous contributions in manufacturing the materials used in this work. I also want to thank SIKA for providing the superficial protections used in this project. Furthermore, I am grateful to Águas de Portugal and EPAL, in particular, to Eng.º Nuno Reis,

for granting me access to their facilities, which has been essential to the success of this project. Their support and collaboration have been invaluable, and I am deeply appreciative of their contributions.

I would also like to thank Jónatas Valença and Bruno Santos, for the cooperation in the development of the fibre rating development ratios presented in this thesis.

I am also thankful to the Portuguese Foundation for Science and Technology (FCT), for the financial support provided through the EcoCoRe doctoral program (scholarship (PD/BD/113640/2015) and the Durable-FRP project - Towards Durability Design of FRP Composites for Civil Engineering Structures (grant PTDC/ECI-EGC/4609/2020), funded by FCT through national funds under the Lisbon Regional Operational Program (PORLisboa), and co-financed by the European Regional Development Fund (ERDF) through the COMPETE - Operational Program for Competitiveness Factors (POFC).

I feel incredibly grateful to have had the support and companionship of so many wonderful people during my journey. In office 2.45, Tiago Morgado and Lourenço Fernandes, my emotional co-supervisors, played an essential role in making this experience the best it could be.

I would also like to express my gratitude to my colleagues at IST from the Core Group, who provided me with help, support, and friendship throughout this entire period. I especially want to thank Mário Garrido, João Firmo, João Sousa, Francisco Nunes, Luís Valarinho, Adriana Azevedo, Inês Rosa, Pietro Mazzuca, and Eloisa Castilho for their unwavering support, motivation, playfulness and guidance.

I am also deeply grateful for my friends Beatriz, Catarina, and Cláudia, who have been a constant source of support and joy throughout this journey. Tiago, in particular, has been an amazing friend, offering emotional support, patience, and understanding during late nights and difficult times.

Lastly, I want to express my deepest gratitude to my late grandparents, uncles, cousins, and most importantly, my core family: my parents, Helena and José, and my dear sister Isabel. They have been the anchors that kept me grounded throughout this journey, providing unwavering support and encouragement, even when we were far apart.

I cannot express how much their love and guidance have meant to me, especially during the times when I felt overwhelmed and uncertain. Their faith in me never wavered, and they never hesitated to remind me of my strengths and potential. Their unwavering support and love have given me the courage to pursue my dreams and overcome the challenges that came my way.



UNIÃO EUROPEIA

Fundo Europeu de  
Desenvolvimento Regional

# Table of contents

<b>PART I INTRODUCTION .....</b>	<b>1</b>
<b>1. INTRODUCTION.....</b>	<b>2</b>
1.1. CONTEXT AND MOTIVATION.....	2
1.2. OBJECTIVES AND METHODOLOGY.....	3
1.3. MAIN SCIENTIFIC CONTRIBUTIONS.....	5
1.4. DOCUMENT OUTLINE .....	6
<b>2. GENERAL REVIEW OF GFRP MATERIALS AND STRUCTURES .....</b>	<b>9</b>
2.1. INTRODUCTORY REMARKS .....	9
2.2. GFRP CONSTITUENTS.....	9
2.2.1. <i>Fibres</i> .....	9
2.2.2. <i>Polymeric matrix</i> .....	10
2.2.3. <i>Fillers</i> .....	11
2.2.4. <i>Additives</i> .....	11
2.2.5. <i>The fibre-matrix interface in FRP composite materials</i> .....	12
2.3. FRP PRODUCTION PROCESSES .....	13
2.3.1. <i>Pultrusion</i> .....	13
2.3.2. <i>Moulding</i> .....	15
2.4. FRP CONNECTION TECHNOLOGY.....	16
2.5. TYPICAL PROPERTIES OF PULTRUDED GFRP PROFILES.....	17
2.6. FRP APPLICATIONS IN CIVIL ENGINEERING.....	18
<b>3. PART I REFERENCES.....</b>	<b>21</b>
<b>PART II DEVELOPMENT OF AN INSPECTION, DIAGNOSIS AND REHABILITATION SYSTEM FOR GFRP CONSTRUCTIONS .....</b>	<b>25</b>
<b>4. CHARACTERIZATION OF THE INSPECTION, DIAGNOSIS AND REHABILITATION SYSTEM PROPOSED ....</b>	<b>29</b>
4.1. INTRODUCTORY REMARKS .....	29
4.2. STATE-OF-THE-ART REVIEW OF INSPECTION, DIAGNOSIS AND REHABILITATION SYSTEMS .....	29
4.3. NORMATIVE AND FUNCTIONAL REQUIREMENTS .....	35
4.4. OUTLINE OF PROPOSED SYSTEM FOR GFRP CONSTRUCTIONS .....	35
4.5. CONCLUDING REMARKS .....	36
<b>5. ANOMALIES IN GFRP CONSTRUCTIONS.....</b>	<b>39</b>
5.1. INTRODUCTORY REMARKS .....	39
5.2. CLASSIFICATION SYSTEM OF THE ANOMALIES .....	39
5.3. CHARACTERIZATION OF THE ANOMALIES.....	40
5.3.1. <i>A.N-Me.01 - Biological colonization</i> .....	40
5.3.2. <i>A.N-Me.02 - Discolouration/loss of gloss</i> .....	41
5.3.3. <i>A.N-Me.03 - Fibre blooming</i> .....	41
5.3.4. <i>A.N-Me.04 - Inclusion</i> .....	42
5.3.5. <i>A.N-Me.05 - Stains</i> .....	42
5.3.6. <i>A.N-Me.06 - Surface marks</i> .....	43
5.3.7. <i>A.N-Me.07 - Wear damage</i> .....	44
5.3.8. <i>A.N-Me.08 - Debris accumulation</i> .....	44
5.3.9. <i>A.Me.01 - Corrosion of metallic components</i> .....	45
5.3.10. <i>A.Me.02 - Cracking</i> .....	45
5.3.11. <i>A.Me.03 - Crushing</i> .....	46
5.3.12. <i>A.Me.04 - Debonding</i> .....	46
5.3.13. <i>A.Me.05 - Delamination</i> .....	47
5.3.14. <i>A.Me.06 - Excessive deflection</i> .....	47
5.3.15. <i>A.Me.07 - Geometrical imperfections</i> .....	47
5.3.16. <i>A.Me.08 - Indentation/perforation</i> .....	48
5.3.17. <i>A.Me.09 - Incorrect curing of adhesive</i> .....	48

5.3.18.	<i>A.Me.10 - Incorrect curing of resin</i> .....	48
5.3.19.	<i>A.Me.11 - Loose connections</i> .....	49
5.3.20.	<i>A.Me.12 - Member failure</i> .....	49
5.3.21.	<i>A.Me.13 - Voids</i> .....	49
5.4.	CLASSIFICATION OF THE CAUSES OF THE ANOMALIES .....	50
5.4.1.	<i>C.P. - Production causes</i> .....	50
5.4.2.	<i>C.D. - Design causes</i> .....	51
5.4.3.	<i>C.I. - Installation causes</i> .....	52
5.4.4.	<i>C.S. - In-service causes</i> .....	52
5.5.	ANOMALY FORMS.....	53
5.6.	CONCLUDING REMARKS .....	53
<b>6.</b>	<b>DIAGNOSIS TECHNIQUES</b> .....	<b>55</b>
6.1.	INTRODUCTORY REMARKS .....	55
6.2.	DIAGNOSIS TECHNIQUES DESCRIPTION .....	55
6.2.1.	<i>I.01 - Visual inspection</i> .....	55
6.2.2.	<i>I.02 - Tap test</i> .....	56
6.2.3.	<i>I.03 - Barcol hardness measurement</i> .....	57
6.2.4.	<i>I.04 - Infrared thermography</i> .....	57
6.2.5.	<i>I.05 - Ultrasonic test</i> .....	58
6.2.6.	<i>I.06 - Moisture meter test</i> .....	59
6.3.	DIAGNOSIS TECHNIQUES FORMS .....	60
6.4.	CONCLUDING REMARKS .....	60
<b>7.</b>	<b>REHABILITATION TECHNIQUES</b> .....	<b>63</b>
7.1.	INTRODUCTORY REMARKS .....	63
7.2.	REHABILITATION TECHNIQUES DESCRIPTION .....	63
7.2.1.	<i>R.01 - Bonding/bolting of strengthening elements</i> .....	63
7.2.2.	<i>R.02 - Strengthening with filling elements</i> .....	64
7.2.3.	<i>R.03 - Application of surface coating</i> .....	64
7.2.4.	<i>R.04 - Surface sanding/cleaning</i> .....	65
7.2.5.	<i>R.05 - Replacement of affected elements</i> .....	65
7.2.6.	<i>R.06 - Protection/tightening of bolted connections</i> .....	65
7.3.	REHABILITATION TECHNIQUES FORMS .....	66
7.4.	CONCLUDING REMARKS .....	68
<b>8.</b>	<b>CORRELATION MATRICES</b> .....	<b>69</b>
8.1.	INTRODUCTORY REMARKS .....	69
8.2.	ANOMALIES - PROBABLE CAUSES CORRELATION MATRIX .....	69
8.3.	INTER-ANOMALIES CORRELATION MATRIX .....	71
8.4.	ANOMALIES - DIAGNOSIS TECHNIQUES CORRELATION MATRIX .....	73
8.5.	ANOMALIES - REHABILITATION TECHNIQUES CORRELATION MATRIX.....	74
8.6.	CONCLUDING REMARKS .....	75
<b>9.</b>	<b>INSPECTION SYSTEM VALIDATION AND DATA ANALYSIS</b> .....	<b>77</b>
9.1.	INTRODUCTORY REMARKS .....	77
9.2.	INSPECTION PLANNING .....	78
9.2.1.	<i>Inspection forms</i> .....	79
9.2.2.	<i>Validation forms</i> .....	79
9.3.	CHARACTERIZATION OF THE SAMPLE.....	80
9.4.	VALIDATION OF THE CLASSIFICATION SYSTEMS .....	81
9.4.1.	<i>Validation and analysis of the anomalies classification system</i> .....	81
9.4.2.	<i>Validation and analysis of the causes classification system</i> .....	83
9.4.3.	<i>Validation and analysis of the diagnosis techniques classification system</i> .....	85
9.4.4.	<i>Validation and analysis of the rehabilitation techniques classification system</i> .....	86
9.5.	VALIDATION OF THE CORRELATION MATRICES .....	86
9.5.1.	<i>Validation of the anomalies-causes matrix</i> .....	87

9.5.2.	<i>Validation of the inter-anomalies matrix</i> .....	91
9.6.	DATA ANALYSIS .....	92
9.6.1.	<i>Anomaly frequency</i> .....	92
9.6.2.	<i>Anomaly severity level</i> .....	93
9.6.3.	<i>Influence of age on anomaly occurrence</i> .....	94
9.7.	ANALYSIS OF ANOMALIES IN DIFFERENT ENVIRONMENTAL CONDITIONS.....	95
9.7.1.	<i>Indoor and outdoor location</i> .....	95
9.7.2.	<i>Exposure to ultra violet radiation</i> .....	96
9.7.3.	<i>Exposure to chemical environments</i> .....	97
9.7.4.	<i>Exposure to wind/rain</i> .....	97
9.7.5.	<i>Exposure to moisture</i> .....	98
9.7.6.	<i>Exposure to other environmental agents</i> .....	99
9.8.	GFRP CONSTRUCTIONS: GOOD PRACTICES OBSERVED .....	99
9.8.1.	<i>Profile constructions</i> .....	99
9.8.2.	<i>Grating constructions</i> .....	101
9.8.3.	<i>Stair constructions</i> .....	102
9.9.	CONCLUDING REMARKS .....	103
<b>10.</b>	<b>PART II REFERENCES</b> .....	<b>105</b>
<b>PART III DURABILITY OF GFRP COMPOSITES EXPOSED TO DIFFERENT ENVIRONMENTAL CONDITIONS</b> .....		<b>109</b>
<b>11.</b>	<b>EXPERIMENTAL PROGRAMME AND INITIAL CHARACTERIZATION OF GFRP MATERIAL</b> .....	<b>113</b>
11.1.	INTRODUCTORY REMARKS.....	113
11.2.	MATERIALS.....	113
11.2.1.	<i>Material selection</i> .....	114
11.2.2.	<i>Material production</i> .....	114
11.3.	CHARACTERISATION METHODS AND TEST SETUP .....	116
11.3.1.	<i>Inorganic mass content</i> .....	117
11.3.2.	<i>Colour</i> .....	117
11.3.3.	<i>Gloss</i> .....	117
11.3.4.	<i>Barcol hardness</i> .....	117
11.3.5.	<i>Dynamic mechanical analysis</i> .....	118
11.3.6.	<i>Tensile tests</i> .....	118
11.3.7.	<i>Compressive tests</i> .....	119
11.3.8.	<i>Flexural tests</i> .....	120
11.3.9.	<i>In-plane shear tests</i> .....	121
11.3.10.	<i>Interlaminar shear strength tests</i> .....	121
11.4.	CHARACTERISATION OF UNAGED GFRP MATERIALS .....	122
11.4.1.	<i>Summary of properties</i> .....	122
11.4.2.	<i>Dynamic mechanical analysis</i> .....	124
11.4.3.	<i>Tensile properties</i> .....	124
11.4.4.	<i>Compressive properties</i> .....	125
11.4.5.	<i>Flexural properties</i> .....	126
11.4.6.	<i>In-plane shear properties</i> .....	127
11.4.7.	<i>Interlaminar shear strength</i> .....	128
11.5.	COMPARISON BETWEEN UP_WV_0 AND VE_WV_0.....	129
11.6.	CONCLUDING REMARKS.....	129
<b>12.</b>	<b>EXPOSURE OF GFRP COMPOSITES TO CHEMICAL ENVIRONMENTS</b> .....	<b>131</b>
12.1.	INTRODUCTORY REMARKS.....	131
12.2.	LITERATURE REVIEW .....	131
12.2.1.	<i>Preliminary remarks</i> .....	131
12.2.2.	<i>Review of studies on the effects of alkaline and acidic environments</i> .....	135
12.2.2.1.	Studies on polymeric materials and matrices .....	135
12.2.2.2.	Studies on GFRP composites .....	135
12.2.3.	<i>Summary of chemical exposure literature review</i> .....	138

12.3.	DESCRIPTION OF THE TEST PROGRAMME.....	139
12.4.	RESULTS AND DISCUSSION .....	141
12.4.1.	<i>Visual inspection</i> .....	141
12.4.2.	<i>Colour variation</i> .....	142
12.4.3.	<i>Gloss variation</i> .....	147
12.4.4.	<i>Compressive tests</i> .....	150
12.4.5.	<i>In-plane shear tests</i> .....	154
12.4.6.	<i>Interlaminar shear strength tests</i> .....	158
12.4.7.	<i>Effect of surface protection coating on mechanical properties for vapour exposure</i> .....	162
12.5.	CONCLUDING REMARKS.....	165
<b>13.</b>	<b>EXPOSURE OF GFRP COMPOSITES TO WEATHERING .....</b>	<b>167</b>
13.1.	INTRODUCTORY REMARKS.....	167
13.2.	LITERATURE REVIEW .....	167
13.2.1.	<i>Preliminary remarks</i> .....	167
13.2.2.	<i>Review of studies on the effects of UV radiation and weathering</i> .....	169
13.2.2.1.	Studies on polymeric materials and matrices .....	169
13.2.2.2.	Studies on FRP composites.....	169
13.2.3.	<i>Summary</i> .....	172
13.3.	EXPERIMENTAL STUDY - NATURAL AND ACCELERATED WEATHERING .....	172
13.3.1.	<i>Description of the test programme</i> .....	172
13.3.2.	<i>Results and discussion</i> .....	176
13.3.2.1.	Colour variation.....	176
13.3.2.2.	Gloss variation.....	181
13.3.2.3.	Dynamical mechanical analysis .....	184
13.3.2.4.	Mechanical properties .....	186
13.3.2.5.	Progression of fibre blooming through image analysis .....	195
13.4.	FIELD STUDY .....	198
13.4.1.	<i>Overview of surveyed constructions</i> .....	198
13.4.1.1.	25 <sup>th</sup> of April Bridge .....	198
13.4.1.2.	Colombo Centre rooftop .....	199
13.4.1.3.	Lisbon Oceanarium.....	200
13.4.2.	<i>Description of test programme</i> .....	200
13.4.3.	<i>Results and discussion</i> .....	201
13.4.3.1.	Inorganic mass content .....	201
13.4.3.2.	Dynamic mechanical analysis .....	201
13.4.3.3.	Mechanical properties .....	201
13.5.	CONCLUDING REMARKS.....	207
<b>14.</b>	<b>PART III REFERENCES.....</b>	<b>209</b>
<b>PART IV CONCLUSIONS AND FUTURE DEVELOPMENTS .....</b>		<b>217</b>
<b>15.</b>	<b>CONCLUSIONS AND FUTURE DEVELOPMENTS.....</b>	<b>219</b>
15.1.	PRELIMINARY REMARKS.....	219
15.2.	CONCLUSIONS.....	219
15.2.1.	<i>Inspection, diagnosis and rehabilitation system</i> .....	219
15.2.2.	<i>Exposure of GFRP composites to chemical environments</i> .....	220
15.2.3.	<i>Exposure of GFRP composites to weathering</i> .....	221
15.3.	FUTURE DEVELOPMENTS .....	222
<b>APPENDIX</b> .....		<b>225</b>

## List of figures

Figure 2.01 - Pultrusion process used for manufacturing GFRP profiles.....	14
Figure 2.02 - Examples of 1 <sup>st</sup> and 2 <sup>nd</sup> generation FRP profiles.....	15
Figure 2.03 - Moulded grating cross-section reinforcement and moulded grating with plate reinforcement.....	16
Figure 2.04 - Examples of different connection technology.....	17
Figure 2.05 - FRP applications in Civil engineering.....	19
Figure 2.06 – Examples of FRP structures in civil engineering.....	20
Figure 4.01 - Examples of the anomalies presented in ASTM D2563-R02.....	30
Figure 4.02 - Examples of the anomalies detected in the Pontresina footbridge.....	31
Figure 4.03 - Examples of the repair techniques applied in the Pontresina footbridge.....	31
Figure 4.04 - Examples of the anomalies .....	32
Figure 4.05 - Proposed organization of the inspection and diagnosis system of GFRP elements.....	36
Figure 5.01 - Examples of the A-N.Me.01 anomaly - biological colonization.....	41
Figure 5.02 - Examples of the A-N.Me.02 anomaly - discolouration/loss of gloss.....	41
Figure 5.03 - Examples of the A-N.Me.03 anomaly - fibre blooming.....	42
Figure 5.04 - Schematic example of the occurrence of the A-N.Me.04 anomaly - inclusion.....	42
Figure 5.05 - Examples of the A-N.Me.05 anomaly - stains.....	43
Figure 5.06 - Examples of the A-N.Me.06 anomaly - surface marks.....	44
Figure 5.07 - Examples of the A-N.Me.07 anomaly - wear damage.....	44
Figure 5.08 - Examples of the A-N.Me.08 anomaly - debris accumulation.....	45
Figure 5.09 - Examples of the A-Me.01 anomaly - corrosion of metallic components.....	45
Figure 5.10 - Examples of the A-Me.02 anomaly - cracking.....	46
Figure 5.11 - Examples of the A-Me.03 anomaly - crushing.....	46
Figure 5.12 - Examples of the A-Me.04 anomaly - debonding.....	47
Figure 5.13 - Examples of the A-Me.05 anomaly - delamination.....	47
Figure 5.14 - Examples of the A-Me.07 anomaly - geometrical imperfections.....	48
Figure 5.15 - Examples of the A-Me.08 anomaly - indentation/perforation.....	48
Figure 5.16 - Examples of the A-Me.11 anomaly - loose connections.....	49
Figure 5.17 - Examples of the A-Me.12 anomaly - member failure.....	49
Figure 5.18 - Examples of the A-Me.11 anomaly - voids.....	50
Figure 5.19 - Examples of occurrence of anomalies due to causes of the production stage.....	51
Figure 5.20 - Examples of occurrence of anomalies due to causes of the design stage.....	51
Figure 5.21 - Examples of occurrence of anomalies due to causes of the installation stage.....	52
Figure 5.22 - Examples of occurrence of anomalies due to causes of the in-service stage.....	52
Figure 5.23 - A-N-Me.01 anomaly (biological colonization) form.....	54
Figure 6.01 - Barcol impressor .....	57
Figure 6.02 - Schematic functioning system of thermography.....	58
Figure 6.03 - Schematic functioning system of ultrasonic testing.....	58
Figure 6.04 - Moisture meter .....	59
Figure 6.05 - I.04 diagnosis technique (Infrared thermography) form.....	61
Figure 7.01 - Illustrative scheme of the R.01 rehabilitation technique - Bonding/bolting of strengthening elements.....	64
Figure 7.02 - Application of the R.02 rehabilitation technique - Strengthening with filling elements.....	64
Figure 7.03- Application of the R.03 rehabilitation technique - Application of surface coating.....	65
Figure 7.04- Application of the R.04 rehabilitation technique - Surface sanding/cleaning.....	65

Figure 7.05 - R.03 rehabilitation form - Protection/tightening of bolted connections.....	67
Figure 9.01 - Types of structures considered. ....	77
Figure 9.02 - Location of the inspected installations. ....	78
Figure 9.03 - Distribution of installations and number of substructures per year .....	81
Figure 9.04 - Absolute frequency of occurrence of each anomaly.....	82
Figure 9.05 - Frequency of occurrence of each anomaly relative to the number substructures.....	82
Figure 9.06 - Frequency of the most probable causes by groups .....	84
Figure 9.07 - Frequency distribution of the anomalies probable causes. ....	84
Figure 9.08 - Frequency of suggested diagnosis techniques. ....	85
Figure 9.09 - Frequency of suggestion of the rehabilitation techniques.....	86
Figure 9.10 - Frequency of occurrence of each anomaly per type of substructures. ....	93
Figure 9.11 - Severity levels of anomaly A.Me.02. ....	94
Figure 9.12 - Frequency of occurrence of each anomaly per time period.....	94
Figure 9.13 - Frequency of occurrence of each anomaly by indoor and outdoor substructures. ....	95
Figure 9.14 - Frequency of occurrence of each anomaly according to exposure (high/low/nil) to UV radiation.....	96
Figure 9.15 - Frequency of occurrence of each anomaly according to exposure to chemically aggressive environments (high/low/nil).....	97
Figure 9.16 - Frequency of occurrence of each anomaly according to exposure to wind/rain (high/low/nil) .....	98
Figure 9.17 - Frequency of occurrence of each anomaly by moisture exposed substructures.....	98
Figure 9.18 - Examples of the most common connections of profile constructions and the support. ....	100
Figure 9.19 - Examples of the most common connections between profiles. ....	100
Figure 9.20 - Examples of gratings constructions.....	102
Figure 9.21 - Examples of stair constructions.....	102
Figure 11.01 - Production of pultruded materials. ....	115
Figure 11.02 - CNC cutting machine used for specimen cutting. ....	116
Figure 11.03 - Equipment used for some of the physical characterisation tests.....	118
Figure 11.04 - DMA test equipment and setup .....	118
Figure 11.05 - Tensile tests setup and typical failure mode.....	119
Figure 11.06 - Compressive tests setup and typical failure mode.....	120
Figure 11.07 - Flexural tests setup and typical failure mode. ....	120
Figure 11.08 - In-plane shear test setup and typical failure mode.....	121
Figure 11.09 - Interlaminar shear strength test setup and typical failure mode.....	122
Figure 11.10 - Representative DMA curves of UP_WV_0 and VE_WV_0 profiles. ....	124
Figure 11.11 - Representative stress-strain curves of tensile tests: (a) UP and (b) VE profiles. ....	125
Figure 11.12 - Representative stress-strain curves of compressive tests: (a) UP and (b) VE profiles.....	126
Figure 11.13 - Representative stress-strain curves of flexural tests: (a) UP and (b) VE profiles. ....	127
Figure 11.14 - Representative shear stress-strain curves of in-plane shear tests: (a) UP and (b) VE profiles.....	127
Figure 11.15 - Representative load-displacement curves of interlaminar shear tests: (a) UP and (b) VE profiles.....	128
Figure 11.16 - Representative curves of mechanical tests of UP_WV_0 and VE_WV_0 .....	130
Figure 12.01 - SEM images of fractured sections of GFRP vinylester specimens after 30 days exposure to: (a) H <sub>2</sub> SO <sub>4</sub> solution (30%, 60 °C); (b) H <sub>2</sub> SO <sub>4</sub> solution (pH 5, 90 °C).....	137
Figure 12.02 - Changes in appearance of GFRP vinylester specimens, after exposure to: (a) H <sub>2</sub> SO <sub>4</sub> solution (30%, 60 °C), (b) NaOH solution (10%, 60 °C), (c) H <sub>2</sub> SO <sub>4</sub> solution (pH 5, 90 °C) .....	137
Figure 12.03 - Specimens set-up to chemical exposure. ....	140

Figure 12.04 - Photographic survey of polyester (UP) specimens exposed to chemical ageing, after 16 weeks of exposure.	143
Figure 12.05 - Photographic survey of vinylester (VE) specimens exposed to chemical ageing, after 16 weeks of exposure.	144
Figure 12.06 - UP specimens colour change ( $\Delta E^*$ ) during chemical ageing.	145
Figure 12.07 - VE specimens colour change ( $\Delta E^*$ ) during chemical ageing.	146
Figure 12.08 - Gloss retention of UP specimens during chemical ageing.	148
Figure 12.09 - Gloss retention of VE specimens during chemical ageing.	149
Figure 12.10 - Representative stress-strain curves of compressive tests of unaged materials and after 16 weeks of immersion in chemical ageing at 23 °C and 70 °C.	150
Figure 12.11 - Compressive strength retention during chemical ageing.	153
Figure 12.12 - Representative stress-strain curves of in-plane shear tests of unaged materials and after 16 weeks of immersion in chemical ageing at 23 °C and 70 °C.	154
Figure 12.13 - In-plane shear strength retention during chemical ageing.	157
Figure 12.14 - Representative load-displacement curves of interlaminar shear tests of unaged materials and after 16 weeks of immersion in chemical ageing at 23 °C and 70 °C.	158
Figure 12.15 - Interlaminar shear strength retention during chemical ageing.	161
Figure 12.16 - Compressive, in-plane shear, and interlaminar shear strength retention during chemical vapour ageing with superficial protection.	163
Figure 12.17 - Variations between the compressive, in-plane shear, and interlaminar shear strength retention during chemical ageing with and without superficial protection.	164
Figure 13.01 - Structure for natural weathering exposure (LNEC rooftop).	174
Figure 13.02 - Average monthly temperature and relative humidity (HR) during natural weathering.	174
Figure 13.03 - QUV chamber (LNEC laboratory).	175
Figure 13.04 - Specimens colour variation ( $\Delta E^*$ ) during weathering (without superficial protection).	178
Figure 13.05 - Specimens colour variation ( $\Delta E^*$ ) during weathering (with superficial protection).	179
Figure 13.06 - Specimens schematic colour variation during QUV accelerated weathering.	180
Figure 13.07 - Specimens gloss retention during weathering (without superficial protection).	182
Figure 13.08 - Specimens gloss retention during weathering (with superficial protection).	183
Figure 13.09 - DMA results during weathering.	185
Figure 13.10 - Representative stress-strain curves in compression, in-plane shear and tension of unaged materials and materials exposed to accelerated weathering (QUV - 6000h) and natural weathering (NW - 20 months).	187
Figure 13.11 - Retention of mechanical properties of UP and VE specimens after 6000 h of QUV accelerated weathering.	189
Figure 13.12 - Retention of mechanical properties of UP specimens for 10 and 20 months of natural weathering.	192
Figure 13.13 - Retention of mechanical properties of VE specimens for 10 and 20 months of natural weathering.	193
Figure 13.14 - Comparison of effects of QUV accelerated and natural weathering on mechanical properties of UP and VE specimens without superficial protection.	194
Figure 13.15 - Fibre blooming image analysis.	195
Figure 13.16 - Evolution of fibre blooming ratio on UP and VE specimens exposed to (a) QUV and (b) NW.	197
Figure 13.17 - 25 <sup>th</sup> of April Bridge and specimen grating location.	198
Figure 13.18 - Colombo Centre and specimen profile location.	199
Figure 13.19 - Lisbon Oceanarium and specimen profile location.	200
Figure 13.20 - Aged and unaged specimens prepared for testing: Lisbon Oceanarium (left), Colombo Centre (centre), 25 <sup>th</sup> of April Bridge (right) - unaged (above), aged (below).	201
Figure 13.21 - DMA results as function of exposure (field study).	203

Figure 13.22 - Mechanical properties of unexposed and exposed specimens (field study).....	204
Figure 13.23 - Retention of stiffness- and strength-related properties vs. exposure period for outdoor natural weathering by climate, Class II.....	205
Figure 13.24 - Retention of stiffness- and strength-related properties vs. exposure period for outdoor natural weathering, Class III.....	206

## List of tables

Table 2.01 - Typical mechanical properties of pultruded GFRP profiles (standard shapes) from different pultrusion manufacturers and minimum values indicated in European standard EN 13706-3. ....	18
Table 4.01 - List of anomalies suggested for FRP elements in different studies.....	33
Table 4.02 - List of Non-destructive techniques suggested for FRP elements in different studies. ....	34
Table 4.03 - Functional requirements for GFRP elements.....	35
Table 5.01 - Proposed classification system for anomalies in GFRP elements.....	40
Table 5.02 - Proposed classification system for the causes of the anomalies .....	50
Table 6.01 - Advantages and limitations of the I.01 diagnosis technique - Visual inspection. ....	56
Table 6.02 - Advantages and disadvantages of the I.02 diagnosis technique - tap test. ....	56
Table 6.03 - Advantages and limitations of the I.03 diagnosis technique - Barcol hardness measurement. ....	57
Table 6.04 - Advantages and limitations of the I.04 diagnosis technique - Infrared thermography.....	58
Table 6.05 - Advantages and limitations of the I.05 diagnosis technique - Ultrasonic test.....	59
Table 6.06 - Advantages and limitations of the I.06 diagnosis technique - Moisture metre test. ....	60
Table 8.01 - Correlation matrix between anomalies and probable causes .....	70
Table 8.02 - Correlation matrix inter-anomalies.....	72
Table 8.03 - Percentage correlation matrix inter-anomalies (%). ....	73
Table 8.04 - Correlation matrix between anomalies and inspection techniques.....	74
Table 8.05 - Correlation matrix between anomalies and rehabilitation techniques.....	75
Table 9.01 - Sample and elements characterization.....	80
Table 9.02 - Comparison between the initial values of the theoretical correlation matrix $C_t$ , and the values obtained through the data of the field inspections $C_{ac}$ . ....	88
Table 9.03 - Analysis, based on the sample, of the cases of discrepancy with the theoretical correlation matrix and probable causes .....	89
Table 9.04 - Comparison between the theoretical ( <b><math>C_{kj}^{theoric}</math></b> ) and validated ( <b><math>C_{kj}^{validated}</math></b> ) inter-anomalies matrix .....	91
Table 11.01 - Designation of the different series of material formulations.....	114
Table 11.02 - Physical and mechanical properties and corresponding standards.....	116
Table 11.03 - Summary of properties of polyester profiles.....	123
Table 11.04 - Summary of properties of vinylester profiles. ....	123
Table 12.01 - Most relevant physical and chemical, moisture induced, degradation mechanisms, adapted from [III.17]. ....	132
Table 12.02 - Mechanical properties reduction, adapted from Gentry <i>et al.</i> [III.50]. ....	138
Table 12.03 - Chemical ageing environments conditions. ....	139
Table 13.01 - Natural and accelerated weathering environmental conditions.....	173
Table 13.02 - Superficial protection thickness.....	173
Table 13.03 - Weathering data for the natural weathering environment, LNEC weather station.....	175
Table 13.04 - DMA results for QUV accelerated and natural weathering. ....	186
Table 13.05 - QUV accelerated weathering fibre blooming ration by exposure time (% of fibres).....	196
Table 13.06 - Natural weathering fibre blooming ration by exposure time (%). ....	196
Table 13.07 - Summary of properties of the field study specimens. ....	203



# Part I

Introduction



## **Preamble**

The durability limitations of traditional materials used in construction (e.g., steel, reinforced concrete) have influenced design practice and regulation, and, together with the requirement for increasing construction speed, they have promoted the development of new structural materials, lighter, non-corrodible and with higher strength.

In this context, pultruded glass fibre reinforced polymer (GFRP) composites have been increasingly used over the last years in the construction sector, namely in pedestrian and road bridges, in buildings, including frames, roofs and cladding, and also in other constructions, such as walkways, handrails and decking structures.

However, some factors have been hindering the further use of GFRP composites in civil engineering, such as: (i) the insufficient knowledge of their durability for different environmental conditions; (ii) the absence of maintenance plans; (iii) inadequate maintenance or rehabilitation measures; (iv) the evidence of degradation under long-term exposure to different environmental conditions; and (v) the uncertainty about their long-term in-service performance.



# 1. Introduction

## 1.1. Context and motivation

In recent years fibre reinforced polymer (FRP) composites have become increasingly popular in civil engineering projects. These composites are made of a polymeric matrix reinforced with different types of fibres, such as carbon, glass, basalt or aramid.

FRP composites now have a diverse range of applications in civil engineering, including the repair and strengthening of concrete, steel and masonry structures. They are also used in the manufacturing of wind turbine blades [I.01], in sewage pipelines [I.02], in components for building facades [I.03], and in the construction of new structures, such as pedestrian and road bridges, including cable-stayed bridges [I.04].

The most significant advantages of FRP composites are their high strength-to-weight ratio, high strength and fatigue resistance, which makes them ideal for use in new load-bearing structures and also in the rehabilitation of existing structures. Furthermore, FRP composites have: (i) high resistance to corrosion (a critical factor in many civil engineering projects); (ii) good resistance to aggressive and chemically adverse environments; (iii) electromagnetic transparency, and (iv) good electrical insulation.

FRP composites offer design flexibility, as they can be moulded into various shapes and sizes (laminates, sheets, rebars, sandwich panels and pultruded profiles), making them suitable for use in custom structures. They are also convenient to install, as they are lightweight and can be cut to size on the construction site, reducing the time and costs associated with construction.

However, FRP composites have a few drawbacks, namely their higher production (initial) cost compared to traditional materials, such as steel and reinforced concrete. Furthermore, FRP composites are still not well known by practitioners and users (namely when compared to traditional construction materials), and there is still limited experience with their use in civil engineering projects.

Despite the empirical evidence of the good performance of FRP composites when exposed to relatively harsh environmental conditions, durability has been identified by several authors as one of the most critical gaps between necessary knowledge and acquired knowledge [I.05]. Studies on this subject are still limited, and the results presented are sometimes contradictory. This is particularly relevant given the fact that unlike other industries that use FRP composites, most civil engineering structures are designed for 50 or 100 years. In this respect, it is worth referring that in some studies, the conditions used for accelerated ageing are not consensual and can sometimes be considered too demanding, causing excessive degradation and leading to conservative estimates of the durability of GFRP materials.

FRP composites can be found in relatively old structures and, even though ensuring an improved performance compared to traditional materials, they may still exhibit anomalies and might require maintenance or rehabilitation at different stages of their service life. However, only scarce information is available in the technical and scientific literature on this important subject.

Extending the knowledge about the durability of FRP composites and consolidating the

information available about the long-term performance of these materials are paramount factors for increasing the acceptance of FRP composites as mainstream structural materials. These are also critical issues towards the development of reliable regulation in this field [I.06]. This is the context in which this thesis is framed.

## 1.2. Objectives and methodology

The main objective of the present thesis was to obtain a comprehensive understanding of the behaviour of GFRP composite materials during their service life, namely by: **(A)** developing an inspection, diagnosis and rehabilitation system that enables managing this type of constructions during their service life; and **(B)** evaluating the durability of pultruded GFRP profiles for civil engineering applications.

**Objective A, the development of an inspection, diagnosis and rehabilitation system for GFRP constructions**, was addressed through the following tasks: A1) development of a classification system of anomalies and respective causes; A2) creation of a system of inspection and diagnosis techniques; A3) determination of the most common and appropriate maintenance and rehabilitation techniques, A4) validation of the proposed system through a large scale field study, and A5) statistical analysis of the results obtained in the field study.

Task A1 intended to comprehensively understand and classify the anomalies that occur in FRP structures. To achieve this goal, the following procedure was followed: (i) a comprehensive literature review was conducted to identify the reported anomalies and the respective causes in FRP structures; (ii) in addition to the literature review, data were collected from producers and end-users to further complement and validate the findings from step (i); (iii) the findings from steps (i) and (ii) were used to develop a classification system for the anomalies and their causes in FRP structures; and (iv) an anomalies-causes and inter-anomalies matrix was created to visually depict the relationship between the anomalies and their causes, as well as the relationship between different anomalies; and (v) finally, an anomaly form was created.

Tasks A2 and A3 intended to identify and categorize the non-destructive diagnosis and rehabilitation techniques that can be applied *in situ*, specifically in the context of civil engineering. The following procedure was followed for both tasks: (i) a thorough literature review was conducted to identify the non-destructive diagnosis/rehabilitation techniques that could be used in the assessment of FRP structures; (ii) the findings from the literature review were used to create the anomalies-diagnosis/rehabilitation technique matrix, which visually depicts the relationship between the anomalies and the corresponding diagnosis/rehabilitation techniques; and, finally, (iii) a diagnosis/rehabilitation technique form was created.

Task A4 comprised a field study that involved a thorough inspection of GFRP facilities located in mainland Portugal. The goal of this part of the study was to identify the anomalies present in these facilities, their causes, and the most appropriate diagnosis and rehabilitation techniques. The following procedure was followed: (i) a detailed inspection survey was conducted on GFRP facilities of different

ages and located in various environments (in mainland Portugal); (ii) during the inspections, visual observations were made to identify the anomalies present at different levels, including the material, structural members, and connections; (iii) the causes of the anomalies were also determined through the inspection process, and (iv) the most appropriate diagnosis and rehabilitation techniques were identified for each of the anomalies detected.

Finally, task A5 involved the analysis and summary of the information gathered from the field inspections and validation forms. The following procedure was adopted: (i) all the data collected from the inspections and validation forms were analysed and combined to validate the inspection system previously developed in tasks A1 to A3; (ii) the analysis of the data allowed for the determination of the most common anomalies occurring in the GFRP facilities, both in general and in each of the different environments detected during the inspections; (iii) the applicability of the diagnosis and rehabilitation techniques proposed in tasks A2 and A3 was also assessed based on the findings from the field inspections; and (iv) data and information gathered were analysed in order to assess the good practices observed.

The overall purpose of **objective B** was to **evaluate the durability of pultruded GFRP profiles for civil engineering applications**. To achieve this goal, the following tasks were carried out: B1) determination of the most conditioning environments for GFRP profiles, based on the information gathered in objective A, and assessment of their effects on GFRP profiles; B2) characterization of the long-term material properties (mechanical, physical, and aesthetical) of GFRP profiles when subjected to the ageing environments selected in task B1; and B3) collection of GFRP samples from in-service structures, characterization of their long-term material properties and comparison with the corresponding initial properties.

Task B1 included the initial characterization of the GFRP materials used to assess the effects of the selected environments. This task was supported by a comprehensive literature review that allowed: (i) identifying the most relevant factors affecting the durability of GFRP materials for the selected environments, concerning both constituent materials (type of fibre, polymer resin, use of surface veils and UV stabilizers additives) and surface protections (coatings); (ii) defining the materials to be used in the experimental campaign, including the nature of the polymeric matrix, fibre architecture, additives, and superficial protections; and (iii) the initial characterization of the mechanical, physical, viscoelastic, chemical, and aesthetical properties of the materials through various experimental tests. To develop this task, two types of commercial "off-the-shelf" pultruded GFRP profiles were produced by ALTO, Perfis Pultrudidos, Lda. These profiles were made of polyester and vinylester resins and a total of 12 different formulations were produced, comprising different combinations of using surface veil and contents of UV stabilizer additives.

Task B2 intended to characterize the long-term durability behaviour of selected pultruded GFRP profiles through two comprehensive experimental programs. These programs included: (i) chemical ageing in water, alkaline, and acidic environments; and (ii) outdoor (natural) and QUV (artificial) accelerated weathering. In both programs, various mechanical, physical, and aesthetic properties were

monitored, and their changes were thoroughly analysed and discussed.

Finally, task B3 involved the identification of some of the oldest in-service structures made of pultruded GFRP profiles in Portugal. Three structures were selected, for which initial characterisation tests were available or possible, and the physical and mechanical properties of their aged GFRP materials were evaluated to assess the level of degradation over time. The results were used to quantify the actual degradation of the GFRP materials for in service conditions under different types of environmental exposure.

It is important to note that while the results obtained from controlled laboratory tests and artificial ageing are significant, correlating them with the results of natural weathering is a challenging task. This is because the environmental aggressiveness is difficult to quantify and there are many factors that can influence the material and structural behaviour and their complex interactions, such as changing temperatures, humidity levels, direct contact with water, creep, fatigue, and ultraviolet radiation. Therefore, natural weathering studies provide a more reliable representation of the long-term behaviour of GFRP materials.

### **1.3. Main scientific contributions**

The research conducted in this thesis has made significant contributions to the understanding of the durability and in-service performance of pultruded GFRP materials and structures. Through the development of the inspection and diagnostic system, as well as the thorough field studies, it was possible to assess the actual in-service performance of GFRP composite materials and structures under various environmental conditions. This information is most valuable in determining whether current design specifications and material choices are adequate, and, where necessary, to make modifications to better suit specific types of environmental exposure.

The investigation into the durability of GFRP materials has greatly enhanced the knowledge about the long-term behaviour of these composite materials when subjected to various ageing conditions likely to be found in civil engineering applications. This part of the research involved a substantial amount of experiments, including approximately 2000 mechanical characterization tests. The results of these tests provided a wealth of data about the physical and mechanical properties of pultruded GFRP materials made from either polyester or vinylester resins after exposure to different environmental conditions. The research also shed light on the impact of chemical ageing on these materials, filling an important gap in the current technical literature. Moreover, the correlation of results from 6,000 hours of QUV artificial ageing tests with natural weathering studies provided valuable insights into the long-term behaviour of these materials used in outdoor conditions. The significance of fibre blooming (observed over relatively short exposure periods) was emphasized and quantified during the weathering process.

The field study further allowed for a direct comparison of the performance of unexposed and exposed GFRP materials to different environmental conditions, allowing a more accurate degradation assessment. The results of this research have important implications for the design and use of pultruded

GFRP materials in real applications.

The following SCI-indexed journal publications resulted or are expected to result from the contributions described above:

- Castelo, A., Correia, J.R., Cabral-Fonseca, S., de Brito, J. (2020). “Inspection, diagnosis and rehabilitation system for all-fibre-reinforced polymer constructions”. *Construction and Building Materials*, 253, 119160.  
<https://doi.org/10.1016/j.conbuildmat.2020.119160>
- Castelo, A., Correia, J.R., Cabral-Fonseca, S., de Brito, J. (2020). “In-Service Performance of Fibre-Reinforced Polymer Constructions Used in Water and Sewage Treatment Plants”. *Journal of Performance of Constructed Facilities*, 34(4), 04020059.  
[https://doi.org/10.1061/\(ASCE\)CF.1943-5509.0001449](https://doi.org/10.1061/(ASCE)CF.1943-5509.0001449)
- Castelo, A., Correia, J.R., Cabral-Fonseca, S., de Brito, J. (in preparation). “Chemical resistance to alkaline exposure of pultruded GFRP profiles”.
- Castelo, A., Correia, J.R., Cabral-Fonseca, S., de Brito, J. (in preparation). “Chemical resistance to acidic exposure of pultruded GFRP profiles”.
- Castelo, A., Correia, J.R., Cabral-Fonseca, S., de Brito, J. (in preparation). “Natural and artificial accelerated weathering of pultruded GFRP profiles”.
- Castelo, A., Correia, J.R., Cabral-Fonseca, S., de Brito, J. (in preparation). “The effects of natural weathering on GFRP structures: Case studies in Portugal”.

#### 1.4. Document outline

This thesis is organized in 15 chapters, which were grouped into the following four parts:

- **Part I** - Introduction (chapters 1 to 3).
- **Part II** - Development of an inspection, diagnosis and rehabilitation system for GFRP constructions (chapters 4 to 10).
- **Part III** - Durability of GFRP composites exposed to different environmental conditions (chapters 11 to 14).
- **Part IV** - Conclusions and future developments (chapter 15).

In **Part I**, the present **chapter 1** introduces the thesis subject, describing its context, motivation, objectives, methodology and the main scientific contributions. Next, **chapter 2** presents a brief overview concerning pultruded GFRP materials, addressing their constituent materials, manufacturing processes, structural shapes, physical and mechanical properties, connection technology and main applications in civil engineering. **Chapter 3** presents the bibliographical references for Part I.

In **Part II**, the development of an inspection, diagnosis, and rehabilitation system for GFRP constructions is presented. **Chapter 4** presents a state-of-the-art review along with an outline of the proposed system. In **Chapter 5**, a classification system for anomalies detected in GFRP constructions

is proposed with the aim of standardizing the designation and description of these anomalies. The classification system of the probable direct and indirect causes of the anomalies is also presented, along with detailed forms for each anomaly. **Chapters 6 and 7** present a classification system for *in-situ* and non-destructive diagnosis tests and rehabilitation techniques, respectively, which can be applied in civil engineering. At the end of each chapter, the information related to each technique is summarized in a form. In **Chapter 8**, the correlation matrices between anomalies and probable causes, anomalies and diagnosis techniques, anomalies and rehabilitation techniques, and inter-anomalies are developed. **Chapter 9**, based on the 410 inspections performed on GFRP facilities, presents the validation of the proposed anomaly classification system developed in previous chapters, calibrating the adopted procedures and developed correlation matrices. Furthermore, this chapter presents a comprehensive statistical analysis of the data collected during the inspections, leading to insightful conclusions regarding the observed best practices. **Chapter 10** presents the bibliographical references for Part II.

**Part III** presents the part of the study which investigated the durability of GFRP composites under various environmental conditions. **Chapter 11** provides an overview of the experimental program, including the materials selection and production process. The chapter also describes the physical and mechanical characterization methods used and presents the results of initial characterization tests for the selected materials. **Chapter 12** focuses on the effects of chemical ageing on pultruded GFRP composites; it includes a literature review, the description of the experimental program and then the presentation and discussion of results related to various physical and mechanical properties. **Chapter 13** investigates the impact of QUV accelerated and natural weathering on the durability of pultruded GFRP composites; the chapter also includes a literature review, the description of the experimental program and characterization techniques, and finishes with the presentation and discussion of results related to various physical and mechanical properties. **Chapter 14** presents the bibliographical references for Part III.

Finally, **Part IV** presents **chapter 15**, which summarizes the main conclusions that can be drawn from the research performed in this thesis and indicates future directions of research in this field.

## **2. General review of GFRP materials and structures**

### **2.1. Introductory remarks**

The use of conventional materials in the rehabilitation of civil infrastructure is often constrained due to a multitude of factors. These encompass rapid degradation within aggressive environments, limited compatibility of materials with existing structures, and a significant increase in weight when employing conventional materials, particularly steel, for rehabilitation. Considering these constraints, there arises a need to develop new materials and technologies capable of augmenting structural performance in a functional, efficient, and durable manner.

Glass fibre reinforced polymer (GFRP) profiles have emerged in infrastructure rehabilitation as a material with great potential. They have advantages such as high stiffness-to-weight and strength-to-weight ratios, low weight, durability in aggressive environments, resistance to fatigue and corrosion, electromagnetic transparency, electrical insulation, and the ability to produce any form. Additionally, according to Pritchard [I.07], the use of GFRP composite profiles can also be cost-effective compared to conventional materials, considering the benefits associated with their durability, reduced maintenance costs and increased lifespan, and lightness, which facilitates their application.

### **2.2. GFRP constituents**

Composite materials result from the macroscopic combination of, at least, two distinct materials that are interconnected through a finite interface. One of the constituents are the reinforcing fibres, which provide most of the stiffness and mechanical strength along their direction. The other main constituent is the polymeric matrix, which binds the different components and transfers the loads applied to the composite profile to the reinforcing fibres. The existence of a reinforcement material (fibres) distinguishes a composite material from a polymeric material. Fillers and additives are sometimes added to the matrix of composite materials in order to improve given characteristics, such as electromagnetic properties, electrical conductivity, and flammability, or, in case of fillers, simply to reduce costs [I.08].

#### **2.2.1. Fibres**

Fibres that can be used as constituents to impart mechanical strength and stiffness to composite materials can come from various sources, both natural and synthetic. In civil engineering, the fibres most frequently used are glass (G), aramid (A) (or Kevlar (K)), carbon (C) and, more recently, basalt (B). The choice of fibre type will depend on the assessment of environmental conditions, strength, stiffness, durability, and required cost [I.09].

In the application of FRP composite profiles as a structural material, the fibres are responsible for most of the mechanical properties. However, fibres are a constituent that, on its own, exhibits brittleness. When a member is subjected to an external load, the applied force is transferred to the fibres through the fibre-matrix interface. This highlights the importance of interaction among the different constituents of the composite material. The matrix plays a synergistic role in containing the spread of

fibre breaks and transferring the external load to various fibres, thus enhancing their resistance. It is therefore important to define the amount and orientation of fibres according to the type of structure and the loads it will be subjected to [I.10]. Of the fibres mentioned, glass fibres are the most widely used in construction, mainly due to their high strength and relatively low cost. Other advantages include temperature resistance, isotropic thermal expansion, good adhesion to polymer matrices, and good chemical resistance. However, they have a lower modulus of elasticity than other fibres and exhibit reduced resistance to moisture, fatigue, creep (rupture), and alkaline environments [I.11].

Various types of glass fibres are commercially available, including E, S, AR, and C fibres. C fibres present improved corrosion resistance, while AR fibres are characterized by improved resistance to alkalis. E and S fibres are the most widely used, especially the former. E fibres have high mechanical strength, chemical resistance, and good electrical insulation. S fibres have higher mechanical strength than E-fibres, but are more onerous [I.12].

Fibres are produced as continuous filaments and are usually applied in the form of rovings, yarns, or chopped fibres. Rovings are the continuous filaments that are not twisted, whereas yarns are the filaments that are twisted. In addition, these fibres and also short fibres can be further processed in order to produce mats, sheets and fabrics, with random or oriented reinforcement in several directions, such as chopped (short fibres) or continuous (long fibres) strand mats and fabrics (woven, stitched, braided and knitted). In some cases, reinforcing fibres can be combined through textile processes into a three-dimensional framework.

Lubricants and anti-static agents are generally applied to the fibres to protect them from damage during manufacturing and to improve their handling characteristics. Resinous binder agents are also applied to the fibres to help agglomerate the filaments into rovings and improve the adhesion between the fibres and the composite matrix. These products also protect the fibres from environmental degradation [I.13].

### **2.2.2. Polymeric matrix**

The polymeric matrix, in accordance with the reinforcing fibres, is a base component in the production of a composite material. It plays a crucial role in the material's strength and durability [I.08].

The first function of the matrix is to bind the reinforcing fibres and agglomerate the various constituents, giving rise to a composite material. Alongside this function, the matrix allows external stresses applied to the material to be distributed throughout the various fibres, increasing the material's resistance and ensuring that the fibres remain in their intended position. The involvement of the fibres also protects them from environmental degradation agents, enhances their resistance to abrasion, and prevents curvature due to compression stresses. When selecting the matrix for a given composite material, it is crucial to evaluate whether the matrix is chemically, thermally, and mechanically compatible with the reinforcing fibres [I.14].

The synthetic polymers used as the matrix of a composite material can be of two types: thermosetting or thermoplastic. Thermosetting polymers present a three-dimensional structure that results from a curing process, usually by the action of heat, which causes polymerization chemical

reactions. After the curing process, the material is in its final state, in the form of an insoluble and infusible product, meaning that due to the crosslinking experienced during the curing process, the material's state is not reversible. In the case of thermoplastic polymers, the material can alternate between a plastic and a rigid state when heated and cooled, respectively. Thermoplastic polymers have the advantage of being reprocessible, but due to their high viscosity, they do not allow for easy fibre impregnation and they do not enable the adhesion features that characterize thermosetting resins [I.15]; yet, they present higher resistance to impacts and micro-fractures, mainly due to their greater ductility and toughness.

Thermosetting polymers are the most widely used in the production of FRP composites, mainly due to their ability to adhere to and impregnate fibres, which allows for better stress transference and physical support against fibre instability under compression actions. This capacity is achieved at an intermediate polymerization level, corresponding to a reduced viscosity liquid state [I.12]. They also provide better thermal and chemical stability and lower shrinkage and relaxation. In the case of thermoplastic resins, the high degree of viscosity makes the manufacture of FRP composites challenging through a viable production system, particularly in combination with continuous fibres.

Among thermosetting polymers, unsaturated polyester and vinylester resins are the most widely used. Their main advantages are reduced viscosity, reduced curing time, dimensional stability, and low cost. They are also characterized by high chemical and electrical resistance and good mechanical performance [I.12]. Volume shrinkage during processing is a drawback as it can result in internal stresses that can lead to debonding at the fibre-matrix interface.

### **2.2.3. Fillers**

Filling materials (or "fillers") are inorganic constituents used without structural functionality and with the aim of improving given characteristics, such as fire reaction (due to their inorganic origin), material toughness, flow, thermal conductivity, and electromagnetic insulation. The use of filling materials increases the viscosity of the resin and reduces shrinkage during the curing process. As a result, it reduces the appearance of cracks in areas of discontinuity and in areas with a high resin content. Fillers also improve the chemical resistance and the resistance to environmental degradation agents. On the other hand, they negatively affect the mechanical resistance of the composite material, although they do favour an increase in stiffness [I.16]. Their application also has the advantage of reducing the costs of the final product and they can represent about 50% of the total weight of the matrix of a GFRP profile intended for non-structural purposes [I.15]. The most used filler substances are calcium carbonate, alumina, kaolin, and calcium sulphate. Alumina and calcium sulphate are generally used to reduce flammability and smoke production during a fire situation [I.11].

### **2.2.4. Additives**

Among the constituents of an FRP composite material, there are often additives aimed at improving its properties and facilitating processing. Used in small quantities, they are integrated into the final product based on the specific properties required for the matrix, the degradation agents to

which the material will be subject to, and the intended colour [I.10].

The most common objectives with the use of additives are to reduce shrinkage, to decrease the level of voids, and to reduce flammability and the production of toxic smoke in case of fire. By adding metal particles, it is possible to improve the electrical conductivity and to increase the electromagnetic interference by using conductive materials. In the opposite situation, when one aims at reducing the attraction of electrical charges that can cause fires, electric shocks, or attract dust, anti-static agents are used. The effects of ultraviolet radiation, such as loss of gloss, discolouration, cracking, and chalking, can be reduced by adding ultraviolet stabilizers (blockers). Polymer oxidation can be delayed or inhibited using antioxidants. The use of foam precursors promotes an increase in thermal insulation capacity and a reduction in shrinkage. In terms of aesthetics, it is also possible to achieve the desired colouration through the use of dyes [I.12].

### **2.2.5. The fibre-matrix interface in FRP composite materials**

An FRP composite material consists of a combination of a polymeric resin and reinforcing fibres, each with their own physical, chemical and mechanical properties. The fibre-matrix interface plays a crucial role in combining and establishing synergies between the properties of the constituents. Optimizing the connections at the fibre-matrix interface improves the performance of the composite material, particularly its mechanical characteristics, properties that the constituents (reinforcing fibres and matrix) could not achieve individually. Adhesion between the matrix and the fibres is, however, greatly influenced by hygrothermal effects and moisture diffusion, which can lead to chemical reactions and plasticization phenomena that affect the durability of the FRP composite material [I.17].

The main constituent contact area is another factor with a significant impact on the mechanical resistance of the FRP composite material. A larger interface area allows for better load transfer between the matrix and the reinforcing fibres and, consequently, it improves the mechanical resistance of the FRP material [I.17]. However, the resistance and stiffness of the fibre-matrix interface is also influenced by the angle between the applied loads and the fibres. The most favourable stiffness and resistance values at the interface are obtained when the directions of the loads and fibres coincide, and these values highly depend on the bonding area and connections established between the constituents of the FRP composite material [I.12].

The fibre-matrix interface, although not a constituent material of an FRP composite, can also be physically differentiated from the other constituent materials through the connections established between the reinforcing fibres and the matrix. In cases where strong connections are established, a finite zone is generated that establishes a continuity between the fibres and the matrix and has mechanical and physical characteristics intermediate to the two constituents [I.18]. For this reason and because the interface is an area of bonding between the matrix and the fibres, there are some characteristic impacts in this zone due to the main degradation agents, the loads applied to the FRP composite material, and the internal stresses that may arise as a result of these two reasons, and that affect the durability of the composite [I.17]. However, the interface is not always physically identifiable, particularly in cases where the connections between the constituents are weak [I.19].

In the studies carried out on FRP composite materials, several authors highlighted the role of the fibre-matrix interface, which, although not a distinct constituent, is becoming increasingly relevant due to its physical, mechanical, and chemical particularities, and the influence it has on the durability of the FRP composite material [I.17].

### **2.3. FRP production processes**

There are various production methods with specific attributes and suitability for the functionality of the composite material to be produced [I.14]. In the case of the production of profiles for structural applications, the pultrusion process is the most commonly used, due to its advantages and economic competitiveness [I.15]. Due to its ease of fabrication, moulding is the most common production method for gratings. It is worth referring that the manufacturing process has significant influence in the quality of produced composites, namely in the curing degree, the void content, and also in the quality of the impregnation of reinforcing fibres by the polymeric matrix, among other aspects.

#### **2.3.1. Pultrusion**

Pultrusion is a manufacturing process for composite materials. The process involves pulling a mixture of fibres and resins through a heated die to form a continuous, uniform profile. Pultrusion is widely used to produce FRP products with different thin-walled cross-sections, such as I-, H-, channels, angles, tubes and rods, for a variety of applications, including construction, transportation, and infrastructure.

The fibre reinforcement is mainly based on continuous and parallel fibres (rovings), which can be complemented with mats that provide transverse reinforcement. The use of surface veils (reinforcing mats that allow for a higher amount of superficial content of polymeric matrix) increases the environmental resistance of the composite [I.14].

The pultrusion manufacturing process [I.20] can be broken down into several steps:

- **Preparation:** In this step, the fibres and resin are prepared for the pultrusion process. The fibres are positioned in coils upstream the pultrusion line and the resins are mixed with any necessary additives, such as pigments or fillers.
- **Loading:** The fibres and resins are loaded into a machine, which typically consists of a pulling mechanism, a heating die, and a cooling system. The fibres are fed into the machine in a loose form, such as a mat or tow, and the resins are fed into the machine as a liquid (generally in an open bath system).
- **Heating:** The fibres and resins are pulled through a heated die, where the temperature is controlled to ensure proper curing of the resin. The die is designed to shape the profile of the final product, and the temperature and pressure conditions are optimized to ensure proper wetting of the fibres by the resin and curing.
- **Cooling:** After exiting the die, the composite profile is cooled to room temperature. This is done to solidify the resin and prevent warping or deformations in the final product.
- **Cutting:** The final composite profile is cut to the desired length by a moving saw at the end of

the pultrusion line.

- Finishing: The composite profile can be sanded or finished in any other way necessary to meet the desired specifications.

The main advantages of this method are the speed of profile production, combined with the economic competitiveness of reduced production and equipment costs compared to other manufacturing processes. It also allows for control of the quantity of fibres and their direction, ensuring high quality [I.21]. The automation of the process and constant production speed favour the uniformity of the profile, not only in terms of shape, but also of characteristics along the profile, allowing for the optimization of the efficiency of the constituents of the FRP composite material and the production of various types of sections [I.22]. Figure 2.01 shows a scheme of the pultrusion process for GFRP profiles.

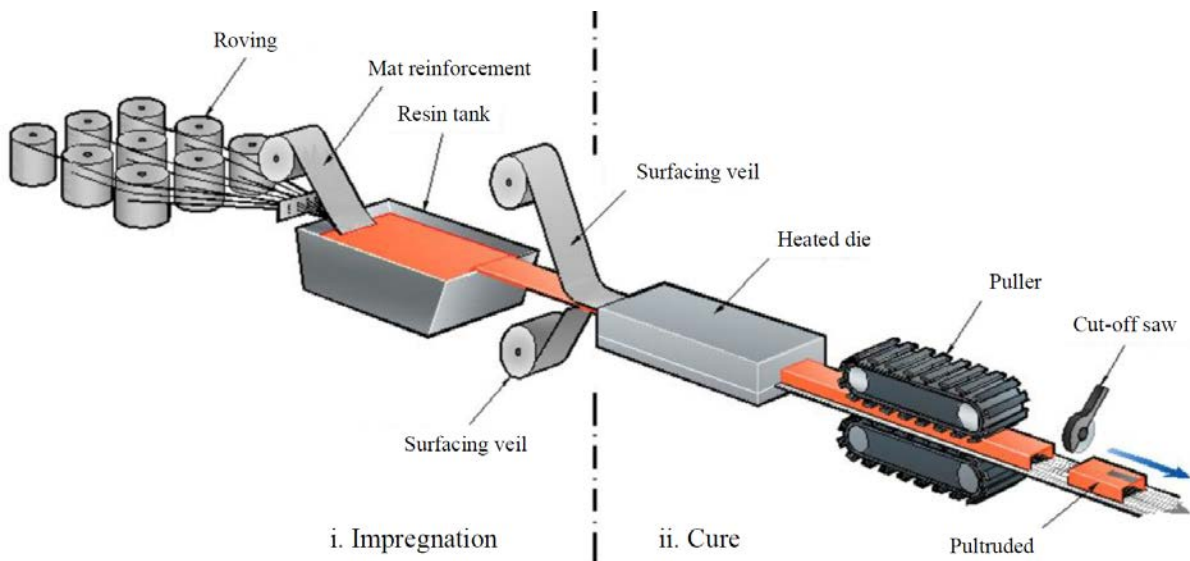
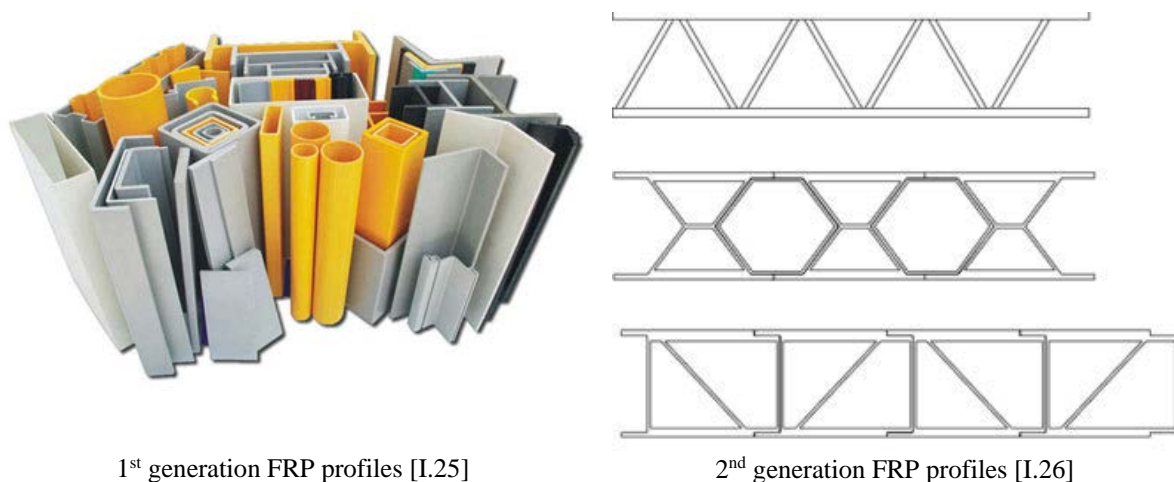


**Figure 2.01 - Pultrusion process used for manufacturing GFRP profiles, adapted from [I.23].**

The disadvantage of the pultrusion process is the restriction of production to profiles with a constant cross-section. Some innovative moulds have been developed that allow for slight changes in the profile cross-section, but these comprise limited variations with a smooth transition [I.14].

The pultrusion process may yield several different types of structural components: rebars, pre-stress tendons, sandwich panels and structural profiles. Regarding profiles, the so-called first-generation shapes started being developed in the 1950s and their structural sections initially mimicked those of metallic profiles, with thin-walled open sections (Figure 2.02 - left). One key reason for this choice was compatibility with existing traditional construction systems. In fact, many industries had well-established systems and infrastructure that had been designed to accommodate metallic profiles. By making FRP profiles with similar shapes, these could be easily integrated into these existing systems without requiring major modifications. Another reason is familiarity for engineers and designers. Engineers and designers who are familiar with metallic profiles can more easily design FRP profiles that have similar shapes. This can help to speed up the design process and reduce the learning curve (although their response presents notable differences). Aesthetics also plays a key role in the design of FRP profiles. In some applications, such as architectural and construction projects, the appearance of

the profiles is important. By making FRP profiles with similar shapes to metallic profiles, the appearance can be maintained while taking advantage of the other benefits of FRP composites. However, due to their inherent sensitivity to buckling issues (namely when constituted by glass fibres), the second generation of pultruded profiles was developed considering a multicellular panels structural principle, aiming at applications in floors and decks. With multicellular (closed-form) panels, the buckling issues are mitigated (Figure 2.02 - right). These FRP pultruded deck panels usually present lower depths than the first-generation profiles and thus they are more limited in terms of free span between supports. Transverse connections between adjacent panels are generally performed by mechanical interlock and/or adhesive bonding [I.24], as explained ahead.



1<sup>st</sup> generation FRP profiles [I.25]

2<sup>nd</sup> generation FRP profiles [I.26]

**Figure 2.02 - Examples of 1<sup>st</sup> and 2<sup>nd</sup> generation FRP profiles.**

### 2.3.2. Moulding

The production process of FRP moulded gratings involves several stages, and the materials used, as for pultrusion, play a crucial role in determining the quality of the final product. Typically, glass fibres are used as reinforcing material and they provide the gratings with their strength and stiffness, and the resin most often used is polyester.

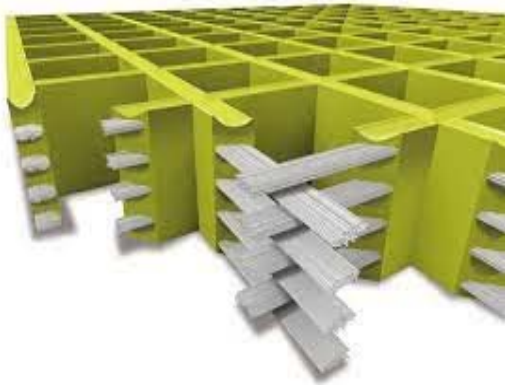
The first stage in the production process is the preparation of the mould. The mould is typically made of metal and it is designed to the specifications required for the particular grating product. Once the mould is ready, a gel coat is applied to the surface to provide a smooth finish and prevent any contamination of the resin during the casting process.

The next stage is the application of the reinforcing materials. The reinforcing materials used in FRP moulded gratings are usually glass fibre rovings - Figure 2.03 (left) presents a moulded grating cross-section with the typical fibre reinforcement orientations - or mats and woven fabrics, when a plate is applied on the grating, as shown in Figure 2.03 (right). These materials are laid into the mould in the desired pattern and orientation, and then a layer of resin is applied to saturate and wet out the reinforcing fibres.

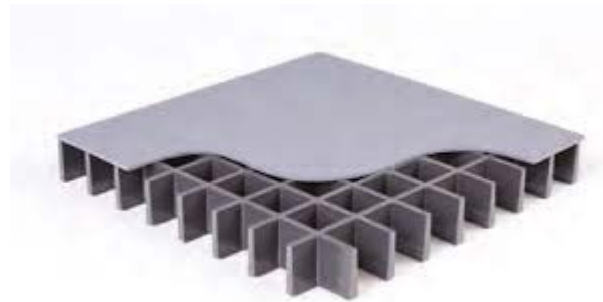
After the resin has been applied, the mould is placed in a controlled environment, such as a heated oven or a press, where the resin cures and the gratings take shape. The curing process is a critical stage in the production of FRP moulded gratings, as it determines the mechanical properties and final

quality of the product.

The final stage is the demoulding and post-processing of the gratings. The gratings are removed from the mould and any excess material is trimmed.



Fibre reinforcement orientations [I.27]



Moulded grating plate application [I.28]

**Figure 2.03 - Moulded grating cross-section reinforcement and moulded grating with plate reinforcement.**

## 2.4. FRP connection technology

FRP profiles and gratings can be connected to each other or to other structural members using several connection technologies, as shown in Figure 2.04. The choice of connection technology depends on factors such as the type of FRP material, the load requirements, the environmental conditions, and the desired performance.

Initially, bolted connections were used to connect pultruded GFRP profiles and gratings, mimicking metallic construction. However, it was soon found out that GFRP has a distinct material behaviour compared to steel [I.11]. In particular, it was found that high stress concentrations develop in the bolt-plate contact surface, which are more critical in the GFRP material as it does not present a ductile behaviour and is orthotropic, with much lower transverse and shear properties.

Although bonded connections are still rarely used in the construction industry, they distribute stresses more efficiently along the bonded surfaces, thus avoiding the stress concentrations induced by bolted connections. However, uncertainties regarding their long-term behaviour to in-service conditions, and the lack of design guidance have delayed their widespread use [I.05].

Hybrid connections, involving a combination of bolted and bonded connections, are another possible solution. Although the stiffness of hybrid connections is mainly provided by the adhesive, the surface-to-surface pressure applied by the bolts may prevent the effect of deficient bonding execution and increase bonding performance [I.11].

Interlock connections are another potential option, allowing pultruded GFRP panels to be connected with a grooving and friction mechanism, which can be complemented with bolting and/or bonding. This type of connection presents great potential as it allows for a very fast and easy execution at the construction site. However, despite being adequate from a conceptual point of view, this system presents significant technical limitations, such as high geometrical tolerance requirements [I.11].



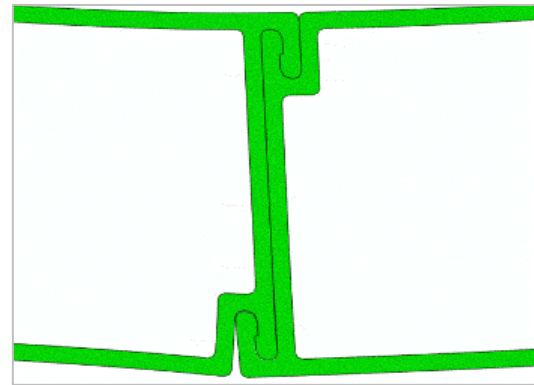
Bolted connection



Hybrid connection



Bolted connections with grips in gratings



Interlock connection between GFRP panels

**Figure 2.04 - Examples of different connection technology.**

## 2.5. Typical properties of pultruded GFRP profiles

The properties of pultruded GFRP profiles depend primarily on the characteristics and content of their constituent materials (e.g., fibre architecture and polymeric matrix) and also on the interaction between the fibres and the polymeric matrix. The structural use of GFRP composite materials is closely related to their mechanical and physical properties and durability, and the subsequent level of maintenance during service life.

Despite the different types of constituent materials and manufacturing processes, there are certain aspects that are common to all pultruded elements, namely their orthotropic behaviour, with higher mechanical properties in the longitudinal pultrusion direction. Comparing to the main competitors (steel profiles), GFRP profiles have relatively high longitudinal strength and low elastic moduli and shear properties. Table 2.01 presents the information reported in the technical specifications of GFRP producers and the European standard EN 13706-3 [I.29].

**Table 2.01 - Typical mechanical properties of pultruded GFRP profiles (standard shapes) from different pultrusion manufacturers and minimum values indicated in European standard EN 13706-3.**

	<i>C. Pultrusions</i>	<i>Fibreline</i>	<i>Top Glass</i>	<i>Alto<sup>(3)</sup></i>	<i>Strongwell</i>	<i>Summary</i>	<i>EN 13706-3<sup>(4)</sup></i>
<b>Material properties<sup>(1-2)</sup></b>							
Tensile strength 0° [MPa]	208-317	240	300-400	450	138-207	138-450	170-240
Tensile strength 90° [MPa]	52-82	50	20-30		48-69	20-82	30-50
Tensile modulus 0° [GPa]	17-29		22-26		12-18	12-29	17-23
Tensile modulus 90° [GPa]	6-10		7-8		5-7	5-10	5-7
Compressive strength 0° [MPa]	227-258	240	160-220	350	165-207	160-350	
Compressive strength 90° [MPa]	113-138	70	55-70		103-121	55-138	
Compressive modulus 0° [GPa]	21		15-18	23	12-18	12-23	
Compressive modulus 90° [GPa]	7-8		6-7		5-7	5-8	
Flexural strength 0° [MPa]	227-258	240	300-400	450	207-241	207-450	170-240
Flexural strength 90° [MPa]	76-86	100	60-70		69-124	60-300	70-100
Flexural modulus 0° [GPa]	11-14			20	8-11	8-20	
Flexural modulus 90° [GPa]	6-7		6-7		6-9	6-9	
Interlaminar shear strength 0° [MPa]	31	25			31	25-31	15-25
In-plane shear strength 0° [MPa]	48		20-30			20-48	
<b>Full-section properties</b>							
Modulus of Elasticity [GPa]	19-22	23-28	25	28	17-19	17-25	17-23
Shear modulus [GPa]	2.9	3.0	2.4-3.0		2.9	2.4-3.0	
<b>Physical properties</b>							
Barcol hardness [°B]	45		45-50	50	40-45	40-50	
Water absorption [% max]	0.6		0.4	0.15	0.6	0.2-0.6	
Density [g/cm <sup>3</sup> ]	1.66-1.93		1.80-2.00	1.8	1.66-1.94	1.65-2.10	
Thermal exp. coeff. 0° [10 <sup>-6</sup> /K]	8		9-11	11	7-8	5-15	
Thermal conductivity [W/m.K]	0.58		0.3-0.35		0.58	0.3-0.58	
<b>Electrical properties</b>							
Dielectric Str. 0° [kV/mm]	1.58		5-10		1.38	1.4-10	
Dielectric constant [50-60 Hz]	5.2		5			5	

(1) Properties are available in the manufacturers technical data sheets; (2) 0° and 90° refer to the longitudinal and transverse directions, respectively; (3) ALTO supplied the profiles for the present thesis; (4) EN 13706 range values correspond to E17 (lower grade) and E23 (upper grade) minimum material requirements.

## 2.6. FRP applications in civil engineering

As mentioned, FRP composite materials are being increasingly used in the construction industry as a structural alternative to traditional materials. These materials can be used in conjunction with or as a replacement of traditional materials, and they are already being used in four distinct areas: concrete reinforcement with FRP, rehabilitation and strengthening of existing structures, new hybrid structures, and entirely composite new structures.

When GFRP profiles are used in conjunction with traditional materials, the most common application is in concrete reinforcement, where they can be used as a substitute for steel rebars, or in the strengthening of concrete members or joints, as laminates or sheets (as shown in Figure 2.05 - top). While there are already several tested solutions that combine concrete with GFRP profiles, the practical

use of these solutions is still limited to niche markets, such as bridges. This is due to the corrosion resistance of GFRP profiles, which reduces maintenance and rehabilitation costs [I.12].

In the rehabilitation and/or strengthening of structures, as shown in Figure 2.05 (bottom), pultruded FRP profiles and CFRP strips are being used as an alternative to timber, steel, and reinforced concrete. For example, these components are being used to strengthen timber structural members and replace steel structures in chemically aggressive environments, and they are also being used to replace bridge decks.



Reinforced concrete slab with GFRP rebars [I.30]



Repair (and protection) of Vasco da Gama Bridge columns with CFRP sheets [I.31]



Strengthening of timber beams with CFRP laminates [I.32]



Metallic bridge with new FRP deck system [I.33]

**Figure 2.05 - FRP applications in Civil engineering.**

In Portugal, GFRP profiles and gratings are being used as an alternative material in various infrastructures, both alone and in combination with other materials. Their application is more common in chemically aggressive environments or in environments favourable to corrosion phenomena, as water and sewage treatment plants, mainly as secondary elements, such as stairs, handrails and floor gratings, as presented in Part II and section 13.4. Recently, two different hybrid bridge prototypes incorporating pultruded profiles were developed and studied at IST. Gonilha *et al.* [I.34] investigated the structural behaviour of a pedestrian bridge with pultruded GFRP girders and slabs made of steel fibre reinforced self-compacting concrete (SFRSCC) - Figure 2.06 (top left); this footbridge was installed in the city of Ovar. Sá *et al.* [I.35] studied the behaviour of a different pedestrian bridge concept comprising steel girders and second-generation pultruded GFRP multicellular decks; this footbridge was built in the city of Viseu - Figure 2.06 (top right).

The first all-composite pedestrian bridge, the Aberfeldy bridge (Figure 2.06 - bottom left), was built in the United Kingdom in 1992. It includes a GFRP deck suspended from GFRP towers by aramid

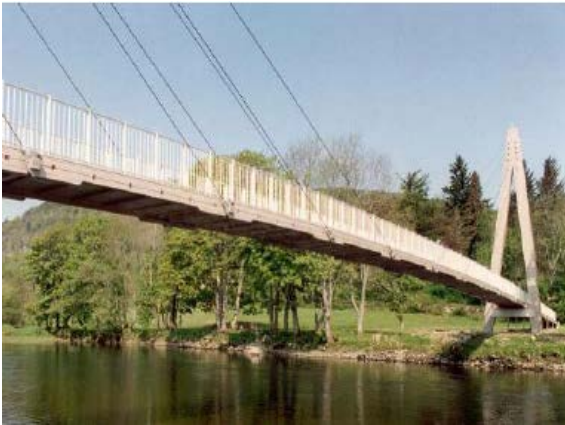
fibre reinforced polymer (AFRP) cables. Several new bridges were subsequently built using this composite material, including the Pontresina bridge (Switzerland, 1997), the Kolding bridge (Denmark, 1997), and the Lleida bridge (Spain, 2001). The Eyecatcher building (Figure 2.06 - bottom right), built in Switzerland in 1999, is a landmark in terms of building construction using FRP materials and is still the tallest residential/office building with composite structure.



Ovar pedestrian bridge with GFRP girders [I.36]



Viseu pedestrian bridge with GFRP deck [I.37]



Aberfeldy footbridge – United Kingdom [I.32]



Eyecatcher building – Switzerland [I.39]

**Figure 2.06 – Examples of FRP structures in civil engineering.**

### 3. Part I references

- [I.01] Bank, L.C., Arias, F.R., Yazdanbakhsh, A., Gentry, T.R., Al-Haddad, T., Chen, J.F., Morrow, R. (2018). “Concepts for reusing composite materials from decommissioned wind turbine blades in affordable housing”. *Recycling*, 3(1), 3.  
<https://doi.org/10.3390/recycling3010003>
- [I.02] Alabtah, F.G., Mahdi, E., Eliyan, F.F. (2021). “The use of fibre reinforced polymeric composites in pipelines: A review”. *Composite Structures*, 276, 114595.  
<https://doi.org/10.1016/j.compstruct.2021.114595>
- [I.03] Keller, T., Theodorou, N., Vassilopoulos, A., Castro, J. (2015). “Effect of natural weathering on durability of pultruded glass fibre-reinforced bridge and building structures”. *Journal of Composites for Construction*, 20(1), 04015025-1, 9.  
[https://doi.org/10.1061/\(ASCE\)CC.1943-5614.0000589](https://doi.org/10.1061/(ASCE)CC.1943-5614.0000589)
- [I.04] Yang, Y., Fahmy, M. F., Guan, S., Pan, Z., Zhan, Y., Zhao, T. (2020). “Properties and applications of FRP cable on long-span cable-supported bridges: A review”. *Composites Part B: Engineering*, 190, 107934.  
<https://doi.org/10.1016/j.compositesb.2020.107934>
- [I.05] Kharbari, V.M., Chin, J.W., Hunston, D., Benmokrane B., Juska, T., Morgan, R., Lesko, J.J., Sorathia, U., Reynaud D. (2003). “Durability gap analysis for fibre-reinforced polymer composites in civil infrastructure”. *Journal of Composites for Construction*, 7(3), 238-247.  
[https://doi.org/10.1061/\(ASCE\)1090-0268\(2003\)7:3\(238\)](https://doi.org/10.1061/(ASCE)1090-0268(2003)7:3(238))
- [I.06] CEN (2022) “CEN/TS 19101: 2022. Design of fibre-polymer composites.” Brussels, Belgium: European Committee for Standardization.
- [I.07] French, M.A., Pritchard, G. (1992). “Environmental stress corrosion of hybrid fibre composites”. *Composites Science and Technology*, 45(3), 257-263.  
[https://doi.org/10.1016/0266-3538\(92\)90087-J](https://doi.org/10.1016/0266-3538(92)90087-J)
- [I.08] Cabral-Fonseca, S. (2005). “Materiais compósitos de matriz polimérica reforçada com fibras usados na engenharia civil - Características e aplicações.”. Laboratório Nacional de Engenharia Civil, ICTM 35, Lisboa 2005.
- [I.09] Van Den Einde, L., Zhao, L., Seible, F. (2003). “Use of FRP composites in civil structural applications”. *Construction and Building Materials*, 17(6-7), 389-403.  
[https://doi.org/10.1016/S0950-0618\(03\)00040-0](https://doi.org/10.1016/S0950-0618(03)00040-0)
- [I.10] Groover, M.P. (2010). “Fundamentals of Modern Manufacturing: Materials. Processes and Systems”. 4<sup>th</sup> Ed., Lehigh University Willey.
- [I.11] Correia, J.R. (2008). “GFRP pultruded profiles in civil engineering: hybrid solutions, bonded connections and fire behaviour”. PhD Thesis, Instituto Superior Técnico, University of Lisbon, 2008.
- [I.12] Bank, L.C. (2006). “Composites for construction: structural design with FRP materials”. John Wiley & Sons, New Jersey.

- [I.13] Keller, T. (2002). "Overview of fibre-reinforced polymers in bridge construction". *Structural engineering international*, 12(2), 66-70.  
<https://doi.org/10.2749/101686602777965595>
- [I.14] Karbhari, V. M. (2007). "Chapter 2: Fabrication, quality and service-life issues for composites in civil engineering". In: *Durability of composites for civil structural applications*, pp. 13-30, Woodhead Publishing, Swanston.  
<https://doi.org/10.1533/9781845693565.1.13>
- [I.15] Correia, J. R. (2023). "Chapter 7: Pultrusion of advanced composites". In Bai, J., editor: *Advanced Fibre-Reinforced Polymer (FRP) Composites for Structural Applications*, pp. 137-177. Woodhead Publishing, Swanston.  
<https://doi.org/10.1016/B978-0-12-820346-0.00007-1>
- [I.16] Lackey, E., Vaughan, J.G., Patki, R. (2003). "Enhanced pultrusion using photocure to supplement standard thermal cure". In *Proceedings of the COMPOSITES 2003 - Convention and Trade Show Composites Fabricators Association Composites*, 1-3 October, Anaheim, USA.
- [I.17] Sethi, S., Ray, B.C. (2010). "Interface Assessment in Composite Materials". In the proceedings of RETMAC-2010 - International Conference on Recent Trends in Materials and Characterization, 14-15 February, Surathkal, India.
- [I.18] Chin, J.W., Nguyen, T., Aouadi, K. (1997). "Effects of environmental exposure on fibre-reinforced plastic (FRP) materials used in construction". *Journal of Composites, Technology and Research*, 19(4), 205-213.
- [I.19] Davis, A., Sims, D. (1983). "Weathering of polymers". Springer Science & Business Media, London.
- [I.20] Meyer, R. (1985). "Handbook of pultrusion technology". London: Chapman & Hall.  
<https://doi.org/10.1007/978-1-4684-7764-1>
- [I.21] Geier, M.H. (1994). "Quality handbook for composite materials". London: Chapman & Hall.
- [I.22] Keller, T. (1999). "Towards structural forms for composite fibre materials". *Structural Engineering International*, 9(4), 297-300.  
<https://doi.org/10.2749/101686699780481673>
- [I.23] Landesmann, A., Seruti, C.A., Batista, E.D.M. (2015). "Mechanical properties of glass fibre reinforced polymers members for structural applications". *Materials Research*, 18, 1372-1383.  
<https://doi.org/10.1590/1516-1439.044615>
- [I.24] Bakis, C. E., Bank, L. C., Brown, V., Cosenza, E., Davalos, J. F., Lesko, J. J., Triantafillou, T. C. (2002). "Fibre-reinforced polymer Composites for Construction - State-of-the-art review". *Journal of composites for construction*, 6(2), 73-87.  
[https://doi.org/10.1061/\(ASCE\)1090-0268\(2002\)6:2\(73\)](https://doi.org/10.1061/(ASCE)1090-0268(2002)6:2(73))
- [I.25] FIBREMAN - Fibreglass Channel and Structural Building Components  
<https://fibremen.ca/fibreglass-channel/> - visited on February 2023.

- [I.26] Liu, Z. (2007). “Testing and analysis of a fibre-reinforced polymer (FRP) bridge deck” PhD Thesis, Virginia Polytechnic Institute and State University, 2007
- [I.27] Strongwell product catalogue.  
<https://www.strongwell.com/wp-content/uploads/2017/01/Duradek-vs-Duragrate-Flyer.pdf> - visited on February 2023.
- [I.28] MTH Industrial Solutions - Grating Products  
<https://irp-cdn.multiscreensite.com/0f36ca8f/files/uploaded/Fibreglass%20%28FRP%29%20Grating%20Catalog.pdf> - visited on February 2023
- [I.29] CEN (2002) “Reinforced plastic composites - Specifications for pultruded profiles - Part 3: Specific requirements”. EN 13706-3. Brussels, Belgium: European Committee for Standardization.
- [I.30] Chen, R.H.L., Choi, J., GangaRao, H.V., Kopac, P.A. (2008) “Steel Versus GFRP Rebars?”. Public Roads - US Department of Transportation - Federal Highway Administration, 72(2), FHWA-HRT-08-006
- [I.31] S&P - Reforço de pilares de ponte - Viaduto Sul da Ponte Vasco da Gama - Lisboa, Portugal  
<https://www.sp-reinforcement.pt/pt-PT/projectos/reforco-de-pilares-de-ponte-viaduto-sul-da-ponte-vasco-da-gama-lisboa-portugal> - visited in February 2023
- [I.32] Kasal, B., Yan, L. (2021) “Fibre-Reinforced Polymers as Reinforcement for Timber Structural Elements”. In: Branco, J., Dietsch, P., Tannert, T., editors: Reinforcement of Timber Elements in Existing Structures. RILEM State-of-the-Art Reports, vol 33. Springer, Cham.  
[https://doi.org/10.1007/978-3-030-67794-7\\_4](https://doi.org/10.1007/978-3-030-67794-7_4)
- [I.33] CW - Composites World - New Bridge Deck Bests Early FRP Systems  
<https://www.compositesworld.com/articles/new-bridge-deck-bests-early-frp-systems> - visited on February 2023
- [I.34] Gonilha, J. A., Barros, J., Correia, J. R., Sena-Cruz, J., Branco, F. A., Ramos, L. F., Gonçalves, D., Alvim, M., Santos, T. (2014) “Static, dynamic and creep behaviour of a full-scale GFRP-SFRSCC hybrid footbridge”. Composite Structures, 118, 496-509.  
<https://doi.org/10.1016/j.compstruct.2014.08.009>
- [I.35] Sá, M.F., Gomes, A.M., Correia, J.R., Silvestre, N. (2011) “Creep behaviour of pultruded GFRP elements–Part 1: Literature review and experimental study”. Composite Structures, 93(10), 2450-2459.  
<https://doi.org/10.1016/j.compstruct.2011.04.013>
- [I.36] CIVITEST - Ovar inaugura ponte somente com 4 cm de espessura  
<https://www.civitest.pt/2016/03/15/ovar-inaugura-ponte-somente-com-4-cm-de-espessura/> - visited on February 2023
- [I.37] Sá, M., Correia, J., Gomes, A., Silvestre, N. (2019). “Ponte Pedonal Híbrida GFRP-aço do Parque da Feira S. Mateus, Viseu, Portugal”. Construção Magazine, vol. 90, pp. 38-39.
- [I.38] Rizkalla, S., Dawood, M., Shahawy, M. (2006) “FRP for transportation and civil engineering

infrastructure: reality and vision”. In Proceedings of the 85th annual transportation research board (TRB) meeting, Washington, DC.

- [I.39] Correia, J.R. (2015). “Chapter 11: Fibre-Reinforced Polymer (FRP) Composites”. In: Gonçalves, M., Margarido, F., editors: *Materials for Construction and Civil Engineering*, pp.501-566. Springer, Cham, Switzerland.  
[https://doi.org/10.1007/978-3-319-08236-3\\_11](https://doi.org/10.1007/978-3-319-08236-3_11)

# **Part II**

Development of an inspection, diagnosis and rehabilitation system for GFRP constructions



## Preamble

The use of an inspection, diagnosis and rehabilitation system can influence decision-making concerning the design and maintenance operations of structural and non-structural elements at every stage, from design and production to the service stage.

An inspection system can assist in the detection, assessment and prevention of the most common types of anomalies that can occur in any given construction element.

This second part of the thesis presents the development of such a system for fibre reinforced polymer (FRP) constructions. With the development of this system, the most common anomalies are described, and the most suitable diagnosis and rehabilitation techniques are allocated to each anomaly.

The validation of the inspection system was based on an extensive field survey of existing FRP constructions, under real service life conditions. Such a survey also provided a better understanding of the short- and long-term behaviour of FRP construction elements, namely through the data analysis of the information gathered.

The work presented in this part resulted in the following publications:

- Castelo, A., Correia, J. R., Cabral-Fonseca, S., & de Brito, J. (2020). Inspection, diagnosis and rehabilitation system for all-fibre-reinforced polymer constructions. *Construction and Building Materials*, 253, 119160.  
<https://doi.org/10.1016/j.conbuildmat.2020.119160>
- Castelo, A., Correia, J. R., Cabral-Fonseca, S., & de Brito, J. (2020) “In-Service Performance of Fibre-Reinforced Polymer Constructions Used in Water and Sewage Treatment Plants”. *Journal of Performance of Constructed Facilities*, 34(4), 04020059.  
[https://doi.org/10.1061/\(ASCE\)CF.1943-5509.0001449](https://doi.org/10.1061/(ASCE)CF.1943-5509.0001449).



## **4. Characterization of the inspection, diagnosis and rehabilitation system proposed**

### **4.1. Introductory remarks**

This chapter first presents a state-of-the-art review of inspection systems for fibre reinforced polymer (FRP) elements, comprising different materials (e.g. fibres, resins) and manufacturing techniques (e.g. pultrusion, filament winding), as well as the main functional requirements GFRP (glass fibre reinforced polymer) elements must fulfil when applied in the construction sector. Next, the chapter presents the outline of the inspection, diagnosis and rehabilitation system proposed within this thesis.

It is worth referring that in the scope of this study, two main types of GFRP elements used in civil engineering applications were investigated: pultruded profiles and moulded gratings. Initially, the use of these components in primary structural applications was restricted to pilot applications or research projects, but they are now gradually finding their own way in mainstream construction. Even though most of the applications of GFRP profiles in civil construction are still related with non-structural elements or secondary structures (e.g. roof and decking structures [II.01], handrail frames), some applications can be found in full-scale primary structures (e.g. pedestrian [II.02] and vehicular [II.03] bridges, emergency housing [II.04] and current buildings [II.05]).

The field study conducted in the frame of this thesis was done in collaboration with two composites manufacturing companies (ALTO and STEP) and with a primary end-user of composite materials, EPAL, a Portuguese public water management company that has a vast number of GFRP constructions often exposed to aggressive environments. The field inspections included a thorough survey of GFRP constructions located all over the country, with different ages and located in different types of environments (e.g. coastal areas, chemically aggressive environments, outdoor exposure, and water immersion). These constructions were the object of detailed inspections (visual observations complemented with field tests) to identify their anomalies at different levels - material, structural element and connections - as well as the corresponding causes. The most suitable diagnosis and rehabilitation techniques and maintenance operations were suggested and registered.

### **4.2. State-of-the-art review of inspection, diagnosis and rehabilitation systems**

For civil engineering constructions, several diagnosis and inspection systems have been developed for different types of structural and non-structural elements. At IST, several inspection systems have been developed for various building construction components, such as concrete members [II.06], ceramic tiling [II.07], coatings for industrial floors [II.08], and exterior claddings of pitched roofs [II.09]. Such systems are not yet available for FRP composite materials, due to their recent applications and specific characteristics.

In this regard, most of the information for FRP materials is available from other applications, such

as aeronautical and mechanical engineering, in which these materials have a much longer history of use and where a much better understanding of their behaviour exists, namely when compared to civil engineering.

Apart from the European Standard EN 13706 [I.01] and the American Standards ASTM D4385-02 (for pultruded products) [II.11], ASTM D2563-R02 (for GFRP laminates) [II.12] and ASTM D2562-R02 (for moulded FRP's) [II.13], there is scarce information available in the technical and scientific literature on the type of anomalies/defects that can occur in GFRP elements, especially throughout their service life.

EN 13706 [I.01], which specifies some of the main properties that pultruded GFRP components must present and mentions some of the anomalies that may occur at the manufacturing stage (presented in Table 4.01), is only focused on the production stage of FRP materials and thus lacks the anomalies that occur during the service life of the materials, in particular the ones associated with the exposure to environmental agents. For some of the anomalies, this standard also presents the recommended tolerances for production acceptance.

The above-mentioned ASTM standards [II.11]-[II.13] mention some of the anomalies that may occur at the production stage (presented in Table 4.01); even though each standard is specific a given type of manufacturing process, they all present a very similar list of anomalies that can be detected at the production stage. These standards specify some of the acceptance criteria upon fabrication for three different levels of product quality defined on the design of the product. Some examples of these anomalies are presented in Figure 4.01.

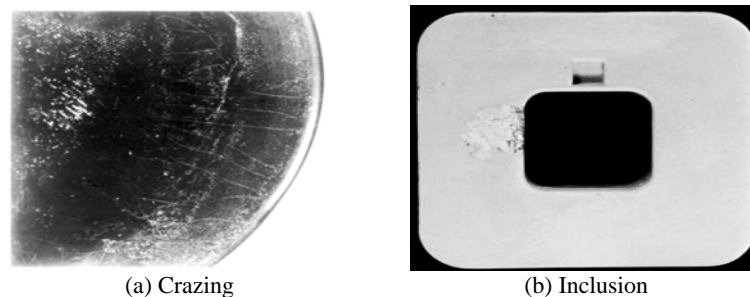


**Figure 4.01 - Examples of the anomalies presented in ASTM D2563-R02, adapted from [II.12].**

The 19-year-old Pontresina GFRP-truss footbridge, in Switzerland [II.02],[II.14], has been thoroughly studied, inspected and tested during its service life. Such field and laboratory studies allowed obtaining extensive knowledge on the behaviour of the GFRP materials used in that specific application (and structural system). These studies allowed the determination of some of the anomalies and their progression between consecutive surveys, as well as the identification of some of the rehabilitation techniques that can be applied in GFRP constructions.

During a field inspection of the Pontresina footbridge conducted in 2005 [II.14], anomalies were classified in five basic damage categories: crushing of flanges, longitudinal cracks in the profiles, fibre blooming on exposed surfaces, surface degradation of upper cut ends of shapes, and localized surface damages. Some examples of these anomalies are presented in Figure 4.02. The only diagnosis technique applied in the inspection of the footbridge was visual inspection. Several rehabilitation techniques were applied in order to minimize and mitigate the anomalies, in most cases simple methods, such as adding bonded GFRP sections and plates to the bridge local crushing damage and by sealing the unprotected

surfaces and cracks. Examples of such repair techniques are presented in Figure 4.03. The inspection of this case study showed that durability is primarily affected by inappropriate constructive detailing and manufacturing (as in reinforced concrete and steel bridges).

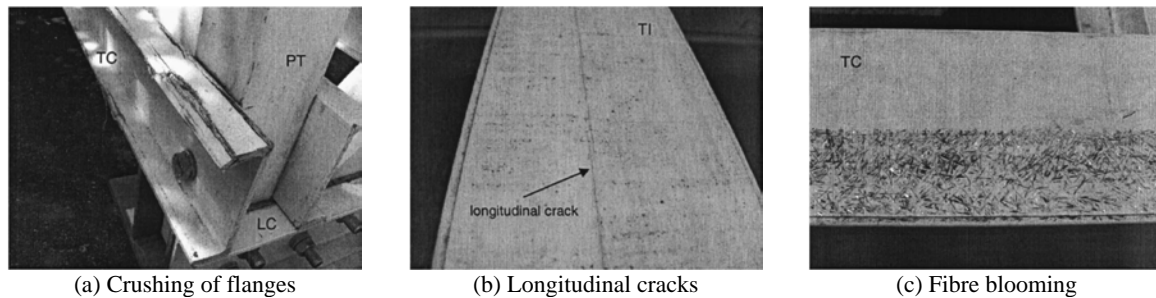


**Figure 4.02 - Examples of the anomalies detected in the Pontresina footbridge [II.14].**

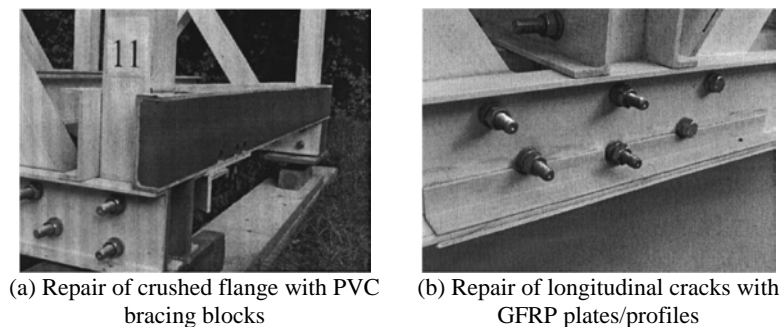


**Figure 4.03 - Examples of the repair techniques applied in the Pontresina footbridge [II.14].**

In the Pontresina footbridge inspection performed in 2014 [II.02], the anomalies detected were different and were classified into new four main categories: fibre blooming, longitudinal cracks in profiles, cracks in adhesive bonds and crushes from impact. In this inspection, fibre blooming was classified in three categories in accordance to its severity level, a new feature compared to the 2005 inspection. The only inspection technique applied was still visual inspection. The rehabilitation techniques applied in the 2005 inspection seemed to be intact and no debonding of the repair profiles had occurred. However, all the repair profiles seemed to have developed fibre blooming, due to lack of the protecting surface veil and absence of any surface protection.

In Norway [II.15], guidelines for non-destructive techniques (NDT) for GFRP oil pipe systems and tanks were published and are already implemented. This document indicates the NDT's that are usually applied for these materials in civil engineering applications, as well as the most common anomalies that can be found during inspection of different structural locations. In this inspection system, the elements to be inspected are produced with different techniques (filament winding, centrifugal casting, continuous winding and hand lay-up) compared to the ones more often used for civil engineering applications. However, the type of anomalies included in such guidelines are a relevant source for the inspection system developed in this thesis. These guidelines divided the possible anomalies in four stages in accordance to their life stage: (i) manufacturing; (ii) prefabrication and receiving; (iii) design; and (iv) installation and commissioning. These guidelines considered the anomalies presented in Table 4.01. Some examples are presented in Figure 4.04: cracks (Figure 4.04 (a)), fracture (Figure 4.04 (b)), lack of adhesive (Figure 4.04 (c)). For each of the

anomalies, the most suitable NDT technique is presented. This study considered visual inspection as the main NDT technique and the remaining NDT's considered are presented in Table 4.02

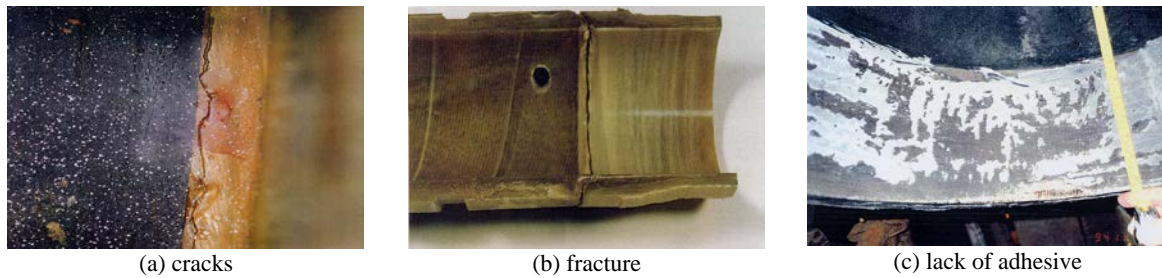


**Figure 4.04 - Examples of the anomalies presented in [II.15].**

Since this system assigns potential anomalies to specific life stages, it becomes easier for the manufacturer, end user and/or inspector to identify the most critical/common anomalies that can be detected in each of the elements during the inspection.

In the USA, the National Cooperative Research Program developed a comprehensive report [II.16], which involved the inspection of hundreds of FRP bridge decks in-service. This report presents some of the most commonly detected anomalies in FRP materials used in bridge decks and recommends the inspection techniques that should be applied to each of the anomalies. The division of the anomalies was made by areas in which they may occur (e.g. panel-to-panel connections, bolted connections, approach joints, edges and closeouts). This anomaly sorting system can be useful when inspecting a construction by areas. However, when inspecting an entire construction, this system becomes more complicated and repetitive, since most of the anomalies can occur in more than one specific area. The inspection methods used in this report are NDT's (presented in Table 4.02) and are considered easy to apply in-situ.

In the USA, the FRP technology group of a chemical company reported [II.17] the most common anomalies found in laminated GFRP elements, indicating their description and possible causes, although not specifying the end-use. This study presents six occasions in which FRP equipment should be inspected: (i) during fabrication; (ii) after fabrication; (iii) after transportation; (iv) after installation; (v) after a specified period of use; and (vi) when changing type of use. The anomalies presented in this study, listed in Table 4.01, were not categorized.

When analysing the data presented in Table 4.01, only one anomaly is presented in every study - cracks. There are also other anomalies that are mentioned in more than 50% of the studies considered: blister/pimples, chips, crazing, delamination, inclusions, dry spots, resin pockets, burns, scratches, voids and wrinkles. There are 15 anomalies mentioned only once, however some are specific to different manufacturing processes (e.g. wormholes, black marking) and others only occur in the-service stage of the structure (e.g. corrosion, excess adhesive) that are not mentioned in most of studies presented.

The anomalies collected in different references were a starting point for the development of the inspection system presented in chapter 4. However, the data collected had to be complemented with information from end-users and a preliminary set of inspections to identify anomalies that are not considered in any of the studies presented before.

**Table 4.01 - List of anomalies suggested for FRP elements in different studies.**

EN 13706 [I.01]	ASTM D4385-02 [II.11]	ASTM D2563-R02 [II.12]	ASTM D2562-R02 [II.13]	Pontresina Bridge [II.02],[II.14]	Norway guideline [II.15]	NCRP [II.16]	Dow chemical company [II.17]
Blister	Blister Black marking	Blister/Pimple	Blister/pimple			Blister	Blister
Crack Crater	Crack Chip/crater Crazing	Crack Chip/pit Crazing	Crack/fracture Chip/pit Crazing	Crack	Crack/fracture Chip/pit Crazing	Crack	Crack Crater Crazing
Delamination Die parting line	Delamination Die parting line Discolouration	Delamination		Crushing	Delamination		Delamination
Dullness Exposed underlayer	Under-cure blooming Exposed underlayer					Discolouration	
Fibre prominence	Fibre bridging Fibre blooming Fibre prominence	Lack of fill out Fisheye		Fibre blooming	Excess/lack of adhesive	Fibre blooming	Fisheye
Folded reinforcement Fracture	Folded reinforcement Fracture				Uneven wall thickness		
Grooving Inclusion	Glassiness Grooving Inclusion	Inclusion	Inclusion		Geometrical imperfections		
Internal dry fibre Internal shrinking cracks	Dry fibre Internal shrinking cracks	Dry spot Shrink mark Pre-gel	Dry spot		Inclusion Incorrect dimensions Dry spots		Dry spots
Resin rich area Saw burn Scale Stop mark	Reinforcement distortion Resin rich area Saw burn/burn Scale Stop mark Scuffing	Resin pocket/resin rich edge Burned Orange peel	Resin pocket Orange peel		Lack of fibres Burn		Resin pocket Burn
Under cure Voids	Insufficient cure Voids	Air bubble/voids	Air bubble	Superficial damages Surface degradation	Wear scratch Impact damage Inadequate curing Voids	Scratches	Scratches
Wrinkle depression	Wire brush surface Wrinkle depression	Wrinkles Wormhole				Wrinkles	Wrinkles

Regarding the inspection techniques [II.17]-[II.21], several studies indicate the most suitable NDT's that can be applied in GFRP elements (presented in Table 4.02). Nevertheless, some of these studies were carried out for specific applications different from those of the construction sector (aerospace, mechanic and naval engineering). Therefore, the scope of some of these techniques concern specific anomalies, aiming at increasing the manufacturing quality control, which sometimes can be considered too strict for the construction sector.

When analysing the data presented in Table 4.02, none of the presented NDT's is considered in all studies. Visual inspection is the NDT that is more often considered in these studies. Acoustic emission, radiography, thermography and ultrasonic testing are present in more than 63% of the studies considered. Six of the techniques are only considered in one of the studies presented, which can be related with the specificities of the applications of the corresponding industries.

It is worth referring other studies regarding anomalies and inspection techniques for FRP elements used in structural strengthening of existing structures, namely previous studies focused on the bonding/bolting of FRP plates in the retrofitting of reinforced concrete elements (beams/slabs) [II.22]-[II.24]. These studies present the anomalies that can occur by retrofitting elements with FRP components. However, in these studies the FRP materials applied (carbon fibres and epoxy resins) differ from the ones commonly used in all-FRP constructions (glass fibres and polyester/vinylester resins). Yet, some of their conclusions can be related and applied in the development of this inspection system.

**Table 4.02 - List of non-destructive inspection techniques suggested for FRP elements in different studies.**

Pontresina bridge [II.02],[II.14]	Norway guideline [II.15]	NCRP [II.16]	Dow chemical company [II.17]	Amory & Wang [II.18]	Fowler et al. [II.19]	Bossi & Giurgiutiu [II.20]	Tappi Association [II.21]
	Acoustic emission Barcol hardness	Acoustic testing	Acoustic emission Barcol hardness	Acoustic emission	Acoustic emission		
						Bond inspection Dye penetrant Electromagnetic techniques Embedded sensor	
		Modal analysis		Holography			
	Pressure test	Load testing			Mechanical vibration Optical methods		
	Radiography	Radiography		Radiography	Radiography	Radiography Shearography Tap testing	Radiography
	Thermography	Tap testing Thermal testing		Video thermography	Thermography	Thermography	Thermography
	Ultrasonic	Ultrasonic testing		Ultrasonic	Ultrasounds	Ultrasonic testing Visual inspection	Ultrasonic
Visual inspection	Visual inspection	Visual inspection	Visual inspection		Visual inspection	Visual inspection	Visual inspection

### 4.3. Normative and functional requirements

As in any constructive system, material or structure, there are a few basic requirements that structural and non-structural GFRP elements must fulfil to guarantee its adequate use. Some of these requirements are common for all the materials used in the construction sector (e.g. fire resistance) and even though there are scarce studies in this subject specifically related to GFRP constructions [I.01], the applicable requirements can be drawn/adapted from different materials [II.25], [II.26]. In this thesis, these requirements were divided into five groups, as presented in Table 4.03: safety, functional, durability, economic and other.

These functional requirements involve meeting different demands and maintaining a satisfactory performance during service life, with respect to the initial design. Therefore, the development of the current study is very important to guarantee that GFRP constructions appropriately satisfy those requirements and avoid the occurrence of anomalies, maintaining a good performance.

**Table 4.03 - Functional requirements for GFRP elements.**

Safety requirements	Mechanical resistance to permanent loads and live loads	
	Fire safety	Combustibility
		Flammability
		Velocity of flame propagation
		Heat potential of materials
		Opacity and toxicity of gases and fumes
	Resistance to normal use	Fire resistance
		Punching
Environmental agents		
Accidental impact		
Functional requirements	Circulation comfort	Floor horizontality and flatness
		Floor resilience
	Visual comfort	Straightness of the edges
		Absence of superficial defects
		Flatness and horizontality of the floor
		Colour uniformity
	Gloss uniformity	
Tactile comfort	Absence of physiological or tactile discomfort	
Durability requirements	Performance maintenance	Mechanical resistance
		Dimensional stability
		Chemical resistance
Cleaning, maintenance and repair		
Economic requirements	Global costs	Construction costs
		Cleaning, maintenance and repair costs
Other requirements	Geometrical stability	
	Constructive process	
	Sustainability	

### 4.4. Outline of proposed system for GFRP constructions

Based on the information gathered in the literature review and that provided by the manufacturing companies and end-user industries, an inspection, diagnosis and rehabilitation system was developed within this thesis. An initial version of the inspection system was used for the first applications of the field study. After a preliminary test, the system was modified/improved to incorporate the new information gathered. At the end of the field study, the system was validated

through data analysis of the information gathered.

The flow chart presented in Figure 4.05 illustrates the structure of the inspection, diagnosis and rehabilitation system. The system is composed of four groups of entities (anomalies, probable causes, diagnosis methods and rehabilitation techniques). For each of these groups, a classification system is proposed to facilitate the application of the system. The objective of this system is to correlate the classification systems and assist in the inspection of existing structures, as well as in the design of new GFRP constructions and in the rehabilitation of existing ones.

The four classification systems are related through correlation matrixes that were developed for the following subject pairs: (i) anomalies-causes, which correlates the list of anomalies with the list of probable causes; (ii) inter-anomalies, which correlates the occurrence of each given anomaly with other simultaneous anomalies; (iii) anomalies-diagnosis techniques, which correlates the list of anomalies with the list of the inspection and diagnosis techniques; and (iv) anomalies-rehabilitation techniques, which correlates the list of anomalies with the most suitable rehabilitation techniques that can be applied to these materials. Also, a detailed form was created containing the information gathered for each anomaly, diagnosis and rehabilitation technique.

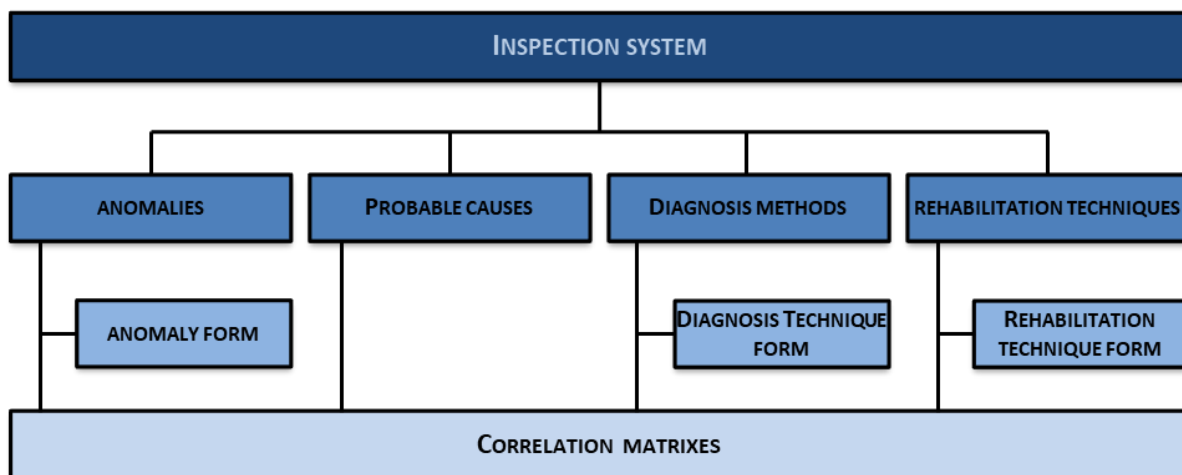


**Figure 4.05 - Proposed organization of the inspection and diagnosis system of GFRP elements.**

#### **4.5. Concluding remarks**

Although ensuring an improved performance compared to traditional materials, GFRP elements may exhibit anomalies and might require maintenance or rehabilitation at different stages of their service life. Even though GFRP structural elements can be found in relatively old structures (10-20 years), there is still no comprehensive and validated classification of the most relevant anomalies/defects that can occur in this type of constructions, from production to structural use (service stage), as well as the corresponding most probable causes and possible consequences.

In this regard, most of the information on FRP materials is available from other applications, such as aeronautical and mechanical engineering, in which these materials have a much longer history of use and where a much better understanding about their behaviour was obtained, namely when compared to civil engineering applications.

Normative and functional requirements are a subject that should be considered at different stages of the construction process (design, fabrication, installation and use). However, with the occurrence of anomalies in most of the existing GFRP constructions, the requirements presented in Table 4.03 may not be fulfilled, in particular the functional and durability requirements, mostly due to the lack of knowledge about the long-term behaviour of these materials. To fulfil the durability requirements, designers and users must consider the materials' behaviour when subjected to different environmental conditions and the associated degradation. However, in this regard, many degradation phenomena underwent by GFRP materials are still not fully understood; in fact, many recent studies have been addressing the long-term durability of GFRP materials under different types of environmental exposure, both accelerated and natural (e.g. [II.27]-[II.29]).

The outline of the inspection, diagnosis and rehabilitation system presented herein is coherent with other systems previously developed at IST for other structural and non-structural elements [II.06]-[II.09].



## **5. Anomalies in GFRP constructions**

### **5.1. Introductory remarks**

Despite the current and growing concern about the quality and durability of constructions, when a given structure is in use some of its requirements may not be met and some anomalies may occur. These can be more or less severe and should be eliminated during routine maintenance operations. Ignoring the occurrence of a given anomaly can lead to its further development, the occurrence of other anomalies and the degradation of the construction.

With the development of an inspection system, in order to optimize and facilitate the inspection and diagnosis of GFRP constructions, it becomes essential to establish a classification system that gathers all the scattered information presented in other studies and reports, leading to a standardized designation and organization of the anomalies that may occur.

In this context, this chapter presents a characterization of the anomalies likely to occur in GFRP constructions, in terms of their visual aspect and possible consequences. This chapter also proposes a classification system for the most probable causes (direct and indirect) of those anomalies, which are in the origin of their occurrence. The anomalies-causes association is presented in a correlation matrix, which also helps determining the correlation values between the occurrence of multiple anomalies. At the end of the chapter, an example of an anomaly form is presented. The anomaly forms of all anomalies identified as being potentially relevant are included in Appendix I.

### **5.2. Classification system of the anomalies**

After the analysis of the literature, of different case studies and based on the information provided by manufacturing and construction companies working with GFRP constructions, a preliminary list of anomalies was defined. This list of anomalies was established based only on the visual aspect that each anomaly presents. This criterion allows an anomaly to be detected in several zones of a GFRP structure (surface and/or bulk of the element, structure, structural element and connection), differing only on the possible causes that led to the development of the anomaly.

To allow for an easier application of the inspection system, the anomalies were classified in two groups (Table 5.01). These groups were created with the purpose of classifying the anomalies according to the properties affected and the changes in visual appearance they cause. The two groups created for this purpose are (i) mechanical and (ii) non-mechanical anomalies, depending on whether the anomalies affect the mechanical performance of a given GFRP element.

Non-mechanical anomalies (A.N-Me) are the ones that do not affect the mechanical properties of the material, structural element or the connections between members, and are generally detected at the surface of the element. Although they do not immediately affect the mechanical properties of the GFRP material, these anomalies can create the necessary conditions for the development of mechanical anomalies at a further stage of degradation. In order to determine whether an anomaly affects the mechanical performance, an advanced stage of development of the anomaly is considered in the analysis.

If, in an advanced stage of development, the effect of the anomaly is considered not to affect the mechanical performance of the element, then the anomaly is categorized as non-mechanical.

Mechanical anomalies (A.Me) are the ones that have the potential to affect the mechanical properties of the material, structural element or connections. Mechanical anomalies resulting from the production stage (some of which are addressed in EN 13706 [I.01]) should have already been discarded at the quality control system of production (factory) or at installation (on-site). Thus, anomalies with these origins should not occur during the in-service stage of GFRP constructions. The inclusion of these anomalies in this classification system is therefore also part of a quality control perspective for both producers and users.

**Table 5.01 - Proposed classification system for anomalies in GFRP elements.**

<b>ANOMALIES IN GFRP ELEMENTS</b>		
<b>#</b>	<b>NON-MECHANICAL (A.N-Me)</b>	<b>MECHANICAL (A.Me)</b>
01	Biological colonization	Corrosion of metallic elements
02	Discolouration/loss of gloss	Cracking
03	Fibre blooming	Crushing
04	Inclusions	Debonding
05	Stains	Delamination
06	Superficial marks	Excessive deflection
07	Wear damage	Geometrical imperfections
08	Debris accumulation	Indentation/perforation
09		Incorrect curing of adhesive
10		Incorrect curing of resin
11		Loose connections
12		Member failure
13		Voids

### **5.3. Characterization of the anomalies**

#### **5.3.1. A.N-Me.01 - Biological colonization**

This anomaly consists of the appearance of biological matter (plants, fungi, animals) on the surface of GFRP elements. It usually occurs in areas with high humidity or permanently immersed and in constructions with lack of maintenance. The development of this anomaly involves the degradation of the aesthetical appearance and, due to moisture accumulation, it may eventually cause the reduction of mechanical performance. If not repaired, the development of this anomaly may possibly affect significant areas of GFRP elements that will become covered with the biological matter.

Figure 5.01 presents three examples of this anomaly: Figure 5.01(a) illustrates the moss growth at the edges of a moulded grating, mostly due to the accumulation of water and small debris in that area; Figure 5.01 (b) shows a nest of wasps inside a pultruded profile; and Figure 5.01(c) shows the development of lichens at the surface of a profile.

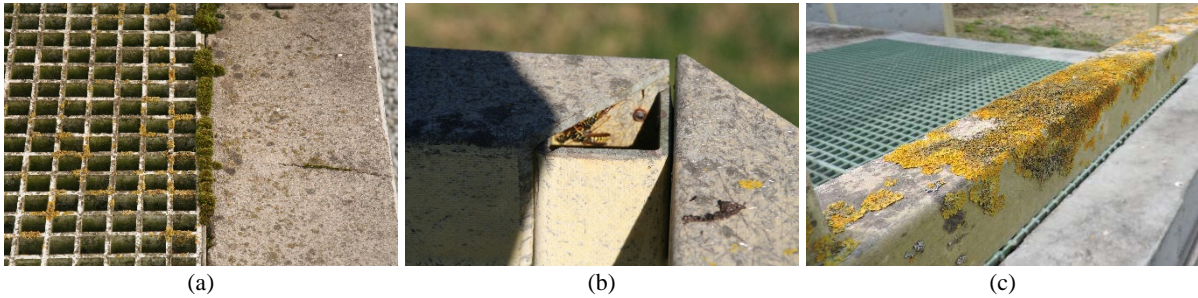


**Figure 5.01 - Examples of the A-N.Me.01 anomaly - biological colonization.**

### **5.3.2. A.N-Me.02 - Discolouration/loss of gloss**

This anomaly is related with the degradation of the surface layer of the polymeric matrix, causing a change of colour and brightness at the surface of the element. Even though it is usually associated with exposure of the elements to solar radiation (in particular UV radiation, which usually affects only a few microns of material next to the surface [II.29]), it may also occur when the elements are exposed to wet and dry cycles, permanent immersion [II.27] and/or exposure to saline or chemical environments.

Another reason for the occurrence of this anomaly is related with incorrect formulation, mixing or curing of the matrix of the GFRP element. In this situation, the anomaly should have been detected at previous stages, rather than during the service stage, namely in the scope of quality control procedures during production and installation.

Figure 5.02 presents two examples of this anomaly. In both cases, the degradation was caused by exposure of the elements to the exterior environmental agents, namely rain and UV radiation.

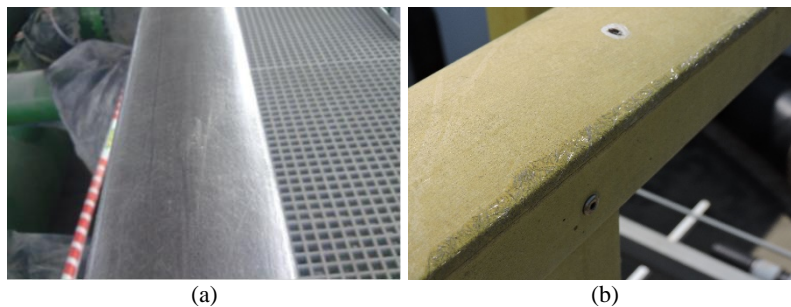


**Figure 5.02 - Examples of the A-N.Me.02 anomaly - discolouration/loss of gloss.**

### **5.3.3. A.N-Me.03 - Fibre blooming**

This anomaly is strictly related with the occurrence of discolouration/loss of gloss, described in the preceding section. The fibre blooming phenomenon consists of the appearance at the elements' surface of the inner fibres of the cross-section (those located closer to the surface), caused by the degradation of the surface layer of the polymer matrix. This anomaly is usually associated with exposure to UV radiation or chemically aggressive environments.

Figure 5.03 presents four examples of this anomaly: Figure 5.03(a) shows the fibre blooming phenomenon due to UV exposure on the lateral side of a moulded grating; Figure 5.03(b) shows fibre blooming on the longitudinal fibres of a moulded grating after the loss of a superficial layer of the element; Figure 5.03(c) illustrates fibre blooming at the top surface of a hand-rail due to UV exposure;

and Figure 5.03(d) shows fibre blooming along part of the section of a GFRP profile where the surface veil was misaligned during the production process.

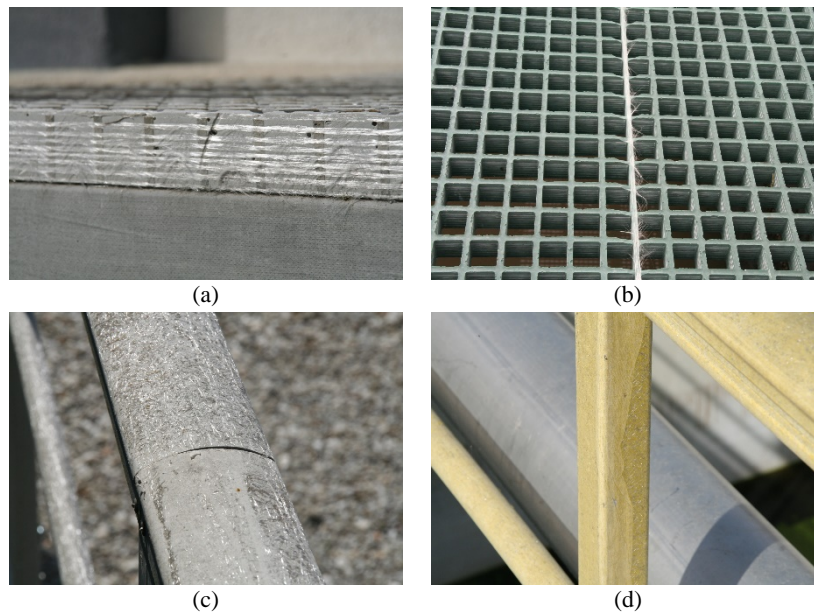


**Figure 5.03 - Examples of the A-N.Me.03 anomaly - fibre blooming.**

In addition to the functional problem it may cause (e.g. users' tactile discomfort in handrails), this anomaly promotes accumulation of water/moisture, development of biological colonization and degradation of the uppermost fibres by direct exposure to the environmental agents.

This anomaly can be avoided by using UV additives, including a surface veil in the fibre architecture (as shown in Figure 5.02 b) and/or applying a surface coating (e.g. paint, enamel or gel coating).

#### **5.3.4. A.N-Me.04 - Inclusion**

This anomaly, which in practice can only be traced during the production stage, consists of the inclusion of an anomalous material inside the cross-section of the GFRP composite, namely in the bulk of the material. This anomaly can be caused by inadequate maintenance/cleaning or isolation of the pultrusion or moulding equipment. These inclusions are usually very small in size and in such case, they typically do not affect the mechanical properties of the material. Figure 5.04 presents a schematic example of an inclusion (black material) inside the bulk of a tubular profile.

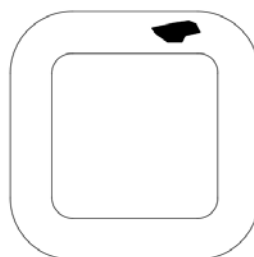


**Figure 5.04 - Schematic example of the occurrence of the A-N.Me.04 anomaly - inclusion.**

#### **5.3.5. A.N-Me.05 - Stains**

This anomaly consists of spots/stains on the surface of the profile. It can be related with several factors, either concerning singular events (e.g. accidental spills) or continuous exposure to an aggressive

environment (e.g. water accumulation, nuts/bolts oxidation)

Figure 5.05 presents four examples of this anomaly: Figure 5.05(a) shows stains on a moulded grating resulting from accidental spills of paint; Figure 5.05(b) shows stains on the top surface of a closed moulded grating due to the continued deposition of chemical vapours; Figure 5.05(c) illustrates stains in the permanently wet region of a GFRP ladder; and Figure 5.05(d) shows stains on a GFRP ladder caused by an accidental iron oxide spill.

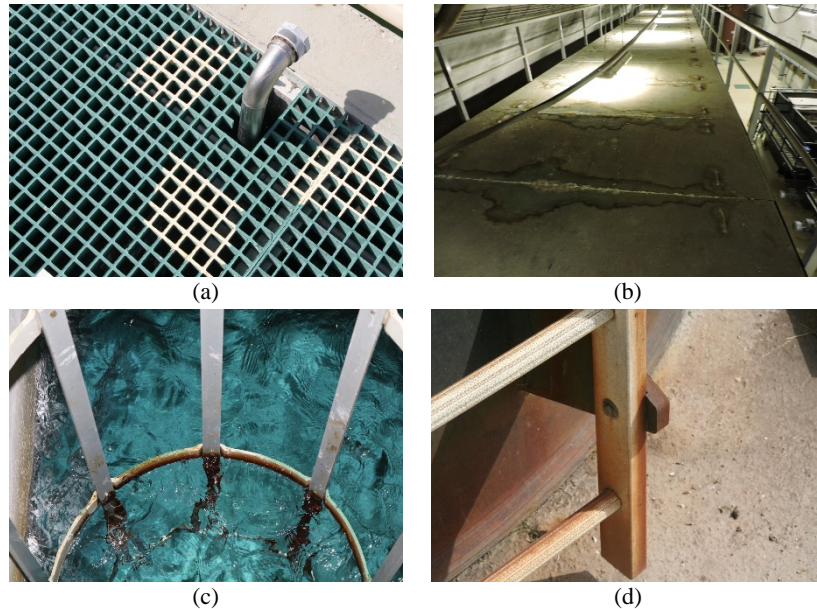


**Figure 5.05 - Examples of the A-N.Me.05 anomaly - stains.**

### **5.3.6. A.N-Me.06 - Surface marks**

This anomaly scopes a total of eight distinct anomalous situations: blisters, craters, saw burns, scaling, grooving, scratches, stop/pull marks, die parting lines and wrinkle depressions. Even though these anomalies have different characteristics, they have a similar visual appearance, namely by revealing themselves as small irregularities at the elements' surface.

These anomalies have several possible causes, and can occur during the production, installation and in-service stages. Irregularities are usually considered irrelevant to the mechanical properties because of their small size. However, their occurrence can involve a more aggressive (local) exposure to environmental agents, leading to an easier deterioration of the matrix protective layer and exposure of the fibres.

In the European standard EN 13706 [I.01] and in the American standards ASTM D4385 [II.11] and ASTM D2563 [II.12], acceptance levels are defined for each of the anomalies. If these criteria are not met (e.g. maximum diameter of blisters/craters, maximum depth of die parting lines) the material should in principle be discarded at the production stage and not applied in a structure.

Figure 5.06 presents five examples of this anomaly: Figure 5.06 (a) shows scratches on top of a closed (covered) moulded grating; Figure 5.06 (b) shows scratches on the top surface of a profile due to abrasion during the in-service stage; Figure 5.06 (c) illustrates the grooving effect on the surface layer of a profile caused during the production stage; Figure 5.06 (d) shows the die parting line of a profile originated from the production stage; and Figure 5.06 (e) shows the wrinkling effect on the

surface layer of a profile caused during the production stage.

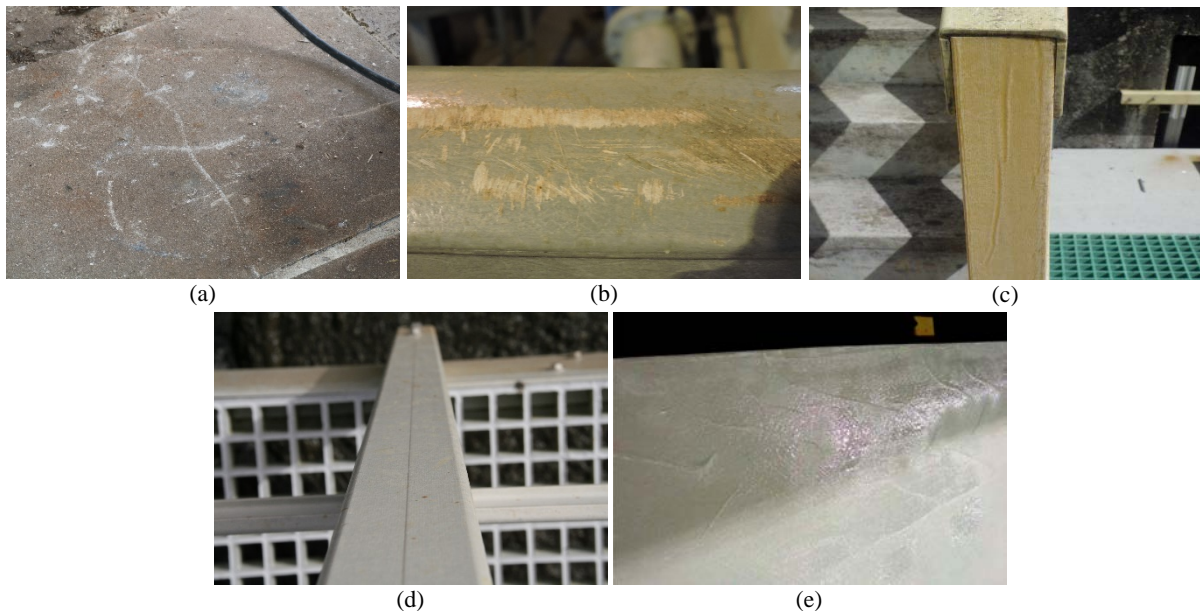


**Figure 5.06 - Examples of the A-N.Me.06 anomaly - surface marks.**

### **5.3.7. A.N-Me.07 - Wear damage**

This anomaly consists of the degradation of the surface layers, protection or coating of the GFRP elements, due to normal or incorrect use of the elements at different stages.

Figure 5.07 presents two examples of this anomaly: Figure 5.07(a) presents the degradation by surface wear during the transportation stage, while Figure 5.07(b) shows the loss of a portion of the protection layer of a closed moulded grating in one of its corners.



**Figure 5.07 - Examples of the A-N.Me.07 anomaly - wear damage.**

### **5.3.8. A.N-Me.08 - Debris accumulation**

This anomaly consists of the accumulation of debris on the gratings and profiles by deposition or by splattering. Even though this anomaly does not influence the mechanical properties of the materials, it allows higher exposure to the environmental agents due to increased water accumulation, it promotes biological colonization and detracts from the visual appearance of the construction.

Figure 5.08 presents three examples of this anomaly: Figure 5.08(a) shows accumulation of debris on top a closed grating; Figure 5.08(b) illustrates accumulation of debris in the open spaces of a grating; and Figure 5.08(c) shows accumulation of debris by splattering on a profile of a handrail.

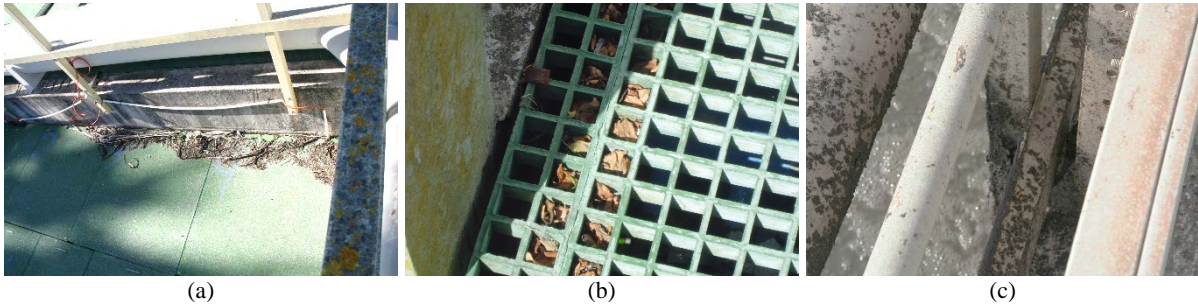


**Figure 5.08 - Examples of the A-N.Me.08 anomaly - debris accumulation.**

### 5.3.9. A.Me.01 - Corrosion of metallic components

This anomaly consists of the corrosion of metallic components (bolts, steel plates and/or profiles) included in the structure, used mainly in connections between elements. The corrosion process may occur due to lack of protection or improper choice and/or application of the metallic components. The evolution of this anomaly can lead to loose connections or to the formation of stains due to the iron oxides that are formed by the corrosion process.

Figure 5.09 presents two examples of this anomaly: Figure 5.09(a) shows the corrosion of the metallic bolts and washers on a connection zone of a profile (bi-metallic corrosion); and Figure 5.09(b) illustrates the corrosion of metallic elements of a connection point of a moulded grating.



**Figure 5.09 - Examples of the A-Me.01 anomaly - corrosion of metallic components.**

### 5.3.10. A.Me.02 - Cracking

This anomaly can occur in any structural component, either at the material level or in bonded/bolted connections between elements. The causes behind this anomaly are diverse and can occur at any stage of the life cycle of GFRP constructions (production, installation and in-service).

Figure 5.10 presents six examples of this anomaly: Figure 5.10(a) shows the cracking in a profile of a ladder, namely in a connection zone, due to bolts over-tightening; Figure 5.10(b) and (c) show the cracking in a connection zone between a profile and its fixing point, also due to bolts over-tightening, which caused excessive local transverse bending of the profiles' walls; Figure 5.10(d) shows the matrix cracking of some profiles, most likely due to lack of shrinkage additives at the production stage; Figure 5.10(e) and (f) show cracking between a vertical profile of a handrail, at the intersection with an horizontal profile. The cracking illustrated in Figure 5.10(e) is due to an accidental impact and incorrect detailing (the cross-section reduction of the vertical component at the joints seems largely excessive) and the crack depicted in Figure 5.10(f) occurred during the installation phase.

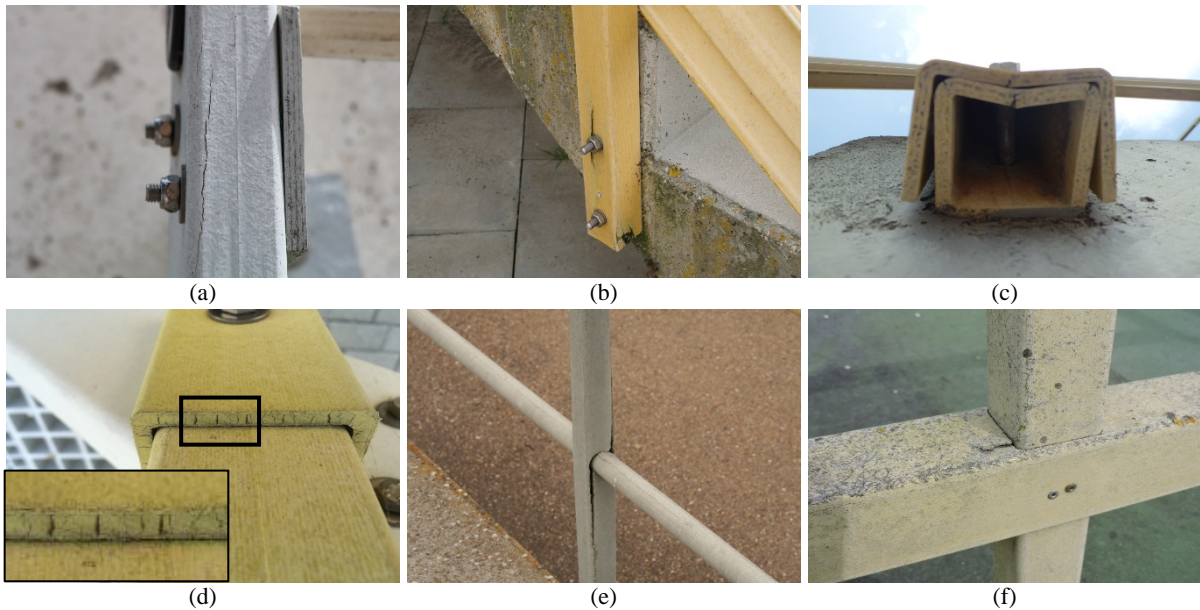


**Figure 5.10 - Examples of the A-Me.02 anomaly - cracking.**

### **5.3.11. A.Me.03 - Crushing**

This anomaly consists of crushing (by compression) of a structural element, occurring more frequently in connection zones or at the ends of the elements. The causes that lead to the appearance of this anomaly are, in general, associated with an incorrect design or installation.

Figure 5.11 presents three examples of this anomaly: Figure 5.11(a) shows crushing of a connection zone between a profile and its fixing point, due to bolts over tightening; Figure 5.11(b) shows cracking of a connection zone between two profiles, due to an accidental impact; and Figure 5.11(c) shows crushing of a border of a grating, due to an accidental impact.

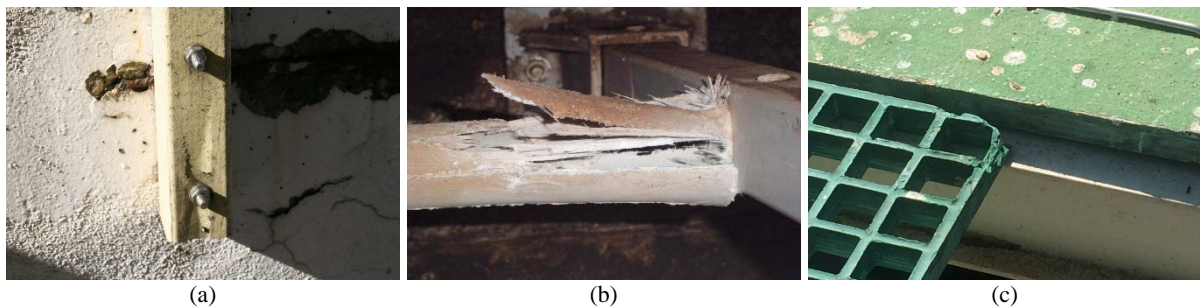


**Figure 5.11 - Examples of the A-Me.03 anomaly - crushing.**

### **5.3.12. A.Me.04 - Debonding**

This anomaly consists of the detachment of two structural elements in a bonded connection. It is generally caused by a wrong choice/application of the adhesive or incorrect treatment of the surfaces of the elements to be bonded, in terms of roughness and cleaning. It can also be caused by incorrect design, namely excessive loading and/or deformation (as presented in Figure 5.12 (a)), as these connections are generally much stiffer than bolted ones. Figure 5.12 (b) presents the debonding between two profiles in the Pontresina Bridge, due to excessive bending of a GFRP adherend.

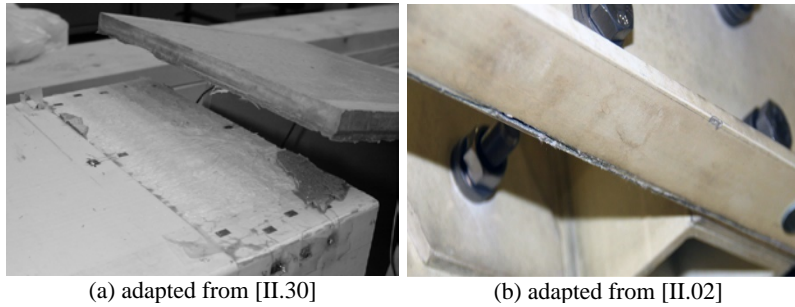


**Figure 5.12 - Examples of the A-Me.04 anomaly - debonding.**

### 5.3.13. A.Me.05 - Delamination

This anomaly consists of the separation (delamination) between different layers of fibrous reinforcement of FRP profiles, which can lead to a considerable reduction of the mechanical properties of the elements. The causes for this anomaly are usually related to production, due to an insufficient binding of the matrix between the layers of fibre reinforcement, an accidental impact or excessive loading.

Figure 5.13 presents three examples of this anomaly: Figure 5.13(a) shows the (superficial) delamination of a profile at an intersection point between two profiles during the installation phase, due to friction/impact between the two elements; Figure 5.13(b) shows the in-depth delamination of an inner reinforcing profile at a connection point most likely due to poor workmanship during the production phase; and Figure 5.13(c) shows the delamination of a profile ending, due to an accidental impact.

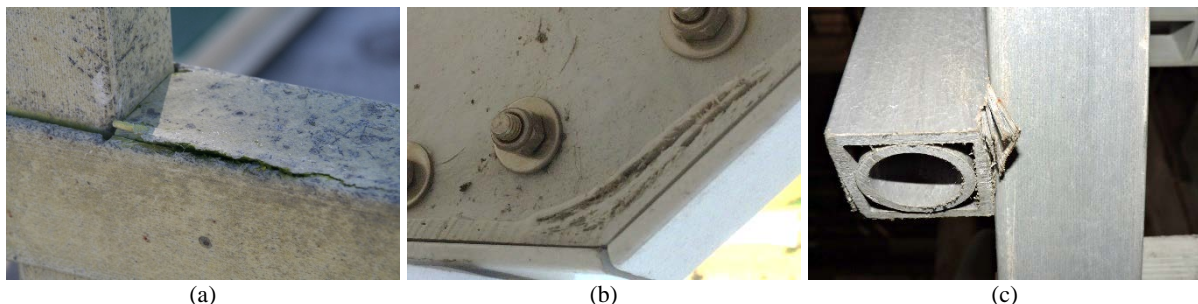


**Figure 5.13 - Examples of the A-Me.05 anomaly - delamination.**

### 5.3.14. A.Me.06 - Excessive deflection

This anomaly consists of the excessive deformation of structural elements (usually the vertical displacement of horizontal members), with reference to the acceptable deflection for such type of elements. This anomaly is usually related to incorrect design, incorrect use of the structure or change in use. In this respect, the importance of shear deformations in GFRP structures (in addition to bending deformations) and of duly accounting for the effects of creep is highlighted.

### 5.3.15. A.Me.07 - Geometrical imperfections

This anomaly reveals itself through the application of profiles with incorrect dimensions (production phase), with excessive deviations (namely exceeding the tolerances defined in EN 13706 [I.01]), or profiles with cuts incorrectly executed (installation phase), leading to the existence of imperfections in connection zones or current zones.

Figure 5.14 depicts two examples of this anomaly: Figure 5.14(a) shows the incorrect drilling

and cutting of a profile in a connection zone; and Figure 5.14(b) shows incorrect cutting of a profile in the middle of the element, with a very significant local reduction of stiffness and strength.



**Figure 5.14 - Examples of the A-Me.07 anomaly - geometrical imperfections.**

### **5.3.16. A.Me.08 - Indentation/perforation**

This anomaly consists of a partial or total indentation (perforation) of one or more surfaces of a pultruded profile or a grating by an external element. Figure 5.15 presents two examples of this anomaly: Figure 5.15(a) shows the indentation of a profile and Figure 5.15(b) shows the indentation of a grating.

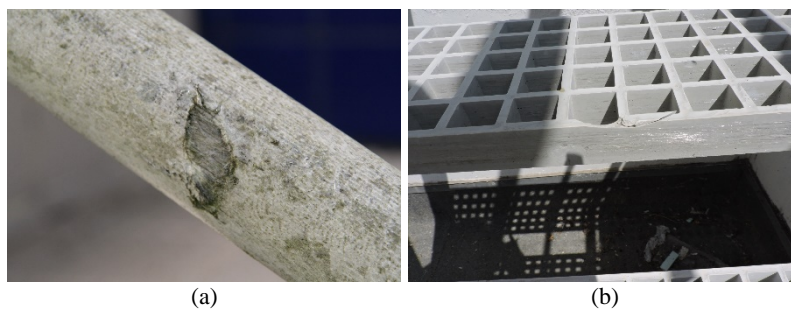


**Figure 5.15 - Examples of the A-Me.08 anomaly - indentation/perforation.**

### **5.3.17. A.Me.09 - Incorrect curing of adhesive**

This anomaly consists of incorrect curing of the adhesive used in bonded connections between structural or non-structural members. This anomaly occurs during the installation phase of the structure, typically caused by inappropriate environmental conditions (in terms of temperatures and/or relative humidity) or incorrect mixture/formulation of the components, and it can compromise the mechanical behaviour of the bonded connection and of the structure, especially if it does not include a backup or redundant system (e.g. bolts).

### **5.3.18. A.Me.10 - Incorrect curing of resin**

This anomaly consists of the incorrect curing of the polymeric resin of the GFRP material during the production phase. Like the previous anomaly, this one can also considerably affect the short-term mechanical properties of the GFRP elements, as well as their long-term performance (creep) and durability when subjected to environmental agents. This anomaly is less likely to occur in FRP components produced by pultrusion (since the resin matrix experiences high temperatures inside the curing die), being potentially more relevant in composite parts produced by hand layup or vacuum infusion.

### 5.3.19. A.Me.11 - Loose connections

This anomaly consists of bolted connections in which there are missing components (e.g. nuts or washers) or in which they were loosely applied (e.g. with insufficient tightening) or not retightened during maintenance operations. It can lead to lower structural performance of bolted connections, in terms of strength and stiffness, and may eventually lead to other anomalies (e.g. indentation due to the absence of washers). Figure 5.16 presents two examples of this anomaly: Figure 5.16(a) shows (several) missing metallic elements in a bolted connection, while Figure 5.16(b) illustrates a connection with an under tightened nut (actually, it is completely loose).



Figure 5.16 - Examples of the A-Me.11 anomaly - loose connections.

### 5.3.20. A.Me.12 - Member failure

This anomaly, which may occur during the in-service stage, consists of failure (rupture) of a structural or non-structural member. This can occur in different ways, e.g. at the connections between section walls (typically the flanges and webs of profiles with thin-walled sections), or at the edges of the laminates of the members. A given member is considered to have failed when its mechanical performance has been seriously compromised with respect to the loads it is expected to sustain.

Figure 5.17 presents three examples of this anomaly: Figure 5.17 (a), (b), and (c) show the rupture of the web-flange junction of different profiles, resulting in a substantial reduction of their mechanical performance. In Figure 5.17 (b), this rupture occurs between the web and flanges of the profile, with permanent deformations outside their original plane, and in Figure 5.17 (c) this rupture occurs at the connection point between a profile and its supporting structure, due to excessive bending and lack of nuts in the bolting system.

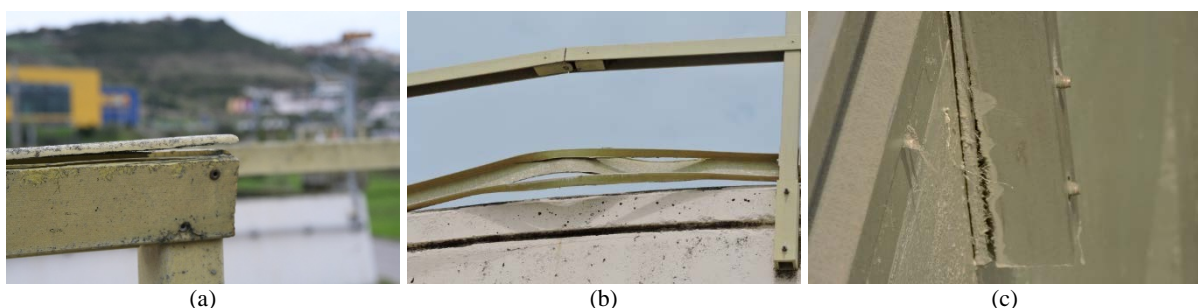


Figure 5.17 - Examples of the A-Me.12 anomaly - member failure.

### 5.3.21. A.Me.13 - Voids

This anomaly consists of the appearance of voids (air pockets) inside the GFRP material or the adhesive used in bonded connections. This anomaly can only occur at the production stage. Figure 5.18

presents two examples of this anomaly: Figure 5.16(a) shows voids inside a profile (that would likely evolve to delamination), and Figure 5.16 (b) shows a superficial void on a profile.

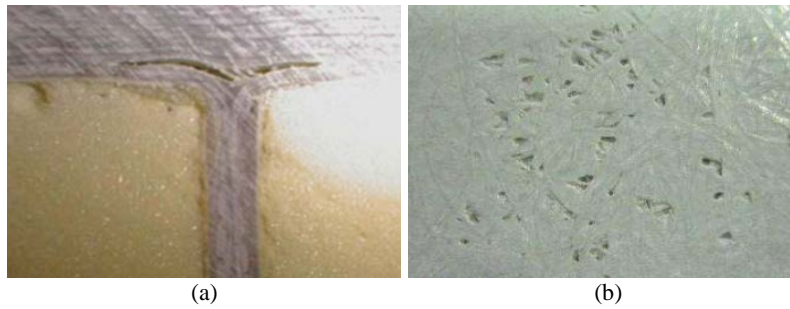


Figure 5.18 - Examples of the A-Me.11 anomaly - voids.

#### 5.4. Classification of the causes of the anomalies

The purpose of this thesis is not to thoroughly study each of the causes presented, but rather to group them according to the moment/action in which they influence the occurrence of a given anomaly. Table 5.02 presents a proposal of the classification system of the probable causes according to a chronological order of occurrence. Therefore, production causes or errors come first, followed by project/design errors, installation causes and in-service causes.

Table 5.02 - Proposed classification system for the causes of the anomalies

CAUSES GROUPS	CAUSES NAMES
<b>PRODUCTION CAUSES</b>	C.P.01 Incorrect cure conditions of the resin (temperature, humidity and duration)
	C.P.02 Excess of resin
	C.P.03 Inadequate quality/mixture/formulation of resin components
	C.P.04 Dripped resin or small air bubbles
	C.P.05 Inadequate maintenance/cleaning/isolation of pultrusion equipment
	C.P.06 Incorrect layout of fibres/mats
	C.P.07 Incorrect positioning of die metallic parts
	C.P.08 Inadequate handling of profiles or cutting element
<b>DESIGN CAUSES</b>	C.D.01 Inadequate structural design/material selection
	C.D.02 Inadequate connection design /material selection
	C.D.03 Lack of surface veil/UV additives/surface coating
<b>INSTALLATION CAUSES</b>	C.I.01 Incorrect installation or prefabrication
	C.I.02 Incorrect application of adhesive (e.g. thickness, voids, position, cure)
	C.I.03 Inadequate quality/mixture/formulation of adhesive components
	C.I.04 Inadequate treatment of bonding surfaces
	C.I.05 Incorrect temperature and/or humidity cure conditions for adhesive
	C.I.06 Over/under tightening of bolted connections
<b>IN- SERVICE CAUSES</b>	C.S.01 High humidity/permanently wet/excessive wet-and-dry cycles environmental condition
	C.S.02 Exposure to UV radiation
	C.S.03 Exposure to chemical/saline environment
	C.S.04 Loss of tightening/unprotected bolted connection
	C.S.05 Vandalism/accidental impact/use wear/change of use or inadequate use
	C.S.06 Lack of maintenance

In general, an anomaly in this type of material is not usually related with a single factor but with a set of related factors that, from the production phase to the in-service phase, allow for the development of the anomaly.

##### 5.4.1. C.P. - Production causes

Several anomalies may arise from the production phase of GFRP elements. This phase is one of the most important for the long- and short-term performance of GFRP constructions, since it may affect the

physical and mechanical properties of the elements. This is the largest group of possible causes of anomalies, which may be related to the characteristics of the production process (generally pultrusion for profiles and casting for moulded gratings). Most of the causes in this group are directly related with the polymeric resin of the matrix of the profiles, or to the incorrect handling of the fibres.

Figure 5.19 presents two examples of anomalies that occur due to causes of the production stage. Figure 5.19(a) shows the occurrence of the fibre blooming anomaly due to a misalignment of the superficial protection layer at the production stage (C.P.06). Figure 5.19(b) shows the occurrence of superficial marks on the entire section of the pultruded profile due to the misalignment of the die metallic parts at the production stage (C.P.07).



**Figure 5.19 - Examples of occurrence of anomalies due to causes of the production stage.**

#### **5.4.2. C.D. - Design causes**

The causes associated with design are generally related with lack of knowledge about the mechanical behaviour of composite materials and to lack of consensual codes for design of GFRP constructions. Anomalies associated with these causes are related with incorrect design of the various components of the structure and their connections (bolted or bonded), with insufficient/inappropriate detailing and inadequate specifications of the materials for the environmental conditions to which the structure is or will be exposed (e.g. type of resin, additives, fibre architecture and surface protection). Thus, this type of causes could be mitigated by a better knowledge of the GFRP material and/or more appropriate constructive details for this type of structures, and the development of applicable regulation (ongoing).

Figure 5.20 presents three examples of anomalies that occur due to causes at the design stage. Figure 5.20 (a) shows the cracking of a GFRP connection element due to an inadequate connection design (C.D.02). Figure 5.20 (b) shows the (bi-metallic) corrosion of a metallic connection element due to inadequate connection design/material choice (C.D.02). Figure 5.20 (c) shows the debris accumulation in a moulded grating due to an incorrect structural design (C.D.01).

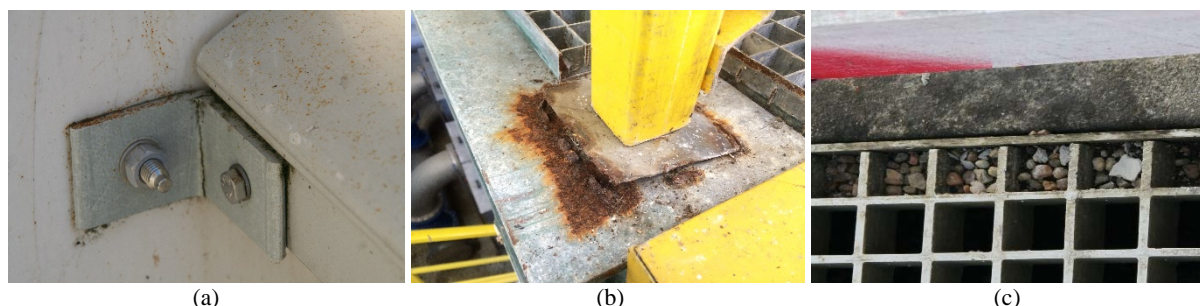


**Figure 5.20 - Examples of occurrence of anomalies due to causes of the design stage.**

### 5.4.3. C.I. - Installation causes

Most causes of this group are related with incorrect installation of the elements and their connections. Generally, these causes are associated with lack of knowledge about the best construction techniques for this type of structures and/or insufficiently trained or low skilled workforce. The causes associated with the installation of GFRP constructions should not have a high incidence, since most of the elements are at least partially pre-assembled in the factory.

Figure 5.21 presents three examples of anomalies that occur due to causes of the installation stage. Figure 5.21 (a) shows the occurrence of indentations due to the incorrect handling of a cutting tool during installation (C.I.01). Figure 5.21 (b) shows the crushing of a connection zone due to bolts' over tightening (C.I.06). Figure 5.21 (c) shows a geometrical imperfection (existence of excessive drill holes) made during the installation stage (C.I.01).

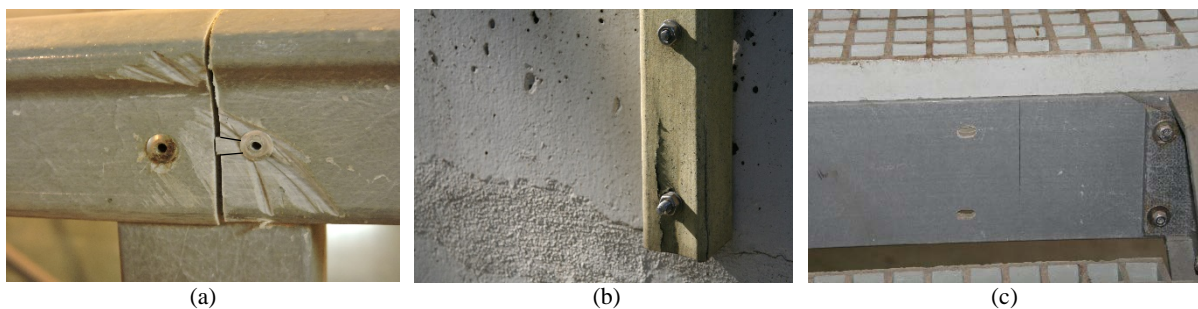


**Figure 5.21 - Examples of occurrence of anomalies due to causes of the installation stage.**

### 5.4.4. C.S. - In-service causes

The causes associated to the in-service stage are usually related to the exposure of the GFRP elements to the atmospheric conditions, misuse or change in the type of use of the constructions. Some of the anomalies detected during the in-service stage may also result from causes originated from previous stages. The implementation of service plans (conditions in which the structure should be used) and inspection and/or maintenance plans would help reducing the incidence of anomalies detected during this stage.

Figure 5.22 presents two examples of anomalies that occur due to causes of the in-service stage. Figure 5.22 (a) shows the occurrence of biological colonization, loss of gloss and fibre blooming - these three anomalies are related with the exposure of the material to environmental conditions: rain (C.S.01) and UV radiation (C.S.02). Figure 5.22 (b) shows a member failure of a profile due to inadequate use (C.S.05).



**Figure 5.22 - Examples of occurrence of anomalies due to causes of the in-service stage.**

## 5.5. Anomaly forms

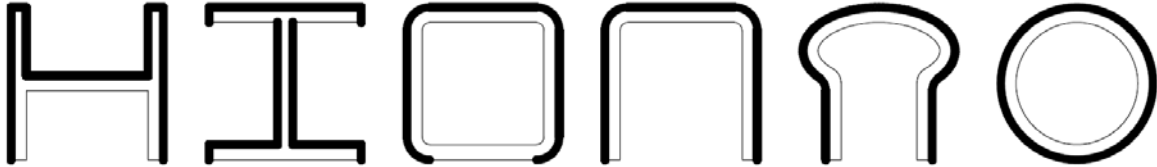
For each anomaly, diagnosis technique and rehabilitation technique (described ahead), a comprehensive form was developed in the frame of the present thesis. As exemplified in Figure 5.23 for anomaly “Biological colonization”. each anomaly form contains the following information: (i) a generic picture of the anomaly; (ii) a brief description of the anomaly; (iii) possible causes of the anomaly; (iv) possible consequences of the appearance/development of the anomaly; (v) details to be inspected (characteristics related to the detected anomaly that may be relevant to the diagnosis); (vi) inspection methods that can be performed *in situ* (in order to further characterize the anomaly in terms of extent, severity and stage of evolution); (vii) rehabilitation techniques to eliminate the anomaly and/or its causes; (viii) classification parameters of the anomaly (which may be the result of tests carried out and that allow assessing the severity level of the anomaly); and (ix) severity level/repair emergency (which was defined to vary between 0 and 4). The remaining anomaly forms can be found in Appendix I. The techniques presented in sections (vi) and (vii), are presented in the following chapters.

## 5.6. Concluding remarks

In this chapter the main anomalies likely to occur in GFRP elements were presented and classified according to the properties they can affect, in a standardized and descriptive anomaly form. The classification system is divided in two groups: mechanical and non-mechanical anomalies, comprising a total of 21 anomalies (13 mechanicals and 8 non-mechanical).

The most probable causes for the occurrence of the anomalies were also presented and classified in four groups according to the life stage in which they may affect the GFRP constructions (production, design, installation and in-service), comprising a total of 23 causes.

A standardized form for each anomaly was also presented containing the most important aspect of each of the anomalies.

<b>ANOMALY FORM - A.N-ME.01</b>	
<b>ANOMALY NAME</b>	
Biological colonization	
<b>ANOMALY DESCRIPTION</b>	
Biological colonization consists of biological matter on the surface of GFRP elements. This anomaly usually occurs in zones with high humidity/permanently wet environmental conditions.	
<b>POSSIBLE CAUSES</b>	
- High humidity environmental condition (C.S.01)	- Lack of maintenance (C.S.06)
- Permanently wet environmental condition (C.S.01)	
<b>POSSIBLE CONSEQUENCES</b>	
- Aesthetical appearance	- Reduction of mechanical properties (due to moisture exposure)
- Increase of water retention	
<b>DETAILS TO INSPECT</b>	
- Affected area	- Exposure to UV radiation
- Source of water/humidity	
<b>INSPECTION METHODS</b>	
- Visual inspection (IM.01)	- Radiography (IM.07)
- Infrared thermography (IM.04)	- Moisture meter (IM.08)
<b>REHABILITATION TECHNIQUES</b>	
- Application of superficial coating (water repellent coating) (R.03)	- Superficial cleaning (R.04)
<b>CLASSIFICATION PARAMETERS</b>	
- Conditions for progression of the anomaly (Y/N)	- Aesthetical significance of the element
<p>- Superficial area affected (<math>A_f</math> (%)) = <math>100 \times \text{Area with biological colonization/superficial and outer exposed area of 1 meter of profile} \times 100</math></p> <p>The considered superficial and outer exposed area is suggested in the diagrams below, for some of the most common types of profiles. The highlighted areas are the most commonly exposed areas to solar radiation on a horizontal profile, as such, the most probable area to the occurrence of biological colonization.</p>	
	
<b>SEVERITY LEVEL / REPAIR EMERGENCY</b>	
0 - Small biological colonization ( $A_f < 20\%$ )	
1 - High biological colonization ( $A_f > 20\%$ ) and/or high aesthetical significance of the element	

**Figure 5.23 - A.N-Me.01 anomaly (biological colonization) form.**

## 6. Diagnosis techniques

### 6.1. Introductory remarks

When an anomaly is observed, in some cases the associated causes can be immediately identified; otherwise, an appropriate diagnosis technique must be applied to determine the exact cause (or, at least, the most probable causes) and extent of such anomaly. A careful diagnosis should consider several factors from design to in-service exposure. The correct identification of the cause(s) of a given anomaly allows, in most cases, the elimination of such anomaly, or at least preventing further development of the anomaly.

The application of a diagnosis technique during an inspection must take into consideration the conditions for the application of that technique *in-situ* when an anomaly is detected. Therefore, most of the techniques that should be applied during an inspection should deliver instant or semi-instant results and should not damage the structure/element being inspected.

The diagnosis techniques included in the inspection system for FRP constructions presented herein can be applied *in-situ* and without damaging the structural elements. These techniques are usually considered as Non-Destructive Techniques (NDT) and in most cases they were adapted from other industries that also use FRP materials (e.g. naval, mechanical, aerospace), generally with a longer history of use than civil engineering applications. The following NDT's were considered relevant for this study: (i) visual inspection; (ii) tap test; (iii) Barcol hardness measurement; (iv) thermography; (v) ultrasonic test; and (vi) moisture meter test.

Some of the techniques considered in the state-of-the-art review, acoustic emission and radiography, were not introduced in the current inspection system due to economic factors, and due to restrictive applicability in some cases (e.g. use of radiation). These techniques, even though showing great applicability for anomaly sizing and depth of some of the anomalies considered, are applied to achieve a greater quality control of the materials and study the anomalies that can occur at the production stage.

### 6.2. Diagnosis techniques description

#### 6.2.1. I.01 - Visual inspection

Visual inspection is the primary method of inspection of all structural composites, since most of the anomalies can be detected at the surface [II.16]. It is recommended that visual inspection should always be used as the initial method of inspection as an aid to any additional instrumented NDT.

This technique is highly applicable in the detection of the most common surface anomalies. However, in some cases visual inspection should not be used as a stand-alone method for inspection of structural GFRP elements. In fact, there are several limitations to this method, including its inability to detect some types of internal delamination and cracks, the difficulty in using it in painted composites or GFRP materials with poor surface quality, and its inability to detect missing reinforcement. In an opaque material, the method is limited to the detection of surface defects.

In order to improve the detection of some anomalies and the results obtained by using this diagnosis technique, several tools/equipment can be used [II.19]. The most common tools/equipment are:

- Magnifying glass and microscope to enlarge small defects;
- Photographic and video recording equipment, used to obtain the appearance of the anomaly for archive and subsequent analysis (e.g. photographic camera, drones, scanning equipment);
- Dye penetrant, used to aid in the detection of superficial cracks or delamination and improve the contrast between defects and the underlying material;
- A calliper/ruler, used to determine the thickness and cross-section dimensions of the elements, and the thickness/depth of cracks;
- A level and laser, used to determine the deflection of a given element/structure.

The main advantages and limitations of this type of diagnosis technique are presented in Table 6.01.

**Table 6.01 - Advantages and limitations of the I.01 diagnosis technique - Visual inspection.**

<b>Advantages</b>	<b>Limitations</b>
Fast and inexpensive Instantaneous interpretation of large areas Generally little to no equipment expenses No coupling equipment required	Baseline properties are difficult to establish Highly susceptible to human misinterpretation Unable to detect interior anomalies

### **6.2.2. I.02 - Tap test**

This NDT technique consists of tapping the surface of a GFRP element with a metallic element (e.g. a coin or a light hammer) in order to detect the variation in local stiffness, by interpreting the difference of the sound produced. This method, although frequently used, has some limitations, such as the type of defect and its real size. This method is also influenced by the surrounding environment, the operator's sensibility and the tapping force [II.20].

Most of these limitations can be discarded by using semi-automatic systems, where the structure is tapped with an instrumented hammer in several locations and a load cell, placed at the tip of the hammer and recording the interacting force. This allows the comparison between the local stiffness of two/different sections of the element.

This method is very intuitive and allows a fast verification of the elements' properties. Being a manual method, it can be applied locally or in large surfaces, in any direction and with small manoeuvring space.

The main advantages and limitations of this diagnosis technique are presented in Table 6.02.

**Table 6.02 - Advantages and disadvantages of the I.02 diagnosis technique - tap test.**

<b>Advantages</b>	<b>Limitations</b>
Low equipment cost Compact and lightweight system No coupling equipment required	Difficult to correlate between sound and actual defect Little to no capability of identifying defect size Requires high consistency of operator labour Influenced by surrounding environment

### 6.2.3. I.03 - Barcol hardness measurement

In this technique, the composites surface hardness is determined using a Barcol impressor or hardener tester, illustrated in Figure 6.01. The relative depth of the impressor's indenter provides a comparative measurement of the material's hardness along the surface of the element.



**Figure 6.01 - Barcol impressor (adapted from [II.31]).**

The Barcol hardness test is most commonly used to determine the degree of resin/adhesive cure [II.32] and to identify possible superficial delamination in FRP materials.

The main advantages and limitations of this diagnosis technique are presented in Table 6.03.

**Table 6.03 - Advantages and limitations of the I.03 diagnosis technique - Barcol hardness measurement.**

Advantages	Limitations
Low equipment cost Compact and lightweight system No coupling equipment required	Little to no capability of defect sizing Demands high operator consistency

### 6.2.4. I.04 - Infrared thermography

Infrared and thermal testing uses the heat transfer rate of materials to detect subsurface anomalies by measuring the surface temperature or surface temperature rates of change, as shown in Figure 6.02.

When applying this technique, when the material has no anomaly affecting the local thermal properties, it creates an even emission of infrared radiation after heating (Figure 6.02 (b)). However, if there is an enclosure material/void with a different heat transfer coefficient from the GFRP, it will create an uneven emission of infrared radiation in the location of the anomaly as shown in Figure 6.02(c).

Thermography is limited by its sensitivity, at the production stage, to measure voids and inclusions, but it is very useful for the detection of in-service damage, such as delamination.

Thermography has a high sensibility to delamination, cracks, voids and moisture ingress and it can be applied passively or actively. In the passive mode, heating by natural surroundings can be used as the source. In the active mode, various moderate heat sources can be used. In many cases, moderate heating with a hair dryer or heat blanket for a few seconds is sufficient to generate heat into a composite with sufficient sensitivity to detect subsurface anomalies.

Thermography has the advantages of allowing for on-site testing, the speed of application, and being a remote testing procedure. Pulse infrared thermographic inspection has proven to be a fast, accurate, reliable and cost-effective NDT [II.19] [II.20]. The main advantages and limitations of this diagnosis technique are

summarized in Table 6.04.

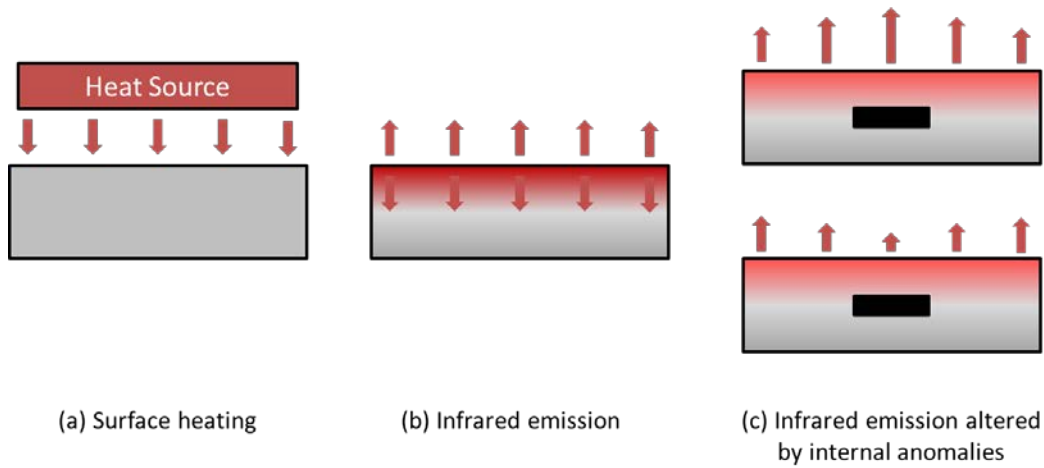


Figure 6.02 - Schematic functioning system of thermography.

Table 6.04 - Advantages and limitations of the I.04 diagnosis technique - Infrared thermography.

Advantages	Limitations
Rapid 'mapping' of large surface areas Particularly suitable for composites and components with low thickness	Susceptible to temperature fluctuations Requires coupling equipment (infra-red camera)
	Requires a highly uniform heat source

### 6.2.5. I.05 - Ultrasonic test

Ultrasonic testing (UT) uses ultrasonic sound waves to test objects for their compactness and, hence, quality. The ultrasound wave is generated by a mechanical vibration from a transducer that converts an electrical signal into mechanical motion and vice versa. By inputting a short pulse of electrical energy or a tone burst to the transducer, a pressure pulse is generated that, when coupled to the composite element, creates an ultrasound wave. This wave travels in the composite material at a particular frequency and velocity from the transmitter to the receiver, as seen in Figure 6.03 (a, b, and c). For the most common specifications for composite inspection, the frequency used will usually range from 1 MHz to 5 MHz [II.20].

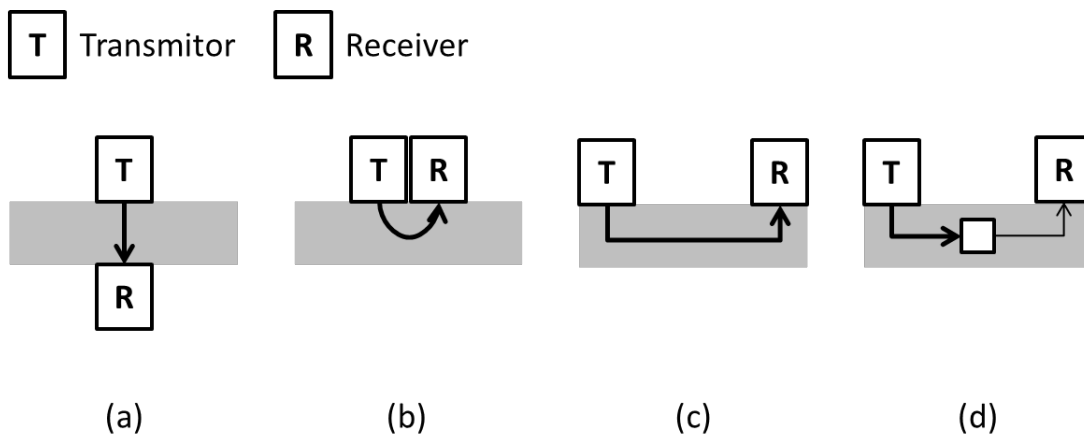


Figure 6.03 - Schematic functioning system of ultrasonic testing.

The detection of anomalies in the elements, such as delamination or inclusions, is a function of the transmission or reflection of the ultrasound across the material. The very low transmission and very high reflection that are associated with air pockets explain why delamination and debonding are easy to detect with ultrasonic tests, as seen in Figure 6.03 (d). Inclusions that are not bonded into the composite are also easy to detect, but inclusions in the bulk of the material are only detectable if the acoustic significance of the inclusion material is different from that of the composite. Even though this technique can easily detect inclusions and debonding, it does not have the capability to determine the depth and extension of the anomaly.

The main advantages and limitations of this diagnosis technique are presented in Table 6.05.

**Table 6.05 - Advantages and limitations of the I.05 diagnosis technique - Ultrasonic test.**

Advantages	Limitations
Highly sophisticated equipment at relatively low cost	Requires wide experience and background knowledge (especially with composite materials)
High mobility	Little to no capability of defect sizing
	Difficult to apply on rough/uneven surfaces

#### 6.2.6. I.06 - Moisture meter test

Measurement/monitoring of the moisture level can be done using the digital thermo-hygrometer devices. When the objective is to measure the amount of free water in the materials (water accumulated in cracks and macro pores that can be evaporated), a moisture meter is generally used (Figure 6.04). This device can only detect whether the surface of the material has free water, but it does not allow determining the depth of the water absorption.

This equipment determines the amount of water inside GFRP elements, making it possible to (qualitatively) correlate this parameter with the level of degradation and mechanical properties of the material [II.34]. Even though this technique can easily detect moisture, it does not have the capability to determine the depth of the anomaly.

The main advantages and limitations of this diagnosis technique are presented in Table 6.06.



**Figure 6.04 - Moisture meter (adapted from [II.33]).**

**Table 6.06 - Advantages and limitations of the I.06 diagnosis technique - Moisture meter test.**

Advantages	Limitations
Compact and lightweight system High mobility	Little to no capability of defect sizing (depth) Difficult to apply on rough/uneven surfaces

### **6.3. Diagnosis techniques forms**

As exemplified in Figure 6.05, for infrared thermography, the diagnosis technique forms developed in this thesis contain the following data: (i) a brief description of the principles of the technique and a photo illustrating its application; (ii) the objectives of the test/technique; (iii) the necessary equipment; (iv) any special requirements; (v) a detailed description of the test method; (vi) the main advantages and limitations of the technique. The forms concerning the remaining diagnosis techniques can be found in Appendix II.

### **6.4. Concluding remarks**

In this chapter, the most suitable diagnosis techniques for FRP composites used in civil engineering applications were presented. A total of six diagnosis techniques were selected to be included in the inspection system; all the techniques presented can be applied in-situ and when applied alone or combined they allow for a comprehensive characterization and definition of the extension of the anomalies detected.

Laboratory techniques that allow determining the physical and mechanical properties of FRP materials were not included in this study. Even though the use of these techniques has great advantages in durability studies, they are not within the scope of the techniques that can be applied in field inspection of GFRP constructions, since most of the mechanical properties are determined by destructive testing. These techniques are usually applied for forensic engineering in case of accidents, structural malfunctioning and/or durability studies.

A standardized form for each diagnosis technique was also presented, containing the most important features of each technique.

<b>DIAGNOSIS TECHNIQUE FORM - I.04</b>	
<b>DIAGNOSIS TECHNIQUE DESIGNATION</b>	
Infrared thermography	
<b>OBJECTIVES</b>	
To evaluate the differences between the thermal conductivity of different areas of the GFRP elements. Infrared thermography has high sensitivity to delamination, cracks, voids and moisture ingress.	
<b>NECESSARY EQUIPMENT</b>	
Thermographic camera sensitive to infrared radiation, thermoelectric sensors to control the temperature of the elements, digital recording equipment to save the thermographic results obtained.	
<b>METHOD DESCRIPTION</b>	
1. Taking advantage of the heating caused by solar radiation (or any other means), observation of the thermographic images obtained through infrared thermography equipment; 2. Recording the images/videos collected on the digital recording equipment; 3. Analysing the recorded images/videos and diagnose accordingly.	
<b>TECHNIQUE ADVANTAGES</b>	
The application of this technique, besides the acquisition costs of the equipment, is economical and efficient. This technique can be applied without any contact with the elements to be inspected and can be applied to general areas instead of localized points. This technique allows recording the analysed surface and can detect anomalies at an early stage.	
<b>TECHNIQUE LIMITATIONS</b>	
The analysis of the thermographic images is considered as a starting point to more localized tests in the possibly affected areas. The interpretation of the thermographic images requires a qualified professional with experience in the thermal behaviour of GFRP materials. The depth and thickness of the anomaly cannot be determined with this method.	

**Figure 6.05 - I.04 diagnosis technique (Infrared thermography) form.**



## **7. Rehabilitation techniques**

### **7.1. Introductory remarks**

This chapter describes the rehabilitation techniques likely to be applied to GFRP constructions presenting anomalies. The rehabilitation techniques applicable to GFRP elements can be considered preventive and/or corrective. The same technique can be considered both preventive and corrective, depending on the anomaly it is applied to. While these techniques primarily aim to rehabilitate, some cases also allow them to function as reinforcement. However, it's important to highlight that the main focus of the discussed techniques is not to reinforce GFRP structures.

Preventive techniques are generally applied to prevent the occurrence of a given anomaly. These techniques can be applied at the construction site after the elements are in place, but preventive techniques should preferably be considered during the design stage. As there is still some uncertainty regarding the long-term behaviour of GFRP materials, there are no guidelines on how to completely prevent the occurrence of different anomalies at the design stage.

On the other hand, corrective techniques aim at correcting and eliminating a given anomaly. After the application of a corrective technique, the application of a preventive technique should also be considered to prevent the reoccurrence of the anomaly and extend the service life of that GFRP construction.

The rehabilitation techniques considered relevant for this study are the following: (i) Bonding/bolting of strengthening elements; (ii) Strengthening with filling elements; (iii) Application of surface coating; (iv) Surface sanding/cleaning; (v) Replacement of affected elements; and (vi) Protection/tightening of bolted connections.

### **7.2. Rehabilitation techniques description**

#### **7.2.1. R.01 - Bonding/bolting of strengthening elements**

This technique consists of bonding or bolting other elements (profiles or plates) on specific areas of an affected element, as shown in Figure 7.01. The bonding/bolting of strengthening elements is typically used to rehabilitate mechanical anomalies. This technique can be used to repair an affected element (e.g. cracked, crushed), as shown in Figure 4.03 (b), or it can be used to increase the stiffness or strength of that element (e.g. excessive deflection). If this technique is to be applied to an entire element, other rehabilitation techniques should be considered as an alternative, such as R.05 (replacement of affected elements, described ahead).

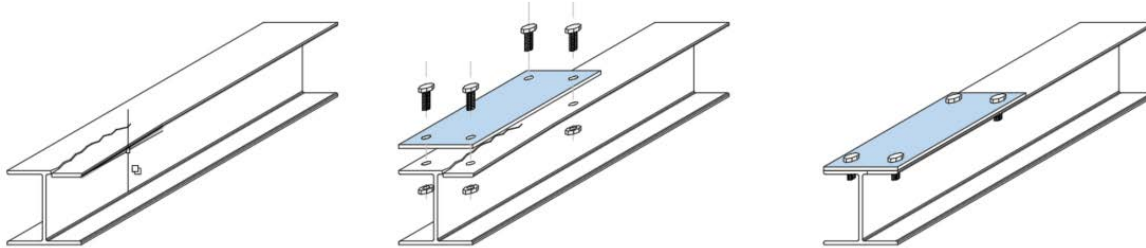


**Figure 7.01 - Illustrative scheme of the R.01 rehabilitation technique - Bonding/bolting of strengthening elements.**

### **7.2.2. R.02 - Strengthening with filling elements**

This technique consists of bonding filling elements with adequate stiffness and strength (e.g. polyurethane foam) to an affected element, as shown in Figure 7.02. As an example, this technique was applied in the Pontresina Bridge, as shown in Figure 4.03(a). This technique is typically used to rehabilitate cracked and crushed elements due to accidental impacts and can also be used as a preventive method when there is an incorrect design or choice of cross section in a GFRP structure, as mentioned in section 4.2.

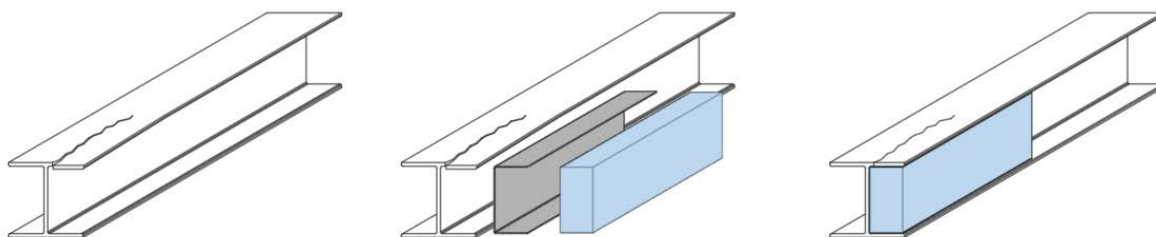


**Figure 7.02 - Application of the R.02 rehabilitation technique - Strengthening with filling elements.**

### **7.2.3. R.03 - Application of surface coating**

This technique is used to rehabilitate non-mechanical anomalies. The application of a surface coating (as shown in Figure 7.03) prevents the accumulation of water and creates an exterior surface protection and sacrifice layer to the environmental agents, in particular exposure to UV radiation and moisture. This technique can also be applied during the installation of the GFRP structure in order to prevent some of the most common anomalies (e.g. biological colonization, loss of gloss and fibre blooming). The use and application of this technique is being considered in natural and accelerated ageing in Part III of this thesis, in order to reduce the occurrence of some anomalies and reduce the effects of exposure of GFRP elements to UV radiation and other environmental agents.

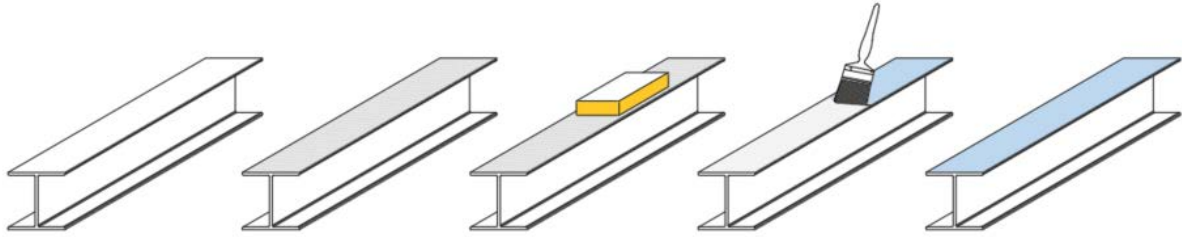


**Figure 7.03- Application of the R.03 rehabilitation technique - Application of surface coating.**

#### **7.2.4. R.04 - Surface sanding/cleaning**

Cleaning of GFRP construction elements should be a periodic operation, executed to eliminate dirt, parasitic vegetation, debris and biological growth (as shown in Figure 7.04). Several chemical and mechanical methods could be used according to the material to remove (e.g. sponge, soft brush, low pressure water jet, water, bleach, paint thinner). To avoid introducing unacceptable damage to the GFRP elements, the initial technique applied in the cleaning operations should be as little aggressive as possible. This technique is also used as a preparatory measure (surface preparation) for other rehabilitation techniques (e.g. R.03 - Application of surface coating), being used, for instance, when repairing effects of fibre blooming.

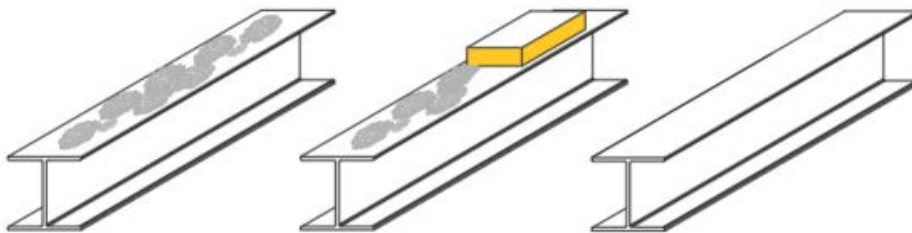


**Figure 7.04- Application of the R.04 rehabilitation technique - Surface sanding/cleaning.**

#### **7.2.5. R.05 - Replacement of affected elements**

When the deterioration of an element is too significant and it is limited to one or few elements that do not affect adjacent elements, repair can be done by replacing the affected elements. Due to its cost and possible complexity in removing the affected elements from the construction, this technique should only be applied if the other techniques cannot be applied and/or their application becomes too expensive.

#### **7.2.6. R.06 - Protection/tightening of bolted connections**

The application of this technique (exemplified in Figure 7.05) concerns bolted connections, in which the metallic elements may be noticeably deteriorated by corrosion, were loose in the installation stage or could have become loose/lost during the in-service stage. Under these circumstances, this technique may involve surface sanding and coating of a corroded element, tightening a loose element or placing a new bolting element when it is missing.

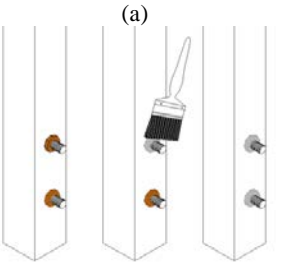
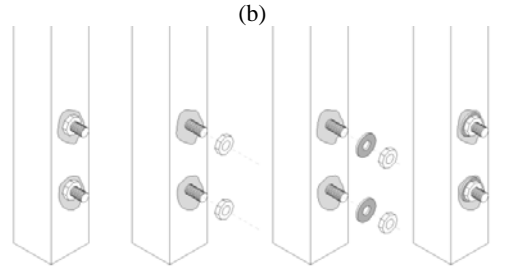
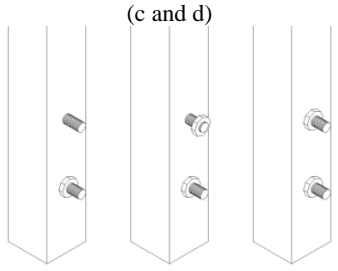
Another issue is concerned with the occurrence of stains around the screw holes, indicating the accumulation of water between the screw and the GFRP element, typically penetrating through the

edges of the hole. This situation can be stopped by adding a plastic washer between the GFRP element and the metallic nuts.

### **7.3. Rehabilitation techniques forms**

For each rehabilitation technique presented above, a rehabilitation form was prepared that contains the following elements: (i) elements to rehabilitate; (ii) materials to apply; (iii) necessary equipment; (iv) description of the rehabilitation technique; (v) estimated labour and time; (vi) estimated cost; (vii) recommendations and special precautions; and (viii) technique limitations.

As an example, Figure 7.05 presents the form of rehabilitation technique R.06 - Protection/tightening of bolted connections. The forms of the remaining rehabilitation techniques can be found in Appendix III. This Appendix also includes complementary information about the forms, including the procedure used to estimate labour, time and costs.

<b>REHABILITATION TECHNIQUE FORM - R.06</b>					
<b>REHABILITATION TECHNIQUE DESIGNATION</b>					
R.06 - Protection/tightening of bolted connection					
<b>TECHNIQUE DESCRIPTION</b>					
The application of this technique concerns bolted connections, in which the metallic elements may be noticeably deteriorated by corrosion (a), were loose in the installation stage (c) or could have become loose/lost during the in-service stage (d). Insufficient sealing of bolted connections can lead to stains around the screw holes, due to the accumulation of water between the screw/nut and the GFRP element (b).					
<b>MATERIALS TO APPLY</b>					
(a) primary paint and anti-corrosion paint		(c) stainless steel nuts (if necessary)			
(b) plastic washers		(d) stainless steel nuts and bolts			
<b>NECESSARY EQUIPMENT</b>					
(a) cleaning material (cloth, water, solvent materials, brush), mechanical or manual pickling and/or sanding material (wire brush, sanding sheet, mechanical sander, water/sand jet) and painting equipment (paints and brushes).					
(b) cleaning material (cloth, water, solvent materials, brush), manual or mechanical wrench.					
(c) cleaning material (cloth, water, solvent materials, brush), manual or mechanical wrench, stainless steel nuts.					
(d) cleaning material (cloth, water, solvent materials, brush), manual or mechanical wrench, stainless steel nuts and bolts.					
<b>DESCRIPTION OF THE REHABILITATION TECHNIQUE</b>					
(a) 1. Clean the rusted element; 2. Pickle and/or sand the rusted layer of the bolted element; 3. Clean the un-rusted surface; 4. Apply primary paint layer; 5. Apply anti-corrosive paint.					
(b) 1. Remove existing metallic nuts; 2. Clean the superficial area between the screw and the GFRP element; 3. Place plastic washers between the GFRP element and metallic bolt; 4. Tighten the bolting elements.					
(c and d) 1. Clean the metallic elements; 2. Place the metallic elements missing (if necessary); 3. Tighten the bolting elements.					
					
<b>ESTIMATED LABOUR AND TIME*</b>					
(a) 1 worker x 8 hours: rehabilitation of 48 elements		(c) 1 worker x 8 hours: rehabilitation of 96 elements			
(b) 1 worker x 8 hours: rehabilitation of 32 elements		(d) 1 worker x 8 hours: rehabilitation of 96 elements			
<b>ESTIMATED COST*</b>					
(a) 1.25 €/element	(b) 1.00 €/element	(c) 1.00 €/element	(d) 0.50 €/element		
<i>* Values estimated and described in appendix III</i>					
<b>RECOMMENDATIONS AND SPECIAL PRECAUTIONS</b>					
General recommendations: The use of personal protective equipment is recommended in all situations. The electric tools should be used correctly and in accordance with the specifications and safety manuals of the equipment.					
(a) make sure that the existing rust has been removed from the metallic elements before applying the primary paint layer; let the primary paint layer completely dry before applying the anti-corrosive paint layer. The paints should be applied at the temperatures recommended by the manufacturers, should not be applied while raining or if the moisture level of the substrate is excessive.					
(b) check that the stains are due to the presence of water between the metallic elements and the GFRP, and it is not due to other causes; choose the plastic/stainless steel washers in accordance with the size of the bolting elements (inner and outer diameters of the washer).					
(c and d) check the appropriate tightening force of the elements, take special precaution not to over tighten the bolting elements, in order not to damage the GFRP elements.					
<b>TECHNIQUE LIMITATIONS</b>					
These techniques may be difficult to apply in elevated structures (that require the use of a ladder) and in structures with hidden/partially obstructed bolted connections.					

**Figure 7.05 - R.03 rehabilitation form - Protection/tightening of bolted connections.**

#### **7.4. Concluding remarks**

In this chapter, a total of six rehabilitation techniques for GFRP constructions, suitable for civil engineering applications, were presented and described. A standardized form for each rehabilitation technique was also presented, containing the most important features of each technique.

The rehabilitation of GFRP elements must be considered as a preventive measure when design is not completely detailed or appropriate to guarantee a durable construction. Even though the rehabilitation of GFRP elements is the more conventional and sustainable path, in some cases, due to the specificity of these materials, the most suitable rehabilitation technique may be the substitution of the affected elements.

## 8. Correlation matrices

### 8.1. Introductory remarks

In the scope of inspection systems, the development of correlation matrixes is intended to facilitate the work of field inspectors, by (i) relating the anomalies with their most probable causes, (ii) correlating the occurrence of different anomalies, (iii) relating the anomalies with the most adequate diagnosis technique(s) and (iv) relating the anomalies with the most appropriate rehabilitation technique(s). The development of these matrices was adapted from the work developed by other authors [II.35], [II.07].

Apart from the “inter-anomalies” matrix, all matrices have a correlation value that may vary between 0 and 2. The value 0 refers to a situation of “**no correlation**” between the two variables; the value 1 refers to a case of “**small correlation**” between the two variables, and the value 2 refers to a scenario of “**great correlation**” between the two variables of the matrix [II.35].

The validation of the matrices was based on a field work conducted within the thesis (described ahead in Chapter 8), which allowed the comparison of the theoretical and real values included in the matrices; As such, some of the values defined at an initial stage changed (these values are highlighted in blue in the correlation matrices).

### 8.2. Anomalies - probable causes correlation matrix

Table 8.01 presents a correlation matrix where anomalies correspond to columns and causes are organized in rows. This correlation matrix was defined in accordance with the list of anomalies and causes presented in Table 5.01 and Table 5.02, respectively.

The correlation coefficient is based on the correlation level between each anomaly and each cause. The coefficient varies between 0 and 2, as per the following description [II.06]: 0 - there is no correlation (direct or indirect) between the anomaly and the cause; 1 - indirect cause of the anomaly, related to the beginning of the decay process; secondary cause of the deterioration process, not essential to its development; or 2 - direct cause of the anomaly, associated with the final stage of the deterioration process; when it occurs, it is one of the main reasons for the deterioration process and it is essential to its development.

When analysing the correlation matrix presented in Table 8.01, considering the anomaly A.N-Me.03 (fibre blooming) as an example, the following comments are prompted:

- The correlation between fibre blooming and the installation causes have a coefficient of 0, since most of the installation causes are correlated with bonded/bolted connections, not affecting fibre blooming;
- Also, fibre blooming has a correlation of 1 with causes C.P.06 (incorrect layout of fibres/mats) and C.D.03 (lack of surface veil/UV additives/surface coating), since these causes themselves do not directly cause the start of fibre blooming, but allow a faster progression of the anomaly;
- As expected, the fibre blooming anomaly has a correlation coefficient of 2 with cause

C.S.02 (exposure to UV radiation); in fact, UV radiation is the environmental agent that causes more degradation to the superficial layer of the matrix that prevents the appearance of fibres at the surface of the profile.

As another example, when analysing the correlation matrix presented in Table 8.01, considering the anomaly A.Me.02 (cracks), the following comments are prompted:

- The correlation between cracking and C.P.04 (dripped resin or small air bubbles) has a coefficient of 0, because there is no correlation between these two factors;
- Also, cracking has a correlation of 1 with causes C.D.01 (Inadequate structural design/material selection) and C.D.02 (Inadequate connection design /material selection), since these causes themselves do not directly cause the occurrence of cracking, but can lead to its occurrence;
- As expected, the cracking anomaly has a correlation coefficient of 2 with cause C.S.05 (Vandalism/accidental impact/use wear/change of use or inadequate use) due to the occurrence of damages in the materials that can lead to cracking.

**Table 8.01 - Correlation matrix between anomalies and probable causes**

CAUSES		ANOMALIES																				
		NON-MECHANICAL (A.N-Me)								MECHANICAL (A.Me)												
		01	02	03	04	05	06	07	08	01	02	03	04	05	06	07	08	09	10	11	12	13
PRODUCTION	C.P.01	0	1	0	0	0	1	0	0	0	0	0	0	1	0	0	0	0	2	0	0	0
	C.P.02	0	0	0	0	0	0	0	0	0	1	0	0	0	0	0	0	0	2	0	0	0
	C.P.03	0	1	0	0	0	0	0	0	0	1	0	0	1	0	0	0	0	2	0	0	0
	C.P.04	0	0	0	0	0	1	0	0	0	0	0	0	0	0	0	0	0	0	0	0	2
	C.P.05	0	0	0	2	0	1	0	0	0	0	0	0	0	0	1	0	0	0	0	0	0
	C.P.06	0	0	1	0	0	1	0	0	0	1	0	0	1	0	0	0	0	0	0	0	1
	C.P.07	0	0	0	0	0	2	0	0	0	0	0	0	0	0	0	0	0	0	0	0	0
	C.P.08	0	0	0	0	0	1	0	0	0	0	0	0	0	0	0	0	0	0	0	0	0
DESIGN	C.D.01	0	0	0	0	0	0	1	0	0	1	1	0	0	1	0	1	0	0	0	2	0
	C.D.02	0	0	0	0	0	0	0	0	2	1	0	1	0	0	1	0	0	0	0	0	0
	C.D.03	1	1	1	0	0	0	1	1	0	0	0	0	0	0	0	0	0	0	0	0	0
INSTALLATION	C.I.01	0	0	0	0	0	1	0	0	0	1	0	2	1	0	2	1	0	0	0	0	0
	C.I.02	0	0	0	0	0	0	0	0	0	2	0	2	0	0	0	0	2	0	0	0	2
	C.I.03	0	0	0	0	0	0	0	0	0	2	0	1	0	0	0	0	2	0	0	0	1
	C.I.04	0	0	0	0	0	0	0	0	0	0	0	2	0	0	0	0	0	0	0	0	0
	C.I.05	0	0	0	0	0	0	0	0	0	1	0	1	0	0	0	0	2	0	0	0	0
	C.I.06	0	0	0	0	0	0	0	0	0	2	1	0	0	0	0	0	0	0	2	1	0
IN-SERVICE	C.S.01	1	1	0	0	1	0	0	0	1	0	0	0	0	0	0	0	0	0	0	0	0
	C.S.02	1	2	2	0	0	0	0	0	0	0	0	0	0	0	0	0	0	0	0	0	0
	C.S.03	0	1	1	0	0	0	0	0	1	0	0	0	0	0	0	0	0	0	0	1	0
	C.S.04	0	0	0	0	0	0	0	0	1	0	0	0	0	0	0	0	0	2	0	0	0
	C.S.05	0	0	0	0	2	1	2	0	0	2	2	0	0	1	0	2	0	0	0	2	0
	C.S.06	2	0	0	0	1	0	0	2	1	0	0	0	0	0	0	0	0	0	1	1	0

*\*blue cells represent the values changed during the validation of the anomalies and probable causes matrix.*

### 8.3. Inter-anomalies correlation matrix

The anomalies detected in GFRP elements can occur isolated or be associated with other anomalies that develop simultaneously. Fibre blooming is one of the examples of an anomaly that may be correlated with other anomalies. For fibre blooming to occur, degradation of the superficial matrix layer must have occurred *a priori*, leading to a discolouration/loss of gloss of the element and, in a further stage, to fibre blooming.

Therefore, a correlation index between anomalies is proposed, in order to establish probabilities of occurrence of other anomalies when one of them is already observed. In this way, an inter-anomalies matrix was developed based on the anomaly-causes correlation matrix.

The correlation index between anomaly  $k$  and anomaly  $j$  is obtained according to a method proposed by Brito [II.06], which has been followed and applied in the present study, as follows:

- For each detected anomaly (anomaly  $k$ ), read the corresponding column in the anomaly-causes correlation matrix;
- For each detected anomaly (anomaly  $j$ ), read the corresponding column in the anomaly-causes correlation matrix;
- The product of the indices of these two columns corresponding to the anomalies  $k$  and  $j$  of the anomaly-cause correlation matrix is calculated per column;
- The various products are added in order to obtain the correlation index of each  $CI_{kj}$  anomaly, translated in the following expression,

$$CI_{kj} = \sum_{i=1}^N c_{ki}c_{ji}$$

with  $N$  being the total number of causes.

Applying this method, it is possible to obtain the correlation matrix presented in Table 8.02.

The inter-anomaly index obtained as explained above by itself is not always clear enough given that the absolute value of the index has no physical meaning for the user. Moreover, in some way, all the anomalies can correlate to other anomalies and the degree of correlation is not always very clear. In any case, a higher absolute value of the correlation index may help identifying an anomaly that is more likely to occur simultaneously to an anomaly that is being considered, compared to another one that presents a lower index.

Therefore, it is useful to establish a percentage correlation between anomalies by determining the percentage of the actual correlation index relative to a possible maximum theoretical correlation index, which shows the probability of occurrence of a given anomaly with the detection of other anomalies.

**Table 8.02 - Correlation matrix inter-anomalies**

		ANOMALIES																						
		NON-MECHANICAL (A.N-Me)								MECHANICAL (A.Me)														
		01	02	03	04	05	06	07	08	01	02	03	04	05	06	07	08	09	10	11	12	13		
ANOMALIES	NON-MECHANICAL (A.N-Me)	01	■	2	1	0	4	0	1	4	3	0	0	0	0	0	0	0	0	2	2	0		
		02	2	■	6	0	2	0	1	0	2	1	0	0	4	0	0	0	0	6	0	1	1	
		03	1	6	■	0	0	1	1	0	1	1	0	0	1	0	0	0	0	0	0	1	1	
		04	0	0	0	■	0	2	0	0	0	0	0	0	0	0	2	0	0	0	0	0	0	
		05	4	2	0	0	■	0	0	2	4	0	0	0	0	0	0	0	0	0	0	3	1	0
		06	0	0	1	2	0	■	1	0	0	3	2	0	1	0	2	1	0	0	0	2	2	0
		07	1	1	1	0	0	1	■	0	0	4	4	0	0	2	0	1	0	0	0	4	0	0
		08	4	0	0	0	2	0	0	■	2	0	0	0	0	0	0	0	0	0	0	2	2	0
	MECHANICAL (A.Me)	01	3	2	1	0	4	0	0	2	■	2	0	2	0	0	2	0	0	0	3	2	0	
		02	0	1	1	0	0	3	4	0	2	■	10	10	3	4	3	2	10	4	4	10	8	
		03	0	0	0	0	0	2	4	0	0	10	■	0	0	4	0	2	0	0	2	9	0	
		04	0	0	0	0	0	0	0	0	2	10	0	■	0	0	5	0	8	0	0	0	5	
		05	0	4	1	0	0	1	0	0	0	3	0	0	■	0	0	0	0	6	0	0	3	
		06	0	0	0	0	0	0	2	0	0	4	4	0	0	■	0	0	0	0	0	4	0	
		07	0	0	0	2	0	2	0	0	2	3	0	5	0	0	■	0	0	0	0	0	0	
		08	0	0	0	0	0	1	1	0	0	2	2	0	0	0	0	■	0	0	0	2	0	
09		0	0	0	0	0	0	0	0	0	10	0	8	0	0	0	0	■	0	0	0	6		
10		0	6	0	0	0	0	0	0	0	4	0	0	6	0	0	0	0	■	0	0	2		
11		2	0	0	0	3	0	0	2	3	4	2	0	0	0	0	0	0	0	■	3	0		
12		2	1	1	0	1	2	4	2	2	10	9	0	0	4	0	2	0	0	0	■	0		
13		0	1	1	0	0	2	0	0	0	8	0	5	3	0	0	0	6	2	0	0	■		

With this calculation, the correlation matrix becomes asymmetric, since the probability of occurrence of anomaly  $j$  when anomaly  $k$  is found is not necessarily identical to the probability of the inverse situation. The theoretical percentage correlation index is thus obtained as follows [II.06]:

- For each anomaly  $k$  detected, the corresponding column is read in the anomaly-causes correlation matrix, multiplying by 2 all the correlation indices of the anomaly  $k$  with the causes and adding the sum of these products, in order to obtain the maximum possible theoretical correlation index of any anomaly  $i$  related to anomaly  $k$ ,  $I_{Mk}$ :

$$I_{Mk} = \sum_{i=1}^N (2 \times c_{ki})$$

with  $N$  being the total number of causes.

- To determine the theoretical correlation index of anomaly  $k$  with anomaly  $j$ ,  $CI_{%kj}$ , which determines the probability of occurrence of anomaly  $j$  (column  $j$ ) when anomaly  $k$  (line  $k$ ) is found, the ratio between the correlation index between anomalies (reference anomaly  $k$  and associated anomaly  $j$ ) and the maximum theoretical correlation index of anomaly  $k$  is computed as follows:

$$CI_{%kj} = \frac{CI_{kj}}{I_{Mk}} \times 100$$

Applying this procedure, the values presented in Table 8.03 were obtained.

As mentioned before, this table presents the probability of occurrence of a given anomaly (column) when another one (row) is detected. As an example, the probability of occurrence of the anomaly A.N-Me.08 (debris accumulation), when the anomaly A.N-Me.01 (biological colonization) is detected is 83%. However, the (inverse) probability of occurrence of the anomaly A.N-Me.01 when the anomaly A.N-Me.08 occurs is only 50%. This apparent disparity can be explained as follows: whenever there is debris accumulation, it is very probable that there is also biological colonization, whereas biological colonization can occur without debris accumulation.

**Table 8.03 - Percentage correlation matrix inter-anomalies (%)**

		ANOMALIES																							
		NON-MECHANICAL (A.N-Me)								MECHANICAL (A.Me)															
		01	02	03	04	05	06	07	08	01	02	03	04	05	06	07	08	09	10	11	12	13			
ANOMALIES	NON-MECHANICAL (A.N-Me)	01	25	30	0	38	0	13	83	25	0	0	0	0	0	0	0	0	0	0	20	14	0		
		02	40	60	0	13	11	13	17	17	3	0	0	38	0	0	0	0	50	0	7	0			
		03	30	38	0	0	6	13	17	8	3	0	0	13	0	0	0	0	0	0	7	8			
		04	0	0	0	0	11	0	0	0	0	0	0	0	0	25	0	0	0	0	0	0			
		05	30	6	0	0	11	50	33	17	13	50	0	0	50	0	50	0	0	10	36	0			
		06	0	13	10	50	25	25	0	0	13	25	11	38	25	38	38	0	17	0	14	25			
		07	10	6	10	0	50	11	17	0	17	63	0	0	75	0	63	0	0	0	43	0			
		08	50	6	10	0	25	0	13	17	0	0	0	0	0	0	0	0	0	0	20	14	0		
	MECHANICAL (A.Me)	01	30	13	10	0	25	0	0	33	7	0	11	0	0	25	0	0	0	30	14	0			
		02	0	6	10	0	50	22	63	0	17	88	56	38	75	38	75	83	33	40	57	58			
		03	0	0	0	0	50	11	63	0	0	23	0	0	75	0	63	0	0	20	50	0			
		04	0	0	0	0	11	0	0	17	33	0	25	0	63	25	67	0	0	0	0	42			
		05	0	19	10	0	0	17	0	0	10	0	11	0	25	13	0	33	0	0	0	8			
		06	0	0	0	0	25	6	38	0	0	10	38	0	0	0	38	0	0	0	29	0			
		07	0	0	0	50	0	17	0	0	17	10	0	28	25	0	25	0	0	0	0	0			
		08	0	0	0	0	50	17	63	0	0	20	63	11	13	75	25	0	0	0	43	0			
		09	0	0	0	0	0	0	0	0	0	33	0	44	0	0	0	0	0	0	0	50			
		10	0	38	0	0	0	11	0	0	0	13	0	0	50	0	0	0	0	0	0	0			
		11	20	0	0	0	13	0	0	33	25	13	25	0	0	0	0	0	0	0	21	0			
		12	20	6	10	0	63	11	75	33	17	27	88	0	0	100	0	75	0	0	30	0			
		13	0	0	10	0	0	17	0	0	0	23	0	28	13	0	0	0	50	0	0	0			

### 8.4. Anomalies - diagnosis techniques correlation matrix

Table 8.04 presents the correlation matrix between anomalies and their potential diagnosis methods. The correlation is intended to aid in the selection of the most appropriate diagnosis method for each anomaly.

The correlation coefficient is based on the correlation level between each anomaly (column) and each diagnosis method (row). The coefficient can vary between 0 and 2, as per the following description [II.06]: 0 - there is no correlation (direct or indirect) between the anomaly and the diagnosis method; 1 - diagnosis method suitable for the characterization of a given anomaly, although it has limitations in terms of technical performance or cost, reducing its scope of application; or 2 - diagnosis

method suitable for the characterization of a given anomaly, whose execution requires little technical support and equipment, increasing its scope of application.

Table 8.04 shows that there are anomalies with more than one diagnosis method with different correlation coefficients. This is because the methods are limited in terms of application scope and may only be suitable for application in given technical and economic situations, depending on the level of the anomaly, or because each method allows the characterization of one parameter of the anomaly and it is necessary to complete the data collected by using more than one method.

As seen in Table 8.04, using the method I.04 (infrared thermography) as an example, it is inferred that this method has no application (correlation coefficient of 0) on the detection of some anomalies, such as loss of gloss (A.N-Me.02) or surface marks (A.N-Me.06). This method has the capability of detecting cracks (A.Me.2), but it does not have the capability to fully quantifying (e.g. extension, depth) the anomaly. However, this method has the capacity to detect and estimate the area affected by delamination (A.N-Me.05); similarly, the method is not able to quantify the depth of this anomaly.

**Table 8.04 - Correlation matrix between anomalies and inspection techniques**

INSPECTION TECHNIQUE	ANOMALIES																				
	NON-MECHANICAL (A.N-Me)								NON-MECHANICAL (A.N-Me)												
	01	02	03	04	05	06	07	08	01	02	03	04	05	06	07	08	09	10	11	12	13
I.01	2	2	2	0	2	2	2	2	2	2	2	1	1	2	2	2	2	1	2	2	
I.02	0	0	0	0	0	0	0	0	0	1	0	2	2	0	0	1	1	0	1	0	1
I.03	0	1	0	0	0	0	0	0	0	0	0	0	1	0	0	0	0	0	2	0	0
I.04	1	0	0	1	1	0	0	0	0	1	1	2	1	2	0	1	0	0	0	0	0
I.05	0	0	0	2	1	0	0	0	0	2	1	2	2	0	0	1	0	0	0	0	0
I.06	1	0	0	0	2	0	0	0	0	0	0	0	0	0	0	0	0	0	0	0	0

### 8.5. Anomalies - rehabilitation techniques correlation matrix

Table 8.05 presents the correlation matrix between anomalies and their potential rehabilitation techniques. This correlation allows selecting the most appropriate rehabilitation technique(s) for each anomaly.

The correlation coefficient is based on the correlation level between each anomaly (column) and each rehabilitation technique (row). The coefficient can vary between 0 and 2, as per the following description [II.06]: 0 - there is no correlation between the anomaly and the rehabilitation technique; 1 - rehabilitation method suitable for the recovery of a given anomaly, although it has limitations in terms of entirely repairing the anomaly and/or eliminating its causes; 2 - most suitable rehabilitation method for the recovery of a given anomaly, in terms of entirely repairing the anomaly and/or eliminating its causes.

As seen in Table 8.05, using the method R.03 (application of surface coating) as an example, it is inferred that this method has no application (correlation coefficient of 0) on most of the mechanical anomalies, such as cracking (A.Me.02) or delamination (A.Me.05). This method has the capability of

rehabilitating wear damage (A.N-Me.7), but it does not have the capability to fully rehabilitate the anomaly in case of extensive damage. However, this method has the capacity to fully rehabilitate the occurrence of the stains (A.N-Me.05) and loss of gloss (A.N-Me.02).

**Table 8.05 - Correlation matrix between anomalies and rehabilitation techniques**

REHABILITATION TECHNIQUE	ANOMALIES																						
	NON-MECHANICAL (A.N-Me)								NON-MECHANICAL (A.N-Me)														
	01	02	03	04	05	06	07	08	01	02	03	04	05	06	07	08	09	10	11	12	13		
R.01	0	0	0	0	0	0	0	0	0	2	2	2	2	2	1	1	2	1	1	0	0		
R.02	0	0	0	0	0	0	0	0	0	2	2	0	0	0	0	0	0	0	0	0	0		
R.03	1	2	2	0	2	1	1	0	1	0	0	0	0	0	0	0	0	0	0	0	0		
R.04	2	0	0	0	2	2	0	2	1	0	0	0	0	0	0	0	0	0	0	0	0		
R.05	0	0	1	2	1	2	2	0	2	2	2	2	2	0	2	2	1	2	2	0	2		
R.06	0	0	0	0	1	0	0	0	2	0	0	0	0	1	0	0	0	0	2	0	0		

### 8.6. Concluding remarks

This chapter presented the correlation matrices of the inspection, diagnosis and rehabilitation system for GFRP constructions, which are an essential tool for any inspection system. For a given anomaly, the matrices allow identifying the most common anomalies that can also be found, the most probable causes of that anomaly and its most appropriate diagnosis and rehabilitation techniques.

With this final tool, the inspection, diagnosis and rehabilitation system is now completed. It was validated based on the field study described in the following chapter, in which extensive data were collected regarding existing GFRP constructions exposed to different environments.



## 9. Inspection system validation and data analysis

### 9.1. Introductory remarks

The initial purpose of this chapter is to present the information gathered during the field inspections of a total of 410 GFRP substructures with anomalies and, subsequently, the analysis and validation of the classification systems and correlation matrices presented in the preceding chapters.

The effectiveness of the validation of an inspection system is greatly dependent on the size, diversity and information gathered from the inspected installations. The greater the representativeness of the sample, the broader the applicability of the system.

The inspections' information was documented in inspection and validation forms presented below. These forms contain all the important information necessary to characterize a given GFRP substructure and allow a comparison between different substructures and different inspections. In each installation inspected there were several substructures, each one differentiated from the others, by its location in each installation, the type of materials used, the constructive technique, the type of exposure to environmental agents and, when applicable, its age.

These substructures were categorized in three types of structures: profiles, gratings and stairs. As the name indicates, profile structures were made only of pultruded profiles (Figure 9.01 (a-b)) and gratings structures were made only of moulded gratings (Figure 9.01 (c-d)). However, the stair structures were considered to be a particular type of structure, in terms of materials (some were made only of profiles (Figure 9.01 (f)), and others had a combination of profiles and gratings (Figure 9.01 (e))) and in terms of constructive techniques (type of fixtures and connections), so these structures were studied separately, in order to better interpret the data gathered.



**Figure 9.01 - Types of structures considered.**

In this chapter, a brief introduction is firstly made regarding the planning of the inspections to the

various installations. Subsequently, a brief description of the information gathered is presented and the validation of the proposed classification systems (for anomalies, causes and diagnosis and rehabilitation techniques) is made and justified. At the end of the chapter a data analysis of the different elements is presented regarding different aspects (e.g. environmental exposure, location).

## 9.2. Inspection planning

During the field work, an extensive inspection campaign was carried out in 31 installations of the EPAL Company, spread across mainland Portugal, as presented in Figure 9.02. These structures included water treatment plants, sewage treatment plants and sewage pumping stations.

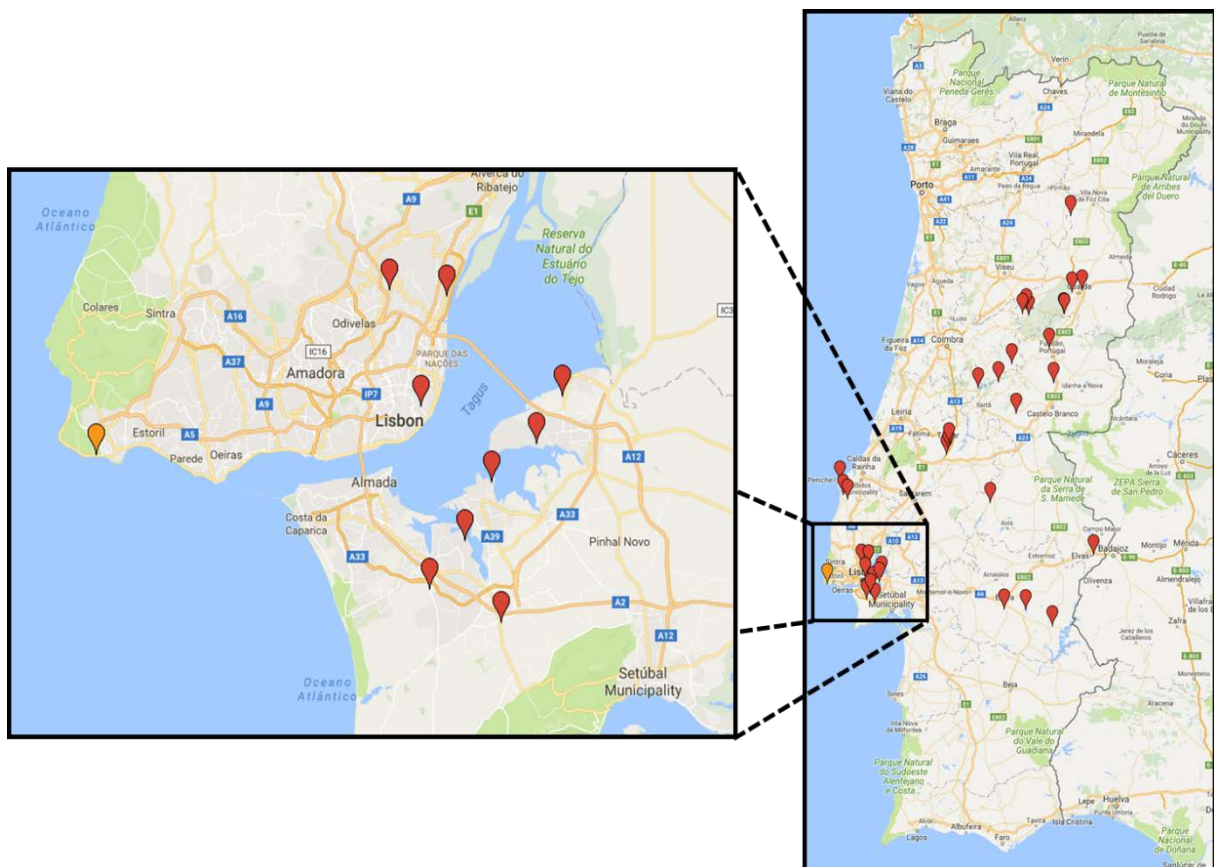


**Figure 9.02 - Location of the inspected installations.**

The main objective of the inspections was to detect anomalies in the structures, to determine the most probable causes of their occurrence and to allocate the most appropriate diagnosis and rehabilitation techniques when applicable, in order to validate the proposed system.

Another objective was to determine whether current maintenance routines were applied to the inspected structures, and to identify the characteristics of the structures, their most sensitive areas (e.g. surface/bulk, span/edge, connection) and the types of environment they were subjected to (exterior/interior, direct/indirect UV exposure).

The information gathered in the inspection forms, although comprehensive, does not indicate the location of each substructure within the installation. Thus, prior to the inspection, a detailed plant of the installation had to be obtained in order to identify the location of each of the individual

substructures to be inspected.

### **9.2.1. Inspection forms**

The inspections forms, presented in Appendix IV, are designed to contain detailed information regarding each of the substructures, and additional information on the characterization of the anomalies detected. In particular, the inspection forms contain the following elements:

- Header: the numeric code of the inspection, its date, the person responsible for it and his/her function, and its purpose;
- For each installation: its denomination; geographic location; general description; year of construction; date of posterior constructions (when applicable); type of surrounding (urban, maritime or countryside); distance from the sea; Portuguese climatic zone; construction description; contacts established; contact name; and observations;
- For each substructure: its numeric code, the picture index number, the location of the substructure; its general description; type of FRP elements used (profiles, gratings); materials used (types of fibres, and resin); type of application (structural, flooring, guardrail, staircase, other); type of connections (bolted or bonded); type(s) of pultruded profile(s) (dimensions, geometry); type(s) of grating(s); type of finishing; substructure description; chemical exposure; UV radiation exposure; exposure to rain/wind; moisture exposure; and other observations.

During the inspections some difficulties were encountered in filling out the forms, due to the scarce information provided by the original design elements. Some of the structures inspected did not seem to have a blueprint with the design and specifications of the materials applied on-site. The lack of this important information leads to an uninformed working base and does not allow interpreting the data by type of material and age.

### **9.2.2. Validation forms**

The validation forms, presented in Appendix V, were designed to gather the necessary information in order to validate the proposed inspection system. For each of the substructures inspected, the anomalies detected were registered, in accordance with the classification system presented in chapter 4. The characterization of the anomalies was made considering several parameters (when applicable), such as:

- Conditions for the anomaly progression (Y(yes)/N(no));
- Location of the anomaly detected - connection (c), span (s) or edges (e);
- Recurring anomaly (Y/N/NI(no information));
- Stabilized anomaly (Y/N/NI);
- Anomaly affecting other elements of the structure (Y/N);
- Element needing replacement (Y/N);
- Level of severity (0 - Low; 1 - Intermediate; 2 - High);

- Aesthetical appeal (0 - Low; 1 - Intermediate; 2 - High);
- Crack width/perforation depth (mm);
- Anomaly affecting the connections (Y/N).

For each of the anomalies registered in the validation form, the most probable causes detected, and the most appropriate diagnosis and rehabilitation techniques were also registered.

### 9.3. Characterization of the sample

As mentioned, during this inspection campaign, a total of 410 GFRP substructures were inspected, from 31 plants. Table 9.01 presents a description of the full sample and characteristics of the elements that were inspected.

**Table 9.01 - Sample and elements characterization**

<b>SAMPLE CHARACTERIZATION</b>	
Geographical location	Of the 31 infrastructures, 8 were located in the district of Guarda, 3 in Castelo Branco, 3 in Santarém, 1 in Leiria, 2 in Portalegre, 5 in Lisbon, 6 in Setúbal and 3 in Évora.
Infrastructure typology	9 were water treatment plants (WTP) and 22 were sewage treatment plants (STP).
General location	Of the 410 substructures, 22% were located in the interior (indoors) and 78% were on the exterior (outdoors).
Chemical exposure	3% of the sample had high chemical exposure, 13% low chemical exposure and 84% no chemical exposure.
UV exposure	79% of the sample was exposed to intense UV radiation, 16% to low UV radiation and 6% to no UV radiation.
Moisture exposure	17% of the sample was permanently dry, 81% had cycles between wet and dry and 1% was permanently wet.
Rain/wind exposure	79% of the sample was exposed to wind and rain, 5% had low exposure to wind and rain and 16% had no exposure to wind or rain.
Surroundings	14% of the sample had an urban surrounding and 86% had a rural surrounding.
Distance from the sea	19% of the sample was less than 1 km away from the sea, 13% was between 1 km and 5 km away from the sea and 68% of the sample was more than 5 km away from the sea.
<b>ELEMENTS CHARACTERIZATION</b>	
	57% of the elements inspected were made of profiles, 25% were gratings and 18% were stairs.
Elements colour	28% of the elements were yellow, 67% were grey, 1% were red and 4% were green.
Surface protection	6% of the elements had surface protection and 94% not.

The effectiveness of the validation of an inspection system is greatly dependent on the size and diversity of the information gathered from the inspected installations. The greater the representativeness of the sample, the broader the applicability of the system. In this respect, the sample used in the present field study is deemed as significant.

During the preparation of the field study, there was some difficulty in obtaining detailed design information regarding the FRP structures of the various installations. In most cases, there were no formal design elements (calculations/drawings) or material specifications. However, due to the specificities of the FRP structures analysed (relatively simple) and the anomalies they presented, the definition of the most indicated intervention strategy was generally straightforward. Based on this limitation, a “lessons learned” section was included ahead (subchapter 8.8), where the most common types of anomalies are discussed, and some constructive solutions are presented to be implemented at

the design stage.

As mentioned, in many cases it was not possible to obtain fully detailed information about the type of constituent materials. However, it was possible to conclude that all FRP elements were made of glass fibres and that virtually all of them were produced with polyester resin, due to their lower cost in comparison to other types of resin.

Figure 9.03 presents the distribution of installations and substructures per year. It shows that the distribution of the numbers of substructures and installations over the years is quite similar; moreover, the number of substructures and installations built between 2005 and 2007 is much higher (when large investments in water treatment and sewage facilities were made). It is worth referring that, for the cases where it was not possible to determine the exact age of each substructure, it was assumed to be the same as that of the installation where it is located (given the relatively short age of the various installations, this assumption is reasonable).

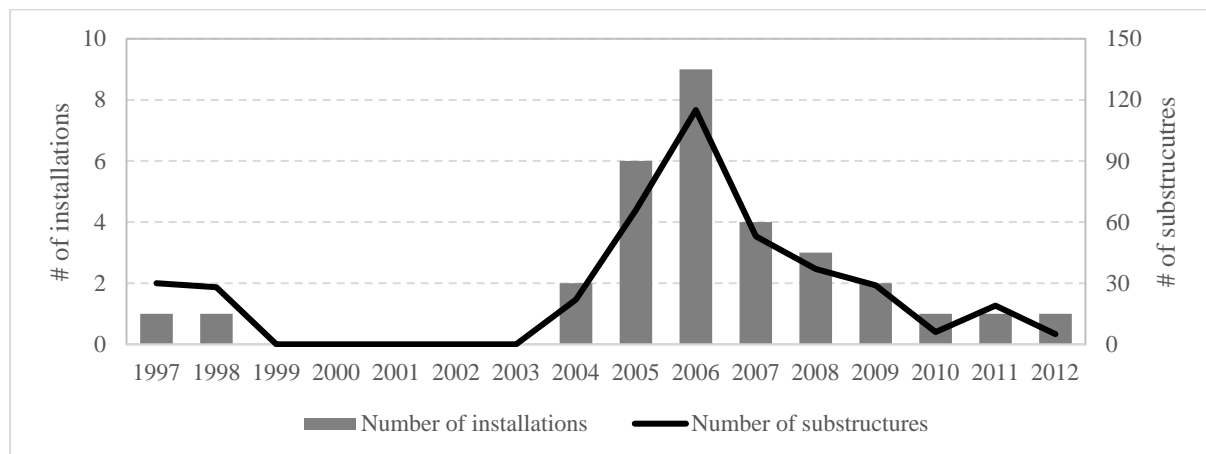


**Figure 9.03 - Distribution of installations and number of substructures per year**

## 9.4. Validation of the classification systems

The validation and data analysis presented in this study follow the classification system presented in chapters 4 to 6. All anomalies, causes, diagnosis techniques and rehabilitation techniques are thus mentioned according to their designation in the system and the relevant acronym.

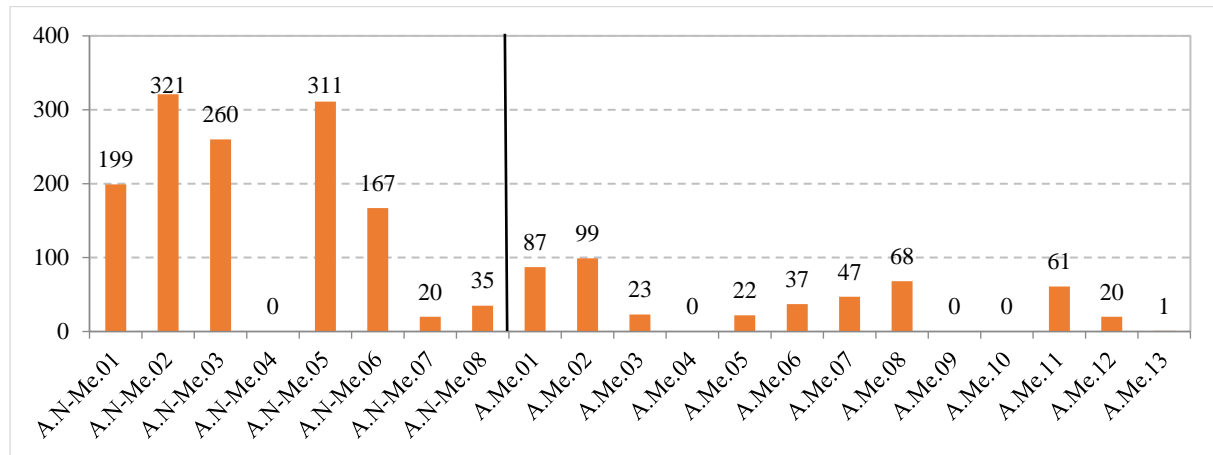
### 9.4.1. Validation and analysis of the anomalies classification system

During the inspections, a total of 1,778 anomalies were detected in the 410 substructures, resulting in an average of 4.3 anomalies per substructure. These values change in accordance with the type of substructure that was inspected - profiles, gratings or ladders - that showed an average number of 4.7, 3.6 and 4.1 anomalies per substructure, respectively. These figures are of the same order of magnitude.

Figure 9.04 and Figure 9.05 illustrate the absolute and relative frequency of occurrence of each anomaly in the 410 substructures inspected. It can be seen that there is a much higher incidence of non-mechanical anomalies, with emphasis on anomalies **A.N-Me.02** (discolouration/loss of loss), **A.N-Me.05** (stains) and **A.N-Me.03** (fibre blooming), which occur, respectively, in 78%, 76% and 63% of all

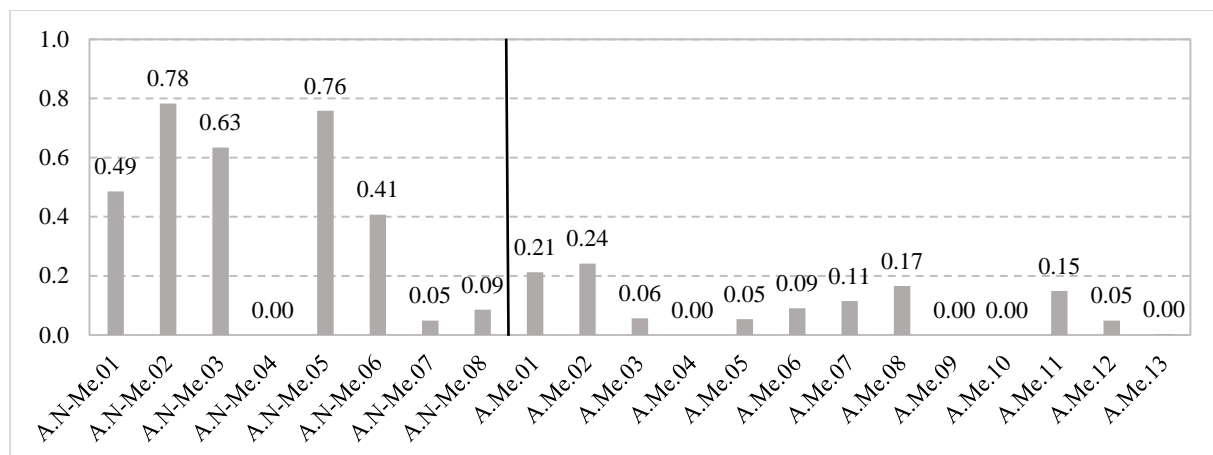
substructures.

The most common mechanical anomalies were **A.Me.02** (cracking), **A.Me.01** (corrosion of mettalic components) and **A.Me.08** (indentations/perforations), which occur respectively in 24%, 21% and 17% of all substructures.



**A.N-Me.01** - Biological colonization; **A.N-Me.02** - Discolouration/loss of gloss; **A.N-Me.03** - Fibre blooming; **A.N-Me.04** - Inclusion; **A.N-Me.05** - Stains; **A.N-Me.06** - Surface marks; **A.N-Me.07** - Wear damage; **A.N-Me.08** - Debris accumulation; **A.Me.01** - Corrosion of metallic components; **A.Me.02** - Cracking; **A.Me.03** - Crushing; **A.Me.04** - Debonding; **A.Me.05** - Delamination; **A.Me.06** -Excessive deflection; **A.Me.07** - Geometrical imperfections; **A.Me.08** - Indentation/perforation; **A.Me.09** - Incorrect curing of adhesive; **A.Me.10** - Incorrect curing of resin; **A.Me.11** - Loose connections; **A.Me.12** - Member failure; **A.Me.13** - Voids

**Figure 9.04 - Absolute frequency of occurrence of each anomaly.**



**A.N-Me.01** - Biological colonization; **A.N-Me.02** - Discolouration/loss of gloss; **A.N-Me.03** - Fibre blooming; **A.N-Me.04** - Inclusion; **A.N-Me.05** - Stains; **A.N-Me.06** - Surface marks; **A.N-Me.07** - Wear damage; **A.N-Me.08** - Debris accumulation; **A.Me.01** - Corrosion of metallic components; **A.Me.02** - Cracking; **A.Me.03** - Crushing; **A.Me.04** - Debonding; **A.Me.05** - Delamination; **A.Me.06** -Excessive deflection; **A.Me.07** - Geometrical imperfections; **A.Me.08** - Indentation/perforation; **A.Me.09** - Incorrect curing of adhesive; **A.Me.10** - Incorrect curing of resin; **A.Me.11** - Loose connections; **A.Me.12** - Member failure; **A.Me.13** - Voids

**Figure 9.05 - Frequency of occurrence of each anomaly relative to the number substructures.**

Even though anomalies generally have an independent behaviour, there are anomalies that can influence the detection or non-detection of other anomalies. As an example, fibre blooming is always preceded by loss of gloss. Biological colonization and fibre blooming can conceal superficial marks and small cracks. When considering this, even though the inspections were carried out as meticulously as possible, there may be very small discrepancies in the values obtained, by default, in the frequency

of some anomalies.

As shown in Figure 9.04, there are some anomalies that did not occur during the inspections, namely: **A.N-Me.04** (inclusions), **A.Me.04** (debonding), **A.Me.09** (incorrect curing of adhesive) and **A.Me.10** (incorrect curing of resin). Anomaly **A.N-Me.04** was not detected by the method used during the inspections (visual inspection), possibly because sometimes it only occurs in the bulk of the material. The use of other inspection methods, such as infrared thermography, would have the capability to detect such anomalies.

Anomalies **A.Me.04** (debonding) and **A.Me.09** (incorrect curing of adhesive) were not detected during the inspections because they are strictly related with bonded connections, and all the connections inspected in the sample were metallically bolted. Anomaly **A.Me.10** (incorrect curing of resin) was not detected because it reveals itself as a viscous surface without gloss after pultrusion and, during the inspection, the loss of gloss was always attributed to other causes rather than incorrect curing of the resin. Moreover, the material inspected was always hard (*i.e.*, not consistent with incorrectly cured material).

Nevertheless, these anomalies should remain in the system, so that this system can be also applied at a production stage for quality control and for structures that have bonded connections rather than bolted ones.

The anomalies classification system is thus considered validated since most anomalies were detected at least once during the inspections. The anomalies that were not detected were commented upon and kept in the system.

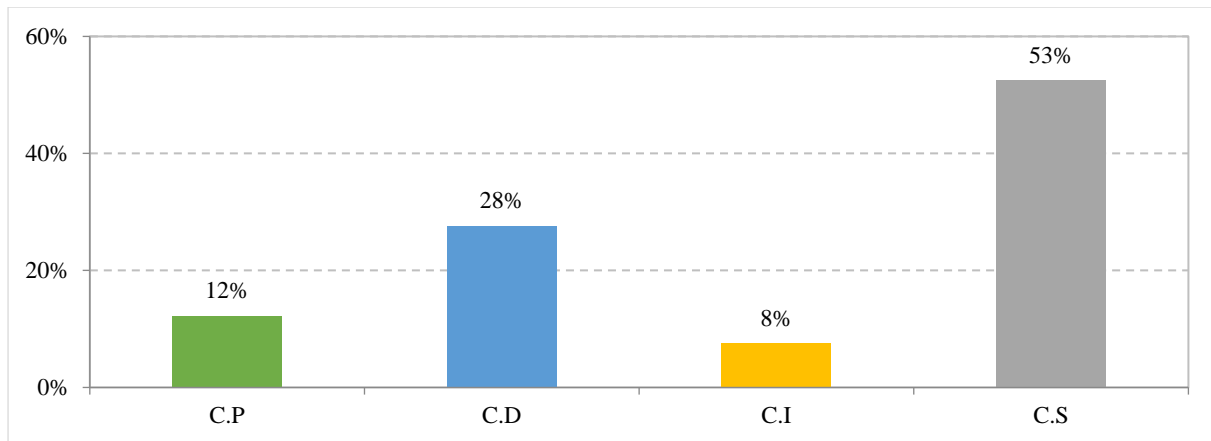
#### **9.4.2. Validation and analysis of the causes classification system**

For all anomalies, a set of possible causes was considered that could be the primary or indirect causes for the development of each anomaly. The causes were divided in four groups according to the different stages of the service life to which they correspond: production; design; installation; in-service.

As shown in Figure 9.06, the highest rate of probable causes occurs during the in-service stage of the structures, mainly because of the effect of environmental agents in the materials.

The second most frequent group of probable causes concerns the design stage. This result shows that there is still some uncertainty and lack of knowledge when designing this type of structures, especially regarding their long-term behaviour when exposed to different environmental agents. A better understanding of these materials and a correct design (in terms of cross-section, fibre architecture, additives, surface protection and construction techniques) would allow for an easier and more widespread introduction of these materials in the construction industry. The lack of widely accepted design guidance is a quite significant drawback in this regard.

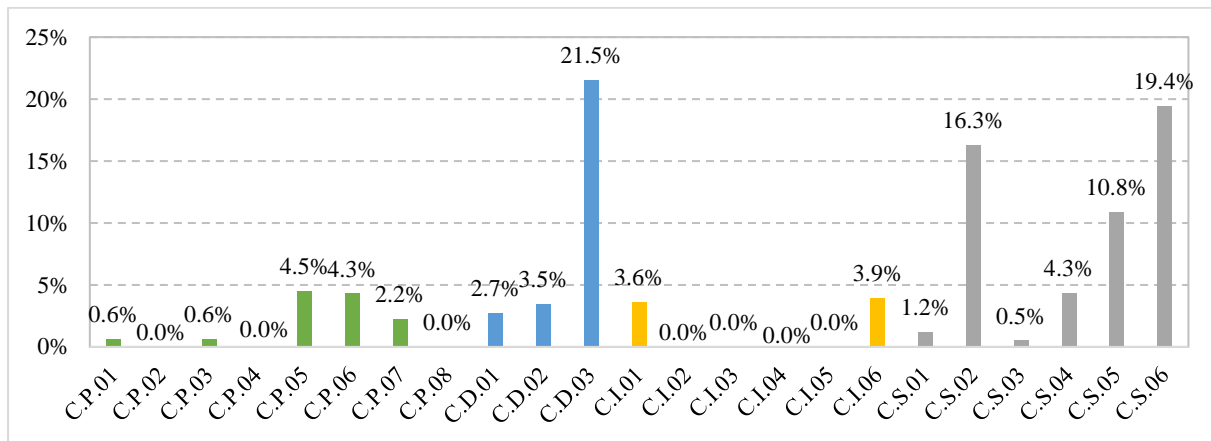
A total of 3,271 causes were associated with the 1,778 anomalies, resulting in an average of about 1.83 causes by anomaly. This value shows that most anomalies are associated with one or two causes, which have a high correlation value between them.



C.P. - Production causes; C.D. - Design causes; C.I. - Installation causes; C.S. - In-service causes.

**Figure 9.06 - Frequency of the most probable causes by groups**

When analysing the frequency of the probable causes of the anomalies detected, presented in Figure 9.07, as expected, the causes with higher frequency are the ones associated with the most common types of anomalies detected.



**C.P.01** - Incorrect cure conditions of the resin (temperature, humidity and duration); **C.P.02** - Excess of resin; **C.P.03** - Inadequate quality/ mixture/formulation of resin components; **C.P.04** - Dripped resin or small air bubbles; **C.P.05** - Inadequate maintenance/cleaning/isolation of pultrusion equipment; **C.P.06** - Incorrect layout of fibres/mats; **C.P.07** - Incorrect positioning of die metallic parts; **C.P.08** - Inadequate handling of profiles or cutting element; **C.D.01** - Inadequate structural design/material selection; **C.D.02** - Inadequate connection design /material choice; **C.D.03** - Lack of surface veil/UV additives/surface coating; **C.I.01** - Incorrect installation or prefabrication; **C.I.02** - Incorrect application of adhesive (e.g. thickness, voids, position, cure); **C.I.03** - Inadequate quality/mixture/formulation of adhesive components; **C.I.04** - Inadequate treatment of bonding surface; **C.I.05** - Incorrect temperature and/or humidity cure conditions for adhesive; **C.I.06** - Over/under tightened bolted connection; **C.S.01** - High humidity/permanently wet/excessive wet-and-dry environmental condition; **C.S.02** - Exposure to UV radiation; **C.S.03** - Exposure to chemical/saline environment; **C.S.04** - Loss of tightening/unprotected bolted connection; **C.S.05** - Vandalism/accidental impact/use wear / Change of use or inadequate use; **C.S.06** - Lack of maintenance

**Figure 9.07 - Frequency distribution of the anomalies probable causes.**

The development of discolouration/loss of gloss (**A.N-Me.02**) and fibre blooming (**A.N-Me.03**) is strictly associated with exposure to UV radiation (**C.S.02**) and lack of a surface veil / UV additives / surface coating (**C.D.03**) to protect the external surface of the materials. The high frequency of cause **C.S.06** (lack of maintenance) is mainly related with the occurrence of surface marks (**A.N-Me.06**).

There are some causes that were not registered during the inspections. These are associated with two groups: the production group and the installation group.

The causes that were not attributed to the production stage group indicate that, due to a higher

quality control, they may no longer have an active part on the occurrence of anomalies during the in-service stage (at least, for the sample included in the inspection). However, that these causes should remain in the system, in order to allow the application of the system during the production stage by the manufacturers.

The causes that were not associated with any anomaly at the inspected plants are strictly related with bonded connections, which were not detected during the inspections. However, these causes should also remain in the system, in order to allow the application of the inspection system to GFRP constructions with bonded connections.

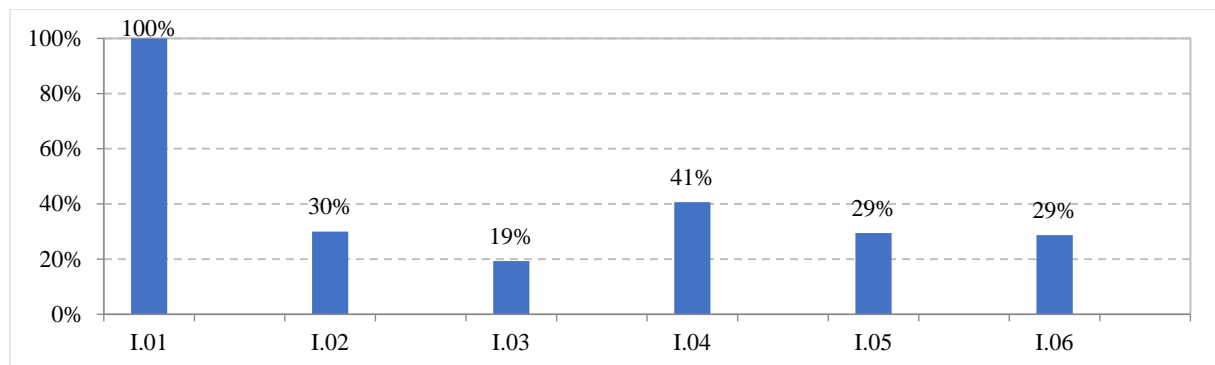
### 9.4.3. Validation and analysis of the diagnosis techniques classification system

As mentioned, the diagnosis methods chosen as part of this system should be executable *in situ* and with a low degree of complexity and should not cause damage to the construction. The objective of these criteria is to avoid the need of extremely specialized personnel or equipment and the use of complex, onerous and destructive methods. With the development of the inspection system, a total of six diagnosis techniques were considered: **I.01** - Visual inspection; **I.02** - Tap test; **I.03** - Barcol hardness measurement; **I.04** - Infrared thermography; **I.05** - Ultrasonic test, and **I.06** - Moisture meter test.

A total of 4,409 diagnosis techniques were allocated to the 1,778 detected anomalies, resulting, on average, in about 2.5 diagnosis techniques per anomaly. The total number of recommended diagnosis techniques (4,409) is higher than the number of anomalies (1,778), because for many of the anomalies more than one technique can be applied, or a combination of several techniques may be necessary for an efficient and complete diagnosis.

For all detected anomalies, visual inspection was the diagnosis technique primarily suggested, as most of the anomalies are easily detected and diagnosed, such as **A.N-Me.01** (biological colonization), **A.N-Me.02** (loss of gloss/discolouration) and **A.N-Me.03** (fibre blooming).

A conclusion to be drawn from Figure 9.08 is that all diagnosis techniques proposed in the classification system are likely to be used in GFRP elements, as they have been registered at least once during the inspections.



**I.01** - Visual inspection; **I.02** - Tap testing; **I.03** - Barcol hardness; **I.04** - Thermography; **I.05** - Ultrasonic; **I.06** - Moisture meter  
**Figure 9.08 - Frequency of suggested diagnosis techniques.**

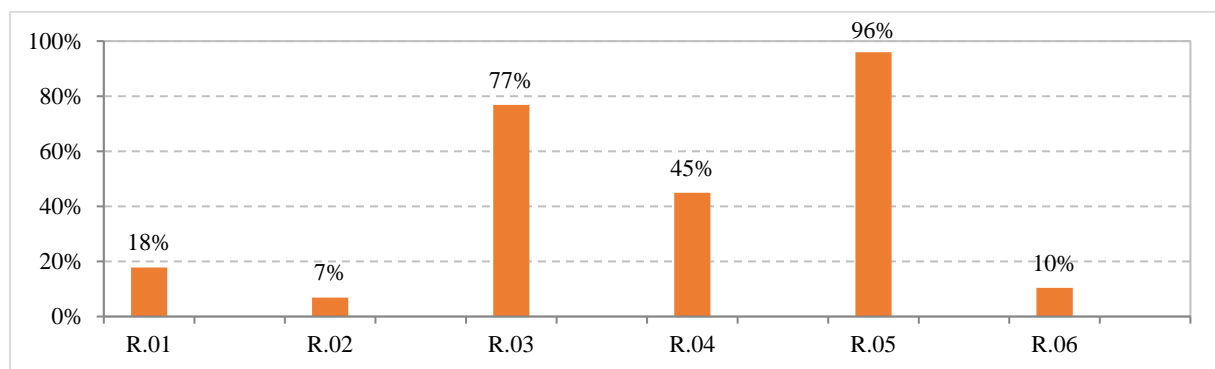
Apart from visual inspection (suggested every time), there is a relatively even distribution of the different diagnosis techniques, with a more frequent occurrence of thermography; this technique can be used in the detection of anomaly **A.N-Me.05** (stains), which has a high number of occurrences.

#### 9.4.4. Validation and analysis of the rehabilitation techniques classification system

In the inspection system, six rehabilitation techniques were considered: **R.01** - Bonding/bolting of strengthening elements; **R.02** - Strengthening with filling elements; **R.03** - Application of surface coating; **R.04** - Superficial sanding/cleaning; **R.05** - Replacement of affected element, and **R.06** - Protection/tightening of bolted connection.

In GFRP constructions there is a limited number of rehabilitation techniques due to the specific characteristics of these composite materials. Since these materials are modular, the structural members or parts can be easily replaced if necessary, rather than repaired. Figure 9.09 presents the frequency of the different rehabilitation techniques recommended, when considering the total anomalies identified in the survey. As shown in Figure 9.09, the percentage of cases where replacement of the affected element is suggested per number of anomalies (**R.05**) is high.

Due to the high number of outdoor substructures and the high frequency of anomalies related to UV radiation (**A.N-Me.01**, **A.N-Me.02** and **A.N-Me.03**), a maintenance technique such as **R.03** (application of superficial coating) is the most suitable to prevent, maintain and repair the damages that occur due to UV radiation.



**R.01** - Bonding/bolting of strengthening elements; **R.02** - Strengthening with filling elements; **R.03** - Application of surface coating; **R.04** - Superficial sanding/cleaning; **R.05** - Replacement of affected element; **R.06** - Protection/tightening of bolted connection.

**Figure 9.09 - Frequency of suggestion of the rehabilitation techniques.**

Also, a higher frequency of maintenance/cleaning (**R.04**) would help maintain, clean and protect most of the structures that were inspected and, in some cases, prevent the development of some of the most frequent anomalies, such as biological colonization (**A.N-Me.01**).

#### 9.5. Validation of the correlation matrices

During the field inspection, for each of the anomalies detected, direct and indirect causes were attributed. This allowed validating the correlation matrices, in which the previously presented criteria were used:

- 0 - if there is no correlation between the two variables;
- 1 - if there is an indirect correlation between the two variables, or an improbable direct cause;
- 2 - if there is a direct cause between the two variables.

The correlations matrices presented before have been validated and calibrated. In the following subchapters their validation process is presented.

### 9.5.1. Validation of the anomalies-causes matrix

The correlation index  $C_{ac}$  obtained from the information gathered in the field study can be determined using the following method, adapted from [II.07]:

$$(f_1 + f_2) \geq 0 \Rightarrow C_{ac} = 1 ; (f_1 > f_2) \wedge \left(f_2 > \frac{1}{3}\right) \Rightarrow C_{ac} = 2 : \text{ and } \textit{remaining cases} \Rightarrow C_{ac} = 0,$$

where  $f_i$  is the relative frequency of occurrence in which the degree of correlation 1 between the anomaly and the cause was attributed, and  $f_2$  is the relative frequency of occurrence in which the degree of correlation 2 between the anomaly and the cause was attributed.

This method allows comparing the initial values of the correlation matrix  $C_i$  and the values obtained through the data of the field inspections  $C_{ac}$ . The results of this comparison are presented in Table 9.02. The values in green represent a good agreement between the two values, the values in yellow a slight disagreement between the two values, and the values in orange a significant disagreement between the two values.

Table 9.02 shows that for 32% of the cases there was a good correlation (green), in 41% of the cases there was a slight disagreement (yellow) and in 27% of the cases there was a significant disagreement (orange). However, if the undetected anomalies (A.N-Me.04, A.Me.04, A.Me.09 and A.Me.10) are not considered those figures change to respectively 37% (good correlation, green), 45% (slight disagreement, yellow) and only 18% (significant disagreement, orange).

Table 9.03 presents the justification for the final values adopted for  $C_f$  for each of the cases where a slight (yellow) or significant (orange) disagreement was observed. The validated correlation matrix between the anomalies and causes is the one presented previously in Table 8.01.

**Table 9.02 - Comparison between the initial values of the theoretical correlation matrix  $C_t$ , and the values obtained through the data of the field inspections  $C_{ac}$ .**

CAUSES		ANOMALIES																				
		NON-MECHANICAL (A.N-Me)							MECHANICAL (A.Me)													
		01	02	03	04	05	06	07	08	01	02	03	04	05	06	07	08	09	10	11	12	13
C.P.01	$C_t$	0	2	0	0	0	1	0	0	0	2	0	0	2	0	1	0	0	2	0	0	0
	$C_{ac}$	0	1	0	0	0	0	0	0	0	0	0	0	0	0	0	0	0	0	0	0	0
C.P.02	$C_t$	0	0	0	0	0	0	0	0	0	1	0	0	0	0	0	0	0	2	0	0	0
	$C_{ac}$	0	0	0	0	0	0	0	0	0	0	0	0	0	0	0	0	0	0	0	0	0
C.P.03	$C_t$	0	1	0	0	0	0	0	0	0	1	0	0	2	0	0	0	0	2	0	0	0
	$C_{ac}$	0	1	0	0	0	0	0	0	0	0	0	0	0	0	0	0	0	0	0	0	0
C.P.04	$C_t$	0	0	0	0	0	2	0	0	0	0	0	0	0	0	0	0	0	0	0	0	2
	$C_{ac}$	0	0	0	0	0	0	0	0	0	0	0	0	0	0	0	0	0	0	0	0	2
C.P.05	$C_t$	0	0	0	2	0	1	0	0	0	0	0	0	0	0	1	0	0	0	0	0	0
	$C_{ac}$	0	0	0	0	0	1	0	0	0	0	0	0	0	0	0	0	0	0	0	0	0
C.P.06	$C_t$	0	0	0	0	0	1	0	0	0	1	0	0	2	0	0	0	0	0	0	0	1
	$C_{ac}$	0	0	1	0	0	1	0	0	0	0	0	1	0	0	0	0	0	0	0	0	1
C.P.07	$C_t$	0	0	0	0	0	2	0	0	0	0	0	0	0	0	0	0	0	0	0	0	0
	$C_{ac}$	0	0	0	0	0	1	0	0	0	0	0	0	0	0	0	0	0	0	0	0	0
C.P.08	$C_t$	0	0	0	0	0	1	1	0	0	0	0	0	0	0	2	0	0	0	0	0	0
	$C_{ac}$	0	0	0	0	0	0	0	0	0	0	0	0	0	0	0	0	0	0	0	0	0
C.D.01	$C_t$	0	0	0	0	0	0	1	0	0	2	2	0	0	2	0	1	0	0	0	1	0
	$C_{ac}$	0	0	0	0	0	0	1	0	0	1	1	0	0	1	0	0	0	0	0	2	0
C.D.02	$C_t$	0	0	0	0	0	0	0	0	2	1	0	1	0	0	2	0	0	0	0	0	0
	$C_{ac}$	0	0	0	0	0	0	0	0	1	1	0	0	0	0	0	0	0	0	0	0	0
C.D.03	$C_t$	1	1	1	0	0	0	0	0	0	0	0	0	0	0	0	0	0	0	0	0	0
	$C_{ac}$	1	1	1	0	0	0	1	0	0	0	0	0	0	0	0	0	0	0	0	0	0
C.I.01	$C_t$	0	0	0	0	0	1	0	0	0	1	0	2	0	0	2	1	0	0	0	0	1
	$C_{ac}$	0	0	0	0	0	1	0	0	0	1	0	0	1	0	2	0	0	0	0	0	0
C.I.02	$C_t$	0	0	0	0	0	0	0	0	0	2	0	2	0	0	1	0	2	0	0	0	2
	$C_{ac}$	0	0	0	0	0	0	0	0	0	0	0	0	0	0	0	0	0	0	0	0	0
C.I.03	$C_t$	0	0	0	0	0	0	0	0	0	2	0	1	0	0	0	0	2	0	0	0	2
	$C_{ac}$	0	0	0	0	0	0	0	0	0	0	0	0	0	0	0	0	0	0	0	0	0
C.I.04	$C_t$	0	0	0	0	0	0	0	0	0	0	0	2	0	0	0	0	0	0	0	0	0
	$C_{ac}$	0	0	0	0	0	0	0	0	0	0	0	0	0	0	0	0	0	0	0	0	0
C.I.05	$C_t$	0	0	0	0	0	0	0	0	0	2	0	0	0	0	0	0	2	0	0	0	0
	$C_{ac}$	0	0	0	0	0	0	0	0	0	0	0	0	0	0	0	0	0	0	0	0	0
C.I.06	$C_t$	0	0	0	0	0	0	0	0	0	2	0	0	0	0	0	0	0	0	1	1	0
	$C_{ac}$	0	0	0	0	0	0	0	0	0	1	1	0	0	0	0	0	0	0	2	0	0
C.S.01	$C_t$	1	1	0	0	2	0	0	0	1	0	0	0	0	0	0	0	0	0	0	0	0
	$C_{ac}$	1	1	0	0	1	0	0	0	1	0	0	0	0	0	0	0	0	0	0	0	0
C.S.02	$C_t$	1	2	2	0	0	0	0	0	0	0	0	0	0	0	0	0	0	0	0	0	0
	$C_{ac}$	1	2	2	0	0	0	0	0	0	0	0	0	0	0	0	0	0	0	0	0	0
C.S.03	$C_t$	0	1	1	0	0	0	0	0	1	0	0	0	0	0	0	0	0	0	0	2	0
	$C_{ac}$	0	1	1	0	0	0	0	0	0	0	0	0	0	0	0	0	0	0	0	0	0
C.S.04	$C_t$	0	0	0	0	1	0	0	0	1	0	0	0	0	0	0	2	0	0	0	0	0
	$C_{ac}$	0	0	0	0	0	0	0	0	1	0	0	0	0	0	0	0	0	0	2	0	0
C.S.05	$C_t$	0	0	0	0	1	1	2	0	0	1	1	0	1	0	0	2	0	0	0	0	0
	$C_{ac}$	0	0	0	0	1	1	1	0	0	2	2	0	0	0	1	0	0	0	0	2	0
C.S.06	$C_t$	2	0	0	0	0	1	0	2	1	0	0	0	0	0	0	0	0	0	0	1	0
	$C_{ac}$	2	0	0	0	1	0	0	2	1	0	0	0	0	0	0	0	0	0	1	0	0

\* The values in green represent a good agreement between the two values, the values in yellow a slight disagreement between the two values, and the values in orange a significant disagreement between the two values.

**Table 9.03 - Analysis, based on the sample, of the cases of discrepancy with the theoretical correlation matrix and probable causes**

( $C_t$  - theoretical correlation value;  $C_{ac}$  - correlation value from the field inspections;  $C_f$  - final correlation value)

Anomalies (no. of occurrences)	Cause	$C_t$	$C_{ac}$	$C_f$	Justification
A.N-Me.02 (321)	C.P.01	2	0	1	This cause was not detected in the sample but may be detected at the production stage.
A.N-Me.03 (260)	C.P.06	0	1	1	This cause was not initially considered as significant for this anomaly, but the shifting of the mats in the profile can lead to the occurrence of the anomaly.
A.N-Me.04 (0)	C.P.05	2	0	2	The anomaly was not detected during the inspection. The correlation value should remain the same.
A.N-Me.05 (311)	C.S.01	2	1	1	In most cases, the cause was considered to be indirect. In accordance, the value was changed.
	C.S.04	1	0	1	This cause was not detected during the inspections but should remain in the matrix since an unprotected bolted connection can allow a stain by moisture ingress.
	C.S.06	0	1	1	This cause was not initially considered as significant for this anomaly, but lack of maintenance leads to a higher number of stains.
A.N-Me.06 (168)	C.P.01	1	0	0	This cause was not detected during the inspection and appears to have no correlation with the anomaly.
	C.P.04	2	0	1	This cause was not detected during the inspection. However, an indirect correlation should be considered at the production stage.
	C.P.07	2	1	2	This cause should remain as a direct cause, since it was identified as such in several of these anomalies.
	C.P.08	1	0	0	This cause was not detected during the inspection, and appears to have no correlation with the anomaly
	C.S.06	1	0	0	have no correlation with the anomaly
A.N-Me.07 (20)	C.P.08	1	0	0	This cause was not detected during the inspection and appears to have no correlation with the anomaly.
	C.D.03	0	1	1	This cause was not initially considered for this anomaly, but lack of surface coating can accelerate the occurrence of the anomaly
	C.S.05	2	1	2	This cause should remain as a direct cause, since it was identified as such in several of these anomalies
A.Me.01 (87)	C.D.02	2	1	2	This cause should remain as a direct cause, since it was identified as such in several of these anomalies
	C.S.03	1	0	1	This cause was not detected during the inspection. However, an indirect correlation should be considered at the production stage.
A.Me.02 (99)	C.P.01	2	0	0	This cause was not detected during the inspection, and appears to have no correlation with the anomaly
	C.P.02	1	0	1	This cause was not detected during the inspection. However, an indirect correlation should be considered at the production stage.
	C.P.03	1	0	1	
	C.P.06	1	0	1	
	C.D.01	2	1	1	This cause was detected during the inspections, but never as a direct factor. Thus, an indirect correlation should be considered.
	C.I.02	2	0	2	This cause was not detected during the inspection. However, a direct correlation should be considered at the installation stage for bonded connections.
	C.I.03	2	0	2	
	C.I.05	2	0	1	
C.I.06	2	1	2	This cause should remain a direct cause, since it was identified as such in several of these anomalies	
C.S.05	1	2	2	This cause was not initially considered as a direct cause, but in accordance with the data collected, the correlation value was changed	
A.Me.03 (23)	C.D.01	2	1	1	This cause was detected during the inspections, but never as a direct factor. Thus, an indirect correlation should be considered.
	C.I.06	0	1	1	This cause was not initially considered an indirect cause, but in accordance with the data collected, the correlation value was changed
	C.S.05	1	2	2	
A.Me.04 (0)	C.D.02	1	0	1	The anomaly was not detected during the inspection. The correlation values should remain the same.
	C.I.01	2	0	2	
	C.I.02	2	0	2	
	C.I.03	1	0	1	
	C.I.04	2	0	2	

**A.N-Me.02** - Discolouration/loss of gloss; **A.N-Me.03** - Fibre blooming; **A.N-Me.04** - Inclusion; **A.N-Me.05** - Stains; **A.N-Me.06** - Surface marks; **A.N-Me.07** - Wear damage; **A.Me.01** - Corrosion of metallic components; **A.Me.02** - Cracking; **A.Me.03** - Crushing; **A.Me.04** - Debonding; **C.P.01** - Incorrect cure conditions of the resin; **C.P.02** - Excess of resin; **C.P.03** - Inadequate quality/ mixture/formulation of resin components; **C.P.04** - Dripped resin or small air bubbles; **C.P.05** - Inadequate maintenance/ cleaning/ isolation of pultrusion equipment; **C.P.06** - Incorrect layout of fibres/mats; **C.P.07** - Incorrect positioning of die metallic parts; **C.P.08** - Inadequate handling of profiles or cutting element; **C.D.01** - Inadequate structural design/material selection; **C.D.02** - Inadequate connection design /material choice; **C.D.03** - Lack of surface veil/UV additives/surface coating; **C.I.02** - Incorrect application of adhesive; **C.I.02** - Incorrect application of adhesive; **C.I.03** - Inadequate quality/mixture/formulation of adhesive components; **C.I.04** - Inadequate treatment of bonding surface; **C.I.05** - Incorrect temperature and/or humidity cure conditions for adhesive; **C.I.06** - Over/under tightened bolted connection; **C.S.01** - High humidity/permanently wet/excessive wet-and-dry environmental condition; **C.S.03** - Exposure to chemical/saline environment; **C.S.04** - Loss of tightening/unprotected bolted connection; **C.S.05** - Vandalism / Accidental impact / Use wear/change of use or improper use; **C.S.06** - Lack of maintenance

**Table 9.03 - Analysis, based on the sample, of the cases of discrepancy with the theoretical correlation matrix and probable causes (continued).**

( $C_t$  - theoretical correlation value;  $C_{ac}$  - correlation value from the field inspections;  $C_f$  - final correlation value)

Anomalies (no. of occurrences)	Cause	$C_t$	$C_{ac}$	$C_f$	Justification
A.Me.05 (22)	C.P.01	2	0	1	This cause was not detected during the inspection. However, an indirect correlation should be considered at the production phase.
	C.P.03	2	0	1	This cause was not detected during the inspection. However, an indirect correlation should be considered at the production phase.
	C.P.06	2	1	1	This cause was detected during the inspections, but never as a direct factor. Thus, an indirect correlation should be considered.
	C.I.01	0	1	1	This cause was not initially considered an indirect cause, but in accordance with the data collected, the correlation value was changed
A.Me.06 (37)	C.D.01	2	1	2	This cause should remain a direct cause, since it was identified as such in several of these anomalies
	C.S.05	1	0	1	This cause was not detected during the inspection. However, an indirect correlation should be considered at the in-service stage.
A.Me.07 (47)	C.P.01	1	0	0	This cause was not detected during the inspection and appears to have no correlation with the anomaly.
	C.P.05	1	0	1	This cause was not detected during the inspection. However, an indirect correlation should be considered at the production stage.
	C.P.08	2	0	0	This cause was not detected during the inspection and appears to have no correlation with the anomaly.
	C.D.02	2	0	1	This cause was not detected during the inspection. However, an indirect correlation should be considered at the design phase.
	C.I.02	1	0	0	This cause was not detected during the inspection and appears to have a low correlation with the anomaly.
A.Me.08 (68)	C.D.01	1	0	1	This cause was not detected during the inspection. However, an indirect correlation should be considered at the design phase.
	C.I.01	1	0	1	This cause was not detected during the inspection. However, an indirect correlation should be considered at the installation stage.
	C.S.04	2	0	0	This cause was not detected during the inspection and appears to have a low correlation with the anomaly.
	C.S.05	2	1	2	This cause should remain a direct cause, since it was identified as such in several of these anomalies
A.Me.09 (0)	C.I.02	2	0	2	The anomaly was not detected during the inspection. The correlation values should remain the same.
	C.I.03	2	0	2	
	C.I.05	2	0	2	
A.Me.10 (0)	C.P.01	2	0	2	The anomaly was not detected during the inspection. The correlation values should remain the same.
	C.P.02	2	0	2	
	C.P.03	2	0	2	
A.Me.11 (61)	C.I.06	1	2	2	This cause was not initially considered a direct cause, but in accordance with the data collected, the correlation value was changed
	C.S.04	0	2	2	This cause was not initially considered an indirect cause, but in accordance with the data collected, the correlation value was changed
	C.S.06	0	1	1	This cause was not initially considered an indirect cause, but in accordance with the data collected, the correlation value was changed
A.Me.12 (20)	C.D.01	1	2	2	This cause was not initially considered a direct cause, but in accordance with the data collected, the correlation value was changed
	C.I.06	1	0	1	This cause was not detected during the inspection. However, an indirect correlation should be considered at the installation stage.
	C.S.03	2	0	1	This cause was not detected during the inspection. However, an indirect correlation should be considered at the design phase.
	C.S.05	0	2	2	This cause was not initially considered a direct cause, but in accordance with the data collected, the correlation value was changed
	C.S.06	1	0	1	This cause was not detected during the inspection. However, an indirect correlation should be considered at the installation stage.
A.Me.13 (1)	C.I.01	1	0	0	This cause was not detected during the inspection, and appears to have no correlation with the anomaly.
	C.I.02	2	0	2	This cause associated with this anomaly was not detected during the inspection, due to lack of bonded connections in the sample.
	C.I.03	2	0	2	The correlation values should remain the same.

**A.Me.05** - Delamination; **A.Me.06** -Excessive deflection; **A.Me.07** - Geometrical imperfections; **A.Me.08** - Indentation/perforation; **A.Me.09** - Incorrect curing of adhesive; **A.Me.10** - Incorrect curing of resin; **A.Me.11** - Loose connections; **A.Me.12** - Member failure; **A.Me.13** - Voids; **C.P.01** - Incorrect cure conditions of the resin; **C.P.02** - Excess of resin; **C.P.03** - Inadequate quality/ mixture/formulation of resin components; **C.P.05** - Inadequate maintenance/ cleaning/ isolation of pultrusion equipment; **C.P.06** - Incorrect layout of fibres/mats; **C.P.08** - Inadequate handling of profiles or cutting element; **C.D.01** - Inadequate structural design/material selection; **C.D.02** - Inadequate connection design /material choice; **C.I.01** - Incorrect installation or prefabrication; **C.I.02** - Incorrect application of adhesive; **C.I.03** - Inadequate quality/mixture/formulation of adhesive components; **C.I.05** - Incorrect temperature and/or humidity cure conditions for adhesive; **C.I.06** - Over/under tightened bolted connection; **C.S.01** - High humidity/permanently wet/excessive wet-and-dry environmental condition; **C.S.03** - Exposure to chemical/saline environment; **C.S.04** - Loss of tightening/unprotected bolted connection; **C.S.05** - Vandalism / Accidental impact / Use wear/change of use or improper use; **C.S.06** - Lack of maintenance

### 9.5.2. Validation of the inter-anomalies matrix

With the changes made in the correlation matrix anomalies - probable causes a new inter-anomalies correlation matrix was obtained (Table 8.03). The comparison between the two inter-anomalies matrices is presented in Table 9.04. In that table, for the correlation between the two anomalies, the upper value was obtained from the theoretical values of the anomalies-causes matrix, and the lower value was obtained from the validated anomalies-causes matrix.

**Table 9.04 - Comparison between the theoretical ( $C_{\%kj}^{theoric}$ ) and validated ( $C_{\%kj}^{validated}$ ) inter-anomalies matrix**

		A.N-Me.01	A.N-Me.02	A.N-Me.03	A.N-Me.04	A.N-Me.05	A.N-Me.06	A.N-Me.07	A.N-Me.08	A.Me.01	A.Me.02	A.Me.03	A.Me.04	A.Me.05	A.Me.06	A.Me.07	A.Me.08	A.Me.09	A.Me.10	A.Me.11	A.Me.12	A.Me.13
A.N-Me.01	$C_{\%kj}^{theoric}$	0	25	38	0	25	9	0	100	25	0	0	0	0	0	0	0	0	0	0	20	0
	$C_{\%kj}^{validated}$	0	25	30	0	38	0	13	83	25	0	0	0	0	0	0	0	0	0	20	14	0
A.N-Me.02	$C_{\%kj}^{theoric}$	40	0	75	0	25	9	0	0	17	14	0	0	43	0	11	0	0	50	0	20	0
	$C_{\%kj}^{validated}$	40	0	60	0	13	11	13	17	17	3	0	0	38	0	0	0	0	50	0	7	0
A.N-Me.03	$C_{\%kj}^{theoric}$	30	38	0	0	0	0	0	0	8	0	0	0	0	0	0	0	0	0	0	20	0
	$C_{\%kj}^{validated}$	30	38	0	0	0	6	13	17	8	3	0	0	13	0	0	0	0	0	0	7	8
A.N-Me.04	$C_{\%kj}^{theoric}$	0	0	0	0	0	9	0	0	0	0	0	0	0	0	11	0	0	0	0	0	0
	$C_{\%kj}^{validated}$	0	0	0	0	0	11	0	0	0	0	0	0	0	0	25	0	0	0	0	0	0
A.N-Me.05	$C_{\%kj}^{theoric}$	20	13	0	0	0	5	25	0	25	3	17	0	7	0	0	33	0	0	0	0	0
	$C_{\%kj}^{validated}$	30	6	0	0	0	11	50	33	17	13	50	0	0	50	0	50	0	0	10	36	0
A.N-Me.06	$C_{\%kj}^{theoric}$	20	13	0	50	13	0	38	50	8	14	17	13	36	0	33	25	0	17	0	10	38
	$C_{\%kj}^{validated}$	0	13	10	50	25	0	25	0	0	13	25	11	38	25	38	38	0	17	0	14	25
A.N-Me.07	$C_{\%kj}^{theoric}$	0	0	0	0	25	14	0	0	0	11	67	0	14	50	11	42	0	0	0	10	0
	$C_{\%kj}^{validated}$	10	6	10	0	50	11	0	17	0	17	63	0	0	75	0	63	0	0	0	43	0
A.N-Me.08	$C_{\%kj}^{theoric}$	40	0	0	0	0	9	0	0	17	0	0	0	0	0	0	0	0	0	0	20	0
	$C_{\%kj}^{validated}$	50	6	10	0	25	0	13	0	17	0	0	0	0	0	0	0	0	0	20	14	0
A.Me.01	$C_{\%kj}^{theoric}$	30	13	13	0	38	5	0	50	0	6	0	13	0	0	22	17	0	0	0	30	0
	$C_{\%kj}^{validated}$	30	13	10	0	25	0	0	33	0	7	0	11	0	0	25	0	0	0	30	14	0
A.Me.02	$C_{\%kj}^{theoric}$	0	31	0	0	13	23	50	0	17	0	83	56	64	100	44	42	100	67	100	40	63
	$C_{\%kj}^{validated}$	0	6	10	0	50	22	63	0	17	0	88	56	38	75	38	75	83	33	40	57	58
A.Me.03	$C_{\%kj}^{theoric}$	0	0	0	0	13	5	50	0	0	14	0	0	7	100	0	33	0	0	0	20	0
	$C_{\%kj}^{validated}$	0	0	0	0	50	11	63	0	0	23	0	0	0	75	0	63	0	0	20	50	0
A.Me.04	$C_{\%kj}^{theoric}$	0	0	0	0	0	9	0	0	17	25	0	0	0	0	44	17	50	0	0	0	50
	$C_{\%kj}^{validated}$	0	0	0	0	0	11	0	0	17	33	0	0	25	0	63	25	67	0	0	0	42
A.Me.05	$C_{\%kj}^{theoric}$	0	38	0	0	13	23	25	0	0	25	17	0	0	0	11	17	0	67	0	0	13
	$C_{\%kj}^{validated}$	0	19	10	0	0	17	0	0	0	10	0	11	0	0	25	13	0	33	0	0	8
A.Me.06	$C_{\%kj}^{theoric}$	0	0	0	0	0	0	25	0	0	11	67	0	0	0	0	17	0	0	0	20	0
	$C_{\%kj}^{validated}$	0	0	0	0	25	6	38	0	0	10	38	0	0	0	0	38	0	0	0	29	0
A.Me.07	$C_{\%kj}^{theoric}$	0	13	0	50	0	27	25	0	33	22	0	50	14	0	0	17	17	17	0	0	25
	$C_{\%kj}^{validated}$	0	0	0	50	0	17	0	0	17	10	0	28	25	0	0	25	0	0	0	0	0
A.Me.08	$C_{\%kj}^{theoric}$	0	0	0	0	50	14	63	0	17	14	67	13	14	50	11	0	0	0	0	10	6
	$C_{\%kj}^{validated}$	0	0	0	0	50	17	63	0	0	20	63	11	13	75	25	0	0	0	0	43	0
A.Me.09	$C_{\%kj}^{theoric}$	0	0	0	0	0	0	0	0	0	33	0	38	0	0	11	0	0	0	0	0	50
	$C_{\%kj}^{validated}$	0	0	0	0	0	0	0	0	0	33	0	44	0	0	0	0	0	0	0	0	50
A.Me.10	$C_{\%kj}^{theoric}$	0	38	0	0	0	9	0	0	0	22	0	0	57	0	11	0	0	0	0	0	0
	$C_{\%kj}^{validated}$	0	38	0	0	0	11	0	0	0	13	0	0	50	0	0	0	0	0	0	0	0
A.Me.11	$C_{\%kj}^{theoric}$	0	0	0	0	0	0	0	0	0	6	0	0	0	0	0	0	0	0	0	10	0
	$C_{\%kj}^{validated}$	20	0	0	0	13	0	0	33	25	13	25	0	0	0	0	0	0	0	0	21	0
A.Me.12	$C_{\%kj}^{theoric}$	20	13	25	0	0	5	13	50	25	11	33	0	0	50	0	8	0	0	50	0	0
	$C_{\%kj}^{validated}$	20	6	10	0	63	11	75	33	17	27	88	0	0	100	0	75	0	0	30	0	0
A.Me.13	$C_{\%kj}^{theoric}$	0	0	0	0	0	27	0	0	0	28	0	50	14	0	22	8	67	0	0	0	0
	$C_{\%kj}^{validated}$	0	0	10	0	0	17	0	0	0	23	0	28	13	0	0	0	50	0	0	0	0

\* The values in green represent a good agreement between the two values, the values in yellow a slight disagreement between the two values, and the values in orange a significant disagreement between the two values.

In order to better visualize the adjustments that were made, the matrix was divided in four colours: white (difference between the coefficients lower than 10%); green (difference between the coefficients between 10% and 25%); yellow (difference between the coefficients between 25% and 50%) and orange (difference between the coefficients higher than 50%).

Table 9.04 indicates that in 73% of the cases the adjustment is considered very good (difference lower than 10%), in 18% of the cases it was considered good (differences between 10% and 25%), in 7% of the cases it was considered reasonable (differences between 25% and 50%) and in only 1% of the cases it was considered bad (difference higher than 50%). These results validate the inter-anomalies correlation.

## 9.6. Data analysis

### 9.6.1. Anomaly frequency

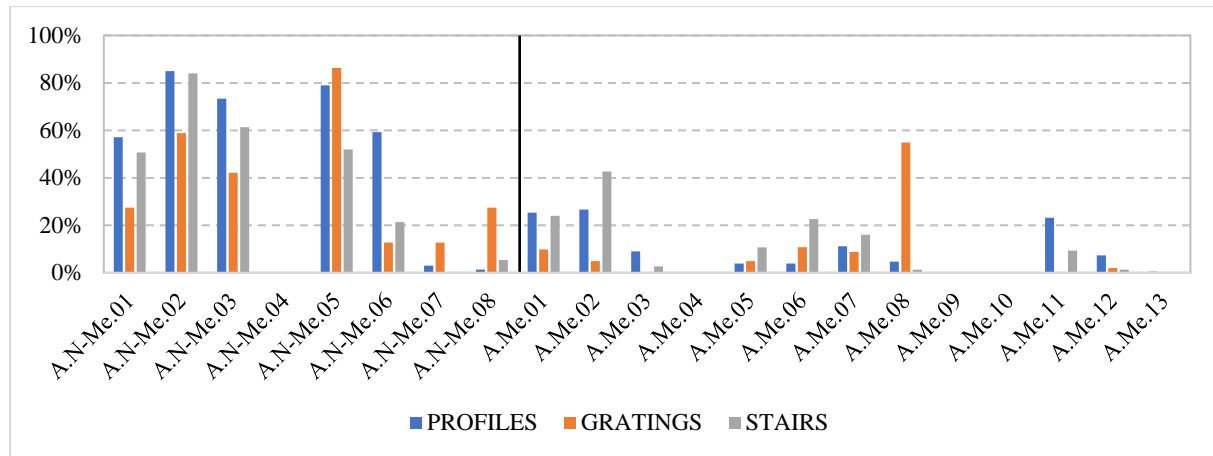
By comparing the type of substructure with the frequency of each anomaly (Figure 9.10), structures made of GFRP profiles present a similar frequency of non-mechanical anomalies to the other types of substructures (profiles - 76%, gratings - 74%, stairs - 68%). Nevertheless, the location (vertical, handrails, ground/floor) of the structures is relevant to the type of anomalies that may occur.

Grating structures present a much higher occurrence of anomalies **A.N-Me.08** (debris accumulation) and **A.Me.08** (indentation) than the other types of substructures. Anomaly **A.N-Me.08** has a higher frequency in this particular type of structure due to the geometry of the grating components and its location at a ground/floor level, which allows a much easier accumulation of debris (namely in the grid spaces), especially at the support points. Anomaly **A.Me.08** is also related with the location of this type of substructure - being at the floor level, these structures suffer a larger number of impacts, leading to a higher number of indentations. Also, due to their orientation (horizontal) and location (floor), gratings present a higher ratio of stains (**A.N-Me.05**), due to spills and/or water accumulation.

When analysing the anomalies that occur in stairs, there is a much higher occurrence of **A.Me.02** (cracking) and **A.Me.06** (excessive deflection) than in other types of structures; in fact, these two anomalies can be related, since most of the cracking found in stairs were located at connection points, which can be related to the excessive deflection of these structures. Most of the stair structures are installed vertically (as shown in Figure 9.01 (f), parallel to the wall). In these cases, the distance between vertical fastenings is sometimes excessive and the stair structure has a low inertia to perpendicular movements, deflecting very easily. This may contribute to a higher occurrence of cracking in the vertical profiles next to the fastenings as presented in Figure 5.10 (a). A reduction of the distance between fastenings, or a more robust vertical profile would help decreasing the occurrence of this anomaly in this type of structure. There are already dimensioning guidelines that should be applied in the design of new structures.

There are some anomalies that occur almost exclusively in some types of substructures such as anomalies **A.N-Me.08**, **A.Me.08** and **A.Me.11** (loose connections), and there are some others that do not occur at all or have a very low incidence in different types of substructures - **A.Me.03** (cracking), **A.Me.12** (member failure) and **A.Me.13** (voids). The anomaly **A.Me.11** only occurs in the connections of the profiles and stairs structures, but not in grating structures, because most of these are simply

supported at their borders. The anomalies **A.Me.12** and **A.Me.13** have a very low incidence, the former due to the gravity of the anomaly when detected (usually the structure has already been removed or repaired), and the latter due to the difficulty of detection of the anomaly by visual inspection.



**A.N-Me.01** - Biological colonization; **A.N-Me.02** - Discolouration/loss of gloss; **A.N-Me.03** - Fibre blooming; **A.N-Me.04** - Inclusion; **A.N-Me.05** - Stains; **A.N-Me.06** - Surface marks; **A.N-Me.07** - Wear damage; **A.N-Me.08** - Debris accumulation; **A.Me.01** - Corrosion of mettalic components; **A.Me.02** - Cracking; **A.Me.03** - Crushing; **A.Me.04** - Debonding; **A.Me.05** - Delamination; **A.Me.06** -Excessive deflection; **A.Me.07** - Geometrical imperfections; **A.Me.08** - Indentation/perforation; **A.Me.09** - Incorrect curing of adhesive; **A.Me.10** - Incorrect curing of resin; **A.Me.11** - Loose connections; **A.Me.12** - Member failure; **A.Me.13** - Voids

**Figure 9.10 - Frequency of occurrence of each anomaly per type of substructures.**

### 9.6.2. Anomaly severity level

Even though an anomaly can occur in many of the substructures, its severity level will not necessarily be constant. In this inspection system, the severity levels are five, between 0 and 4, with the following meaning: 0 - Not concerning severity level, and the evolution of the anomaly must be monitored; 1 - Medium-to-low level of concern, and the evolution of the anomaly must be monitored; 2 - Needs medium-term intervention in up to one year; 3 - Medium-to-high level of concern, with a need for intervention in up to six months; and 4 - high level of concern with a need for immediate intervention in up to three months.

The severity level and the classification parameters are different for every anomaly, and not all of them range the five severity levels. As an example, anomaly **A.Me.02** (cracking) is categorized according to the following parameters: (i) crack width (mm); (ii) location of the anomaly (mid-span, matrix, adhesive, connection); (iii) conditions for progression of the anomaly; and (iv) aesthetical significance of the element.

With those parameters, the anomaly **A.Me.02** can be categorized in the following five severity levels: 0 - crack width lower than 0.5 mm with no conditions for progression and low aesthetical significance of the element; 1 - crack width lower than 0.5 mm with no conditions for progression and high aesthetical significance of the element; 2 - mapped cracking; crack width lower than 0.5 mm with conditions for progression; 3 - crack width higher than 0.5 mm with no conditions for progression; 4 - crack width higher than 0.5 mm with conditions for progression. Figure 9.11 presents an example of each of the severity levels of anomaly **A.Me.02**.

In total, anomaly **A.Me.02** was detected 99 times, with the following distribution of severity

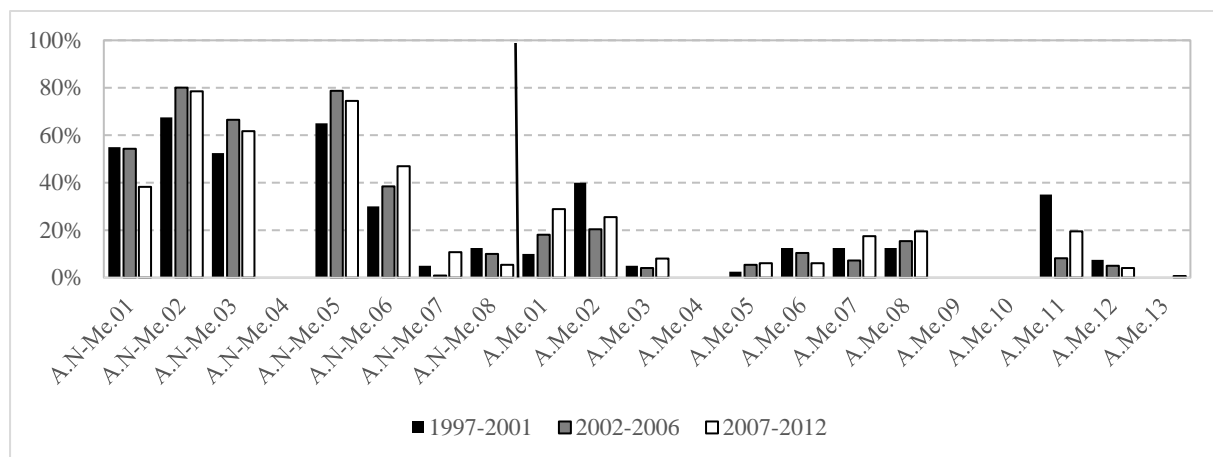
levels: 15% in level 0, 33% in level 1, 31% in level 2, 8% in level 3 and 12% in level 4.



**Figure 9.11 - Severity levels of anomaly A.Me.02.**

### 9.6.3. Influence of age on anomaly occurrence

The frequency of occurrence of each anomaly per substructure when considering the respective age is compared in Figure 9.12. The results show that, as expected, the occurrence of some the most common non-mechanical anomalies is less frequent in more recent structures: **A.N-Me.01** (biological colonization), **A.N-Me.02** (discolouration/loss of gloss) and **A.N-ME.03** (fibre blooming). This is naturally due to the gradual development of these anomalies. However, this trend is not so clear when considering older structures, possibly due to the smaller number of older substructures in the sample and/or due to inherent characteristics of the FRP materials applied before (different compositions of fillers and resins in the matrix).



**A.N-Me.01** - Biological colonization; **A.N-Me.02** - Discolouration/loss of gloss; **A.N-Me.03** - Fibre blooming; **A.N-Me.04** - Inclusion; **A.N-Me.05** - Stains; **A.N-Me.06** - Surface marks; **A.N-Me.07** - Wear damage; **A.N-Me.08** - Debris accumulation; **A.Me.01** - Corrosion of mettalic components; **A.Me.02** - Cracking; **A.Me.03** - Crushing; **A.Me.04** - Debonding; **A.Me.05** - Delamination; **A.Me.06** - Excessive deflection; **A.Me.07** - Geometrical imperfections; **A.Me.08** - Indentation/perforation; **A.Me.09** - Incorrect curing of adhesive; **A.Me.10** - Incorrect curing of resin; **A.Me.11** - Loose connections; **A.Me.12** - Member failure; **A.Me.13** - Voids

**Figure 9.12 - Frequency of occurrence of each anomaly per time period.**

Anomalies **A.N-Me.06** (surface marks) and **A.N-Me.07** (wear damage) seem to occur more frequently in more recent structures, which *a priori* could be considered as an unexpected result. This can be explained by the recent increase of application of grating substructures, where these anomalies occur more frequently.

When considering mechanical anomalies, the frequency of anomaly **A.Me.01** (corrosion of mettalic components) was expected to increase significantly with age, due to the longer exposure to environmental agents of metallic components used in FRP connections. However, the results obtained show an opposite trend and the explanation is as follows: in older structures, the connections between elements was frequently made with plastic elements instead of mettalic ones, and the application of mettalic connections has increased in recent years; quite often the mettalic elements applied are not the most suitable for these structures, in

particular the ones exposed to more aggressive environments (where stainless steel is not always used).

There is also a significant increase in the frequency of occurrence of the anomalies **A.Me.02** (cracking) and **A.Me.11** (loose connections) with age; this result is logical, as older structures have higher probability of suffering from accidental impacts, wear, change of use, loss of tightening or simply ageing of the materials.

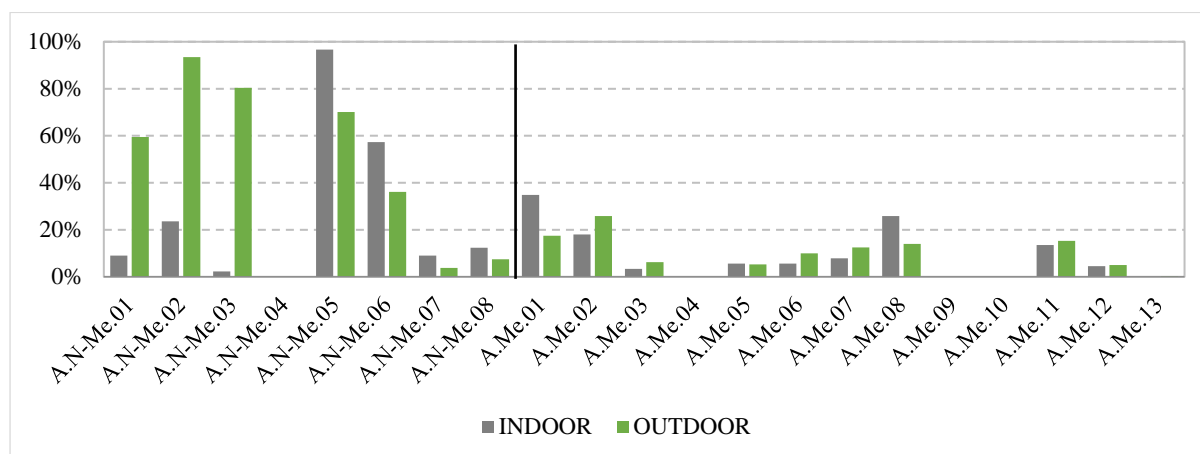
For some mechanical anomalies, **A.Me.05** (delamination), **A.Me.06** (excessive deflection) **A.Me.07** (geometrical imperfections) and **A.Me.08** (indentation/perforation), the frequency of occurrence is relatively constant for FRP structures with different ages. This is possibly due to the fact that these anomalies are usually associated with design, production or installation causes, and therefore they do not present an evolutive nature, and also because FRP construction techniques and design practice did not change significantly during the period under analysis.

## 9.7. Analysis of anomalies in different environmental conditions

### 9.7.1. Indoor and outdoor location

When analysing the differences between the anomalies that occur in indoor substructures (inside a building), and those that occur in outdoor substructures, as shown in Figure 9.13, there is a considerable difference on the frequency of non-mechanical anomalies.

In outdoor substructures, as expected, the development of UV-related anomalies - **A.N-Me.02** (discolouration/loss of gloss) and **A.N-ME.03** (fibre blooming) - has a much higher incidence when compared to indoor structures. Also, the exposure to wet and dry cycles (rain) in outdoor structures leads to a much higher incidence of anomaly **A.N-Me.01** (biological colonization), which is also logical, whereas the lack of wet and dry cycles (due to rain) in indoor structures leads to a higher incidence of anomaly **A.N-Me.05** (stains).



**A.N-Me.01** - Biological colonization; **A.N-Me.02** - Discolouration/loss of gloss; **A.N-Me.03** - Fibre blooming; **A.N-Me.04** - Inclusion; **A.N-Me.05** - Stains; **A.N-Me.06** - Surface marks; **A.N-Me.07** - Wear damage; **A.N-Me.08** - Debris accumulation; **A.Me.01** - Corrosion of mettalic components; **A.Me.02** - Cracking; **A.Me.03** - Crushing; **A.Me.04** - Debonding; **A.Me.05** - Delamination; **A.Me.06** -Excessive deflection; **A.Me.07** - Geometrical imperfections; **A.Me.08** - Indentation/perforation; **A.Me.09** - Incorrect curing of adhesive; **A.Me.10** - Incorrect curing of resin; **A.Me.11** - Loose connections; **A.Me.12** - Member failure; **A.Me.13** - Voids

**Figure 9.13 - Frequency of occurrence of each anomaly by indoor and outdoor substructures.**

In the case of anomaly **A.N.Me.06** (superficial marks), there is a higher frequency in indoor structures. Even though this anomaly was more frequently observed in indoor structures, in outdoor

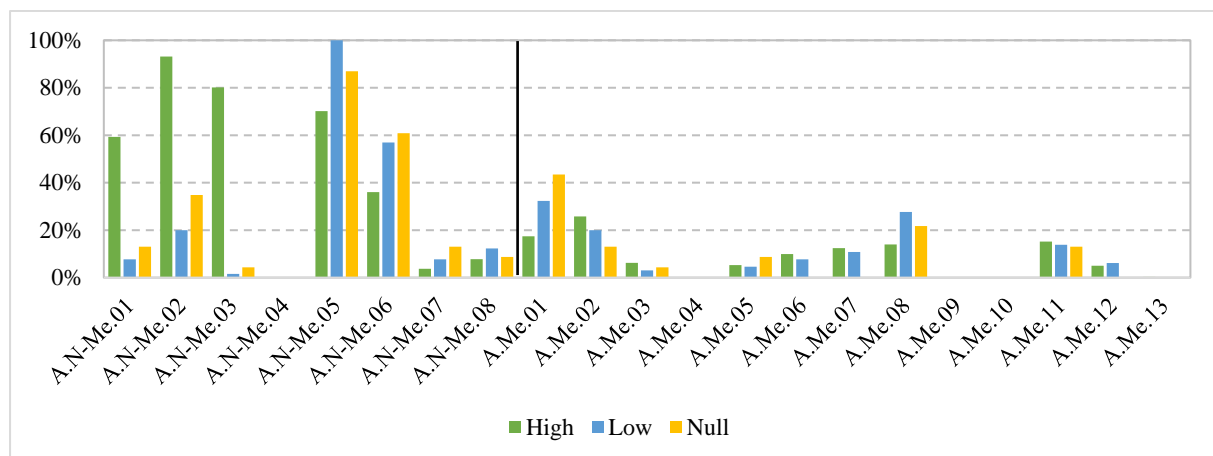
structures the detection of this anomaly can be restricted by other anomalies, such as biological colonization and fibre blooming.

When analysing mechanical anomalies, the difference between the incidence of anomalies that occur in indoor and outdoor structures is not significant. This should be attributed to the overall good weathering resistance (i.e. little changes in mechanical properties) of GFRP composite materials.

### 9.7.2. Exposure to ultra violet radiation

Figure 9.14 compares the behaviour of the substructures in terms of type of exposure to UV radiation. There is a much higher incidence of anomalies **A.N-Me.01** (biological colonization), **A.N-Me.02** (discolouration/loss of gloss) and **A.N-Me.03** (fibre blooming) in exposure environments with high UV radiation, when compared to other exposure environments. This was an expected result, since these anomalies are directly related to exposure to sunlight (for biological development) and degradation of the profiles matrix by UV radiation, respectively.

The more frequent occurrence of anomaly **A.Me.02** (cracking) under high exposure to UV radiation is related to the fact that, as shown in Figure 9.13, this anomaly occurs more frequently in substructures located outdoors. Even though exposure to UV radiation can make the materials' matrix more fragile and more susceptible to cracking, it is not considered to be the most relevant contribution to the development of this anomaly outdoor, but rather the occurrence of accidental impacts and mainly to the over tightening of the bolts at the connection points, because of the type of installation system applied (shown in Figure 5.10 a, b and c).



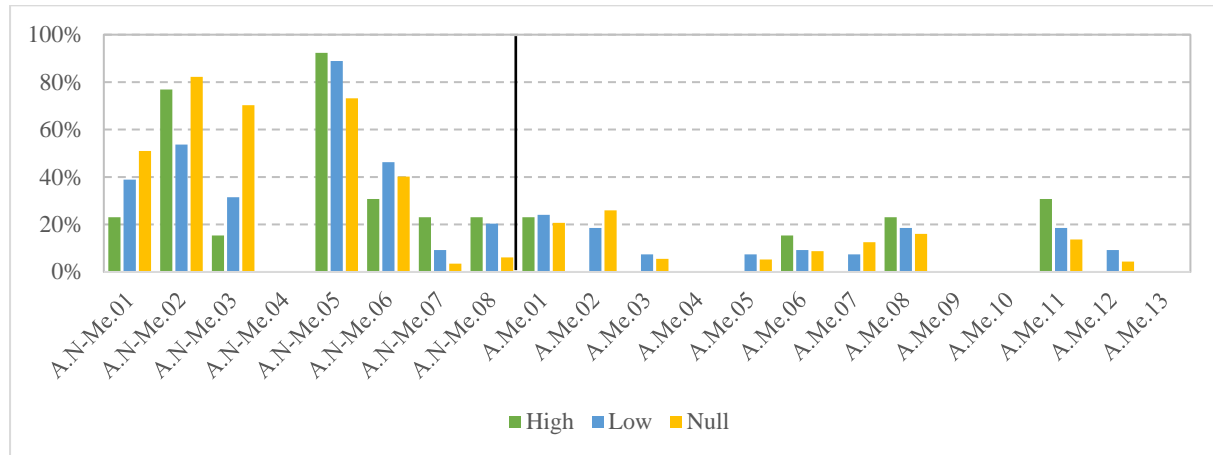
**A.N-Me.01** - Biological colonization; **A.N-Me.02** - Discolouration/loss of gloss; **A.N-Me.03** - Fibre blooming; **A.N-Me.04** - Inclusion; **A.N-Me.05** - Stains; **A.N-Me.06** - Surface marks; **A.N-Me.07** - Wear damage; **A.N-Me.08** - Debris accumulation; **A.Me.01** - Corrosion of mettalic components; **A.Me.02** - Cracking; **A.Me.03** - Crushing; **A.Me.04** - Debonding; **A.Me.05** - Delamination; **A.Me.06** -Excessive deflection; **A.Me.07** - Geometrical imperfections; **A.Me.08** - Indentation/perforation; **A.Me.09** - Incorrect curing of adhesive; **A.Me.10** - Incorrect curing of resin; **A.Me.11** - Loose connections; **A.Me.12** - Member failure; **A.Me.13** - Voids

**Figure 9.14 - Frequency of occurrence of each anomaly according to exposure (high/low/nil) to UV radiation.**

Anomalies **A.Me.06** (excessive deflection), **A.Me.07** (geometrical imperfections) and **A.Me.12** (member failure) were not detected in the environments with no exposure to UV radiation. Naturally, the lack of observation of these anomalies in this type of environment should not be attributed to the specific conditions in indoor environment (with no natural lighting), but rather to the small significance of this environment in the sample (6% of all substructures).

### 9.7.3. Exposure to chemical environments

Figure 9.15 compares the anomalies that occur under exposure to different types of chemical environments. Non-mechanical anomalies in substructures exposed to high chemical aggressiveness are those that present a greater variation of occurrence, when compared with substructures exposed to high intensity UV radiation.



**A.N-Me.01** - Biological colonization; **A.N-Me.02** - Discolouration/loss of gloss; **A.N-Me.03** - Fibre blooming; **A.N-Me.04** - Inclusion; **A.N-Me.05** - Stains; **A.N-Me.06** - Surface marks; **A.N-Me.07** - Wear damage; **A.N-Me.08** - Debris accumulation; **A.Me.01** - Corrosion of mettalic components; **A.Me.02** - Cracking; **A.Me.03** - Crushing; **A.Me.04** - Debonding; **A.Me.05** - Delamination; **A.Me.06** -Excessive deflection; **A.Me.07** - Geometrical imperfections; **A.Me.08** - Indentation/perforation; **A.Me.09** - Incorrect curing of adhesive; **A.Me.10** - Incorrect curing of resin; **A.Me.11** - Loose connections; **A.Me.12** - Member failure; **A.Me.13** - Voids

**Figure 9.15 - Frequency of occurrence of each anomaly according to exposure to chemically aggressive environments (high/low/nil).**

The chemically aggressive environments (3% of all substructures) are mostly found in indoor structures (70%); the types of anomalies that occur in these structures and their frequency is partially limited by the anomalies detected in indoor structures, shown in Figure 9.13, since indoor structures have a very low frequency of anomalies related to UV exposure, namely **A.N-Me.02-03** (loss of gloss/fibre blooming). However, anomaly **A.N-Me.02** (loss of gloss) has a similar incidence in highly aggressive environments, when compared to structures that are not exposed to chemical environments but are outdoors, due to the corrosion of the matrix by the chemical agents, which presents a similar visual appearance to the degradation caused by UV radiation.

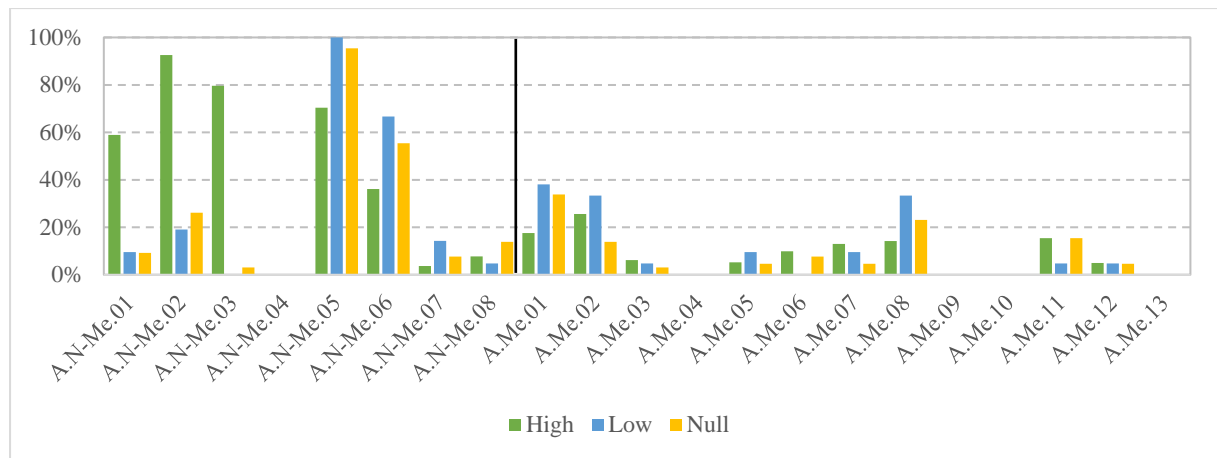
Anomaly **A.N-Me.03** (fibre blooming) occurs in indoor and chemically aggressive environments due to the corrosion of the matrix by the vapour of chemical agents and not by exposure to UV radiation, which is the main cause of this anomaly for outdoor exposure.

The fact that most of the mechanical anomalies present a nil or very low frequency of occurrence does not necessarily allow concluding that these anomalies do not occur in these types of environments. In fact, the sample for chemically aggressive environments was relatively small, and this may also explain why no cases were detected during the inspections.

### 9.7.4. Exposure to wind/rain

When analysing the exposure of the substructures to wind and rain, shown in Figure 9.16, the anomaly distribution shows a very similar frequency distribution to that exhibited in terms of exposure of the structures to UV radiation; in fact, the distribution between high, low, and nil exposure are relatively identical.

The structures that present a high/low/nil exposure to wind/rain are practically the same that have the same type of exposure (high/low/nil) to UV radiation; therefore, it becomes difficult to distinguish which type of anomaly occurs exclusively due to a particular type of environment.

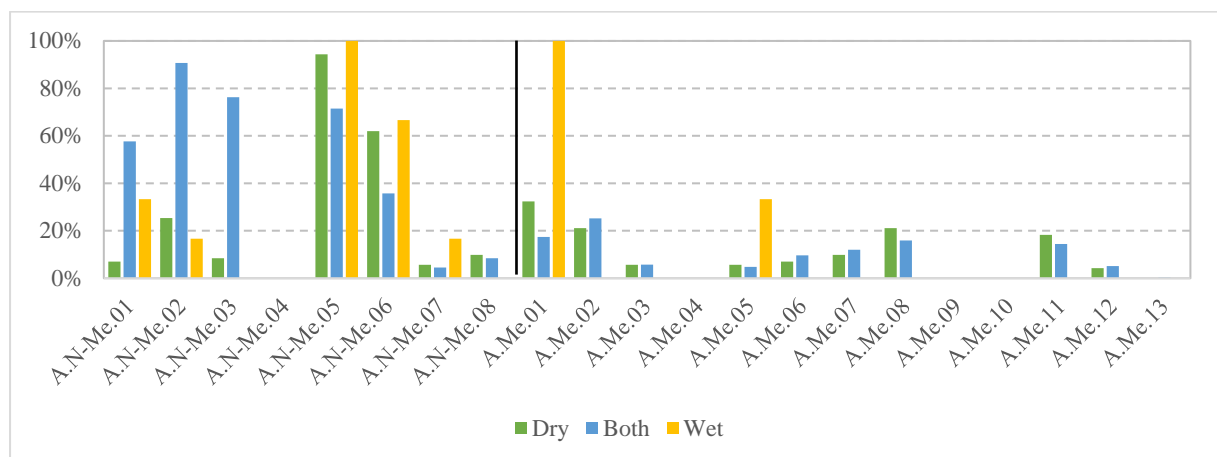


**A.N-Me.01** - Biological colonization; **A.N-Me.02** - Discolouration/loss of gloss; **A.N-Me.03** - Fibre blooming; **A.N-Me.04** - Inclusion; **A.N-Me.05** - Stains; **A.N-Me.06** - Surface marks; **A.N-Me.07** - Wear damage; **A.N-Me.08** - Debris accumulation; **A.Me.01** - Corrosion of mettalic components; **A.Me.02** - Cracking; **A.Me.03** - Crushing; **A.Me.04** - Debonding; **A.Me.05** - Delamination; **A.Me.06** -Excessive deflection; **A.Me.07** - Geometrical imperfections; **A.Me.08** - Indentation/perforation; **A.Me.09** - Incorrect curing of adhesive; **A.Me.10** - Incorrect curing of resin; **A.Me.11** - Loose connections; **A.Me.12** - Member failure; **A.Me.13** - Voids

**Figure 9.16 - Frequency of occurrence of each anomaly according to exposure to wind/rain (high/low/nil).**

### 9.7.5. Exposure to moisture

When analysing the state of the substructures exposed to different environments of moisture (permanently dry, wet and dry cycles and permanently dry), the data shown in Figure 9.17 reveal a higher occurrence of anomalies **A.N-Me.01** (biological colonization), **A.N-Me.02** (discolouration/loss of gloss) and **A.N-Me.03** (fibre blooming) when the substructures are exposed to wet and dry cycles, which usually corresponds to outdoor structures (also exposed to UV radiation).



**A.N-Me.01** - Biological colonization; **A.N-Me.02** - Discolouration/loss of gloss; **A.N-Me.03** - Fiber blooming; **A.N-Me.04** - Inclusion; **A.N-Me.05** - Stains; **A.N-Me.06** - Surface marks; **A.N-Me.07** - Wear damage; **A.N-Me.08** - Debris accumulation; **A.Me.01** - Corrosion of mettalic components; **A.Me.02** - Cracking; **A.Me.03** - Crushing; **A.Me.04** - Debonding; **A.Me.05** - Delamination; **A.Me.06** -Excessive deflection; **A.Me.07** - Geometrical imperfections; **A.Me.08** - Indentation/perforation; **A.Me.09** - Incorrect curing of adhesive; **A.Me.10** - Incorrect curing of resin; **A.Me.11** - Loose connections; **A.Me.12** - Member failure; **A.Me.13** - Voids

**Figure 9.17 - Frequency of occurrence of each anomaly by moisture exposed substructures.**

The data also show that 100% of the inspected substructures that are permanently wet present anomalies **A.N-Me.05** (stains) and **A.Me.01** (corrosion of mettalic components), which is logical. There

is also a much higher occurrence of delamination (**A.Me.05**) in substructures that are permanently wet, which should be associated to the well-known detrimental effects of permanent exposure to moisture on the mechanical properties of GFRP composites (e.g. [II.28],[II.29]).

The fact that most of the mechanical anomalies present a nil or very low frequency of occurrence does not allow concluding that these anomalies do not occur in this type of environment, but rather that these anomalies were not detected in these substructures, which have a small significance in the sample (1% of all substructures).

#### **9.7.6. Exposure to other environmental agents**

In this study, other exposure environments were also considered, such as the type of surrounding (countryside and urban) and distance from the sea. However, the data acquired did not show any relevant distinguishable characteristics or effects, and therefore exposure to these environmental agents is not analysed or presented here.

### **9.8. GFRP constructions: good practices observed**

During the inspection campaign several constructive techniques and details of the inspected constructions were registered and documented in order to determine which would be the most adequate to apply in these constructions.

As it is common in different civil engineering projects, some aspects are expected to be fully detailed, planned and studied. However, due to the uncertainty about the long-term behaviour of GFRP materials, some aspects of the project are sometimes neglected at an early design stage (e.g. surface protection) which can lead to the appearance of structural deficiencies during the service stage of the constructions.

In fact, most of the inspected constructions did not present any project or design. These constructions were built taking into consideration the knowledge acquired by the construction companies. Furthermore, in more recent structures, there seems to be an evolution in the constructive techniques used leading to fewer anomalies. Some of these cases will be presented below.

#### **9.8.1. Profile constructions**

When analysing the profile constructions, there are several areas that are more sensible and prone to the occurrence of anomalies. One of these areas is the connection between the profiles and the supporting element, Figure 9.18 presents some examples of the most common types of connections. These connections were usually with metallic elements (Figure 9.18 (a, b)), plastic elements (Figure 9.18 (c, d)) and more prominently with bolted fixtures (Figure 9.18 (d) and (e)).

The connections with metallic elements were the most stable, but some of the elements appeared corroded (Figure 5.20 (b)). For this type of connection, all the metallic elements used should be of stainless steel and manufactured specifically for these constructions.

The connections with plastic elements were more uncommon. The ones presented in Figure 9.18 (c) were in good state and had a high stiffness. Whereas, the connections presented in Figure 9.18 (d) were made with adapted sections of current pultruded profile sections, had a lower stiffness and were sometimes cracked, if not broken, between the web and flanges of the connection profile (Figure 5.20 (a)).

The bolted connections to the support (the most common type of connection inspected on profiles) is considered suitable for these types of constructions (Figure 9.18 (e)). However, as mentioned before, it is common to find cracks in these connections due to an overtightening of the bolts during the installation (Figure 5.10 (b)). This problem can usually be resolved with the increase of stiffness provided by adding a secondary profile outside (Figure 5.10 (c)) or inside (the most adequate solution - Figure 9.18 (f)) the main profile.

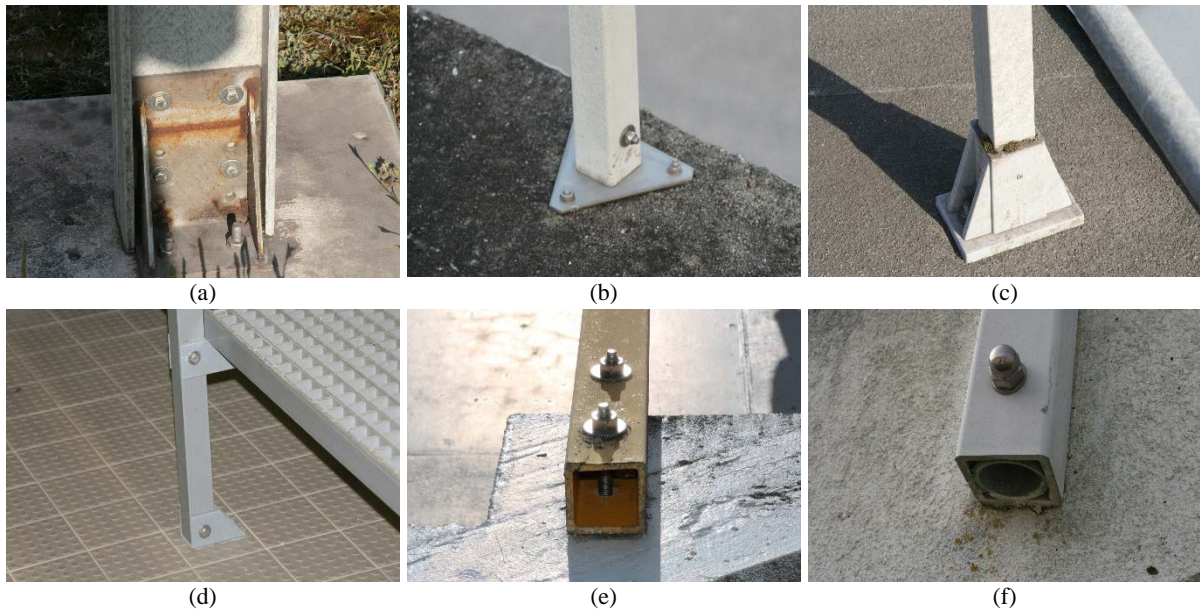


**Figure 9.18 - Examples of the most common connections of profile constructions and the support.**

The connection between profiles is also a sensible area in these constructions. These connections can be made with metallic and plastic elements, some of which are presented in Figure 9.19.

The connections between profiles with metallic elements (Figure 9.19 (a)) in accordance with was mentioned before present a higher stability. However, if the correct materials are not applied (e.g. stainless steel, aluminium), can present other anomalies such as corrosion (Figure 9.19 (b)).

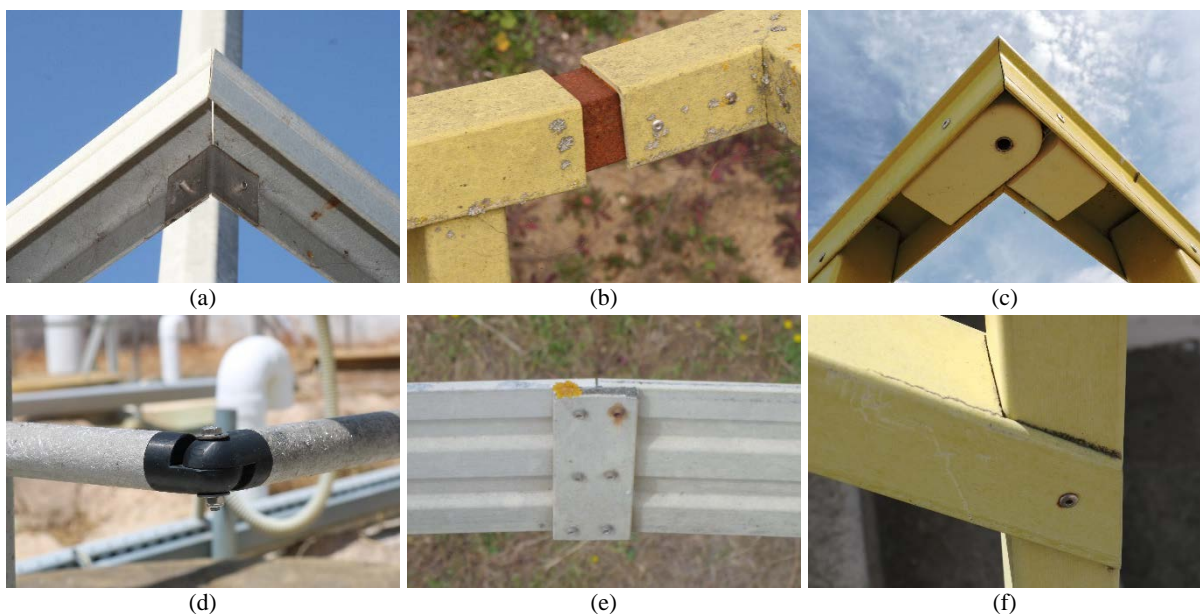


**Figure 9.19 - Examples of the most common connections between profiles.**

In order to avoid the problem of corrosion with the metallic elements usually another GFRP or

plastic element is used in the connection between profiles, as shown in (Figure 9.19 (c) to (f)). However, the use of plastic elements in these connections always require the use of complementary metal elements (e.g. bolts, rivets), these elements should also be of stainless steel in order to avoid their corrosion.

In the connection between profiles, the most common anomalies are cracking (Figure 5.10(f)) and loose connections (Figure 5.16(a)); therefore, the constructive technique applied should avoid the occurrence of such anomalies.

The examples shown in Figure 9.19(c) for omega and c-shaped profiles and in Figure 9.19(d) for circular profiles are the best examples on how to connect these profiles, since they guarantee a certain level of flexibility to accidental impacts. Whereas, the example presented in Figure 9.19(e) using a small GFRP plate to connect the two profiles is sensitive to accidental impacts and often leads to failure of the connection by shear-out of the plate or the profile (Figure 5.21(a)). In the example presented in Figure 9.19(f) the section of a profile was cut so as to fit into the other profile. This type of connection between profiles was often used and frequently led to cracking (Figure 9.19(f)), delamination (Figure 5.13(a)) or section failure of the profile.

As a general comment to these structures, all elements in exterior environments should have in its fibre architecture a superficial layer of polyester veil, in order to mitigate the occurrence of fibre blooming. As studied in chapter 12, the use of superficial protection reduces the occurrence of loss of gloss, fibre blooming and biological colonization, however the application of these protections slightly increases the initial cost of installation and maintenance operations.

### **9.8.2. Grating constructions**

When analysing the grating constructions, as mentioned before, these are typically located at a ground level and are very susceptible to spills (Figure 5.05 (a)), accidental impacts and debris accumulation (Figure 5.08 (b)), which are difficult anomalies to mitigate through constructive techniques since they cannot be foreseen during the design stage.

During the fabrication process of a grating (moulded casting, see section 2.3.2) the top side of the mould is always more irregular and has thicker layer of resin. In outdoor applications, this side should always be put faced up in order to mitigate the occurrence of fibre blooming (Figure 9.20 (a)).

In these constructions one of the most sensitive areas are the edges of the grating. When the gratings are cut and left with live edges, these can be easily crushed during the life stage of the construction (Figure 9.20 (b)). One way to reduce the occurrence of this anomaly is to protect the border of the grating with an L-shaped profile (Figure 9.20 (c)).

When these constructions have larger spans and are only simply supported on opposing edges, there is usually an effect of excessive deflection mid-span of the unsupported edges. When the end-users are walking between a succession of these profiles, this excessive deflection between the edges can lead to a feeling of unsafety. This deflection can be mitigated by fixing the supported edges (Figure 9.20 (d)) in order to restrain their rotation and the gratings should be bolted together by the edges (Figure 9.20 (e)) in order to prevent the possible difference in deflection between the gratings and increase the overall stiffness of the construction.

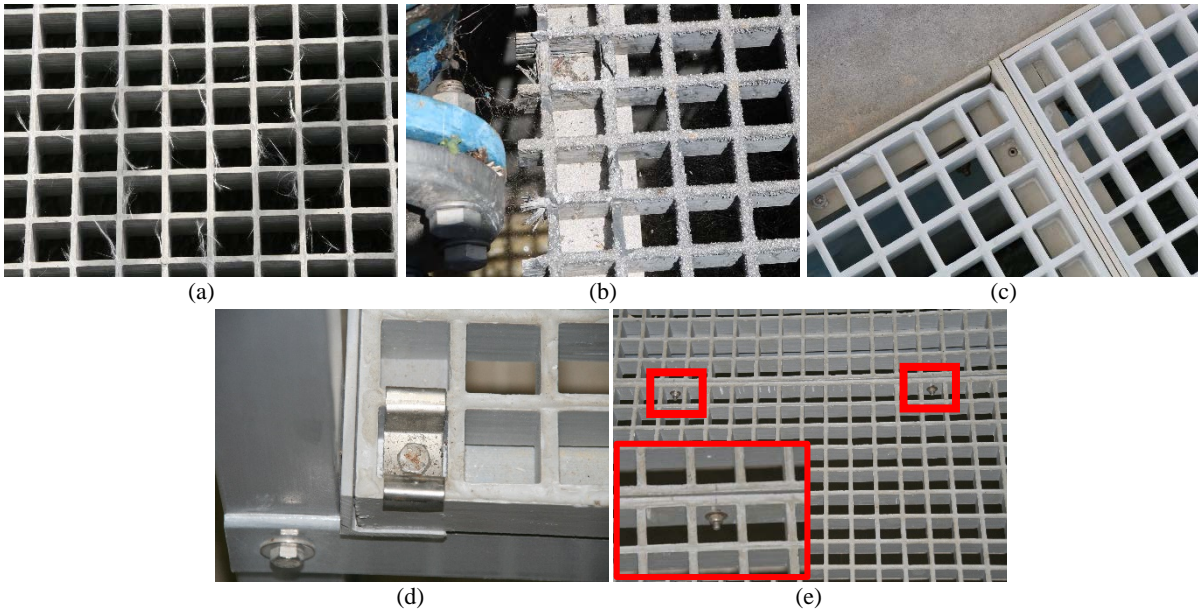


**Figure 9.20 - Examples of gratings constructions.**

### 9.8.3. Stair constructions

There are three primary anomalies in stair constructions that can be mitigated at a design stage: corrosion of metallic elements, cracking and excessive deflections. The corrosion of metallic elements (Figure 9.21 (a)) can be avoided by using stainless steel in all the fixtures necessary for these constructions.

The cracks and excessive deflections are related with the types of connections these constructions have to their support, since most of the anomalies detected are found at connection points. These connections can be made with metallic elements (Figure 9.21 (b)) or plastic/GFRP elements (Figure 9.21 (c)). The metallic connections present a higher stiffness in comparison to the plastic/GFRP connections and, as such, reduces the lateral deflection of the structure.

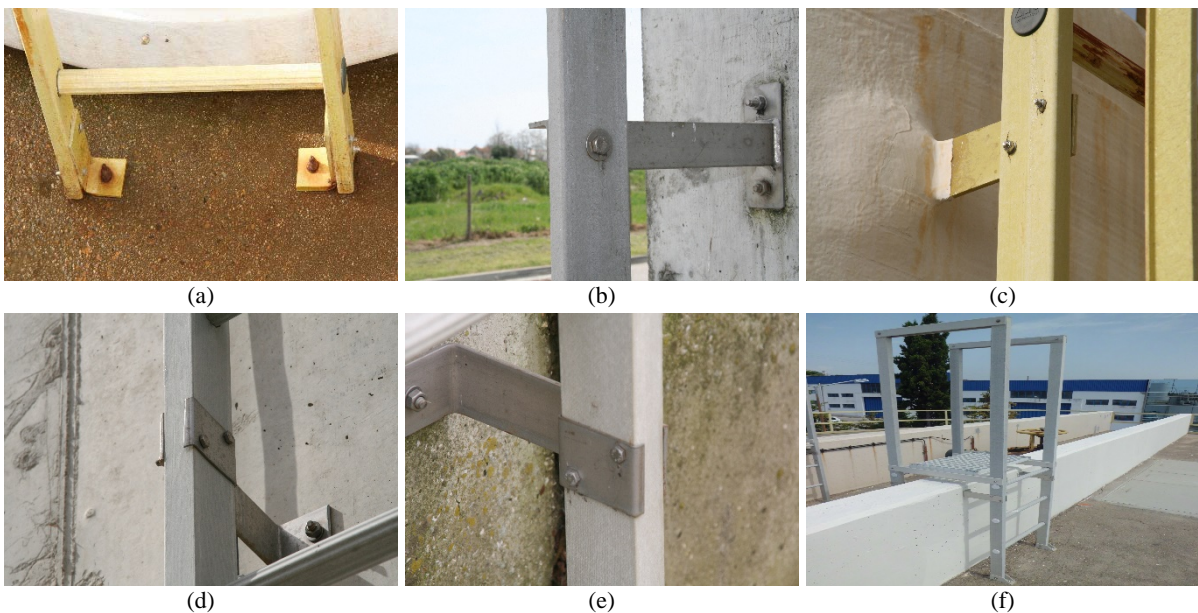


**Figure 9.21 - Examples of stair constructions.**

Most of the stair structures are installed vertically (as shown in Figure 8.01 (f), parallel to the wall). In these cases, the distance between fastenings is sometimes excessive and the stair structure has a low inertia to perpendicular movements. This may contribute to a higher occurrence of cracking in the vertical profiles

next to the fastenings as presented in Figure 4.10 (a). A reduction of the distance between fastenings, or a more robust vertical profile would help decrease the occurrence of this anomaly in this type of structure.

Also, at the connection points, there is an excessive tightening of the metallic bolts, leading to cracking of the vertical profiles, which have a thin wall cross-section. This anomaly can be mitigated with the application of a reinforcing metallic element (Figure 9.21 (d-e)).

In stair constructions that require an extension of the vertical profile without connection to the support, as shown in Figure 9.01 (f), the type of reinforcing structure, presented in Figure 9.21 (f), should be applied in order to reduce the deflection of these extensions and consequent occurrence of anomalies at the connection points. The application of this type of reinforcement besides increasing the stability of the structure also increases the safety of end-users.

As a general comment to these structures, all elements in exterior environments should have in its fibre architecture a superficial layer of polyester veil, in order to mitigate the occurrence of fibre blooming.

### 9.9. Concluding remarks

The data analysis reported here was based on the field inspection of 31 infrastructures containing 410 GFRP substructures. This campaign helped identifying the most common anomalies that can be found during the use stage of GFRP constructions.

It was found out that non-mechanical anomalies have a much higher incidence than mechanical anomalies, with emphasis on anomalies **A.N-Me.02** (discolouration/loss of gloss), **A.N-Me.05** (stains) and **A.N-Me.03** (fibre blooming). Among the mechanical anomalies, the most common are **A.Me.01** (corrosion of metallic components) and **A.Me.08** (indentations/perforations).

The environmental conditions the structures are exposed to were found to have a decisive impact on the types of anomalies that can be detected during the service stage. Three main factors were identified as being the most conditioning: location of the structure (indoor or outdoor), chemical aggressiveness of the environment, and exposure to UV radiation.

The most probable causes associated with the anomalies detected were found to be related with the in-service phase (exposure to the environmental agents) and the design stage; for the latter, there is still lack of knowledge and guidance on how to properly design and detail this type of structures when considering their long-term behaviour.

For all the anomalies detected, visual inspection was the diagnosis technique primarily suggested, as most of the anomalies are easily detected and diagnosed; this is the case of anomalies **A.N-Me.01** (biological colonization), **A.N-Me.02** (discolouration/loss of gloss) and **A.N-Me.03** (fibre blooming).

There are only a few rehabilitation techniques that can effectively be applied in GFRP constructions for civil engineering applications. During inspections, it was found that most structures lacked continuous maintenance procedures, which could help preventing the occurrence of some of the anomalies. It was also found that the rehabilitation of some of the GFRP elements would significantly help to reduce the detection of some of the most common anomalies (biological colonization, fibre blooming and discolouration).



## 10.Part II references

- [II.01] Garrido, M., Correia, J.R., Keller, T., Branco, F.A. (2016). “Connection systems between composite sandwich floor panels and load-bearing walls for building rehabilitation”. *Engineering Structures*, 106, 209-221.  
<https://doi.org/10.1016/j.engstruct.2015.10.036>
- [II.02] Keller, T., Theodorou, N., Vassilopoulos, A., Castro, J. (2015). “Effect of natural weathering on durability of pultruded glass fibre-reinforced bridge and building structures”. *Journal of Composites for Construction*, 20(1), 04015025-1 - 9.  
[https://doi.org/10.1061/\(ASCE\)CC.1943-5614.0000589](https://doi.org/10.1061/(ASCE)CC.1943-5614.0000589)
- [II.03] Knippers, J., Pelke, E., Gabler, M., Berger, D. (2007). “The FRP Bridge in Friedberg Germany: Design, Analysis and Material Tests”. In the proceedings of the ABSE Symposium: Improving Infrastructure Worldwide, 19-21 September, Weimar, Germany.  
<https://doi.org/10.2749/222137807796158147>
- [II.04] Castelo, A. (2014). “Emergency Constructions in Catastrophe Affected Regions. Development of a Constructive Solution in Advanced Composite Materials”. MSc Dissertation in Civil Engineering, IST, University of Lisbon (In Portuguese).
- [II.05] Keller, T. (2001). “Recent all-composite and hybrid fibre-reinforced polymer bridges and buildings”. *Progress in Structural Engineering and Materials*, 3(2), 132-140.  
<https://doi.org/10.1002/pse.66>
- [II.06] De Brito, J. (1992). “Development of a Concrete Bridge Management System”. PhD Thesis in Civil Engineering, IST, Technical University of Lisbon (In Portuguese).
- [II.07] Silvestre, J.D., de Brito, J. (2009). “Ceramic tiling inspection system”. *Construction and Building Materials*, 23(2), 653–668.  
<https://doi.org/10.1016/j.conbuildmat.2008.02.007>
- [II.08] Garcia, J., de Brito, J. (2008). “Inspection and diagnosis of epoxy resin industrial floor coatings”. *Journal of Materials in Civil Engineering*, 20(2), 128–136.  
[https://doi.org/10.1061/\(ASCE\)0899-1561\(2008\)20:2\(128\)](https://doi.org/10.1061/(ASCE)0899-1561(2008)20:2(128))
- [II.09] Garcez, N., Lopes, N., de Brito, J., Silvestre, J.D. (2012). “System of inspection, diagnosis and repair of external claddings of pitched roofs”. *Construction and Building Materials*, 35, 1034-1044.  
<https://doi.org/10.1016/j.conbuildmat.2012.06.047>
- [II.10] CEN (2002) “Reinforced plastic composites - Specifications for pultruded profiles - Part 2: Methods of test and general requirements”. EN 13706-2. Brussels, Belgium: European Committee for Standardization.
- [II.11] ASTM International (2002) “Standard Practice for Classifying Visual Defects in Thermosetting Reinforced Plastic Pultruded Products”. ASTM D4385-02, West Conshohocken, Pennsylvania, USA.
- [II.12] ASTM International (2002) “Standard Practice for Classifying Visual Defects in Glass-

- Reinforced Plastic Laminate Parts”. ASTM D2563-R02, West Conshohocken, Pennsylvania, USA.
- [II.13] ASTM International (2002) “Standard Practice for Classifying Visual Defects in Parts Molded from Reinforced Thermosetting Plastics”. ASTM D2562-R02, West Conshohocken, Pennsylvania, USA.
- [II.14] Keller, T., Bay, Y., Vallée, T. (2007) “Long-term performance of a glass fibre-reinforced polymer truss bridge”. *Journal of Composites for Construction*, 11(1), 99-108.
- [II.15] Norwegian Oil and Gas Association (1997), “Recommended Guidelines for NDT of GRP Pipe Systems and Tanks”.
- [II.16] National Cooperative Highway Research Program (2006) “Report 564: Field Inspection of In-Service FRP Bridge Decks”.
- [II.17] Cowley, T.W. (1997). “A recommended FRP inspection procedure for the end-user”. In the proceedings of the Corrosion 97 - Annual Corrosion Conference of the National Association of Corrosion Engineers. NACE International, pp.349/1-9, 9-14 March, New Orleans, USA.
- [II.18] Amory, R.L., Wang, D.S. (1985), “State-of-the-Art Review on Composite Material Fatigue/Damage Tolerance”. B & M Technological Services, Inc. Cambridge, United States.
- [II.19] Fowler, T., Kinra, V.K., Maslov, K., Moon, T.J. (2001). “Inspecting FRP Composite Structures with Nondestructive Testing.” Research Report 1892-1, Texas department of transportation, United States.
- [II.20] Bossi, R.H., Giurgiutiu, V. (2014). “Chapter 15: Nondestructive testing of damage in aerospace composites”. In Irving, P.E., Soutis, C., editor: *Polymer Composites in the Aerospace Industry*, pp. 413-448. Woodhead Publishing, Swanston.  
<http://dx.doi.org/10.1016/B978-0-85709-523-7.00015-3>
- [II.21] Tappi Association (2016). “Guidelines for Inspecting Used FRP Equipment, Technical Information Paper TIP 0402-28”. Georgia, United States.
- [II.22] Oehlers, D.J. (2001). “Development of design rules for retrofitting by adhesive bonding or bolting either FRP or steel plates to RC beams or slabs in bridges and buildings”. *Composites: Part A*, 32(9), 1345-55.  
[https://doi.org/10.1016/S1359-835X\(01\)00089-6](https://doi.org/10.1016/S1359-835X(01)00089-6)
- [II.23] Rizkalla, S., Rosenboom, O., Miller, A., Walter, C. (2005). “Value engineering and cost effectiveness of various fibre reinforced polymer (FRP) repair systems.”. FHWA/NC/2006-39, North Carolina State University.
- [II.24] Rosenboom, O., Walter, C., Rizkalla, S. (2009). “Strengthening of prestressed concrete girders with composites: installation, design, and inspection”. *Construction and Building Materials*, 23(4), 1495–507.  
<https://doi.org/10.1016/j.conbuildmat.2007.11.010>
- [II.25] Garcia, J., Brito, J. (2006). “Functional requirements of industrial floor coatings”. Nascimento, J.M., (1985) “Functional requirement of flooring elements”. In the proceedings of QIC2006,

- LNEC (National laboratory of Civil Engineering), 21-24 November, Lisbon, Portugal (in Portuguese).
- [II.26] Rato, V.M. (2002) “Conservation of Historical Heritage: Principles of Intervention”. MSc Dissertation in Construction, IST, University of Lisbon. (In Portuguese).
- [II.27] Correia, J.R., Cabral-Fonseca, S., Branco, F.A., Ferreira, J.G., Eusébio, M.I., Rodrigues, M.P. (2006). “Durability of pultruded glass-fibre-reinforced polyester profiles for structural applications”. *Mechanics of Composite Materials*, 42(4), 325-338.  
<https://doi.org/10.1007/s11029-006-0042-3>
- [II.28] Sousa, J.M.; Correia, J.R.; Cabral-Fonseca, S. (2016). “Durability of glass fibre reinforced polymer pultruded profiles: comparison between QUV accelerated exposure and natural weathering in a Mediterranean climate”. *Experimental Techniques*, 40(1), 207-219.  
<https://doi.org/10.1007/s40799-016-0024-x>
- [II.29] Sousa, J.M., Correia, J.R., Cabral-Fonseca, S., Diogo, A.C. (2014). “Effects of thermal cycles on the mechanical response of pultruded GFRP profiles used in civil engineering applications”. *Composite Structures*, 116, 720-731.  
<https://doi.org/10.1016/j.compstruct.2014.06.008>
- [II.30] Castro San Román, J. (2005) "System ductility and redundancy of FRP structures with ductile adhesively-bonded joints." PhD Thesis in Civil Engineering, École Polytechnique Fédérale de Lausanne.  
<https://doi.org/10.5075/epfl-thesis-3214>
- [II.31] Texas instruments product catalogue  
<http://www.txinstruments.com/products/barcol-hardness-tester/935.html>, visited in December 2018.
- [II.32] Reichold (2009). “FRP inspection guide - An Inspection Guide for Fibre-Reinforced Plastic (FRP) Equipment”. Reichold, Inc., North Carolina, USA.
- [II.33] Ryobitools product catalogue  
<https://www.ryobitools.com/power-tools/products/details/pinless-moisture-meter>, visited in September 2018
- [II.34] Böer, P., Holliday, L., Kang, T.H.K. (2014). “Interaction of environmental factors on fibre-reinforced polymer composites and their inspection and maintenance: A review”. *Construction and Building Materials*, 50, 209-218.  
<https://doi.org/10.1016/j.conbuildmat.2013.09.049>
- [II.35] Walter, A., de Brito, J.; Lopes, J. (2005). “Current flat roof bituminous membranes waterproofing systems - inspection, diagnosis and pathology classification”. *Construction and Building Materials*, vol. 19(3), pp. 233-242.  
<https://doi.org/10.1016/j.conbuildmat.2004.05.008>



# **Part III**

Durability of GFRP composites exposed to different environmental conditions



## Preamble

In recent years, a significant number of studies about the durability of FRP materials was carried out. However, some knowledge gaps remain and, therefore, to enable their widespread use in the construction sector, it is essential to understand in further depth their long-term behaviour when exposed to various environmental agents.

This third part of the thesis presents an experimental investigation aimed at assessing the effects of the exposure to different environmental agents on the performance of pultruded GFRP materials with different resin systems, with and without surface veil, different content of UV stabilizer additives, and with or without superficial protections.

The experimental programme carried out in the scope of the thesis allowed assessing the effects of chemical (alkaline and acidic) environments, and natural and artificial weathering (including UV radiation) on the physical, thermomechanical and mechanical properties of pultruded GFRP materials. Furthermore, real GFRP structures were selected to assess the effects of natural weathering on the physical and mechanical properties of pultruded GFRP materials under actual in-service conditions.

The work presented in this part resulted in the following publications:

- Castelo, A., Correia, J.R., Cabral-Fonseca, S., de Brito, J. (in preparation). “Chemical resistance to alkaline exposure of pultruded GFRP profiles”.
- Castelo, A., Correia, J.R., Cabral-Fonseca, S., de Brito, J. (in preparation). “Chemical resistance to acidic exposure of pultruded GFRP profiles”.
- Castelo, A., Correia, J.R., Cabral-Fonseca, S., de Brito, J. (in preparation). “Natural and artificial accelerated weathering of pultruded GFRP profiles”.
- Castelo, A., Correia, J.R., Cabral-Fonseca, S., de Brito, J. (in preparation). “The effects of natural weathering on GFRP structures: Case studies in Portugal”.



## **11. Experimental programme and initial characterization of GFRP material**

### **11.1. Introductory remarks**

As explained in chapter 1 and discussed in [I.01], there is a gap in the knowledge about the durability of FRP composite materials used in civil engineering applications. In fact, despite the increasing use of these materials in the construction sector, there are still some concerns and doubts about their behaviour under long-term exposure to different environmental conditions.

In Part II, a list of the most common anomalies likely to be found in FRP constructions was created and validated. Some of these anomalies were related to construction methods and installation procedures. Other anomalies that were detected in the field inspections could be correlated directly with the type of environments the FRP materials were exposed to during their service life. Among the environmental agents that were identified, besides exposure to moisture (which has been the object of several studies in the past), exposure to UV radiation and exposure to chemical agents proved to be particularly relevant. Accordingly, in this Part III, an experimental programme was developed to assess the durability of GFRP elements, in terms of their remaining properties under different environmental conditions, including those that were deemed as being particularly relevant and for which less information is available in the literature. This experimental programme is presented in more detail in the following sections.

When studying the performance of FRP composite materials, their physical and mechanical properties can vary in accordance with several features, such as the type of polymeric matrix, the type of reinforcing fibres, the fibre content, the fibre architecture, and the additives used (e.g., pigments or flame retardants). In the development of this experimental programme, pultruded GFRP materials and configurations most commonly used in civil engineering applications were considered, and an attempt was made to correlate the results of the experimental programme carried out in laboratory conditions with results of tests performed on GFRP elements applied in real constructions in service conditions.

In this chapter, the different pultruded GFRP materials used in the experimental programme performed in the laboratory are presented, and the experiments carried out to characterise them are described. Results obtained in these tests are then used as reference for the discussion of the results obtained after exposure of the same GFRP materials to the different types of ageing (chapters 12 and 13).

### **11.2. Materials**

As mentioned, for this experimental programme, the most common pultruded GFRP materials commercially available were used and combined to obtain a wide variety of application possibilities and to determine the most suitable one for each type of exposure environment.

All materials applied in the experimental programme were manufactured by pultrusion (described in Part I), by *ALTO Perfis Pultrudidos, Portugal*.

### 11.2.1. Material selection

For the manufacturing, two alternative resin systems were used: an isophthalic polyester resin AROPOL™ IS 4698 (UP), provided by ASHLAND, and a bisphenol A vinyl ester urethane resin ATLAC 580 (VE), provided by DSM - their technical sheets are provided in Appendix VI. The UP resin was selected since it has the widest use in most structural applications, being appropriate for standard purpose without stringent durability requirements. On the other hand, the VE resin has a higher demand when more aggressive environments are considered due to its higher chemical resistance and stability.

Both resins have a light grey colour, given by an added pigment. For some of the samples, a benzotriazole UV stabilizer additive, provided by Ciba, was added. The manufacturer of this UV stabilizer additive specifies a use range of up to 0.5% in mass of polymeric matrix. Therefore, three levels of UV stabilizer additive content were formulated into the resin, to assess the potential influence of this constituent in the durability of the pultruded GFRP materials: 0% (no UV stabilizer additive), 0.25% and 0.50%. The technical sheet of this additive is also provided in Appendix VI.

Both pultruded GFRP materials, produced with UP and VE resins, have an identical type of E-glass fibre reinforcement, regardless of the type of matrix resin, comprising: (i) unidirectional rovings, with a saline sizing and linear density of 4800 tex; (ii) two outer layers of chopped strand mats (CSM), with weight of 300 g/m<sup>2</sup>; and (iii) a non-woven fibre mat as a central layer with density of 500 g/m<sup>2</sup> - the production scheme is illustrated in Figure 11.01.

Some samples have a surface polyester non-woven veil, which was used to evaluate its effectiveness in preventing the fibre blooming phenomenon (caused by UV radiation).

A total of 12 series of different specimens was considered, as detailed in Table 11.01. The designation of the specimens follows the following labelling: resin type (polyester - UP or vinyl ester - VE), presence of surface veil (with veil - WV, no veil - NV), and % of UV stabilizer additive [0 (no additive), 0.25 or 0.50 (%)].

**Table 11.01 - Designation of the different series of material formulations.**

Type of resin	% UV stabilizer additive	Surface veil	Designation
Polyester	No additive (0%)	Yes	UP_WV_0
		No	UP_NV_0
	Mixture 1 (0.25%)	Yes	UP_WV_025
		No	UP_NV_025
	Mixture 2 (0.50%)	Yes	UP_WV_050
		No	UP_NV_050
Vinylester	No additive (0%)	Yes	VE_WV_0
		No	VE_NV_0
	Mixture 1 (0.25%)	Yes	VE_WV_025
		No	VE_NV_025
	Mixture 2 (0.50%)	Yes	VE_WV_050
		No	VE_NV_050

### 11.2.2. Material production

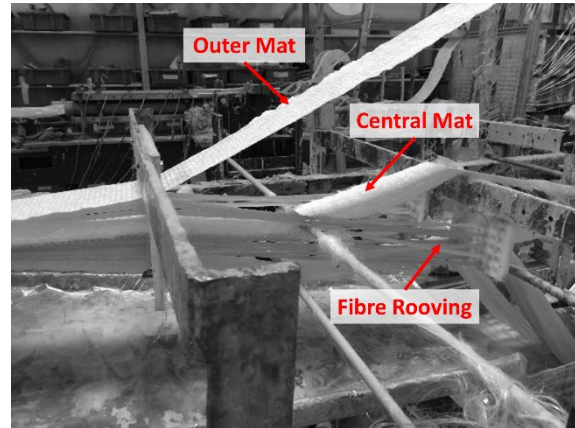
The manufactured GFRP profiles have uniform geometry, with rectangular cross section of

100 mm (width) by 6.5 mm (thickness) and were cut into plates approximately 3 m long. After production, all profiles were cut into smaller plates (30 cm or 90 cm long), according to the different exposure environments and were placed in an oven, set at 80 °C, for 7 days; this procedure had the following goals: to guarantee a high (and uniform) curing degree in all specimens, and to prevent (or minimize) the occurrence of post-curing phenomena under exposure to the ageing environments.

The production of the pultruded GFRP materials was made to order, considering the material needs for the experimental programme. Therefore, some formulations were produced in very small batches and others in larger batches (as they correspond to “off-the-shelf” profiles, more often used).



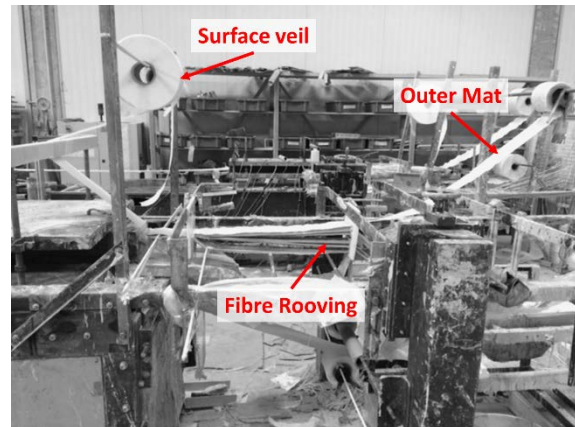
(a) Materials without surface veil



(b) Materials without surface veil - arrangement of reinforcing fibres



(c) Materials with surface veil



(d) Materials with surface veil - arrangement of reinforcing fibres



(e) Finished material after exiting the pultrusion die

**Figure 11.01 - Production of pultruded materials.**

The profile quantities produced were as follows: UP\_WV\_0 and VE\_WV\_0 - 81 m each; UP\_NV\_0 - 57 m; VE\_NV\_0 and the 4 mixtures with 0.25% of UV stabilizer additive - 12 m each; and the 4 remaining mixtures with 0.50% UV stabilizer additive - 6 m each.

### 11.3. Characterisation methods and test setup

All test series were subjected to a comprehensive set of experimental characterisation tests to determine their physical, thermomechanical and mechanical behaviour. As presented in Table 11.02, the following physical and thermomechanical properties were analysed: (i) inorganic content (by calcination tests); (ii) colour; (iii) gloss; (iv) Barcol hardness; and (v) glass transition temperature, by dynamic mechanical analysis (DMA). The following mechanical properties were analysed: (i) tensile properties; (ii) compressive properties; (iii) flexural properties; (iv) in-plane shear properties; and (v) interlaminar shear strength. The mechanical properties were always determined in the longitudinal direction of the fibres.

**Table 11.02 - Physical and mechanical properties and corresponding standards.**

Type of property	Properties	Standard
<b>Physical</b>	Inorganic content	ISO 1172
	Colour	ISO 11664-4
	Gloss	ISO 2813
	Barcol hardness	ASTM D2583
	Glass transition temperature (DMA)	ISO 6721
<b>Mechanical</b>	Tensile properties	ISO 527-4
	Compressive properties	ASTM D6641
	Flexural properties	ISO 14125
	In-plane shear properties	ASTM D5379
	Interlaminar shear strength	ASTM D2344

Whenever necessary, the specimens were cut down to the size required by each test standard specification, using a CNC cutting machine, as shown in Figure 11.02. This cutting system allowed obtaining a uniform and very precise sizing in all specimens.



**Figure 11.02 - CNC cutting machine used for specimen cutting.**

### **11.3.1. Inorganic mass content**

The inorganic mass content (IMC) of each GFRP material was measured using the calcination method, described in ISO 1172 [III.02]. The specimens were heated to 800 °C, in a muffle furnace, for a minimum period of 8 h. This process allows burning the resin matrix and the polyester surface veil, revealing fibres and inorganic fillers. By weighing test specimens, in an analytical balance, before and after calcination, it is possible to determine the inorganic content (in mass). Three specimens were tested for each material.

### **11.3.2. Colour**

Colour measurements were determined in accordance with the EN ISO/CIE 11664: Part 4 [III.03], according to the colour space CIE L\*a\*b\* 1976, using a HunterLAB MiniScan XE Plus colourimeter (Figure 11.03 - left). A total of 4 colour measurements were made per specimen and the results were averaged. The following parameters were used in the colour measurements: (i) scale: CIELAB; (ii) area: 4.91 cm<sup>2</sup>; (iii) geometry: d/8; (iv) illuminant: D65; (daylight); (v) observer: 10° and (vi) with specular gloss and UV component included. Colour measurements were obtained before and after exposure to the different environmental conditions, or after pre-determined periods of environmental exposure, to calculate the colour changes. Results for the unaged materials are presented ahead in this chapter, while results obtained for the aged materials are presented in the following chapters.

### **11.3.3. Gloss**

Gloss was determined in accordance with the ISO 2813 [III.04], at an angle of 60°, using a Novo-Gloss Statistical Glossmeter (Figure 11.03, centre). A total of 10 gloss measurements were made per test specimen and per direction, and the results were averaged. Gloss measurements were obtained before and after the exposure to the different environmental conditions, or after pre-determined periods of exposure. Results for the unaged materials are presented ahead in this chapter, while results obtained for the aged materials are presented in the following chapters.

### **11.3.4. Barcol hardness**

Barcol hardness was evaluated in accordance with ASTM D2583 [III.05], using a Barber-Colman Impressor (Rockford, Illinois, USA) (Figure 11.03 - right). A total of 10 measurements were made per test specimen and the results were averaged. These properties were obtained before and after exposure to the different environmental conditions, or for pre-determined periods of time for continuous exposures.



HunterLAB MiniScan XE Plus

Novo-Gloss statistical glossmeter

Barcol hardness impressor

**Figure 11.03 - Equipment used for some of the physical characterisation tests.**

### 11.3.5. Dynamic mechanical analysis

The glass transition temperature ( $T_g$ ) and the temperature-dependent mechanical behaviour were determined according to ISO 6721: Parts 1 and 5 [III.06], by dynamic mechanical analysis, using a Q800 DMA analyser from TA instruments (Figure 11.04). The test specimens, with dimensions of  $60 \times 15 \times 6.5$  mm, were tested in a three-point bending configuration, from room temperature to  $200^\circ\text{C}$  (in air), at a heating rate of  $2^\circ\text{C}/\text{min}$ , and at a constant frequency of 1 Hz and a strain amplitude of  $15\ \mu\text{m}$ .

The  $T_g$  was determined in accordance with ASTM E1640 [III.07], from the peak of the loss factor ( $\tan \delta$ ) curve and from the storage modulus ( $E'$ ) curve as the extrapolated onset of its sigmoidal change.



Q800 DMA analyser



Three-point bending test setup

**Figure 11.04 - DMA test equipment and setup.**

### 11.3.6. Tensile tests

The tensile properties were determined according to ISO 527: Parts 1 and 4 [III.08], using an Instron universal testing machine (UTM), with 250 kN of capacity. The tests were performed under

displacement control, at a speed of 2 mm/min. The test specimens had dimensions of  $300 \times 25 \times 6.5$  mm and the setup is shown in Figure 11.05.

The deformations in the central part of the test specimens were measured with a video extensometer, comprising a high-definition Sony XCG 5005E video camera with a Fujinon Fujifilm HF50SA-1 lens. The video extensometer continuously monitored the position of 13 target dots marked on the test specimens. Eleven targets were marked vertically, spaced 1 cm from the test specimens' centre, and three targets were marked horizontally, spaced 0.5 cm from the test specimens' centre. The variation of their coordinates was used to determine the tensile strains. In order to obtain more accurate results, all test specimens were superficially painted with a white acrylic matte spray paint and the targets were marked with a black pen.

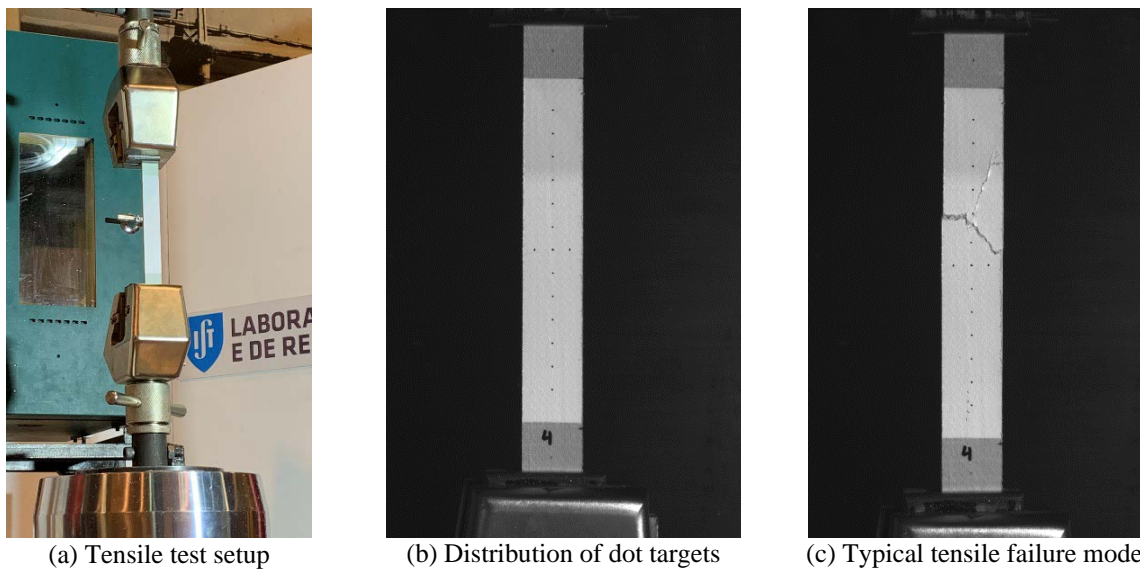
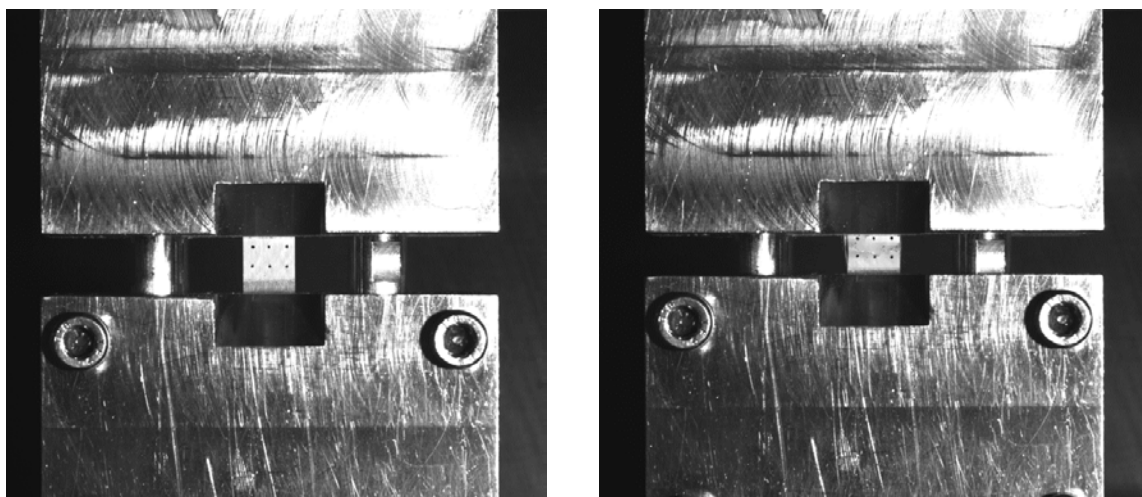


**Figure 11.05 - Tensile tests setup and typical failure mode.**

The axial stress was determined by dividing the applied load by the average cross-section dimensions (an average of three measurements was considered by direction), whereas the strains were measured with the video extensometer outputs, containing the relative position of the targets. The tensile modulus was determined from the slope of the stress *vs.* strain curves, considering strain values ranging between 0.001 and 0.005 mm/mm (for which the response was linear).

### **11.3.7. Compressive tests**

The compressive properties were determined according to ASTM D6641/D6641M [III.10], rendering to the combined load compression (CLC) test procedure. The tests were performed using an Instron 1343 universal testing machine (UTM) with 250 kN of capacity. The tests were conducted under displacement control, at a speed of 1 mm/min. The test specimens had dimensions of  $140 \times 12 \times 6.5$  mm and the test setup is shown in Figure 11.06.



(a) Distribution of dot targets

(b) Typical compressive failure mode

**Figure 11.06 - Compressive tests setup and typical failure mode.**

The deformations in the central part of the test specimens were measured with the same video extensometer used in the tensile tests. The video extensometer continuously monitored the position of 6 target dots marked on the surface of the test specimens. The targets were arranged in two rows with three targets spaced 0.5 cm from the test specimens' centre. The variation of their coordinates was used to determine the strains. As for the tensile tests, in order to obtain more accurate results, all test specimens were superficially painted with a white acrylic matte spray paint and the targets were marked with a black pen.

The axial stresses and strains were determined using the same method described in the tensile tests. The compressive modulus was determined from the slope of the stress vs. strain curves within the linear branch of the curves, considering strains between 0.001 and 0.005 mm/mm.

### 11.3.8. Flexural tests

The flexural properties were obtained according to ISO 14125 [III.11], using an Instron 1343 universal testing machine (UTM), with 250 kN of capacity. Tests were conducted under displacement control, at a speed of 2 mm/min, with a test span of 130 mm. The test specimens had dimensions of  $195 \times 15 \times 6.5$  mm and the test setup is shown in Figure 11.07.



(a) Flexural test setup

(b) Typical flexural failure mode

**Figure 11.07 - Flexural tests setup and typical failure mode.**

The flexural stress was determined by dividing the applied load by the average value of the cross-section flexural modulus (an average of three measurements was made by direction), whereas the strains were assessed through the midspan vertical displacement (crosshead displacement of test machine). The flexural modulus was determined (estimated) from the slope of the flexural stress vs. strain curves, with strains varying approximately from 0.0005 to 0.0025 mm/mm (for which the response was linear).

### 11.3.9. In-plane shear tests

The in-plane shear properties were obtained according to ASTM D5379/D5379M [III.09], using an Instron 1343 universal testing machine (UTM) with 250 kN of capacity. Tests were carried out under displacement control, at a speed of 2 mm/min. The test specimens had dimensions of  $76 \times 20 \times 6.5$  mm, comprising a notch at the middle part, and the setup is shown in Figure 11.08.

The deformations in the central notch of the test specimens were measured with the same video extensometer already described in the tensile tests. The video extensometer continuously monitored the position of 8 target dots marked on the surface of the test specimens, forming two square grids with sides of 10 mm and 6 mm, equally spaced from the centre of the test specimens. In general, all results were obtained from the 10mm grids, only when the results were unreliable the 6mm grid was used. The variation of their coordinates was used to determine the shear strains. To obtain more accurate results, all specimens were superficially painted with a white acrylic matte spray paint and the targets were marked with a black pen.

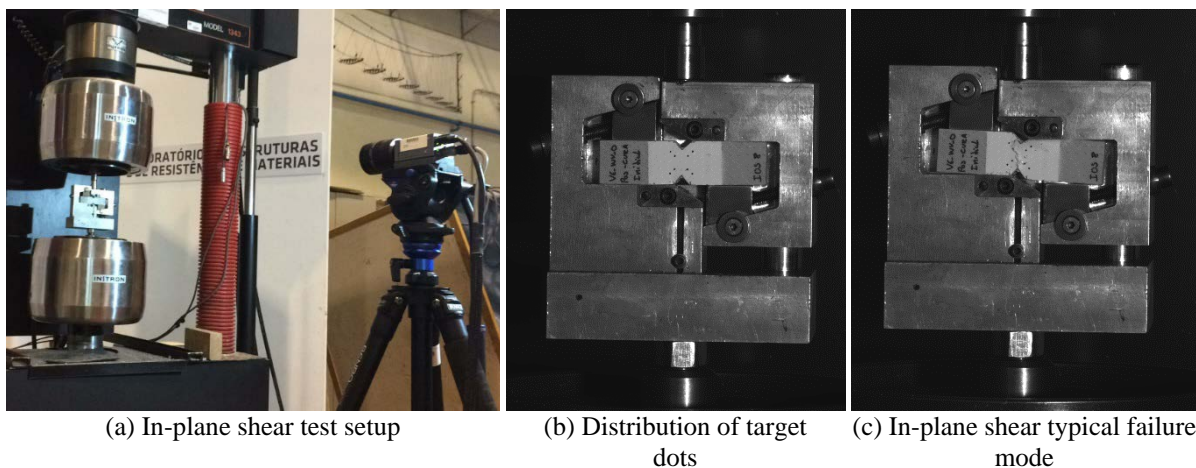


**Figure 11.08 - In-plane shear test setup and typical failure mode.**

The shear stress was determined by dividing the applied load by the average cross-section dimensions of the central notched section (an average of three measurements was made by direction), whereas the shear strains were assessed through the video extensometer outputs, containing the relative position of the targets. The shear modulus was determined from the slope of the shear stress vs. strain curves within the linear branch of the curves, considering strains between 0.002 and 0.006.

### 11.3.10. Interlaminar shear strength tests

The interlaminar shear strength was obtained according to ASTM D2344 [III.12], using an Instron 1343 universal testing machine (UTM) with 250 kN of capacity. The tests were performed under

displacement control, at a speed of 1 mm/min, with a test span of 26 mm. The test specimens had dimensions of  $39 \times 13 \times 6.5$  mm and the setup is shown in Figure 11.09.

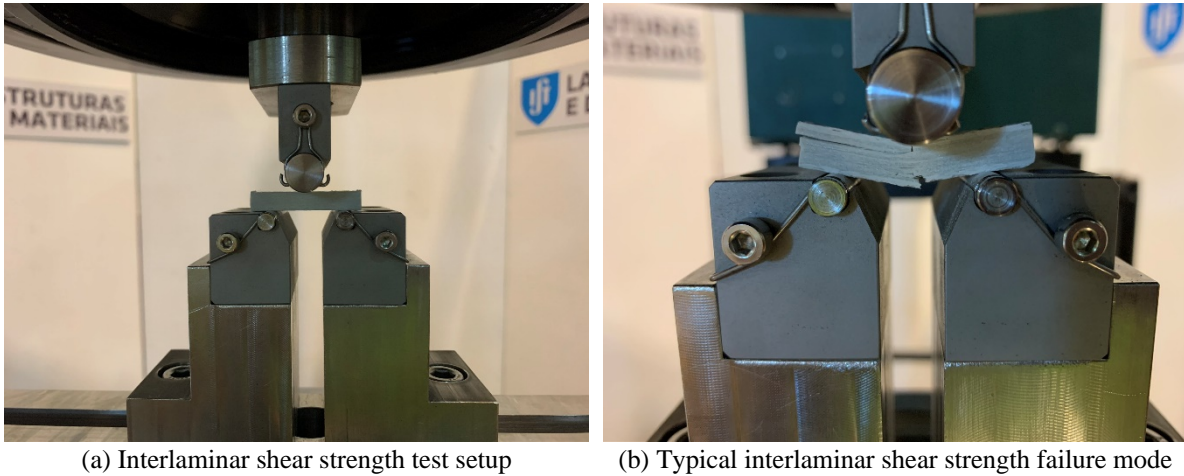


**Figure 11.09 - Interlaminar shear strength test setup and typical failure mode.**

The interlaminar shear stresses were estimated as indicated in ASTM D2344 [III.12], by dividing the applied load at midspan by the average cross-section dimensions (an average of three measurements was made by direction), whereas the midspan displacements were measured through the midspan vertical displacement (crosshead displacement of test machine).

## **11.4. Characterisation of unaged GFRP materials**

### **11.4.1. Summary of properties**

The main properties obtained in the material characterization tests of the GFRP materials are presented in Table 11.03 and Table 11.04 for UP and VE profiles, respectively. It is highlighted that the results obtained refer only to the longitudinal direction, as no tests were performed in the transversal direction. The values obtained for the various properties are in accordance with the typical values exhibited by pultruded GFRP materials referred in chapter 2.

Although the profiles were produced from the same constituent materials (fibres and resin), they present slightly different physical and mechanical properties among the various formulations.

**Table 11.03 - Summary of properties of polyester profiles.**

Property	Method	Unit	UP_WV_0	UP_NV_0	UP_WV_025	UP_NV_025	UP_WV_050	UP_NV_050
IMC	Calcination	[%]	71.9 ± 1.06	72.5 ± 0.62	71.6 ± 1.29	73 ± 1.73	72.4 ± 1.03	69.3 ± 1.54
Colour	CIE L*a*b* 1976	L*/a*/b*	79.38 / -4.12 / 3.64	78.99 / -3.84 / 3.35	81.12 / -1.32 / 3.08	80.79 / -1.11 / 4.52	81.47 / -1.13 / 5.22	80.87 / -0.93 / 6.05
Gloss	Glossmeter	(-)	23.4 ± 0.8	22 ± 0.9	26.5 ± 0.9	32.6 ± 1.9	30.7 ± 1.2	22.3 ± 1.4
$T_g$	DMA	$T_g$ ( $E'_{onset}$ ) [°C]	104.1 ± 2.8	--	--	--	--	--
		$T_g$ ( $\tan \delta$ ) [°C]	125.4 ± 2.0	--	--	--	--	--
Mechanical property	Tensile tests	$\sigma_{tu}$ [MPa]	432.7 ± 34.3	521.4 ± 11.5	438.7 ± 26.5	449.7 ± 27.2	470.7 ± 34.8	451.4 ± 26.6
		$E_t$ [GPa]	42.4 ± 0.63	42.0 ± 0.98	43.0 ± 1.3	43.0 ± 1.65	42.5 ± 1.83	37.5 ± 1.76
	Compressive tests	$\sigma_{cu}$ [MPa]	725 ± 62.1	805.1 ± 24.6	607.2 ± 25.2	613 ± 26.8	560.8 ± 39.6	593.1 ± 41.2
		Flexural tests	$\sigma_{fu}$ [MPa]	554.1 ± 14.5	497.6 ± 24.4	477.2 ± 26.8	489.6 ± 21.4	551.1 ± 20.4
	$E_f$ [GPa]		32.3 ± 1.35	32.5 ± 0.62	32.6 ± 0.58	32.0 ± 0.42	31.8 ± 1.36	29.0 ± 0.56
	In-plane shear tests	$\tau_{max}$ [MPa]	62.9 ± 1.51	63.3 ± 2.15	52.3 ± 2.39	51.9 ± 1.27	45.9 ± 3.74	54.4 ± 0.46
		G [GPa]	3.6 ± 0.36	3.0 ± 0.32	4.2 ± 0.72	3.2 ± 0.18	3.0 ± 0.23	3.0 ± 0.52
	Interlaminar shear tests	$\sigma_{sbs}$ [MPa]	40.6 ± 2.1	41 ± 1.75	39.9 ± 0.55	38.1 ± 0.47	31.2 ± 3.1	38.1 ± 1.2

**Table 11.04 - Summary of properties of vinylester profiles.**

Property	Method	Unit	VE_WV_0	VE_NV_0	VE_WV_025	VE_NV_025	VE_WV_050	VE_NV_050
IMC	Calcination	[%]	73.7 ± 0.34	71.6 ± 0.49	70.4 ± 1.14	71 ± 1.3	71.6 ± 0.49	70.7 ± 0.47
Colour	CIE L*a*b* 1976	L*/a*/b*	80.86 / -0.81 / 4.92	79.89 / -1.57 / 5.54	80.44 / -1.02 / 4.38	79.64 / -1.15 / 4.58	79.36 / -1.02 / 4.48	78.79 / -1.35 / 5.33
Gloss	Glossmeter	(-)	11.7 ± 0.4	28.4 ± 1.9	46.2 ± 2.1	44.3 ± 1.8	57.5 ± 2.4	47.7 ± 1.6
$T_g$	DMA	$T_g$ ( $E'_{onset}$ ) [°C]	98.9 ± 5.6	--	--	--	--	--
		$T_g$ ( $\tan \delta$ ) [°C]	118.2 ± 4.3	--	--	--	--	--
Mechanical property	Tensile tests	$\sigma_{tu}$ [MPa]	475.4 ± 16.9	471.3 ± 13.0	421.8 ± 23.6	420.4 ± 39.8	444.6 ± 26.7	439.4 ± 8.37
		$E_t$ [GPa]	39.3 ± 1.6	43.4 ± 1.12	41.9 ± 0.23	39.8 ± 0.47	37.4 ± 1.12	40.7 ± 1.32
	Compressive tests	$\sigma_{cu}$ [MPa]	753 ± 29.76	540 ± 42.8	633.2 ± 58.42	567.7 ± 47.0	555.9 ± 122.2	545.3 ± 55.4
		Flexural tests	$\sigma_{fu}$ [MPa]	563.6 ± 14.9	546.7 ± 15.4	531.8 ± 15.42	585.8 ± 12.1	563.3 ± 7.61
	$E_f$ [GPa]		32 ± 1.23	32.9 ± 0.58	30.2 ± 0.14	32.8 ± 0.7	30.2 ± 1.17	32.2 ± 0.61
	In-plane shear tests	$\tau_{max}$ [MPa]	71.9 ± 0.13	64 ± 1.08	64.5 ± 2.52	66.6 ± 1.91	57.4 ± 1.28	56.4 ± 2.99
		G [GPa]	4.7 ± 0.07	3.4 ± 0.22	3.8 ± 0.5	4.5 ± 0.25	3.9 ± 0.54	3.5 ± 0.33
	Interlaminar shear tests	$\sigma_{sbs}$ [MPa]	41.5 ± 0.87	42.6 ± 2.13	36 ± 0.67	36.1 ± 0.52	31.8 ± 1.09	34.2 ± 0.52

### 11.4.2. Dynamic mechanical analysis

The results of the dynamic mechanical analysis of the two reference GFRP profiles, made with polyester (UP) and vinyl ester (VE) resins with no UV stabilizer additive (0%) and with (WV) surface veil, are presented in Figure 11.10, namely the storage modulus,  $E'$  (left axis - dashed lines), and the loss factor,  $\tan \delta$  (right axis - continuous lines).

The  $E'$  curves display a sigmoidal shape commonly seen in polymers and fibre reinforced polymers. The steep reduction of  $E'$  started at 104.1 °C and 98.9 °C for the UP and VE profiles, respectively. From a mechanical point of view, these temperatures correspond to the beginning of a steep decrease in the profiles' flexural stiffness. Additionally, the VE profile had higher values of initial  $E'$  and a steeper drop in the  $E'$  curve compared to the UP profile.

The  $\tan \delta$  curves show the typical peaks at elevated temperature associated to the glass transition process; those peaks occur for higher temperatures compared to the onset reduction of  $E'$ , namely for 125.4 °C (UP) and 118.2 °C (VE), the peak value being lower for the VE profile.

The  $T_g$  values obtained from both the  $\tan \delta$  curve and the onset of the  $E'$  curve were slightly higher for the UP profile than for the VE profile.

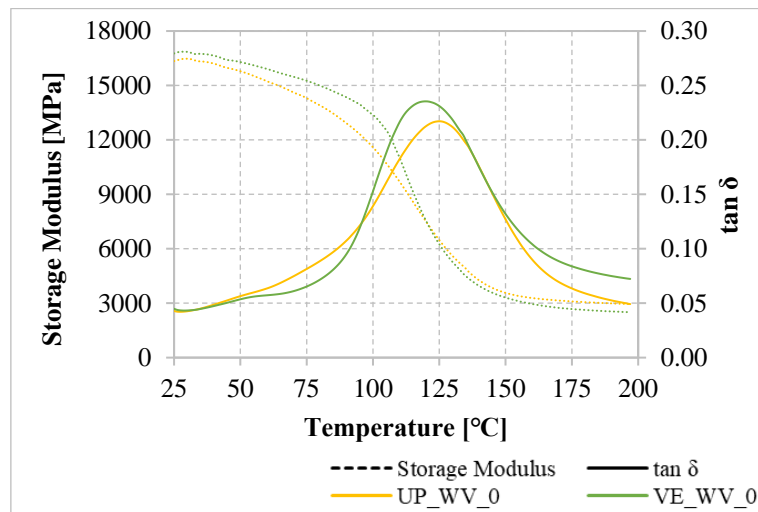


Figure 11.10 - Representative DMA curves of UP\_WV\_0 and VE\_WV\_0 profiles.

### 11.4.3. Tensile properties

Figure 11.11 presents the tensile response of the various GFRP profiles made with polyester (UP) and vinyl ester (VE) resins, with different contents of UV stabilizer additive (0%, 0.25% and 0.50%) and with (WV) or without (NV) surface veil.

In general, all types of profiles presented linear elastic behaviour until brittle rupture, which is the typical response of this type of GFRP composites in the longitudinal direction. The characteristic failure mode observed in this test is illustrated in Figure 11.05 (c), involving delamination and fibre rupture within the central part of the specimens (i.e., outside the grips).

Most UP profiles presented a tensile strength that ranged from ~430 MPa to ~470 MPa. However, the UP\_NV\_0 profiles presented significantly higher tensile strength than the remaining UP series, approximately 520 MPa. Since the same type of fibres and fibre architecture was used in the

former series, relative differences should be attributed to a better curing process in this specific series.

The VE profiles of the various series presented more uniform tensile strength, which ranged between ~420 MPa and ~470 MPa, thus being very similar to that of the UP series.

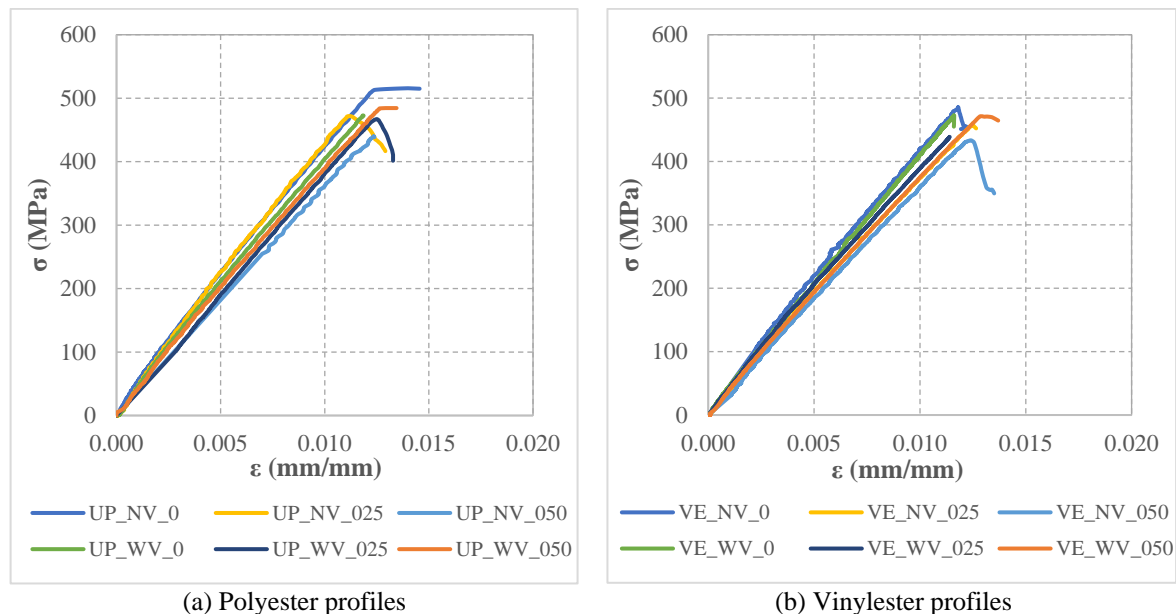


**Figure 11.11 - Representative stress-strain curves of tensile tests: (a) UP and (b) VE profiles.**

The tensile modulus was similar for all types of profiles, regardless of the type of resin, surface veil and UV stabilizer additive, ranging from approximately 37 GPa and 43 GPa. This result is expected as the (longitudinal) tensile modulus depends essentially on the fibre reinforcement ratio in the load direction, which was the same in all series.

The tensile properties obtained are slightly above the typical ranges of variation referred in chapter 2 for pultruded GFRP profiles.

#### 11.4.4. Compressive properties

Figure 11.12 presents the compressive response of the various GFRP profiles made with UP and VE resins, with different contents of UV stabilizer additive and with/without surface veil.

It was not possible to determine with sufficient accuracy the compressive modulus for all materials. Even though some tests present a clear and well-defined stress vs. strain curve, most of the results presented significant scatter, which was due to: (i) the reduced gage length associated with this specific test setup (CLC method); and (ii) the insufficient precision of the video extensometer for the determination of strains (for that gauge length).

In general, for all types of profiles, the stress-strain curves obtained in the compressive tests (the ones that were well-defined) reflect a linear elastic behaviour until failure, as expected, since this is the typical behaviour of this type of GFRP profiles under compression. The characteristic failure mode is shown in Figure 11.06 (b), involving delamination and fibre kinking in the gauge (free) length.

The compressive strength of UP profiles typically ranged between ~560 MPa and 607 MPa. However, for series UP\_WV\_0 and UP\_NV\_0, somehow the average compressive was higher, 725 MPa and 805 MPa, respectively. In the VE profiles, the compressive strength ranged between

~540 MPa and 630 MPa. In this case, series VE\_WV\_0 presented more different results, with a compressive strength of ~750 MPa.

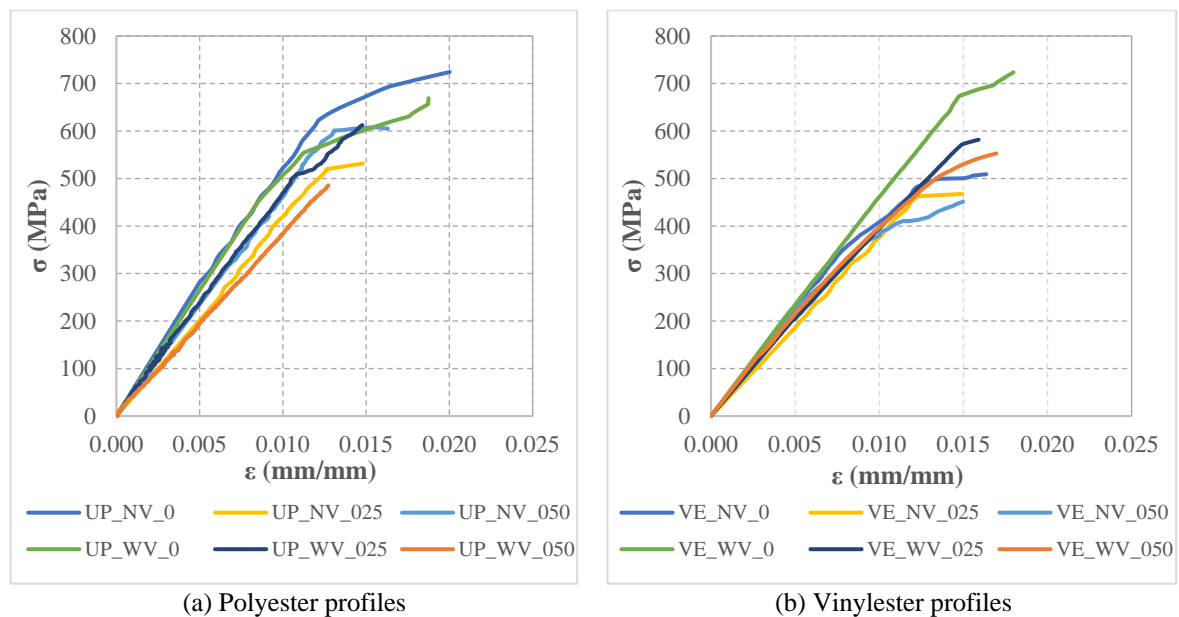


**Figure 11.12 - Representative stress-strain curves of compressive tests: (a) UP and (b) VE profiles.**

As mentioned in section 11.2.2, the series UP\_WV\_0, UP\_NV\_0 and VE\_WV\_0 were the first to be manufactured and the volume of material that was produced in those series was much higher than for the remaining series. Therefore, it is likely (but it was not possible to confirm) that the resin mixture could have been slightly different, due to the volume mixtures produced; moreover, as mentioned above, the environmental conditions during production and curing (temperature, relative humidity) may have also been different among the various series (in the plant where the profiles were produced those environmental conditions are not controlled), which can also justify the relative differences encountered for this particular property.

Regardless of the variations mentioned above, the results obtained for the compressive properties of the various profiles are above the ranges of variation reported in the literature indicated in chapter 2.

#### 11.4.5. Flexural properties

Figure 11.13 presents the flexural response of the various GFRP profiles made with UP and VE resins, with different contents of UV stabilizer additive and with/without surface veil.

For all types of profiles, in general, the flexural tests indicated linear elastic behaviour until failure, as expected. The flexural strength of the UP profiles ranged from ~470 MPa to 550 MPa. For the VE profiles, the flexural strength was higher than that exhibited by the UP profiles, ranging from ~550 MPa to 585 MPa. The higher flexural strength of the VE profiles can be due to the better performance provided by its polymeric matrix, which is quite important under bending.

The flexural modulus was similar for all types of profiles, ranging between ~29 GPa and 33 GPa. This was an expected result, as the flexural modulus (similarly to the tensile modulus) depends essentially on the type of reinforcing fibres and their architecture, which was identical in all series. The characteristic failure mode observed in the flexural tests is illustrated in Figure 11.07 (b).

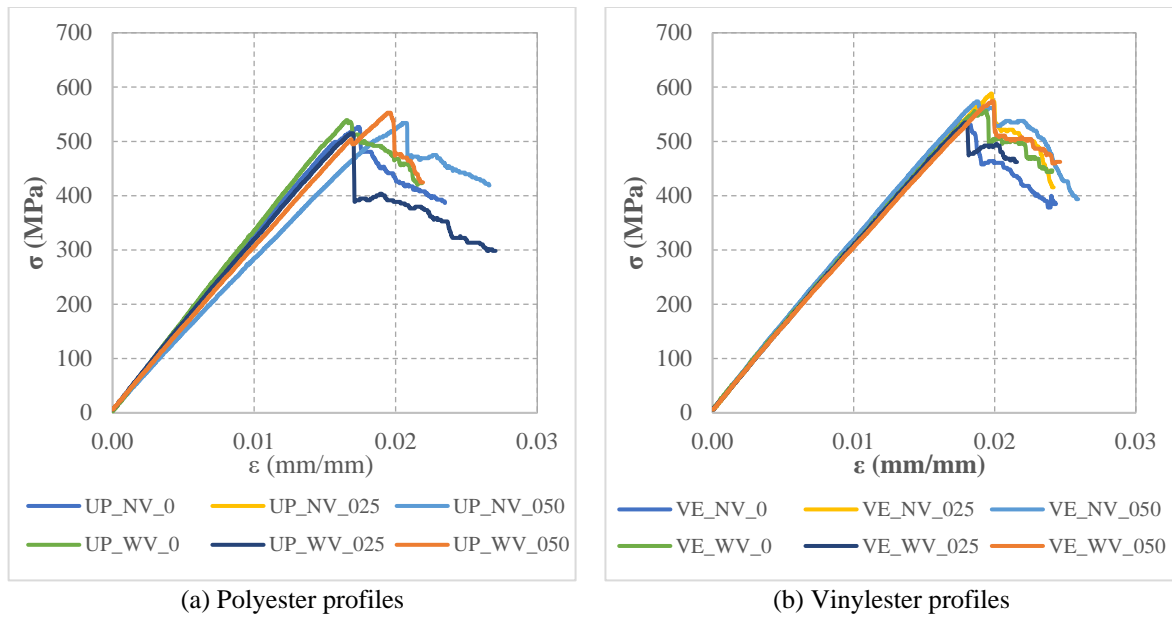


**Figure 11.13 - Representative stress-strain curves of flexural tests: (a) UP and (b) VE profiles.**

The results obtained for the flexural properties of the various profiles are above the range of variation reported in the literature for pultruded GFRP profiles shown in chapter 2, as for the tensile and compressive properties.

#### 11.4.6. In-plane shear properties

Figure 11.14 presents the in-plane shear response of the various GFRP profiles made with UP and VE resins, with different contents of UV stabilizer additive and with/without surface veil.

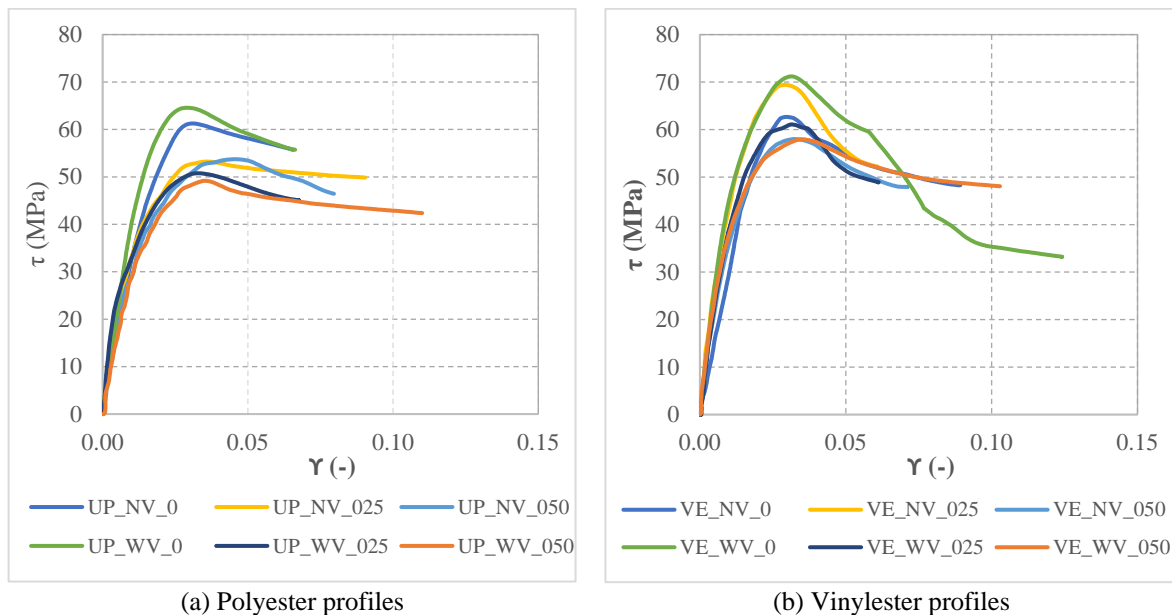


**Figure 11.14 - Representative shear stress-strain curves of in-plane shear tests: (a) UP and (b) VE profiles.**

For all types of specimens, the response was initially linear. Then, the response became non-linear, with progressive stiffness reduction, until a shear stress peak was attained. After this peak, there was a relatively soft shear stress reduction until failure; in some specimens, a relatively stable stress plateau was observed. The typical failure mode, involving a vertical crack oriented along the central V-notch, is presented in Figure 11.08 (c).

Most UP profiles presented an in-plane shear strength that ranged from ~45 MPa to 55 MPa. However, the profiles with no UV stabilizer additives, UP\_NV\_0 and UP\_WV\_0, presented a higher in-plane shear strength of ~63 MPa. It is worth referring that the in-plane shear strength of profiles containing mostly unidirectional reinforcement is mostly a matrix-dominated property.

The VE profiles presented a more uniform in-plane shear strength among the various series, which ranged from ~56 MPa to 65 MPa for most series. In this case, the exception was the VE\_WV\_0 profile, also without UV stabilizer additives, which presented a higher in-plane shear strength of ~73 MPa.

As mentioned above, when presenting and discussing the tensile properties, the above-mentioned differences in the in-plane shear strength of the various series could also be due to the different production volumes and/or to differences in the environmental conditions during manufacturing and curing.

The shear modulus was similar in all types of profiles, ranging from ~30 GPa and 43 GPa. In general, the VE profiles presented a higher shear modulus than the UP profiles, which could be due to the higher shear modulus of the vinylester resin; note that the shear modulus of pultruded profiles comprising essentially unidirectional reinforcement is also very much influenced by the shear modulus of the polymeric matrix.

The in-plane shear properties obtained for both types of profiles are above the typical ranges of variation reported in the literature for pultruded GFRP materials, described in chapter 2.

#### 11.4.7. Interlaminar shear strength

Figure 11.15 presents the interlaminar shear response of the various GFRP profiles made with UP and VE resins, with different contents of UV stabilizer additive and with/without surface veil. The typical failure mode observed in these tests, involving the fibre-matrix delamination in horizontal planes, is presented in Figure 11.09 (b).

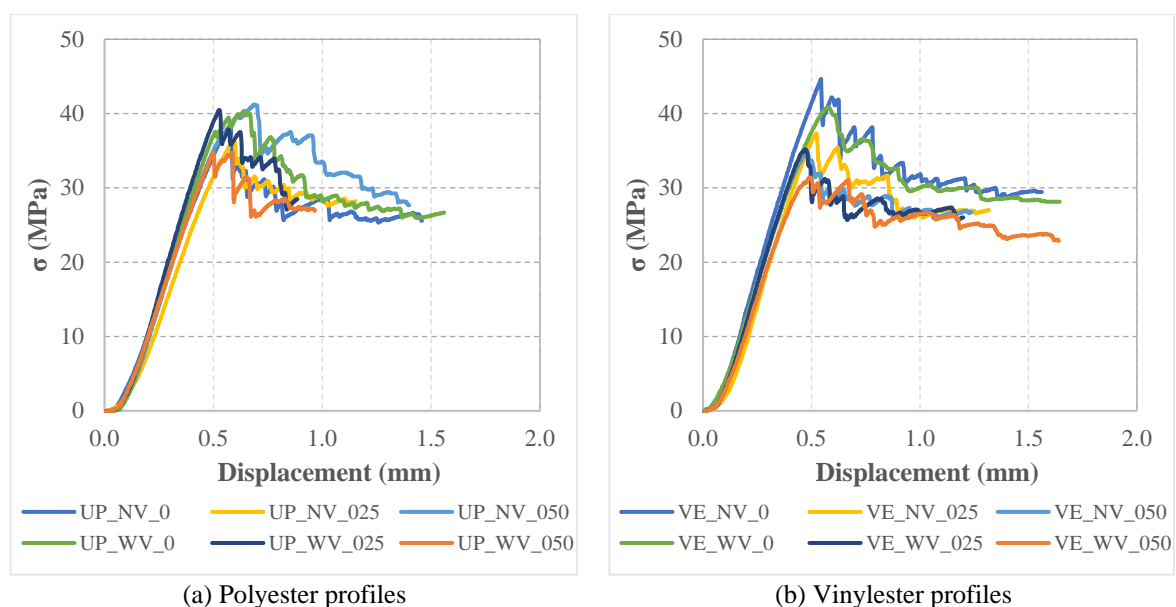


**Figure 11.15 - Representative load-displacement curves of interlaminar shear tests: (a) UP and (b) VE profiles.**

In general, all profiles presented the same type of behaviour and maximum interlaminar shear stress, before the first delamination. For the UP profiles, the interlaminar shear strength ranged from ~38 MPa to 41 MPa, while for the VE profiles it ranged from ~34 MPa to 42 MPa; somehow, the UP\_WV\_050 and VE\_WV\_050 series presented a lower strength of ~31 MPa.

The interlaminar shear strength results obtained are in-line with the typical results exhibited by pultruded GFRP profiles, as described in chapter 2.

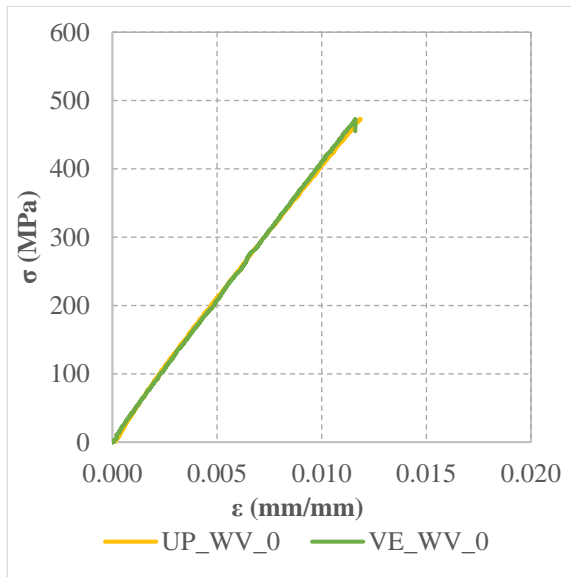
### **11.5. Comparison between UP\_WV\_0 and VE\_WV\_0**

As explained in the following chapters, the UP\_WV\_0 and VE\_WV\_0 series are the two reference types of profiles used in all ageing environments. Therefore, Figure 11.16 presents a comparison between the mechanical responses of these two types of profiles obtained in the different characterisation tests.

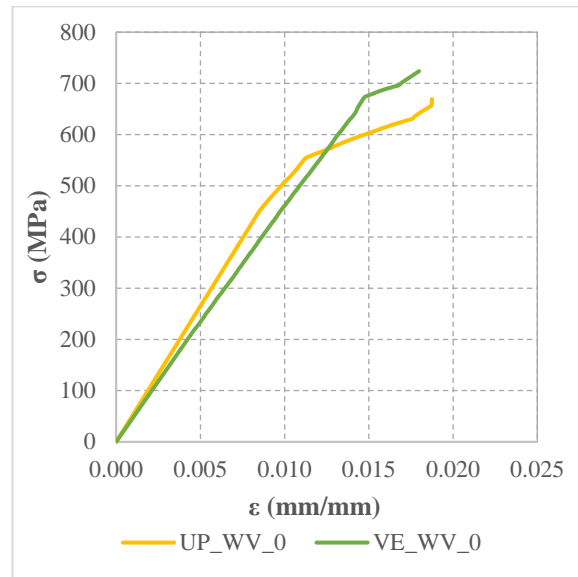
In general, the mechanical response of both types of profiles, which present similar fibre content and architecture, differing only in the type of polymeric matrix, is comparable. The most relevant differences are the following: the VE\_WV\_0 series presents (slightly) higher strength for all types of loading, which is likely due to the improved performance of the VE resin compared to the UP resin; however, the UP\_WV\_0 series presents (slightly) higher tensile and flexural moduli.

### **11.6. Concluding remarks**

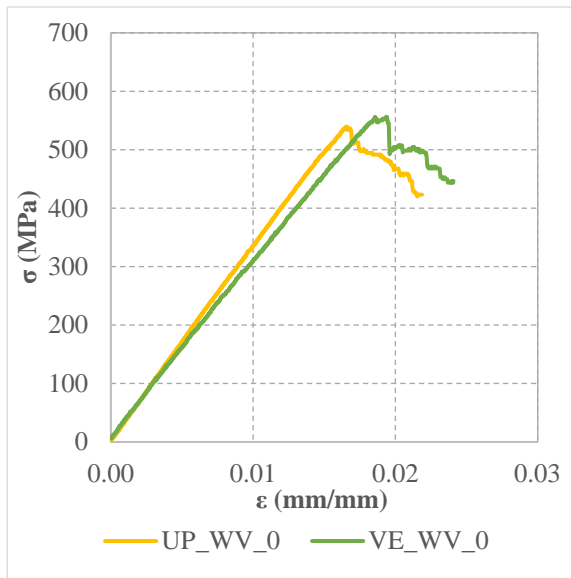
This chapter presented an overview of the test programme carried out in the scope of the present thesis. In particular, it explained the options made in the development of the experimental programme, namely regarding the materials and different typologies of GFRP profiles used in the experiments. In total, 12 materials were considered, comprising 2 types of resins, 3 contents of UV stabilizer additives and 2 types of superficial finishing (with or without superficial veil). The chapter then presented an overview of the test methodologies used for the characterisation of the physical, thermomechanical and mechanical properties of the different materials; in total, 10 test methods were presented: (i) five to assess physical and thermomechanical properties (inorganic mass content, colour, gloss, Barcol hardness, and glass transition temperature), and (ii) five to assess mechanical properties (tensile, compressive, flexural, in-plane shear, and interlaminar shear). In the final part of the chapter, the results of the initial characterisation tests were presented and analysed. These results will serve as a reference for the ageing tests presented in the next chapters. These chapters also provide additional information about the experimental programme, concerning both the laboratory study and the field study.



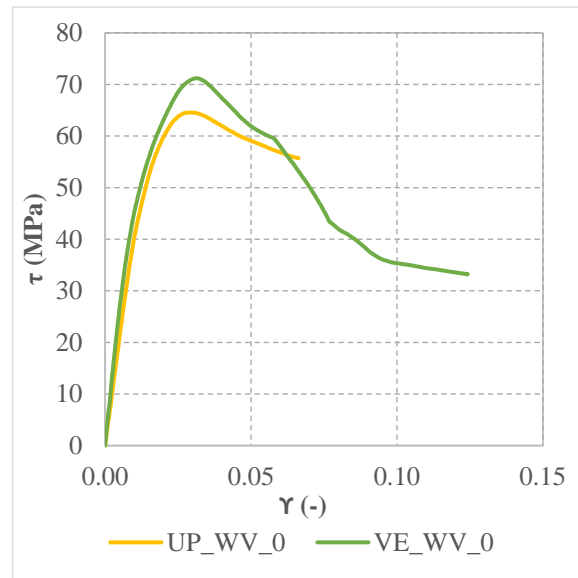
(a) Tensile test



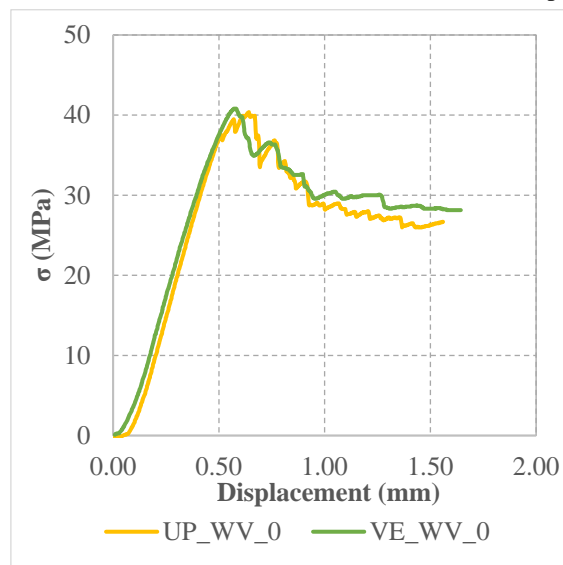
(b) Compressive test



(c) Flexural test



(d) In-plane shear test



(e) Inter-laminar shear test

**Figure 11.16 - Representative curves of mechanical tests of UP\_WV\_0 and VE\_WV\_0.**

## **12.Exposure of GFRP composites to chemical environments**

### **12.1. Introductory remarks**

There is already a relatively long history of use of pultruded GFRP profiles in a wide range of applications, some of them in corrosive or chemically aggressive environments. Indeed, the construction industry has seen a rise in the use of GFRP materials in those environments, precisely due to their improved resistance to chemicals, namely when compared to conventional materials, such as reinforced concrete or steel; this is the case of the infrastructures inspected in Part II (water and wastewater treatment plants).

Despite the growing use of GFRP materials, there is still a lack of knowledge regarding their behaviour when exposed to chemically aggressive environments, including for profiles made with the most common types of resins and fibres. Although several studies have been carried out to investigate the behaviour of GFRP composites exposed to chemical environments, most of them addressed materials not commonly used in civil engineering applications. Therefore, there is a research gap in this area.

This chapter begins by presenting a brief literature review on the effects of exposure to chemical environments (alkaline and acidic) on GFRP composites. Next, a test program developed to assess the physical and mechanical changes that occur in GFRP profiles after exposure to such chemicals is presented. Subsequently, the results obtained in those laboratory tests are presented and discussed. Finally, the main conclusions obtained from the experiments are summarized.

### **12.2. Literature review**

#### **12.2.1.Preliminary remarks**

A considerable number of variables influence the durability performance of FRP composite materials, such as the type of polymeric matrix (resin, fillers and additives), the type of fibre reinforcement (type of reinforcing fibres, fibre architecture), the manufacturing process, the type of exposure (type and aggressiveness of environmental conditions - temperature, type of chemical agent and concentration), and the duration of exposure. This section presents and discusses the main findings of previous studies reported in the literature on this subject; they have been selected based on the production technique (pultrusion) and constituent materials (glass fibres and polyester/vinylester resins), considering the type of pultruded GFRP profiles more often used in civil engineering (also used in the test programme).

In civil engineering applications, composites are typically not exposed to concentrated chemicals directly. Therefore, the effects of chemicals on GFRP composites are usually studied in aqueous solutions. However, since exposure does not always involve immersion, it is important to study the durability performance of GFRP materials when they are exposed to chemicals in both liquid and vapour phases. Therefore, it is also relevant to take into account the effects of exposure to moisture.

#### **Exposure to moisture (water)**

Composite materials can be exposed to moisture and aqueous environments through direct contact with rain, humidity, moisture, or immersion in aqueous solutions. Moisture can penetrate into

the GFRP matrix and cause degradation of the composite structure, leading to a reduction in mechanical properties. The effects of moisture exposure in composites has been comprehensively reviewed by Liu *et al.* [III.13], Pritchard & Jones [III.14], Kharbari *et al.* [I.01], Schutte [III.15], Sousa [III.16] and Svetlick [III.17], among others.

The impact of moisture absorption on the deterioration of GFRP materials can be understood by examining the effect of water on (i) the reinforcing fibres, (ii) the polymeric matrix, and (iii) the fibre-matrix interphase. Such impact can be divided into two categories: physical and chemical.

Physical ageing refers to the temporary modification of the polymer properties, which are mainly influenced by temperature, but can partially revert upon drying - it encompasses **plasticization**, **swelling** and **relaxation** of the polymer matrix. Chemical ageing may occur after prolonged exposure and may lead to irreversible degradation of the polymer matrix, the fibres, and the fibre-matrix interface. It mainly encompasses **hydrolysis** of the polymer matrix, causing chain scission and also damaging the fibre-matrix bond, or even resulting in pitting damage to the fibres [III.18], [III.19]. Changes in physical and mechanical properties may involve a combination of both types of ageing, with one or the other being more prevalent, according to the nature of the GFRP material and the characteristics of the environment.

A summary of the degradation mechanisms mentioned above, caused by moisture, and their classification is presented in Table 12.01.

**Table 12.01 - Most relevant physical and chemical, moisture induced, degradation mechanisms, adapted from [III.17].**

Classification	Degradation mechanism		Location			Reversibility
			Fibre	Matrix	Interphase	
Physical	Plasticization			X	X	Yes <sup>a</sup>
	Swelling			X		Yes <sup>a</sup>
	Relaxation			X	X	No
Chemical	Hydrolysis	Chain scission		X		No <sup>a</sup>
		Pitting	X			No <sup>a</sup>
		Debonding			X	No <sup>a</sup>
	Leaching		X	X	X	No

<sup>a</sup> - Processes which have been reported both as irreversible and reversible

**Plasticization** occurs when the water molecules penetrate into the polymeric matrix (filling the empty voids between the polymer macromolecules) and interact with the polymeric chains, reducing their intermolecular forces and increasing chain mobility [III.20]. This leads to: (i) a reduction in the glass transition temperature ( $T_g$ ) and an increase in the polymer ability to deform under load; and (ii) a reduction in the mechanical properties of the composite (strength and modulus) [III.21], [III.22].

**Swelling** occurs when the water molecules penetrate into the matrix and cause the polymer chains to expand, leading to an increase in the volume of the composite. This expansion can result in the formation of voids and micro-cracks in the matrix [III.23], reducing the mechanical properties of the composite (strength and modulus). Also, the fibre-matrix interphase can be a convenient channel for water ingress [III.24], and the water absorbed there can cause differential swelling of the interface and promote the propagation of micro-cracks [III.25], [III.26].

**Relaxation** in a polymeric matrix and in the fibre-matrix interphase, due to water-penetrant swelling effects, allows macro-molecular movement of the reticulated network of the polymeric matrix and the redistribution of voids and water inside the composite. This phenomenon can further widen the initial cracks and channels, and create new cracks and voids, thereby allowing additional water to penetrate the composite, further promoting the various degradation mechanisms [III.27], [III.28].

**Hydrolysis** is an irreversible chemical reaction between water and the polymeric matrix, leading to the breakdown of the polymer chains and reducing the cross-linking density [III.29], thus causing a reduction of mechanical properties. Hydrolysis of GFRP composites can also result in the formation of voids in the matrix, through the hydrolytic molecular bond cleavage and consequent formation of water-soluble fragments [III.30], which weakens the polymeric structure and reduces the overall performance of the composite. Hydrolysis of the ester groups is the primary reason for chemical degradation of the unsaturated polyester and vinylester matrices [III.31], the former resin being more affected [III.32].

**Leaching** is the release of low molecular weight soluble components from the composite polymeric matrix. These particles can be dissolved in the water and leached away along the interface [III.33], particularly at high temperatures, resulting in an apparent weight loss of the composite [III.34]. When these events extend to the fibre reinforcement and the fibre-matrix interphase, the weight loss becomes permanent [III.35].

The degradation of the mechanical properties of composites occurs through a combination of the physical and chemical mechanisms described above. The different mechanical properties of composites are not affected in the same way by moisture. In fact, flexural and shear properties, which are generally matrix- and interface-dominated (with such dependence being a function of the fibre architecture, in case of shear), generally present significant reductions for prolonged exposure; on the other hand, tensile strength and modulus, which are fibre-dominated, are usually much less affected [III.36].

In general, the more moisture is absorbed by the composite material the more likely it is that its properties will deteriorate and the changes upon drying will be less reversible. Long-term exposure to moisture at higher temperatures increases the degradation rate, generally causing irreversible changes that permanently affect the properties of composite materials.

### **Exposure to alkaline and acidic environments**

As mentioned, GFRP composites can degrade in both alkaline and acidic environments. When such chemicals are dissolved in aqueous solutions, to some extent they act similarly to moisture. In fact, those solutions can diffuse into the composite material and interact with its constituents, causing the same degradation mechanisms presented above, including the formation of cracks and voids in the polymeric matrix, and resulting in a reduction of mechanical properties. However, alkaline and acidic solutions contribute in different manners to the degradation process (as explained ahead) and some studies have shown that alkaline environments have a more aggressive impact on the mechanical properties of composites than acidic environments [III.37].

Alkaline solutions, including sodium hydroxide (NaOH), potassium hydroxide (KOH) and calcium hydroxide (Ca(OH)<sub>2</sub>), are commonly used in various industrial processes (water and wastewater

treatment), and they can also simulate pore solutions of concrete (relevant for composites applied as reinforcing bars or strengthening strips, or for hybrid structures, combining components made of GFRP with those made of conventional materials, such as concrete or steel).

Previous studies have shown that the extent of degradation in GFRP composites immersed in alkaline solutions depends on several factors, including the type and concentration of the alkaline solution, temperature, and immersion time. In general, higher concentrations of alkaline solutions and longer immersion times result in a higher degree of degradation [III.38]. Additionally, the type of alkaline solution has also been shown to have a significant effect, with NaOH being the most aggressive among those that are usually tested.

In alkaline environments, there is a higher concentration of hydroxyl ions ( $\text{OH}^-$ ) in the aqueous solution that diffuses into the composite, reacting differently with each of the composite constituents. In the polymeric matrix, they react with the ester groups present in polyester and vinylester resins, breaking their polymeric chains (hydrolysis). Since polyester resins have a higher number of ester groups in comparison to vinylester resins, the former are generally more susceptible to hydrolysis and considered less chemically stable in alkaline environments [III.39]. The stability of vinylester resins can be attributed to a higher polymeric conversion rate and to a more compact microstructure.

The degradation of glass fibres in an alkaline environment can be categorized into two mechanisms: (i) etching, which occurs when the hydroxyl ions break the silica-oxygen bonds in the glass fibres, resulting in loss of surface area and reduction of tensile strength [III.40]; and (ii) leaching, which is the diffusion of the alkali ions (e.g.  $\text{Na}^+$  ions) out of the glass structure of the fibre by the hydroxyl ions [III.41]. Both mechanisms occur in the presence of water, and their effects are more severe in the presence of an alkaline solution.

Acidic solutions, including hydrochloric acid (HCl) and sulphuric acid ( $\text{H}_2\text{SO}_4$ ), are also present in various industrial processes (water and wastewater treatment) and, in some cases, in urban rain water. As for alkaline solutions, a number of variables affect the degradation that occurs due to exposure to acidic solutions, such as the type of acid and the concentration of the acidic solution, the temperature, and the period of exposure.

In acidic solutions, hydrolysis degradation of the ester groups of the polymeric matrix also occurs. However, without the presence of high concentration of hydroxyl ions (found in alkaline environments), this reaction only occurs with the hydroxyl ions contained in the water of the acidic solution, thus, it occurs at a much slower pace when compared to alkaline environments.

Glass fibres, when exposed to an acidic environment, suffer a more pronounced leaching effect (in comparison to the neutral environment), in which the diffusion of the alkali ions (e.g.  $\text{Na}^+$  ions) out of the structure of the glass fibres occurs due to the presence of hydrogen ions ( $\text{H}^+$ ) in the acidic solution [I.07]. These anions diffuse into the voids of the matrix and are transferred into the fibre-matrix interphase, weakening the bond strength, and gradually decreasing the mechanical properties of GFRP composites [III.43].

## 12.2.2. Review of studies on the effects of alkaline and acidic environments

### 12.2.2.1. Studies on polymeric materials and matrices

The study of Pradchar *et al.* [III.44], [III.45] intended to examine the impact of temperature changes on the flexural strength of  $60 \times 25 \times 2$  mm unsaturated polyester specimens exposed to acidic solutions for 10 days. The specimens were exposed to three solutions - freshwater, 20 wt% hydrochloric acid (HCl), and 20 wt% sulphuric acid ( $H_2SO_4$ ) - and were also exposed to the vapour phase of those solutions to determine the effect of vapour condensation. Two methods were used to expose the specimens to different environmental conditions: (i) isothermal immersion at a constant temperature of 80 °C; and (ii) immersion under thermal cycles, consisting of a 24-hour cycles, starting at 80 °C and fluctuating from 80 °C to 40 °C for periods of 1 h; both temperature increasing and decreasing periods were also set for 1 h, and the remaining 12 h were set for room temperature at 20 °C.

Under the isothermal immersion condition, the flexural strength decreased 2.4% in water, 34.5% in HCl, and 19.4% in  $H_2SO_4$ . When exposed to the vapour phase of those solutions, the reductions in flexural strength were lower, especially for the acids, 2.3% in water, 23.1% in HCl, and 8.2% in  $H_2SO_4$ .

For immersion under thermal cycles, the decrease in flexural strength was higher compared to the isothermal immersion condition (except for HCl): 9.8% in water, 17.8% in HCl, and 19.8% in  $H_2SO_4$ . When exposed to the vapour phase, the decrease was even higher, namely for the acids: 21.0% in water, 26.7% in HCl, and 20.2% in  $H_2SO_4$ .

Comparing the results of the two conditions, for the cyclic temperature condition, the decrease in flexural strength was greater in the vapour phase than in the liquid phase, which suggests that dew condensation occurred in the material and may reduce its lifespan when exposed to acid vapours. Additionally, HCl solution caused the greatest decrease in flexural strength compared to water or  $H_2SO_4$ .

### 12.2.2.2. Studies on GFRP composites

Nishizaki & Meiarashi [III.46] conducted a study to investigate the effects of water immersion and exposure to high humidity on pultruded specimens made from glass fibre-reinforced vinylester. The specimens had a cross-sectional area of  $68 \times 15 \times 3$  (length  $\times$  width  $\times$  thickness, in mm). The researchers immersed the specimens in water at 40 °C for 380 days, in water at 60 °C for 434 days, and exposed them to a vapour phase at 60 °C with relative humidity of 85% for 423 days. The study found that, during immersion, the flexural strength of the specimens decreased by 20% at 40 °C and 38% at 60 °C. When exposed to the vapour phase, the flexural strength of the specimens decreased by 23%, which was significantly less than the reduction caused by immersion at the same temperature. Through the analysis of SEM images, the authors concluded that these reductions were caused by debonding between the fibres and the matrix.

In the study conducted by Bazli *et al.* [III.47], the effect of exposure to various aggressive environments on the flexural strength of different vinylester GFRP pultruded profiles was examined. The researchers selected 5 cross-sections and subjected them to alkaline solutions with pH 13.6 and 12.7, simulating pore solutions of concrete with potassium hydroxide (KOH), sodium hydroxide (NaOH), and calcium hydroxide ( $Ca(OH)_2$ ), as well as an acidic solution of hydrochloric acid with pH

3.5. All profiles were immersed for 147 days at 20 °C. The authors found that, during immersion, the weakening of the bond between the fibres and the matrix resulted in the development of microcracks at the interface, leading to a decrease in mechanical properties. The reduction in flexural strength varied within the different profile types due to their geometry and cross-section shape. However, the reduction in the alkaline environments was always greater compared to the acidic environment. For the cross-section of 20 × 15 × 7 mm (length × width × thickness, in mm), flexural strength decreased by 43.9% in the 13.6 pH solution, 39.7% in the 12.7 pH solution, and 15.6% in the 3.5 pH solution.

Sonawala *et al.* [III.48] investigated the degradation of glass isophthalic polyester (IPE) pultruded specimens, with a cross-section of 100 × 25 × 3.75 mm (length × width × thickness, in mm), when immersed in brine (5% NaCl) and a 10% sodium hydroxide (NaOH) solution over a period of 270 days at 25 °C, both with and without a polyethylene terephthalate (PET) and C-glass surface veil. The authors found that, after 270 days of immersion in brine, the IPE composite experienced a 31% reduction in tensile strength and a 30% reduction in flexural strength. However, immersion in NaOH resulted in major physical and chemical degradation of the composite (hydrolysis), leading to a 95% reduction in tensile strength and a 79% reduction in flexural strength. The effect of the surface veils on the degradation in brine was also analysed. The application of the C-glass veil did not result in significant changes in the properties of the IPE laminates, but the addition of the PET veil caused a further decrease of 8% in tensile strength and 25% in flexural strength. This further decrease observed with the application of the PET veil was attributed to an increase in water absorption of the composite into the bulk of the material. In the case of immersion in the alkaline solution, the same level of property reduction was observed, regardless of which veil was applied: 95% and 79% reductions in tensile and flexural strengths, respectively.

In a study by Feng *et al.* [III.49], the long-term performance of pultruded GFRP vinylester plates in corrosive environmental conditions was analysed. The plates were immersed in four different solutions with varying concentrations and temperatures for 90 days. The environmental conditions included: (i) H<sub>2</sub>SO<sub>4</sub> with a pH 5 at 60 °C; (ii) H<sub>2</sub>SO<sub>4</sub> with a pH 5 at 90 °C; (iii) a 30% solution of H<sub>2</sub>SO<sub>4</sub> at 60 °C; and (iv) a 10% solution of NaOH at 60 °C. The results indicated that the flexural strength of the plates decreased with exposure time in acidic solutions, and that the acid concentration and temperature had a significant impact on the flexural properties. For the cross-section of 100 × 15 × 8 mm (length × width × thickness, in mm), the flexural strength decreased in solution (i) by 16%. The increase in concentration and temperature of the acidic solution led to flexural strength reductions of 34% and 77% (solutions (iii) and (ii), respectively). The flexural strength in the alkaline solution at 60 °C (iv) decreased by 29%, having resulted in a more pronounced degradation effect on the mechanical properties than the acidic solution at the same temperature. The changes in the flexural modulus in the acidic solution (i) had little significance (1%), while the alkaline solution led to a decrease of 15%. The increase in concentration and temperature of the acidic solution led to a decrease of 39% and 37%, respectively.

In Figure 12.01, fibre pull-out and debonding between the fibres and matrix are illustrated. The delamination between the fibre layers of the composite was the main failure mechanism when they were

subjected to flexure, which can be observed in Figure 12.01 (b). The visual aspect of the specimens at different exposure times is shown in Figure 12.02, where it is noted that the specimens exposed to acidic solutions showed a deeper change in colour compared to those exposed to alkaline environments. In specimens exposed to the acidic solution at 60 °C, the fibre resurgence was more visible than in those exposed to the same solution at 90 °C.

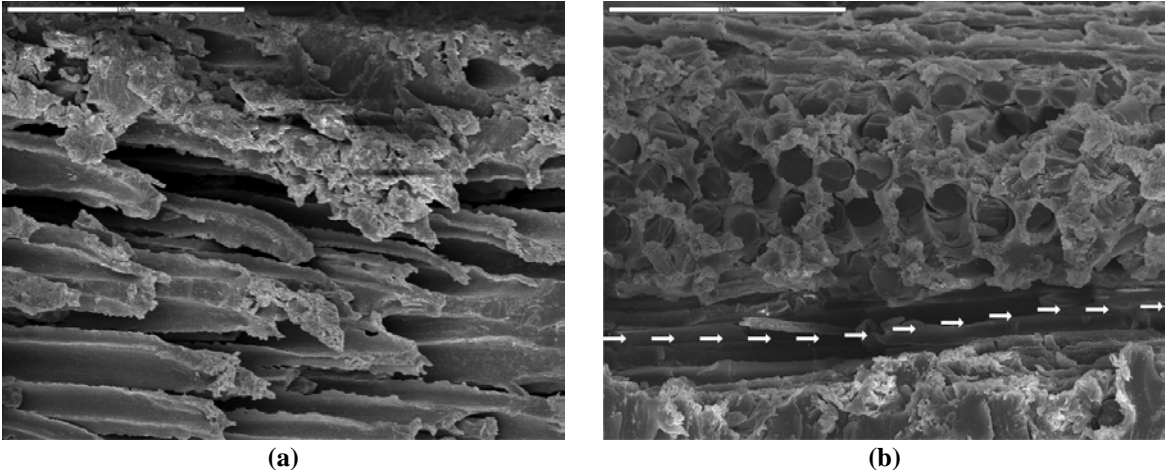


Figure 12.01 - SEM images of fractured sections of GFRP vinylester specimens after 30 days exposure to: (a) H<sub>2</sub>SO<sub>4</sub> solution (30%, 60 °C); (b) H<sub>2</sub>SO<sub>4</sub> solution (pH 5, 90 °C), adapted from [III.49].

		Exposure time				
		Virgin Sample	7 days	15 days	30 days	90 days
a)						

Figure 12.02 - Changes in appearance of GFRP vinylester specimens, after exposure to: (a) H<sub>2</sub>SO<sub>4</sub> solution (30%, 60 °C), (b) NaOH solution (10%, 60 °C), (c) H<sub>2</sub>SO<sub>4</sub> solution (pH 5, 90 °C), adapted from [III.49].

In a study by Gentry *et al.* [III.50], the performance of pultruded GFRP composites with vinylester resin, with a thickness of 6 mm, exposed to different environmental conditions for 28 days was examined. Three different environments were tested: deionized water, ammonia solution (3% volume), and acetic acid solution (pH 3). The study considered two immersion temperatures (23 °C and 80 °C) and evaluated the tensile, flexural, and inter-laminar shear strengths. The results obtained are

summarized in Table 12.02, showing that the alkaline environment (ammonia solution) led to the highest reduction for all properties and for both temperatures - thus, it was the most conditioning environment. Immersion in the acidic solution, at lower temperatures, led to an increase in flexural and shear strengths, although both properties presented a reduction following immersion in deionized water. The increase in properties was attributed to an improvement at the fibre-matrix interphase, but this effect was lost at the higher temperature (80 °C), resulting in higher reductions in interphase related properties.

**Table 12.02 - Mechanical properties reduction, adapted from Gentry *et al.* [III.50].**

Environment	Temperature	Tensile strength retention	Flexural strength retention	Interlaminar shear strength retention
Deionized water	23 °C	98%	96%	96%
	80 °C	70%	43%	76%
Ammonia solution	23 °C	83%	86%	75%
	80 °C	61%	27%	62%
Acetic acid solution	23 °C	92%	108%	101%
	80 °C	60%	44%	74%

Cordeiro *et al.* [III.51] analysed the behaviour of pultruded GFRP vinylester profiles immersed in an alkaline solution with 1.0% NaOH, 1.4% KOH, and 0.16% Ca(OH)<sub>2</sub> (pH 13). After exposure to such solution at 40 °C for 120 days, they analysed changes in tensile strength and spectrophotometer colour variations. For the cross-section of 127 × 5 × 5 mm (length × width × thickness, in mm), the tensile strength presented reductions of about 20% and 40% after 90 and 120 days of exposure, respectively. The loss in tensile strength was correlated with fibre-matrix delamination, and fibre degradation. The colour variation of the specimens was based on the ANOVA statistical analysis by using the CIE 1976 L\*a\*b\* colour system, and showed that the discolouration of the specimens ( $\Delta E^*$ ) after 120 days was perceptible to the naked eye, as the vinylester resin lightened ( $\Delta E^* \approx 12.2$ ). The authors stated the colour variation was not directly related with the reduction in mechanical properties. It was however important for the aesthetical aspect of several projects, especially for outdoor applications.

### 12.2.3. Summary of chemical exposure literature review

There is a general lack of studies about the durability of pultruded GFRP composites used in civil engineering applications when exposed to chemicals. Moreover, the few studies available present significant variations in the test programmes, namely with respect to: (i) test specimens (resin, type of profile, geometry); (ii) environmental conditions (chemical composition, duration, and temperature); and (iii) characterised properties.

This review shows that most studies that evaluated the performance in terms of retention of mechanical properties only assessed a single property, such as the flexural strength or the tensile strength. Furthermore, there is a lack of information on the behaviour of these materials under conditions other than immersion, which may not be representative of real-world industrial applications, namely vapour exposure. Additionally, there is limited data on the physical and non-mechanical performance of these materials in various environmental conditions.

In spite of those limitations, the results available allow assessing some features concerning the

behaviour of GFRP materials exposed to chemical environments. It was found that the fibre-matrix interface appears to have lower resistance to acidic environments, especially at higher temperatures, while the matrix has lower resistance to alkaline environments. It was also shown that exposure to higher concentrations of those chemicals and to higher temperatures results in a higher decrease of mechanical properties. In general, the data analysed show that alkaline environments cause a higher decrease in flexural properties compared to acidic environments, due to the higher degradation of the matrix. In terms of tensile properties, the acidic environments lead to a higher decrease in comparison to alkaline environments, due to the degradation of the fibre-matrix interphase that occurs in the former, leading to premature fibre pull-out under stress.

The information available in the literature is relatively limited concerning two aspects addressed in the present study: (i) the effects of immersion vs vapour exposure; and (ii) the effects of superficial protections. A universal testing methodology for composite materials has yet to be established [III.52], and the design of accelerated tests is critical. The setup of those tests must reflect the real-world environmental conditions that composites will experience.

### 12.3. Description of the test programme

The effects of chemical exposure was studied on the two reference GFRP profiles, made with the two alternative resins, comprising surface veil but without UV stabilizer additive (UP\_WV\_0 and VE\_WV\_0, presented in section 10.2), since they are the materials most often used in real applications; it was also assumed that the UV stabilizer additive has no significant effect on the chemical resistance of the materials. Both materials were exposed to three chemical conditions (neutral, acidic and alkaline), two types of exposure (immersion and vapour), three temperatures (23, 50 and 70 °C) and four different periods (1, 4, 8 and 16 weeks), as summarized in Table 12.03. Also, in order to assess the level of surface protection that can be conferred to the specimens in vapour, the *SikaCor EG5 system* (by Sika) was selected, comprising 2-pack acrylic polyurethane with high chalking resistance and colour retention; two layers of that superficial protection were applied to all sides of the specimen with an average final thickness of  $0.11 \pm 0.03$  mm.

**Table 12.03 - Chemical ageing environments.**

Material	Exposure period (weeks)	Exposure temperature (°C)	Chemical condition	Type of exposure
UP_WV_0	1, 4, 8, 16	23, 50, 70	Neutral (Water) Acidic (H <sub>2</sub> SO <sub>4</sub> ) Alkaline (NaOH)	Immersion Vapour (with and without superficial protection)
VE_WV_0				

The selection of exposure periods and temperatures was based on the methodology provided in ISO 175 [III.53], which defines 16 weeks for a long-term test. To monitor the evolution of the effects of chemical exposure, characterization tests were scheduled with intermediate durations of 1, 4, and 8 weeks. ISO 175 [III.53] defines that the preferred test temperatures are 23 °C (as reference temperature) and 70 °C; in addition, an intermediate recommended temperature of 50 °C was selected. In the initial characterization, presented in section 10.4, the mean values determined for the  $T_g$  of the considered

GFRP materials with UP and VE resins were 104 °C and 99 °C, respectively. Thus, the highest exposure temperature considered (70 °C) is approximately 30 °C below the lowest  $T_g$  of the materials.

The conditions of the chemical environments to which the GFRP materials were subjected to were selected based on the information collected during the inspections carried out on the structures described in Part II. Demineralized water ( $H_2O$ ) was selected as the reference environment, a sulphuric acid ( $H_2SO_4$ ) solution was used for the acidic environment, and a sodium hydroxide ( $NaOH$ ) solution was used for the alkaline environment. The concentration of the solutions was as indicated in ASTM D543-14 [III.54], comprising a 10% solution for the sodium hydroxide and a 30% solution for the sulphuric acid; both solutions were obtained by dilution of concentrated reagents.

The GFRP samples, with size of 100 × 300 × 6.5 mm, were subjected to each chemical condition by immersion (liquid phase) and exposure to vapour (vapour phase). The samples were subjected to the different exposure conditions placed inside polypropylene containers, as shown in Figure 12.03. The immersed samples were stacked using a separator made of the same material that ensured an appropriate space between them, and submerged with a volume of 1.5 litre per specimen. The samples subjected to the vapour phase were suspended in other identical containers, but in this case only a volume of 0.5 litre per specimen was added. Both containers were capped and sealed with mastic in order to minimize evaporation losses.

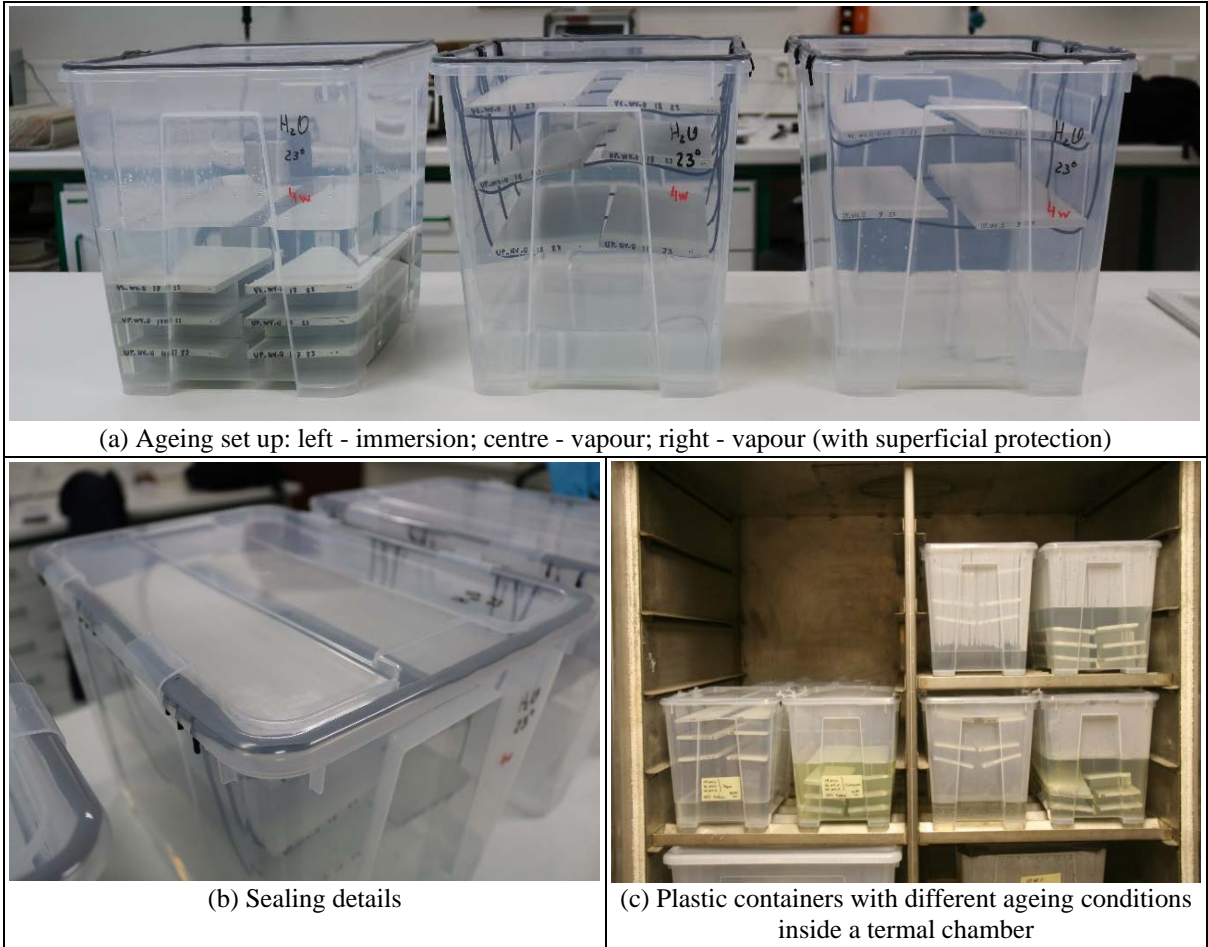


**Figure 12.03 - Specimens set-up to chemical exposure.**

After exposure to each of the chemical environmental conditions, the samples were rinsed in tap water and placed in an oven at 80 °C for one week to dry until constant mass, in order to reduce the

reversible damages presented before being cut down to the size required by each test standard specification. To evaluate the effects of the chemical environments, samples were collected at predefined times and the following physical properties were analysed: (i) colour; and (ii) gloss. In addition, in order to complement the lack of information in the literature, the following mechanical properties were analysed: (i) compressive properties; (ii) in-plane shear properties; and (iii) interlaminar shear strength. All properties were determined in accordance with the characterisation methods described in section 10.3, and the main results are also presented in appendix VII. For colour and gloss assessment, the properties of each specimen were measured before and after the exposure periods. Before testing, the superficial protection coating was not removed from the specimens; given its very small thickness, its effect on the mechanical properties was considered negligible.

## **12.4. Results and discussion**

In this section, the experimental results of the tests performed on GFRP materials exposed to different chemical environmental conditions are presented and discussed. Properties of profiles with UP and VE resins, determined in accordance with the characterisation methods described in section 11.2, are presented in terms of remaining properties compared to the initial ones obtained in unaged specimens.

### **12.4.1. Visual inspection**

A visual inspection was performed during the chemical ageing of both materials, to try to establish a damage metric that could be correlated with the mechanical performance of the materials. This visual inspection comprised the assessment of colour and gloss changes and surface finishing (texture).

Figure 12.04 and Figure 12.05 display photographs of test specimens exposed to the higher temperatures (50 °C and 70 °C) and the longest period (16 weeks) of immersion and exposure to vapour in the three types of conditions (neutral, acidic, and alkaline), for UP and VE specimens, respectively. Visual inspection of the test specimens shows that some ageing conditions caused significant changes in the colour and the gloss, as well as in the surface texture. The changes are particularly evident in the UP material that has been immersed in the alkaline solution at the highest temperature.

In general, and for both materials, exposure to different environments caused a progressive yellowing and lightening. This trend was more pronounced with longer exposure times and higher temperatures. However, variations in this pattern were observed, depending on the type of resin used and the specific exposure conditions.

In addition, these images indicate that some specimens undertook severe degradation, as evidenced by changes in colour, dimensions, texture, and other visible marks. Some specimens (e.g. UP\_WV\_0 immersed in an alkaline environment) showed signs of cracking and flaking, which might be indicative of severe degradation of mechanical properties (assessed ahead).

During inspections carried out in the field study (part II, section 9.7.3), substructures exposed to aggressive chemical environments showed three common types of anomalies, listed here in order of frequency: stains, loss of gloss, and superficial marks. It was found that these anomalies were also observed in most specimens after undergoing chemical ageing in laboratory experimental campaigns.

### 12.4.2. Colour variation

Figure 12.06 presents the effects of different chemical ageing conditions on the colour change of specimens made of UP resin, in terms of the variation of parameter  $\Delta E^*$ . This parameter, determined through the CIE  $L^*A^*B^*$  coordinate system, creates a vector between the original measurement and the final coordinate after exposure. The greater the value of this parameter, the greater the distance between the two points (i.e. the colour change). The variation of the coordinates  $L^*$  (black-white axis),  $a^*$  (green-red axis) and  $b^*$  (blue-yellow axis) reflects the colour variation between measurements.

When exposed to water at 23 °C and 50 °C, UP specimens presented a very similar behaviour, in both phases (liquid and vapour), with a relatively low change in colour ( $\Delta E^* \approx 2$ ). For the same temperatures, immersion in the acidic environment presented variations like those of the immersion in water; however, immersion in the alkaline environment caused a very significant change in colour ( $\Delta E^* \approx 10$ , lightening and blueing). When exposed to 70 °C, the immersion in the acid environment (yellowing) and alkaline environment (lightening) showed similar and significant colour changes, in comparison to that observed due to immersion in water.

In the vapour phase, the colour change was very consistent at all exposure temperatures, except in the case of the acidic environment at 70 °C, which led to a significant colour change ( $\Delta E^* \approx 10$ , yellowing). For UP specimens exposed to immersion, an increase in temperature led to a significant colour change in all environments; at 70 °C, similar effects on colour change resulted from acidic and alkaline environments and alkaline environments only had more impact at lower temperatures. For UP specimens, the highest  $\Delta E^*$  value (11.0) was measured after 8 weeks of immersion in an acidic environment.

Figure 12.07 presents the effects of different chemical ageing conditions on the colour change of VE specimens. Exposure of VE material to the liquid and vapour phases, at 23 °C and 50 °C, caused similar colour changes, for all environments ( $\Delta E^* \approx 6$ ); however, these colour changes were more significant than those observed for the UP material. At 70 °C, the acidic environment caused a greater colour change (yellowing) when compared to the other environments, in both phases. For the VE specimens, the highest  $\Delta E^*$  value (12.6) was measured after 16 weeks of immersion in an acidic environment.

The colour changes for VE specimens immersed in the alkaline environment at 50 °C ( $\Delta E^* = 7$ ) was lower than the results obtained by Cordeiro *et al.* [III.50], which for VE laminates presented a  $\Delta E^* = 12$  (lightening) when immersed in an alkaline environment at 40 °C. This could be due to differences in the chemical solutions, the initial colour of the specimens or the matrix formulation.

For both materials exposed to the vapour phase, coating the specimens with SIKA protection led to much less pronounced colour changes (except for the acidic environment at 70 °C), which means that the application of a coating provides, at least, protection against changes in aesthetic appearance.

The results obtained with both types of materials showed that higher temperatures promoted a significant colour change in all environments, with significant colour changes occurring at 70 °C. It was found that the VE material is more susceptible to colour changes when compared to the UP material, even in neutral environments and lower temperatures.

		Neutral environment (H <sub>2</sub> O)	Acidic environment (H <sub>2</sub> SO <sub>4</sub> )	Alkaline environment (NaOH)
50 °C	Immersion	UP.WV.0 50°C 16w I H <sub>2</sub> O	UP.WV.0 50°C 16w I H <sub>2</sub> SO <sub>4</sub>	UP.WV.0 50°C 16w I NaOH
	Vapour	UP.WV.0 50°C 16w V H <sub>2</sub> O	UP.WV.0 50°C 16w V H <sub>2</sub> SO <sub>4</sub>	UP.WV.0 50°C 16w V NaOH
70 °C	Immersion	UP.WV.0 70°C 16w I H <sub>2</sub> O	UP.WV.0 70°C 16w I H <sub>2</sub> SO <sub>4</sub>	
	Vapour	UP.WV.0 70°C 16w V H <sub>2</sub> O	UP.WV.0 70°C 16w V H <sub>2</sub> SO <sub>4</sub>	UP.WV.0 70°C 16w V NaOH

Figure 12.04 - Photographic survey of polyester (UP) specimens exposed to chemical ageing, after 16 weeks of exposure.

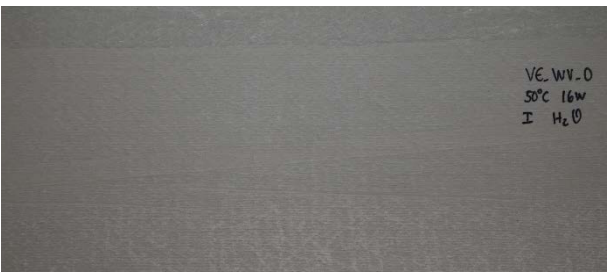
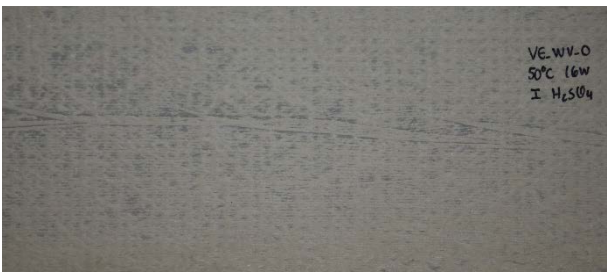
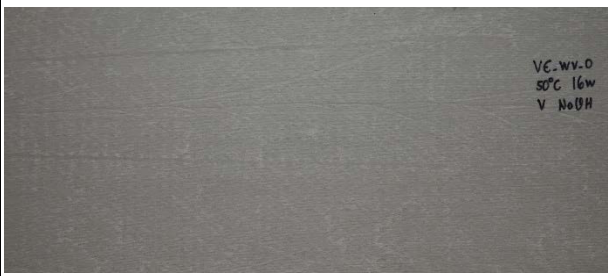
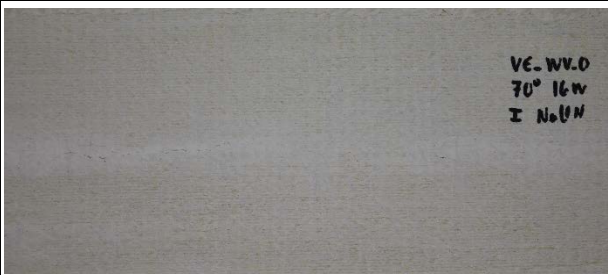
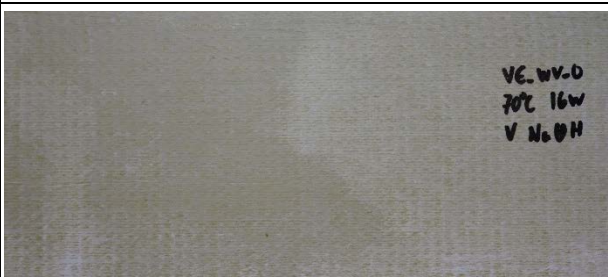
		Neutral environment (H <sub>2</sub> O)	Acidic environment (H <sub>2</sub> SO <sub>4</sub> )	Alkaline environment (NaOH)
50 °C	Immersion	 <p>VE-WV-0 50°C 16w I H<sub>2</sub>O</p>	 <p>VE-WV-0 50°C 16w I H<sub>2</sub>SO<sub>4</sub></p>	 <p>VE-WV-0 50°C 16w I NaOH</p>
	Vapour	 <p>VE-WV-0 50°C 16w V H<sub>2</sub>O</p>	 <p>VE-WV-0 50°C 16w V H<sub>2</sub>SO<sub>4</sub></p>	 <p>VE-WV-0 50°C 16w V NaOH</p>
70 °C	Immersion	 <p>VE-WV-0 70°C 16w I H<sub>2</sub>O</p>	 <p>VE-WV-0 70°C 16w I H<sub>2</sub>SO<sub>4</sub></p>	 <p>VE-WV-0 70°C 16w I NaOH</p>
	Vapour	 <p>VE-WV-0 70°C 16w V H<sub>2</sub>O</p>	 <p>VE-WV-0 70°C 16w V H<sub>2</sub>SO<sub>4</sub></p>	 <p>VE-WV-0 70°C 16w V NaOH</p>

Figure 12.05 - Photographic survey of vinyl ester (VE) specimens exposed to chemical ageing, after 16 weeks of exposure.

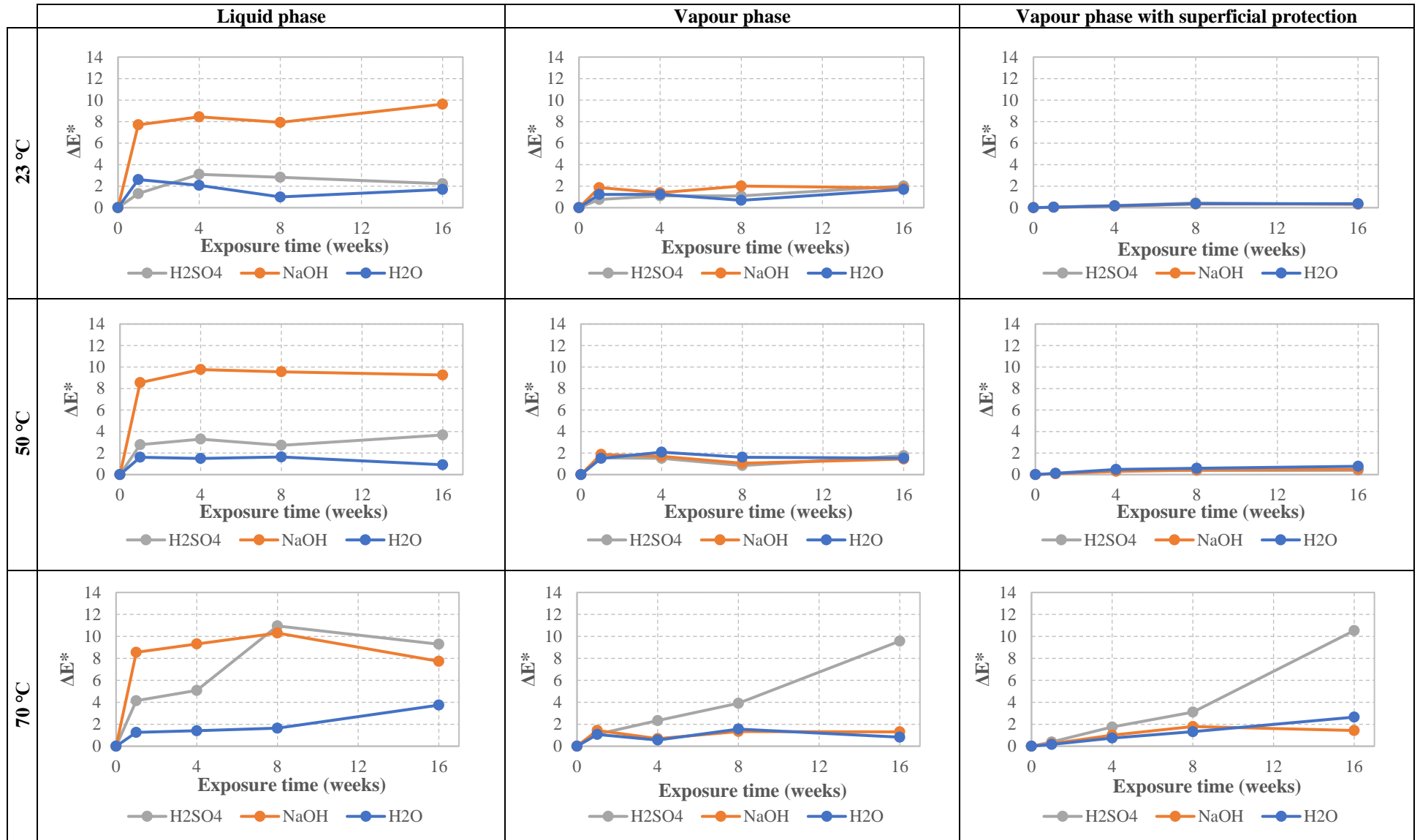


Figure 12.06 - UP specimens colour change ( $\Delta E^*$ ) during chemical ageing.

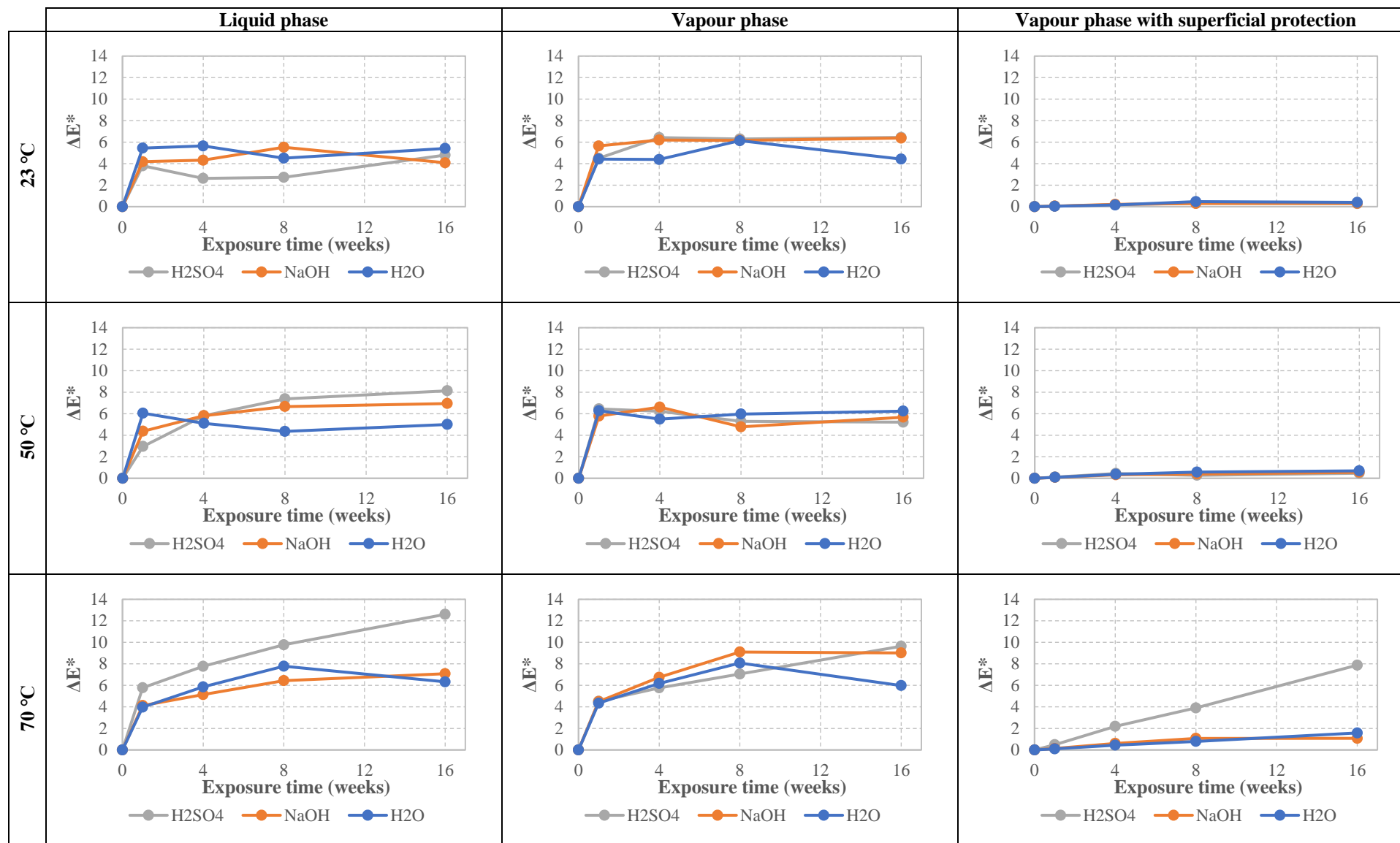


Figure 12.07 - VE specimens colour change ( $\Delta E^*$ ) during chemical ageing.

### 12.4.3. Gloss retention

The specimens that were exposed to the different chemical ageing, showed a progressive loss of gloss. This tendency was more pronounced with longer periods of exposure. However, in the most aggressive environments (alkaline liquid phase for UP), the highest loss of gloss occurred at the early stages of the exposure.

Figure 12.08 shows the results of gloss changes for the UP material. When immersed in water, for the temperatures of 23 °C and 50 °C, the specimens presented similar gloss variations. However, unlike what could be expected *a priori*, specimens immersed in water at 70 °C showed a less pronounced loss of gloss when compared to those immersed at lower temperatures.

When immersed in the alkaline solution, all UP specimens experienced a significant decrease in gloss at all temperatures, becoming almost negligible after 16 weeks. This variation mainly occurred at the initial periods of exposure.

UP specimens immersed in the acidic solution showed a progressive loss of gloss with time, with small variations between the various temperatures. Except for immersion at 70 °C, the gloss change in acidic solution was less compared to water.

In vapour phase, the gloss changes of UP material were very similar in all environments and directly related to both exposure time and temperature; the alkaline environment was the most aggressive, particularly in shorter periods of exposure, with a gloss change of around 55%.

The results of gloss changes in VE profiles (Figure 12.09), show a very similar behaviour in the specimens immersed in water at all temperatures. At 23 °C, the gloss change was similar in all environments and was never less than 50% of the original value.

Immersion in the alkaline solution, for 16 weeks, at the highest temperatures (50 °C and 70 °C) led to a gloss reduction of approximately 80%. In comparison, the UP specimens retained no gloss for the same conditions.

Contrary to what happened in the UP material, immersion of VE material in the acidic solution caused a loss of gloss that was always greater than that of immersion in water. In the vapour phase, the loss of gloss was never higher than 40%, with a similar behaviour in both UP and VE specimens.

The analysis of the surface protection effect of the SIKA coating shows that, in the vapour phase, the loss of gloss was similar in all environments, being greater at higher temperatures. Furthermore, the surface protection behaviour of the coating was similar for both materials, as would be expected, since the analysed characteristic is independent of the substrate.

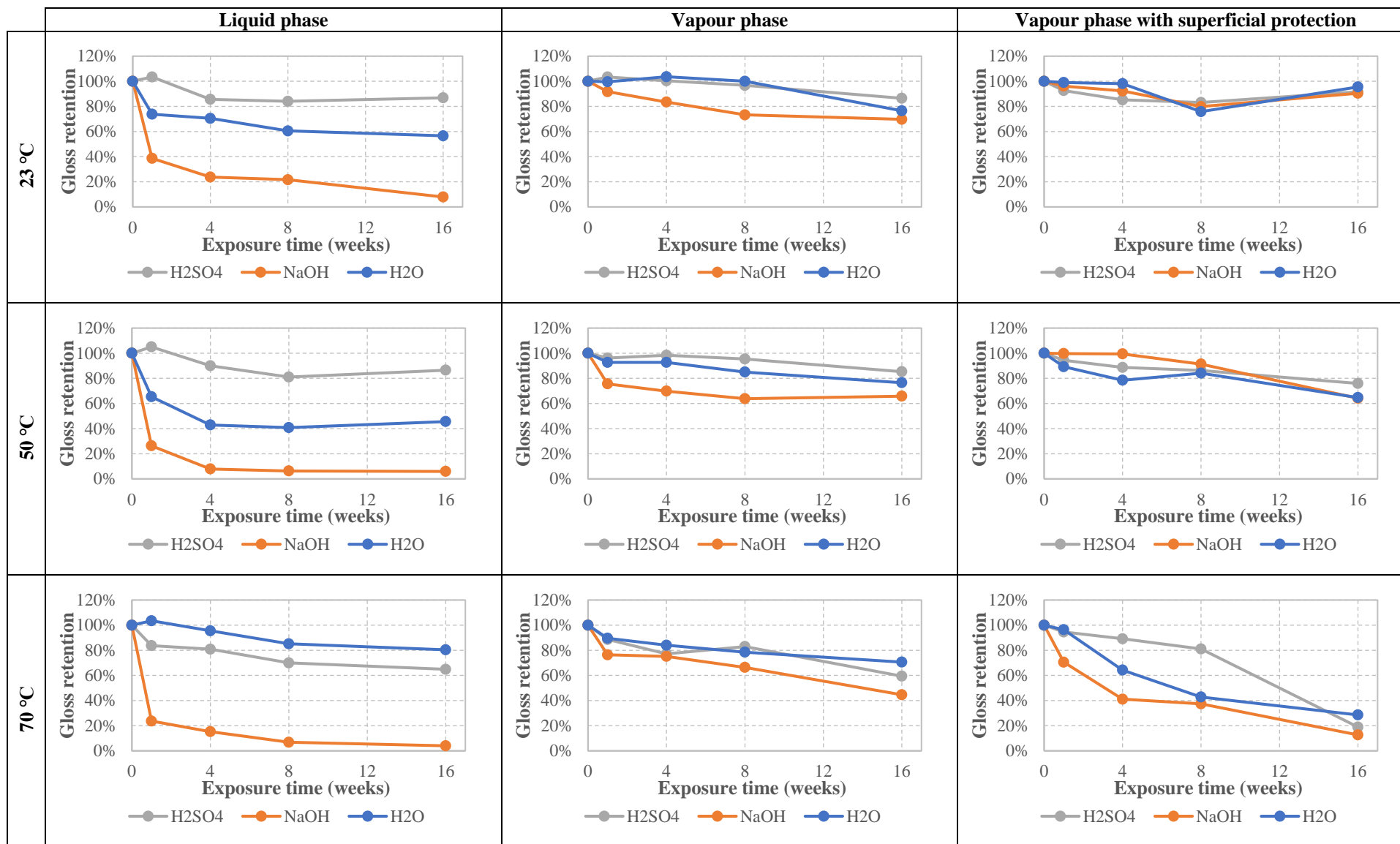


Figure 12.08 - Gloss retention of UP specimens during chemical ageing.

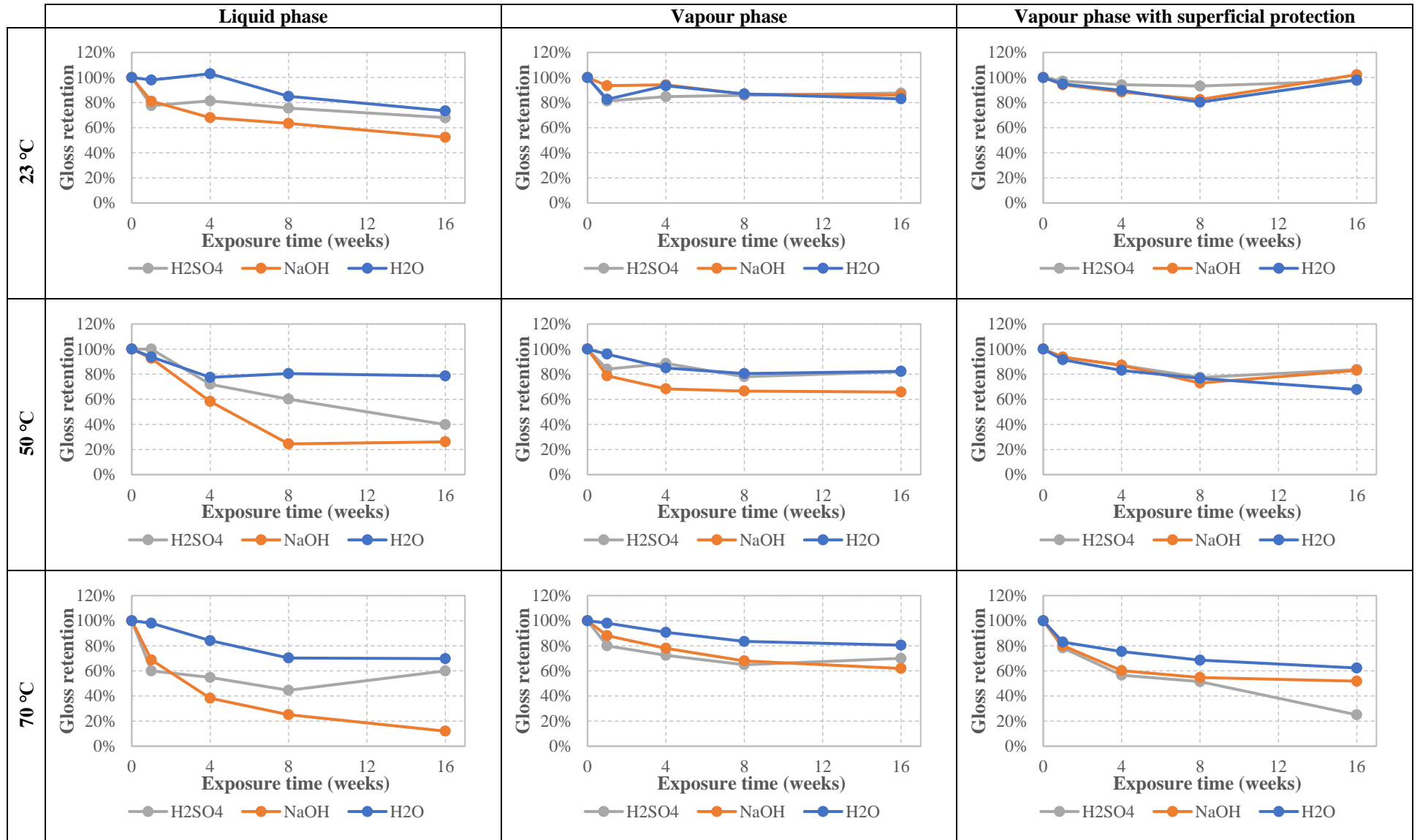


Figure 12.09 - Gloss retention of VE specimens during chemical ageing.

#### 12.4.4. Compressive tests

Figure 12.10 shows the compressive response of representative UP and VE specimens for each of the different chemical environments, at temperatures of 23 °C and 70 °C, after 16 weeks. For most materials, it was not possible to determine the compressive modulus with sufficient accuracy due to the reduced gage length associated with the specific test setup (CLC method) and the insufficient precision of the video extensometer for that gage length. In fact, while some tests provided a clear and consistent stress vs. strain curve, most results exhibited significant scatter. The UP curve for alkaline immersion at 70 °C is not illustrated since the material was too damaged to be tested.

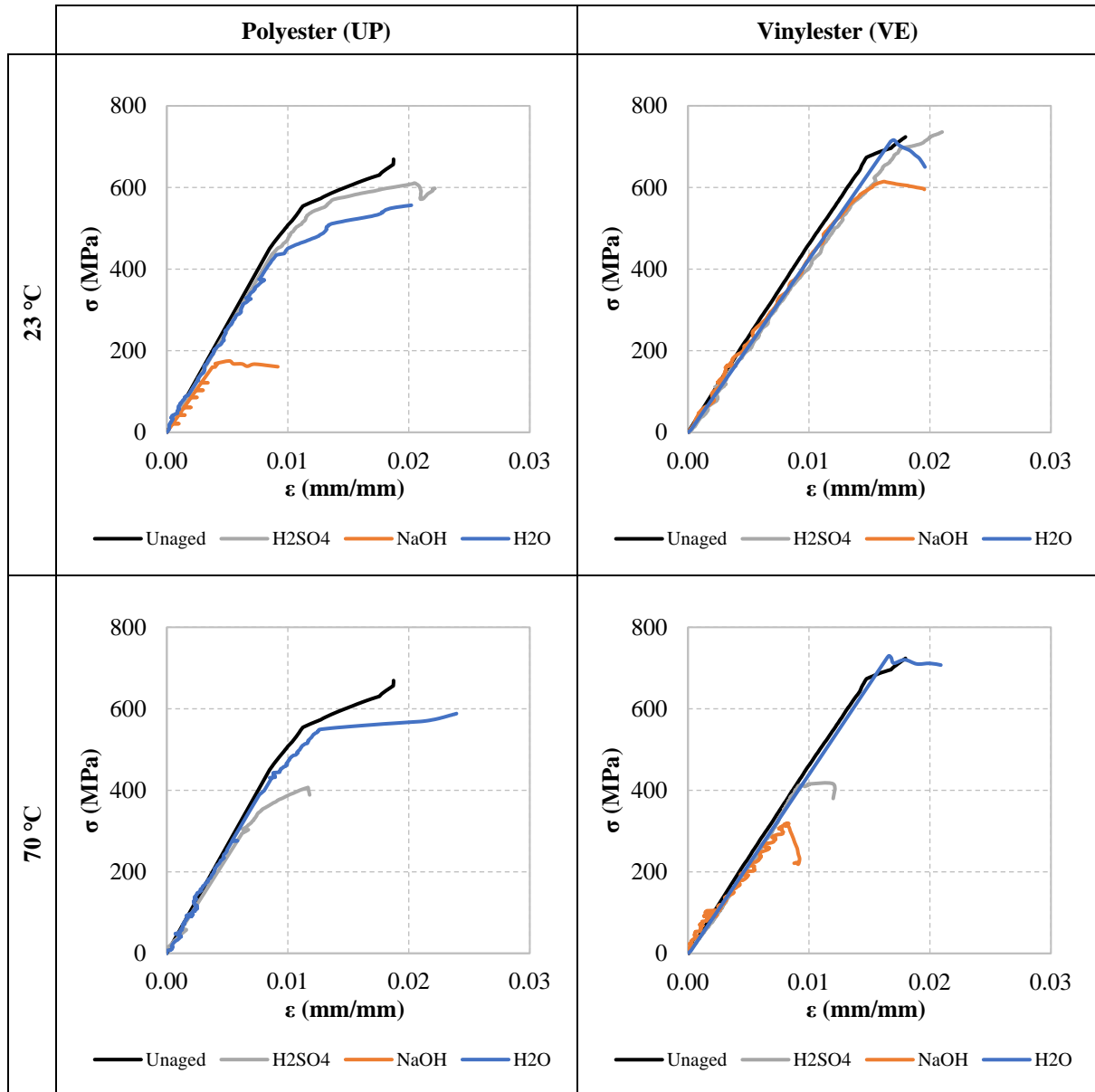


Figure 12.10 - Representative stress-strain curves of compressive tests of unaged materials and after 16 weeks of immersion in chemical ageing at 23 °C and 70 °C.

As the experimental curves show, the specimens presented linear responses with similar slope until damage initiation occurred, which was followed by a non-linear ascending branch until failure. However, the specimens immersed in the alkaline solution, at both temperatures, presented a non-linear descending branch after damage initiation, which may indicate the occurrence of loss of effectiveness

in the adhesion between the fibres and the matrix.

The effects of different ageing conditions on the compressive strength of the UP and VE materials is illustrated in Figure 12.11, which plots the average values (with error bars as standard deviation). In general, for all ageing environments, the compressive strength decreased with increasing exposure periods.

**Immersion in water** caused similar and relatively small reduction in compressive strength for both materials. This reduction in compressive strength was more pronounced with increasing temperature and exposure period, with maximum reductions of 16% (UP - 70 °C/16 weeks) and 14% (VE - 50 °C/16 weeks). For the VE specimens, the exposure to 50 °C/16 weeks was more damaging than the exposure to 70 °C/16 weeks (9% reduction vs. 14%).

**Immersion in the acidic environment** of the UP specimens caused similar reductions of compressive strength to those observed in water at lower temperatures (23 °C and 50 °C). In acidic immersion at 70 °C and for longer exposure periods (16 weeks), exposure to acidic environment caused a higher reduction in compressive strength, with a maximum of 40%. On the other hand, VE specimens showed a progressive reduction in compressive strength during the first 8 weeks (20%) of acidic immersion at 23 °C, with a (somewhat unexpected) recovery of that property after 16 weeks of exposure (only 4% reduction). At the higher temperatures (50 °C and 70 °C), specimens exhibited very similar progressions of compressive strength, with a maximum reduction of 44% after 16 weeks of exposure. The results show that the UP material, when compared to the VE material, presents better performance, measured by its compressive strength, when immersed in acidic solutions.

**Immersion in the alkaline environment** caused large reductions in the compressive strength of the UP specimens, particularly for longer periods of exposure. After 16 weeks of exposure, the reduction of this property at 23 °C was very expressive (73%), and at the higher temperatures of 50 °C and 70 °C, the compressive strength became negligible. This reduction is compatible with the significant degradation visually observed in the test specimens after exposure (Figure 12.04). Regarding the VE material, results show a similar behaviour when specimens were immersed in alkaline and acidic environments, with a maximum reduction of 50% (70 °C/16 weeks). These results show that the VE material demonstrates superior compressive strength performance when exposed to alkaline solutions compared to the UP material.

When exposed to the **vapour phase**, both materials showed improved performance compared to liquid phase exposure. A similar trend of reduction of compressive strength was observed with longer exposure periods and higher temperatures. For the UP specimens, exposure to water vapour became the most conditioning environment, with a maximum reduction of 23% (70 °C/16 weeks), which is slightly higher than the reduction observed in immersion. Under the same conditions, acidic and alkaline environments caused property reductions of 16% and 10%, respectively. For VE specimens, acid vapour exposure became the most conditioning environment with a maximum reduction of compressive strength of 40% (70 °C/8 weeks). Exposure to water vapour caused a property reduction of 20% (50 °C/8 weeks) and exposure to alkaline environment caused a 12% reduction (70 °C/16 weeks). It was also observed

that, in some of the environments and for both materials, there was an increase in compressive strength after 16-weeks of exposure (compared to preceding periods), which may be related to a post-cure phenomenon that occurred during longer periods of exposure (except for acidic vapour at 23 °C, the compressive strength after 16 weeks never exceeded the initial strength).

When comparing the two materials, they exhibit distinct behaviours in the two exposure phases. In the liquid phase (immersion), the VE material outperformed the UP material even at higher temperatures and longer exposure periods, mainly in alkaline environments. However, in the vapour phase, the materials exhibited a similar performance, with UP even presenting better performance in some cases.

For both UP and VE materials, the alkaline environment had the greatest impact on the compressive strength reduction, especially at higher temperatures, which is in agreement with the conclusions drawn in other studies [III.48], [III.49].

In the existing literature, information on the influence of chemical ageing on the mechanical properties analysed herein is relatively scarce, with most studies being limited to only one property, typically flexural strength. However, Sonawala *et al.* [III.48] analysed the effect of alkaline solutions on the tensile strength and reported a 95% reduction for a UP material after 270 days at 25 °C, which is consistent with the results obtained in this study.

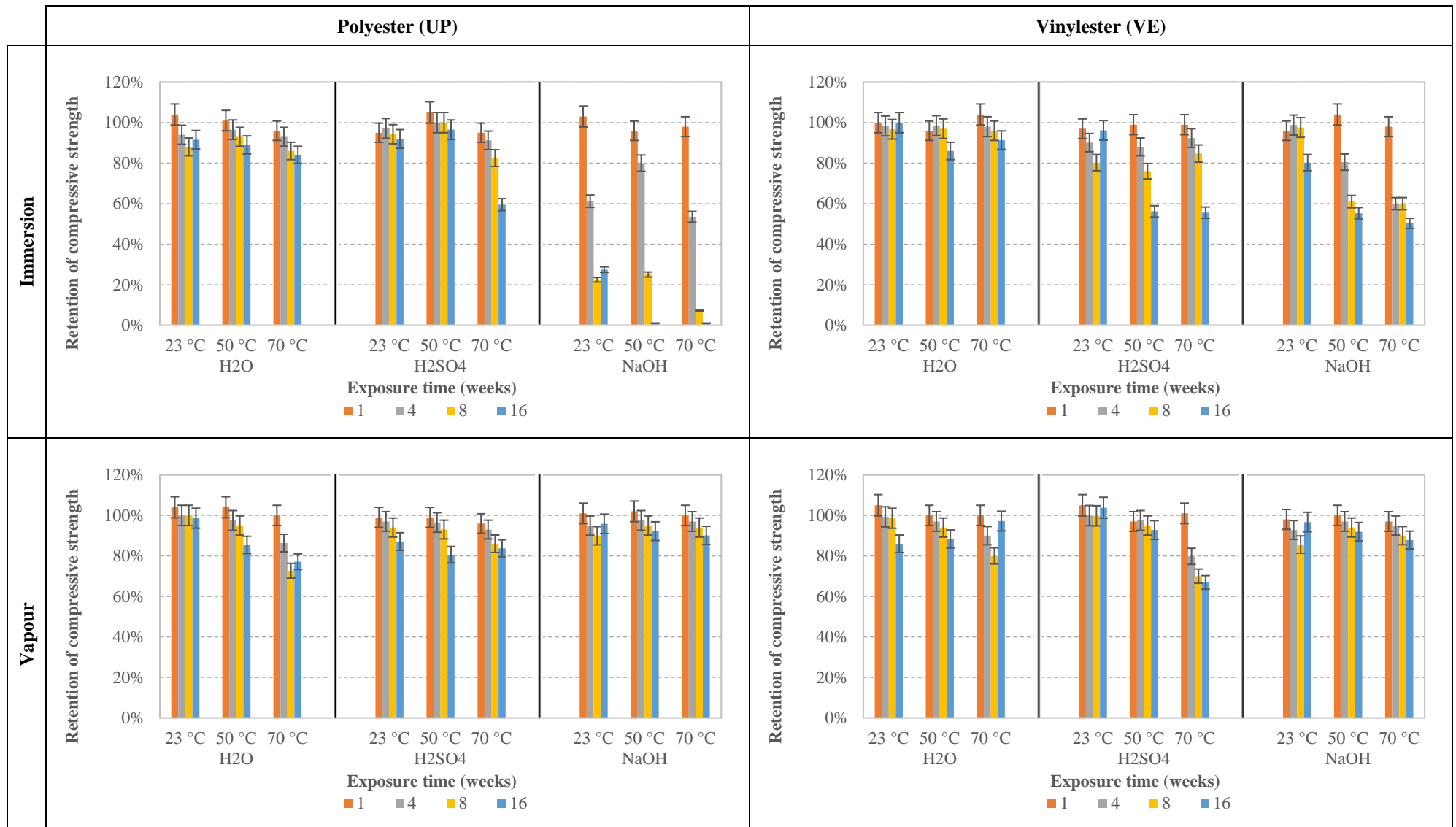
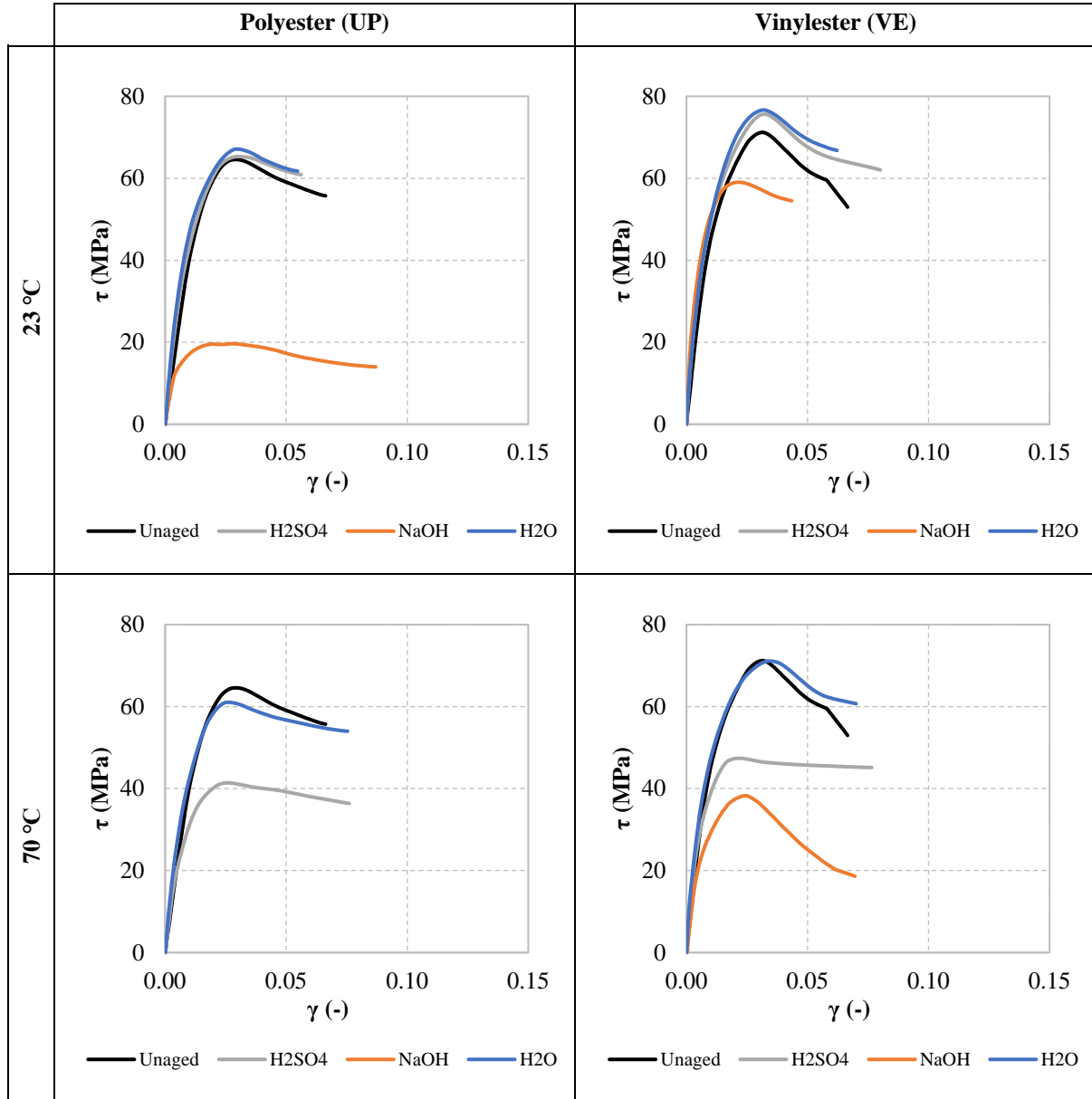


Figure 12.11 - Compressive strength retention during chemical ageing.

### 12.4.5. In-plane shear tests

Figure 12.12 shows the in-plane shear response of representative UP and VE specimens for each of the different chemical environments, at the temperatures of 23 °C and 70 °C, after 16 weeks. The shear stress vs. distortion curve for the UP material under alkaline immersion at 70 °C could not be illustrated since the material was too damaged to be tested.



**Figure 12.12 - Representative stress-strain curves of in-plane shear tests of unaged materials and after 16 weeks of immersion in chemical ageing at 23 °C and 70 °C.**

For both materials and all types of exposure, the mechanical response was initially linear. Then, the response became non-linear, with a progressive stiffness reduction, until a shear stress peak was attained. After this peak, there was a relatively soft shear stress reduction until failure.

The effects of different ageing conditions on the in-plane shear strength of the UP and VE materials is shown in Figure 12.13, which plots the average value (with error bars as standard deviation). In general, the in-plane shear strength decreased with increasing exposure periods, regardless of the

ageing environment. It should be noted, however, that this decrease was significantly more intense for immersion in the alkaline solution, even at the lowest temperature.

When subjected to **immersion in water**, at various temperatures, both materials exhibited a comparable and relatively low decrease in their in-plane shear strength. The reduction in in-plane shear strength became increasingly apparent as the temperature and duration of exposure increased, reaching a maximum of 16% (for UP at 70 °C/16 weeks) and 11% (for VE at 50 °C/8 weeks). These results are consistent with those reported by Sousa [III.16], who investigated similar materials but for longer periods of exposure (up to 2 years). It was also observed that, at 23 °C, there was an increase in in-plane shear strength after 16 weeks of exposure, which may be related to a post-cure phenomenon that occurred during longer periods of exposure. In-line with what was observed for compressive strength, the exposure to 50 °C was more damaging for the VE specimens than the exposure to 70 °C/16 weeks, which caused only a 2% reduction.

**Immersion in the acidic environment** at 23 °C presented a similar behaviour to the immersion in water, for both materials. On the other hand, for higher temperatures, immersion in acidic solution was more damaging, with a larger reduction of in-plane shear strength with temperature and exposure periods. The maximum reductions were 31% (UP - 70 °C/16 weeks) and 35% (VE - 70 °C/16 weeks).

The **immersion in the alkaline environment** resulted in a major reduction of the in-plane shear strength of the UP specimens, mainly for the longer exposure periods, which is in line with the results obtained for compressive strength. The reduction of in-plane shear strength at 23 °C was particularly pronounced, reaching 72% after 16 weeks of exposure. Furthermore, at higher temperatures (50 °C and 70 °C/16 weeks), that property became negligible. For the VE specimens, results show a similar behaviour for the highest temperatures (50 °C and 70 °C), with a maximum in-plane shear reduction of 50% (70 °C/16 weeks). The results show that, in general, the VE material presents a better in-plane shear strength performance, compared to the UP material, when immersed in alkaline solutions. Since this mechanical property is greatly influenced by the matrix nature, the better chemical resistance of VE matrix to the alkaline environment results in a better performance of the VE profile (when compared to UP), which is also in line with the relative performance observed in terms of compressive strength.

Both materials showed an enhanced performance in the **vapour phase**, in comparison to their liquid phase exposure (the same was observed in the compression tests). The general effects of exposure to vapour on the in-plane shear strength comprised a small decreasing trend with increasing time and temperature of exposure. Exposure to water vapour of both materials, at the highest temperature, was the most conditioning environment, leading to a maximum reduction of 22% (70 °C/8 weeks) for UP and 18% (70 °C/8 weeks) for VE; similarly to the compressive strength, the property reduction in the water vapour phase was (slightly) higher than the reduction observed in water immersion. Exposure to acidic and alkaline vapour caused a reduction of the in-plane shear strength of the UP material, reaching a maximum after 8 weeks of exposure: reductions of 15% and 14% at 50 °C in acidic and alkaline environments, respectively. For VE specimens, exposure to water vapour was shown to be the most aggressive, resulting in a maximum reduction of the in-plane shear strength of 18% (70 °C/8 weeks).

Exposure to acidic vapour caused a property reduction of 7% (50 °C/8 weeks), and exposure to alkaline vapour caused a reduction of 10% (70 °C/8 weeks). For both materials, the maximum reductions were reached at 8 weeks of exposure, since an increase of in-plane shear strength occurred after 16 weeks of exposure; this phenomenon may be attributed to a post-cure effect occurring during prolonged periods of exposure.

Unlike the results of the compression tests, the VE material showed better performance in terms of in-plane shear strength retention for both phases and in all environments, especially in alkaline immersion. This is because this property is very much dependent on the matrix (especially for composites with quasi-unidirectional fibre reinforcement), which may explain the superior performance of the VE material.

Overall, the alkaline environment was the one that had the largest effect in reducing the in-plane shear strength for both materials, particularly at higher temperatures. This finding is consistent with similar studies where the property reduction in alkaline immersion was always greater compared to acidic immersion [III.47].

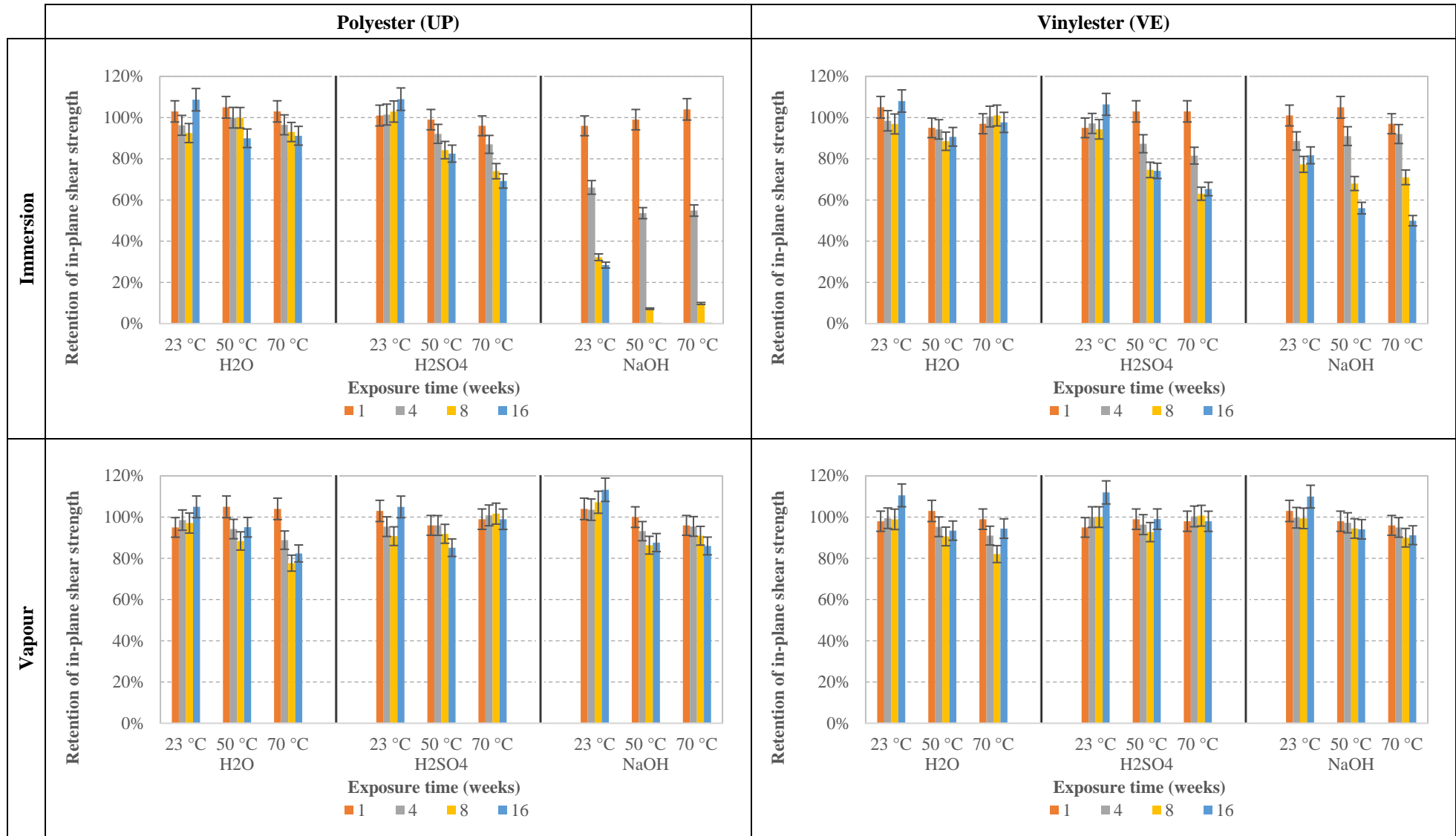
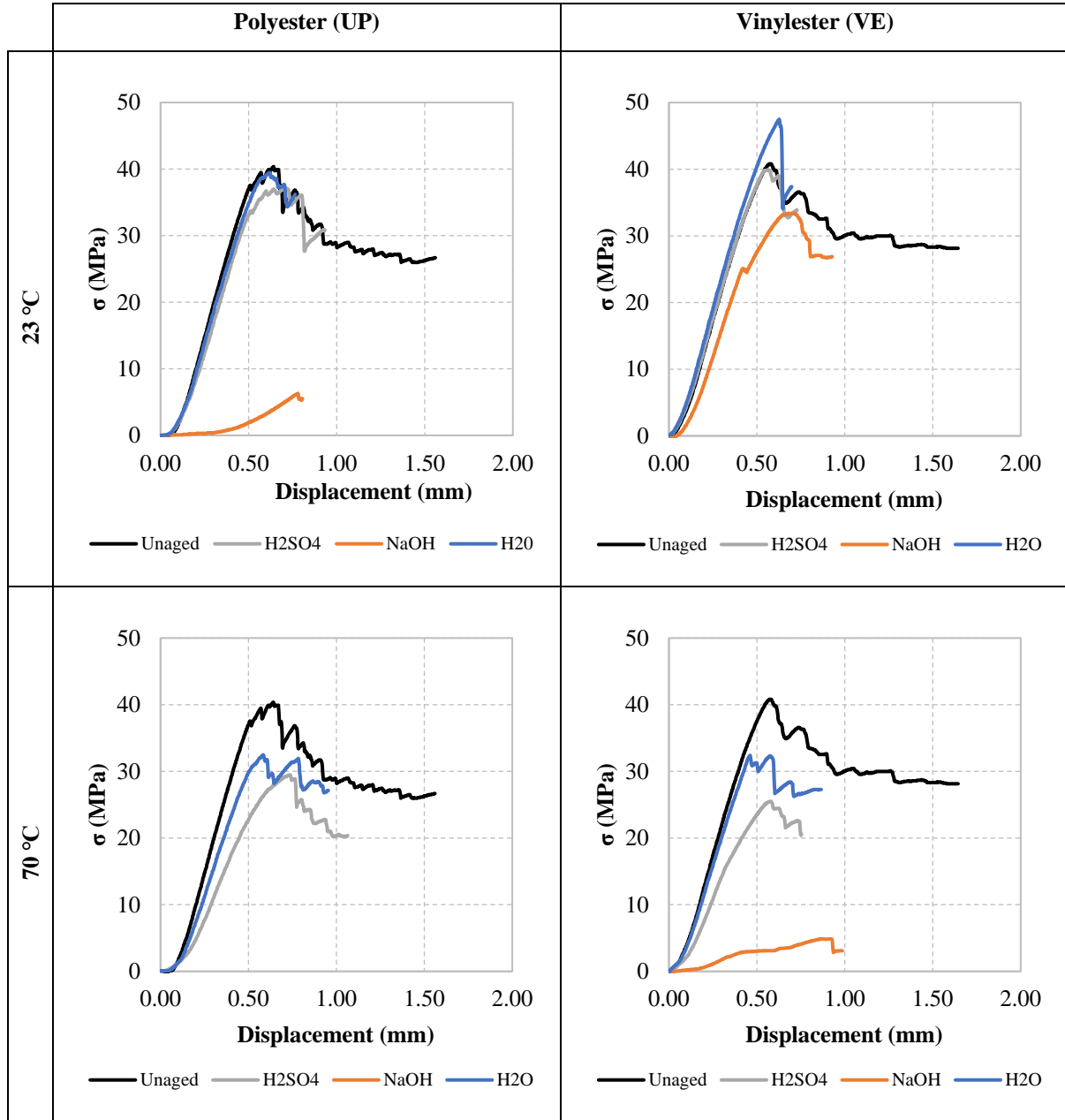


Figure 12.13 - In-plane shear strength retention during chemical ageing.

### 12.4.6. Interlaminar shear strength tests

Figure 12.14 presents the interlaminar shear response (interlaminar shear stress vs. midspan displacement) of representative UP and VE specimens for each of the different chemical environments, at the temperatures of 23 °C and 70 °C, after 16 weeks. The curve for the UP material under alkaline immersion at 70 °C could not be obtained since the material was too damaged to be tested.



**Figure 12.14 - Representative load-displacement curves of interlaminar shear tests of unaged materials and after 16 weeks of immersion in chemical ageing at 23 °C and 70 °C.**

As illustrated by the representative curves, after a toe region (due to adjustments in the setup), most specimens presented a linear response until the first interlaminar delamination occurred. However, some of the specimens exposed to the alkaline environment presented a different interlaminar shear response until the first delamination. In the case of UP and VE specimens exposed to the alkaline environment at 23 °C and 70 °C, respectively, the experimental curves exhibited a completely different behaviour, showing a major

loss of stiffness and strength for those conditions compared to the corresponding unaged materials. These observations suggest a loss of effectiveness in the adhesion between the fibres and the matrix, which is consistent with the behaviour observed in the compressive test curves.

Figure 12.15 presents the effect of different ageing conditions on the interlaminar shear strength of UP and VE materials, displaying the average value with standard deviation as error bars.

The interlaminar shear strength of the UP and VE specimens decreased when **immersed in water**, particularly with longer exposure periods and higher temperatures, in line with the other mechanical properties presented before. The maximum reduction observed was 13% (70 °C/16 weeks) for the UP specimens and 18% for the VE specimens under the same conditions. These figures compare well with results reported by Sousa [III.16] for similar materials and comparable periods of water immersion.

When **immersed in the acidic environment**, the UP specimens presented a similar behaviour to those immersed in water at lower temperatures (23 °C and 50 °C). However, at 70 °C, these specimens experienced a higher reduction in interlaminar shear strength, with a maximum of 27%, after 16 weeks. In contrast, the VE specimens exhibited a greater reduction in interlaminar shear strength compared to water immersion, particularly at higher temperatures (50 °C and 70 °C), with a maximum reduction of 40% (70 °C/16 weeks). Overall, these results suggest that the acidic environment has a more severe effect on the interlaminar shear strength of VE specimens (relative to UP specimens), especially at elevated temperatures.

**Immersion in the alkaline environment** of UP specimens caused significant reductions in interlaminar shear strength, especially for longer exposure periods. After 16 weeks of exposure at 23 °C, the interlaminar shear strength was substantially reduced (by 84%). At the highest temperatures of 50 °C and 70 °C, the interlaminar shear strength was reduced to zero. On the other hand, and in contrast to the previously presented mechanical properties, a very significant effect of the alkaline immersion was observed on the interlaminar shear strength of the VE specimens (90% reduction, after 16 weeks, at 70 °C).

These results suggest that, in terms of interlaminar shear strength, the UP material is more resistant to immersion in water and in acidic solutions, while the VE material is more resistant to immersion in alkaline solutions. Moreover, the results indicate that, except for the 16 weeks of exposure, the UP and VE specimens immersed in the alkaline environment exhibited more damage at 50 °C than at 70 °C. However, the reason for this variation remains unclear, as it contradicts what one would expect *a priori* and also the results observed in other mechanical properties, where this behaviour did not occur.

Exposure to water **vapour phase** was more conditioning than water immersion for both materials, with maximum reductions of 28% and 20% for the UP and VE specimens, respectively, under the same exposure conditions of 70 °C/16 weeks. This indicates that, in accordance with the previous properties, the material had a more significant property reduction in water when exposed to its vapour phase than when exposed to its liquid phase. For UP specimens, acidic and alkaline vapour exposure caused interlaminar shear strength reductions of 14% (70 °C/8 weeks) and 8% (70 °C/16 weeks), respectively. For VE specimens, acidic and alkaline environments caused interlaminar shear strength reductions of 13% (70 °C/8 weeks) and 12% (70 °C/16 weeks), respectively. The same post-curing effect, observed in other analysed mechanical properties, seems to justify some resistance recovery after 16

weeks of exposure, for both materials.

The two materials showed different performance in terms of retention of interlaminar strength in distinct environments: (i) the UP material performed better than VE when exposed to water and acidic environments in their liquid phase; while (ii) the VE material performed better than UP in alkaline environments in the liquid phase and in both water and acidic environments in the vapour phase.

In a study by Pradchar *et al.* [III.44], the effect of water exposure on the flexural strength of resin specimens was investigated. The specimens were subjected to water in both liquid and vapour phases for 10 days. The study found that after immersion in water and exposure to vapour, the flexural strength decreased by 10% and 21%, respectively. This difference was attributed to the materials not reaching full saturation in the vapour phase, which created a more damaging effect at the surface of the material and created microcracks. The same phenomenon could have occurred in the tested specimens, explaining why exposure to the vapour phase led to a greater reduction compared to the liquid phase.

In contrast, the results obtained by Nishizaki & Meiarashi [III.46] on the effects of water immersion and exposure to high humidity on GFRP pultruded vinylester specimens showed that, during immersion, the flexural strength of the specimens decreased by 20% at 40 °C and 38% at 60 °C, while exposure to the vapour phase decreased the flexural strength by only 23%. Therefore, for the same temperature, immersion in water caused a higher reduction compared to the vapour phase, which is contradictory to the results obtained in this study and those of Pradchar *et al.* [III.44]. Further studies should be developed to clarify this aspect.

As reported by Gentry *et al.* [III.50], the interlaminar shear strength of vinylester pultruded GFRP composites under water, acidic, and alkaline immersion was studied for a period of 28 days. The results showed an interlaminar shear strength retention of 96% (water), 101% (acidic), and 75% (alkaline) at 23 °C. In comparison, the results obtained in this study for 4 weeks of exposure presented retentions of 98% (water), 102% (acidic) and 96% (alkaline). However, for immersion at 80 °C, Gentry *et al.* presented interlaminar shear strength retentions of 76% (water), 74% (acidic), and 62% (alkaline). In the present study, at 70 °C, interlaminar shear strength retentions after 4 weeks were 98% (water), 89% (acidic) and 90% (alkaline). In spite of the differences in those elevated temperatures, the specimens tested in this study presented a higher overall mechanical performance. It should be mentioned that the same improvement of the interlaminar shear strength after immersion in acidic solutions for small periods was also reported in the study by Gentry *et al.*, which the authors attributed to an improvement in the fibre-matrix interphase. In their study, the alkaline environment had the greatest impact on the reduction of interlaminar shear strength, which is also in agreement with the results obtained in this study.

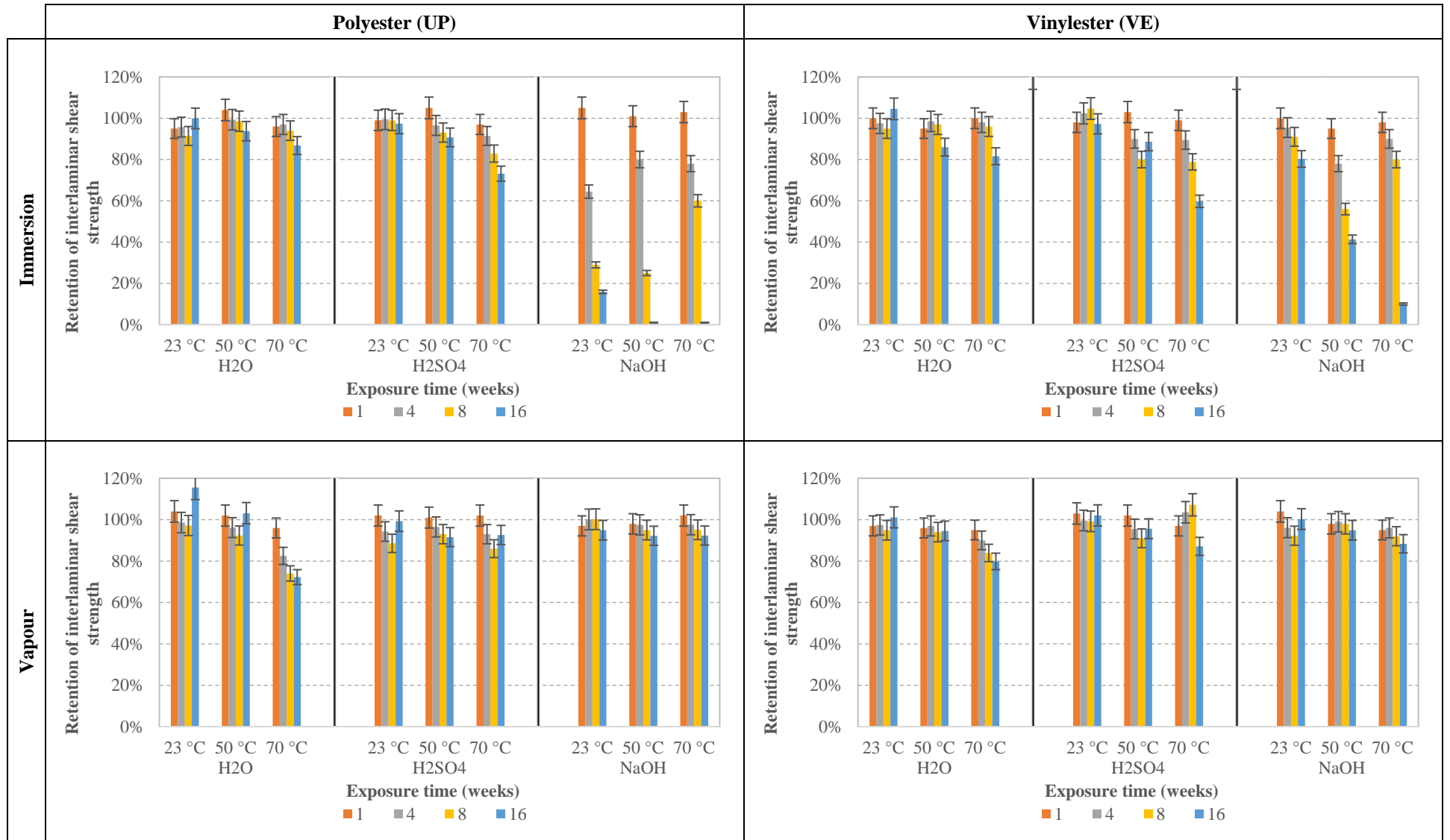


Figure 12.15 - Interlaminar shear strength retention during chemical ageing.

#### **12.4.7. Effect of surface protection coating on mechanical properties for vapour exposure**

The mechanical properties (compressive, in-plane shear, and interlaminar shear strengths) of the UP and VE materials with a surface protection coating (SIKA), exposed to different vapour conditions, are illustrated in Figure 12.16. Figure 12.17 presents the difference in property retention between specimens with and without surface protection. A positive value indicates that the surface protection had a favourable impact, whereas a negative value means that the surface protection had an unfavourable effect.

The results show that, for some environments, as expected, the mechanical properties of protected specimens showed a lower degree of degradation compared to the corresponding unprotected specimens. The surface protection appeared to be more effective when exposed to water vapour and at higher temperatures. For example, the UP material exposed to water vapour for 16 weeks at 70 °C showed an improvement in the three mechanical properties analysed in comparison to the unprotected material: 20% for in-plane shear strength, and 4% and 6% (both within the experimental uncertainty) for compressive strength and interlaminar shear strength, respectively. However, the same UP protected material subjected to the same environment and exposure time but at 23 °C showed a higher deterioration in the three mechanical properties analysed compared to the unprotected material: 10%, 27% and 18% for in-plane shear strength, compressive strength and interlaminar shear strength, respectively. This could be due to post-curing effects at 70 °C (for some reason, more impactful in unprotected specimens) outweighing the potential degradation when exposed to water vapour.

In addition, coated specimens exposed to acid vapour at 70 °C for 16 weeks showed an improvement in compressive strength (5% for UP and 17% for VE), which is in-line with the results obtained for water vapour; once again, this could be due to post-curing effects outweighing the potential degradation. However, it was observed that the application of the surface protection coating was not always fully effective. For instance, the UP material exposed to alkaline vapour at 70 °C for 16 weeks presented an additional reduction of 25% in compressive strength and 14% in interlaminar shear strength, and an 11% improvement in in-plane shear strength compared to the unprotected material; therefore, in these cases, the use of surface coatings did not provide a clear improvement of strength retention. No clear reason could be identified for the fact that the protection coating in some cases was associated to further degradation of mechanical properties. Additional studies should be conducted in the future to address this point.

It is worth noting that the reduction in mechanical properties, for specimens exposed to vapour with protection, followed similar trends to those observed for specimens exposed to vapour without protection, with compressive strength showing the highest reduction among the properties tested.

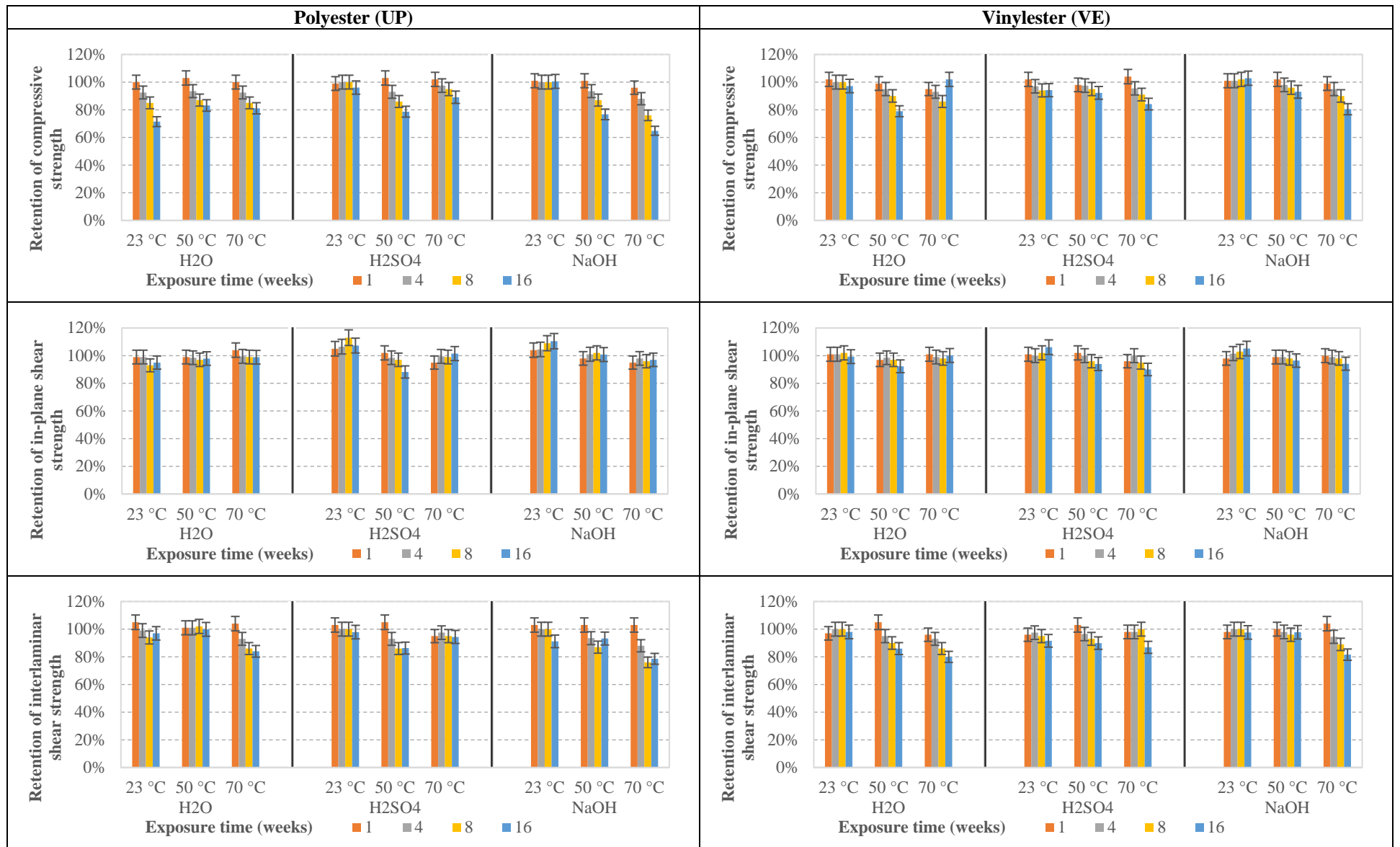


Figure 12.16 - Compressive, in-plane shear, and interlaminar shear strength retention during chemical vapour ageing with superficial protection.

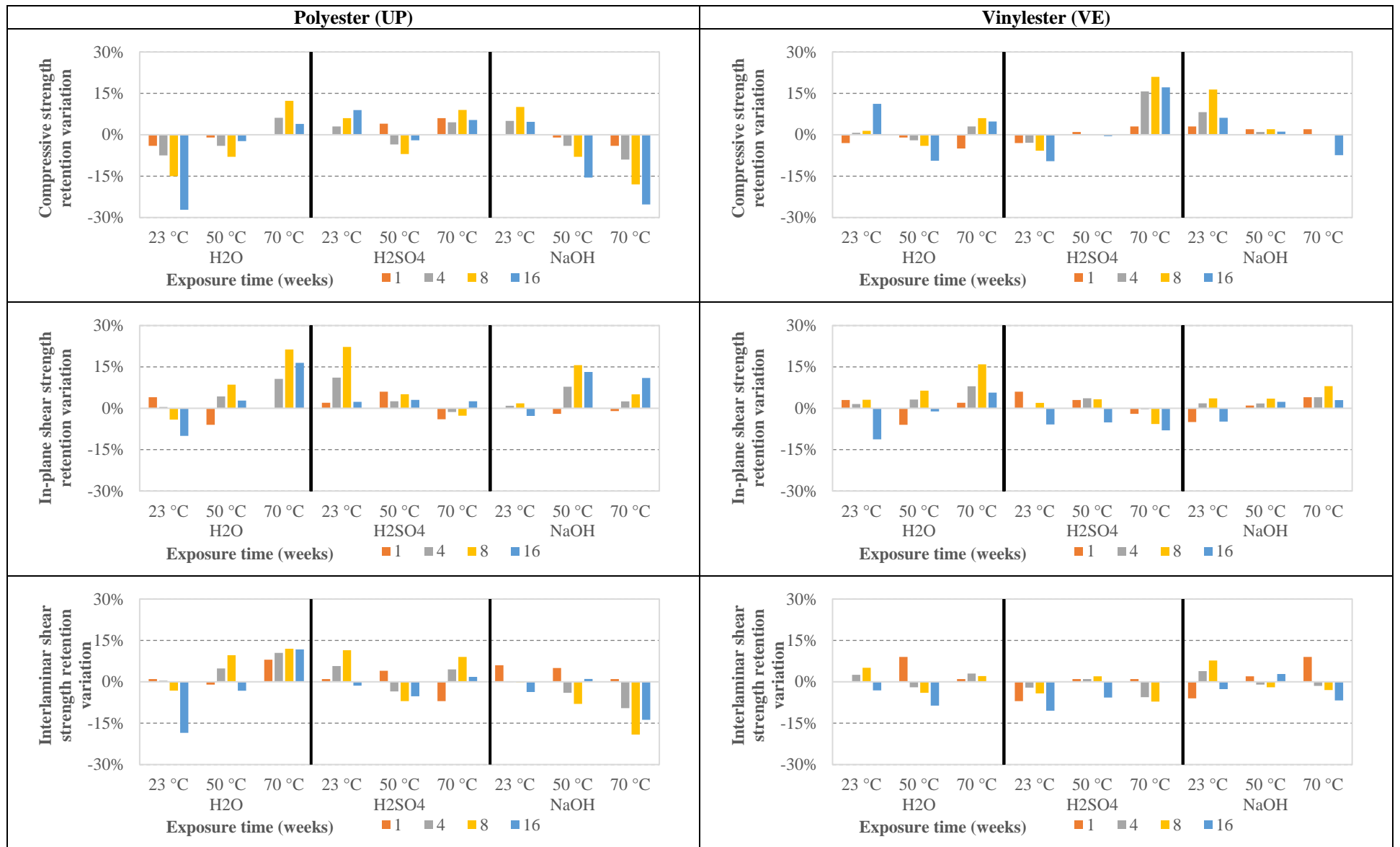


Figure 12.17 - Variations between the compressive, in-plane shear, and interlaminar shear strength retention during chemical ageing with and without superficial protection.

## 12.5. Concluding remarks

The results of the experimental study presented in this chapter provide important information about the effects of different chemical environments and exposure temperatures on the properties of pultruded UP and VE composite materials. After exposure to the different conditions, the materials showed different degrees of visual surface changes, such as alteration in colour, in gloss, and in some cases the presence of flaking and cracking (e.g., UP\_WV\_0 at 50 °C and 70 °C after 16 weeks of immersion in the alkaline solution). The study showed that these signs of material damage should be considered as indicative of possible degradation of mechanical performance.

In general, the specimens exposed to the different chemical environments showed a progressive yellowing, accompanied by loss of gloss, with more pronounced changes observed in exposures at higher temperatures and longer periods of exposure. The UP material showed more pronounced colour changes in alkaline environments, while the VE material was more susceptible to colour changes overall. Regarding gloss changes, the results showed a progressive transition from a glossy to a matte surface finish, with the most substantial loss of gloss being observed at the beginning of the exposure in alkaline environments.

In terms of mechanical properties, the results showed that at the reference temperature (23 °C), immersion in water and in the acidic solutions did not significantly change the performance of both materials. On the other hand, immersion in the alkaline environment caused much more extensive degradation in both materials, especially for longer exposure periods. The UP material suffered a more significant reduction in interlaminar shear strength, with a maximum reduction of 84% after 16 weeks of exposure, while the VE material experienced a maximum reduction of only 23% after 8 weeks of exposure.

In general, increasing temperature had a very significant effect in accelerating the degradation of the mechanical properties, especially for longer exposure periods. This effect, although present in the acidic environment, was more pronounced in the alkaline environments, where a complete loss of mechanical strength was observed in all properties of UP specimens after 16 weeks of exposure to both 50 °C and 70 °C.

Considering the effect of the exposure duration, during the first 4 weeks, there was no significant impact on the mechanical properties of the materials, while in some cases exposure for 16 weeks resulted in significant changes. Yet, in some cases, particularly under exposure to the degradation agents in their vapour phase, a period of 8 weeks proved to be the most conditioning, likely due to the occurrence of the post-cure phenomenon at 16 weeks. These results highlight the importance of considering long exposure periods, even in laboratory studies.

Considering only the longest exposure period (16 weeks) and the average reduction for each environment, it was found that, for the UP material, the most affected property was compressive strength and the least affected one was in-plane shear strength. In the case of the VE material, interlaminar shear strength was the most affected property, while in-plane shear strength was the least affected one.

As discussed before, exposure to water vapour was found to be the most conditioning exposure among the three vapour environments and, in most cases, it resulted in a higher reduction compared to water immersion. This result was somewhat unexpected, although the literature available in this respect is not fully consistent, presenting some contradictory results. For both materials, exposure to acidic and alkaline environments generally showed better performance in the vapour phase compared to the liquid phase.

Regarding the use of a superficial coating protection, the results obtained in this study do not seem to show a clear effect on the strength retention of both materials - for some conditions, as expected, the coating had a positive effect, leading to less degradation of mechanical properties; on the other hand, for other conditions, unprotected specimens presented less degradation. However, these results are only valid for the type of protection used in this study (an epoxy resin coating) and cannot be generalized. Indeed, further investigations are necessary to assess the effects of different types of coating, such as a water vapour impermeable protection, on the strength retention of composite materials.

Overall, the results obtained indicate that the UP material performed better in water environments, the VE material performed better in alkaline environments, and both materials performed similarly in the acidic environment. These results highlight the importance of material selection during the design stage, when considering the type of in-service chemical exposure. While the results obtained provide a wealth of experimental data, they are sometimes inconsistent, and therefore, cannot serve as the basis for the development of degradation models. This also highlights the importance of further investigations. When developing degradation models, it is crucial to consider the reduction in mechanical properties, and those properties should not become negligible, which was the case of the results obtained in the alkaline environments. In this respect, further investigation is required regarding two aspects: (i) whether the exposure temperatures for accelerated ageing were excessively high for the materials studied herein; and/or (ii) whether the concentration of the alkaline solution was too high. To obtain answers to these questions, a broader range of temperatures and concentrations should be explored.

## 13. Exposure of GFRP composites to weathering

### 13.1. Introductory remarks

It is now possible to find FRP composite structures that are in-service already for long periods of exposure to natural weathering conditions. Natural weathering includes the exposure to several environmental effects, such as (i) temperature and (ii) moisture, acting in isolation or combined, and (iii) UV radiation, which is given particular attention in this chapter.

In the spectrum of solar radiation, the UV component is the most aggressive, since it has enough energy to initiate several photochemical reactions that may lead to irreversible degradation of the superficial layer of polymeric and FRP composite materials. This superficial degradation, which has been reported to be around 10  $\mu\text{m}$  deep in the case of polymeric materials [III.13], can lead to changes in the aesthetical (e.g., discolouration) and mechanical performance of polymeric and FRP composite materials [I.18].

As discussed below, several studies have been carried out about the behaviour of GFRP composites when exposed to natural weathering. Also, some studies analysed the behaviour of such composites when exposed to accelerated (artificial) weathering, namely in QUV chambers, which accelerate the effects of UV radiation and moisture diffusion into the materials; in some studies, an attempt was also made to compare the effects of accelerated and natural weathering.

This chapter first presents a literature review regarding the effects of exposure to natural weathering on GFRP composites, with particular focus on the effects of UV radiation. Next, the chapter presents the description of a test programme carried out within the scope of the present thesis to assess, in laboratory conditions, the weathering performance of pultruded GFRP composites. Subsequently, a field study is presented, in which pultruded GFRP specimens were collected from three structures exposed to natural weathering for about 20 years, for which it was possible to determine the variation of mechanical properties, by testing also unaged material. The final part of the chapter presents and discusses the results obtained in both experiments.

### 13.2. Literature review

#### 13.2.1. Preliminary remarks

A considerable number of variables influence the weathering performance of FRP composite materials, such as the type of polymeric matrix (resin, filler and additives), the type of fibre reinforcement, the manufacturing process, the type of exposure (nature and aggressiveness of environmental conditions), and the duration of exposure. This section presents and discusses the main findings of previous studies reported in the literature on this subject; they have been selected based on their relevance to civil engineering applications in terms of materials, manufacturing processes, and environmental exposure conditions, with particular relevance being given to the effects of UV radiation.

In the study developed by Chin *et al.* [I.18], the following degradation sequence was defined for **UV-induced degradation** of composite materials: (i) loss of surface gloss; (ii) surface discolouration (such as fading and discolouration); (iii) chalking; (iv) flaking of surface resin; (v)

pitting; (vi) microcracking; (vii) blistering; (viii) severe loss of resin from outer surface, with fibres not yet visible; (ix) severe loss of resin from outer surface, with fibres already visible (“fibre blooming” - see Figure 13.15 (a)); (x) fibres visible and loosened from the surface; and (xi) delamination of topmost ply. Loss of gloss and chalking are caused by the erosion of fragmented polymer chains from the surface of the polymer. For some polymers, yellowing is a result of photo-oxidation of unreacted double bonds in incompletely cured resins or the formation of conjugated double bonds [I.19]. Polymers containing styrene crosslinks, such as vinylester and isophthalic polyester, are particularly susceptible to UV-induced yellowing [III.56]. Although the degradation of the surface layer may not have a (direct) significant impact on the mechanical properties of GFRP components [III.57], it can affect their overall behaviour and, in the long term, it can promote the degradation of other environmental agents. In fact, changes in aesthetic properties, such as gloss loss and colour change as well as, chalking do not directly correlate with the decay of mechanical properties, but they can increase the risk of moisture and other aggressive agents penetrating faster into the bulk of the material [III.58]. After prolonged exposure, more severe damage, such as surface crazing and cracking, may occur. Cracking is often caused by chain scission reactions initiated by UV exposure, where the fragments resulting from it take up more volume than the original polymers, causing stresses that lead to crack formation. If the degradation products are volatile or gaseous, pore and pit formation may also occur [III.59], [III.60]. The surface morphological features resulting from UV exposure can also serve as sites for moisture sorption and fracture initiation, leading to degradation of mechanical properties.

In what concerns the effects of the exposure of FRP composites to other environmental agents, namely moisture and temperature, which may involve thermal cycles and freeze and thaw cycles, the reader is referred to the comprehensive reviews by Pritchard & Jones [III.14] (moisture), Juska *et al.* [III.61] (temperature and thermal cycles) and Karbhari [III.62] (freeze-thaw cycles). The basic mechanisms associated to **moisture-induced degradation**, already reviewed in chapter 12, involve plasticization, hydrolysis and swelling; and they can cause significant reversible and irreversible damage in FRP composite materials and their mechanical properties [III.63], [III.64]. Short-term exposure to **elevated temperatures** causes softening of the resin and increased viscoelasticity; therefore, when the material temperature approaches or exceeds the glass transition temperature ( $T_g$ ), there is a marked reduction in the stiffness- and strength-related properties of composite materials, especially of matrix-dominated properties [III.65]. The effects of long-term exposure to elevated temperature are not well documented in the literature, although they are generally expected to promote post-curing and hence to potentially improve mechanical properties, if they do not exceed the  $T_g$ . Exposure to **sub-zero temperatures** can cause polymer matrix embrittlement, possibly increasing its strength and stiffness; however, it may also lead to brittle failure modes and reduced stress transfer between fibres and matrix. Low temperatures may also cause matrix hardening and micro-cracking, facilitating the ingress and degradation by environmental agents [III.66]-[III.68]. Due to the dissimilar thermal expansion coefficients of the fibre reinforcement and the polymeric matrix, **thermal cycles** can generate stresses due to fluctuating temperatures and result in fibre-matrix bond degradation; however,

for Mediterranean climates, the effects on the mechanical properties of pultruded FRP materials have been reported to be relatively limited [III.69], [III.70]. **Freeze-thaw cycles**, including also the effects of water freezing in the pores of FRP materials, can result in accelerated degradation compared to thermal cycles, due to the formation and expansion of water deposits, in addition to the effects of moisture induced swelling and drying, and sub-zero polymer matrix embrittlement [III.66].

### **13.2.2. Review of studies on the effects of UV radiation and weathering**

#### **13.2.2.1. Studies on polymeric materials and matrices**

UV radiation absorbed in the presence of oxygen can cause chemical changes in polymeric materials, including the formation of oxygen-containing functional groups, chain scission, branching, crosslinking and rearrangement processes [III.60].

Chin *et al.* [I.18] studied the effects of accelerated UV exposure on cast films of non-UV stabilized vinylester and isophthalic polyester irradiated with a Xenon arc light source. After 1200 h of UV exposure, both materials showed significant surface erosion in the form of cratering and cracking, as observed through atomic force microscopy. However, no changes in the  $T_g$  of the exposed specimens were observed following the exposure period.

Signor *et al.* [III.71] also studied the effects of UV exposure on non-reinforced vinylester resins using a Xenon arc light source and observed that the ultimate tensile strain was very sensitive to degradation, with up to 40% reduction after 4000 h of exposure. Additionally, they found that, after exposure, the near surface region hardness and modulus, studied using an atomic force microscopy (AFM) nanoindentation technique, had a significant increase.

#### **13.2.2.2. Studies on FRP composites**

Bogner *et al.* [III.72] conducted a study to compare the degradation suffered by pultruded GFRP specimens made from different polymeric matrices (polyester and vinylester) after being exposed to UV radiation in a QUV chamber (fluorescent light source) for 10000 h and also in Florida outdoor natural weathering. The results showed that the specimens with a polyester matrix had better resistance to UV radiation than those with vinylester matrix in terms of appearance. In terms of mechanical properties, for accelerated weathering, there was no change in the flexural strength of the specimens with polyester matrix, while the specimens with vinylester matrix lost 4% of their flexural strength. For natural weathering, the unsaturated polyester specimens retained their performance, but the vinylester specimens lost 28% of their initial flexural strength and modulus. Both types of specimens showed signs of gloss loss, chalking and surface erosion.

Segovia *et al.* [III.73] studied the behaviour of different glass fibre unsaturated polyester composites and found that they exhibited 15% to 20% reductions in tensile modulus and strength, after being exposed to accelerated exposure to UV radiation for 7000 h. The tensile strain at failure exhibited reductions ranging from 20% to 56%, which were attributed to the brittleness induced in the resin and fibre-matrix interface. Most of the degradation occurred primarily in the surface resin, whereas the glass fibre reinforcement presented no signs of deterioration.

Cabral-Fonseca *et al.* [III.74] studied the effects of UV radiation on pultruded GFRP composites made of unsaturated polyester and vinylester resins. These materials were exposed to artificial accelerated weathering in a QUV chamber for 3000 h. The results showed that the effects of UV radiation on the mechanical properties of the vinylester composite were minimal, while the unsaturated polyester composite experienced a 21% reduction in tensile strength. Chemical changes at the surface of both materials were also observed through FTIR analysis. The authors noted that the effects of UV radiation were mostly confined to the surface layer of the material, causing only slight (vinylester) to moderate (polyester) reductions in mechanical properties, but significant changes in appearance, namely loss of gloss and colour change.

Nishizaki *et al.* [III.75] determined the effects of applying a superficial protection on the durability performance of pultruded GFRP plates made of E-glass fibres and vinylester resin under 10-year outdoor exposure in Tsukuba (Japan). The specimens were first coated with an epoxy coating and then coated with an acrylurethane resin top coating. In the case of unprotected specimens, the tensile and in-plane shear strengths decreased 23% and 33%, respectively, compared to unaged reference specimens. For unpainted specimens, a slight increase of the modulus of elasticity was observed, probably because of resin post-curing. In the case of painted specimens, the tensile and in-plane shear strengths were similar to the ones of the unaged material, and this was attributed to the protection provided by the surface paints.

In the same study, Nishizaki *et al.* [III.75] investigated the durability of pultruded GFRP plates with various laminate systems and volume ratios of longitudinal reinforcing fibres (12%, 26%, and 43%). The authors examined the differences in tensile performance of specimens removed from the plates after 1 and 10 years of exposure to natural weathering, in the same conditions. They found that the two systems with the lowest fibre content exhibited tensile strength reductions of approximately 17% and tensile modulus increases of around 4% after 10 years. Conversely, the specimens with a higher percentage of longitudinal fibres displayed increases in tensile strength and modulus of 7% and 29%, respectively. No significant changes were observed after 1 year.

Sousa *et al.* [III.76] conducted a study on the durability of pultruded profiles made with E-glass fibres and unsaturated polyester (UP) or vinylester (VE) resins. The profiles were exposed to both outdoor natural weathering in Lisbon for 42 months and to QUV accelerated weathering for 3000 h. The results showed that both natural and accelerated weathering caused significant changes in gloss and colour. Both UP and VE profiles showed yellowness and extremely low gloss retention, due to resin photo-chemical degradation. FTIR analysis confirmed the occurrence of chemical changes in both materials and, along with mechanical testing, confirmed that the effects of UV exposure are mainly confined to the top few microns of the surface, leading to much smaller changes in mechanical properties when compared to hygrothermal ageing [III.16]. It appears that the most damaging effects of UV radiation on GFRP composites are not due to direct exposure to radiation, but rather to the acceleration of the degradation caused by other agents, such as moisture. DMA analysis showed slight changes in  $T_g$  for both artificial accelerated and natural ageing, but also indicated the existence of post-

curing effects due to moisture and high temperature exposure, which was confirmed by mechanical testing. Tensile, flexural, and interlaminar shear strengths showed some changes throughout the exposure time, which at some point seemed to have been affected by post-curing phenomena. Flexural strength was the most affected resistance property (22% loss for the VE profile). Tensile and flexural moduli showed higher signs of degradation, which was maximum in the UP profile (33% and 37% reduction for tensile and flexural moduli, respectively). Interlaminar shear strength showed some initial degradation for both profiles; however, significant property gain was reported for the longer exposure periods. In general, the VE profile presented higher mechanical properties and stability to degradation compared with the UP profile, which is consistent with earlier findings. However, such higher performance was not observed in terms of  $T_g$  variation, which may also be due to differences in the initial curing degree of both resins. Overall, QUV artificial accelerated and natural ageing could be correlated, particularly in what concerns colour and gloss changes: 2000-3000 h of QUV exposure caused similar aesthetic degradation to 30-40 months of natural ageing in Lisbon city centre. In general, it was also possible to correlate changes in thermomechanical ( $T_g$ ) and mechanical properties after exposure to those two environments - mechanical properties were of the same order of magnitude and exhibited comparable variation trends; for tensile strength, such correlation was not so strong, most likely because the influence of post-curing caused by those two environments was different.

Klamer *et al.* [III.77] examined the effects of 13-year exposure to outdoor humidity and water conditions in Werkendam, the Netherlands, of GFRP plates, with polyester resin. The plates were placed on a pontoon, submerged and above water level. The authors did not specify the manufacturing process of the plates but reported that they had a relatively low fibre content compared to typical values in pultrusion. The plates that were exposed above water level, and therefore not subjected to degradation by direct contact with water, displayed less degradation. However, except for interlaminar shear strength, all mechanical properties decreased after exposure. The tensile strength showed reductions between 16% and 33% for the plates above and below water level, respectively. The tensile modulus showed smaller variations, between 7% and 10% for the same type of plates.

Keller *et al.* [III.78] evaluated the effects of natural ageing on pultruded GFRP components of a building structure (in Basel city centre) and a pedestrian bridge (in Pontresina, an alpine environment), after 15 and 17 years of service, respectively. They performed a detailed inspection of both structures, complemented by full-scale tests representative of in-service conditions, and coupon tests for mechanical characterization (only for the pedestrian bridge). The authors observed that the mechanical performance of the pedestrian bridge profiles was significantly affected by the combined presence of thermal cycling and strong ultraviolet (UV) radiation, especially in the profiles' upper flange - 32% (flange) and 17% (web) tensile strength reductions. However, the tensile modulus showed small variations - 2% in the flanges and 5% in the web. UV radiation was also responsible for the appearance of fibres at the surface (fibre blooming), as stated in Part II - Figure 3.03 (c). In both structures, serviceability and structural safety levels were not compromised and, even though some mechanical anomalies were detected (and rehabilitated), they should not become critical in the near future (see

remaining parts of Figure 3.03). In the building structure, colour changes were identified near the bolted connections of the profiles, related to the increased sensitivity of these areas to water absorption (as the bolt holes were not sealed). Based on the results obtained, the authors recommended the use of surface protection systems in GFRP structures exposed to adverse environmental conditions.

In another study, Sousa [III.16] evaluated the durability of GFRP components installed in a transportation service viaduct in Oeiras, Portugal. The study, which spanned a period of 11 years, focused on the substructure supporting the deck of the railway viaduct and examined the effects of partial exposure to UV radiation and other weathering elements in a Mediterranean climate on the structural, mechanical, physical and aesthetic performance of the GFRP components. The investigation revealed that, while there were reductions in tensile and flexural strengths of 11% and 8%, respectively, there were insignificant changes in stiffness-related properties. These variations are believed to be the result of competing post-curing effects on the polymeric matrix and degradation mechanisms due to environmental exposure, in this case an environment with high moisture, next to the coast. The colour variation of the material was also studied, and was already perceptible by visual observation, with a  $\Delta E^*$  value of 6.31.

### **13.2.3. Summary**

The literature review presented above indicates that UV radiation is a significant factor for the deterioration of GFRP materials. Previous studies have shown that UV exposure involves various degradation mechanisms, including changes in colour and gloss, chalking, microcracking, and severe loss of resin from outer surface (with fibre blooming), among other effects.

The effects of UV radiation are mainly confined to the surface layer of the material and, in the short-term, they do not significantly impact the mechanical properties of GFRP composites. However, UV exposure can accelerate the degradation caused by other agents, such as moisture, that act together with UV radiation in outdoor applications. Previous studies have also shown that vinylester matrix resins are more susceptible to UV-induced yellowing and deterioration than polyester matrix resins. Additionally, some studies have shown that the use of surface coatings can protect GFRP materials from the effects of UV radiation and thus extend their service life.

The information available in the literature is relatively limited concerning two aspects addressed in the present study: (i) the effects of incorporating surface veils and UV additives in the fibre reinforcement and polymeric matrix, respectively; (ii) the effects of superficial protections, and (iii) the results of very long exposure to outdoor weathering - in fact, the maximum duration reported in the literature is only 17 years, much lower than the typical service life of most civil engineering structures - 50 or 100 years.

## **13.3. Experimental study - natural and accelerated weathering**

### **13.3.1. Description of the test programme**

In order to determine the effects of weathering on pultruded GFRP composites, two different types of ageing environments were considered - natural and accelerated weathering, the latter in a QUV

chamber - in both cases with varying duration of exposure, as presented in Table 13.01.

All 12 types of specimens presented in 11.2.1, differing in the type of resin (isophthalic polyester, UP, and vinylester, VE), the use of surface veil (with, WV, or without, NV) and the use of a UV stabilizer additive (0, 0.25% and 0.50% of content), were used in this experimental study; they were considered to assess the influence of those parameters on the durability performance of pultruded GFRP composites for natural and accelerated weathering. Due to space restrictions in the QUV chamber of LNEC, some of the specimens exposed to natural weathering were not included in the accelerated weathering study. The specimens excluded were the ones with superficial protections for the UP resin with 0.50% of content of UV absorber additive, and for the VE resin with 0.25% and 0.50% of content of UV absorber additive.

To assess the level of surface protection that can be conferred to pultruded GFRP composites, the following two coatings were selected: (i) the *SikaCor EG 5* system, comprising a 2-pack acrylic polyurethane with high chalking resistance and colour retention; and (ii) the *CIN 7P-600 C-THANE® RPS HS* coating, based on an aliphatic polyurethane enamel - the technical specifications of the coatings are presented in Annex VI. These coatings were selected after consultation with specialized coating companies and also based on the current practice in recent rehabilitation works of pultruded GFRP constructions. Two layers of those superficial protections were applied to the exposed sides of the specimens, according to the data presented in Table 13.02, and their application can be considered in-line with the technical specifications of the manufacturers.

**Table 13.01 - Natural and accelerated weathering environmental conditions.**

Material	Natural weathering		QUV accelerated weathering	
	Exposure period	Superficial protections	Exposure period	Superficial protections
UP_WV_0	10 and 20 months	With and without superficial protections	Up to 6000 h (assessment every 300 h)	With and without superficial protections
UP_NV_0				
UP_WV_025				
UP_NV_025				
UP_WV_050				Without superficial protections
UP_NV_050				
VE_WV_0				
VE_NV_0				
VE_WV_025				With and without superficial protections
VE_NV_025				
VE_WV_050				
VE_NV_050				

**Table 13.02 - Superficial protection thickness.**

Superficial protection	Specified dry thickness (per layer)	1 <sup>st</sup> layer thickness	2 <sup>nd</sup> layer thickness	Total thickness
<i>SikaCor EG 5</i> system	0.06-0.08 mm	0.06 ± 0.03 mm	0.05 ± 0.02 mm	0.11 ± 0.02 mm
<i>CIN 7P-600 C-THANE® RPS HS</i>	0.035-0.05mm	0.05 ± 0.04 mm	0.04 ± 0.02 mm	0.09 ± 0.02 mm

The natural weathering involved exposure to Lisbon city centre (urban) environment; the GFRP materials were placed in the roof of LNEC main building, where temperature, relative humidity, and UV radiation are continuously monitored by means of a weather station, located at latitude of 38.77°N,

longitude of 9.13°W, and 100 m above the sea level. This station includes a combined sensor for measuring air temperature and relative humidity, a dark globe temperature sensor, a global solar radiation sensor, and a UV component radiation sensor. The test specimens were exposed for 10 and 20 months (approximately 1 and 2 years) and placed on the structures shown in Figure 13.01 at an angle of 45° with the horizontal plane, oriented towards south. Additional specimens were prepared for longer periods of exposure to be tested after the completion of this thesis.

The data from the weather station during the natural weathering exposure is presented in Figure 13.02 and Table 13.03. The specimens started to be exposed to natural weathering on 04/10/2017, were first collected on 06/08/2018 (after 10 months) and were finally collected on 10/06/2019 (after 20 months).



**Figure 13.01 - Structure for natural weathering exposure (LNEC rooftop).**

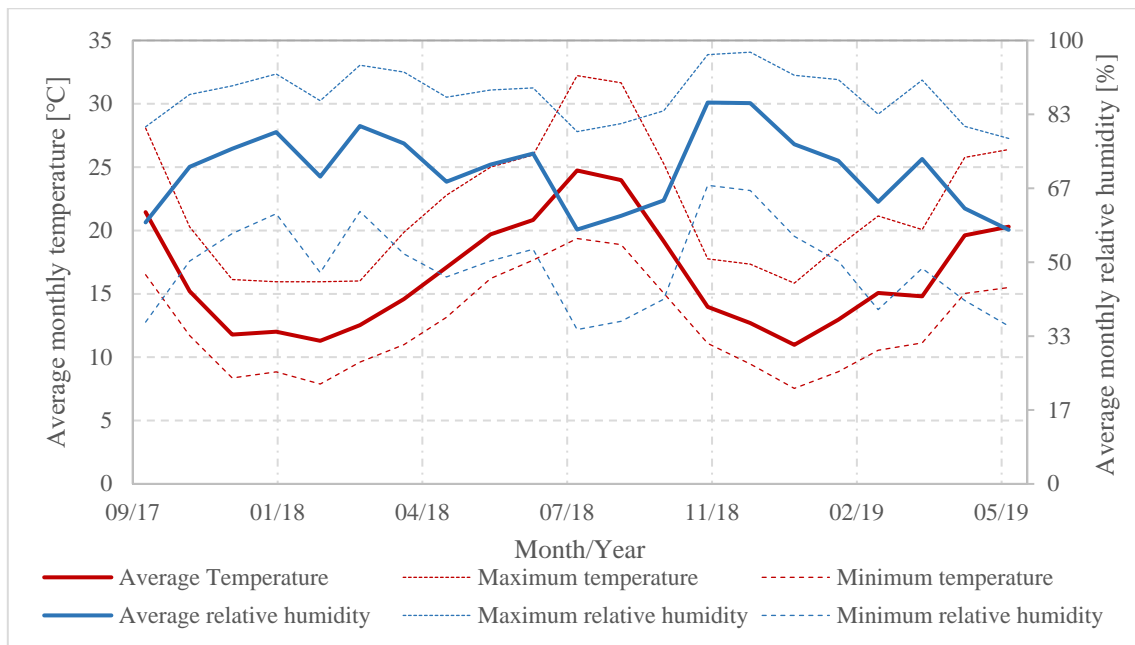


**Figure 13.02 - Average monthly temperature and relative humidity (HR) during natural weathering.**

**Table 13.03 - Weathering data for the natural weathering environment, LNEC weather station.**

Year	Month	Average temperature (°C)	Average relative humidity (%)	Solar radiation (KJ/m <sup>2</sup> )	UV radiation (KJ/m <sup>2</sup> )
2017	October*	21.5 ± 2.6	59.0 ± 17.6	534592	16525
	November	15.2 ± 1.7	71.5 ± 13.4	503102	13644
	December	11.8 ± 2.2	75.6 ± 13.5	577271	11192
2018	January	12.0 ± 1.7	79.3 ± 9.2	622903	11949
	February	11.3 ± 1.9	69.3 ± 14.0	508773	14534
	March	12.5 ± 1.5	80.7 ± 9.9	351435	16341
	April	14.6 ± 2.6	76.8 ± 7.4	348101	19861
	May	17.1 ± 2.5	68.2 ± 10.6	484793	24525
	June	19.7 ± 3.3	72.0 ± 8.7	577737	22839
	July	20.8 ± 0.7	74.5 ± 3.8	586426	25167
	August	24.7 ± 4.4	57.4 ± 15.0	587237	25541
	September	24.0 ± 2.5	60.5 ± 12.1	567060	22068
	October	19.1 ± 3.4	63.9 ± 17.0	610959	19804
	November	14.0 ± 1.5	86.0 ± 6.5	688130	10901
	December	12.7 ± 1.4	85.9 ± 5.6	752964	10762
2019	January	11.0 ± 1.5	76.6 ± 11.8	625793	13033
	February	13.0 ± 1.8	72.9 ± 9.1	553983	15105
	March	15.1 ± 1.8	63.6 ± 15.2	615286	22523
	April	14.8 ± 2.3	73.3 ± 9.5	597902	20848
	May	19.6 ± 3.6	62.1 ± 17.2	605859	26176
	June*	20.3 ± 4.4	57.3 ± 14.8	195331	8621

\* These months values only consider the days of exposure and not the full month

The QUV chamber used in the experiments, shown in Figure 13.03, is an artificial accelerated weathering equipment, allowing exposing materials to alternating cycles of UV light and moisture. The laboratory simulation of the damaging effects of sunlight is provided by fluorescent UV lamps, which is alternated with exposure to moisture caused by constant condensation of de-ionized water at 50 °C. Cycling sets were prepared according to parts 1 and 3 of ISO 4892-3, alternating 8 h of UV radiation at 50 °C (dry cycle) with 4 h without UV radiation at 60 °C and with moisture (wet cycle). The fluorescent lamps used in the QUV chamber were UVA-340 type, providing an irradiance of 0.76 W/(m<sup>2</sup>nm) at 340 nm, which reproduces the most relevant part of the sun's spectrum, between 290 and 350 nm.



**Figure 13.03 - QUV chamber (LNEC laboratory).**

After exposure to each of the weathering conditions, the specimens were rinsed in tap water and placed in an oven at 80 °C for one week to dry the free water out of the specimens. Next, for all weathering conditions, the following physical properties were analysed: (i) colour; (ii) gloss; (iii) Barcol hardness<sup>1</sup> and (iv)  $T_g$ , by dynamic mechanical analysis (DMA). For the QUV accelerated weathering, the compressive and in-plane shear properties were analysed. For the natural weathering, the tensile, compressive and in-plane shear properties were analysed.

All properties were determined in accordance with the characterisation methods described in section 10.3, and the main results are also presented in appendix VII. For colour and gloss assessment, the properties of each specimen were measured before and after the exposure periods. Before testing, the superficial protections were not removed from the specimens; given their very small thickness, their effect on the mechanical properties was considered negligible.

### **13.3.2. Results and discussion**

#### **13.3.2.1. Colour variation**

Figure 13.04 presents the effects of environmental exposure on the colour change of UP and VE specimens, with and without superficial protection, in terms of the variation of parameter  $\Delta E^*$ . This parameter, determined through the CIE  $L^*A^*B^*$  coordinate system, creates a vector between the original measurement and the final coordinate after exposure. The greater the value of this parameter, the greater the distance between the two points (i.e., the colour change). The variation of the coordinates  $L^*$  (black-white axis),  $a^*$  (green-red axis) and  $b^*$  (blue-yellow axis) reflects the colour variation between measurements.

The results obtained show that for both types of exposure, the VE specimens exhibit a greater change in colour than UP specimens, especially for the lower exposure durations - possible reasons are discussed ahead. After an initial increase, which is quite steep in QUV, the colour change in VE specimens appears to stabilize or even reduce. In contrast, UP specimens exhibit a more gradual change in colour; for QUV exposure, for most types of specimens, there is a peak in colour change at around 300-500 h (VE) and 1250 h (UP), which is then followed by a stabilization plateau for the rest of the exposure period in UP specimens and a slight reduction in VE specimens; for Natural Weathering (NW), this stabilization trend is only observed for some types of specimens.

Comparing the QUV and NW exposures, it was found that after 42 weeks (10 months) of NW exposure, the values of colour change are similar (or, at least, they present the same order of magnitude) to those of QUV exposure for 1250 h and 336 h, respectively for UP and VE specimens.

This change in colour is not consistent with the results obtained by Bogner *et al.* [III.72] and by Sousa *et al.* [III.76] - in both studies a higher colour variation was reported for UP specimens compared to VE specimens. Two reasons may explain this difference: (i) the specific characteristics of the VE resin used in this study, which can be closer to an epoxy resin - this latter type of resin is known to have a higher colour variation when exposed to UV radiation compared to UP resins; (ii) the dissimilar initial

---

<sup>1</sup> Barcol hardness did not present significant changes due to weathering; therefore, results are not presented next.

colour of the specimens, both UP\_NV\_0 and UP\_WV\_0 had an initial slightly greener colour than all other specimens, and in comparison to the remaining UP profiles, they always present a lower colour variation in both weathering conditions.

The incorporation of UV additive absorbers in the polymeric matrix and of a surface veil in the fibre architecture did not have a clear effect on the colour change. For longer exposure periods to QUV, VE specimens with surface veil seem to have a distinct behaviour, presenting higher colour change, compared to those without surface veil - this could be due to the constituent material of the veil (polyester), which has a distinct behaviour to the bulk polymer. However, for NW, such a trend is not (yet) clear and the same occurs for UP specimens for both types of exposure. This result is expected, since the main effect of using a surface veil is basically to create a higher matrix content next to the surface of the composite component.

Figure 13.05 shows the colour change ( $\Delta E^*$ ) of GFRP specimens, containing the two types of superficial protections. This series of tests essentially aimed at assessing the behaviour of the superficial protections, rather than of the GFRP substrates. As expected, in general, the behaviour of the various GFRP specimens comprising a given type of superficial protection was very similar.

Regarding the VE specimens protected with the SIKA protective coating, exposure to QUV accelerated weathering caused a cyclic pattern of colour change, with increasing and decreasing branches throughout the exposure time. This behaviour seems to have been caused by a micro-decomposition of the superficial layer of the paint, which was released as fine dust upon cleaning the specimens. This phenomenon occurred with some regularity, which is reflected in the “saw-tooth” pattern of the colour change curve. On the other hand, UP specimens protected with the CIN protection coating presented more regular variation of colour change, which seems to reflect a higher stability to weathering of this specific coating, which also presented lower magnitude of colour change.

For both superficial protections, the change of colour following exposure to QUV accelerated weathering was very reduced and almost negligible in comparison to the change of colour without superficial protection - this means that both paints are less sensitive to colour changes than the bulk GFRP materials. The change of colour in specimens exposed to NW was greater than in those exposed to QUV, which could be due to the superficial protection's sensitivity to other environmental agents absent in the QUV chamber, such as atmospheric pollution, wind, particle erosion, and other regions of the full spectrum of sunlight (long-wave UV, visible and infrared).

Figure 13.06 depicts a representation of the colour change of the specimens, obtained by converting the CIE L\*a\*b\* colour scheme to an RGB based colour scheme. It can be seen that there is yellowing in all specimens without superficial protection, due to UV radiation exposure. The colour of the superficial protections remained practically unchanged during the entire test periods. Even though the  $\Delta E^*$  values changed between measurements, the small variations that were measured by the equipment are not detectable by the human eye.

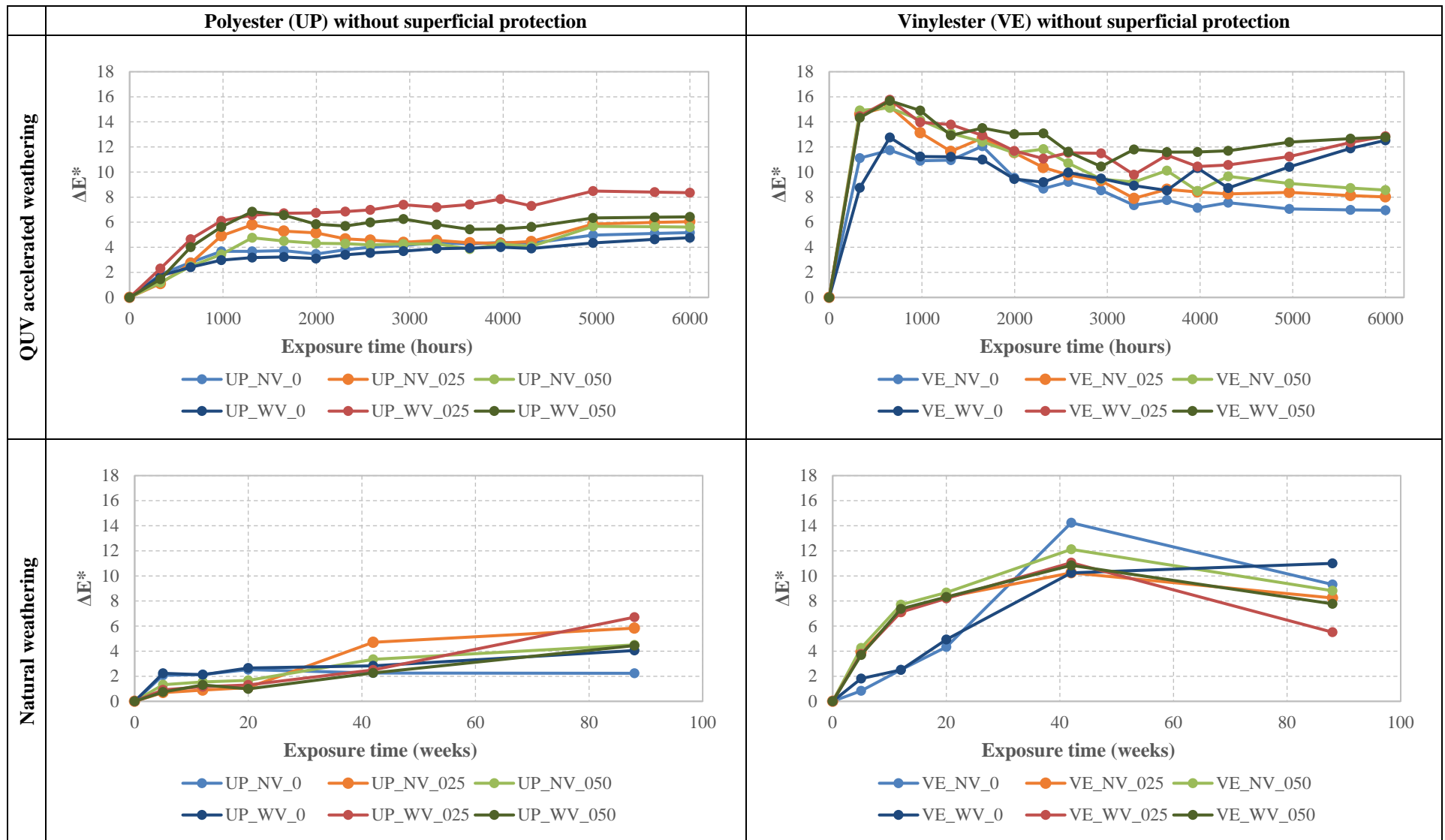


Figure 13.04 - Specimens colour variation ( $\Delta E^*$ ) during weathering (without superficial protection).

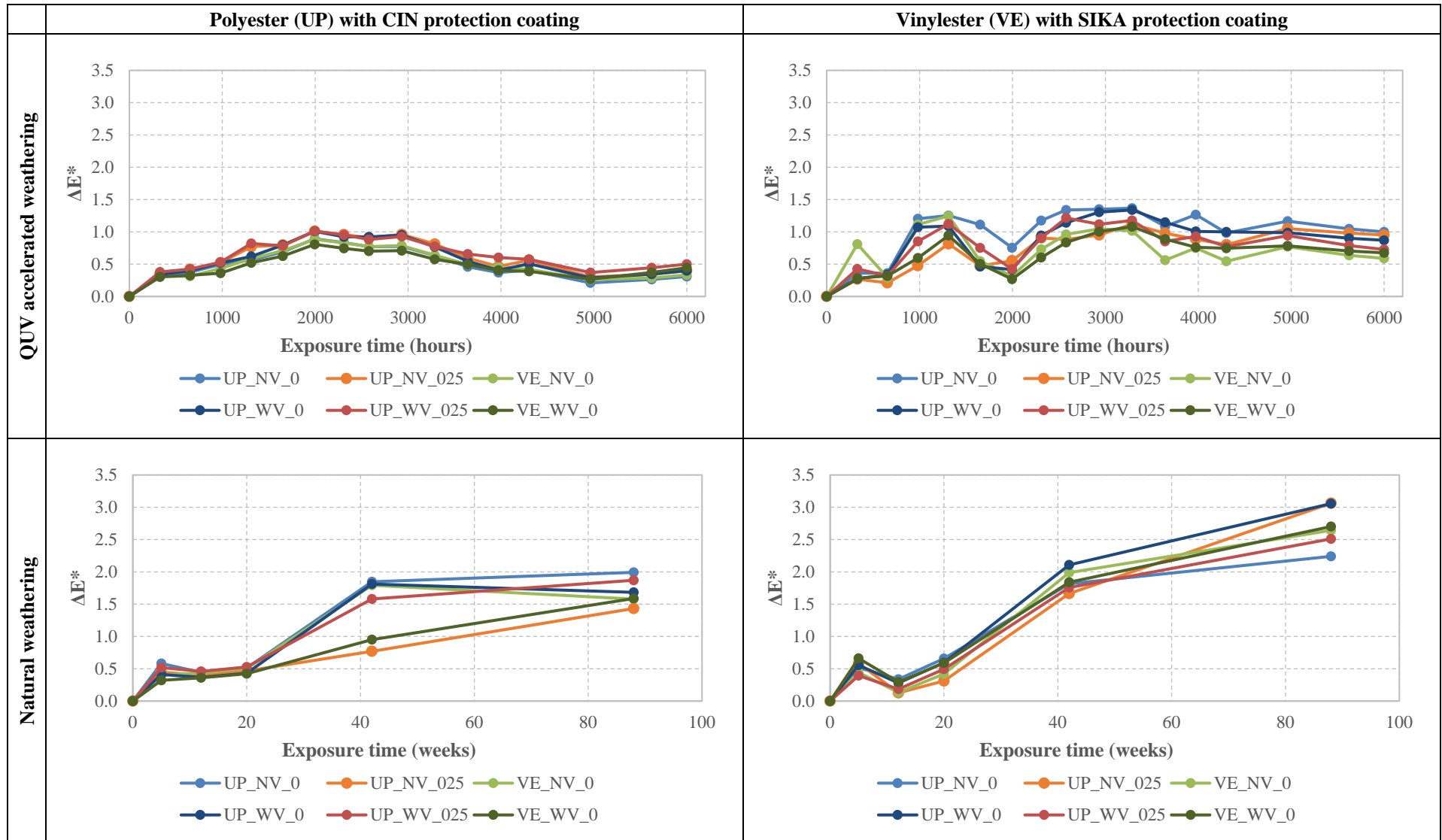


Figure 13.05 - Specimens colour variation ( $\Delta E^*$ ) during weathering (with superficial protection).

Colour variation during QUV accelerated weathering						
	0 weeks(0 h)	2 weeks (330 h)	6 weeks (982 h)	14 weeks (2310 h)	24 weeks (3973 h)	36 weeks (6000 h)
UP_WV_0						
UP_WV_050						
VE_WV_0						
VE_WV_050						
UP_WV_0 CIN						
UP_WV_0 SIKA						

Figure 13.06 - Specimens schematic colour variation during QUV accelerated weathering.

### 13.3.2.2. Gloss retention

Figure 13.07 presents the effects of weathering exposure on the gloss variation of UP and VE specimens, with and without superficial protection.

For UP specimens exposed to QUV accelerated weathering, after 2000 h the gloss became negligible, remaining constant for the subsequent exposure period. Similarly, for VE specimens, after 1000 h of QUV exposure, the gloss also became negligible and remained unchanged for the rest of the exposure period. Previous studies available in the literature have also (consensually) reported the loss of gloss in pultruded GFRP materials after exposure to both accelerated and natural weathering [III.76]; as for the colour variation, the degradation mechanisms that cause the loss of gloss phenomenon occur at the very surface layer of the materials [III.74].

As expected, for both materials, the exposure periods causing greater variation (loss) of gloss coincide with the greatest variations in colour. For UP specimens, for most series, 20 months of exposure to NW had a similar effect on the loss of gloss to 2000 h of QUV exposure. For VE specimens, 10 months of exposure to NW caused similar loss of gloss to 1000 h of exposure to QUV accelerated weathering.

Figure 13.08 presents the effects of weathering exposure on the gloss variation of specimens with superficial protections; as for the colour variation, these results reflect mostly the effects of weathering on the surface protections, rather than on the GFRP substrates. Once again, as expected, the behaviour was similar for all specimens.

For all specimens protected with the SIKA coating, the gloss measured became negligible (below 0.1) after 2000 h of QUV exposure and subsequently it remained roughly unchanged. For all specimens protected with the CIN protection coating, during the entire QUV exposure period of 6000 h, the gloss never became negligible (minimum value of 0.4).

Comparatively, only after all specimens protected with the SIKA coating lost all gloss after 2000 h of QUV exposure did all specimens protected with the CIN coating start to lose their initial gloss - this indicates the much higher efficacy of the latter protection. The variation of gloss in NW and QUV presents the same global development; in specimens with the CIN coating, there is an initial plateau for QUV exposure, which is still being observed after 90 weeks of NW exposure (when the experiments were completed). However, the specimens protected with the SIKA coating exposed to NW present an initial period where they retain a significant part of their gloss; such an effect is not observed for QUV exposure, where the initial reduction is very steep: after 336 h of QUV exposure, the loss of gloss was up to 50%. This could be due to the presence and deposition of atmospheric particles (e.g., dust, pollution, pollen) on the specimens' surface, which were not present in the QUV chamber and may have delayed the loss of gloss process in NW. Also, the initial exposure to NW occurred in the winter period, which has a lower solar radiation exposure.

In some specimens with surface protection, the coating was removed using acetone, to assess (visually) the colour and gloss of the surface. It was observed that the samples retained their grey colour and high gloss; however, the properties could not be quantified as it was not possible to guarantee the complete removal of the surface protection.

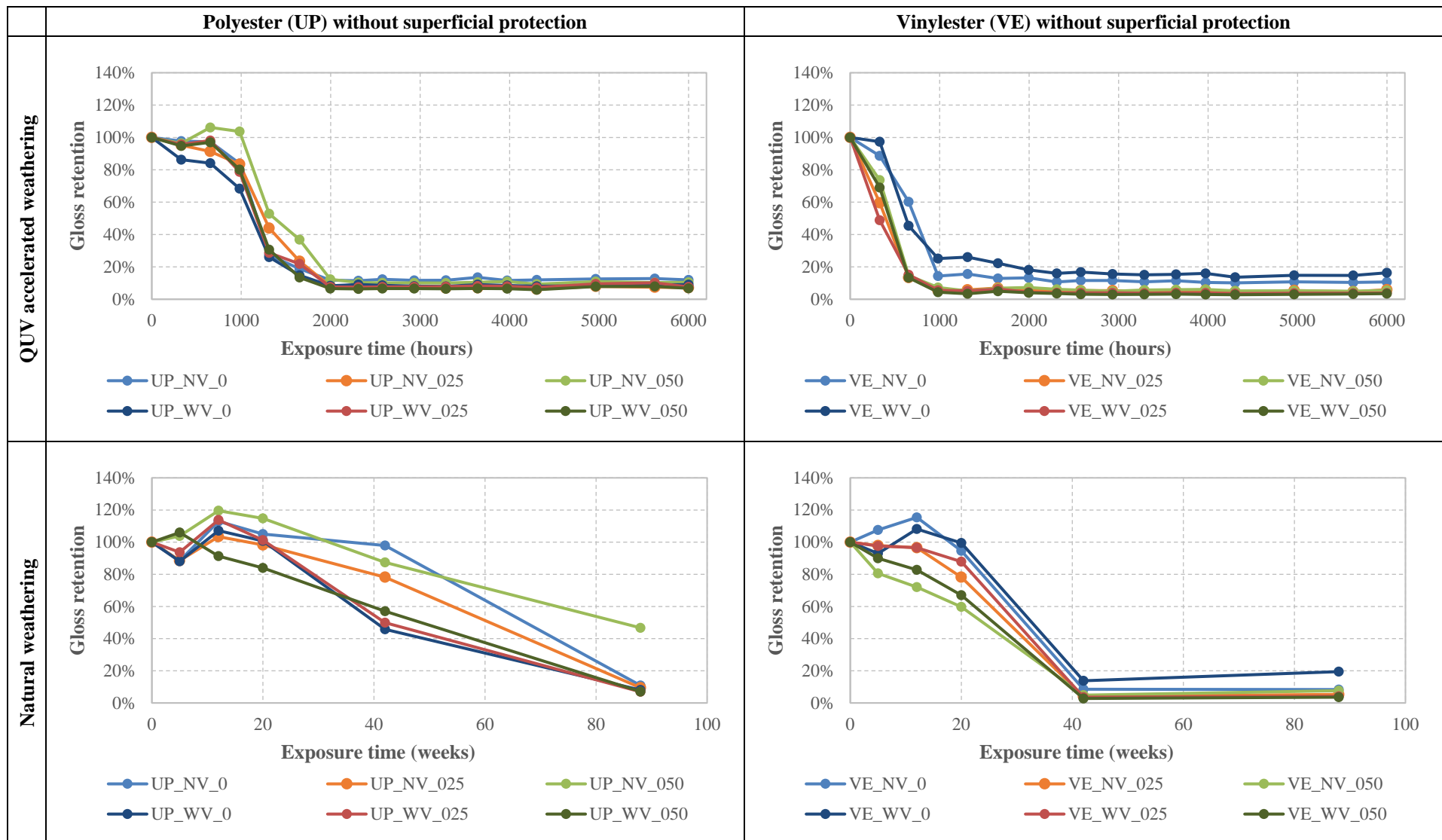


Figure 13.07 - Specimens gloss retention during weathering (without superficial protection).

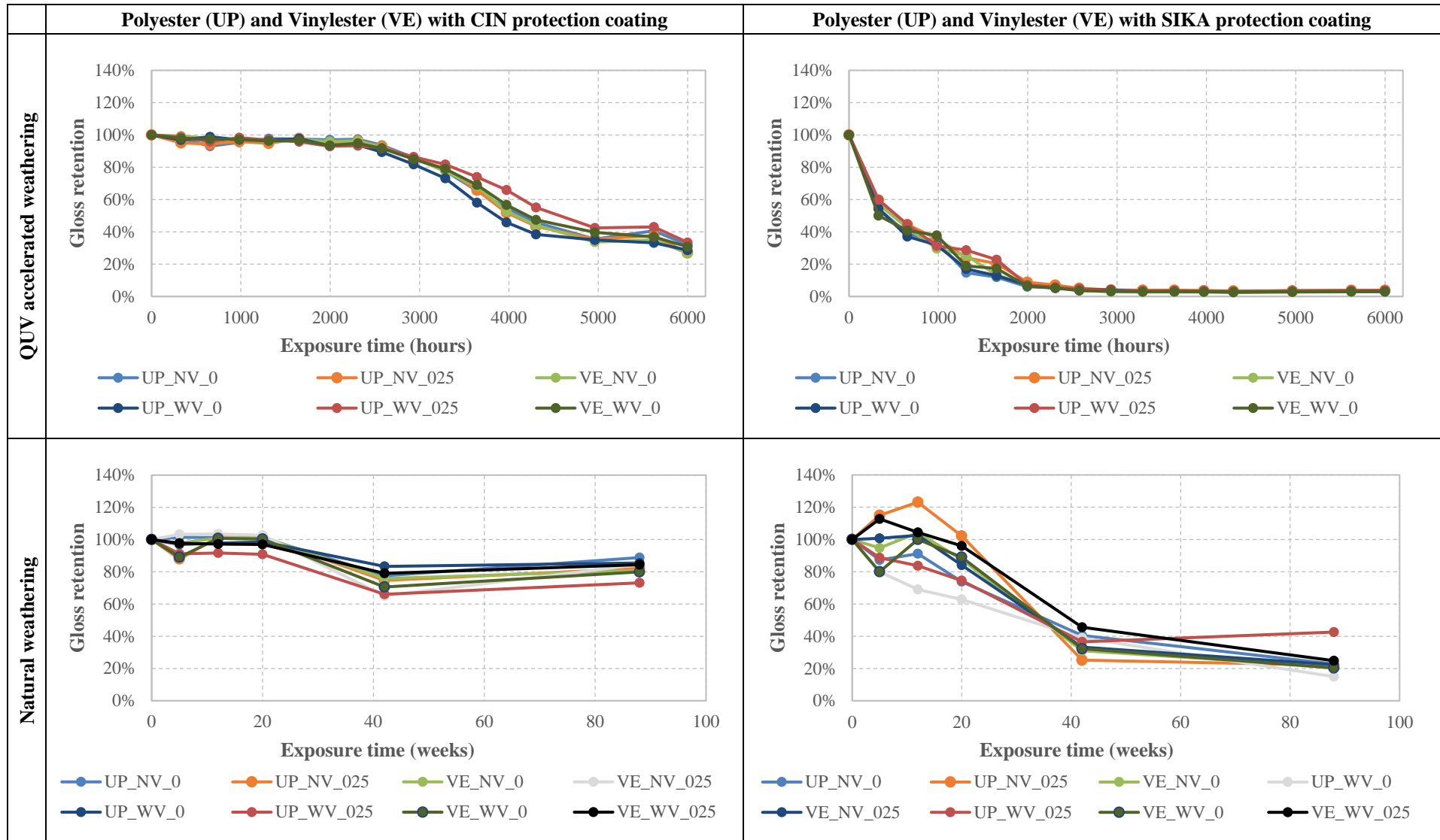


Figure 13.08 - Specimens gloss retention during weathering (with superficial protection).

### 13.3.2.3. Dynamical mechanical analysis

Figure 13.09 presents the DMA curves, namely the storage modulus,  $E'$  (left axis - dashed lines), and the loss factor,  $\tan \delta$  (right axis - continuous lines), for both weathering conditions: NW (20 months of exposure) and QUV accelerated weathering (6000 h of exposure). The results are presented only for the reference specimens produced with both types of resins, without surface veil and no UV additives (UP\_WV\_0 and the VE\_WV\_0 specimens), in both cases with and without the superficial protections. Table 13.04 presents the  $T_g$  estimates obtained from the storage modulus and loss factor curves.

During the tests, the superficial protections applied before exposure were not removed from the specimens. Although their thickness is small, both the storage modulus and the  $\tan \delta$  curves reflect the presence of the superficial protections, as they contributed to the thermomechanical response of the DMA specimens. In the storage modulus curves, the presence of the coatings is reflected in a more or less pronounced peak prior to the decay stage of the curve; on the other hand, in what concerns the loss factor, the coatings also result in a preliminary peak or a shoulder in the curve. Due to the influence of the coatings, for some storage modulus curves, it was not possible to obtain an accurate estimate of  $T_g$ .

For UP specimens under QUV accelerated weathering, the height of the  $\tan \delta$  curve peak remained unchanged with the exposure, while the storage modulus values decreased in the glassy plateau (25 °C). Such reduction was quite pronounced in specimens with superficial protections; yet, this reduction should be related also with the additional thickness corresponding to the coating (when computing the storage modulus, a homogenous material was assumed). The  $T_g$  of the UP specimens remained similar for all test series, with only very slight reductions - thus, there was no significant influence of either QUV exposure or surface protections.

For the VE specimens under QUV accelerated weathering, the height of the  $\tan \delta$  curve peak remained unchanged for the unprotected material and somehow it increased for the specimens with the two superficial protections - no clear reason was identified to justify such variation. Similarly to the UP specimens, the storage modulus values of the VE specimens decreased in the glassy plateau (25 °C). Similarly to the UP specimens, the  $T_g$  value remained similar for the unprotected VE specimen; however, it presented relevant reductions for both VE specimens with superficial protection - once again, no clear reason could be identified to justify such reduction.

For the UP profiles under NW exposure, contrary to the QUV exposure, the height of the  $\tan \delta$  curve peak reduced with the NW exposure. However, the storage modulus values decreased in the glassy plateau (25 °C). The  $T_g$  of the UP specimens remained consistent across all test series, with only minor increases being observed as a result of NW exposure. Accordingly, there was no notable overall effect on  $T_g$  resulting from either surface protection or NW exposure.

In what concerns the VE specimens under NW exposure, as for the QUV exposure, the height of the  $\tan \delta$  curve peak remained unchanged for the unprotected material and it increased for specimens with superficial protections. However, there was a slight  $T_g$  reduction in unprotected and protected specimens, as shown in Table 13.04.

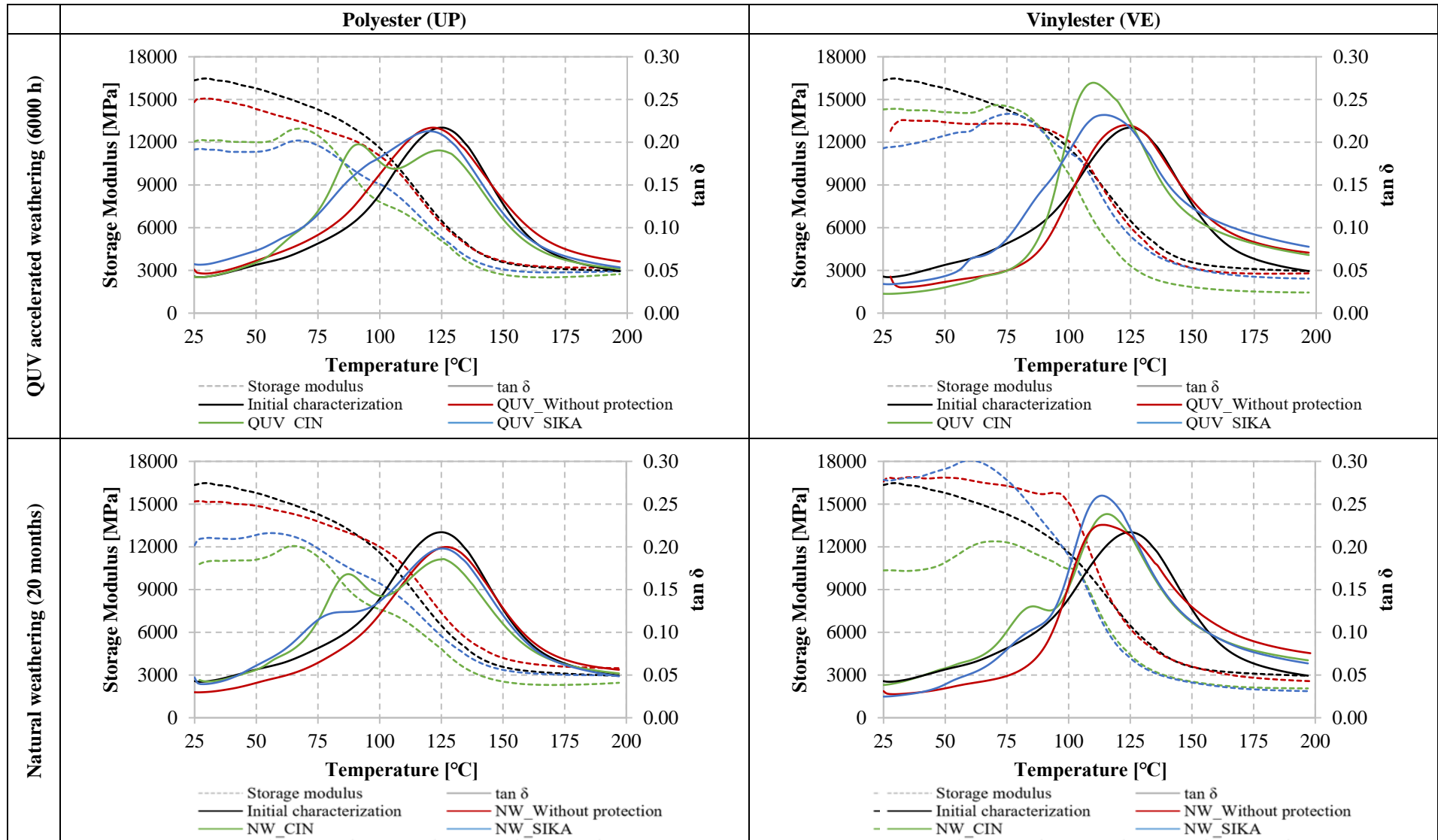


Figure 13.09 - DMA results during weathering.

Figure 13.09 shows that almost all VE specimens after weathering exposure present a slight left shift in the  $\tan \delta$  curve. However, due to the large scatter in the results presented in Table 13.04, this effect is not considered significant.

**Table 13.04 - DMA results for QUV accelerated and natural weathering.**

Type of conditioning		UP_WV_0		VE_WV_0	
		$T_g$ ( $E'_{\text{onset}}$ ) [°C]	$T_g$ ( $\tan \delta$ ) [°C]	$T_g$ ( $E'_{\text{onset}}$ ) [°C]	$T_g$ ( $\tan \delta$ ) [°C]
<b>Initial characterization</b>		104.1 ± 2.8	125.4 ± 2.0	98.9 ± 5.6	118.2 ± 4.3
<b>QUV weathering (6000 h)</b>	<b>Without protection</b>	95.6 ± 6.5	121.5 ± 0.1	95.0 ± 1.0	123.4 ± 1.2
	<b>CIN</b>	78.8 ± 3.9	124.6 ± 1.2	89.9 ± 5.7	111.1 ± 1.4
	<b>SIKA</b>	102.9 ± 14.6	119.7 ± 0.9	96.7 ± 4.5	115.7 ± 1.5
<b>Natural weathering (20 months)</b>	<b>Without protection</b>	105.6 ± 9.9	127.9 ± 0.9	98.9 ± 4.2	114.9 ± 3.0
	<b>CIN</b>	98.0 ± 2.4	128.0 ± 1.1	100.3 ± 8.3	115.6 ± 1.0
	<b>SIKA</b>	92.6 ± 15	126.2 ± 0.9	92.8 ± 7.7	113.4 ± 0.4

### 13.3.2.4. Mechanical properties

The mechanical properties of UP and VE materials are presented and compared with the initial ones obtained from testing unaged specimens, as presented in section 10.4.

Figure 13.10 shows the mechanical response in compression, in-plane shear and tension of representative UP and VE specimens for each of the properties tested, after 6000 hours of accelerated weathering conditions (QUV) and 20 months of natural weathering (NW).

When subjected to compression, both representative materials exhibited linear responses with similar slopes until damage initiation occurred, which was followed by a non-linear ascending branch until rupture. The experimental curves indicate that the in-plane shear mechanical response was initially linear and then became non-linear with a progressive stiffness reduction until a shear stress peak was attained; following this peak, there was a relatively soft shear stress reduction until failure. Regarding the mechanical response observed in the tensile tests, which were only performed for natural weathering conditions, all types of profiles exhibited linear elastic behaviour until brittle rupture.

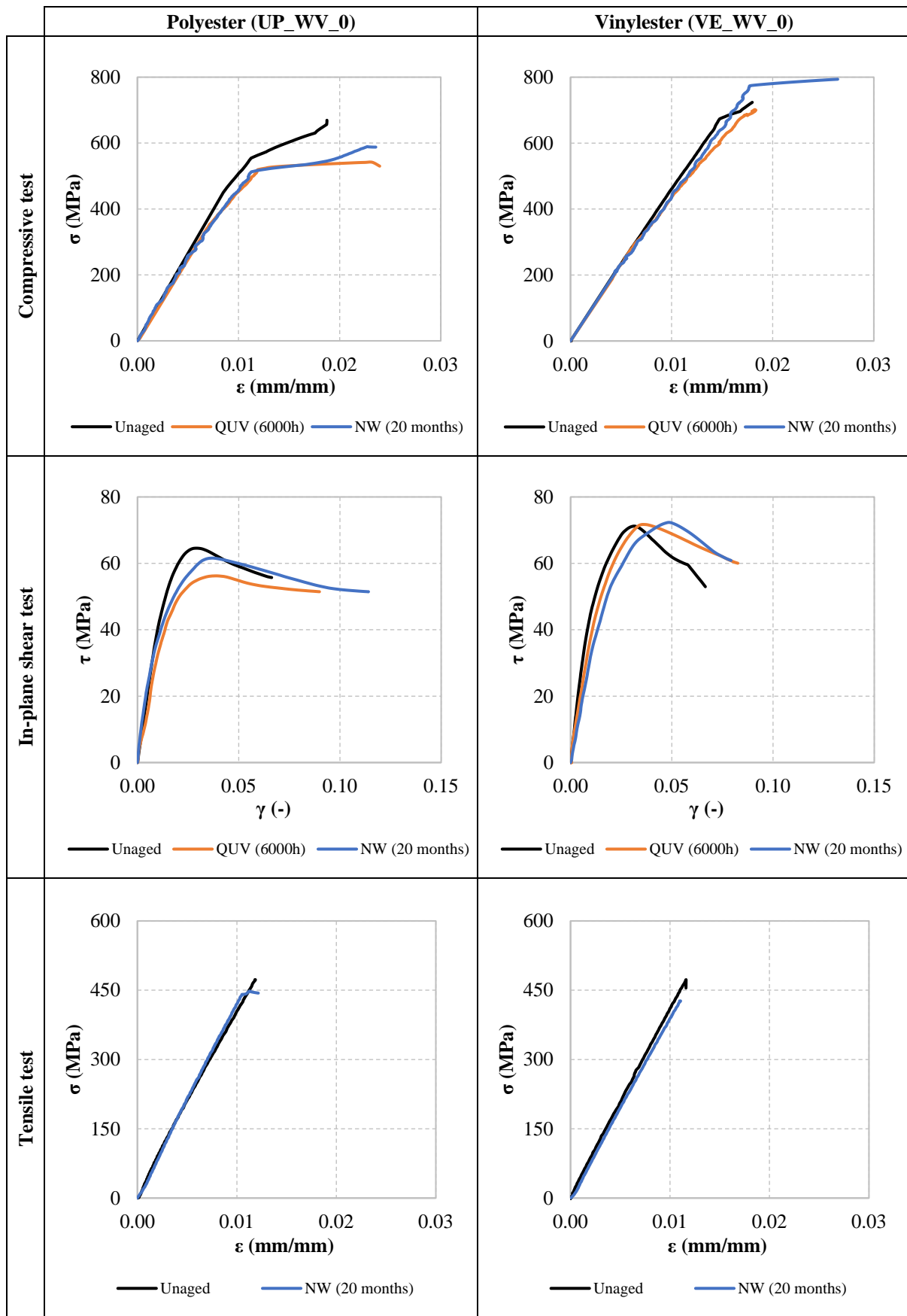


Figure 13.10 - Representative stress-strain curves in compression, in-plane shear and tension of unaged materials and materials exposed to accelerated weathering (QUV - 6000h) and natural weathering (NW - 20 months).

### QUV accelerated weathering

Figure 13.11 shows the effects of 6000 h of QUV accelerated weathering on the mechanical properties of UP and VE specimens, namely in the retention of in-plane shear strength and compressive strength. For both types of resins, specimens were tested (i) with and without surface veil, (ii) with three different ratios of UV additive (0%, 0.25% and 0.50%), and (iii) with two different coatings (CIN and SIKA).

For the reference **UP specimens**, without surface veil and no superficial protection, the mean values of in-plane shear strength and compressive strength retention were 91% and 75%, respectively. In general, the use of surface veil did not influence the retention of those mechanical properties and the use of surface coatings also did not have a clear effect. On the other hand, the use of UV stabilizer additive consistently provided higher retention of those mechanical properties, which are both significantly influenced by the mechanical properties of the polymeric matrix; the results obtained do not show a clear correlation between such performance increase and the ratio of UV additive. It thus seems that the incorporation of UV additive improved the mechanical properties of the UP resin regardless of the incorporation ratio used.

For the reference **VE specimens** (no surface veil, no surface protection), the mean values of in-plane shear strength and compressive strength retention were 96% and 127%, respectively. These figures indicate better overall weathering resistance of the (reference) VE resin specimens compared to their UP counterparts; in addition, the (significant) compressive strength increase also suggests the occurrence of post-curing of the VE resin, which, however, was not reflected in the  $T_g$  values obtained from DMA. For most test series, the use of surface veil did not have a significant effect on strength retention, especially for in-plane shear; yet, for compression, the use of surface veil somehow had a clear detrimental effect on strength retention in specimens without UV additive - no clear reason could be identified for this result. Similarly to UP specimens, the use of surface coatings did not have a clear influence on the strength retention of VE specimens.

In the literature, the information about the influence of QUV accelerated weathering in the mechanical properties analysed herein is relatively scarce. However, Cabral-Fonseca *et al.* [III.74] and Sousa *et al.* [III.76] both reported that the weathering effects (including UV radiation) on the mechanical properties of pultruded GFRP laminates with VE resin were reduced, while equivalent GFRP laminates with UP resin experienced a higher reduction in mechanical properties; those results are in-line with those obtained herein for the unprotected specimens without UV stabilizer additives. With both these protective features, UP specimens can obtain similar performance to VE specimens; for instance, UP and VE GFRP profiles (with and without veil) with 0.5% of UV stabilizer additive appear to fully retain the initial mechanical properties in both tests. However, since the scatter of the results obtained was relatively high regarding the effects of the four parameters assessed (type of resin, use of surface veil, UV additive and superficial protection), further studies are warranted.

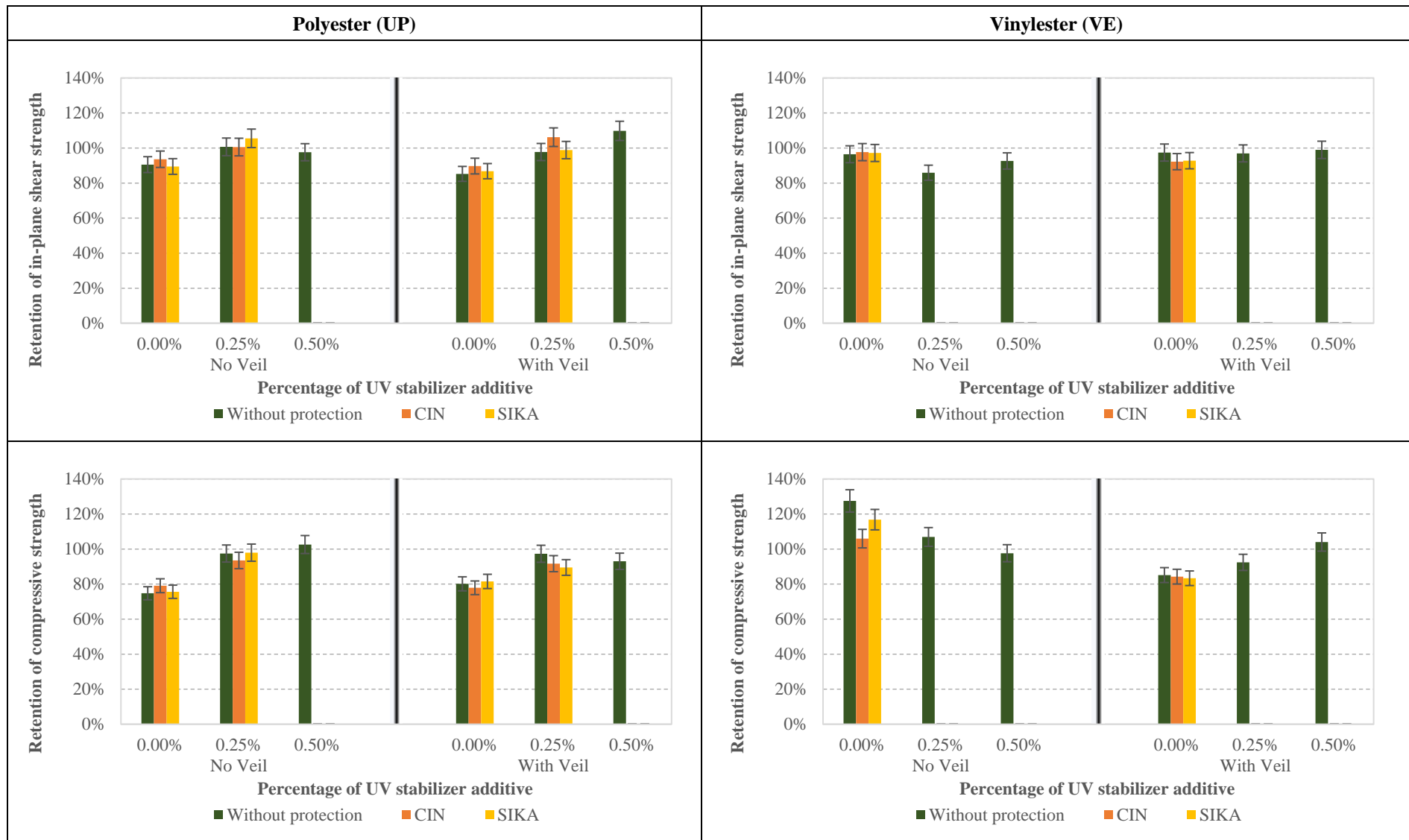


Figure 13.11 - Retention of mechanical properties of UP and VE specimens after 6000 h of QUV accelerated weathering.

## Natural weathering

The effects of 10 and 20 months of NW on the mechanical properties of UP and VE specimens are presented in Figure 13.12 and Figure 13.13, respectively, namely in terms of retention of in-plane shear strength, tensile strength and compressive strength. For both types of resins, specimens were tested (i) with and without surface veil, (ii) with three different ratios of UV additive (0%, 0.25% and 0.50%), and (iii) with two different coatings (CIN and SIKA).

For the reference **UP specimens**, without surface veil and no superficial protection, after 20 months of exposure, the mean values of in-plane shear strength, tensile strength and compressive strength retention were 101%, 91% and 68%, respectively.

In what concerns the in-plane shear strength, for specimens with no surface veil, the use of UV stabilizer additive and superficial protections did not influence the retention of that mechanical property. However, for specimens with surface veil, the use of UV stabilizer additive provided an increase of in-plane shear strength, particularly when combined with superficial protection, even though the same effect was not registered in the other properties.

Regarding the tensile strength, unlike the in-plane shear strength, for specimens with no surface veil, the use of UV stabilizer additive provided higher strength retention, particularly when combined with superficial protection. However, for specimens with surface veil, the use of UV stabilizer additive led to a slightly lower retention of tensile strength, and the use of surface coatings did not have a clear influence on such property retention.

The compressive strength was the property with the highest overall reduction. The use of UV stabilizer additives led to an improvement in property retention, when combined with the CIN protection coating. There was no clear influence of the use of surface veil on compressive strength retention. Somehow, the application of the SIKA protection coating had a detrimental effect on property retention, in particular for specimens without UV stabilizer additive, with an incremental reduction of 20% (UP\_NV\_0) - no clear reason could be identified for this result.

For the reference **VE specimens**, without surface veil and no superficial protection, after 20 months of exposure, the mean values of in-plane shear strength, tensile strength and compressive strength retention were 98%, 94% and 101%, respectively. These figures indicate better overall weathering resistance of the (reference) VE resin specimens compared to their UP counterparts; in addition, the compressive strength increase also highlights the occurrence of post-curing of the VE resin (as mentioned, not reflected in the  $T_g$  values obtained from DMA).

As per the in-plane shear strength and tensile strength, the use of surface veil, UV stabilizer additive and superficial protection did not appear to have a significant effect on strength retention; in particular for the tensile strength, the strength retention for the longer exposure period was in general very high.

Regarding the compressive strength, the property retention was the lowest among all mechanical properties. Somehow, the increase in the ratio of UV stabilizer additive and the use of superficial protection led to a lower strength retention - no clear reasons could be identified to explain these specific results. The use of a surface veil, without considering the superficial protection, did not seem to affect

the strength retention. The maximum reduction of compressive strength was registered for all the specimens with veil and with superficial protection (~30%).

In the study of Nishizaki *et al.* [III.75], pultruded GFRP specimens with VE resin presented a 33% reduction of in-plane shear strength after 10 years of outdoor exposure in Japan, which reflects a much higher degradation compared to the results obtained here for the reference VE specimens (2%). Yet, it is worth referring that the exposure period used in their study was longer; in addition, the authors mentioned that after 1 year no significant changes were observed, which seems to be consistent with the relatively low degradation observed in the present study after nearly 2 years of exposure.

Sousa *et al.* [III.76] also exposed pultruded GFRP specimens to a Mediterranean environment and, after 102 months of natural weathering, UP and VE GFRP specimens presented 84% and 97% of tensile strength retention, respectively, which compare with 91% (UP) and 94% (VE) obtained in the current study for the reference materials - although there are differences in the exposure periods used in both studies (102 vs. 20 months), it is clear that VE specimens present better performance in terms of tensile strength retention.

Figure 13.14 compares the retention of mechanical properties of UP and VE specimens without any superficial protection after undergoing QUV accelerated weathering and NW.

In terms of in-plane shear strength, for almost all UP and VE specimens, the property retention after 6000 h of QUV accelerated weathering is more comparable to the property retention after 10 months of NW; yet, for all exposure conditions, the retention values present the same order of magnitude. For UP specimens, the compressive strength retention after 6000 h of QUV weathering is slightly lower than that after 10 months of NW, but always higher than that after 20 months of NW; hence, it can be concluded that for UP specimens 6000 h of QUV weathering compares to NW exposure between 10 (closer) and 20 months. In contrast, for VE specimens (with the exception of VE\_WV\_0), the compressive strength retention after 6000 h of QUV weathering is always higher than after 20 months of NW and, in most cases, it is also higher than after 10 months of NW. This result indicates that NW was more damaging to most VE specimens than QUV exposure, likely due to the exposure to different environmental agents. Hence, for most VE specimens, QUV weathering can be considered less damaging than or equivalent to 10 months of NW in terms of compressive strength retention.

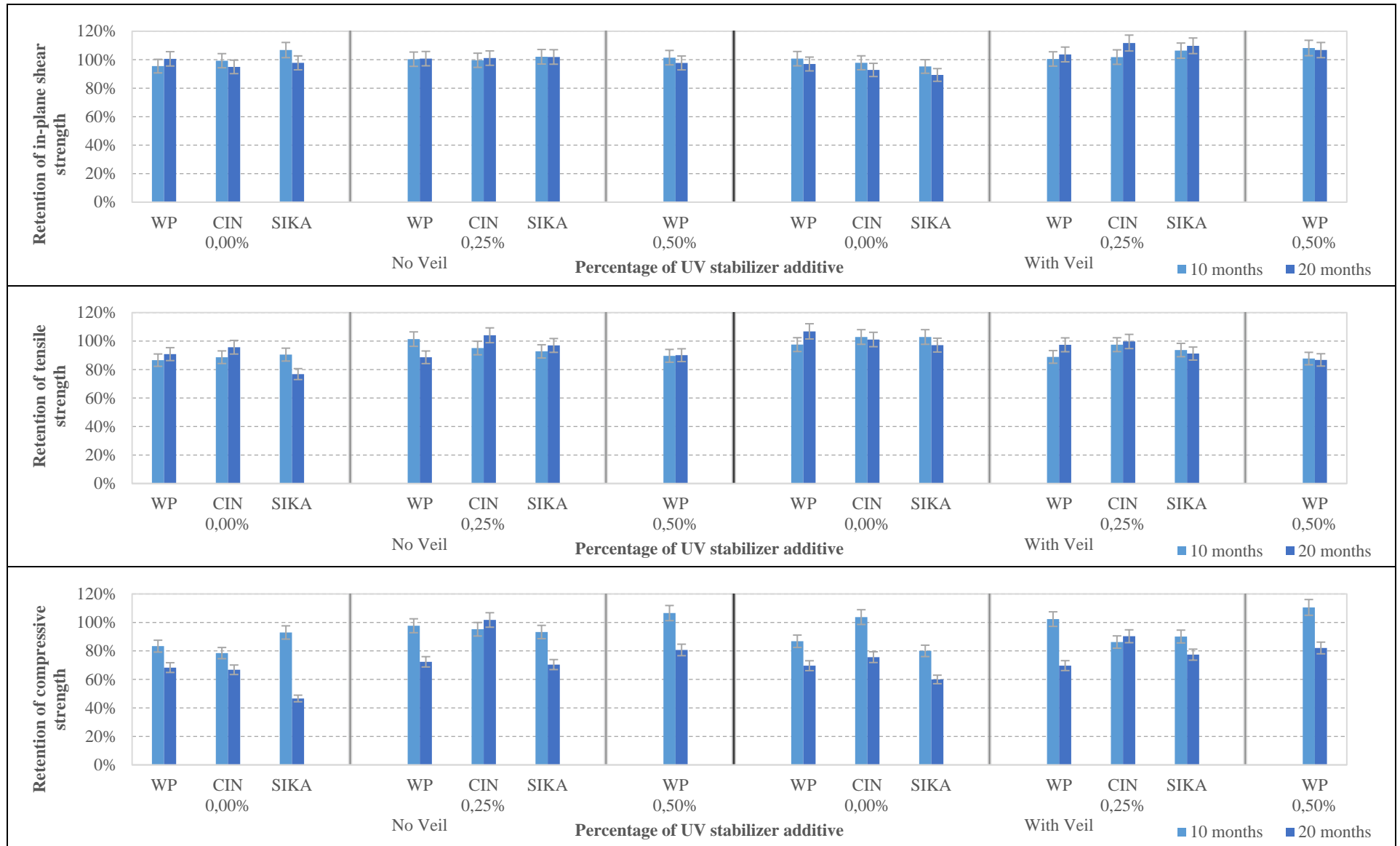


Figure 13.12 - Retention of mechanical properties of UP specimens for 10 and 20 months of natural weathering.

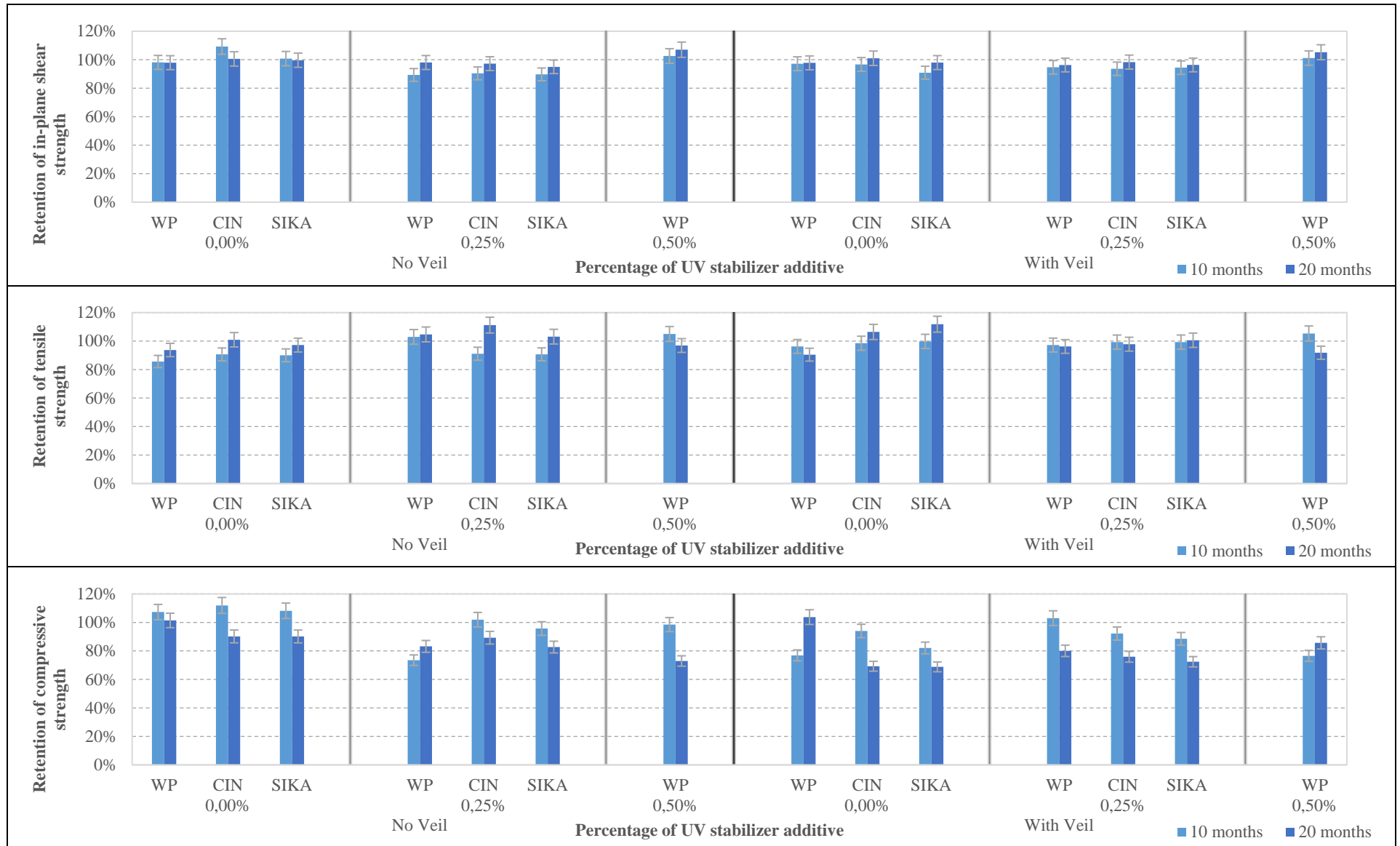
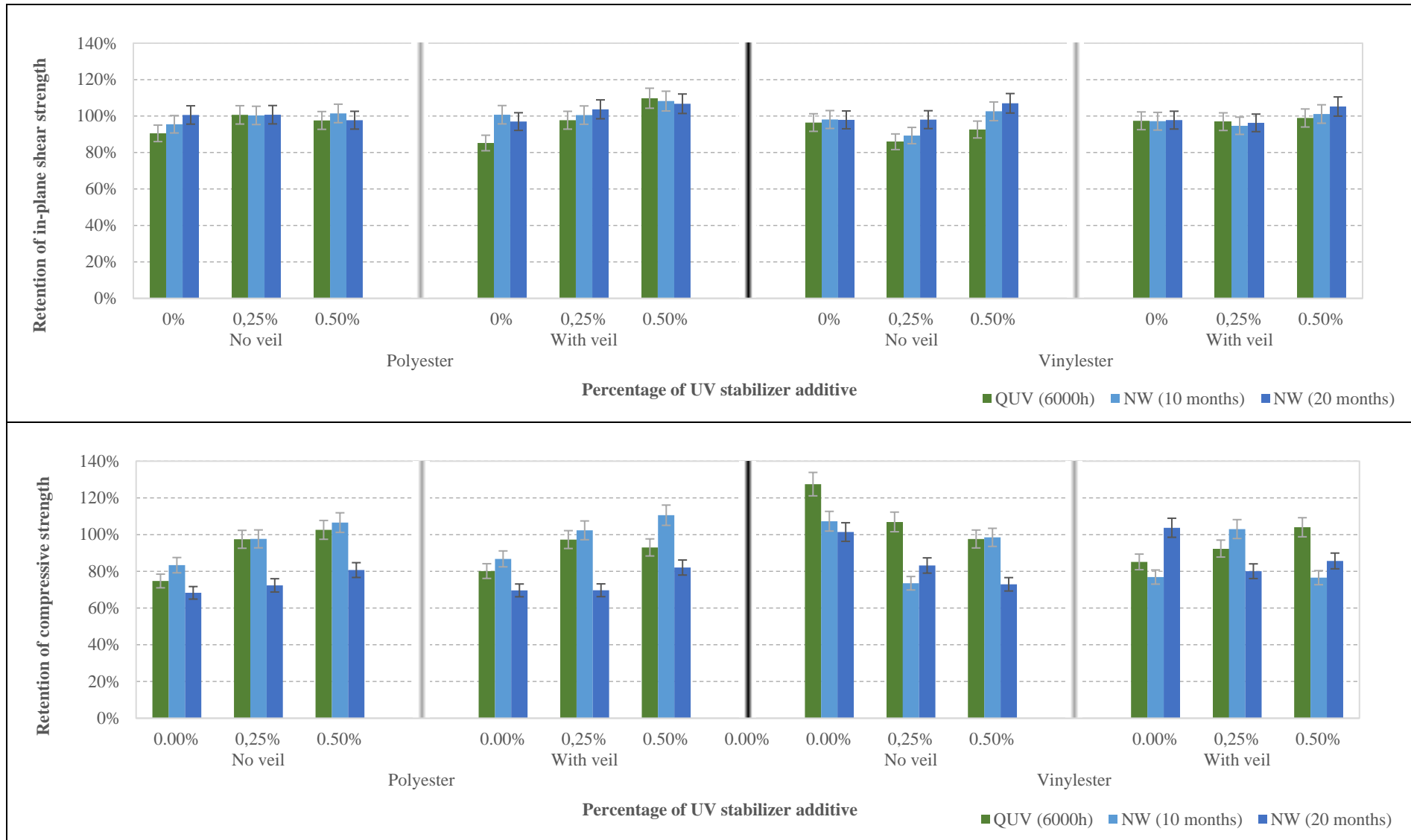


Figure 13.13 - Retention of mechanical properties of VE specimens for 10 and 20 months of natural weathering.



**Figure 13.14 - Comparison of effects of QUV accelerated and natural weathering on mechanical properties of UP and VE specimens without superficial protection.**

### 13.3.2.5. Progression of fibre blooming through image analysis

To evaluate the appearance and evolution of the fibre blooming phenomenon due to UV photodegradation, a segmentation and measurement method based on image processing was implemented. In pair with every colour and gloss measurement, referred in section 13.3.1, a Dino-Lite Edge Digital Microscope AM7915MZT equipment was used; and a total of 10 images were taken from each specimen, as shown in Figure 13.15(a)). In a first step, the image was converted to grayscale; due to the non-uniform light distribution, the Sauvola method [III.79] was then used to compute a threshold map for each image. This map allowed to segment the fibre blooming from the background according to local conditions of brightness (Figure 13.15(b)). Segmentation maps referring to fibre blooming enable to quantify its relative area in the image, which was then averaged for the entire set of 10 images of each specimen. Table 13.05 and Table 13.06 show the fibre blooming ratio evolution with exposure time for QUV accelerated weathering and natural weathering, respectively.

(a) Picture of specimen VE\_NV\_0, after 6000 h of QUV accelerated weathering exposure



(b) Picture of the above specimen after the software analysis (49.5% image area of fibres)

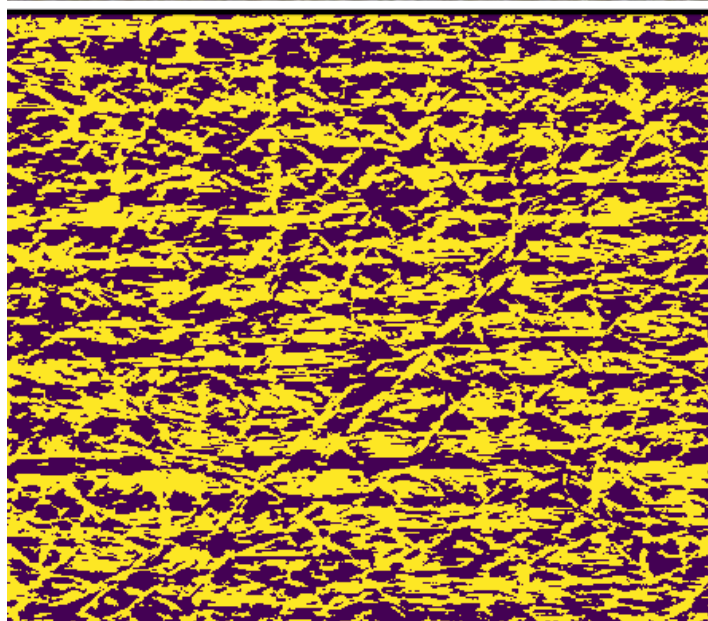


Figure 13.15 - Fibre blooming image analysis.

**Table 13.05 - QUV accelerated weathering fibre blooming ratio by exposure time (% of fibres).**

Hours	UP_NV_0	UP_NV_025	UP_NV_050	VE_NV_0	VE_NV_025	VE_NV_050
1312	26.46 ± 0.52	26.75 ± 0.71	24.3 ± 1.34	23.41 ± 0.74	22.18 ± 0.45	18.62 ± 0.91
1652	31.21 ± 0.35	30.08 ± 0.69	29.16 ± 2.69	27.05 ± 2.12	24.39 ± 0.83	20.48 ± 1.67
1996	41.32 ± 1.86	36.54 ± 1.53	34.37 ± 1.77	31.70 ± 2.29	30.12 ± 1.64	28.63 ± 3.40
2578	47.52 ± 0.74	40.58 ± 1.16	39.16 ± 1.48	37.12 ± 2.97	37.14 ± 2.94	34.02 ± 2.30
2933	46.21 ± 0.65	40.62 ± 0.97	38.09 ± 1.98	36.51 ± 2.13	39.28 ± 1.05	40.29 ± 2.42
3288	45.78 ± 0.91	43.03 ± 1.21	39.24 ± 1.25	41.08 ± 1.98	42.64 ± 1.47	41.57 ± 1.94
3643	45.36 ± 1.88	45.45 ± 2.04	44.42 ± 1.71	45.65 ± 2.69	46.01 ± 2.75	42.84 ± 2.29
3973	45.60 ± 1.31	44.66 ± 1.34	45.73 ± 1.61	46.52 ± 2.66	46.81 ± 2.74	46.59 ± 3.62
4303	43.82 ± 1.16	43.50 ± 1.43	45.69 ± 2.02	47.88 ± 2.42	46.25 ± 2.52	46.47 ± 3.43
4963	44.72 ± 1.58	42.80 ± 1.30	45.11 ± 2.26	45.21 ± 2.13	47.42 ± 1.93	43.55 ± 2.56
5623	45.14 ± 1.05	39.17 ± 1.67	42.22 ± 1.36	43.12 ± 3.24	45.28 ± 2.40	44.00 ± 1.75
6000	43.43 ± 0.96	44.70 ± 1.62	45.85 ± 1.39	48.27 ± 2.54	47.04 ± 1.36	44.51 ± 3.08

**Table 13.06 - Natural weathering fibre blooming ratio by exposure time (%).**

Weeks	UP_NV_0	UP_NV_025	UP_NV_050	VE_NV_0	VE_NV_025	VE_NV_050
42	42.67 ± 2.07	41.59 ± 2.57	38.99 ± 2.43	21.56 ± 1.48	20.86 ± 1.52	21.20 ± 2.20
88	49.25 ± 1.24	49.03 ± 1.65	46.52 ± 1.04	36.72 ± 1.75	38.23 ± 2.03	32.24 ± 2.94

It is worth referring that, for both weathering conditions - accelerated (QUV) and natural - the fibre blooming phenomenon only occurred in specimens without the non-woven polyester surface veil and no superficial protection - in fact, only specimens from UP\_NV and VE\_NV series presented fibre blooming. This result highlights the effectiveness of both strategies in preventing the occurrence of fibre blooming, which is known to (i) have detrimental effects on the functionality of GFRP constructions (e.g., in handrails and guardrails), and to (ii) increase the retention of moisture and biological colonization.

Figure 13.16 depicts the evolution of the fibre blooming ratio for the different types of UP and VE specimens (with varying UV additive ratio) exposed to QUV and NW. For both types of exposure, the evolution of the fibre blooming ratio seems to present two stages (clearer in QUV, partly due to the higher number of measurements): an initial stage with a roughly linear increase of fibre blooming ratio, followed by a non-linear stage with reduction of the increase rate of fibre blooming ratio, which tends to a plateau.

The results obtained for QUV accelerated weathering exposure (Figure 13.16 (a)) show that the UP profiles exhibited a higher rate of fibre blooming development (slope of the curves) in comparison to the VE profiles - even though the VE profiles exhibited a faster photochemical degradation, as seen in the colour variation measurements, they experienced less chalking (loss of the superficial layer) in comparison to the UP profiles, which resulted in a slower rate of occurrence of fibre blooming. Figure 13.16 (a) also shows that, for both types of profiles, the fibre blooming ratio attained a plateau ranging from 43% to 48%, which was similar for specimens produced with both types of resins and did not seem to depend on the UV additive content - in other words, in the long-term, the extent of fibre blooming in profiles produced with UP and VE resins is identical and is not influenced by the UV

additive content.

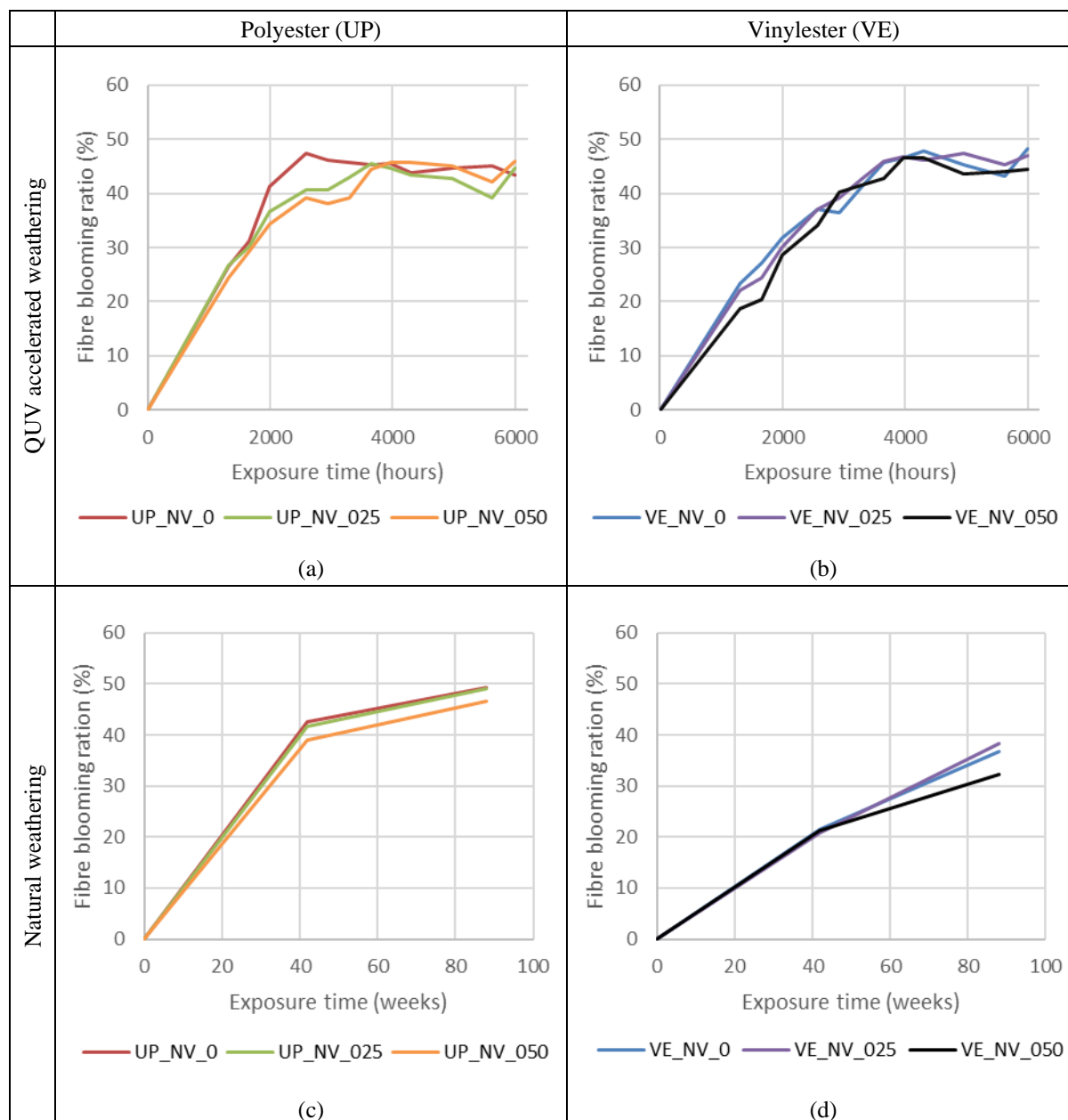


Figure 13.16 - Evolution of fibre blooming ratio on UP and VE specimens exposed to (a) QUV and (b) NW.

The results obtained for NW exposure (Figure 13.16 (c and d)) show that, similarly to QUV accelerated weathering, the UP specimens present a higher initial rate of fibre blooming development in comparison to the VE specimens. After 20 months (88 weeks) of NW exposure, the UP specimens seem to have already reached the stabilization plateau value obtained in the QUV accelerated weathering experiments - in this respect, results are quite consistent; on the other hand, for the VE specimens, although the rate of fibre blooming presents a decreasing trend with the exposure period, such plateau was not yet attained.

## 13.4. Field study

### 13.4.1. Overview of surveyed constructions

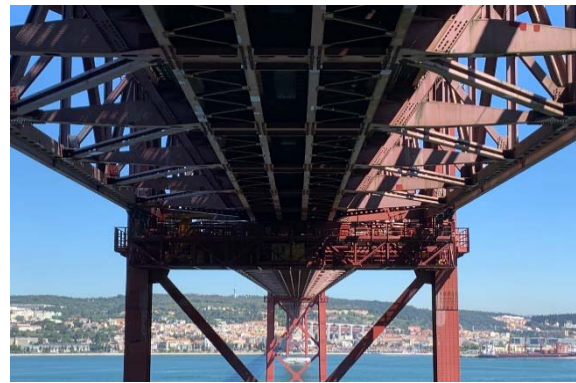
To complement the investigation presented in Part II and the experimental study described in the preceding section (which comprised limited duration of weathering exposure), an additional field survey was carried out, in collaboration with manufacturers and installers of pultruded GFRP structures. This study focused on some of the older pultruded GFRP structures built in Portugal, for which original material not subjected to any direct weathering exposure (e.g., sun light, moisture, and wind) was available. Three GFRP installations, described next, could be identified and considered for the present study. For each of them, specimens of profiles exposed to natural weathering were collected, prepared and subjected to mechanical tests alongside unexposed (identical) specimens from the same production batches. This allowed assessing the actual effects of natural weathering on the mechanical properties of such pultruded GFRP profiles.

#### 13.4.1.1. 25<sup>th</sup> of April Bridge

The 25<sup>th</sup> of April Bridge, open to traffic in 1966, is a suspension bridge over the Tagus River connecting the cities of Lisbon and Almada. Due to the need to serve an increasing population and also due to structural repair needs, in 1998, the bridge was subjected to a large-scale intervention, in the scope of which a lower deck was added, and a railway track installed. As shown in Figure 13.17, the floor between the train tracks is composed of GFRP gratings, made of interconnected small “I” and circular cross-section profiles. The “I” profiles (with dimensions of  $25 \times 15 \times 4$  mm) have a superficial protection on the upper flange made of a mixture of sand and resin in order to make the grating anti-slip.



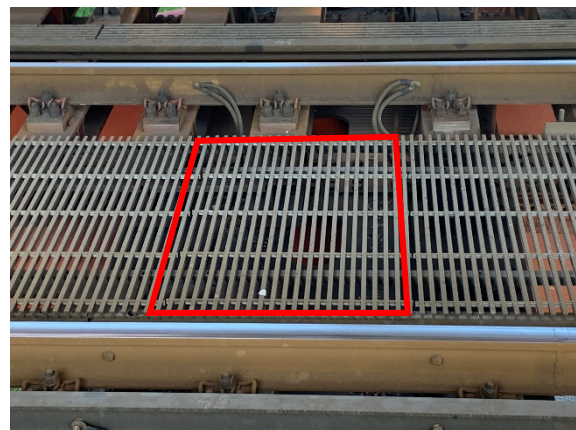
(a) 25<sup>th</sup> of April Bridge - overview



(b) Bridge lower deck - bottom view



(c) Bridge lower deck - upper view



(d) Grating removed for specimen extraction

**Figure 13.17 - 25<sup>th</sup> of April Bridge and specimen grating location.**

A grey grating was removed from the lower deck floor, upon inspection, on May 2019 - it was thus exposed to natural weathering for a period of approximately 21 years. Considering the location of the bridge, and the position of the grating, the following environmental agents were relevant: reduced (direct) UV radiation, temperature variations, moisture, saline condensation (the bridge is very close to the sea) and polluting agents from the bridge's traffic. The reference (unexposed) specimen was an excess grating that was not used at the time of installation and was kept inside the bridge's massifs; therefore, it was not subjected to relevant weathering exposure (these components are not acclimatized, but have very high thermal inertia and the zone where the reference specimen was stored was buried).

#### 13.4.1.2. Colombo Centre rooftop

The Colombo Centre (Figure 13.18), located in Lisbon and inaugurated in 1997, comprises a shopping mall, two office towers (built later) and a food court. In the centre's rooftop, several GFRP structures were installed in order to provide an aesthetical protection to the centre's chilling and exhaustion devices. The selected structure for specimen extraction, illustrated in Figure 13.18 (c) and (d), is pitched at a 50° angle with the horizontal plane, and west-southwest oriented.

A green "H" shaped pultruded profile (with dimensions of 50 × 50 × 3 mm) was collected during an inspection carried out in July 2019 - the material was thus in service for a period of approximately 22 years. The unaged and replacement profiles were collected from the manufacturer's warehouse, which were stored and unused since the time of the original installation.

Considering the location of the Colombo Centre, and the position of the profiles, the following environmental agents can be considered as relevant: continuous (direct) UV radiation, temperature variations, moisture, and polluting agents from the centre's surrounding traffic.



(a) Colombo Centre - overview



(b) GFRP shading structures in the rooftop



(c) Structure selected for specimen collection



(d) Profiles removed for specimen extraction

**Figure 13.18 - Colombo Centre and specimen profile location.**

### 13.4.1.3. Lisbon Oceanarium

The Lisbon Oceanarium (Figure 13.19) is located in the Expo district of Lisbon and was inaugurated in 1998 for the World Exhibition. Inside the Oceanarium, over its main tank, a GFRP walkway structure with profiles and gratings was installed due to their non-corrosive properties (Figure 13.19 (b) and (c)). A yellow SHS shaped profile (with dimensions of  $40 \times 40 \times 3.2$  mm) was collected upon an inspection carried out in July 2019, resulting in an exposure period of approximately 21 years. The unaged and replacement specimens were collected from the manufacturer's warehouse, which were stored and unused since the time of the original installation. The environmental conditions above the main water tank (where the walkway is installed) are artificially set to a 21 °C temperature and 81% relative humidity. Considering the location of the specimens, the following environmental agents are considered as relevant: saline condensation and moisture.



(a) Lisbon Oceanarium - overview



(b) GFRP walkway structure above main tank



(c) GFRP walkway structure above main tank



(d) Profiles removed for specimen extraction

Figure 13.19 - Lisbon Oceanarium and specimen profile location.

### 13.4.2. Description of test programme

After removal from the corresponding structures, the collected specimens (grating and profiles) were cut down to the size required by each test standard (Table 11.02) using a CNC cutting machine (Figure 13.20). This procedure provided a uniform and very precise sizing for all specimens.

The following physical properties were analysed (3 specimens were considered for each of the tests): (i) inorganic content; and (ii) glass transition temperature, by dynamic mechanical analysis (DMA). The following mechanical properties were analysed: (i) tensile properties; (ii) compressive properties; (iii) flexural properties; and (iv) in-plane shear properties. All properties were determined according to the characterisation methods described in section 10.3. In flexural and

interlaminar shear tests, the specimens were tested with the top surface (exposed to UV radiation in constructions located outdoors) subjected to compressive stresses.

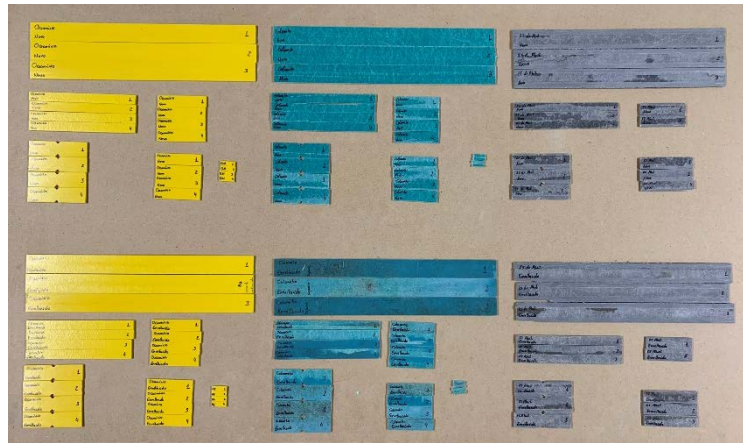


**Figure 13.20 - Aged and unaged specimens prepared for testing: Lisbon Oceanarium (left), Colombo Centre (centre), 25<sup>th</sup> of April Bridge (right) - unaged (above), aged (below)**

### **13.4.3. Results and discussion**

#### **13.4.3.1. Inorganic mass content**

The inorganic mass content (IMC) of the profiles corresponding to each case study (which comprises glass fibre reinforcement and inorganic filler), exposed and unexposed to weathering, was estimated in accordance with the methodology described in section 10.3.1. The results obtained are presented in Table 13.07, showing that the IMC of the profiles used in the 25<sup>th</sup> of Abril and Colombo Centre is similar to the fibre content of the specimens used in the experimental study, whereas the IMC of specimens used in the Oceanarium is much lower, which is consistent with the much lower mechanical properties for some types of loading (more fibre-dominated), namely for tension and flexure. For each case study, unexposed and exposed specimens present quite similar IMC values, confirming that they were produced in the same batch.

#### **13.4.3.2. Dynamic mechanical analysis**

The DMA experimental curves, shown in Figure 13.21, include the storage modulus,  $E'$  (left axis - dashed lines), and the loss factor,  $\tan \delta$  (right axis - continuous lines). In general, environmental exposure did not have a very significant effect on the shape of the DMA curves nor on the corresponding  $T_g$  estimates (Table 13.07), namely considering the scatter of test data.

In the 25<sup>th</sup> of April Bridge and in the Oceanarium, due to the weathering exposure, the height of the  $\tan \delta$  curve peak decreased and the storage modulus values in the glassy plateau (25 °C) increased; in the Colombo Centre, the trends were precisely inverse, which can be due to the more aggressive and continuous sun exposure in this latter environment. In any case, as mentioned, the changes in  $T_g$  estimates were not very significant.

#### **13.4.3.3. Mechanical properties**

The mechanical properties of the unaged and aged specimens obtained from the three different case studies are presented in Table 13.07 and Figure 13.22.

Overall, the results show that the mechanical properties of the pultruded GFRP materials used in the three case studies remained relatively unchanged due to the weathering exposure. This said, there were some variations in specific properties of the specimens collected from each location that are discussed next.

The specimens extracted from the 25<sup>th</sup> of April Bridge exhibited a slight strength increase for all tests, the highest occurring in tension, with 15% increase. On the other hand, the elastic modulus did not present any relevant changes; the most notable change occurred in the flexural test, for which a 10% decrease occurred, but associated to quite high scatter.

The specimens extracted from the Colombo Centre roof presented a slight to moderate reduction in all strength- and stiffness-related mechanical properties due to the weathering exposure (consistent with DMA results); the most relevant reduction occurred in compressive strength (19%), and in flexural strength (12%) and flexural modulus (17%).

Finally, the specimens extracted from the Oceanarium presented a reduction of most strength-related properties, the most notable occurring in tension (24%); in compression, the strength increased 10%, but this figure is associated to high scatter. The elastic moduli presented reductions in tension (10%) and flexure (7%), in both cases within the experimental uncertainty, and an increase in shear (13%).

Keller *et al.* [I.03] and Sousa [III.16] also evaluated the performance of GFRP components extracted from in-service structures in order to determine the effects of weathering on the reduction of mechanical properties and also the influence of the in-service exposure conditions on the performance of those infrastructures. Keller *et al.* [I.03] studied a footbridge located in a relatively harsher environment (alpine climate) in comparison with the ones studied herein. However, the reduction of tensile strength exhibited by the walls of the GFRP profiles after 17 years of exposure - 32% (flange) and 17% (web) - is comparable to the tensile strength reduction obtained for the Oceanarium (24%). Sousa [III.16] studied a transportation service viaduct subjected to a more comparable environment (Mediterranean - Lisbon) to the ones considered in the present study and reported reductions of tensile and flexural strengths of 11% and 8%, respectively, after 11 years of exposure. In the present study, the results obtained for outdoor exposure in the 25<sup>th</sup> of April Bridge and in the Colombo Centre were of the same order of magnitude, with a lower reduction of tensile strength and a similar reduction of flexural strength.

In summary, this experimental (field) study allowed quantifying the changes in the mechanical properties of pultruded GFRP materials with over 20 years of in-service exposure to different environments. The changes obtained are low to moderate and the set of data obtained is quite relevant given the lack of long-term durability studies *in situ*. Additional research (and data) is needed to understand in further depth the underlying causes for the changes in mechanical properties due to the various environmental agents and to allow predicting the service life of this type of FRP composite structures.

**Table 13.07 - Summary of properties of the field study specimens.**

Property	Method	Unit	25 <sup>th</sup> of April Bridge		Colombo Centre		Lisbon Oceanarium	
			Unexposed	Exposed	Unexposed	Exposed	Unexposed	Exposed
IMC	Calcination	[%]	71.8 ± 0.37	68.7 ± 0.01	67.5 ± 0.7	69.6 ± 0.9	49.7 ± 0.89	50.8 ± 0.91
$T_g$	DMA	$T_g (E'_{onset}) [°C]$	90.6 ± 0.8	95.0 ± 4.3	135.5 ± 6.4	130.0 ± 2.8	65.7 ± 0.9	66.5 ± 1.7
		$T_g (\tan \delta) [°C]$	103.5 ± 3.5	104.7 ± 7.6	142.5 ± 0.7	142.5 ± 2.1	103.0 ± 4.2	99.8 ± 0.3
Mechanical property	Tensile tests	$\sigma_{tu}$ [MPa]	323.1 ± 19.6	371.6 ± 20.7	444.8 ± 40.4	432.6 ± 17.8	255.7 ± 27	193.8 ± 34.3
		$E_t$ [GPa]	37.9 ± 1.9	37.3 ± 1.5	36.8 ± 1	35.3 ± 1.6	17.8 ± 1.4	16.1 ± 1.6
	Compressive tests	$\sigma_{cu}$ [MPa]	485.4 ± 38.8	514.9 ± 8.8	604.8 ± 51.4	487.7 ± 77.7	437.7 ± 57.3	482.7 ± 40.1
	Flexural tests	$\sigma_{fu}$ [MPa]	585.6 ± 17.4	590.1 ± 41.2	639.6 ± 41.9	561.4 ± 1.1	312 ± 9.2	281.9 ± 4.8
		$E_f$ [GPa]	36.3 ± 0.7	32.6 ± 4.3	40.8 ± 4.1	33.8 ± 0.6	15.6 ± 0.1	14.5 ± 1.3
	In-plane shear tests	$\tau_{max}$ [MPa]	49.6 ± 0.6	51.4 ± 3.2	61.6 ± 1.1	55.1 ± 1.7	57.6 ± 2.4	54.6 ± 2.5
		$G$ [GPa]	3.2 ± 0.1	3.2 ± 0.3	3.8 ± 0.4	3.3 ± 0.1	2.6 ± 0.1	3.0 ± 0.1

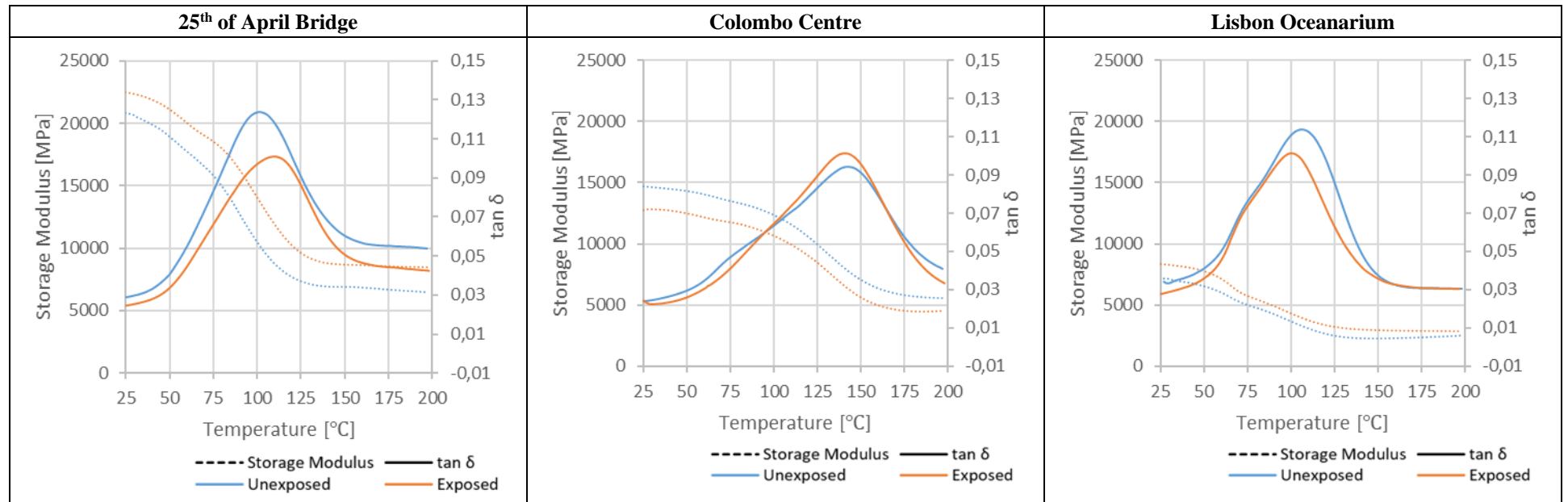


**Figure 13.21 - DMA results as function of exposure (field study).**

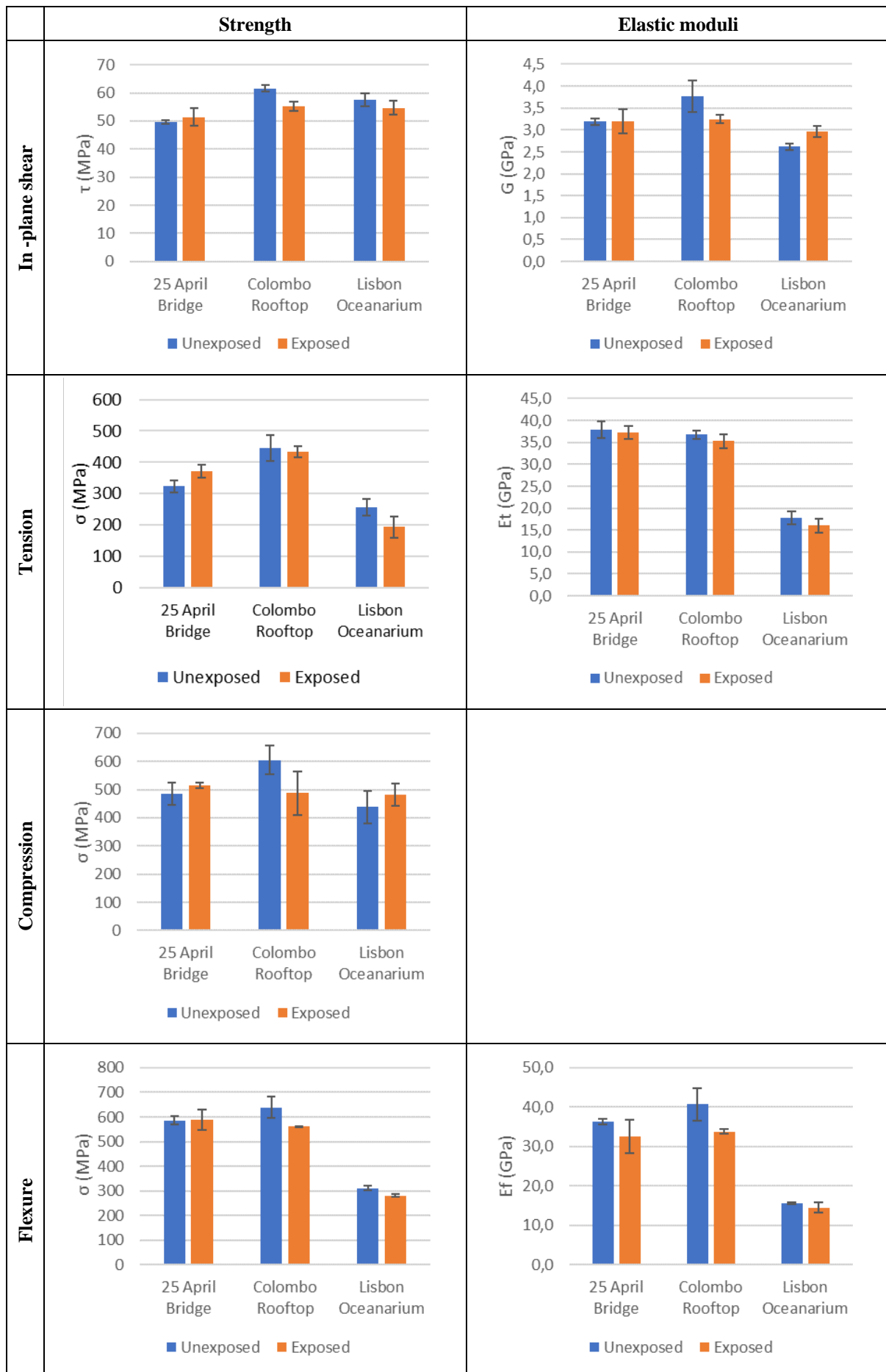


Figure 13.22 - Mechanical properties of unexposed and exposed specimens (field study).

In this respect, in the recent European Technical Specification CEN/TS 19101: 2022, *Design of fibre-polymer composite structures*, the following three exposure classes are defined:

- Class I - indoor exposure;
- Class II - outdoors exposure without continuous exposure to water, or permanent immersion in water, or permanent exposure to a relative humidity higher than 80%, or combined UV-radiation and frequent freeze-thaw cycles;
- Class III - continuous exposure to water (or seawater), or permanent immersion in water (or seawater), or permanent exposure to a relative humidity higher than 80% (material temperature up to 25 °C).

Based on the above-mentioned descriptions, the 25<sup>th</sup> of April Bridge and the Colombo Centre are defined as Class II; the Oceanarium is defined as Class III, since the relative humidity above the main tank is 81% (this value is only very slightly above the threshold of 80% set for class III).

According to CEN/TS 19101:2022, the conversion factors for exposure classes I, II and III are respectively 1.00, 0.85 and 0.60. These values were defined based on a survey of test data reported in the literature [III.80]. Figure 13.23 presents the data considered in that survey for class II (in blue), as well as the results obtained in the present field study (in grey and green). Figure 13.24 shows that the data obtained in the field study are in line with the property retention reported in previous studies (all corresponding to shorter exposure periods), in the (vast) majority of cases exceeding the 0.85 recommended value.

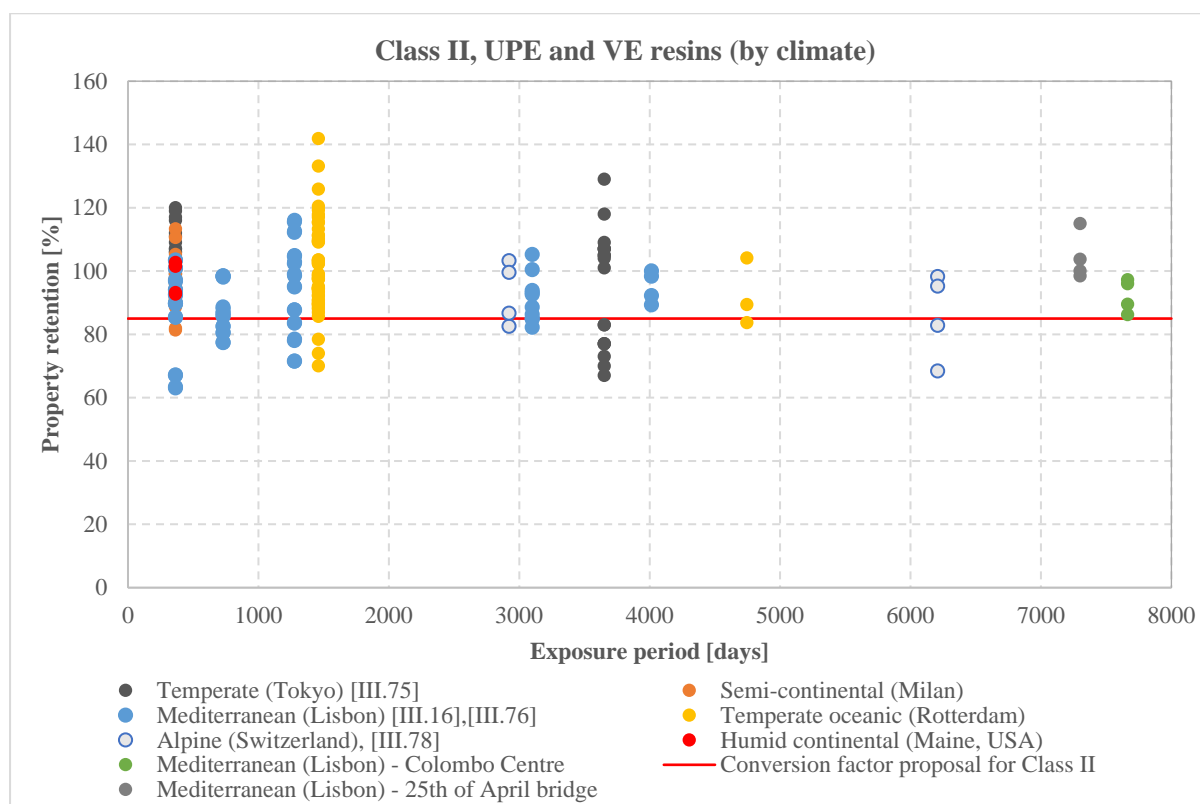


**Figure 13.23 - Retention of stiffness- and strength-related properties vs. exposure period for outdoor natural weathering by climate, Class II (data from the literature [III.80] and present field study).**

Figure 13.24 presents the data considered in that survey for class III (in blue), as well as the results

obtained in the present field study for the Oceanarium (in yellow). The results depicted in Figure 13.24 also show that the data obtained in the field study are in line with the property retention reported in previous studies, with the majority of cases exceeding the recommended value of 0.60. About the aggressiveness of the Oceanarium, as mentioned above, the exposure conditions of this construction (relative humidity of 81%) are close to the threshold of 80%, which defines the boundary of this class - in other words, this environment would correspond to the least aggressive within this exposure class III.

Overall, this analysis indicates (i) the suitability of the provisions given in CEN/TS 19101: 2022 (based on the data available), and (ii) the good weathering performance of the GFRP materials studied herein, which, naturally, needs to be confirmed for longer periods of exposure.

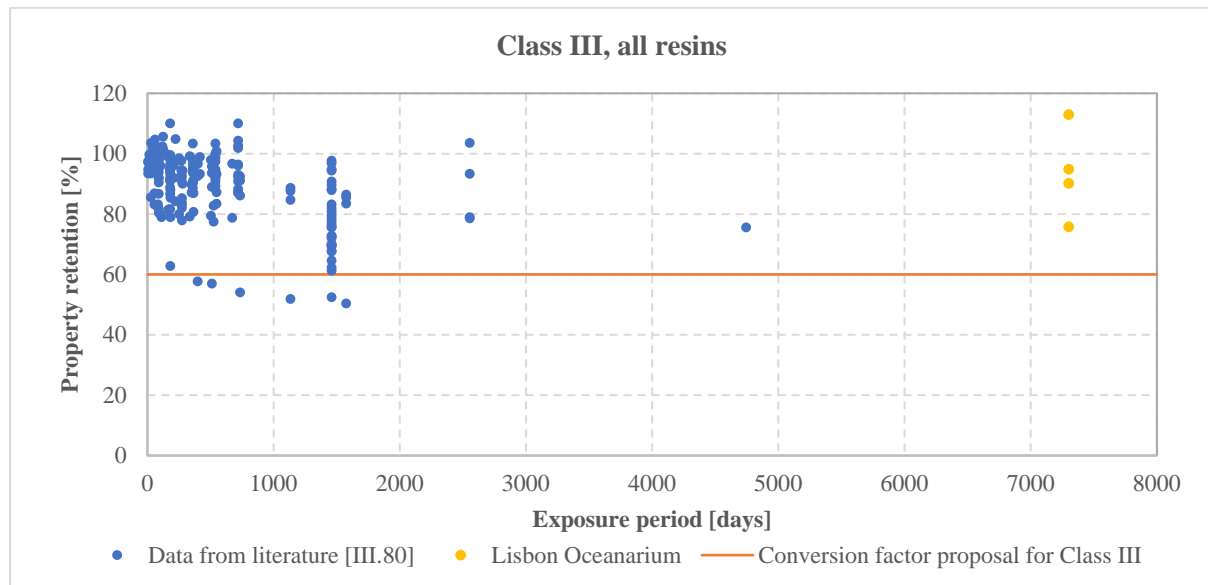


**Figure 13.24 - Retention of stiffness- and strength-related properties vs. exposure period for outdoor natural weathering, Class III (data from the literature [III.80] and present field study).**

### 13.5. Concluding remarks

This section presented and discussed the results of experimental investigations on pultruded GFRP materials exposed to natural weathering and accelerated weathering in artificial conditions using a QUV chamber.

In these experiments, vinylester (VE) specimens exhibited a greater change in colour than polyester (UP) specimens, and this colour change was relevant even for very short exposure periods. The colour changes in VE specimens appeared to stabilize after an initial change, while the UP specimens exhibited a more gradual change in colour, peaking at around 1250 h, and then stabilizing. The addition of UV additive absorbers and surface veil had no effect on the colour change. Longer exposure periods resulted in a distinct behaviour in VE specimens with surface veil compared to those without surface veil.

When UP specimens were exposed to QUV, after 2000 h, the gloss became negligible, and then remained constant for the rest of the exposure period. Similarly, in VE specimens exposed to QUV, after 1000 h of exposure, the gloss became negligible and then remained unchanged for the rest of the exposure period. For both materials, as expected, the exposure times associated to greater loss of gloss coincided with those corresponding to the greatest variation in colour. For UP specimens, 20 months of NW exposure caused similar loss of gloss to 2000 h of QUV exposure. For VE specimens, after 10 months of NW exposure, the loss of gloss was already similar to that caused by 1000 h in QUV.

Regarding the mechanical properties of UP and VE specimens exposed to QUV accelerated weathering for 6000 h, the results obtained show that: (i) the use of UV stabilizer additive consistently provided higher retention of mechanical properties for UP specimens; (ii) VE specimens had better overall UV weathering resistance compared to UP specimens; (iii) the use of surface veil did not have a significant effect on strength retention for most test series, but for compression it somehow had a detrimental effect on strength retention in specimens without UV additive (no clear reasons could be identified to justify this result); (iv) the use of superficial protection did not have a clear influence in the strength retention.

The effects of NW on the mechanical properties of UP and VE specimens after 10 and 20 months of exposure showed that the VE specimens had better overall weathering resistance compared to UP specimens. The use of UV stabilizer additive and superficial protection improved the retention of mechanical properties, but had different effects depending on the type of test. The use of surface veil had a varying effect on the retention of the mechanical properties. In compression, there was a higher overall property reduction, with the maximum property decay occurring in specimens with veil and superficial protection. For both UP and VE specimens, in general, the reductions of in-plane shear and compressive strengths after 6000 h of QUV accelerated weathering were comparable to those after 10 months of NW. The relevance of these findings is limited due to the short duration of the NW exposure; additional results, for longer periods of exposure, are needed.

The field study intended to determine the effects of long-term exposure to different environments on the mechanical properties of pultruded GFRP materials in-service conditions. The study involved collecting specimens from three different case studies: the 25<sup>th</sup> of April Bridge, the

Colombo Centre, and the Lisbon Oceanarium. The results showed that environmental exposure had a low to moderate impact on the mechanical properties of the GFRP profiles applied in those case studies, with some variations observed among the specimens collected from each location. The specimens collected from the 25<sup>th</sup> of April Bridge showed a slight increase in strength, while the specimens extracted from the Colombo Centre showed a slight to moderate reduction in strength- and stiffness-related properties. The specimens collected from the Oceanarium showed a low to moderate reduction in most strength-related properties. These results provide valuable information on the long-term durability of pultruded GFRP materials, but further research is needed to understand better the underlying causes of changes in mechanical properties and to predict the service life of FRP composite structures. The reduction in mechanical properties observed for these case studies support the values of the moisture conversion factors established in the recent European Technical Specification CEN/TS 19101: 2022 for exposure classes II and III.

## 14. Part III references

- [III.01] Kharbari, V.M., Chin, J.W., Hunston, D., Benmokrane B., Juska, T., Morgan, R., Lesko, J.J., Sorathia, U., Reynaud D. (2003) “Durability gap analysis for fibre-reinforced polymer composites in civil infrastructure”. *Journal of Composites for Construction*, 7(3), pp. 238-247. [https://doi.org/10.1061/\(ASCE\)1090-0268\(2003\)7:3\(238\)](https://doi.org/10.1061/(ASCE)1090-0268(2003)7:3(238))
- [III.02] International Organization for Standardization (1999) “Textile-glass-reinforced plastics - Prepregs, moulding compounds and laminates - Determination of the textile-glass and mineral-filler content - Calcination methods”, ISO 1172:1999.
- [III.03] International Organization for Standardization (2019) “Colourimetry; Part 4: CIE 1976 L\*a\*b\* colour space”, ISO 11664:2019.
- [III.04] International Organization for Standardization (2014) “Paints and varnishes. Determination of specular gloss of non-metallic paint films at 20°, 60°, 85°”. ISO 2813:2014.
- [III.05] ASTM International (2001) “Standard Test Method for indentation Hardness of Rigid Plastics by means of a Barcol Impressor”, ASTM D2583-95, West Conshohocken, Pennsylvania, USA.
- [III.06] International Organization for Standardization (1996) “Plastics - Determination of dynamic mechanical properties - Part 1: General principles. Part 5: Flexural vibration - non-resonance method”, ISO 6721:1996.
- [III.07] ASTM International (1999) “Standard test method for assignment of the glass transition temperature by dynamic mechanical analysis”. ASTM E1640-99, West Conshohocken, Pennsylvania, USA.
- [III.08] International Organization for Standardization (1997) “Plastics - Determination of tensile properties - Part 1: General principles. Part 4: Test conditions for isotropic and orthotropic fibre-reinforced plastic composites”, ISO 527:1997.
- [III.09] ASTM International (2011) “Standard test method for shear properties of composite materials by the V-notched beam method”. ASTM D 5379 / D 5379M, West Conshohocken, Pennsylvania, USA.
- [III.10] ASTM International (2011) “Standard Test Method for Compressive Properties of Polymer Matrix Composite Materials Using a Combined Loading Compression (CLC) Test Fixture”. ASTM D 6641 / D 6641M, West Conshohocken, Pennsylvania, USA.
- [III.11] International Organization for Standardization (1997) “Fibre-reinforced plastic composites - Determination of flexural properties”, ISO 14125:1998.
- [III.12] ASTM International (2000) “Standard test method for short-beam strength of polymer matrix composite materials and their laminates”. ASTM D 2344, West Conshohocken, Pennsylvania, USA.
- [III.13] Liu, T., Liu, X., Feng, P. (2020). “A comprehensive review on mechanical properties of pultruded FRP composites subjected to long-term environmental effects”. *Composites Part B: Engineering*, 191, 107958. <https://doi.org/10.1016/j.compositesb.2020.107958>

- [III.14] Jones, F.R. (1999). "Chapter 3: Durability of reinforced plastics in liquid environments." In Pritchard, G., editor: Reinforced plastics durability, pp. 70-110. Woodhead Publishing, Sawston.  
<https://doi.org/10.1533/9781845694876.70>
- [III.15] Schutte, C.L. (1994). "Environmental durability of glass-fibre composites". *Materials Science and Engineering: R: Reports*, 13(7), 265-323.  
[https://doi.org/10.1016/0927-796X\(94\)90002-7](https://doi.org/10.1016/0927-796X(94)90002-7)
- [III.16] Sousa, J. (2018). "Durability of pultruded GFRP profiles and adhesively bonded connections between GFRP adherends". PhD Thesis in Civil Engineering, Instituto Superior Técnico, University of Lisbon.
- [III.17] Svetlik, S. L. (2008). "An investigation in the hygrothermal degradation of an E-glass/vinyl-ester composite in humid and immersion environments". PhD thesis in Civil Engineering, University of California, San Diego.
- [III.18] Antoon, M. K., & Koenig, J. L. (1980). "The structure and moisture stability of the matrix phase in glass-reinforced epoxy composites". *Journal of Macromolecular Science - Reviews in Macromolecular Chemistry*, 19(1), 135-173.  
<https://doi.org/10.1080/00222358008081048>
- [III.19] Mijović, J., & Lin, K. F. (1985). "The effect of hygrothermal fatigue on physical/mechanical properties and morphology of neat epoxy resin and graphite/epoxy composite". *Journal of Applied Polymer Science*, 30(6), 2527-2549.  
<https://doi.org/10.1002/app.1985.070300619>
- [III.20] Thomson, K.W., Wong, T., Broutman, L.J. (1984). "The plasticization of an epoxy resin by dibutylphthalate and water". *Polymer Engineering & Science*, 24(16), 1270-1276.  
<https://doi.org/10.1002/pen.760241610>
- [III.21] Alessi, S., Pitarresi, G., Spadaro, G. (2014). "Effect of hydrothermal ageing on the thermal and delamination fracture behaviour of CFRP composites". *Composites Part B: Engineering*, 67, 145-153.  
<https://doi.org/10.1016/j.compositesb.2014.06.006>
- [III.22] Wang, M., Xu, X., Ji, J., Yang, Y., Shen, J., Ye, M. (2016). "The hygrothermal ageing process and mechanism of the novolac epoxy resin". *Composites Part B: Engineering*, 107, 1-8.  
<https://doi.org/10.1016/j.compositesb.2016.09.067>
- [III.23] Mikols, W.J., Seferis, J.C., Apicella, A., Nicolais, L. (1982). "Evaluation of structural changes in epoxy systems by moisture sorption-desorption and dynamic mechanical studies". *Polymer Composites*, 3(3), 118-124.  
<https://doi.org/10.1002/pc.750030304>
- [III.24] Sethi, S., Ray, B. C. (2015). "Environmental effects on fibre reinforced polymeric composites: Evolving reasons and remarks on interfacial strength and stability". *Advances in Colloid and Interface Science*, 217, 43-67.

- <https://doi.org/10.1016/j.cis.2014.12.005>
- [III.25] Rocha, I.B.C.M., Raijmaekers, S., Nijssen, R.P.L., Van der Meer, F.P., Sluys, L.J. (2017). “Hygrothermal ageing behaviour of a glass/epoxy composite used in wind turbine blades”. *Composite Structures*, 174, 110-122.  
<https://doi.org/10.1016/j.compstruct.2017.04.028>
- [III.26] Gautier, L., Mortaigne, B., Bellenger, V. (1999). “Interface damage study of hydrothermally aged glass-fibre-reinforced polyester composites”. *Composites Science and Technology*, 59(16), 2329-2337.  
[https://doi.org/10.1016/S0266-3538\(99\)00085-8](https://doi.org/10.1016/S0266-3538(99)00085-8)
- [III.27] Tsenoglou, C.J., Pavlidou, S., Papaspyrides, C.D. (2006). “Evaluation of interfacial relaxation due to water absorption in fibre–polymer composites”. *Composites science and technology*, 66(15), 2855-2864.  
<https://doi.org/10.1016/j.compscitech.2006.02.022>
- [III.28] Berens, A. R., Hopfenberg, H. B. (1978). “Diffusion and relaxation in glassy polymer powders: 2. Separation of diffusion and relaxation parameters”. *Polymer*, 19(5), 489-496.  
[https://doi.org/10.1016/0032-3861\(78\)90269-0](https://doi.org/10.1016/0032-3861(78)90269-0)
- [III.29] Zafar, A., Bertocco, F., Schjødt-Thomsen, J., Rauhe, J.C. (2012). “Investigation of the long-term effects of moisture on carbon fibre and epoxy matrix composites”. *Composites Science and Technology*, 72(6), 656-666.  
<https://doi.org/10.1016/j.compscitech.2012.01.010>
- [III.30] Pickett, J. E., Coyle, D. J. (2013). “Hydrolysis kinetics of condensation polymers under humidity ageing conditions”. *Polymer Degradation and Stability*, 98(7), 1311-1320.  
<https://doi.org/10.1016/j.polymdegradstab.2013.04.001>
- [III.31] Boinard, E., Pethrick, R. A., Dalzel-Job, J., Macfarlane, C. J. (2000). “Influence of resin chemistry on water uptake and environmental ageing in glass fibre reinforced composites-polyester and vinyl ester laminates”. *Journal of Materials Science*, 35, 1931-1937.  
<https://doi.org/10.1023/A:1004766418966>
- [III.32] Davies, P., Mazeas, F., Casari, P. (2001). “Sea water ageing of glass reinforced composites: shear behaviour and damage modelling”. *Journal of composite materials*, 35(15), 1343-1372.  
<https://doi.org/10.1106/MNBC-81UB-NF5H-P3ML>
- [III.33] Huang, G., Sun, H. (2007). “Effect of water absorption on the mechanical properties of glass/polyester composites”. *Materials & Design*, 28(5), 1647-1650.  
<https://doi.org/10.1016/j.matdes.2006.03.014>
- [III.34] Lee, S.B., Rockett, T.J., Hoffman, R.D. (1992). “Interactions of water with unsaturated polyester, vinyl ester and acrylic resins”. *Polymer*, 33(17), 3691-3697.  
[https://doi.org/10.1016/0032-3861\(92\)90657-I](https://doi.org/10.1016/0032-3861(92)90657-I)
- [III.35] Abeyasinghe, H.P., Edwards, W., Pritchard, G., Swampillai, G.J. (1982). “Degradation of crosslinked resins in water and electrolyte solutions”. *Polymer*, 23(12), 1785-1790.

[https://doi.org/10.1016/0032-3861\(82\)90123-9](https://doi.org/10.1016/0032-3861(82)90123-9)

- [III.36] Grammatikos, S.A., Evernden, M., Mitchels, J., Zafari, B., Mottram, J.T., Papanicolaou, G.C. (2016). "On the response to hygrothermal ageing of pultruded FRPs used in the civil engineering sector". *Materials & Design*, 96, 283-295.  
<https://doi.org/10.1016/j.matdes.2016.02.026>
- [III.37] Amaro, A.M., Reis, P.N.B., Neto, M.A., Louro, C. (2013). "Effects of alkaline and acid solutions on glass/epoxy composites". *Polymer Degradation and Stability*, 98(4), 853-862.  
<https://doi.org/10.1016/j.polymdegradstab.2012.12.029>
- [III.38] Stamenović, M., Putić, S., Rakin, M., Medjo, B., Čikara, D. (2011). "Effect of alkaline and acidic solutions on the tensile properties of glass-polyester pipes". *Materials & Design*, 32(4), 2456-2461.  
<https://doi.org/10.1016/j.matdes.2010.11.023>
- [III.39] Visco, A.M., Campo, N., Cianciafara, P. (2011). "Comparison of seawater absorption properties of thermoset resins based composites". *Composites Part A: Applied Science and Manufacturing*, 42(2), 123-130.  
<https://doi.org/10.1016/j.compositesa.2010.10.009>
- [III.40] Evans, K.E., Caddock, B.D., Ainsworth, K.L. (1988). "Statistical changes during the corrosion of glass fibre bundles". *Journal of Materials Science*, 23(8), 2926-2930.  
<https://doi.org/10.1007/BF00547471>
- [III.41] Chen, Y., Davalos, J.F., Ray, I., Kim, H.Y. (2007). "Accelerated ageing tests for evaluations of durability performance of FRP reinforcing bars for concrete structures". *Composite Structures*, 78(1), 101-111.  
<https://doi.org/10.1016/j.compstruct.2005.08.015>
- [III.42] French, M.A., Pritchard, G. (1992). "Environmental stress corrosion of hybrid fibre composites". *Composites Science and Technology*, 45(3), 257-263.  
[https://doi.org/10.1016/0266-3538\(92\)90087-J](https://doi.org/10.1016/0266-3538(92)90087-J)
- [III.43] Bagherpour, S., Bagheri, R., Saatchi, A. (2009). "Effects of concentrated HCl on the mechanical properties of storage aged fibre glass polyester composite". *Materials & Design*, 30(2), 271-274.  
<https://doi.org/10.1016/j.matdes.2008.04.078>
- [III.44] Pradchar, P., Aoki, S., Kubouchi, M., Sakai, T. (2015). "The Effect of Cyclic Temperature of Sulfuric Acid on Flexural Property of Matrix Resin for FRP Storage". *Journal of Chemical Engineering of Japan*, 48(8), 670-677.  
<https://doi.org/10.1252/jcej.14we320>
- [III.45] Pradchar, P., Aoki, S., Kubouchi, M., Sakai, T. (2013). "The Effect of Cyclic Water Temperature on Flexural Property of Unsaturated Polyester Resin Under Liquid and Vapor Phase". In the Proceedings of: ICCM19, (pp.1644-1652), Montreal.
- [III.46] Nishizaki, I., Meiarashi, S. (2002). "Long-term deterioration of GFRP in water and moist

- environment". *Journal of Composites for Construction*, 6(1), 21-27.  
[https://doi.org/10.1061/\(ASCE\)1090-0268\(2002\)6:1\(21\)](https://doi.org/10.1061/(ASCE)1090-0268(2002)6:1(21))
- [III.47] Bazli, M., Ashrafi, H., Oskouei, A.V. (2016). "Effect of harsh environments on mechanical properties of GFRP pultruded profiles". *Composites Part B: Engineering*, 99, 203-215.  
<https://doi.org/10.1016/j.compositesb.2016.06.019>
- [III.48] Sonawala, S.P., Spontak, R.J. (1996). "Degradation kinetics of glass-reinforced polyesters in chemical environments: Part I Aqueous solutions". *Journal of Materials Science*, 31, 4745-4756.  
<https://doi.org/10.1007/BF00355857>
- [III.49] Feng, P., Wang, J., Wang, Y., Loughery, D., Niu, D. (2014). "Effects of corrosive environments on properties of pultruded GFRP plates". *Composites Part B: Engineering*, 67, 427-433.  
<https://doi.org/10.1016/j.compositesb.2014.08.021>
- [III.50] Gentry, T.R., Bank, L.C., Barkatt, A., Prian, L. (1998). "Accelerated test methods to determine the long-term behaviour of composite highway structures subject to environmental loading". *Journal of Composites Technology & Research*, 20(1), 38-50.  
<https://doi.org/10.1520/CTR10499J>
- [III.51] Cordeiro, G. C., Vieira, J. D., C6, C. M. (2016). "Tensile properties and colour and mass variations of GFPR composites under alkaline and ultraviolet exposures". *Mat6ria (Rio de Janeiro)*, 21(1), 1-10.  
<https://doi.org/10.1590/S1517-707620160001.0001>
- [III.52] Bank, L.C., Gentry, T.R., Barkatt, A. (1995). "Accelerated test methods to determine the long-term behaviour of FRP composite structures: environmental effects". *Journal of Reinforced Plastics and Composites*, 14(6), 559-587.  
<https://doi.org/10.1177/073168449501400602>
- [III.53] International Organization for Standardization (2010) "Plastics – Methods of test for the determination of the effects of immersion in liquid chemicals", ISO 715:2010.
- [III.54] ASTM International (2014) "Standard Practices For Evaluating The Resistance Of Plastics To Chemical Reagents". ASTM D543-14, West Conshohocken, Pennsylvania, USA.
- [III.55] Davis, A., Sims, D. (1983). "Weathering of polymers". Applied Science Publishers, London, 1983.
- [III.56] Jian, S.Z., Lucki, J., Rabek, J.F., Ranby, B. (1985). "Photooxidation and photostabilisation of unsaturated cross-linked polyesters". ACS Symposium Series, Proceedings of the 187th Meeting of the American Chemical Society.
- [III.57] Chin, J.W., Martin, J., Nguyen, T. (2001). "Chapter 8: Effects of Ultraviolet (UV) Radiation" In: *Gap Analysis for Durability of Fibre Reinforced Polymer Composites in Civil Infrastructure* (pp. 80-99), American Society of Civil Engineers, Virginia.  
[https://doi.org/10.1061/\(ASCE\)1090-0268\(2003\)7:3\(238\)](https://doi.org/10.1061/(ASCE)1090-0268(2003)7:3(238))
- [III.58] Busel, J.P., Lockwood, J.D. (2000). "Product selection guide: FRP composite products for

- bridge applications”. Market Development Alliance FRP Composites Industry (pp. 122-157), Harrison, New York.
- [III.59] Searle, N.D. (2003). “Chapter 8: Environmental Effects on Polymeric Materials”. In Andradý A.L., editor: *Plastics and the Environment*, pp. 313-358. John Wiley & Sons, New York.  
<https://doi.org/10.1002/0471721557.ch8>
- [III.60] Kaczmarek, H. (2002). “Changes in polymer morphology caused by U.V. irradiation, 1. Surface damage”. *Polymer*, 37(2), 189-94.  
[https://doi.org/10.1016/0032-3861\(96\)81086-X](https://doi.org/10.1016/0032-3861(96)81086-X)
- [III.61] Juska, T., Dutta, P., Carlson, L., and Weitsman, J. (2001). “Chapter 5 - Thermal Effects”. In: *Gap Analysis for Durability of Fibre Reinforced Polymer Composites in Civil Infrastructure* (pp. 40-51). American Society of Civil Engineers, Virginia.  
[https://doi.org/10.1061/\(ASCE\)1090-0268\(2003\)7:3\(238\)](https://doi.org/10.1061/(ASCE)1090-0268(2003)7:3(238))
- [III.62] Karbhari, V.M. (2007). “Chapter 4: Durability of composites in sub-zero and freeze-thaw conditions.” In: *Durability of Composites for Civil Structural Applications*, pp. 72-79, Woodhead Publishing, Sawston.  
<https://doi.org/10.1533/9781845693565.1.72>
- [III.63] Garrido, M., Sousa, J. M., Correia, J. R., Cabral-Fonseca, S. (2022). “Prediction of long-term performance and definition of a moisture conversion factor for the durability design of pultruded GFRP profiles under hygrothermal exposure”. *Construction and Building Materials*, 326, 126856.  
<https://doi.org/10.1016/j.conbuildmat.2022.126856>
- [III.64] Sousa, J. M., Garrido, M., Correia, J. R., Cabral-Fonseca, S. (2021). “Hygrothermal ageing of pultruded GFRP profiles: Comparative study of unsaturated polyester and vinyl ester resin matrices”. *Composites Part A: Applied Science and Manufacturing*, 140, 106193.  
<https://doi.org/10.1016/j.compositesa.2020.106193>
- [III.65] Correia, J. R., Keller, T., Garrido, M., Sá, M., Firmo, J. P., Shahid, M. A., Machado, M. (2023). “Mechanical properties of FRP materials at elevated temperature-Definition of a temperature conversion factor for design in service conditions”. *Construction and Building Materials*, 367, 130298.  
<https://doi.org/10.1016/j.conbuildmat.2023.130298>
- [III.66] Dutta, P. K. (1988). “Structural fibre composite materials for cold regions”. *Journal of Cold Regions Engineering*, 2(3), 124-134.  
[https://doi.org/10.1061/\(ASCE\)0887-381X\(1988\)2:3\(124\)](https://doi.org/10.1061/(ASCE)0887-381X(1988)2:3(124))
- [III.67] Dutta, P. K., Hui, D. (1996). “Low-temperature and freeze-thaw durability of thick composites”. *Composites Part B: Engineering*, 27(3-4), 371-379.  
[https://doi.org/10.1016/1359-8368\(96\)00007-8](https://doi.org/10.1016/1359-8368(96)00007-8)
- [III.68] Sapi, Z., Butler, R. (2020). “Properties of cryogenic and low temperature composite materials-a review”. *Cryogenics*, 111, 103190.

- <https://doi.org/10.1016/j.cryogenics.2020.103190>
- [III.69] Sousa, J.M., Correia, J.R., Cabral-Fonseca, S., Diogo, A.C. (2014). “Effects of thermal cycles on the mechanical response of pultruded GFRP profiles used in civil engineering applications”. *Composite Structures*, 116, 720-731.  
<https://doi.org/10.1016/j.compstruct.2014.06.008>
- [III.70] Grammatikos, S.A., Jones, R.G., Evernden, M., Correia, J.R. (2016). “Thermal cycling effects on the durability of a pultruded GFRP material for off-shore civil engineering structures”. *Composite Structures*, 153, 297-310.  
<https://doi.org/10.1016/j.compstruct.2016.05.085>
- [III.71] Sgnor, A.W., VanLandingham, M.R., Chin, J.W. (2003). “Effects of ultraviolet radiation exposure on vinylester resins: characterization of chemical, physical and mechanical damage”. *Polymer Degradation and Stability*, 79(2), 359-368.  
[https://doi.org/10.1016/S0141-3910\(02\)00300-2](https://doi.org/10.1016/S0141-3910(02)00300-2)
- [III.72] Bogner, B.R., Borja, P.P. (1994). “Ultraviolet Light Resistance of Pultruded Composites”. In the proceedings of EPTA 1994 - Conference Proceedings, European Pultrusion Technology Association, Venice.
- [III.73] Segovia, F., Ferrer, C., Salvador, M.D., Amigó, V. (2001). “Influence of processing variables on mechanical characteristics of sunlight aged polyester-glass fibre composites”. *Polymer Degradation and Stability*, 71(1), 179-184.  
[https://doi.org/10.1016/S0141-3910\(00\)00168-3](https://doi.org/10.1016/S0141-3910(00)00168-3)
- [III.74] Cabral-Fonseca, S., Correia, J.R., Rodrigues, M.P., Branco F.A. (2012). “Artificial accelerated ageing of GFRP pultruded profiles made of polyester and vinylester resins: Characterisation of physical-chemical and mechanical damage”. *Strain*, 48 (2), 162-173.  
<https://doi.org/10.1111/j.1475-1305.2011.00810.x>
- [III.75] Nishizaki, I., Sakuraba, H., Tomiyama, T. (2015). “Durability of Pultruded GFRP through Ten-Year Outdoor Exposure Test”. *Polymers*, 7(12), 2494-2503.  
<https://doi.org/10.3390/polym7121525>
- [III.76] Sousa, J., Correia, J.R., Cabral-Fonseca, S. (2016). “Durability of Glass Fibre Reinforced Polymer Pultruded Profiles: Comparison Between QUV Accelerated Exposure and Natural Weathering in a Mediterranean Climate”. *Experimental Techniques*, 40, 207-219.  
<https://doi.org/10.1007/s40799-016-0024-x>
- [III.77] Klamer, E., Tromp, L., de Boer, A., Nijssen, R. (2015). “Long-term effects of wet and outdoor conditions on GFRP”. In IABSE Symposium Report (Vol. 105, No. 14, pp. 1-8), Geneva, Switzerland.
- [III.78] Keller, T., Theodorou, N., Vassilopoulos, A., Castro, J. (2015). “Effect of natural weathering on durability of pultruded glass fibre-reinforced bridge and building structures”. *Journal of Composites for Construction*, 20(1), pp. 04015025-1, 9.  
[https://doi.org/10.1061/\(ASCE\)CC.1943-5614.0000589](https://doi.org/10.1061/(ASCE)CC.1943-5614.0000589)

- [III.79] Sauvola, J., Pietikäinen, M. (2000) “Adaptive document image binarization”. *Pattern Recognition*, 33(2), 225-236.  
[https://doi.org/10.1016/S0031-3203\(99\)00055-2](https://doi.org/10.1016/S0031-3203(99)00055-2)
- [III.80] M. Garrido, J.R. Correia, J. Sena-Cruz (2022), “Background report to paragraph 4.4.7.3(1) to CEN/TS 19101: 2022”. March 2022 (unpublished).

# **Part IV**

Conclusions and future developments



## **15. Conclusions and future developments**

### **15.1. Preliminary remarks**

In recent years, the durability of composite structures used in Civil Engineering applications has become increasingly important, and it is expected that such interest in composite materials will continue to increase. However, there is a growing need to understand in further depth and develop solutions to expand the durability and long-term performance of composite materials. Therefore, the main objective of this investigation was to develop an inspection and diagnosis system to support decision-making activities regarding design and maintenance operations, and to study the durability of GFRP components exposed to different environmental conditions. This chapter presents the main conclusions obtained in this study and provides suggestions for future developments.

### **15.2. Conclusions**

#### **15.2.1. Inspection, diagnosis and rehabilitation system**

Inspection and maintenance activities are crucial in Civil Engineering to ensure the long-term durability of construction facilities. Therefore, diagnosis and inspection systems play a key role in different types of structural members and non-structural elements. These systems must adhere to basic requirements to guarantee an adequate use. In this investigation, these requirements include safety, functionality, durability, economics, and other considerations, which aim at ensuring that GFRP constructions maintain satisfactory performance throughout their service life.

The proposed system, presented in part II, consists of four groups: anomalies, probable causes, diagnosis methods, and rehabilitation techniques, complemented with several forms that include all the necessary information. Each group has a classification system to facilitate the application of the system and to assist in the inspection of existing structures, but it can also be used in the design of new GFRP constructions and the rehabilitation of existing ones. The list of anomalies considered was based on the visual aspect each anomaly presented and they were divided into mechanical and non-mechanical. The system also classified the probable causes, into the following groups: production, project/design, installation, and in-service. Correlation matrices were developed to associate anomalies to causes, anomalies to other anomalies, anomalies to diagnosis techniques, and anomalies to rehabilitation techniques.

The anomalies detected during inspection must be assessed with an appropriate diagnosis technique to determine the exact cause and extent, considering multiple factors from the design stage until in-service exposure. Rehabilitation techniques might be applied as a corrective or preventive measure depending on the anomaly and, in some cases, the substitution of affected elements may be the most suitable alternative.

The validation of the inspection system for GFRP substructures showed that the system is effective in detecting and classifying anomalies, determining causes, and allocating appropriate diagnosis and rehabilitation techniques. The inspection forms were comprehensive and included important information to describe the substructures and compare them among different inspections.

The analysis was based on the inspection of 31 infrastructures that contained 410 GFRP substructures. Apart from validating the system, the inspection campaign intended to identify the most common anomalies found in GFRP constructions during their use stage. It was revealed that, of the 1780 anomalies detected, the non-mechanical anomalies were more prevalent than the mechanical ones, with A.N-Me.02 (discolouration/loss of gloss), A.N-Me.05 (stains), and A.N-Me.03 (fibre blooming) being the most common non-mechanical anomalies, while A.Me.01 (corrosion of metallic components) and A.Me.08 (indentations/perforations) were the most common mechanical anomalies.

Results obtained show that the environmental conditions have a significant impact on the anomalies detected during the service stage, with the location of the structure (indoor or outdoor), chemical aggressiveness of the environment, and exposure to UV radiation being the main conditioning factors. The probable causes associated with the anomalies were found to be related to the in-service and design stages, due to the lack of knowledge and guidance on the proper design and detailing of GFRP structures in view of their long-term behaviour.

Visual inspection was found to be the most effective technique for diagnosing anomalies, with most of them being easily detected by the naked eye. During the inspections, it was found that most structures lacked continuous maintenance to prevent the occurrence of some anomalies and the rehabilitation of GFRP elements to reduce the detection of the most common anomalies, including biological colonization, fibre blooming, and discolouration.

### **15.2.2. Exposure of GFRP composites to chemical environments**

The experimental campaign studying the effects on pultruded GFRP materials when exposed to chemical environments, presented in the beginning of part III, whether alkaline or acidic, is influenced by several variables such as the type of fibre, resin, chemical exposure, solution concentration, and the duration and temperature of exposure.

The study developed in this thesis intended to determine the effect of chemical exposure on GFRP elements with two alternative resins, polyester (UP) and vinylester (VE). Both GFRP composites were exposed to three chemical conditions (neutral, acidic and alkaline), two types of exposure (immersion and vapour), three temperatures (23, 50 and 70 °C), and four different durations (1, 4, 8 and 16 weeks).

The results of the experimental study show that, after exposure to those conditions, the materials exhibited visual surface changes (such as cracking and swelling) and signs of degradation in mechanical performance, which were more pronounced with higher temperatures and longer periods of exposure.

The UP material showed more significant colour changes in alkaline environments, while the VE material was more susceptible to overall colour changes. Gloss changes were also observed, with a progressive transition from a glossy to a matte surface finish, most noticeably at the beginning of the exposure to alkaline environments.

The results show that immersion in water and acidic solutions did not significantly affect the performance of both materials at the reference temperature of 23 °C. Still, immersion in alkaline environments caused extensive degradation, especially for longer exposure periods. The UP material

suffered a more significant reduction in mechanical performance than the VE material.

Increasing temperature had a significant effect on accelerating the degradation of the mechanical properties, especially for longer exposure periods. This effect was more pronounced in alkaline environments, where a complete loss of mechanical strength was observed (for all types of loading) for UP specimens after 16 weeks of exposure at both 50 °C and 70 °C.

Exposure to water vapour was the most conditioning among the three vapour environments and, in most cases, it resulted in a higher reduction compared to water immersion. For vapour exposure, the use of a surface protection coating was also investigated, but the results obtained were not consistent, not allowing to draw clear conclusions about their effectiveness.

In general, the UP material performed better in the water environment, the VE material performed better in the alkaline environment, and both materials performed similarly in the acidic environment. These findings highlight the importance of material selection during the design stage, considering the type of in-service chemical exposure. Further investigation is required to develop degradation models that simulate the long-term reduction in mechanical properties and to explore a broader range of temperatures and concentrations of chemicals.

### **15.2.3. Exposure of GFRP composites to weathering**

The research about the weathering effects on pultruded GFRP elements, presented in chapter 13 of part III, focused on the impact of natural weathering (NW, up to 20 months), accelerated weathering in QUV chamber (up to 6000 hours) and natural weathering in-service conditions (up to approximately 20 years). Weathering includes exposure of GFRP elements to a range of environmental effects, including temperature, moisture and UV radiation, acting alone or in combination.

The experimental tests showed that VE specimens exhibited a greater change in colour than UP specimens, and this colour change was significant even for very short exposure periods. The colour changes in VE specimens appeared to stabilize after the initial change, while the UP specimens exhibited a more gradual change in colour, peaking at around 1250 hours and then stabilizing. The addition of UV additive absorbers and surface veil did not affect the colour change. Longer exposure periods resulted in a different behaviour in VE specimens with surface veil compared to those without surface veil.

When UP specimens were exposed to QUV, after 2000 hours, the gloss became negligible and then remained constant for the rest of the exposure period. Similarly, in VE specimens exposed to QUV, after 1000 hours of exposure, the gloss became negligible and then remained unchanged for the rest of the exposure period. For both materials, the exposure times associated with greater loss of gloss coincided with those corresponding to the greatest variation in colour. For UP specimens, 20 months of NW exposure caused similar loss of gloss to 2000 hours of QUV exposure. For VE specimens, after 10 months of NW exposure, the loss of gloss was similar to that caused by 1000 hours in QUV.

Regarding the mechanical properties of UP and VE specimens exposed to QUV accelerated weathering for 6000 hours, the results obtained show that: (i) the use of UV stabilizer additive consistently provided higher retention of mechanical properties for UP specimens; (ii) VE specimens had better overall UV weathering resistance compared to UP specimens; (iii) the use of surface veil did

not have a significant effect on strength retention for most test series, but for compression it had a detrimental effect on strength retention in specimens without UV additive (no clear reasons could be identified to justify this result); and (iv) the use of superficial protection did not have a clear influence on the strength retention.

The effects of NW on the mechanical properties of UP and VE specimens after 10 and 20 months of exposure showed (confirmed) that the VE specimens had better overall weathering resistance compared to UP specimens. The use of UV stabilizer additive and a surface protection coating improved the retention of mechanical properties but had different effects depending on the type of test. The use of surface veil had a varying effect on the retention of mechanical properties. In compression, there was a higher overall property reduction, with the maximum property decay occurring in specimens with veil and superficial protection. For both UP and VE specimens, in general, the reductions of in-plane shear and compressive strengths after 6000 hours of QUV accelerated weathering were comparable to those after 10 months of NW. However, due to the short duration of the NW exposure, the relevance of these findings is limited, and additional results for longer periods of exposure are needed.

In order to complement the investigation presented above and the results obtained in Part II, an additional field survey was carried out, which focused on some of the older in-service pultruded GFRP structures built in Portugal. The specimens were collected from three case studies: the 25<sup>th</sup> of April Bridge, the Colombo shopping Centre, and the Lisbon Oceanarium. The results indicated that the mechanical properties of the GFRP profiles applied in those case studies were only moderately affected by environmental exposure, with some variations observed between the specimens collected from each location. The specimens collected from the 25<sup>th</sup> of April Bridge showed a slight increase in strength, while those from the Colombo Centre exhibited a slight to moderate reduction in strength- and stiffness-related properties. The Oceanarium specimens showed a low to moderate reduction in most strength-related properties. The variation in mechanical properties measured in these three constructions seems to support the moisture conversion factors defined in the recent European Technical Specification CEN/TS 19101.

These results provide valuable insights about the long-term durability of pultruded GFRP materials, although further research is required to determine the underlying causes of changes in mechanical properties and to predict the service life of FRP composite structures.

### **15.3. Future developments**

The thesis comprised field inspections, data analysis, and experimental studies that contributed to a more comprehensive understanding of the in-service performance and durability of pultruded GFRP elements when exposed to various environmental agents. However, some aspects of the research may require further investigation. These specific aspects are presented in the subsequent paragraphs.

Regarding the inspection, diagnosis, and rehabilitation system proposed, for a further validation of the information provided in this work, it is recommended to conduct further studies and apply the diagnosis and rehabilitation techniques described here in-situ, namely to other types of facilities and locations. Specialized companies could be contacted for this purpose, to monitor not only the application

of the rehabilitation techniques, but also the results obtained (diagnosis) and their performance in the medium-to-long term. In this way, the costs associated with each operation could be assessed more accurately, leading to a more precise analysis of the life cycle cost of FRP constructions and more accurate proactive maintenance plans.

It would be useful to develop an inspection, diagnosis, and rehabilitation software for FRP constructions that could be used on laptop computer devices. By aggregating photos, inspection reports, diagnosis, and rehabilitation information, this software would enable an unskilled person to perform valid inspections of various FRP constructions, with instant access to estimates of material costs, labour, and degree of required specialization. This would allow the end-user to easily understand the cost of rehabilitation *versus* the cost of replacement offered by a company in the sector.

To increase the sample size at a national level, and if possible, at an international level, it is necessary to include a greater quantity of FRP constructions, constructive systems, exposure environments, materials, and applicability of superficial coatings.

The durability study of pultruded components is complex, and material properties can vary significantly between manufacturers. To fully understand the long-term effects of these materials, it would be helpful to explore materials produced by a variety of suppliers and compare the results to those already available; such a study would require knowing, in detail, the physical (e.g. water absorption, void content), thermo-mechanical (e.g.  $T_g$ ) and mechanical properties of those materials. By doing so, it would be possible to build a more comprehensive database of information on this subject and make a more accurate assessment of the factors that influence material performance over time. Investigating alternative combinations of fibre architectures, polymeric resins, and reinforcing fibres could also be useful to gain a deeper understanding of the parameters that affect material durability. The same applies to the study of other properties besides those investigated herein. Altogether, this would allow obtaining a more comprehensive understanding of the long-term durability of pultruded FRP composites and to develop more effective prediction tools and strategies for using these materials in a wider range of applications.

The study of sustainability and life cycle assessment (LCA) is also necessary to increase the competitiveness of FRP solutions compared to traditional structural applications. Further research on these subjects is needed, including LCA from cradle to cradle for several GFRP constructions and service life periods, comparing them with conventional solutions.

The study of GFRP elements exposed to chemical environments has the potential to be further investigated through the development of degradation models that consider the reduction in mechanical properties and a wider range of temperatures and concentrations of different chemicals. Furthermore, it is necessary to clarify the inconsistent results obtained from the use of superficial coating protection in the vapour phase by applying different superficial protections, such as vapour barrier protections.

Additionally, there is a need to examine the long-term performance of GFRP materials exposed to chemical environments. The current study only investigated exposure periods of up to 16 weeks, so investigating longer exposure periods would provide further insights into the lifespan and maintenance requirements of GFRP elements in different chemical environments, enabling better-informed material

selection during the design stage. Moreover, the accelerated conditions used in the experiments should be compared to situations of real exposure to the same types of chemicals, for instance in waste water treatment plants. This would also allow assessing the procedures used in accelerated tests.

Regarding the weathering effect on GFRP elements, future research should explore the impact of other environmental factors, such as moisture, freeze and thaw cycles, polluting agents, and wind, on the durability of these materials. It is also important to investigate the effects of weathering on GFRP elements in additional real applications under in-service conditions, as the ones presented in section 13.4. This would provide valuable information on the long-term performance of GFRP elements and could lead to updates in maintenance and replacement schedules. Different outdoor ageing conditions and climates should also be considered, such as tropical, dry and alpine climates, and longer periods of exposure than those previously studied would be of great value.

Finally, future research could focus on developing new materials or improving existing ones to enhance the durability and resistance of GFRP elements to chemical exposure and weathering. This could involve exploring alternative resins or fibres, as well as investigating the effectiveness of different surface treatments and coatings in protecting GFRP elements from environmental degradation.

# Appendix



## **Appendix list**

Appendix I - Anomaly forms

Appendix II - Diagnosis forms

Appendix III - Rehabilitation forms

Appendix IV - Inspection form

Appendix V - Validation form

Appendix VI - Technical sheets

Appendix VII - Experimental data



**Appendix I**  
Anomaly forms

With the information gathered (anomalies, causes, consequences, diagnosis and rehabilitation techniques) it is now possible to create an individual form for each anomaly.

These forms are an essential tool for the development of the inspection system, as they summarize much of the information studied for each component of the inspection system. For this reason, they should be an integral part of the inspection manual and are indispensable in the inspections of the case studies.

Each anomaly form contains the following information:

- (i) a generic picture of the anomaly;
- (ii) a brief description of the anomaly;
- (iii) possible causes of the anomaly;
- (iv) possible consequences of the appearance/development of the anomaly;
- (v) details to be inspected (characteristics related to the detected anomaly that may be relevant to the diagnosis);
- (vi) inspection methods that can be performed in situ (in order to further characterize the anomaly in terms of extent, severity and stage of evolution);
- (vii) rehabilitation techniques to eliminate the anomaly and/or its causes;
- (viii) classification parameters of the anomaly (which may be the result of tests carried out and that allow assessing the severity level of the anomaly); and
- (ix) severity level/repair emergency, which was defined to vary between 0 and 4:
  - 0 - Not concerning severity level, and the evolution of the anomaly must be monitored;
  - 1 - Medium-to-low level of concern, and the evolution of the anomaly must be monitored;
  - 2 - Needs medium-term intervention in up to one year;
  - 3 - Medium-to-high level of concern, with a need for intervention in up to six months; and
  - 4 - High level of concern with a need for immediate intervention in up to three months.

For some anomalies, the EN 13706-02<sup>1</sup>, presents some conditions that pultruded profiles must present in order to be considered acceptable for structural applications. These requirements are highlighted in blue in the anomaly forms.

---

<sup>1</sup> CEN (2002). "Reinforced plastic composites - Specifications for pultruded profiles - Part 2: Methods of test and general requirements", EN 13706-2. Brussels, Belgium: European Committee for Standardization.

## **NON-MECHANICAL ANOMALIES**

# ANOMALY FORM - A.N-ME.01

## ANOMALY NAME

**Biological colonization**

## ANOMALY DESCRIPTION

This anomaly consists of the appearance of biological matter (plants, fungi, animals) on the surface of FRP elements. It usually occurs in areas with high humidity or permanently immersed, and in constructions with lack of maintenance.



## POSSIBLE CAUSES

- Lack of surface coating (C.D.03)
- High humidity environment condition (C.S.01)
- Permanently wet environmental condition (C.S.01)
- Exposure to UV radiation (C.S.02)
- Lack of maintenance (C.S.06)

## POSSIBLE CONSEQUENCES

- Aesthetical appearance
- Increase of water retention
- Reduction of mechanical properties (due to moisture exposure)

## DETAILS TO INSPECT

- Affected area
- Source of water/humidity
- Exposure to UV radiation

## INSPECTION METHODS

- Visual inspection (I.01)
- Infrared thermography (I.04)
- Moisture meter (I.06)

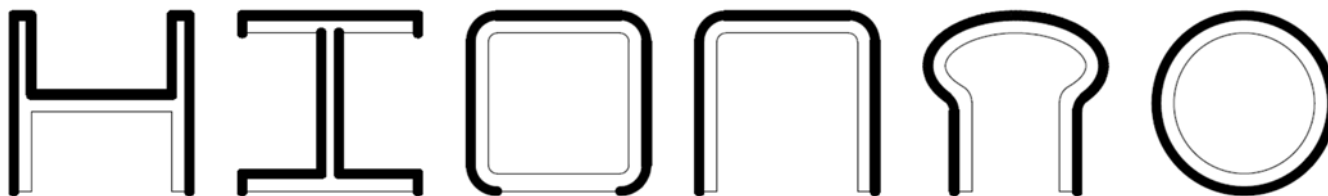
## REHABILITATION TECHNIQUES

- Application of superficial coating (water repellent coating) (R.03)
- Superficial cleaning (R.04)

## CLASSIFICATION PARAMETERS

- Conditions for progression of the anomaly (Y/N)
- Aesthetical significance of the element
- Superficial area affected ( $A_f$  (%) = Area with biological colonization/superficial and outer exposed area of 1 meter of profile  $\times$  100)

The considered superficial and outer exposed area is suggested in the diagrams below, for some of the most common types of profiles. The areas in bold are the most commonly exposed to solar radiation on a horizontal profile; as such, they are where occurrence of biological colonization is most probable.



## SEVERITY LEVEL / REPAIR EMERGENCY

- 0 – Small biological colonization ( $A_f < 20\%$ )
- 1 – Biological colonization ( $A_f \geq 20\%$ ) and/or high aesthetical significance of the element
- 2 –
- 3 –
- 4 –

# ANOMALY FORM - A.N-ME.02

## ANOMALY NAME

**Discoloration / Loss of gloss**

## ANOMALY DESCRIPTION

This anomaly is related with the degradation of the surface layer of the polymeric matrix (or a surface coat), causing a change of colour and brightness at the surface of the element. Even though it is usually associated with exposure of the elements to solar radiation, it may also occur when the elements are exposed to wet and dry cycles, permanent immersion and/or exposure to saline or chemical environments.



## POSSIBLE CAUSES

- Improper cure of resin (C.P.01)
- Improper quality/mixture/formulation of resin (C.P.03)
- Lack of UV additives (C.D.03)
- Excessive wet/dry cycles (C.S.01)
- Permanently wet environmental condition (C.S.01)
- Exposure to UV radiation (C.S.02)
- Exposure to chemical environments (C.S.03)
- Exposure to saline environments (C.S.03)

## POSSIBLE CONSEQUENCES

- Aesthetical appearance
- Reduction of mechanical properties (due to moisture exposure/UV radiation)
- Reduction of mechanical properties (due to improper curing of resin)

## DETAILS TO INSPECT

- Affected area
- Degradation of remaining protective resin
- Type of environmental exposure

## INSPECTION METHODS

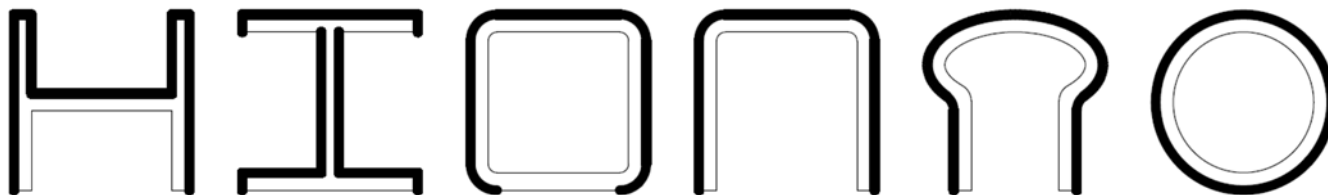
- Visual inspection (I.01)
- Barcol Hardness (I.03)

## REHABILITATION TECHNIQUES

- Application of superficial coating (e.g. varnish/enamel) (R.03)

## CLASSIFICATION PARAMETERS

- Aesthetical significance of the element
  - Loss of gloss due to improper cure of resin (Y/N)
  - Superficial area affected ( $A_g$  (%) = Area with loss of gloss / superficial and outer exposed area of 1 meter of profile  $\times$  100)
- The considered superficial and outer exposed area is suggested in the diagrams below, for some of the most common types of profiles. The areas in bold are the most commonly exposed to solar radiation on a horizontal profile; as such, they are where occurrence of biological colonization is most probable.



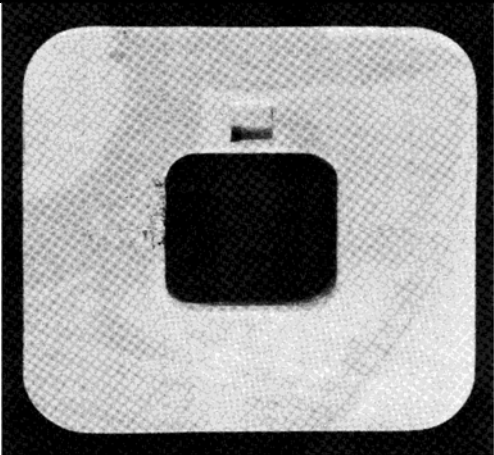
## SEVERITY LEVEL / REPAIR EMERGENCY

- 0 – Superficial affected area ( $A_g < 50\%$ )
- 1 – Superficial affected area ( $A_g \geq 50\%$ ) and/or high aesthetical significance of the element
- 2 –
- 3 – Loss of gloss due to improper cure of resin
- 4 –

# ANOMALY FORM - A.N-ME.03

ANOMALY NAME		
<b>Fibre blooming</b>		
ANOMALY DESCRIPTION		
<p>The fibre blooming phenomenon consists of the appearance at the elements' surface of the outmost fibres of the cross-section (closer to the surface), caused by the degradation of the surface layer of the polymer matrix. This anomaly is usually associated with exposure to UV radiation or chemically aggressive environments</p>		
POSSIBLE CAUSES		
- Incorrect layout of fibres/mats (C.P.06)		
- Inadequate material selection (C.D.02)		
- Lack of surface veil (C.D.03)		
- Lack of UV additives (C.D.03)		
- Lack of surface coating (C.D.03)		
- Exposure to UV radiation (C.S.02)		
- Exposure to chemical environments (C.S.03)		
POSSIBLE CONSEQUENCES		
- Direct exposure of superficial fibres to the environmental conditions		
- Easier ingress of environmental agents into the bulk of the laminate		
- Discomfort and lack of safety in use for certain applications (e.g. handrails)		
- Aesthetical appearance		
DETAILS TO INSPECT		
- Affected area		
- Existence of surface fibres		
- Existence of protective coating		
- Exposure to UV radiation		
- Location of the element on the structure		
INSPECTION METHODS		
- Visual inspection (I.01)		
REHABILITATION TECHNIQUES		
- Application of surface coating (e.g. enamel, paint, varnish) (R.03)		
- Replacement of affected element (R.05)		
CLASSIFICATION PARAMETERS		
- Area with exposed fibres ( $A_f(\%) = \text{Area with exposed fibres} / \text{superficial exposed area of 1 meter of profile} \times 100$ )		
- Element in possible contact with users (Y/N)		
- Aesthetical significance of the element		
SEVERITY LEVEL / REPAIR EMERGENCY		
0 - $A_f < 30\%$		
1 - $A_f \geq 30\%$ and the element is not in possible contact with users and/or high aesthetical significance of the element		
2 - $A_f > 85\%$ and the element is not in possible contact with users		
3 - $A_f > 85\%$ and the element is in possible contact with users		
4 -		

# ANOMALY FORM - A.N-ME.04

ANOMALY NAME	
<b>Inclusion</b>	
ANOMALY DESCRIPTION	
<p>This anomaly, which in practice can only be traced during the production stage, consists of the inclusion of an anomalous material inside the cross-section of the FRP composite, namely in the bulk of the material.</p>	
POSSIBLE CAUSES	
- Improper maintenance of the pultrusion equipment (C.P.05)	
- Improper cleaning of the pultrusion equipment (C.P.05)	
- Improper isolation of the pultrusion equipment (C.P.05)	
POSSIBLE CONSEQUENCES	
- Reduction of mechanical properties	
DETAILS TO INSPECT	
- Size of inclusion	
- Location on the laminate	
INSPECTION METHODS	
- Thermography (I.04)	
- Ultrasonic (I.05)	
REHABILITATION TECHNIQUES	
- Removal of affected element (R.05)	
CLASSIFICATION PARAMETERS	
- Dimension of inclusions (mm)	
- Location on the pultruded profile cross-section	
SEVERITY LEVEL / REPAIR EMERGENCY	
0 - Inclusion inferior to 5 mm in any direction	
1 - Inclusion inferior to 5 mm in any direction and at the surface of the element	
2 - Inclusion superior to 5 mm in any direction and at the surface of the element; more than one inclusion per meter	
3 -	
4 -	

# ANOMALY FORM - A.N-ME.05

<b>ANOMALY NAME</b>	
Stains	
<b>ANOMALY DESCRIPTION</b>	
<p>This anomaly consists of spots/stains on the surface of the FRP component. It can be related with several factors, either concerning singular events (e.g. accidental spills, vandalism) or continuous exposure to an aggressive environment (e.g. water accumulation, nuts/bolts oxidation).</p>	
<b>POSSIBLE CAUSES</b>	
- High humidity environment (C.S.01)	
- Permanently wet environmental condition (C.S.01)	
- Unprotected bolted connection (C.S04)	
- Accidental impact (C.S.05)	
- Vandalism (C.S.05)	
- Use Wear (C.S.05)	
- Change of use or improper use (C.S.05)	
- Lack of maintenance (C.S.06)	
<b>POSSIBLE CONSEQUENCES</b>	
- Discoloration of the profile	
- Reduction of mechanical properties	
- Deterioration of the protective resin	
- Promotes biological colonization	
- Aesthetical appearance	
<b>DETAILS TO INSPECT</b>	
- Stained area	
- Stain depth	
- Origin of stain	
<b>INSPECTION METHODS</b>	
- Visual inspection (I.01)	
- Thermography (I.04)	
- Ultrasonic (I.05)	
- Moisture meter (I.06)	
<b>REHABILITATION TECHNIQUES</b>	
- Application of surface coating (e.g. enamel, paint, varnish) (R.03)	
- Superficial cleaning (R.04)	
- Replacement of affected element (R.05)	
- Protection of bolted connection (R.06)	
<b>CLASSIFICATION PARAMETERS</b>	
- The progression of the stain is stabilized (Y/N)	
- Aesthetical significance of the element	
<b>SEVERITY LEVEL / REPAIR EMERGENCY</b>	
0 - Progression of the stain stabilized and/or low aesthetical significance of the element	
1 - Progression of the stain not stabilized and/or high aesthetical significance of the element	
2 -	
3 -	
4 -	

# ANOMALY FORM - A.N-ME.06

<b>ANOMALY NAME</b>	
<b>Superficial Marks</b>	
<b>ANOMALY DESCRIPTION</b>	
<p>This anomaly comprises eight distinct anomalous situations: blisters, craters, saw burns, scaling, grooving, scratches, stop/pull marks, die parting lines and wrinkle depressions. Even though these anomalies have different characteristics, they have a similar visual appearance, namely by revealing themselves as small irregularities at the elements' surface.</p>	
<b>POSSIBLE CAUSES</b>	
- Incorrect cure conditions of the resin (temperature, humidity, duration) (C.P.01)	
- Improper quality of resin (C.P.03)	- Incorrect layout of fibres/mats (C.P.06)
- Improper mixture of resin components (C.P.03)	- Incorrect positioning of die metallic parts (C.P.07)
- Dripped resin (C.P.04)	- Improper handling of profiles (C.P.08)
- Surface of small air bubbles (C.P.04)	- Improper cutting tool (C.P.08)
- Improper maintenance of the pultrusion equipment (C.P.05)	- Incorrect installation (C.I.01)
- Improper cleaning of the pultrusion equipment (C.P.05)	- Use wear (C.S.05)
- Improper isolation of the pultrusion equipment (C.P.05)	- Change of use or improper use (C.S.05)
<b>POSSIBLE CONSEQUENCES</b>	
- Exposure of fibres to the environmental conditions	
- Deterioration of the protective resin	
- More aggressive exposure to environmental agents (easier ingress of moisture)	
- Aesthetical appearance	
<b>DETAILS TO INSPECT</b>	
Blisters – Size of blister not greater than 15% of width and not greater than 10mm in any direction. No more than 1 per 5m of length	
Crater – Size of crater not greater than 5 mm of diameter and 1 mm in depth. No more than 2 per meter of length for craters between 1 and 5mm.	
Die parting line – the line projection caused by the die parting line shall not extend past the profiles surface by more than 0,20mm.	
Grooving – Maximum material thickness reduction is 10% and groove width is smaller than 3mm.	
Surface porosity – Voids are less than 0.4mm in diameter and 0.4mm in depth. Maximum of 5 voids in 100cm <sup>2</sup> per 0.3m of profile.	
Stop Mark – Permitted unless associated with other superficial marks	
<b>INSPECTION METHODS</b>	
- Visual inspection (I.01)	
<b>REHABILITATION TECHNIQUES</b>	
- Application of superficial coating (R.03)	
- Superficial sanding (R.04)	
- Replacement of affected element (R.05)	
<b>CLASSIFICATION PARAMETERS</b>	
- Aesthetical significance of the element	
<b>SEVERITY LEVEL / REPAIR EMERGENCY</b>	
0 -	
1 - High aesthetical significance of the element	
2 -	
3 -	
4 -	

# ANOMALY FORM - A.N-ME.07

<b>ANOMALY NAME</b>	
<b>Wear damage</b>	
<b>ANOMALY DESCRIPTION</b>	
<p>This anomaly consists of the degradation of the surface layers, protection or coating of the elements, due to the normal or incorrect use of the elements at different stages of their service life.</p>	
<b>POSSIBLE CAUSES</b>	
- Improper handling of profiles (C.P.08)	
- Improper structural design (C.D.01)	
- Improper material selection (C.D.02)	
- Incorrect installation (C.I.01)	
- Vandalism (C.S.05)	
- Use Wear (C.S.05)	
- Change of use or improper use (C.S.05)	
<b>POSSIBLE CONSEQUENCES</b>	
- Reduction of mechanical properties	
- Aesthetical appearance	
<b>DETAILS TO INSPECT</b>	
- Thickness of remaining protective resin	
<b>INSPECTION METHODS</b>	
- Visual inspection (I.01)	
<b>REHABILITATION TECHNIQUES</b>	
- Application of superficial coating (R.03)	
- Replacement of affected element (R.05)	
<b>CLASSIFICATION PARAMETERS</b>	
- Exposure of fibres (Y/N)	
- Are there conditions to the progression of the anomaly (Y/N)	
- Aesthetical significance of the element	
<b>SEVERITY LEVEL / REPAIR EMERGENCY</b>	
0 - Low aesthetical significance of the element	
1 - High aesthetical significance of the element	
2 -	
3 -	
4 -	

# ANOMALY FORM - A.N-ME.08

**ANOMALY NAME**

**Debris accumulation**

**ANOMALY DESCRIPTION**

Debris accumulation is an anomaly that consists on the accumulation of rocks, dirt, sand and debris on the inside of the profile cross sections or gratings.



**POSSIBLE CAUSES**

- Improper structural design (C.D.01)
- Lack of maintenance (C.S.07)

**POSSIBLE CONSEQUENCES**

- Reduction of mechanical properties (due to moisture accumulation)
- Aesthetical appearance

**DETAILS TO INSPECT**

- Type of debris accumulated

**INSPECTION METHODS**

- Visual inspection (I.01)

**REHABILITATION TECHNIQUES**

- Superficial cleaning (R.04)

**CLASSIFICATION PARAMETERS**

- Aesthetical significance of the element

**SEVERITY LEVEL / REPAIR EMERGENCY**

- 0 - Low aesthetical significance of the element
- 1 - High aesthetical significance of the element
- 2 -
- 3 -
- 4 -



## **MECHANICAL ANOMALIES**

# ANOMALY FORM - A.ME.01

ANOMALY NAME	
<b>Corrosion of metallic components</b>	
ANOMALY DESCRIPTION	
<p>This anomaly consists of the corrosion of metallic components (bolts, steel plates and/or profiles) included in the construction, which are used mainly in connections between elements. The corrosion process may occur due to lack of protection or improper choice and/or application of the metallic components.</p>	
POSSIBLE CAUSES	
- Improper connection design (material selection) (C.D.02)	
- High humidity/permanently wet/ excessive wet-and-dry cycles (C.S.01)	
- Exposure to chemical environment (C.S.03)	
- Exposure to saline environment (C.S.03)	
- Unprotected bolted connection (C.S.04)	
- Lack of maintenance (C.S:06)	
POSSIBLE CONSEQUENCES	
- Connection strength and stiffness reduction	
- Aesthetical appearance	
DETAILS TO INSPECT	
- Level of corrosion of metallic elements	
INSPECTION METHODS	
- Visual Inspection (I.01)	
REHABILITATION TECHNIQUES	
- Application of superficial coating (R.03)	
- Superficial cleaning (R.04)	
- Replacement of affected element (R.05)	
- Protection of bolted connection (R.06)	
CLASSIFICATION PARAMETERS	
- Visual inspection of the level of corrosion (punctual, widespread, widespread and intense with increase in volume, widespread and intense with section loss)	
- Are there conditions to the progression of the anomaly (Y/N)	
- Aesthetical significance of the element	
SEVERITY LEVEL / REPAIR EMERGENCY	
0 - No corrosion; low aesthetical significance of the element	
1 - Punctual corrosion of metallic element; high aesthetical significance of the element	
2 - Widespread corrosion of metallic element	
3 - Widespread and intense with increase in volume	
4 - Widespread and intense with section loss	

# ANOMALY FORM - A.ME.02

ANOMALY NAME		
Cracking		
ANOMALY DESCRIPTION		
<p>Cracking is an anomaly that can occur, in every production stage as well as in every part of the structure. The causes that lead to this anomaly are diversified and can affect the element, the matrix and/or the adhesive of a bonded connection between two elements.</p>		
POSSIBLE CAUSES		
- Improper cure conditions of resin (C.P.01)	- Incorrect installation (C.I.01)	
- Excess of resin (C.P.02)	- Incorrect application of adhesive (C.I.02)	
- Improper quality of resin (C.P.03)	- Improper quality of adhesive components (C.I.03)	
- Improper mixture of resin (C.P.03)	- Incorrect cure conditions for adhesive (C.I.05)	
- Improper formulation of resin (C.P.03)	- Over tightening of bolted connections (C.I.06)	
- Incorrect layout of fibres/mats (C.P.06)	- Vandalism (C.S.05)	
- Improper structural design (C.D.01)	- Accidental Impact (C.S.05)	
- Improper cross-section selection (C.D.01)	- Change of use or improper use (C.S.05)	
- Improper connection design (C.D.02)		
POSSIBLE CONSEQUENCES		
- Reduction of mechanical properties	- Connection strength and stiffness reduction	
- Easier ingress of environmental degradation agents	- Possible connection failure	
- Easier ingress of environmental agents to the adhesive bulk	- Aesthetical appearance	
DETAILS TO INSPECT		
- Element cracked	- Cracking width, depth, length and orientation	
- Are there conditions to the progression of the anomaly (Y/N)	- Location of the cracking on the element	
INSPECTION METHODS		
- Visual inspection (I.01)	- Thermography (I.04)	
- Tap testing (I.02)	- Ultrasonic test (I.05)	
REHABILITATION TECHNIQUES		
- Bonding/bolting of reinforcing elements (R.01)	- Replacement of affected element (R.05)	
- Strengthening with filling elements (R.02)		
CLASSIFICATION PARAMETERS		
- Crack width (mm)		
- Location of the anomaly (mid-span, matrix, adhesive, connection)		
- Are there conditions to the progression of the anomaly (Y/N)		
- Aesthetical significance of the element		
SEVERITY LEVEL / REPAIR EMERGENCY		
0 - Crack width inferior to 0,5mm with no conditions for progression; Low aesthetical significance of the element		
1 - Crack width inferior to 0,5mm with no conditions for progression; high aesthetical significance of the element		
2 - Matrix cracking; crack width inferior to 0,5mm with conditions for progression		
3 - Crack width superior to 0,5mm with no conditions for progression		
4 - Crack width superior to 0,5mm with conditions for progression		

# ANOMALY FORM - A.ME.03

ANOMALY NAME	
<b>Crushing</b>	
ANOMALY DESCRIPTION	
<p style="text-align: center;">This anomaly consists of crushing (by compression) of an element, occurring more frequently in connection zones or at the ends of the elements.</p>	
POSSIBLE CAUSES	
- Improper structural design (C.D.01)	
- Improper cross-section selection (C.D.01)	
- Over tightening of bolted connections (C.I.06)	
- Vandalism (C.S.05)	
- Accidental impact (C.S.05)	
- Change of use or improper use (C.S.05)	
POSSIBLE CONSEQUENCES	
- Reduction of mechanical properties	
- Connection strength and stiffness reduction	
- Aesthetical appearance	
DETAILS TO INSPECT	
- Location of the crushed area	
- Causes of crushing	
INSPECTION METHODS	
- Visual inspection (I.01)	
- Tap testing (I.02)	
- Thermography (I.04)	
- Ultrasonic test (I.05)	
REHABILITATION TECHNIQUES	
- Bonding/bolting of reinforcing elements (R.01)	
- Strengthening with filling elements (R.02)	
- Replacement of affected element (R.05)	
CLASSIFICATION PARAMETERS	
- Location of the anomaly (mid-span, flange, connection)	
- Affects mechanical performance (Y/N)	
- Aesthetical significance of the element	
SEVERITY LEVEL / REPAIR EMERGENCY	
0 - Low aesthetical significance of the element	
1 - Does not affect mechanical properties; high aesthetical significance of the element	
2 -	
3 - Affects mechanical performance and on flange of the element	
4 - Other situations	

# ANOMALY FORM - A.ME.04

<b>ANOMALY NAME</b>	
<b>Debonding</b>	
<b>ANOMALY DESCRIPTION</b>	
<p>This anomaly consists of the debonding between two FRP elements or adherends in a bonded connection. It is generally caused by a wrong choice/application of the adhesive or incorrect treatment of the surfaces of the elements to be bonded, in terms of roughness and cleaning. It can also be caused by incorrect design, namely excessive loading and/or deformation, as these connections are generally much stiffer than bolted ones.</p>	
<b>POSSIBLE CAUSES</b>	
- Improper connection design (C.D.02)	
- Incorrect installation (C.I.01)	
- Incorrect application of adhesive (C.I.02)	
- Incorrect quality of adhesive components (C.I.03)	
- Incorrect mixture of adhesive components (C.I.03)	
- Incorrect formulation of adhesive components (C.I.03)	
- Improper treatment of bonding surface (C.I.04)	
- Incorrect cure of adhesive (C.I.05)	
<b>POSSIBLE CONSEQUENCES</b>	
- Connection strength and stiffness reduction	
- More aggressive exposure of both materials and bonded interfaces to environmental agents (easier ingress of moisture)	
<b>DETAILS TO INSPECT</b>	
- Type of debonding (punctual, widespread)	
- Causes for debonding	
- Quality of application	
<b>INSPECTION METHODS</b>	
- Visual inspection (I.01)	
- Tap testing (I.02)	
- Thermography (I.04)	
- Ultrasonic test (I.05)	
<b>REHABILITATION TECHNIQUES</b>	
- Bonding/bolting of strengthening elements (R.01)	
- Replacement of affected element (R.05)	
<b>CLASSIFICATION PARAMETERS</b>	
- Location of debonding (all connection, edges, centre)	
- Are there conditions to the progression of the anomaly (Y/N)	
<b>SEVERITY LEVEL / REPAIR EMERGENCY</b>	
0 – No debonding	
1 – Debonding on the middle of the connection with no conditions for progression	
2 – Debonding on the middle of the connection with conditions for progression; Debonding on edge of the connection with no conditions for progression	
3 – Debonding on edge of the connection with conditions for progression	
4 – Debonding in all connection section	

# ANOMALY FORM - A.ME.05

## ANOMALY NAME

**Delamination**

## ANOMALY DESCRIPTION

This anomaly consists of the separation (delamination) between different layers of fibrous reinforcement of FRP elements, which can lead to a considerable reduction of the mechanical properties of the elements.



## POSSIBLE CAUSES

- incorrect cure of resin (C.P.01)
- Improper quality of resin components (C.P.03)
- Improper formulation/mixture of resin components (C.P.03)
- Incorrect layout of fibres/mats (C.P.07)
- Incorrect installation (C.P.01)

## POSSIBLE CONSEQUENCES

- Reduction of mechanical properties
- More aggressive exposure to environmental agents (easier ingress of moisture)

## DETAILS TO INSPECT

- Condition of delamination (punctual or widespread)
- Causes of delamination

## INSPECTION METHODS

- Visual inspection (I.01)
- Tap testing (I.02)
- Barcol Hardness (I.03)
- Thermography (I.04)
- Ultrasonic test (I.06)

## REHABILITATION TECHNIQUES

- Bonding/bolting of strengthening elements (R.01)
- Replacement of affected element (R.05)

## CLASSIFICATION PARAMETERS

- Condition of delamination (punctual or widespread)
- Are there conditions to the progression of the anomaly (Y/N)

## SEVERITY LEVEL / REPAIR EMERGENCY

- 0 – No delamination
- 1 –
- 2 – Punctual delamination with no conditions for progression
- 3 – Punctual delamination with conditions for progression
- 4 – Widespread delamination

# ANOMALY FORM - A.ME.06

<b>ANOMALY NAME</b>	
<b>Excessive deflection</b>	
<b>ANOMALY DESCRIPTION</b>	
<p>This anomaly consists of the excessive deformation of structural elements (usually the vertical displacement of horizontal members in bending), with reference to the acceptable deflection for such type of elements. This anomaly is usually related to incorrect design, incorrect use of the structure or change in use.</p>	
<b>POSSIBLE CAUSES</b>	
- Improper structural design(C.D.01)	
- Improper cross-section selection (C.D.01)	
- Change of use or improper use (C.S.05)	
<b>POSSIBLE CONSEQUENCES</b>	
- Development of 2 <sup>nd</sup> order effects on structural elements	
- Damage in other structural elements	
- Damage in non-structural elements	
- Damage in connections	
- Aesthetical appearance	
<b>DETAILS TO INSPECT</b>	
- Amplitude of deflection	
- Cause of excessive deflection	
<b>INSPECTION METHODS</b>	
- Visual Inspection (I.01)	
<b>REHABILITATION TECHNIQUES</b>	
- Bonding/bolting of strengthening elements (R.01)	
- tightening of bolted connections (R.06)	
<b>CLASSIFICATION PARAMETERS</b>	
- Magnitude of deflection (mm)	
<b>SEVERITY LEVEL / REPAIR EMERGENCY</b>	
0 - No deflection	
1 -	
2 - Deflection < L/200	
3 - L/100 > Deflection > L/200	
4 - Deflection > L/100	

# ANOMALY FORM - A.ME.07

ANOMALY NAME	
<b>Geometrical imperfections</b>	
ANOMALY DESCRIPTION	
<p>This anomaly reveals itself through the application of elements with incorrect dimensions (production phase), with excessive deviations, or elements with cuts incorrectly executed (installation phase), leading to the existence of imperfections in connection zones or current zones.</p>	
POSSIBLE CAUSES	
- Incorrect maintenance of the pultrusion equipment (C.P.06)	
- Improper handling of cutting element (C.P.08)	
- Incorrect or incomplete (not fully detailed) connection design (C.D.02)	
- Incorrect Installation or prefabrication (C.I.01)	
- Movement during cure of adhesive (C.I.02)	
POSSIBLE CONSEQUENCES	
- Possible strength and stiffness reduction of structural element	
- Higher susceptibility to buckling (second order effects)	
- Development of higher forces/stresses in some parts of the connection	
- Cracking in connection areas	
- Crushing in connection areas	
- Connection strength and stiffness reduction	
- Residual stresses in structural elements	
- Increase of eccentricities in load transfer	
- Aesthetical appearance	
DETAILS TO INSPECT	
- Cause of geometrical imperfection	
- Measurement of the imperfection	
INSPECTION METHODS	
- Visual Inspection (I.01)	
REHABILITATION TECHNIQUES	
- Bonding/bolting of strengthening elements (R.01)	
- Replacement of affected element (R.05)	
CLASSIFICATION PARAMETERS	
- Affects mechanical performance of the element/connection (Y/N)	
- Aesthetical significance of the element	
SEVERITY LEVEL / REPAIR EMERGENCY	
0 - Other cases	
1 - High aesthetical significance of the element	
2 -	
3 - Affects the mechanical performance of the element/connection	
4 -	

# ANOMALY FORM - A.ME.08

<b>ANOMALY NAME</b>	
<b>Indentation/Perforation</b>	
<b>ANOMALY DESCRIPTION</b>	
<p style="text-align: center;">This anomaly consists of a partial or total indentation (perforation) of one or more surfaces of an FRP member by an external element.</p>	
<b>POSSIBLE CAUSES</b>	
- Improper structural design (C.D.01)	
- Improper cross-section selection (C.D.01)	
- Vandalism (C.S.05)	
- Accidental impact (C.S.05)	
- Change of use or improper use (C.S.05)	
<b>POSSIBLE CONSEQUENCES</b>	
- Reduction of mechanical properties (local)	
- More aggressive exposure to environmental agents (easier ingress of moisture)	
- Aesthetical appearance	
<b>DETAILS TO INSPECT</b>	
- Depth and area of perforation	
- Cause of perforation	
<b>INSPECTION METHODS</b>	
- Visual Inspection (I.01)	
- Tap testing (I.02)	
- Thermography (IM.04)	
- Ultrasonic test (IM.05)	
<b>REHABILITATION TECHNIQUES</b>	
- Bonding/bolting of strengthening elements (R.01)	
- Replacement of affected element (R.05)	
<b>CLASSIFICATION PARAMETERS</b>	
- Depth of perforation (mm)	
- Area affected by perforation ( $A_i$ (%)) = (maximum indentation length in longitudinal direction maximum $\times$ maximum indentation length in transversal direction) / (maximum indentation length longitudinal direction $\times$ cross-section width in transversal direction)	
- Aesthetical significance of the element	
<b>SEVERITY LEVEL / REPAIR EMERGENCY</b>	
0 - Other cases	
1 - Depth of indentation $< t/2$ ; High aesthetical significance of the element	
2 - Depth of infentation $> t/2$	
3 - $A_i > 40\%$	
4 -	

# ANOMALY FORM - A.ME.09

## ANOMALY NAME

**Incorrect cure of adhesive**

## ANOMALY DESCRIPTION

The adhesive used in the bonded connections is incorrectly cured, which compromises the effectiveness of the connection.

## POSSIBLE CAUSES

- Incorrect application of adhesive thickness (C.I.02)
- Improper quality of adhesive components (C.I.03)
- Improper mixture of adhesive components (C.I.03)
- Improper formulation of adhesive components (C.I.03)
- Incorrect cure of adhesive (C.I.05)
- Incorrect temperature/humidity cure conditions for adhesive (C.I.05)

## POSSIBLE CONSEQUENCES

- Connection strength and stiffness reduction
- Higher susceptibility to viscoelastic effects

## DETAILS TO INSPECT

- Reason for uncured adhesive

## INSPECTION METHODS

- Visual Inspection (I.01)
- Tap testing (I.02)

## REHABILITATION TECHNIQUES

- Bonding/bolting of strengthening elements (R.01)
- Replacement of affected element (R.05)

## CLASSIFICATION PARAMETERS

- Adhesive incorrectly cured (Y/N)

## SEVERITY LEVEL / REPAIR EMERGENCY

- 0 - Adhesive correctly cured
- 1 -
- 2 -
- 3 - Adhesive incorrectly cured
- 4 -

# ANOMALY FORM - A.ME.10

<b>ANOMALY NAME</b>	
<b>Incorrect cure of resin</b>	
<b>ANOMALY DESCRIPTION</b>	
<p>This anomaly consists of the incorrect curing of the polymeric matrix of the FRP material during the production phase. This anomaly can considerably affect the short-term mechanical properties of the FRP elements, as well as their long-term performance (creep) and durability when subjected to environmental agents.</p>	
<b>POSSIBLE CAUSES</b>	
- Incorrect temperature and/or humidity conditions (C.P.01)	
- Excess of resin (C.P.02)	
- Improper quality of resin components (C.P.03)	
- Improper mixture of resin components (C.P.03)	
- Improper formulation of resin mixture (C.P.03)	
<b>POSSIBLE CONSEQUENCES</b>	
- Reduction of mechanical properties	
- Increase of viscoelasticity	
- Lower durability to environmental agents	
- Possible delamination	
<b>DETAILS TO INSPECT</b>	
-Reason for uncured resin	
<b>INSPECTION METHODS</b>	
- Visual inspection (I.01)	
- Tap testing (I.02)	
- Barcol hardness (I..03)	
<b>REHABILITATION TECHNIQUES</b>	
- Bonding/bolting of strengthening elements (R.01)	
- Replacement of affected element (R.05)	
<b>CLASSIFICATION PARAMETERS</b>	
- Resin incorrectly cured (Y/N)	
- Expected value for barcol bardness	
<b>SEVERITY LEVEL / REPAIR EMERGENCY</b>	
0 - Resin correctly cured	
1 -	
2 -	
3 - Resin incorrectly cured	
4 -	

# ANOMALY FORM - A.ME.11

## ANOMALY NAME

**Loose connections**

## ANOMALY DESCRIPTION

This anomaly consists of bolted connections with missing components (e.g. nuts or washers) or in which they were loosely applied (e.g. with insufficient tightening) or not retightened during maintenance operations.



## POSSIBLE CAUSES

- Under tightening of bolted connection (C.I.06)
- Loss of torque in bolted connection (C.S.04)
- Lack of maintenance (C.S.06)

## POSSIBLE CONSEQUENCES

- Connection strength and stiffness reduction
- Increased wear of the elements

## DETAILS TO INSPECT

- Cause to loosen connection

## INSPECTION METHODS

- Visual inspection (I.01)

## REHABILITATION TECHNIQUES

- Replacement of missing components (R.05)
- Tightening of bolted connection (R.06)

## CLASSIFICATION PARAMETERS

- Loose Connection (Y/N)

## SEVERITY LEVEL / REPAIR EMERGENCY

- 0 - Other cases
- 1 -
- 2 -
- 3 - Loose connection
- 4 -

# ANOMALY FORM - A.ME.12

<b>ANOMALY NAME</b>	
<b>Member Failure</b>	
<b>ANOMALY DESCRIPTION</b>	
<p>This anomaly, which may occur during the in-service stage, consists of failure (rupture) of a structural or non-structural member. It can occur in different ways, e.g. at the connections between section walls (typically the flanges and webs of profiles with thin-walled sections), or at the edges of the laminates of the members.</p>	
<b>POSSIBLE CAUSES</b>	
- Inadequate structural design (C.D.01)	
- Over tightening of bolted connections (C.I.06)	
- Vandalism (C.S.05)	
- Accidental impact (C.S.05)	
- Use wear (C.S.05)	
- Change of use or improper use (C.S.05)	
<b>POSSIBLE CONSEQUENCES</b>	
- Critical reduction of mechanical properties	
- Aesthetical appearance	
<b>DETAILS TO INSPECT</b>	
- Causes of failure	
- Degradation of the material	
<b>INSPECTION METHODS</b>	
- Visual Inspection (IM.01)	
<b>REHABILITATION TECHNIQUES</b>	
- Bonding/bolting of strengthening elements (R.01)	
- Strengthening with filling elements (R.02)	
- Replacement of affected element (R.05)	
<b>CLASSIFICATION PARAMETERS</b>	
- Member failure (Y/N)	
- Structural element (Y/N)	
- Aesthetical significance of the element	
<b>SEVERITY LEVEL / REPAIR EMERGENCY</b>	
0 -	
1 - Failure on a non-structural element; High aesthetical significance of element	
2 -	
3 - Failure on a structural element	
4 -	

# ANOMALY FORM - A.ME.13

ANOMALY NAME		
Voids		
ANOMALY DESCRIPTION		
<p>This anomaly consists of the appearance of voids (air pockets) inside the material of the FRP components or at the adhesive used in bonded connections. This anomaly can only occur at the production stage.</p>		
POSSIBLE CAUSES		
- Incorrect mixture of resin components (C.P.04)		
- Incorrect formulation of resin components (C.P.04)		
- Incorrect layout of fibres/mats (C.P.06)		
- Incorrect application of adhesive (C.I.02)		
- Improper mixture of adhesive components (C.I.03)		
- Movement during cure of adhesive (C.I.02)		
POSSIBLE CONSEQUENCES		
- Reduction of mechanical properties		
- Connection strength and stiffness reduction		
DETAILS TO INSPECT		
- Causes of anomaly		
INSPECTION METHODS		
- Visual inspection (I.01)		
- Tap testing (I.02)		
- Thermography (I.04)		
- Ultrasonic test (I.05)		
REHABILITATION TECHNIQUES		
- Bonding/bolting of strengthening elements (R.01)		
- Replacement of affected element (R.05)		
CLASSIFICATION PARAMETERS		
- Area of cross-section void for pultruded element (%)		
- Area of void for bonded connection (%)		
SEVERITY LEVEL / REPAIR EMERGENCY		
0 - Other cases		
1 -		
2 - Area of cross-section void for pultruded element >2%; Area of void for bonded connection >5%		
3 -		
4 -		

**Appendix II**  
Diagnosis forms

With the information gathered it is now possible to create an individual form for each diagnosis technique.

These forms are an essential tool for the development of the inspection system, as they summarize much of the information studied for each component of the inspection system. For this reason, they should be an integral part of the inspection manual and are indispensable in the inspections of the case studies.

Each diagnosis technique form contains the following information:

- (i) The technique designation and an illustrative picture;
- (ii) the objectives of the test/technique;
- (iii) the necessary equipment;
- (iv) a detailed description of the test method; and
- (v) the main advantages and limitations of the technique

## DIAGNOSIS TECHNIQUE - I.01

DIAGNOSIS TECHNIQUE DESIGNATION	
<b>Visual inspection</b>	
<b>OBJECTIVES</b>	
Visual inspection is the primary method of inspection for all structural composites, since most of the anomalies can be detected at the surface. It is recommended that visual inspection should always be used as the initial method of inspection as an aid to any additional instrumented NDT.	
NECESSARY EQUIPMENT	
In order to avoid injuries, use proper safety precautions and individual protective equipment (IPE). To improve the detection of some anomalies several tools/equipment's can be used, such as: (a) magnifying glass/microscope; (b) photographic and video recording equipment; (c) dye penetrant; (d) a calliper/ruler; and (e) a level and laser.	
TECHNIQUE DESCRIPTION	
1. Put on safety equipment (IPE), when applicable; 2. Inspection of the elements through direct observation aided by other equipment if necessary: (a) to enlarge small objects; (b) to obtain the appearance of the anomaly for archive and subsequent analysis; (c) detection of superficial cracks or delamination and improve the contrast between defects and the underlying material; (d) determine the thickness and cross-section dimensions of the elements, and the thickness/depth of cracks; and (e) determine the deflection of a given element/structure.	
TECHNIQUE ADVANTAGES	
This technique is highly applicable in the detection of the most common surface anomalies and allows the instantaneous interpretation of large areas. In general, there are little to no equipment expenses and there is no coupling equipment necessary.	
TECHNIQUE LIMITATIONS	
This technique is unable to detect some types of internal delamination and cracks, it's of difficult applicability in painted composites or FRP materials with poor surface quality, and its unable to detect missing reinforcement. Moreover, in an opaque material, the method is limited to the detection of surface defects. The baseline properties are difficult to establish, and the interpretation of the anomalies and severity levels are highly susceptible to human misconception	

## DIAGNOSIS TECHNIQUE - I.02

DIAGNOSIS TECHNIQUE DESIGNATION	
Tap testing	
OBJECTIVES	
Detection of stiffness variations in the element through sound. A high frequency clean sound identifies a high stiffness area. A low frequency hollow sound identifies a low stiffness area.	
NECESSARY EQUIPMENT	
In order to avoid injuries, use proper safety precautions and individual protective equipment (IPE). To the production of the sound several equipment's can be used (coin, metallic hammer, rubber hammer, automatic system).	
TECHNIQUE DESCRIPTION	
1. Put on safety equipment (IPE), when applicable; 2. Gently tap the element under inspection and correlate the tapping sound to other areas of the element/other elements.	
TECHNIQUE ADVANTAGES	
This method is very intuitive and allows a fast verification of the elements' properties. Being a manual method, it can be applied locally or in large surfaces, in any direction and with small manoeuvring space. In general, there are little to no equipment expenses and there is no coupling equipment necessary.	
TECHNIQUE LIMITATIONS	
This method, although frequently used, has some limitations: (i) the difficulty to correlate between the sound produced and the type of anomaly/defect; (ii) its low capability of defect sizing. It also demands a high operator consistency and sensibility and it is influenced by the surrounding environment.	

## DIAGNOSIS TECHNIQUE - I.03

<b>DIAGNOSIS TECHNIQUE DESIGNATION</b>	
<b>Barcol hardness</b>	
<b>OBJECTIVES</b>	
Identification of the elements surface hardness, which allows the comparative measurement of the materials hardness through the element.	
<b>NECESSARY EQUIPMENT</b>	
In order to avoid injuries, use proper safety precautions and individual protective equipment (IPE), Barcol impressor	
<b>TECHNIQUE DESCRIPTION</b>	
1. Put on safety equipment (IPE), when applicable; 2- Press the Barcol impressor three times against the element and register the average result in one location; 3. Correlate the surface hardness of the element to other areas of the element, other elements or reference values.	
<b>TECHNIQUE ADVANTAGES</b>	
This method is very intuitive and allows a fast verification of the elements' properties. Being a manual method, it can be applied locally or in large surfaces, in any direction and with small manoeuvring space. In general, besides the acquisition costs of the equipment, there are little to no equipment expenses and there is no coupling equipment necessary.	
<b>TECHNIQUE LIMITATIONS</b>	
This method has some limitations: (i) limited to the detection of resin/adhesive cure degree and possible superficial delamination; (ii) its low capability of defect sizing. It also demands a high operator consistency and sensibility	

## DIAGNOSIS TECHNIQUE - I.04

### DIAGNOSIS TECHNIQUE DESIGNATION

**Infrared thermography**

### OBJECTIVES

To evaluate the differences between the thermal conductivity of different areas of the FRP elements. Infrared thermography has high sensitivity to delamination, cracks, voids and moisture ingress.



### NECESSARY EQUIPMENT

In order to avoid injuries, use proper safety precautions and individual protective equipment (IPE). Thermographic camera sensitive to infrared radiation, thermoelectric sensors to control the temperature of the elements, digital recording equipment to save the thermographic results obtained.

### TECHNIQUE DESCRIPTION

1. Put on safety equipment (IPE), when applicable; 2. Taking advantage of the heating caused by solar radiation (or any other means), observation of the thermographic images obtained through infrared thermography equipment; 3. Recording the images/videos collected on the digital recording equipment; 4. Analysing the recorded images/videos and diagnose accordingly.

### TECHNIQUE ADVANTAGES

The application of this technique, besides the acquisition costs of the equipment, is economical and efficient. This technique can be applied without any contact with the elements to be inspected and can be applied to general areas instead of localized points. This technique allows recording the analysed surface and can detect anomalies at an early stage.

### TECHNIQUE LIMITATIONS

The analysis of the thermographic images is considered a starting point to more localized tests in the possibly affected areas. The interpretation of the thermographic images requires a qualified professional with experience in the thermal behaviour of FRP materials. The depth and thickness of the anomaly cannot be determined with this method. The application of this method is very susceptible to temperature fluctuations and requires a highly uniform heat source. Requires coupling equipment (infra-red camera).

## DIAGNOSIS TECHNIQUE - I.05

<b>DIAGNOSIS TECHNIQUE DESIGNATION</b>	
<b>Ultrasonic test</b>	
<b>OBJECTIVES</b>	
<p>Analysis of the ultrasound speed, through the element, between a transmitter and a receiver. This method allows determining the thickness of the element and the existence of anomalies or discontinuities in the interior of the element</p>	
<b>NECESSARY EQUIPMENT</b>	
<p>In order to avoid injuries, use proper safety precautions and individual protective equipment (IPE). Ultrasonic impulse generator, 2 transducers (transmitter and receiver), cathode ray tube, calibration bar and coupling mass to the element (e.g. Vaseline)</p>	
<b>TECHNIQUE DESCRIPTION</b>	
<p>1. Put on safety equipment (IPE), when applicable; 2. Place the transmitting and receiving transducers in contact with the surface of the element over a thin layer of the coupling mass; 3. Exert the appropriate pressure to prevent the presence of air between the contact surfaces; 4. Apply the ultrasonic pulse through the transmitter and register the propagation velocity on the impulse generator or on the cathodic ray tube; 5. Register the results for posterior analysis and comparison to other areas, physical properties (thickness) and mechanical properties.</p>	
<b>TECHNIQUE ADVANTAGES</b>	
<p>The application of this technique, besides the acquisition costs of the equipment, is economical and efficient. This technique allows a high mobility of mapping through the construction and can easily detect delamination, debonding, voids and inclusions.</p>	
<b>TECHNIQUE LIMITATIONS</b>	
<p>The analysis of the ultrasonic results is considered a starting point to more localized tests in the possibly affected areas. The interpretation of the ultrasonic results requires a qualified professional with experience in the acoustics behaviour of FRP materials. The defect sizing of the anomaly cannot be determined with this method. This method is difficult to apply on rough/uneven surfaces. Requires continuous coupling equipment (transducers).</p>	

## DIAGNOSIS TECHNIQUE - I.06

DIAGNOSIS TECHNIQUE DESIGNATION	
Moisture meter	
OBJECTIVES	
Detection of moisture at the surface and superficial layers of the elements.	
NECESSARY EQUIPMENT	
In order to avoid injuries, use proper safety precautions and individual protective equipment (IPE). Moisture meter	
TECHNIQUE DESCRIPTION	
1. Put on safety equipment (IPE), when applicable; 2. Place the moisture meter in contact with the surface of the element three times and register the average result in one location; 3. Correlate the superficial moisture of the element to other areas of the element, other elements or reference values.	
TECHNIQUE ADVANTAGES	
This method is very intuitive and allows a fast verification of the elements' properties. Being a manual method, it can be applied locally or in large surfaces, in any direction and with small manoeuvring space.	
TECHNIQUE LIMITATIONS	
This technique can only detect whether the surface of the material has free water (water accumulated in cracks and macro pores that can be evaporated), but it does not allow determining the depth of the water absorption. This method is difficult to apply on rough/uneven surfaces.	

**Appendix III**  
Rehabilitation forms

With the information gathered it is now possible to create an individual form for each rehabilitation technique.

These forms are an essential tool for the development of the inspection system, as they summarize much of the information studied for each component of the inspection system. For this reason, they should be an integral part of the inspection manual and are indispensable in the inspections of the case studies.

Each rehabilitation technique form contains the following information:

- (i) The technique designation and description;
- (ii) materials to apply;
- (iii) necessary equipment;
- (iv) description of the rehabilitation technique;
- (v) estimated labour and time;
- (vi) estimated cost;
- (vii) recommendations and special precautions; and
- (viii) technique limitations.

# REHABILITATION TECHNIQUE FORM - R.01

## REHABILITATION TECHNIQUE DESIGNATION

**Bonding/bolting of strengthening element**

### TECHNIQUE DESCRIPTION

This technique consists of bonding (a) or bolting (b) other elements (profiles or plates) on specific areas of an affected element. The bonding/bolting of strengthening elements is typically used to rehabilitate mechanical anomalies. This technique can be used to repair an affected element (e.g. cracked, crushed), or it can be used to increase the stiffness or strength of that element (e.g. excessive deflection). If this technique is to be applied to an entire element, other rehabilitation techniques should be considered as an alternative, such as R.05 (replacement of affected elements).

### MATERIALS TO APPLY

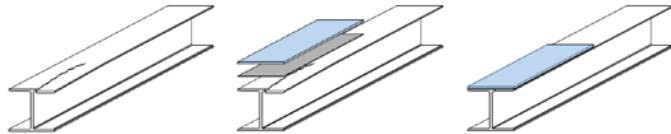
- (a) binding element (e.g. resin), reinforcement plates.  
 (b) stainless steel nuts and bolts, plastic washers, reinforcement plates.

### NECESSARY EQUIPMENT

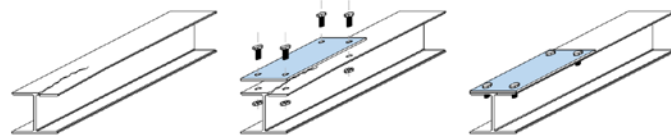
- (a) cleaning material (sponge, cloth, water, solvent materials, brush, low-pressure water jet), mechanical or manual sanding material (wire brush, sanding sheet, mechanical sander), mixing material (mixing cup, bucket, spoon, metal rod), binder spreading material (trowel, metal plate)  
 (b) cleaning material (cloth, water, solvent materials, brush), drill, manual or mechanical wrench.

### DESCRIPTION OF THE REHABILITATION TECHNIQUE

(a) 1. Clean and sand the surface of affected element; 2. Apply the bonding element (e.g. resin); 3. Place the strengthening element and keep it in position; 4. Let the bonding material cure at appropriate temperature and humidity conditions.



(b) 1. Clean the surface of affected element; 2. Execute the drill holes on the affected and strengthening element; 3. Place the washers and metallic elements (screws); 4. Tighten the bolting elements.



### ESTIMATED LABOUR AND TIME\*

- (a) 1 worker × 8 hours: rehabilitation of 75 linear meters | (b) 1 worker × 8 hours: rehabilitation of 130 linear meters

### ESTIMATED COST\*

- (a) 16.75€/linear meter | (b) 14.50€/linear meter

*\*assuming the reinforcement of a web of a I120 pultruded profile (costs estimated with average productivity and cost of labour and materials in Portugal)*

### RECOMMENDATIONS AND SPECIAL PRECAUTIONS

General recommendations: The use of personal protective equipment is recommended in all situations. The electric tools should be used correctly and in accordance with the specifications and safety manuals of the equipment.

- (a) Choose the binder in accordance with the type of environment the construction is exposed, verify the binder as the appropriate conditions of humidity and temperature to cure.  
 (b) Choose the plastic washers in accordance with the size of the bolting elements (inner and outer diameters of the washer); check the appropriate tightening torque of the elements, take special precaution not to over tighten the bolting elements, in order not to damage the FRP elements.

### TECHNIQUE LIMITATIONS

These techniques may be difficult to apply in tall constructions (that require the use of a ladder or scaffolding) and in constructions with hidden/partially obstructed affected elements.

## REHABILITATION TECHNIQUE FORM - R.02

### REHABILITATION TECHNIQUE DESIGNATION

**Strengthening with filling element**

### TECHNIQUE DESCRIPTION

This technique consists of bonding filling elements with adequate stiffness and strength (e.g. polyurethane foam) to an affected element. This technique is typically used to rehabilitate cracked and crushed elements due to accidental impacts and can also be used as a preventive method when there is an incorrect design or choice of cross section in a FRP construction

### MATERIALS TO APPLY

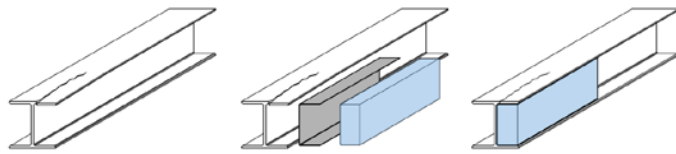
Binding element (e.g. resin), reinforcement filling elements.

### NECESSARY EQUIPMENT

cleaning material (sponge cloth, water, solvent materials, brush, low-pressure water jet), mechanical or manual sanding material (wire brush, sanding sheet, mechanical sander), mixing material (mixing cup, bucket, spoon, metal rod), binder spreading material (trowel, metal plate)

### DESCRIPTION OF THE REHABILITATION TECHNIQUE

1. Clean and sand the surface of affected element; 2. Apply the bonding element (e.g. resin); 3. Place the strengthening element and keep it in position; 4. Let the bonding material cure at appropriate temperature and humidity conditions.



### ESTIMATED LABOUR AND TIME\*

1 worker × 8 hours: rehabilitation of 50 linear meters

### ESTIMATED COST\*

14.75€/linear meter

*\*assuming the strengthening of one side of a I120 pultruded profile (costs estimated with average productivity and cost of labour and materials in Portugal)*

### RECOMMENDATIONS AND SPECIAL PRECAUTIONS

General recommendations: The use of personal protective equipment is recommended in all situations. The electric tools should be used correctly and in accordance with the specifications and safety manuals of the equipment.

(a) Choose the binder and filling element in accordance with the type of environment the construction is exposed, verify the binder as the appropriate conditions of humidity and temperature to cure.

### TECHNIQUE LIMITATIONS

This technique may be difficult to apply in tall constructions (that require the use of a ladder or scaffolding) and in constructions with hidden/partially obstructed affected elements.

## REHABILITATION TECHNIQUE FORM - R.03

### REHABILITATION TECHNIQUE DESIGNATION

**Application of surface coating**

### TECHNIQUE DESCRIPTION

This technique is used to rehabilitate non-mechanical anomalies. The application of a surface coating (e.g. gel coat or conventional painting scheme) prevents the accumulation of water and creates an exterior surface protection and sacrificial layer to the environmental agents. This technique can also be applied during the installation of the FRP construction in order to prevent some of the most common anomalies (e.g. biological colonization, discoloration and loss of gloss, and fibre blooming)

### MATERIALS TO APPLY

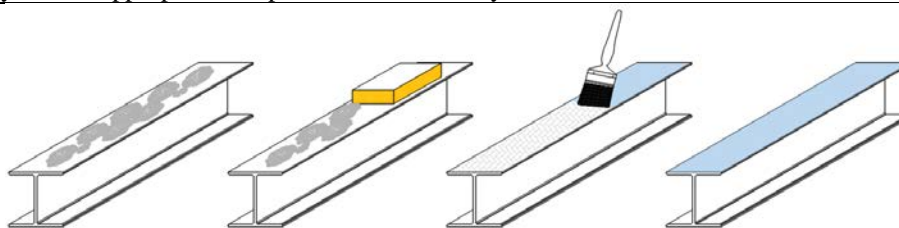
Surface coating (e.g. enamel, paint, resin)

### NECESSARY EQUIPMENT

Cleaning material (sponge, cloth, water, solvent materials, brush, low-pressure water jet), mechanical or manual sanding material (wire brush, sanding sheet, mechanical sander), mixing material (mixing cup, bucket, spoon, metal rod), painting materials (paint, roller, paint tray)

### DESCRIPTION OF THE REHABILITATION TECHNIQUE

1. Clean the surface of affected element; 2. Sand the surface of the element for a better adhesion of the surface coating, when necessary; 3. Mix and apply the surface coating to the element; 4. Let the surface coating dry/cure at appropriate temperature and humidity conditions.



### ESTIMATED LABOUR AND TIME\*

1 worker × 8 hours: rehabilitation of 40 linear meters

### ESTIMATED COST\*

23,75€/linear meter

*\*assuming the coating of the full cross section of a I120 pultruded profile (costs estimated with average productivity and cost of labour and materials in Portugal)*

### RECOMMENDATIONS AND SPECIAL PRECAUTIONS

General recommendations: The use of personal protective equipment is recommended in all situations. The electric tools should be used correctly and in accordance with the specifications and safety manuals of the equipment.

Choose the surface coating in accordance with the type of environment the construction is exposed, verify the binder as the appropriate conditions of humidity and temperature to dry/cure.

### TECHNIQUE LIMITATIONS

This technique may be difficult to apply in tall constructions (that require the use of a ladder or scaffolding).

## REHABILITATION TECHNIQUE FORM - R.04

### REHABILITATION TECHNIQUE DESIGNATION

Surface sanding/cleaning

### TECHNIQUE DESCRIPTION

This technique should be considered as periodic operation, executed to eliminate dirt, parasitic vegetation, debris and biological growth. Several chemical and mechanical methods can be used according to the material to remove. To avoid unacceptable damage to the FRP elements

### MATERIALS TO APPLY

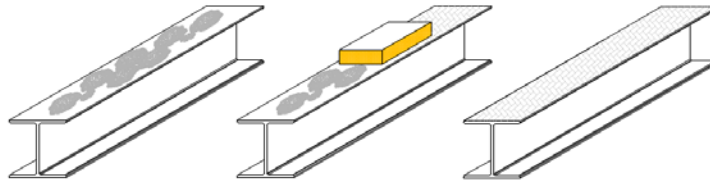
None

### NECESSARY EQUIPMENT

Cleaning material (sponge, cloth, water, solvent materials, brush, low-pressure water jet), mechanical or manual sanding material (wire brush, sanding sheet, mechanical sander, soft water/sand jet),

### DESCRIPTION OF THE REHABILITATION TECHNIQUE

1. Clean/sand the surface of affected element;



### ESTIMATED LABOUR AND TIME\*

1 worker × 8 hours: rehabilitation of 60 linear meters

### ESTIMATED COST\*

2.00€/linear meter

*\*assuming the cleaning of the full cross section of a I120 pultruded profile (costs estimated with average productivity and cost of labour and materials in Portugal)*

### RECOMMENDATIONS AND SPECIAL PRECAUTIONS

General recommendations: The use of personal protective equipment is recommended in all situations. The electric tools should be used correctly and in accordance with the specifications and safety manuals of the equipment.

The initial technique applied in the cleaning operations should be as little aggressive as possible.

### TECHNIQUE LIMITATIONS

This technique may be difficult to apply in tall constructions (that require the use of a ladder or scaffolding).

## REHABILITATION TECHNIQUE FORM - R.05

### REHABILITATION TECHNIQUE DESIGNATION

**Replacement of affected elements**

### TECHNIQUE DESCRIPTION

This technique should only be considered when the deterioration of an element is too significant, and it is limited to one or few elements that do not compromise adjacent elements and the construction. The type of technique will depend on the original type of connection: (a) binded, (b) bolted

### MATERIALS TO APPLY

New FRP elements

### NECESSARY EQUIPMENT

(a) cutting material (grinding wheel, sabre saw, saw), mechanical or manual sanding material (wire brush, sanding sheet, mechanical sander), mixing material (mixing cup, bucket, spoon, metal rod), binder spreading material (trowel, metal plate)

(b) cutting material (grinding wheel, sabre saw, saw), drill, manual or mechanical wrench.

### DESCRIPTION OF THE REHABILITATION TECHNIQUE

(a) 1. Remove the affected element; 2. Prepare the surface for binding element 3. Apply the bonding element (e.g. resin); 4. Place the new element and keep it in position; 4. Let the bonding material cure at appropriate temperature and humidity conditions.

(b) 1. Remove the affected element and bolted connections; 2. Execute the drill holes on the new element; 3. Place the washers and metallic elements (screws); 4. Tighten the bolting elements.

### ESTIMATED LABOUR AND TIME\*

(a) 1 worker × 8 hours: replacement of 10 elements

(a) 1 worker × 8 hours: replacement of 15 elements

### ESTIMATED COST\*

(a) 58.00€/element

(b) 36.00€/element

*\*assuming the replacement of one meter of a I120 pultruded profile (costs estimated with average productivity and cost of labour and materials in Portugal)*

### RECOMMENDATIONS AND SPECIAL PRECAUTIONS

General recommendations: The use of personal protective equipment is recommended in all situations. The electric tools should be used correctly and in accordance with the specifications and safety manuals of the equipment.

Due to its cost and possible complexity in removing the affected elements from the construction, this technique should only be applied if the other techniques cannot be used and/or their application becomes too expensive

### TECHNIQUE LIMITATIONS

This technique may be difficult to apply in tall constructions (that require the use of a ladder or scaffolding) or in elements with many connections.

## REHABILITATION TECHNIQUE FORM - R.06

### REHABILITATION TECHNIQUE DESIGNATION

**Protection/tightening of bolted connections**

#### TECHNIQUE DESCRIPTION

The application of this technique concerns bolted connections, in which the metallic elements may be noticeably deteriorated by corrosion (a), were loose in the installation stage (c), or could have become loose/lost during the in-service stage (d). Insufficient sealing of bolted connections can lead to stains around the screw holes, due to the accumulation of water between the screw/nut and the FRP element (b).

#### MATERIALS TO APPLY

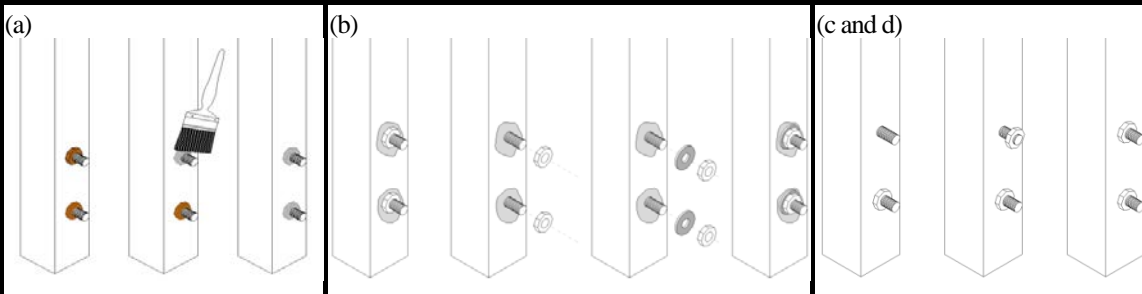
(a) primary paint and anti-corrosion paint	(c) stainless steel nuts (if necessary)
(b) plastic washers	(d) stainless steel nuts and bolts

#### NECESSARY EQUIPMENT

- (a) Cleaning material (cloth, water, solvent materials, brush), mechanical or manual pickling and/or sanding material (wire brush, sanding sheet, mechanical sander, water/sand jet) and painting equipment (paints and brushes).
- (b) Cleaning material (cloth, water, solvent materials, brush), manual or mechanical wrench.
- (c) Cleaning material (cloth, water, solvent materials, brush), manual or mechanical wrench, stainless steel nuts.
- (d) Cleaning material (cloth, water, solvent materials, brush), manual or mechanical wrench, stainless steel nuts and bolts.

#### DESCRIPTION OF THE REHABILITATION TECHNIQUE

- (a) 1. Clean the rusted element; 2. Pickle and/or sand the rusted layer of the bolted element; 3. Clean the un-rusted surface; 4. Apply primary paint layer; 5. Apply anti-corrosive paint.
- (b) 1. Remove existing metallic nuts; 2. Clean the superficial area between the screw and the FRP element; 3. Place plastic washers between the FRP element and metallic bolt; 4. Tighten the bolting elements.
- (c and d) 1. Clean the metallic elements; 2. Place the metallic elements missing (if necessary); 3. Tighten the bolting elements.



#### ESTIMATED LABOUR AND TIME\*

(a) 1 worker × 8 hours: rehabilitation of 64 elements	(c) 1 worker × 8 hours: rehabilitation of 240 elements
(b) 1 worker × 8 hours: rehabilitation of 160 elements	(d) 1 worker × 8 hours: rehabilitation of 240 elements

#### ESTIMATED COST\*

(a) 2.00 €/element	(b) 0.75 €/element	(c) 0.50 €/element	(d) 0.50 €/element
--------------------	--------------------	--------------------	--------------------

*\*estimated with average productivity and cost of labour and materials in Portugal*

#### RECOMMENDATIONS AND SPECIAL PRECAUTIONS

General recommendations: The use of personal protective equipment is recommended in all situations. The electric tools should be used correctly and in accordance with the specifications and safety manuals of the equipment.

(a) Make sure that the existing rust has been removed from the metallic elements before applying the primary paint layer; let the primary paint layer completely dry before applying the anti-corrosive paint layer. The paints should be applied at the temperatures recommended by the manufacturers, should not be applied while raining or if the moisture level of the substrate is excessive.

(b) Check that the stains are due to the presence of water between the metallic elements and the FRP, and it is not due to other causes; choose the plastic/stainless steel washers in accordance with the size of the bolting elements (inner and outer diameters of the washer).

(c and d) Check the appropriate tightening torque of the elements, take special precaution not to over tighten the bolting elements, in order not to damage the FRP elements.

#### TECHNIQUE LIMITATIONS

These techniques may be difficult to apply in tall constructions (that require the use of a ladder or scaffolding) and in constructions with hidden/partially obstructed bolted connections.

**Appendix IV**  
Inspection form



<b>INSPECTION SHEET NUMBER</b>		<b>INSPECTION DATE</b>	
<b>INSPECTOR/FUNCTION</b>			
<b>INSPECTION OBJECTIVE</b>			

<b>I. STRUCTURE DESIGNATION</b>		<b>DENOMINATION</b>	
<b>I.1 – Location</b>			
<b>I.2 – General description</b>			
<b>I.3 – Year of construction</b>		<b>I.4 – Construction Company</b>	
<b>I.5 – Posterior construction</b>	No	Yes	Date
<b>I.6 – Type of surrounding</b>	Urban	Countryside	Maritime
<b>I.7 – Proximity to the sea</b>	< 1 Km	< 5 km	> 5 km
<b>I.8 – Climatic zone</b>	One	Two	Three
<b>I.9 – Construction description</b>			
<b>I.10 – Contacts established</b>	Owner	Design.	Constructor
<b>I.11 – Contact name</b>			
<b>I.12 – Observations</b>			

<b>II.A SUB-STRUCTURE NUMBER</b>		<b>PICTURE INDEX (Y/N)(Name)</b>	
<b>II.1 – Location</b>			
<b>II.2 – General description</b>			Year
<b>II.3 – Type of elements used</b>	Pultruded	Gratings	Other
<b>II.4 – Materials used</b>	Fibres	Glass	Carbon
	Resin	Vinylester	Polyester
<b>II.5 – Type of application</b>	Structural	Flooring	Guardrail
	Staircase	Other	
<b>II.6 – Type of connections</b>	Bolted	Bonded	Both
<b>II.7 – Type(s) of pultruded profile(s) (dimensions)</b>	S/R	C/U	Circle
<b>II.8 – Type(s) of grating(s)</b>	Height		Mesh
<b>II.9 – Type of finishing</b>	Colour	Superficial Protection	
<b>II.10 – Sub-Structure description</b>			
<b>II.11 – Chemical exposure</b>	High	Medium	Low
<b>II.12 – UV radiation exposure</b>	High	Medium	Low
<b>II.13 – Exposure to rain/wind</b>	High	Medium	Low
<b>II.14 – Moisture exposure</b>	P. Wet	Wet/Dry	P. Dry
<b>II.15 – Observations</b>			

<b>II.B SUB-STRUCTURE NUMBER</b>		<b>PICTURE INDEX (Y/N)(Name)</b>	
<b>II.1 – Location</b>			
<b>II.2 – General description</b>			Year
<b>II.3 – Type of elements used</b>	Pultruded	Gratings	Other
<b>II.4 – Materials used</b>	Fibres	Glass	Carbon
	Resin	Vinylester	Polyester
<b>II.5 – Type of application</b>	Structural	Flooring	Guardrail
	Staircase	Other	
<b>II.6 – Type of connections</b>	Bolted	Bonded	Both
<b>II.7 – Type(s) of pultruded profile(s) (dimensions)</b>	S/R	C/U	Circle
<b>II.8 – Type(s) of grating(s)</b>	Height		Mesh
<b>II.9 – Type of finishing</b>	Colour	Superf. Protection	
<b>II.10 – Sub-Structure description</b>			
<b>II.11 – Chemical exposure</b>	High	Medium	Low
<b>II.12 – UV radiation exposure</b>	High	Medium	Low
<b>II.13 – Exposure to rain/wind</b>	High	Medium	Low
<b>II.14 – Moisture exposure</b>	P. Wet	Wet/Dry	P. Dry
<b>II.15 – Observations</b>			

II.C SUB-STRUCTURE NUMBER	PICTURE INDEX (Y/N)(Name)						
II.1 – Location							
II.2 – General description							Year
II.3 – Type of elements used	Pultruded		Gratings		Other		
II.4 – Materials used	Fibres	Glass	Carbon		Other		
	Resin	Vinylester	Polyester		Other		
II.5 – Type of application	Structural		Flooring		Guardrail		
	Staircase		Other				
II.6 – Type of connections	Bolted		Bonded		Both		
II.7 – Type(s) of pultruded profile(s) (dimensions)	S/R	C/U		Circle	I/H		
II.8 – Type(s) of grating(s)	Height			Mesh			
II.9 – Type of finishing	Colour		Superf. Protection				
II.10 – Sub-Structure description							
II.11 – Chemical exposure	High	Medium		Low	Null		
II.12 – UV radiation exposure	High	Medium		Low	Null		
II.13 – Exposure to rain/wind	High	Medium		Low	Null		
II.14 – Moisture exposure	P. Wet	Wet/Dry		P. Dry	Other		
II.15 – Observations							

III. MAINTENANCE						
III.1 – Current maintenance type						
III.2 – Inspection routine						
III.3 – Maintenance actions						
1	Date		Sub-Structure number		Type of intervention	
	Technique applied					
	Materials applied					
2	Date		Sub-Structure number		Type of intervention	
	Technique applied					
	Materials applied					
3	Date		Sub-Structure number		Type of intervention	
	Technique applied					
	Materials applied					

IV. OTHER OBSERVATIONS	

**Appendix V**  
Validation form



<b>VALIDATION SHEET NUMBER</b>		<b>INSPECTION DATE</b>	
<b>SUB-STRUCTURE NUMBER</b>		<b>PICTURE INDEX (Name)</b>	

<b>I. DETECTED ANOMALIES</b>			
<b>NON-MECHANICAL ANOMALIES</b>			
<b>A.N-Me.01</b> Biological colonization		<b>A.N-Me.05</b> Stains	
<b>A.N-Me.02</b> Discoloration/Loss of gloss		<b>A.N-Me.06</b> Superficial marks	
<b>A.N-Me.03</b> Fibre blooming		<b>A.N-Me.07</b> Wear Damage	
<b>A.N-Me.04</b> Inclusion		<b>A.N-Me.08</b> Debris accumulation	
<b>MATERIAL ANOMALIES</b>			
<b>A.Me.01</b> Corrosion of bolted elements		<b>A.Me.08</b> Indentation/Perforation	
<b>A.Me.02</b> Cracking		<b>A.Me.09</b> Incorrect cure of adhesive	
<b>A.Me.03</b> Crushing		<b>A.Me.10</b> Member failure	
<b>A.Me.04</b> Debonding		<b>A.Me.11</b> Incorrect cure of resin	
<b>A.Me.05</b> Delamination		<b>A.Me.12</b> Loose connections	
<b>A.Me.06</b> Excessive deflection		<b>A.Me.13</b> Voids	
<b>A.Me.07</b> Geometrical imperfections			
<b>Observations</b>			

<b>II. ANOMALIES CHARACTERIZATION</b>	<b>ANOMALIES</b>				
<b>(Complete only if applicable to the anomaly)</b>					
<b>Are there conditions for the anomaly progression? (Y/N)</b>					
<b>Anomaly detected at connection (c), mid-span (m) or edges (e)?</b>					
<b>Recurring anomaly (Y/N/NI)?</b>					
<b>Stabilized (Y/N/NI)?</b>					
<b>Affects other elements of the structure (Y/N)?</b>					
<b>Needs replacement (Y/N)?</b>					
<b>Level of severity (0-Low; 1-Intermediate ;2-High)</b>					
<b>Aesthetical appeal (0-Low; 1-Intermediate; 2-High)</b>					
<b>Crack width/perforation depth (mm)</b>					
<b>Affects the connections (Y/N)?</b>					
<b>Observations</b>					

III. PROBABLE CAUSES	ANOMALIES				
(Complete only if applicable to the anomaly) (1- Indirect cause / 2- Direct cause)					
<b>PRODUCTION CAUSES</b>					
C.P.01 Incorrect cure conditions of the resin (temperature, humidity and duration)					
C.P.02 Excess of resin					
C.P.03 Inadequate quality/mixture/formulation of resin components					
C.P.04 Dripped resin or small air bubbles					
C.P.05 Inadequate maintenance/cleaning/isolation of pultrusion equipment					
C.P.06 Incorrect layout of fibres/mats					
C.P.07 Incorrect positioning of die metallic parts					
C.P.08 Inadequate handling of profiles or cutting element					
<b>DESIGN CAUSES</b>					
C.D.01 Inadequate structural design/material selection					
C.D.02 Inadequate connection design /material selection					
C.D.03 Lack of surface veil/UV additives/surface coating					
<b>INSTALLATION CAUSES</b>					
C.I.01 Incorrect installation or prefabrication					
C.I.02 Incorrect application of adhesive (e.g. thickness, voids, position, cure)					
C.I.03 Inadequate quality/mixture/formulation of adhesive components					
C.I.04 Inadequate treatment of bonding surfaces					
C.I.05 Incorrect temperature and/or humidity cure conditions for adhesive					
C.I.06 Over/under tightening of bolted connections					
<b>IN-SERVICE CAUSES</b>					
C.S.01 High humidity/permanently wet/excessive wet-and-dry cycles environmental condition					
C.S.02 Exposure to UV radiation					
C.S.03 Exposure to chemical/saline environment					
C.S.04 Loss of tightening/unprotected bolted connection					
C.S.05 Vandalism/accidental impact/use wear/change of use or inadequate use					
C.S.06 Lack of maintenance					

IV. INSPECTION METHODS	ANOMALIES				
(Complete only if applicable to the anomaly)					
I.01 Visual inspection					
I.02 Tap testing					
I.03 Barcol hardness					
I.04 Thermography					
I.05 Ultrasonic					
I.06 Moisture metre					

V. OTHER OBSERVATIONS

**Appendix VI**  
Technical sheets



# Technical Datasheet

Ashland Performance Materials

RESINA AROPOL IS 4698 [18031]



## AROPOL™ IS 4698



AROPOL IS 4698 is a high viscosity, high reactivity, isophthalic based special purpose resin with good mechanical properties combined with high temperature resistance.

### Typical liquid resin properties

Property	Value	Unit	Method
Viscosity at 25 C, Brookfield	800	mPas	ISO 2555
Styrene content	36	%	SFS 4864
Geltime, SPI	8	min	SPI
Total time	10	min	SPI
Peak exotherm	215	°C	SPI
Acid value	max 20		DS-09-119
Colour, Hazen	max 200		DS-09-056

### Typical cured resin properties

Property	Value	Unit	Method
Tensile strength	680	kg/cm <sup>2</sup>	ASTM D638
Elongation at break	3,6	%	ASTM D638
Flexural strength	1190	kg/cm <sup>2</sup>	ASTM D790
Heat deflection temperature (HDT)	110	C	ASTM D648
Barcol hardness	45		ASTM D2583

### Application and use

AROPOL IS 4698 resin is suitable for production of high quality laminates, surface linings or other composites exposed to a corrosive environment and for production of composites where good mechanical properties are important.

When AROPOL IS 4698 resin is cured at room temperature, following curing system should be followed;

AROPOL IS 4698	100 g
Co-oct (6%)	0,2-0,4 parts
MEKP-50	1,0-2,0 parts

When needed, the resin can be diluted with 10 % styrene to decrease viscosity to 150-300 mPas. To achieve a good surface cure, 5-7 % of a 1 % paraffine solution in styrene, should be added.

AROPOL 4698 resin can be be coloured with standard colourants/pigments used in polyester resins, and it is advisable to add thixotropic additives when working on vertical, inclined surfaces.

At elevated temperatures, using appropriate peroxides, pressed parts with optimal thermal and electrical characteristics are obtained. AROPOL IS 4698 resin is especially formulated for use in pultrusion.



Responsible Care\*

Ashland is committed to the continuous evolution of technology and service solutions that promote health, safety and environmental protection around the world.  
\* Registered service mark of the American Chemistry Council. © Registered trademark and ™ trademark of Ashland Inc.

**ASHLAND**  
With good chemistry great things happen.™

# Technical Datasheet

Ashland Performance Materials



## AROPOL™ IS 4698

Due to excellent mechanical properties and chemical resistance, AROPOL IS 4698 resin is used in manufacturing a variety of products like; water equipment, silos, shunt boxes, protecting plaques, vessels, pipes, protecting screens, ship equipments etc.

Certificates and approvals	The manufacturing, quality control and distribution of products, by Ashland Performance Materials, are complying with one or more of the following programs or standards: Responsible Care, ISO 9001, ISO 9002, ISO 14001 and OHSAS 18001.
Handling and storage	It is highly recommended that all material is stored at stable temperatures under 25°C preferably indoors, and away from direct sunlight. Prolonged storage outside of recommended conditions can influence liquid resin properties like viscosity and gel time. It is also strongly recommended to mix resin thoroughly before use. Shelf life of AROPOL IS 4698 resin is six (6) months.
Notice	<p>All information presented herein is believed to be accurate and reliable, and is solely for the user's consideration, investigation and verification. The information is not to be taken as an express or implied representation or warranty for which Ashland assumes legal responsibility. Any warranties, including warranties of merchantability or non-infringement of intellectual property rights of third parties, are herewith expressly excluded.</p> <p>Since the user's product formulations, specific use applications and conditions of use are beyond the control of Ashland, Ashland makes no warranty or representation regarding the results which may be obtained by the user. It shall be the responsibility of the user to determine the suitability of any of the products mentioned for the user's specific application.</p> <p>Ashland requests that the user reads, understands and complies with the information contained herein and the current Material Safety Data Sheet.</p>



Responsible Care\*

Ashland is committed to the continuous evolution of technology and service solutions that promote health, safety and environmental protection around the world.  
\* Registered service mark of the American Chemistry Council. © Registered trademark and ™ trademark of Ashland Inc.

**ASHLAND**  
With good chemistry great things happen.™

## Chemical/physical nature

Atlac 580 is a high-grade bisphenol A vinyl ester urethane resin, which combines exceptional chemical resistance and an outstanding combination of heat resistance and flexibility. Furthermore Atlac 580 has very good handling and curing properties. Atlac 580 is resistant to many aqueous acidic salts and alkaline solutions. Especially against alkaline media and hot water Atlac 580 has an outstanding performance.

## Major applications

Atlac 580 can be used in all fabrication methods, but is especially adapted to meet the requirements of filament winding, centrifugal casting and spray-up applications. Extra additional of styrene leads to viscosities which are needed for resin injection moulding techniques.

## Principal properties

Atlac 580 has excellent wet-out and deaeration properties. It produces less foam when peroxides are added with less air inhibition, resulting in a tack free cured surface.

Due to its urethane incorporation, Atlac 580 can be thixotropised easily and shows an improved compatibility with aramid fibre reinforcements. Atlac 580 has a low exotherm in curing allowing thick sections to be fabricated.

## Product specifications upon delivery

Property	Range	Unit	TM
Viscosity, 23°C	400 - 500	mPa.s	2013
Solids content, IR	52 - 54	%	2033
NCO content	0.00 - 0.03	%	2220
Appearance	Hazy	-	2265
Water content	600	ppm	2350
Acid value, as such	5 - 7	mg KOH/g	2401
Gel time from 25 to 35°C	33 - 43	minutes	2625
Cure time from 25°C to peak	46 - 61	minutes	2625
Peak temperature	110 - 135	°C	2625
Colour	Yellow	-	4073

## Remarks

Viscosity: 23°C, Physica, Sp. Z2, 100 s<sup>-1</sup>  
 Gelltime: 2,5 g NL49 + 1,0 g NL63 -10 P +  
 1,0 g Butanox M 50

## Properties of the liquid resin (typical values)

Property	Value	Unit	TM
Density, 23°C	appr. 1074	kg/m <sup>3</sup>	2160
Flash point	appr. 33	°C	2800
Stability, no init., dark, 25°C	6	months	-

## Properties of cast unfilled resin (typical values)

Property	Value	Unit	TM
Density, 20°C	1110	kg/m <sup>3</sup>	-
Tensile strength	83	MPa	ISO 527-2
Mod. of elasticity in tension	3.5	GPa	ISO 527-2
Elongation at break	4.2	%	ISO 527-2
Flexural strength	153	MPa	ISO 178
Mod. of elasticity in bending	3.6	GPa	ISO 178
Impact res. - unnotched sp.	15	kJ/m <sup>2</sup>	ISO 179
Heat deflection temp. (HDT)	115	°C	ISO 75-A
Glass transition temp. (Tg)	132	°C	DIN 53445
Hardness	40	Barcol	2604

## Properties of cast filled resin (typical values)

Property	Value	Unit	TM
Glass content	30	%	-
Density, 20°C	1320	kg/m <sup>3</sup>	-
Tensile strength	105	MPa	ISO 527-2
Mod. of elasticity in tension	7.4	GPa	ISO 527-2
Flexural strength	160	MPa	ISO 178
Mod. of elasticity in bending	6.8	GPa	ISO 178
Mod. of elasticity in bending	6.8	GPa	ISO 178
Impact res. - unnotched sp.	115	kJ/m <sup>2</sup>	ISO 179
Glass transition temp. (Tg)	132	°C	DIN 53445
Linear expansion	30 x 10 <sup>-6</sup>	C-1	ASTM D 696
Thermal conductivity	0.21	W/m.k	DIN 52612

## Curing conditions

All properties are measured at 20°C unless otherwise specified.  
 Cure system: 0.5% NL63-10P, 0.5% NL51P and 1.5% Butanox M-50.

All samples were cured during 24 hrs at ambient temperature, followed by a postcure of 3 hrs at 100°C. Glass mat used OCF M 710 or Vetrotex M 113 (450 g/m<sup>2</sup>).

Version: 001610/5.0  
 Date of issue: May 2006

Head office: DSM Composite Resins AG  
 P.O. Box 1227, 8207 Schaffhausen, Switzerland, Tel. +41 (0)52 644 1212  
 Fax. +41 (0)52 644 1200, Internet site: www.dsmcompositeresins.com

Although the facts and suggestions in this publication are based on our own research and are believed reliable, we cannot assume any responsibility for performance or results obtained through the use of our products herein described, nor do we accept any liability for loss or damages directly or indirectly caused by our products. The user is held to check the quality, safety and all other properties of our product prior to use. Nothing herein is to be taken as permission, inducement or recommendation to practise any patented invention without a license.

**Remarks on cure agents**

Butanox M-50 (Methyl ethyl ketones peroxide 50%), NL 51P (Cobalt octoate, 6% solution) and NL63-10P (Dimethylaniline, 10% solution) are AKZO NOBEL products

**Guidelines before use**

Before use, the resin should be conditioned at a well defined, application dependant temperature (usually 15 °C minimum for a MEKP / Co cure). Stir the product before blending.

**Storage guidelines**

The resin should be stored indoors in the original, unopened and undamaged packaging, in a dry place at temperatures between 5°C and 30°C and the properties might change during storage. Shelf life is reduced at higher temperatures.

The shelf life of styrene containing unsaturated polyesters will be significantly reduced when exposed to light. Store in dark and in 100% light tight containers only.

**Material Safety**

A material safety data sheet for the product is available on request.

**Test methods**

Test methods (TM) referred to in the table(s) are available on request.

Version: 001610/5.0  
Date of issue: May 2006

Head office: DSM Composite Resins AG  
P.O. Box 1227, 8207 Schaffhausen, Switzerland, Tel. +41 (0)52 644 1212  
Fax. +41 (0)52 644 1200, Internet site: [www.dsmcompositeresins.com](http://www.dsmcompositeresins.com)

Although the facts and suggestions in this publication are based on our own research and are believed reliable, we cannot assume any responsibility for performance or results obtained through the use of our products herein described, nor do we accept any liability for loss or damages directly or indirectly caused by our products. The user is held to check the quality, safety and all other properties of our product prior to use. Nothing herein is to be taken as permission, inducement or recommendation to practise any patented invention without a license.



## ®TINUVIN P

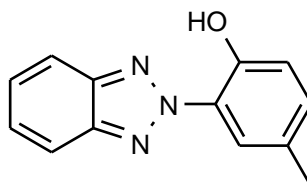
### Benzotriazole UV Absorber

**Characterization**    ®TINUVIN P is an ultraviolet light absorber (UVA) of the hydroxyphenol benzotriazole class, imparting good light stability to a wide variety of polymers during its use.

**Chemical Name**    2-(2H-benzotriazol-2-yl)-p-cresol

**CAS Number**        2440-22-4

**Structure**            ®TINUVIN P



**Molecular weight**    225 g/mol

**Applications**        ®TINUVIN P provides ultraviolet protection in a wide variety of polymers including styrene homo- and copolymers, engineering plastics such as polyesters and acrylic resins, polyvinyl chloride, and other halogen containing polymers and copolymers (e.g. vinylidenes), acetals and cellulose esters. Elastomers, adhesives, polycarbonates, polyurethanes, and some cellulose esters and epoxy materials also benefit from the use of ®TINUVIN P.

**Features/ Benefits**    ®TINUVIN P features a strong absorption of ultraviolet radiation in the 300-400 nm region. It also has a high degree of photostability over long periods of light exposure. The high absorbance combined with photostability and the ability to release absorbed energy in non sensitizing ways make ®TINUVIN P an effective stabilizer against the effects of ultraviolet light.

®TINUVIN P has Food Contact Approvals in rigid and flexible PVC applications for food, consumer care products and pharmaceuticals, preserving the package contents from the detrimental effects of light.

<b>Product Forms</b>	Code:	Appearance:
	®TINUVIN P	slightly yellow powder
	®TINUVIN P FF	slightly yellow, free-flowing granules

**Guidelines for use**    The use levels of ®TINUVIN P range between 0.10% and 0.50%, depending on substrate and performance requirements of the final application. ®TINUVIN P can be used alone or in a variety of blends and combinations with ®IRGAFOS, ®IRGANOX and ®CHIMASSORB stabilizers where often a synergistic performance is observed.

®TINUVIN P may react with various heavy metal ions to form salts or complexes. For example, if ®TINUVIN P comes into contact with iron or cobalt ions, colored complexes are formed. Reducing and oxidizing agents used in polymerization and curing processes have no effect on the stability of ®TINUVIN P.

Distributed by

Date first Edition: Jun-75  
Printing Date: Aug-98

Product Name: ®TINUVIN P

page 1

©Ciba Specialty Chemicals, Inc.

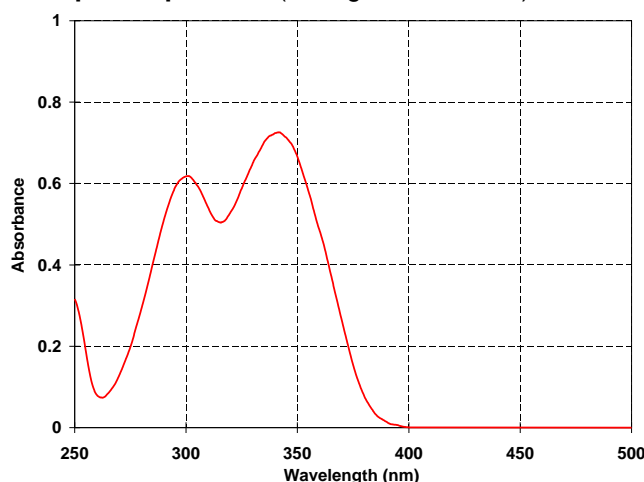
## Physical Properties

Melting Range	128-132°C
Flashpoint	205°C
Specific Gravity (20°C)	1.38 g/cm <sup>3</sup>
Vapor Pressure (20°C)	1.5 E-4 Pa
<b>Solubility (20°C)</b>	% w/w
Water	< 0.01
Acetone	3
Benzene	7
Chloroform	13
Cyclohexane	1
Ethyl acetate	3.5
n-Hexane	0.8
Methanol	0.2
Methylene chloride	16

**Volatility** (pure substance; TGA, heating rate 20°C/min in air)

Weight loss (%)	Temperature (°C)
1.0	153
2.0	170
5.0	190

### Absorption Spectrum (10 mg/l, Chloroform)



®TINUVIN P exhibits strong absorbance in the 300-400 nm region and minimal absorbance in the visible region (> 400 nm) of the spectrum. The absorption maxima are at 301 nm and 341 nm ( $\epsilon = 16150$  l/mol-cm) in chloroform solution.

## Handling & Safety

In accordance with good industrial practice, handle with care and avoid unnecessary personal contact. Protect skin. Prevent contamination of the environment. Avoid dust formation and ignition sources.

For more detailed information please refer to the material safety data sheet.

## Registration

®TINUVIN P is listed on the following Inventories:

Australia: AICS	Canada: DSL	China: First Import
Europe: EINECS	Japan: MITI	Korea: ECL
Philippines: PICCS	USA: TSCA	

®TINUVIN P is approved in many countries for use in food contact applications.

For detailed information refer to our Positive List or contact your local sales office.

**IMPORTANT:** The following supercedes Buyer's documents. **SELLER MAKES NO REPRESENTATION OR WARRANTY, EXPRESS OR IMPLIED, INCLUDING OF MERCHANTABILITY OR FITNESS FOR A PARTICULAR PURPOSE.** No statements herein are to be construed as inducements to infringe any relevant patent. Under no circumstances shall Seller be liable for incidental, consequential or indirect damages for alleged negligence, breach of warranty, strict liability, tort or contract arising in connection with the product(s). Buyer's sole remedy and Seller's sole liability for any claims shall be Buyer's purchase price. Data and results are based on controlled or lab work and must be confirmed by Buyer by testing for its intended conditions of use. The product(s) has not been tested for, and is therefore not recommended for, uses for which prolonged contact with mucous membranes, abraded skin, or blood is intended; or for uses for which implantation within the human body is intended.

**7P-600 C-THANE® RPS HS**  
 (CROMOGLAS RPS HS)  
**Aliphatic Polyurethane Enamel**

Revision: January 2018

**PRODUCT DESCRIPTION** C-Thane RPS HS is an aliphatic polyurethane enamel. Its main properties are:

- High gloss.
- Excellent resistance in weathering.
- High chemical resistance.
- Hard and abrasion resistant, and also, very flexible.
- Good anti-graffiti properties. (Maximum number of cleanings: 3)
- Available in “Colormix Industrial System”. (ICS)
- Fireproof.
- Product ACQPA nº36051.

**INTENDED USES** Topcoat for “long life” painting systems providing excellent chemical resistance in marine environments and high aggressiveness as chemical plants, pulp and paper mills, off shore platforms, refineries, bridges, tanks, etc.,.

<b>PROPERTIES</b>	<b>Finish</b>	Gloss
	<b>Colour</b>	RAL, NCS; other colours on request.
	<b>Components</b>	2
	<b>Mixing ratio (volume)</b>	Resin 7P-601 2 parts Cure 7P-602 1 part
	<b>Pot-life</b>	6 – 8 hours at 20°C
	<b>Volume solids</b>	58,3% (depending on UNE-48274:2003) - Referred to white colour
	<b>Specific weight</b>	1,27 g/mL
	<b>Dry film thickness</b>	35 - 50 µm
	<b>Number of coats</b>	1 – 2
	<b>Theoretical coverage</b>	11,7 m²/L at 50µm Allow for application losses, surface irregularities, etc.
	<b>Application method</b>	Airless or conventional spray, brush or short hair roller for application on floor.

We recommend that the technical data sheet is periodically checked to ensure that it is the most recent version. CIN guarantees that its products conform to the specifications as detailed in the respective technical data sheets. CIN cannot under any circumstances be held responsible for the consequences of technical information given prior to or after purchase of products. This is merely of an advisory nature, given in good faith and to the best of its knowledge, and based on current technical know-how. Claims can only be accepted for products which have manufacturing defects or which do not conform to the purchase order. CIN will, at its discretion, either replace the defective goods or reimburse the customer. CIN cannot accept responsibility for any other loss or damage. All sales are subject to our general terms and conditions of sales that we advise should be read carefully.

**7P-600 C-THANE® RPS HS**  
 (CROMOGLAS RPS HS)  
**Aliphatic Polyurethane Enamel**

Revision: January 2018

**Drying times**

at 23°C and 50 µm:

Dry to touch: 4 hours

Through dry: Max: 12 – 16 hours

Recoat: Min: 12 - 16 hours – Max: Unlimited

Drying times are dependent on temperature, ventilation and film thickness.

Accelerant 25211 can be used in order to reduce drying times. The maximum quantity that can be used is 1 liter for every 20 liters of paint.

If 250 ml (1 can) are used, then drying times at 23 °C and 50 microns thickness are:

Dry to touch: 2 h

Through dry: 5 h

**SURFACE PREPARATION**

Coating performance is proportional to the degree of surface preparation. Refer to application instructions for specific primers being used. Before topcoat, the previous coat, epoxy (or polyurethane when it is coated with itself), must be clean, dry and exempt from any contaminant including salt deposits. If it was necessary, also it is recommended a suitable film roughness. All previous coats must be clean, dry and free of contaminants, including salt deposits. Remove abrasive residues from surface. Adhere to all minimum and maximum topcoat times.

Concrete: Pay attention to complete set (1 month). If necessary, realize the preparation surface using an abrasive sweep, to remove all the laitance. A previous coat of Cromodrol Sealer is recommended. It is also possible to apply a coat of C-Floor E120 as a concrete sealer. For wall structural concrete, see C-Cryl Technical data sheets.

**APPLICATION**

Add cure to resin solution and stir material for 5 minutes. In confined areas ventilate with clean air during application and drying until solvents are removed.

**Environmental applications**

Minimum application temperature 5°C

Relative humidity 0 - 80%

Minimum surface temperature 3°C above dew point

**Application Equipment:**
**Conventional spray**

Recommended

Fluid tip orifice size 0,055 – 0,070 inches (1,39 – 1,77mm)

 Air pressure 3,1 – 4,2 kg/cm<sup>2</sup>

 Fluid pressure 0,7 – 1,4 kg/cm<sup>2</sup>

Thinning 10 – 15 %

**Airless spray**

Recommended

Fluid tip orifice size 0,015 – 0,019 inches (0,38 – 0,48 mm)

Fluid pump 30 : 1

 Fluid pressure 150 – 170 kg/cm<sup>2</sup>

Thinning 0 – 8 %

We recommend that the technical data sheet is periodically checked to ensure that it is the most recent version. CIN guarantees that its products conform to the specifications as detailed in the respective technical data sheets. CIN cannot under any circumstances be held responsible for the consequences of technical information given prior to or after purchase of products. This is merely of an advisory nature, given in good faith and to the best of its knowledge, and based on current technical know-how. Claims can only be accepted for products which have manufacturing defects or which do not conform to the purchase order. CIN will, at its discretion, either replace the defective goods or reimburse the customer. CIN cannot accept responsibility for any other loss or damage. All sales are subject to our general terms and conditions of sales that we advise should be read carefully.

**7P-600 C-THANE® RPS HS**  
 (CROMOGLAS RPS HS)  
**Aliphatic Polyurethane Enamel**

Revision: January 2018

<b>Brush / Roller</b>	
Thinning	5%

Thinner 7Q-680.0000 (CP-81) - Cleaner 7Q-680.0000 (CP-81)

**ADDITIONAL INFORMATION**
**Curing mechanism** – By solvent release and reaction between components

**Volatile Organic Compounds (COV)**

EU limit for this product (cat. A/j): 500 g/L  
 This product contains max. 458 g/L COV. (TVOCC: 41%) \*)  
 Supplying form: < 417 g/L (TVOC: < 37%)  
 VOC Resin: 401 g/L (TVOC: 30%)  
 VOC Cure: 414 g/L (TVOC: 40%)  
 VOC Thinner: 862 g/L (TVOC: 100%)  
 VOC Cleaner: 862 g/L (TVOC: 100%)

\*) The VOC value shown above refers to a ready for use product, as tinted, thinned, etc in accordance with our recommendations. We are not responsible for products obtained by mixing products with are different from those we have recommended and we must draw attention to the responsibility of anyone involved within the supply chain not to infringe Directive 2004/12/CE.

**Flash Point (Closed Cup)**

Resin	30°C
Cure	26°C
Thinner	20°C (7Q-680.0000)
Cleaner	20°C (7Q-680.0000)

**Packaging**

Resin	13,3, 2,7 and 0,5 L
Cure	6,7, 1,3 and 0,25 L

**Storage**

Stored indoors in original containers at 5 to 40°C, Resin: 24 months, Cure: 18 months.

**PAINT SYSTEMS**

Steel: All kind of primers and intermediates epoxy.

Concrete on walls (non-structural): After prepared and sealed surface, to apply two coats of C-Thane RPS-HS thinned at 10%.

Concrete on walls (structural): See C-Cryl Technical Data Sheets.

Concrete floors of low to medium mechanical aggression (&lt;1000 kg): Realize the surface preparation according C-Floor E120 Technical Data Sheet and seal the porosity with the same paint. Apply two coats of C-Thane RPS-HS, with 24 hours between them. Wait 5 – 7 weeks for total curing system.

Concrete floors of very high mechanical effects (&gt;1000 kg): If you want a smooth finish, it is

We recommend that the technical data sheet is periodically checked to ensure that it is the most recent version. CIN guarantees that its products conform to the specifications as detailed in the respective technical data sheets. CIN cannot under any circumstances be held responsible for the consequences of technical information given prior to or after purchase of products. This is merely of an advisory nature, given in good faith and to the best of its knowledge, and based on current technical know-how. Claims can only be accepted for products which have manufacturing defects or which do not conform to the purchase order. CIN will, at its discretion, either replace the defective goods or reimburse the customer. CIN cannot accept responsibility for any other loss or damage. All sales are subject to our general terms and conditions of sales that we advise should be read carefully.

**7P-600 C-THANE® RPS HS**  
 (CROMOGLAS RPS HS)  
**Aliphatic Polyurethane Enamel**

Revision: January 2018

recommended to use the C-Floor products.

Non-metallic surfaces (non-immersion): Including polyester and pvc surfaces or others. In these cases, sand the surface and apply one coat of C-Pox Primer FA. Complete the system with two coats of C-Thane RPS HS. If a better mechanical protection is required, apply a coat of C-Thane Varnish Gloss, Satin or Matt according on requested brightness.

Intumescent paints: Guarantee that the intumescent paint is totally dry before applying the topcoat. In case of aqueous intumescent paints we recommend to carry out a previous test in order to verify the correct behaviour of the topcoat.

**HOMOLOGATIONS AND CERTIFICATES**

Complies the Norm 48274:2003

C-Thane RPS HS is certified according to EN -13501-1 to meet Bs1d0.

This paint system is certified by ACQPA according to standard EN ISO 12944-6 for environments with class C4 in environmental corrosivity, defined in the standard EN ISO 12944-2.

Cincoat Primer IZS920	75 µm
C-Pox S130 FD	125 µm
C-Thane RPS-HS	50 µm

Corrosivity category C4 according to EN ISO 12944-6, high durability of painting system:

C-Pox Primer ZP200 HB	90µm
C-Pox S140 Mio FD	120µm
C-Thane RPS-HS	50µm

Corrosivity category C5M according to EN ISO 12944-6, high durability of painting system:

C-Pox Primer ZN800	75µm
C-Pox S990 Mio FD	85µm
C-Thane RPS-HS	80µm

**SAFETY PRECAUTIONS**

Protect the eyes and skin from contact, gloves, goggles and appropriate clothing should be worn. Keep out of the reach of children. Use only in well ventilated areas. Do not empty into drains. Keep the container properly sealed and stored in the correct place. Take correct measures when transporting the product so as to avoid any accidents that could rupture the can or cause damage to the packaging. Ensure that the container is correctly stacked in a safe area. Do not store or use the product in extreme temperature conditions. Always take account of the appropriate legislation relating to the environmental and Health and Safety at Work. For more information **it is essential to read the label on the container and the product MATERIAL SAFETY DATA SHEET of this product, its components and all complementary products referred on Technical Data Sheet.**

We recommend that the technical data sheet is periodically checked to ensure that it is the most recent version. CIN guarantees that its products conform to the specifications as detailed in the respective technical data sheets. CIN cannot under any circumstances be held responsible for the consequences of technical information given prior to or after purchase of products. This is merely of an advisory nature, given in good faith and to the best of its knowledge, and based on current technical know-how. Claims can only be accepted for products which have manufacturing defects or which do not conform to the purchase order. CIN will, at its discretion, either replace the defective goods or reimburse the customer. CIN cannot accept responsibility for any other loss or damage. All sales are subject to our general terms and conditions of sales that we advise should be read carefully.

# PRODUCT DATA SHEET

## SikaCor® EG-5

### 2-PACK AY-PUR TOP COAT

#### DESCRIPTION

SikaCor® EG-5 is a 2-pack acrylic polyurethane top coat.  
Suitable for use in hot and tropical climatic conditions.

#### USES

SikaCor® EG-5 may only be used by experienced professionals.

In combination with 2-pack primer and intermediate coats of the SikaCor® and Sika® Permacor® product range for heavy duty corrosion protection of steel structures.

Also suitable for submerged steel.

#### CHARACTERISTICS / ADVANTAGES

Combined with 2-pack epoxy primer and intermediate coats:

- Very good corrosion protection properties
- Excellent chemical, weather and colour stability
- Tough elastic and hard but not brittle
- Largely insensitive against shock and impact

#### APPROVALS / CERTIFICATES

- Approved according to German standard 'TL/TP-KOR-Stahlbauten', page 87 and page 94.
- In combination with SikaCor® PUR Accelerator, SikaCor® EG-5 is approved according to German standard 'TL/TP-KOR-Stahlbauten', page 97.

#### PRODUCT INFORMATION

Packaging	SikaCor® EG-5	30 kg and 10 kg net.
Appearance / Colour	RAL and NCS colour shades	
Shelf life	2 years from date of manufacture	
Storage conditions	In originally sealed containers in a cool and dry environment.	
Density	~1.3 kg/l	
Solid content	~61 % by volume ~74 % by weight	

## TECHNICAL INFORMATION

<b>Chemical Resistance</b>	Weather, water, sewage, seawater, smoke, de-icing salts, acid and lye vapours, oils, grease and short term exposure to fuels and solvents.
<b>Temperature Resistance</b>	Dry heat up to +150 °C, short term up to +180 °C Damp heat up to approximately +50 °C In case of higher temperatures please consult Sika.

## SYSTEMS

<b>Systems</b>	<u>Steel:</u> Used as top coat on 2-pack primer and intermediate coats of the SikaCor® and Sika® Permacor® product range.  <u>Galvanized steel, stainless steel and aluminium:</u> 1 x SikaCor® EG-1 or SikaCor® EG-1 VHS 1 x SikaCor® EG-5  In case of light colours a second top coat of SikaCor® EG-5 may become necessary to achieve perfect opacity.
----------------	--

## APPLICATION INFORMATION

<b>Mixing Ratio</b>	Components A : B		
	By weight	90 : 10	
	By volume	7.1 : 1	
<b>Thinner</b>	Sika® Thinner EG If necessary maximum 5 % Sika® Thinner EG may be added to adapt the viscosity.		
<b>Consumption</b>	Theoretical material-consumption/VOC without loss for medium dry film thickness:		
	Dry film thickness	60 µm	80 µm
	Wet film thickness	100 µm	130 µm
	Consumption	~0.130 kg/m <sup>2</sup>	~0.170 kg/m <sup>2</sup>
	VOC	~33.2 g/m <sup>2</sup>	~44.3 g/m <sup>2</sup>
<b>Product Temperature</b>	+5 °C min. / +35 °C max.		
<b>Relative Air Humidity</b>	Maximum 85 %, except the surface temperature is significantly higher than the dew point temperature, it shall be at least 3 °C above dew point. The surface must be dry and free from ice.		
<b>Surface Temperature</b>	Minimum +5 °C 0 °C by adding SikaCor® PUR Accelerator		
<b>Pot Life</b>	+10 °C	~7 h	~5 h *
	+20 °C	~5 h	~3 h *
	+30 °C	~4 h	~2 h *
	(*Adding 1 % by weight SikaCor® PUR Accelerator)		
<b>Drying Stage 6</b>	<b>Dry film thickness 80 µm</b>	(ISO 9117-5)	
	+5 °C	21 h	
	+10 °C	18 h	
	+20 °C	14 h	
	+40 °C	3 h	
	+80 °C	45 min	

Adding 1 % by weight SikaCor® PUR Accelerator

	Dry film thickness 80 µm
0 °C	52 h
+5 °C	18 h
+10 °C	13 h
+20 °C	5 h

(ISO 9117-5)

**Waiting Time / Overcoating** Minimum waiting time until drying stage 6 is achieved to unlimited maximum time.

Prior to further applications possible contamination must be removed (see page 3 surface preparation).

**Drying time** **Final drying time**  
Depending on film thickness and temperature full hardness is achieved after 1 to 2 weeks. Tests of the completed coating system should only be carried out after final curing.

## APPLICATION INSTRUCTIONS

### SURFACE PREPARATION

#### Steel:

Blast cleaning to Sa 2 ½ according to ISO 12944, part 4. Free from dirt, oil and grease.

#### Galvanized steel, stainless steel and aluminium:

Free from dirt, oil, grease and corrosion products. In case of permanent immersion and condensation the surfaces must be slightly sweep blasted with non-ferrous abrasives.

Contaminated surfaces for example galvanized or primed areas we recommend to clean with SikaCor® Wash.

### MIXING

Stir component A very thoroughly using an electric mixer (start slowly, then increase up to approximately 300 rpm). Add component B carefully and mix both components very thoroughly (including sides and bottom of the container). Mix for at least 3 minutes until a homogeneous mixture is achieved. Fill mixed material into clean container and mix again shortly as described above.

### APPLICATION

The method of application has a major effect on achieving uniform thickness and appearance. Spray application will give the best results. The indicated dry film thickness is easily achieved by airless spray. Adding solvents reduces the sag resistance and the dry film thickness. In case of application by roller or brush, additional applications may become necessary to achieve the required coating thickness, depending on type of construction, site conditions, colour shade etc. Prior to major coating operations a test application on site may be useful to ensure the selected application method will provide the requested results.

#### By brush and roller

#### Conventional high pressure spraying:

- Nozzle size 1.5 - 2.5 mm
- Pressure 3 - 5 bar
- Oil and water trap is compulsory

#### Airless-spraying:

- Pressure minimum 180 bar
- Nozzle size 0.38 - 0.53 mm (0.015 - 0.021 inch)
- Spraying angle 40° - 80°

### CLEANING OF EQUIPMENT

SikaCor® Cleaner

Spraying equipment must be rinsed with Sika® Thinner EG before using SikaCor® EG-5.

## BASIS OF PRODUCT DATA

All technical data stated in this Data Sheet are based on laboratory tests. Actual measured data may vary due to circumstances beyond our control.

## LOCAL RESTRICTIONS

Note that as a result of specific local regulations the declared data and recommended uses for this product may vary from country to country. Consult the local Product Data Sheet for the exact product data and uses.

## ECOLOGY, HEALTH AND SAFETY

For information and advice on the safe handling, storage and disposal of chemical products, users shall refer to the most recent Safety Data Sheet (SDS) containing physical, ecological, toxicological and other safety-related data.

## LEGAL NOTES

The information, and, in particular, the recommendations relating to the application and end-use of Sika products, are given in good faith based on Sika's current knowledge and experience of the products when properly stored, handled and applied under normal conditions in accordance with Sika's recommendations. In practice, the differences in materials, substrates and actual site conditions are such that no warranty in respect of merchantability or of fitness for a particular purpose, nor any liability arising out of any legal relationship whatsoever, can be inferred either from this information, or from any written recommendations, or from any other advice offered. The user of the product must test the product's suitability for the intended application and purpose. Sika reserves the right to change the properties of its products. The proprietary rights of third parties must be observed. All orders are accepted subject to our current terms of sale and delivery. Users must always refer to the most recent issue of the local Product Data Sheet for the product concerned, copies of which will be supplied on request.

### SIKA NORTHERN GULF

Bahrain / Qatar / Kuwait  
Tel: +973 177 38188  
sika.gulf@bh.sika.com  
gcc.sika.com

### SIKA SOUTHERN GULF

UAE / Oman / SIC  
Tel: +971 4 439 8200  
info@ae.sika.com  
gcc.sika.com

### SIKA SAUDI ARABIA

Riyadh / Jeddah / Damman  
Tel: +966 11 217 6532  
info@sa.sika.com  
gcc.sika.com



ISO 9001: Sika UAE LLC,  
Sika Gulf B.S.C. (c),  
Sika Saudi Arabia Co. Ltd,  
Sika Qatar LLC  
ISO 14001: Sika UAE LLC,  
Sika Gulf B.S.C. (c),  
Sika Saudi Arabia Co. Ltd  
OHSAS: Sika UAE LLC,  
Sika Gulf B.S.C. (c)

All products are supplied  
under a management  
system certified to conform  
to the requirements of the  
quality, environmental and  
occupational health &  
safety standards ISO 9001,  
ISO 14001 and OHSAS  
18001.

### Product Data Sheet

SikaCor® EG-5

October 2016, Version 02.03  
020602000040000004

SikaCorEG-5-en-AE-(10-2016)-2-3.pdf



## **Appendix VII**

Experimental data



Table 11.03 - Summary of properties of polyester profiles								
Property	Method	Unit	UP_WV_0	UP_NV_0	UP_WV_025	UP_NV_025	UP_WV_050	UP_NV_050
IMC	Calcination	[%]	71.9 ± 1.06	72.5 ± 0.62	71.6 ± 1.29	73 ± 1.73	72.4 ± 1.03	69.3 ± 1.54
Colour	CIE L*a*b* 1976	L*/a*/b*	79.38 / -4.12 / 3.64	78.99 / -3.84 / 3.35	81.12 / -1.32 / 3.08	80.79 / -1.11 / 4.52	81.47 / -1.13 / 5.22	80.87 / -0.93 / 6.05
Gloss	Glossmeter	(-)	23.4 ± 0.8	22 ± 0.9	26.5 ± 0.9	32.6 ± 1.9	30.7 ± 1.2	22.3 ± 1.4
$T_g$	DMA	$T_g$ ( $E'_{onset}$ ) [°C]	104.1 ± 2.8	--	--	--	--	--
		$T_g$ (tan d) [°C]	125.4 ± 2.0	--	--	--	--	--
Mechanical properties	Tensile tests	$\sigma_{tu}$ [MPa]	432.7 ± 34.3	521.4 ± 11.5	438.7 ± 26.5	449.7 ± 27.2	470.7 ± 34.8	451.4 ± 26.6
		$E_t$ [GPa]	42.4 ± 0.63	42.0 ± 0.98	43.0 ± 1.3	43.0 ± 1.65	42.5 ± 1.83	37.5 ± 1.76
	Compressive tests	$\sigma_{cu}$ [MPa]	725 ± 62.1	805.1 ± 24.6	607.2 ± 25.2	613 ± 26.8	560.8 ± 39.6	593.1 ± 41.2
	Flexural tests	$\sigma_{fu}$ [MPa]	554.1 ± 14.5	497.6 ± 24.4	477.2 ± 26.8	489.6 ± 21.4	551.1 ± 20.4	517.9 ± 11.4
		$E_f$ [GPa]	32.3 ± 1.35	32.5 ± 0.62	32.6 ± 0.58	32.0 ± 0.42	31.8 ± 1.36	29.0 ± 0.56
	In-plane shear tests	$t_{max}$ [MPa]	62.9 ± 1.51	63.3 ± 2.15	52.3 ± 2.39	51.9 ± 1.27	45.9 ± 3.74	54.4 ± 0.46
		G [GPa]	3.6 ± 0.36	3.0 ± 0.32	4.2 ± 0.72	3.2 ± 0.18	3.0 ± 0.23	3.0 ± 0.52
	Interlaminar shear tests	$\sigma_{sbs}$ [MPa]	40.6 ± 2.1	41 ± 1.75	39.9 ± 0.55	38.1 ± 0.47	31.2 ± 3.1	38.1 ± 1.2

Table 11.04 - Summary of properties of vinylester profiles								
Property	Method	Unit	VE_WV_0	VE_NV_0	VE_WV_025	VE_NV_025	VE_WV_050	VE_NV_050
IMC	Calcination	[%]	73,7 ± 0,34	71,6 ± 0,49	70,4 ± 1,14	71 ± 1,3	71,6 ± 0,49	70,7 ± 0,47
Colour	CIE L*a*b* 1976	L*/a*/b*	80,86 / -0,81 / 4,92	79,89 / -1,57 / 5,54	80,44 / -1,02 / 4,38	79,64 / -1,15 / 4,58	79,36 / -1,02 / 4,48	78,79 / -1,35 / 5,33
Gloss	Glossmeter	(-)	11,7 ± 0,4	28,4 ± 1,9	46,2 ± 2,1	44,3 ± 1,8	57,5 ± 2,4	47,7 ± 1,6
$T_g$	DMA	$T_g$ ( $E'_{onset}$ ) [°C]	98.9 ± 5.6	--	--	--	--	--
		$T_g$ (tan d) [°C]	118.2 ± 4.3	--	--	--	--	--
Mechanical properties	Tensile tests	$\sigma_{tu}$ [MPa]	475.4 ± 16.85	471.3 ± 12.99	421.8 ± 23.59	420.4 ± 39.8	444.6 ± 26.67	439.4 ± 8.37
		$E_t$ [GPa]	39.3 ± 1.6	42.6 ± 0.28	41.9 ± 0.23	39.8 ± 0.47	37.4 ± 1.12	40.7 ± 1.32
	Compressive tests	$\sigma_{cu}$ [MPa]	753 ± 29.76	540 ± 42.82	633.2 ± 58.42	567.7 ± 47.03	555.9 ± 122.23	545.3 ± 55.38
	Flexural tests	$\sigma_{fu}$ [MPa]	563.6 ± 14.91	546.7 ± 15.43	531.8 ± 15.42	585.8 ± 12.08	563.3 ± 7.61	557.3 ± 16.89
		$E_f$ [GPa]	32 ± 1.23	32.9 ± 0.58	30.2 ± 0.14	32.8 ± 0.7	30.2 ± 1.17	32.2 ± 0.61
	In-plane shear tests	$t_{max}$ [MPa]	71.9 ± 0.13	64 ± 1.08	64.5 ± 2.52	66.6 ± 1.91	57.4 ± 1.28	56.4 ± 2.99
		G [GPa]	4.7 ± 0.07	3.4 ± 0.22	3.8 ± 0.5	4.5 ± 0.25	3.9 ± 0.54	3.5 ± 0.33
	Interlaminar shear tests	$\sigma_{sbs}$ [MPa]	41.5 ± 0.87	42.6 ± 2.13	36 ± 0.67	36.1 ± 0.52	31.8 ± 1.09	34.2 ± 0.52

Figure 12.06 - UP specimens colour change ( $\Delta E^*$ ) during chemical ageing																		
Temperature				23 °C					50 °C					70 °C				
Weeks of exposure				0	1	4	8	16	0	1	4	8	16	0	1	4	8	16
Profile	Exposure phase	Environment	Superficial protection	$\Delta E^*$														
UP_WV_0	Immersion	Acidic	--	0	1.31	3.10	2.83	2.23	0	2.78	3.30	2.72	3.68	0	4.14	5.08	10.95	9.29
		Alkaline	--	0	7.71	8.44	7.93	9.63	0	8.55	9.76	9.56	9.26	0	8.55	9.31	10.31	7.73
		Neutral	--	0	2.61	2.08	1.00	1.69	0	1.62	1.50	1.64	0.92	0	1.26	1.41	1.64	3.74
	Vapour	Acidic	--	0	0.76	1.10	1.09	2.02	0	1.55	1.51	0.84	1.75	0	1.10	2.34	3.91	9.58
		Alkaline	--	0	1.87	1.39	2.01	1.83	0	1.87	1.70	1.05	1.45	0	1.44	0.69	1.34	1.31
		Neutral	--	0	1.23	1.23	0.69	1.70	0	1.51	2.08	1.61	1.53	0	1.07	0.56	1.56	0.82
		Acidic	SIKA	0	0.05	0.19	0.44	0.32	0	0.09	0.38	0.38	0.40	0	0.39	1.75	3.11	10.53
		Alkaline		0	0.04	0.15	0.35	0.34	0	0.07	0.30	0.44	0.49	0	0.22	1.01	1.79	1.43
		Neutral		0	0.04	0.17	0.37	0.37	0	0.12	0.48	0.59	0.77	0	0.17	0.75	1.32	2.65

Figure 12.07 - VE specimens colour change ( $\Delta E^*$ ) during chemical ageing																		
Temperature				23 °C					50 °C					70 °C				
Weeks of exposure				0	1	4	8	16	0	1	4	8	16	0	1	4	8	16
Profile	Exposure phase	Environment	Superficial protection	$\Delta E^*$														
VE_WV_0	Immersion	Acidic	--	0	3.80	2.63	2.73	4.79	0	2.96	5.82	7.39	8.13	0	5.78	7.78	9.77	12.60
		Alkaline	--	0	4.18	4.32	5.52	4.08	0	4.37	5.82	6.66	6.95	0	4.13	5.14	6.44	7.08
		Neutral	--	0	5.45	5.65	4.51	5.41	0	6.06	5.11	4.36	5.00	0	3.98	5.86	7.78	6.33
	Vapour	Acidic	--	0	4.50	6.43	6.29	6.44	0	6.45	6.23	5.29	5.22	0	4.52	5.77	7.06	9.64
		Alkaline	--	0	5.65	6.20	6.17	6.38	0	5.78	6.62	4.78	5.68	0	4.49	6.75	9.10	9.02
		Neutral	--	0	4.42	4.38	6.14	4.42	0	6.28	5.50	5.97	6.24	0	4.35	6.18	8.08	5.99
		Acidic	SIKA	0	0.05	0.18	0.32	0.29	0	0.11	0.45	0.28	0.47	0	0.49	2.20	3.90	7.88
		Alkaline		0	0.05	0.22	0.30	0.30	0	0.08	0.32	0.40	0.56	0	0.13	0.61	1.08	1.08
		Neutral		0	0.04	0.16	0.47	0.40	0	0.09	0.37	0.58	0.69	0	0.10	0.44	0.79	1.58

Figure 12.08 - Gloss retention of UP specimens during chemical ageing																		
Temperature				23 °C					50 °C					70 °C				
Weeks of exposure				0	1	4	8	16	0	1	4	8	16	0	1	4	8	16
Profile	Exposure phase	Environment	Superficial protection	Gloss retention														
UP_WV_0	Immersion	Acidic	--	100%	103%	86%	84%	87%	100%	105%	90%	81%	87%	100%	84%	81%	70%	65%
		Alkaline	--	100%	39%	24%	22%	8%	100%	26%	8%	6%	6%	100%	24%	15%	7%	4%
		Neutral	--	100%	74%	71%	61%	57%	100%	65%	43%	41%	46%	100%	104%	96%	85%	80%
	Vapour	Acidic	--	100%	103%	100%	97%	86%	100%	96%	98%	95%	85%	100%	89%	77%	83%	59%
		Alkaline	--	100%	92%	83%	73%	70%	100%	76%	70%	64%	66%	100%	76%	75%	66%	45%
		Neutral	--	100%	100%	104%	100%	77%	100%	93%	93%	85%	77%	100%	90%	84%	79%	71%
		Acidic	SIKA	100%	93%	85%	83%	92%	100%	94%	89%	86%	76%	100%	95%	89%	81%	19%
		Alkaline		100%	96%	92%	80%	90%	100%	100%	99%	91%	64%	100%	71%	41%	37%	13%
		Neutral		100%	99%	98%	76%	95%	100%	89%	78%	84%	65%	100%	96%	64%	43%	29%

Figure 12.09 - Gloss retention of VE specimens during chemical ageing																		
Temperature				23 °C					50 °C					70 °C				
Weeks of exposure				0	1	4	8	16	0	1	4	8	16	0	1	4	8	16
Profile	Exposure phase	Environment	Superficial protection	Gloss retention														
VE_WV_0	Immersion	Acidic	--	100%	78%	81%	76%	68%	100%	100%	72%	60%	40%	100%	60%	55%	45%	60%
		Alkaline	--	100%	81%	68%	63%	52%	100%	93%	58%	24%	26%	100%	69%	38%	25%	12%
		Neutral	--	100%	98%	103%	85%	73%	100%	94%	78%	81%	79%	100%	98%	84%	70%	70%
	Vapour	Acidic	--	100%	81%	85%	86%	88%	100%	84%	89%	78%	82%	100%	80%	72%	65%	70%
		Alkaline	--	100%	94%	94%	87%	86%	100%	79%	68%	67%	66%	100%	88%	78%	68%	62%
		Neutral	--	100%	83%	93%	87%	83%	100%	96%	85%	81%	82%	100%	98%	91%	84%	81%
		Acidic	SIKA	100%	97%	94%	93%	97%	100%	94%	87%	77%	84%	100%	78%	57%	51%	25%
		Alkaline		100%	94%	88%	82%	102%	100%	94%	87%	73%	83%	100%	80%	60%	55%	52%
		Neutral		100%	95%	90%	80%	98%	100%	92%	83%	77%	68%	100%	83%	75%	69%	62%

**Figure 12.11 - Compressive strength retention during chemical ageing**

Material			Polyester				Vinylester				Polyester				Vinylester				
Weeks of exposure			0	1	4	8	16	1	4	8	16	1	4	8	16	1	4	8	16
Exposure phase	Environment	Temperature	Retention of compressive strength								Error bars								
<b>Immersion</b>	Neutral	23 °C	100.0%	104.0%	94.0%	88.0%	91.5%	100.0%	98.4%	96.7%	100.0%	4.8%	5.0%	4.1%	4.1%	5.2%	5.3%	5.2%	5.0%
		50 °C	100.0%	101.0%	96.5%	93.0%	89.0%	96.0%	98.5%	97.0%	86.0%	4.9%	4.9%	4.9%	4.1%	4.7%	5.1%	5.3%	4.3%
		70 °C	100.0%	96.0%	93.0%	86.0%	84.1%	104.0%	98.0%	96.0%	91.3%	4.9%	4.3%	4.5%	4.4%	4.8%	5.2%	4.4%	4.7%
	Acidic	23 °C	100.0%	95.0%	97.1%	94.3%	92.0%	97.0%	90.1%	80.3%	96.2%	5.1%	4.8%	4.3%	4.6%	5.1%	4.8%	4.0%	4.5%
		50 °C	100.0%	105.0%	100.0%	100.0%	96.5%	99.0%	88.0%	76.0%	56.2%	5.7%	4.9%	4.7%	4.5%	5.4%	4.6%	3.8%	2.9%
		70 °C	100.0%	95.0%	91.3%	82.5%	59.5%	99.0%	92.4%	84.7%	55.5%	4.9%	5.0%	4.5%	2.9%	5.0%	4.9%	4.2%	3.0%
	Alkaline	23 °C	100.0%	103.0%	61.2%	22.4%	27.4%	96.0%	98.8%	97.6%	80.2%	5.5%	3.0%	1.1%	1.2%	4.6%	5.0%	4.7%	4.0%
		50 °C	100.0%	96.0%	80.0%	25.0%	0.0%	104.0%	80.5%	61.0%	55.3%	4.7%	4.2%	1.3%	0.0%	5.1%	3.8%	3.3%	2.7%
		70 °C	100.0%	98.0%	53.5%	7.0%	0.0%	98.0%	60.0%	60.0%	50.3%	5.3%	2.8%	0.3%	0.0%	4.4%	3.1%	2.9%	2.5%
<b>Vapour</b>	Neutral	23 °C	100.0%	104.0%	100.0%	100.0%	98.6%	105.0%	99.3%	98.6%	86.0%	4.9%	5.3%	5.4%	5.3%	5.7%	5.4%	5.3%	4.0%
		50 °C	100.0%	104.0%	97.5%	95.0%	85.4%	100.0%	97.0%	94.0%	88.4%	4.8%	4.5%	4.3%	4.5%	4.7%	4.6%	4.9%	4.8%
		70 °C	100.0%	100.0%	86.4%	72.7%	77.1%	100.0%	90.0%	80.0%	97.2%	5.1%	4.7%	3.6%	3.9%	5.5%	4.8%	4.3%	5.1%
	Acidic	23 °C	100.0%	99.0%	97.0%	94.0%	87.1%	105.0%	99.9%	99.8%	103.8%	4.9%	4.8%	5.0%	4.7%	5.4%	4.9%	5.3%	5.1%
		50 °C	100.0%	99.0%	96.5%	93.0%	80.6%	97.0%	97.5%	95.0%	92.8%	5.4%	4.7%	4.5%	4.4%	5.2%	5.3%	4.6%	4.2%
		70 °C	100.0%	96.0%	93.0%	86.0%	83.7%	101.0%	79.8%	70.0%	66.9%	4.4%	4.4%	4.7%	4.2%	5.4%	4.0%	3.8%	3.3%
	Alkaline	23 °C	100.0%	101.0%	95.0%	89.9%	95.8%	98.0%	92.8%	85.6%	96.7%	5.4%	5.1%	4.2%	5.2%	4.6%	4.9%	4.5%	4.5%
		50 °C	100.0%	102.0%	97.5%	95.0%	92.2%	100.0%	97.0%	94.0%	91.9%	5.3%	5.0%	4.7%	4.8%	5.0%	4.6%	4.9%	4.5%
		70 °C	100.0%	100.0%	97.0%	94.0%	90.1%	97.0%	95.0%	90.0%	87.8%	4.7%	5.3%	5.2%	4.4%	4.5%	5.0%	4.8%	4.2%

**Figure 12.13 - In-plane shear strength retention during chemical ageing**

Material			Polyester				Vinylester				Polyester				Vinylester				
Weeks of exposure			0	1	4	8	16	1	4	8	16	1	4	8	16	1	4	8	16
Exposure phase	Environment	Temperature	Retention of in-plane shear strength								Error bars								
<b>Immersion</b>	Neutral	23 °C	100.0%	103.0%	96.2%	92.5%	108.7%	105.0%	98.4%	96.9%	108.0%	4.9%	5.1%	4.3%	5.2%	4.7%	4.7%	4.7%	5.0%
		50 °C	100.0%	105.0%	100.0%	99.9%	90.0%	95.0%	94.3%	88.5%	90.7%	4.9%	5.2%	5.1%	4.1%	4.4%	4.6%	4.3%	4.7%
		70 °C	100.0%	103.0%	96.5%	93.0%	91.2%	97.0%	100.5%	101.0%	97.7%	5.6%	4.9%	4.8%	4.9%	4.5%	5.0%	5.0%	4.5%
	Acidic	23 °C	100.0%	101.0%	101.5%	102.9%	108.9%	95.0%	97.1%	94.3%	106.4%	4.8%	4.6%	4.9%	4.9%	5.2%	5.2%	5.1%	5.0%
		50 °C	100.0%	99.0%	92.1%	84.2%	82.5%	103.0%	87.3%	74.6%	74.1%	5.0%	4.9%	4.3%	4.0%	4.8%	4.8%	3.4%	3.9%
		70 °C	100.0%	96.0%	87.0%	74.0%	69.2%	103.0%	81.5%	63.0%	65.3%	4.3%	4.4%	3.4%	3.2%	5.6%	4.0%	3.2%	3.6%
	Alkaline	23 °C	100.0%	96.0%	66.1%	32.2%	28.4%	101.0%	88.6%	77.3%	81.7%	5.1%	3.5%	1.6%	1.3%	4.6%	4.2%	3.8%	3.7%
		50 °C	100.0%	99.0%	53.6%	7.2%	0.0%	105.0%	91.0%	68.0%	56.1%	4.9%	2.8%	0.4%	0.0%	5.2%	4.4%	3.4%	3.0%
		70 °C	100.0%	104.0%	54.9%	9.8%	0.0%	97.0%	92.0%	71.0%	50.0%	5.2%	2.8%	0.5%	0.0%	5.3%	4.9%	3.4%	2.5%
<b>Vapour</b>	Neutral	23 °C	100.0%	95.0%	98.6%	97.1%	105.0%	98.0%	99.5%	98.9%	110.6%	4.7%	4.6%	4.9%	4.9%	4.7%	4.9%	4.9%	5.1%
		50 °C	100.0%	105.0%	94.2%	88.4%	95.1%	103.0%	95.3%	90.6%	93.4%	4.9%	4.5%	4.2%	4.3%	4.8%	4.6%	4.4%	4.5%
		70 °C	100.0%	104.0%	88.8%	77.7%	82.4%	99.0%	91.0%	82.1%	94.4%	5.1%	4.4%	4.2%	3.9%	5.0%	4.7%	4.4%	4.6%
	Acidic	23 °C	100.0%	103.0%	95.4%	90.8%	105.0%	95.0%	100.0%	100.0%	112.0%	4.7%	5.2%	4.9%	5.7%	4.3%	4.7%	4.8%	6.0%
		50 °C	100.0%	96.0%	96.0%	91.9%	85.2%	99.0%	96.4%	92.7%	99.0%	4.9%	4.8%	4.2%	4.2%	4.5%	4.9%	4.4%	4.8%
		70 °C	100.0%	99.0%	100.8%	101.7%	99.0%	98.0%	100.3%	100.7%	98.0%	4.9%	5.4%	5.3%	4.8%	5.2%	4.9%	5.3%	4.9%
	Alkaline	23 °C	100.0%	104.0%	103.6%	107.2%	113.3%	103.0%	99.7%	99.4%	110.0%	4.9%	5.5%	5.7%	6.0%	5.5%	5.0%	4.7%	5.6%
		50 °C	100.0%	100.0%	93.2%	86.4%	87.6%	98.0%	97.2%	94.5%	94.1%	4.9%	4.4%	4.1%	4.6%	4.5%	5.1%	4.3%	4.5%
		70 °C	100.0%	96.0%	95.5%	91.0%	86.0%	96.0%	95.0%	90.0%	91.2%	5.1%	4.9%	4.5%	3.9%	4.7%	5.0%	4.7%	4.9%

**Figure 12.15 - Interlaminar shear strength retention during chemical ageing**

Material			Polyester				Vinylester				Polyester				Vinylester				
Weeks of exposure			0	1	4	8	16	1	4	8	16	1	4	8	16	1	4	8	16
Exposure phase	Environment	Temperature	Retention of interlaminar shear strength								Error bars								
<b>Immersion</b>	Neutral	23 °C	100.0%	95.0%	95.7%	91.4%	99.9%	100.0%	97.5%	95.0%	104.6%	4.5%	4.9%	4.6%	4.6%	4.9%	5.1%	4.4%	4.9%
		50 °C	100.0%	104.0%	99.3%	98.6%	93.7%	95.0%	98.5%	97.0%	86.0%	5.4%	5.4%	4.6%	4.5%	4.7%	4.6%	4.8%	4.3%
		70 °C	100.0%	96.0%	97.0%	94.0%	86.8%	100.0%	98.0%	96.0%	81.6%	5.0%	4.6%	5.1%	4.4%	5.2%	5.2%	5.1%	4.3%
	Acidic	23 °C	100.0%	99.0%	99.5%	99.0%	97.4%	98.0%	102.4%	104.7%	97.3%	4.9%	5.1%	5.2%	4.8%	5.2%	4.9%	5.0%	5.0%
		50 °C	100.0%	105.0%	96.5%	93.1%	90.7%	103.0%	90.0%	80.0%	88.7%	4.8%	5.0%	4.7%	4.7%	5.0%	4.9%	4.2%	4.8%
		70 °C	100.0%	97.0%	91.4%	82.9%	73.1%	99.0%	89.4%	78.9%	59.8%	5.0%	5.0%	4.1%	3.8%	4.8%	4.4%	4.3%	3.0%
	Alkaline	23 °C	100.0%	105.0%	64.5%	28.9%	15.9%	100.0%	95.5%	91.0%	80.3%	5.5%	3.3%	1.4%	0.8%	4.7%	4.3%	4.3%	3.9%
		50 °C	100.0%	101.0%	80.0%	25.0%	1.0%	95.0%	78.0%	56.0%	41.3%	4.8%	3.7%	1.3%	0.0%	4.4%	4.0%	2.8%	2.3%
		70 °C	100.0%	103.0%	78.0%	60.0%	1.0%	98.0%	90.0%	80.0%	10.0%	4.7%	4.2%	3.0%	0.0%	5.0%	4.8%	3.8%	0.5%
<b>Vapour</b>	Neutral	23 °C	100.0%	104.0%	98.6%	97.2%	115.5%	97.0%	97.5%	94.9%	101.1%	5.4%	4.5%	4.9%	5.3%	5.1%	4.6%	4.5%	4.7%
		50 °C	100.0%	102.0%	96.2%	92.3%	103.1%	96.0%	97.0%	94.0%	94.6%	5.3%	5.0%	4.9%	4.8%	4.6%	4.7%	4.4%	4.9%
		70 °C	100.0%	96.0%	82.5%	74.0%	72.2%	95.0%	90.0%	83.9%	79.8%	5.0%	3.7%	3.5%	3.3%	5.1%	4.2%	4.2%	4.1%
	Acidic	23 °C	100.0%	102.0%	94.3%	88.6%	99.3%	103.0%	99.6%	99.2%	102.1%	5.4%	4.4%	4.5%	5.3%	4.9%	5.2%	5.3%	5.0%
		50 °C	100.0%	101.0%	96.5%	93.0%	91.6%	102.0%	95.5%	91.0%	95.6%	5.1%	4.7%	5.0%	4.3%	5.2%	5.2%	4.7%	4.8%
		70 °C	100.0%	102.0%	93.0%	86.0%	92.6%	97.0%	103.6%	107.2%	87.1%	5.1%	4.7%	4.5%	4.9%	4.7%	5.3%	4.9%	4.5%
	Alkaline	23 °C	100.0%	97.0%	100.1%	100.2%	94.9%	104.0%	96.1%	92.3%	100.3%	5.2%	5.4%	5.1%	4.4%	4.8%	4.5%	4.7%	4.9%
		50 °C	100.0%	98.0%	97.5%	95.0%	92.2%	98.0%	99.0%	98.0%	94.9%	4.7%	5.3%	4.5%	4.7%	5.4%	5.1%	4.8%	4.8%
		70 °C	100.0%	102.0%	97.6%	95.1%	92.3%	95.0%	96.0%	92.0%	88.3%	5.1%	5.2%	5.1%	4.9%	5.0%	5.0%	4.9%	4.6%

**Figure 12.16 - Compressive, in-plane shear, and interlaminar shear strength retention during chemical vapour ageing with superficial protection**

Material			Polyester				Vinylester				Polyester				Vinylester				
Weeks of exposure		0	1	4	8	16	1	4	8	16	1	4	8	16	1	4	8	16	
Property	Environment	Temperature	Vapour with superficial protection								Error bars								
Retention of compressive strength	Neutral	23 °C	100.0%	100.0%	92.5%	85.0%	71.4%	102.0%	100.0%	100.0%	97.2%	5.4%	4.5%	4.0%	3.8%	4.8%	5.0%	5.5%	4.7%
		50 °C	100.0%	103.0%	93.5%	87.0%	83.1%	99.0%	95.0%	90.0%	79.0%	5.1%	4.5%	4.2%	4.0%	5.0%	4.7%	4.8%	4.0%
		70 °C	100.0%	100.0%	92.5%	85.0%	81.1%	95.0%	93.0%	86.0%	102.0%	5.0%	5.0%	4.4%	4.3%	4.4%	4.6%	4.7%	5.4%
	Acidic	23 °C	100.0%	99.0%	100.0%	100.0%	96.0%	102.0%	97.0%	94.0%	94.2%	4.7%	4.8%	4.6%	4.8%	4.7%	5.0%	5.2%	4.6%
		50 °C	100.0%	103.0%	93.0%	86.0%	78.6%	98.0%	97.5%	95.0%	92.2%	5.5%	4.7%	4.6%	3.8%	5.2%	5.0%	4.6%	4.8%
		70 °C	100.0%	102.0%	97.5%	95.0%	89.1%	104.0%	95.5%	91.0%	84.1%	5.4%	5.3%	4.7%	4.0%	5.1%	4.8%	4.4%	3.8%
	Alkaline	23 °C	100.0%	101.0%	100.0%	100.0%	100.5%	101.0%	101.0%	102.0%	102.8%	4.9%	4.7%	5.0%	4.7%	5.5%	4.7%	5.2%	4.8%
		50 °C	100.0%	101.0%	93.5%	87.0%	76.7%	102.0%	98.0%	96.0%	93.0%	4.6%	4.4%	4.4%	4.1%	5.1%	4.5%	5.1%	4.5%
		70 °C	100.0%	96.0%	88.0%	76.0%	64.8%	99.0%	95.0%	90.0%	80.4%	4.6%	4.6%	3.5%	3.3%	4.8%	4.3%	4.9%	3.9%
Retention of in-plane shear strength	Neutral	23 °C	100.0%	99.0%	99.0%	93.0%	95.0%	101.0%	101.0%	102.0%	99.3%	4.9%	4.9%	4.9%	4.8%	4.7%	4.6%	5.5%	5.1%
		50 °C	100.0%	99.0%	98.5%	97.0%	97.9%	97.0%	98.5%	97.0%	92.3%	4.5%	4.5%	4.6%	4.5%	4.8%	4.9%	4.8%	4.4%
		70 °C	100.0%	104.0%	99.5%	99.0%	98.8%	101.0%	99.0%	98.0%	100.1%	4.9%	5.4%	5.3%	4.7%	5.0%	4.5%	5.4%	4.9%
	Acidic	23 °C	100.0%	105.0%	106.5%	113.0%	107.3%	101.0%	100.0%	102.0%	106.1%	5.1%	5.1%	5.3%	5.0%	4.6%	4.9%	5.5%	5.6%
		50 °C	100.0%	102.0%	98.5%	97.0%	88.2%	102.0%	100.0%	96.0%	93.9%	4.7%	5.0%	4.6%	4.2%	4.8%	5.1%	5.2%	4.9%
		70 °C	100.0%	95.0%	99.5%	99.0%	101.5%	96.0%	100.0%	95.0%	90.0%	5.0%	5.2%	4.9%	5.6%	4.7%	4.8%	4.5%	4.4%
	Alkaline	23 °C	100.0%	104.0%	104.5%	109.0%	110.5%	98.0%	101.5%	103.0%	105.1%	4.8%	5.4%	5.4%	5.5%	4.6%	5.5%	5.7%	5.0%
		50 °C	100.0%	98.0%	101.0%	102.0%	100.8%	99.0%	99.0%	98.0%	96.4%	4.6%	5.2%	4.7%	5.4%	4.7%	4.8%	4.8%	5.3%
		70 °C	100.0%	95.0%	98.0%	96.0%	97.0%	100.0%	99.0%	98.0%	94.2%	4.7%	5.4%	5.0%	5.0%	5.5%	4.7%	4.8%	4.8%
Retention of interlaminar shear strength	Neutral	23 °C	100.0%	105.0%	99.0%	94.0%	97.0%	97.0%	100.0%	100.0%	98.0%	4.7%	4.9%	4.6%	4.7%	4.5%	5.2%	5.1%	4.7%
		50 °C	100.0%	101.0%	101.0%	102.0%	99.9%	105.0%	95.0%	90.0%	86.0%	4.9%	4.7%	5.2%	5.1%	4.8%	5.2%	4.9%	4.4%
		70 °C	100.0%	104.0%	93.0%	86.0%	84.0%	96.0%	93.0%	86.0%	80.0%	5.3%	4.7%	4.6%	4.0%	4.9%	4.4%	4.5%	4.1%
	Acidic	23 °C	100.0%	103.0%	100.0%	100.0%	97.9%	96.0%	97.5%	95.0%	91.6%	4.7%	5.5%	5.1%	4.7%	5.1%	5.0%	4.6%	4.2%
		50 °C	100.0%	105.0%	93.0%	86.0%	86.3%	103.0%	96.5%	93.0%	89.9%	4.8%	4.4%	4.7%	4.2%	5.3%	4.9%	5.0%	4.5%
		70 °C	100.0%	95.0%	97.5%	95.0%	94.4%	98.0%	98.0%	100.0%	86.9%	4.5%	5.2%	4.7%	4.4%	5.1%	4.6%	5.2%	4.5%
	Alkaline	23 °C	100.0%	103.0%	100.0%	100.0%	91.2%	98.0%	100.0%	100.0%	97.6%	5.2%	5.1%	5.0%	4.3%	5.2%	5.3%	5.2%	5.3%
		50 °C	100.0%	103.0%	93.5%	87.0%	93.2%	100.0%	98.0%	96.0%	97.8%	5.4%	4.9%	4.1%	4.9%	4.9%	4.4%	5.2%	4.7%
		70 °C	100.0%	103.0%	88.0%	76.0%	78.6%	104.0%	94.5%	89.0%	81.6%	4.8%	4.4%	3.9%	4.1%	5.6%	4.5%	4.4%	4.0%

**Figure 12.17 - Variations between the compressive, in-plane shear, and interlaminar shear strength retention during chemical ageing with and without superficial protection**

Material			Polyester				Vinylester			
Weeks of exposure			1	4	8	16	1	4	8	16
Property	Environment	Temperature	Vapour with superficial protection							
Retention of compressive strength	Neutral	23 °C	-4.0%	-7.5%	-15.0%	-27.2%	-3.0%	0.7%	1.4%	11.2%
		50 °C	-1.0%	-4.0%	-8.0%	-2.3%	-1.0%	-2.0%	-4.0%	-9.4%
		70 °C	0.0%	6.1%	12.3%	3.9%	-5.0%	3.0%	6.0%	4.8%
	Acidic	23 °C	0.0%	3.0%	6.0%	8.9%	-3.0%	-2.9%	-5.8%	-9.6%
		50 °C	4.0%	-3.5%	-7.0%	-2.0%	1.0%	0.0%	0.0%	-0.5%
		70 °C	6.0%	4.5%	9.0%	5.3%	3.0%	15.7%	21.0%	17.2%
	Alkaline	23 °C	0.0%	5.0%	10.1%	4.7%	3.0%	8.2%	16.4%	6.1%
		50 °C	-1.0%	-4.0%	-8.0%	-15.5%	2.0%	1.0%	2.0%	1.1%
		70 °C	-4.0%	-9.0%	-18.0%	-25.3%	2.0%	0.0%	0.0%	-7.4%
Retention of in-plane shear strength	Neutral	23 °C	-5.0%	0.4%	-4.2%	-20.5%	4.0%	3.5%	7.1%	-1.8%
		50 °C	-3.0%	2.3%	4.7%	-5.2%	1.0%	1.5%	3.0%	-2.3%
		70 °C	8.0%	17.0%	25.0%	26.6%	6.0%	9.0%	14.1%	20.3%
	Acidic	23 °C	3.0%	12.2%	24.4%	8.0%	-2.0%	0.4%	2.8%	4.1%
		50 °C	1.0%	2.0%	4.0%	-3.4%	0.0%	4.5%	5.0%	-1.7%
		70 °C	-7.0%	6.5%	13.0%	8.9%	-1.0%	-3.6%	-12.2%	2.9%
	Alkaline	23 °C	7.0%	4.4%	8.8%	15.6%	-6.0%	5.4%	10.7%	4.9%
		50 °C	0.0%	3.5%	7.0%	8.6%	1.0%	0.0%	0.0%	1.5%
		70 °C	-7.0%	0.4%	0.9%	4.7%	5.0%	3.0%	6.0%	5.8%
Retention of interlaminar shear strength	Neutral	23 °C	1.0%	0.4%	-3.2%	-18.5%	0.0%	2.5%	5.1%	-3.1%
		50 °C	-1.0%	4.8%	9.7%	-3.3%	9.0%	-2.0%	-4.0%	-8.6%
		70 °C	8.0%	10.5%	12.0%	11.8%	1.0%	3.0%	2.1%	0.1%
	Acidic	23 °C	1.0%	5.7%	11.4%	-1.4%	-7.0%	-2.1%	-4.2%	-10.5%
		50 °C	4.0%	-3.5%	-7.0%	-5.3%	1.0%	1.0%	2.0%	-5.7%
		70 °C	-7.0%	4.5%	9.0%	1.8%	1.0%	-5.6%	-7.2%	-0.2%
	Alkaline	23 °C	6.0%	-0.1%	-0.2%	-3.7%	-6.0%	3.9%	7.7%	-2.7%
		50 °C	5.0%	-4.0%	-8.0%	1.0%	2.0%	-1.0%	-2.0%	2.8%
		70 °C	1.0%	-9.6%	-19.1%	-13.8%	9.0%	-1.5%	-3.0%	-6.8%

**Figure 13.04 - Specimens colour variation ( $\Delta E^*$ ) during weathering (without superficial protection)**

Type of weathering	Profile	Superficial protection	$\Delta E^*$																	
			0	330	654	982	1312	1652	1996	2310	2578	2933	3288	3643	3973	4303	4963	5623	6000	
QUV accelerated weathering	Exposure period (hours)		0	330	654	982	1312	1652	1996	2310	2578	2933	3288	3643	3973	4303	4963	5623	6000	
	UP_NV_0	--	0	1.83	2.79	3.68	3.67	3.73	3.46	3.80	4.00	4.14	4.39	4.26	4.38	4.32	4.96	5.10	5.17	
	UP_WV_0	--	0	1.73	2.41	2.97	3.18	3.22	3.10	3.40	3.56	3.70	3.88	3.93	4.01	3.91	4.35	4.63	4.76	
	UP_NV_025	--	0	1.10	2.72	4.92	5.79	5.29	5.15	4.67	4.57	4.39	4.56	4.36	4.32	4.46	5.85	5.98	6.04	
	UP_WV_025	--	0	2.30	4.64	6.11	6.55	6.71	6.74	6.84	6.99	7.39	7.19	7.41	7.84	7.30	8.48	8.40	8.35	
	UP_NV_050	--	0	1.19	2.49	3.43	4.75	4.50	4.32	4.29	4.19	4.26	4.28	3.86	4.25	4.07	5.67	5.63	5.61	
	UP_WV_050	--	0	1.45	4.01	5.62	6.84	6.56	5.84	5.69	5.98	6.25	5.81	5.43	5.46	5.62	6.34	6.40	6.42	
	VE_NV_0	--	0	11.11	11.74	10.90	10.95	12.06	9.54	8.68	9.21	8.54	7.35	7.77	7.14	7.56	7.05	6.98	6.95	
	VE_WV_0	--	0	8.74	12.76	11.23	11.22	11.00	9.44	9.19	9.96	9.48	8.91	8.53	10.31	8.72	10.41	11.88	12.53	
	VE_NV_025	--	0	14.62	15.24	13.14	11.65	12.71	11.54	10.36	9.77	9.30	7.90	8.62	8.41	8.26	8.38	8.12	8.02	
	VE_WV_025	--	0	14.45	15.76	13.96	13.79	12.92	11.69	11.07	11.53	11.49	9.78	11.35	10.44	10.57	11.23	12.36	12.85	
	VE_NV_050	--	0	14.91	15.12	14.15	13.10	12.41	11.52	11.83	10.70	9.44	9.21	10.11	8.49	9.66	9.09	8.72	8.56	
	VE_WV_050	--	0	14.33	15.68	14.90	12.92	13.50	13.03	13.08	11.62	10.44	11.80	11.59	11.60	11.69	12.38	12.66	12.78	
	Natural weathering	Exposure period (weeks)		0	5	12	20	42	88											
UP_NV_0		--	0	2.07	2.13	2.53	2.25	2.23												
UP_WV_0		--	0	2.23	2.12	2.66	2.83	4.05												
UP_NV_025		--	0	0.69	0.89	1.09	4.70	5.83												
UP_WV_025		--	0	0.91	1.16	1.30	2.50	6.71												
UP_NV_050		--	0	1.32	1.55	1.67	3.34	4.50												
UP_WV_050		--	0	0.74	1.30	0.99	2.26	4.44												
VE_NV_0		--	0	0.83	2.51	4.33	14.24	9.32												
VE_WV_0		--	0	1.82	2.50	4.93	10.24	11.00												
VE_NV_025		--	0	3.94	7.15	8.31	10.25	8.25												
VE_WV_025		--	0	3.78	7.12	8.21	11.06	5.51												
VE_NV_050		--	0	4.26	7.70	8.68	12.12	8.82												
VE_WV_050		--	0	3.70	7.37	8.31	10.84	7.77												

**Figure 13.05 - Specimens colour variation ( $\Delta E^*$ ) during weathering (with superficial protection)**

Type of weathering	Profile	Superficial protection	$\Delta E^*$																
			0	330	654	982	1312	1652	1996	2310	2578	2933	3288	3643	3973	4303	4963	5623	6000
QUV accelerated weathering	Exposure period (hours)		0	330	654	982	1312	1652	1996	2310	2578	2933	3288	3643	3973	4303	4963	5623	6000
	UP_NV_0	CIN	0	0.30	0.38	0.49	0.56	0.69	0.89	0.83	0.77	0.77	0.63	0.46	0.37	0.41	0.21	0.26	0.31
	UP_WV_0	CIN	0	0.34	0.40	0.52	0.62	0.79	1.01	0.92	0.92	0.95	0.77	0.54	0.41	0.51	0.29	0.35	0.40
	UP_NV_025	CIN	0	0.34	0.42	0.52	0.77	0.80	1.01	0.96	0.91	0.96	0.81	0.59	0.46	0.56	0.30	0.34	0.40
	UP_WV_025	CIN	0	0.38	0.42	0.53	0.82	0.78	1.01	0.95	0.88	0.93	0.77	0.66	0.60	0.58	0.37	0.44	0.50
	UP_NV_050	CIN	0	0.31	0.31	0.43	0.59	0.71	0.88	0.83	0.77	0.79	0.64	0.49	0.45	0.42	0.26	0.29	0.34
	UP_WV_050	CIN	0	0.30	0.33	0.36	0.52	0.63	0.81	0.74	0.70	0.71	0.58	0.49	0.40	0.39	0.27	0.37	0.44
	VE_NV_0	SIKA	0	0.36	0.36	1.20	1.25	1.11	0.75	1.17	1.34	1.35	1.37	1.08	1.27	0.98	1.17	1.05	1.00
	VE_WV_0	SIKA	0	0.27	0.34	1.07	1.09	0.46	0.42	0.94	1.14	1.31	1.34	1.15	1.01	1.00	0.99	0.90	0.87
	VE_NV_025	SIKA	0	0.27	0.21	0.48	0.81	0.47	0.55	0.91	0.88	0.95	1.12	0.98	0.89	0.80	1.05	0.98	0.95
	VE_WV_025	SIKA	0	0.42	0.32	0.85	1.12	0.75	0.42	0.90	1.22	1.12	1.18	0.85	0.93	0.77	0.94	0.79	0.73
	VE_NV_050	SIKA	0	0.81	0.29	1.11	1.25	0.55	0.32	0.73	0.96	1.05	1.02	0.56	0.75	0.54	0.77	0.64	0.59
	VE_WV_050	SIKA	0	0.28	0.32	0.60	0.94	0.50	0.27	0.60	0.84	1.00	1.08	0.89	0.76	0.75	0.78	0.70	0.68
	Natural weathering	Exposure period (weeks)		0	5	12	20	42	88										
UP_NV_0		CIN	0	0.58	0.44	0.51	1.85	1.99											
UP_WV_0		CIN	0	0.41	0.37	0.43	1.81	1.68											
UP_NV_025		CIN	0	0.45	0.40	0.47	0.77	1.43											
UP_WV_025		CIN	0	0.52	0.46	0.53	1.58	1.87											
UP_NV_050		CIN	0	0.40	0.44	0.50	1.79	1.58											
UP_WV_050		CIN	0	0.32	0.36	0.42	0.95	1.59											
VE_NV_0		SIKA	0	0.52	0.34	0.66	1.81	2.24											
VE_WV_0		SIKA	0	0.56	0.28	0.59	2.11	3.06											
VE_NV_025		SIKA	0	0.58	0.13	0.31	1.66	3.06											
VE_WV_025		SIKA	0	0.39	0.19	0.50	1.76	2.51											
VE_NV_050		SIKA	0	0.44	0.13	0.42	1.99	2.64											
VE_WV_050		SIKA	0	0.66	0.29	0.59	1.84	2.70											

**Figure 13.07 - Specimens gloss retention during weathering (without superficial protection)**

Type of weathering	Profile	Superficial protection	Gloss retention																
QUV accelerated weathering	Exposure period (hours)		0	330	654	982	1312	1652	1996	2310	2578	2933	3288	3643	3973	4303	4963	5623	6000
	UP_NV_0	--	100%	97.7%	97.3%	83.9%	27.3%	18.8%	11.8%	11.4%	12.3%	11.7%	11.8%	13.5%	11.6%	11.9%	12.5%	12.8%	12.0%
	UP_WV_0	--	100%	86.2%	84.1%	68.4%	26.1%	14.8%	8.3%	9.1%	8.6%	8.1%	8.0%	9.1%	8.6%	8.0%	8.5%	8.9%	9.1%
	UP_NV_025	--	100%	95.2%	91.4%	83.4%	44.0%	23.5%	8.0%	7.2%	7.4%	7.3%	6.9%	7.1%	7.2%	6.3%	8.0%	7.4%	7.1%
	UP_WV_025	--	100%	95.7%	98.2%	78.7%	28.7%	21.8%	7.6%	7.5%	7.7%	7.7%	7.8%	8.3%	8.0%	7.3%	9.5%	10.2%	7.6%
	UP_NV_050	--	100%	96.3%	106.2%	103.7%	52.9%	36.9%	12.4%	10.4%	10.2%	10.1%	10.0%	10.6%	10.9%	9.3%	10.9%	10.3%	10.4%
	UP_WV_050	--	100%	94.7%	97.0%	80.1%	30.7%	13.5%	6.6%	6.4%	6.6%	6.6%	6.5%	6.7%	6.5%	5.9%	7.8%	7.9%	6.8%
	VE_NV_0	--	100%	88.7%	60.3%	14.4%	15.7%	12.8%	13.2%	10.7%	11.6%	11.6%	10.8%	11.5%	10.4%	10.1%	10.8%	10.4%	10.7%
	VE_WV_0	--	100%	97.3%	45.4%	25.2%	26.0%	22.3%	18.2%	16.0%	16.8%	15.6%	15.1%	15.4%	16.0%	13.6%	14.8%	14.7%	16.4%
	VE_NV_025	--	100%	59.7%	13.4%	5.6%	5.8%	7.0%	5.7%	5.1%	5.3%	5.3%	5.0%	5.1%	5.6%	4.5%	5.4%	4.7%	5.9%
	VE_WV_025	--	100%	48.8%	15.2%	5.6%	5.1%	6.3%	4.4%	4.0%	4.0%	4.0%	3.7%	4.0%	3.9%	3.5%	3.8%	3.7%	3.9%
	VE_NV_050	--	100%	73.7%	14.6%	7.2%	5.1%	6.8%	7.3%	6.2%	5.6%	5.0%	5.7%	5.9%	6.1%	5.2%	5.3%	5.0%	5.5%
	VE_WV_050	--	100%	69.0%	13.3%	4.4%	3.4%	5.0%	4.0%	3.5%	3.1%	2.9%	3.0%	3.2%	2.9%	2.8%	3.0%	3.2%	3.5%
Natural weathering	Exposure period (weeks)		0	5	12	20	42	88											
	UP_NV_0	--	100%	88.4%	113.0%	105.0%	97.9%	10.9%											
	UP_WV_0	--	100%	88.1%	107.2%	100.7%	45.8%	8.0%											
	UP_NV_025	--	100%	88.5%	103.4%	98.3%	78.2%	9.5%											
	UP_WV_025	--	100%	93.7%	113.8%	101.3%	49.9%	6.9%											
	UP_NV_050	--	100%	103.8%	119.6%	114.8%	87.5%	46.7%											
	UP_WV_050	--	100%	106.0%	91.3%	84.0%	57.1%	7.1%											
	VE_NV_0	--	100%	107.6%	115.4%	94.6%	8.5%	8.3%											
	VE_WV_0	--	100%	93.0%	108.2%	99.5%	13.8%	19.5%											
	VE_NV_025	--	100%	97.9%	96.5%	78.2%	4.1%	5.3%											
	VE_WV_025	--	100%	97.6%	96.6%	87.9%	3.6%	4.1%											
	VE_NV_050	--	100%	80.6%	72.0%	59.8%	4.9%	7.7%											
VE_WV_050	--	100%	89.9%	82.8%	67.0%	2.8%	3.6%												

**Figure 13.08 - Specimens gloss retention during weathering (with superficial protection)**

Type of weathering	Profile	Superficial protection	Gloss retention																	
QUV accelerated weathering	Exposure period (hours)		0	330	654	982	1312	1652	1996	2310	2578	2933	3288	3643	3973	4303	4963	5623	6000	
	UP_NV_0	CIN	100%	98.0%	93.1%	95.4%	97.7%	97.5%	97.0%	97.3%	93.6%	85.9%	77.7%	65.4%	54.7%	45.8%	35.5%	40.7%	31.9%	
	UP_WV_0	CIN	100%	96.9%	98.9%	97.0%	96.8%	97.7%	93.3%	93.8%	89.4%	81.8%	73.1%	58.1%	45.9%	38.4%	35.0%	33.2%	28.7%	
	UP_NV_025	CIN	100%	95.1%	94.3%	96.0%	94.8%	97.8%	93.9%	96.2%	93.0%	85.1%	79.0%	65.8%	51.9%	43.4%	35.5%	37.7%	26.9%	
	UP_WV_025	CIN	100%	98.7%	95.9%	98.3%	96.8%	95.8%	93.0%	93.3%	92.0%	86.4%	81.8%	74.0%	65.9%	55.1%	42.4%	43.1%	33.5%	
	VE_NV_0	CIN	100%	99.4%	97.9%	96.9%	96.8%	97.2%	95.9%	96.4%	92.4%	85.6%	77.4%	68.2%	52.7%	44.1%	33.6%	35.2%	26.7%	
	VE_WV_0	CIN	100%	97.8%	97.5%	97.1%	96.3%	96.7%	93.5%	94.8%	91.7%	85.0%	79.0%	69.0%	56.7%	47.4%	39.7%	36.9%	30.8%	
	UP_NV_0	SIKA	100%	54.3%	38.9%	34.1%	14.7%	12.0%	6.0%	5.3%	4.1%	3.9%	3.4%	3.3%	3.5%	2.9%	3.6%	3.7%	3.5%	
	UP_WV_0	SIKA	100%	54.4%	37.1%	31.9%	17.0%	12.8%	7.0%	5.2%	4.6%	4.0%	3.3%	3.1%	3.1%	2.7%	3.0%	3.2%	3.0%	
	UP_NV_025	SIKA	100%	59.7%	44.5%	35.8%	24.0%	20.3%	8.8%	7.0%	5.0%	4.1%	3.9%	3.9%	3.6%	3.4%	3.5%	3.8%	3.8%	
	UP_WV_025	SIKA	100%	59.9%	44.5%	31.4%	28.7%	22.8%	7.0%	5.8%	4.4%	3.5%	3.5%	3.6%	3.5%	3.2%	3.5%	3.7%	3.8%	
	VE_NV_0	SIKA	100%	57.2%	42.5%	29.6%	25.3%	13.3%	7.0%	5.5%	3.8%	2.8%	2.8%	2.8%	2.7%	2.4%	2.7%	2.9%	2.9%	
	VE_WV_0	SIKA	100%	50.0%	40.8%	37.8%	18.9%	17.3%	6.5%	5.2%	3.6%	3.1%	2.9%	3.1%	2.9%	2.8%	2.9%	3.1%	3.1%	
	Natural weathering	Exposure period (weeks)		0	5	12	20	42	88											
UP_NV_0		CIN	100%	101.4%	101.3%	101.2%	77.5%	88.8%												
UP_WV_0		CIN	100%	96.9%	97.7%	98.6%	83.3%	85.5%												
UP_NV_025		CIN	100%	88.0%	101.4%	101.2%	74.7%	82.1%												
UP_WV_025		CIN	100%	91.1%	91.7%	90.8%	66.1%	73.1%												
VE_NV_0		CIN	100%	97.7%	101.0%	101.5%	75.8%	80.9%												
VE_WV_0		CIN	100%	89.1%	100.7%	100.3%	70.6%	79.9%												
VE_NV_025		CIN	100%	103.2%	103.4%	102.7%	65.0%	84.5%												
VE_WV_025		CIN	100%	97.7%	97.2%	96.9%	79.0%	84.4%												
UP_NV_0		CIN	100%	87.3%	91.2%	73.8%	40.5%	22.8%												
UP_WV_0		CIN	100%	80.0%	69.0%	62.8%	39.0%	15.0%												
UP_NV_025		CIN	100%	115.0%	123.1%	102.2%	25.2%	22.0%												
UP_WV_025		CIN	100%	88.7%	83.7%	74.5%	36.5%	42.6%												
VE_NV_0		CIN	100%	94.7%	104.2%	87.5%	31.0%	21.0%												
VE_WV_0		CIN	100%	80.0%	100.0%	89.0%	32.3%	20.3%												
VE_NV_025	CIN	100%	100.7%	102.6%	84.1%	33.3%	22.4%													
VE_WV_025	CIN	100%	112.7%	104.4%	96.0%	45.6%	24.9%													

**Figure 13.11 - Retention of mechanical properties of UP and VE specimens after 6000 h of QUV accelerated weathering**

Material		Polyester			Vinylester			Polyester			Vinylester			
Type of superficial protection		0	None	CIN	SIKA	None	CIN	SIKA	None	CIN	SIKA	None	CIN	SIKA
Superficial veil	%UV absorber additive	Retention of in-plane shear strength							Error bars					
No veil	0.00%	100.0%	90.5%	93.6%	89.5%	96.5%	97.7%	97.2%	4.3%	4.9%	4.8%	4.7%	4.9%	4.7%
	0.25%	100.0%	100.7%	100.6%	105.5%	85.9%	--	--	5.0%	5.4%	5.8%	4.4%	--	--
	0.50%	100.0%	97.6%	--	--	92.6%	--	--	5.2%	--	--	4.5%	--	--
With veil	0.00%	100.0%	85.2%	89.7%	86.8%	97.4%	92.2%	92.8%	4.3%	4.4%	4.1%	4.4%	4.3%	4.4%
	0.25%	100.0%	97.7%	106.2%	98.8%	96.9%	--	--	4.5%	5.6%	5.0%	5.3%	--	--
	0.50%	100.0%	109.8%	--	--	99.0%	--	--	5.2%	--	--	5.1%	--	--
		Retention of compressive strength							Error bars					
No veil	0.00%	100.0%	74.8%	79.1%	75.6%	127.5%	106.0%	116.8%	3.8%	3.6%	3.6%	6.0%	5.1%	5.6%
	0.25%	100.0%	97.4%	93.5%	97.9%	106.9%	--	--	5.0%	4.8%	5.2%	5.2%	--	--
	0.50%	100.0%	102.6%	--	--	97.6%	--	--	4.8%	--	--	5.3%	--	--
With veil	0.00%	100.0%	80.1%	77.9%	81.5%	85.1%	84.2%	83.3%	3.8%	3.8%	4.5%	4.3%	4.6%	4.1%
	0.25%	100.0%	97.3%	91.7%	89.5%	92.4%	--	--	4.7%	4.6%	4.9%	4.3%	--	--
	0.50%	100.0%	93.0%	--	--	104.0%	--	--	4.5%	--	--	5.3%	--	--

<b>Figure 13.12 - Retention of mechanical properties of UP specimens for 10 and 20 months of natural weathering</b>										
<b>Surface veil</b>			<b>No veil</b>		<b>With veil</b>		<b>No veil</b>		<b>With veil</b>	
<b>Exposure period (months)</b>		<b>0</b>	<b>10</b>	<b>20</b>	<b>10</b>	<b>20</b>	<b>10</b>	<b>20</b>	<b>10</b>	<b>20</b>
<b>%UV absorber additive</b>	<b>Superficial protection</b>	<b>Retention of in-plane shear strength</b>					<b>Error bars</b>			
<b>0.00%</b>	None	100.0%	95.5%	100.6%	100.7%	97.0%	4.4%	5.3%	4.9%	5.2%
	CIN	100.0%	99.3%	95.0%	97.8%	92.8%	5.0%	4.8%	4.5%	4.2%
	SIKA	100.0%	106.8%	97.8%	95.3%	89.3%	5.5%	4.6%	4.3%	4.7%
<b>0.25%</b>	None	100.0%	100.4%	100.8%	100.5%	103.7%	5.2%	5.2%	4.8%	5.5%
	CIN	100.0%	99.6%	101.1%	101.8%	111.7%	4.9%	5.5%	5.1%	6.0%
	SIKA	100.0%	102.1%	101.9%	106.4%	109.8%	5.1%	5.3%	5.6%	5.9%
<b>0.50%</b>	None	100.0%	101.5%	97.7%	108.2%	106.8%	5.2%	5.3%	5.8%	5.2%
		<b>Retention of tensile strength</b>					<b>Error bars</b>			
<b>0.00%</b>	None	100.0%	86.6%	90.8%	97.5%	106.8%	4.5%	5.0%	4.7%	5.1%
	CIN	100.0%	88.7%	95.7%	102.9%	101.1%	4.4%	4.9%	5.6%	5.2%
	SIKA	100.0%	90.5%	76.8%	102.9%	97.2%	4.3%	4.1%	4.8%	4.6%
<b>0.25%</b>	None	100.0%	101.4%	88.6%	88.9%	97.4%	5.2%	4.6%	4.7%	4.5%
	CIN	100.0%	95.1%	104.1%	97.5%	99.7%	4.7%	5.2%	4.8%	5.1%
	SIKA	100.0%	92.8%	96.9%	93.7%	91.2%	4.9%	5.3%	4.7%	4.1%
<b>0.50%</b>	None	100.0%	89.7%	90.1%	87.7%	86.8%	4.3%	4.4%	4.6%	4.0%
		<b>Retention of compressive strength</b>					<b>Error bars</b>			
<b>0.00%</b>	None	100.0%	83.4%	68.3%	86.8%	69.6%	3.9%	3.7%	4.2%	3.8%
	CIN	100.0%	78.5%	66.8%	103.7%	75.6%	4.2%	3.4%	4.7%	3.8%
	SIKA	100.0%	93.0%	46.6%	80.0%	60.0%	4.4%	2.3%	4.0%	3.0%
<b>0.25%</b>	None	100.0%	97.7%	72.4%	102.3%	69.7%	4.9%	3.4%	4.9%	3.4%
	CIN	100.0%	95.2%	101.7%	86.2%	90.3%	4.6%	4.9%	4.4%	5.0%
	SIKA	100.0%	93.3%	70.4%	90.1%	77.4%	4.7%	3.5%	4.6%	4.1%
<b>0.50%</b>	None	100.0%	106.6%	80.7%	110.6%	82.1%	5.1%	4.3%	6.0%	4.3%

<b>Figure 13.12 - Retention of mechanical properties of VE specimens for 10 and 20 months of natural weathering</b>										
<b>Surface veil</b>		<b>No veil</b>			<b>With veil</b>		<b>No veil</b>		<b>With veil</b>	
<b>Exposure period (months)</b>		<b>0</b>	<b>10</b>	<b>20</b>	<b>10</b>	<b>20</b>	<b>10</b>	<b>20</b>	<b>10</b>	<b>20</b>
<b>%UV absorber additive</b>	<b>Superficial protection</b>	<b>Retention of in-plane shear strength</b>					<b>Error bars</b>			
<b>0.00%</b>	None	100.0%	98.1%	97.9%	97.2%	97.8%	5.3%	5.3%	4.8%	4.5%
	CIN	100.0%	109.2%	100.6%	96.7%	101.0%	5.8%	4.7%	5.1%	4.9%
	SIKA	100.0%	100.8%	99.6%	90.9%	98.0%	4.9%	4.8%	4.9%	5.1%
<b>0.25%</b>	None	100.0%	89.3%	98.0%	94.7%	96.3%	4.5%	5.2%	4.6%	4.7%
	CIN	100.0%	90.4%	97.2%	93.7%	98.3%	4.9%	4.5%	4.6%	4.6%
	SIKA	100.0%	89.7%	95.0%	94.4%	96.3%	4.3%	5.1%	4.4%	5.2%
<b>0.50%</b>	None	100.0%	102.6%	107.0%	101.1%	105.2%	5.2%	4.9%	5.2%	4.9%
		<b>Retention of tensile strength</b>					<b>Error bars</b>			
<b>0.00%</b>	None	100.0%	85.7%	93.7%	96.3%	90.5%	4.7%	5.1%	5.0%	4.3%
	CIN	100.0%	90.6%	100.9%	98.5%	106.4%	4.3%	4.6%	4.8%	5.6%
	SIKA	100.0%	90.0%	97.2%	99.8%	111.9%	4.3%	5.0%	4.8%	5.2%
<b>0.25%</b>	None	100.0%	103.0%	104.7%	97.2%	96.2%	5.4%	5.4%	4.9%	4.6%
	CIN	100.0%	91.1%	111.2%	99.3%	97.8%	5.0%	5.9%	5.4%	5.3%
	SIKA	100.0%	90.7%	103.1%	99.3%	100.6%	4.8%	5.0%	4.8%	5.3%
<b>0.50%</b>	None	100.0%	105.0%	96.9%	105.3%	91.8%	4.7%	5.0%	4.8%	4.6%
		<b>Retention of compressive strength</b>					<b>Error bars</b>			
<b>0.00%</b>	None	100.0%	107.3%	101.4%	76.9%	103.7%	5.5%	4.7%	3.9%	5.0%
	CIN	100.0%	111.9%	90.2%	94.0%	69.3%	5.4%	4.2%	4.7%	3.6%
	SIKA	100.0%	108.2%	90.2%	82.1%	68.8%	5.3%	4.7%	3.7%	3.7%
<b>0.25%</b>	None	100.0%	73.5%	83.2%	103.0%	80.1%	3.4%	3.7%	5.5%	3.8%
	CIN	100.0%	101.9%	89.3%	92.2%	75.9%	4.7%	4.5%	4.3%	3.5%
	SIKA	100.0%	95.7%	82.7%	88.5%	72.4%	5.1%	3.9%	4.2%	3.3%
<b>0.50%</b>	None	100.0%	98.5%	72.9%	76.5%	85.7%	5.4%	3.5%	4.1%	4.5%

**Figure 13.14 - Comparison of effects of QUV accelerated and natural weathering on mechanical properties of UP and VE specimens without superficial protection.**

Type of resin			Polyester			Vinylester			Polyester			Vinylester		
Exposure period (months)		0	QUV	10	20	QUV	10	20	QUV	10	20	QUV	10	20
Superficial veil	%UV absorber additive	Retention of in-plane shear strength						Error bars						
No veil	0.00%	100.0%	90.5%	95.5%	100.6%	96.5%	98.1%	97.9%	4.3%	4.4%	5.3%	4.7%	5.3%	5.3%
	0.25%	100.0%	100.7%	100.4%	100.8%	85.9%	89.3%	98.0%	5.0%	5.2%	5.2%	4.4%	4.5%	5.2%
	0.50%	100.0%	97.6%	101.5%	97.7%	92.6%	102.6%	107.0%	5.2%	5.2%	5.3%	4.5%	5.2%	4.9%
With veil	0.00%	100.0%	85.2%	100.7%	97.0%	97.4%	97.2%	97.8%	4.3%	4.9%	5.2%	4.4%	4.8%	4.5%
	0.25%	100.0%	97.7%	100.5%	103.7%	96.9%	94.7%	96.3%	4.5%	4.8%	5.5%	5.3%	4.6%	4.7%
	0.50%	100.0%	109.8%	108.2%	106.8%	99.0%	101.1%	105.2%	5.2%	5.8%	5.2%	5.1%	5.2%	4.9%
		Retention of compressive strength						Error bars						
No veil	0.00%	100.0%	74.8%	83.4%	68.3%	127.5%	107.3%	101.4%	3.8%	3.9%	3.7%	6.0%	5.5%	4.7%
	0.25%	100.0%	97.4%	97.7%	72.4%	106.9%	73.5%	83.2%	5.0%	4.9%	3.4%	5.2%	3.4%	3.7%
	0.50%	100.0%	102.6%	106.6%	80.7%	97.6%	98.5%	72.9%	4.8%	5.1%	4.3%	5.3%	5.4%	3.5%
With veil	0.00%	100.0%	80.1%	86.8%	69.6%	85.1%	76.9%	103.7%	3.8%	4.2%	3.8%	4.3%	3.9%	5.0%
	0.25%	100.0%	97.3%	102.3%	69.7%	92.4%	103.0%	80.1%	4.7%	4.9%	3.4%	4.3%	5.5%	3.8%
	0.50%	100.0%	93.0%	110.6%	82.1%	104.0%	76.5%	85.7%	4.5%	6.0%	4.3%	5.3%	4.1%	4.5%

**Table 13.07 - Summary of properties of the field study specimens / Figure 13.22 - Mechanical properties of unexposed and exposed specimens (field study).**

Property	Method	Unit	25th of April Bridge		Colombo Centre		Lisbon Oceanarium	
			Unexposed	Exposed	Unexposed	Exposed	Unexposed	Exposed
IMC	Calcination	[%]	71.8 ± 0.37	68.7 ± 0.01	67.5 ± 0.7	69.6 ± 0.9	49.7 ± 0.89	50.8 ± 0.91
Tg	DMA	$T_g$ ( $E'_{onset}$ ) [°C]	90.6 ± 0.8	95.0 ± 4.3	135.5 ± 6.4	130.0 ± 2.8	65.7 ± 0.9	66.5 ± 1.7
		$T_g$ (tan d) [°C]	103.5 ± 3.5	104.7 ± 7.6	142.5 ± 0.7	142.5 ± 2.1	103.0 ± 4.2	99.8 ± 0.3
Mechanical property	Tensile tests	$\sigma_{tu}$ [MPa]	323.1 ± 19.6	371.6 ± 20.7	444.8 ± 40.4	432.6 ± 17.8	255.7 ± 27	193.8 ± 34.3
		$E_t$ [GPa]	37.9 ± 1.9	37.3 ± 1.5	36.8 ± 1	35.3 ± 1.6	17.8 ± 1.4	16.1 ± 1.6
	Compressive tests	$\sigma_{cu}$ [MPa]	485.4 ± 38.8	514.9 ± 8.8	604.8 ± 51.4	487.7 ± 77.7	437.7 ± 57.3	482.7 ± 40.1
	Flexural tests	$\sigma_{fu}$ [MPa]	585.6 ± 17.4	590.1 ± 41.2	639.6 ± 41.9	561.4 ± 1.1	312 ± 9.2	281.9 ± 4.8
		$E_f$ [GPa]	36.3 ± 0.7	32.6 ± 4.3	40.8 ± 4.1	33.8 ± 0.6	15.6 ± 0.1	14.5 ± 1.3
	In-plane shear tests	$t_{max}$ [MPa]	49.6 ± 0.6	51.4 ± 3.2	61.6 ± 1.1	55.1 ± 1.7	57.6 ± 2.4	54.6 ± 2.5
		G [GPa]	3.2 ± 0.1	3.2 ± 0.3	3.8 ± 0.4	3.3 ± 0.1	2.6 ± 0.1	3.0 ± 0.1